THE CD4$^+$ T CELL RESPONSE TO HUMAN CYTOMEGALOVIRUS

Yiling Eleanor Lim

Department of Medicine

University of Cambridge

Darwin College

This thesis is submitted for the degree of

Doctor of Philosophy

June 2021

Declaration

This dissertation is the result of my own work and includes nothing which is the outcome of work done in collaboration except as declared in the Preface and specified in the text. It is not substantially the same as any that I have submitted, or, is being concurrently submitted for a degree or diploma or other qualification at the University of Cambridge or any other University or similar institution except as declared in the Preface and specified in the text. I further state that no substantial part of my dissertation has already been submitted, or, is being concurrently submitted for any such degree, diploma or other qualification at the University of Cambridge or any other University or similar institution except as declared in the Preface and specified in the text. It does not exceed the prescribed word limit for the Degree Committee of the Faculties of Clinical Medicine and Veterinary Medicine.

Yiling Eleanor Lim
June 2021

To mum and dad,
for granting me this sojourn.

The CD4$^+$ T Cell Response to Human Cytomegalovirus

Abstract

Human cytomegalovirus (HCMV) is a betaherpesvirus that infects most humans worldwide. In the healthy host, it elicits a broad immune response involving both the innate and adaptive arms of immunity, which is able to limit viral replication and prevent end-organ disease. However, like all herpesviruses, the virus then establishes a lifelong latent infection such that the host is unable to eradicate the virus completely. This then results in periods during which the virus reactivates and can replicate. In an immunocompetent host, this replication is eventually controlled by a robust secondary immune response. However, when this occurs during periods of immunosuppression, such as after solid organ or haematopoietic stem cell transplantation, the virus is then able to multiply rapidly and infect numerous organ systems. Consequently, HCMV is one of the most frequently-occurring viral infections in such patients. Most of the previous studies on HCMV infections in these patients have focused on the CD8$^+$ T cell response, but in recent years, more evidence has come to light that other immune cell populations play a role as well.

In the work presented in this thesis, I have utilised a viral dissemination assay (VDA) to study the responses of peripheral blood mononuclear cells (PBMCs), CD4$^+$ cells, CD8$^+$ T cells, and natural killer (NK) cells to HCMV infection of autologous fibroblasts in healthy HCMV-seropositive and HCMV-seronegative adults, and showed that there were inherent differences in the ability to control HCMV immediate-early (IE) and late gene expression between the PBMCs, CD4$^+$ cells and CD8$^+$ T cells from HCMV-seropositive and HCMV-seronegative individuals. It was also found that the presence of other immune cells in a CD4$^+$ cell population, such as CD14$^+$ monocytes, are essential for CD4$^+$ T cells to recognise HCMV-infected fibroblasts via the MHC Class II antigen presentation pathway. This leads to the production of a cytokine milieu that can limit HCMV dissemination, of which IFN-γ was found to be one of the key cytokines. A small number of plasmacytoid dendritic cells were also present in the CD4$^+$ cell population, although their contribution to overall control by CD4$^+$ cells is yet to be fully determined.

I have also used the VDA to assess the responses of PBMCs, CD4$^+$ cells, CD8$^+$ T cells, and NK cells from kidney and liver transplant patients to HCMV-infected autologous fibroblasts, and shown that this assay may provide a more comprehensive assessment of the immune response to HCMV than measurement of interferon-γ responses of T cells to HCMV peptides, a commonly used method of immune monitoring in these patient groups. I have also compared the responses of the transplant patients to those from healthy adults, and shown that, during periods of CMV viraemia, patients frequently have responses similar to or worse than those from HCMV-seronegative adults, regardless of the HCMV serostatus of the donor or recipient.

Acknowledgements

To my supervisor, **Dr Mark Wills**, thank you for giving me the opportunities, despite my complete naïveté in any lab work, to join your group — first in 2016 to experience lab work, and then again in 2017 for my PhD. Your open-door policy (probably taken advantage of far too much by myself), neverending patience and encouragement has made my learning process over the last 3.5 years very enjoyable and one that I will miss. Thank you also for the chances you gave me to attend and present my work at international conferences, and helping me to publish my work. I apologise deeply for my contribution to the grey hairs on your head.

To **Prof John Sinclair**, thank you also for forwarding my e-mail back in 2016 to Dr Wills, for the advice and comments on my work, and the opportunity to take part in experiments (latency ones!) that I learnt alot from.

There are many that I owe a debt of gratitude to, without whom I would not have been able to complete this project. To **Dr Sarah Jackson**, thank you for assisting with phenotyping advice, proofreading and editing work, and knowing where everything in the laboratory is kept. To **Georgina Okecha**, thank you for teaching me the basics of laboratory techniques, and for being a magician at growing high-titre virus. To **Paula Rayner**, thank you for the friendly chats and also for providing me cells whenever I needed them. To **Dr Charlotte Houldcroft**, thank you for your assistance with the VDAs on the transplant samples, and for the FluoroSpot data. To **Dr Ian Groves**, thank you for teaching me about qPCR, latency techniques, and how to be a master at bad jokes. To my current and erstwhile fellow office-sharers **Marianne Perera, Martin Potts, Dr George Sedikides, Dr Liz Elder** and the late-comer **Mahlaqua Noor**, thank you for the advice, commiserations, shared jokes and most of all, the friendship—your presence has made the endless hours of lab work much more pleasant. Special mention also goes to **Dr Gennaro Iaconis** for his assistance with proofreading parts of this thesis and his contribution to the convivial office atmosphere.

I would also like to thank collaborators at University College London, **Dr Matthew Reeves, Megan McIntosh** and **Dr Claire Atkinson**, for their assistance with sample collection from the transplant recipients; staff at the NIHR Cambridge BRC Cell Phenotyping Hub for sorting and flow cytometry assistance (especially **Nika Romashova**) and also all the other donors who gave blood or tissue samples for my experimental work.

And finally, to **my family**, for their unwavering support through the years, particularly my

parents, without whom I would not have been able to undertake this PhD.

Contents

List of Figures

List of Tables

Abbreviations

AF Alexa Fluor

AIDS acquired immune deficiency syndrome

APC allophycocyanin; antigen presenting cell

ARPE-19 adult retinal pigmented epithelium-19

BDCA blood dendritic cell antigen

BUV Brilliant UltraViolet

BV Brilliant Violet

cDCs conventional dendritic cells

cGAS cyclic guanosine monophosphate–adenosine monophosphate (cGAMP) synthase

CIITA Class II transactivator

CLEC4C C-type lectin domain family 4 member C

CLIP class II-associated invariant chain peptide

Cy cyanine

DNA deoxyribonucleic acid

E:T effector : target

ER endoplasmic reticulum

Fas/FasL FS-7-associated surface antigen (Fas)/Fas ligand

FITC Fluorescein 5-isothiocyanate

GAS Gamma-interferon activated site

GCSF granulocyte colony-stimulating factor

GMCSF granulocyte-macrophage colony-stimulating factor

GO Gene Ontology

HCMV Human Cytomegalovirus

HFFFs human foetal foreskin fibroblasts

HHV Human Herpesvirus

HLA human leucocyte antigen

HSCT haematopoietic stem cell transplant

HUVECs human umbilical vein endothelial cells

IE immediate-early

IFN interferon

IL interleukin

IRF interferon regulatory factor

ISG interferon-stimulated genes

ISRE interferon-stimulated response element

Jak Janus kinase

MACS magnetic-activated cell sorting

MHC major histocompatability complex

MOI multiplicity of infection

N-myc N-myc proto-oncogene

NF-κB nuclear factor κ-light-chain-enhancer of activated B cells

NFAT nuclear factor of activated T cells

NK natural killer

ORFs open reading frames

PBMCs peripheral blood mononuclear cells

PBS phosphate-buffered saline

PCR polymerase chain reaction

pDCs plasmacytoid dendritic cells

PE phycoerythrin

PKR protein kinase R / interferon-induced, double-stranded RNA-activated protein kinase

pp phosphoprotein

RNA ribonucleic acid

SOT solid organ transplant

STAT signal transducer and activator of transcription proteins

STING stimulator of interferon genes

TBS tris-buffered saline

TGF transforming growth factor

TLR toll-like receptor

TNF tumour necrosis factor

TRAIL TNF-related apoptosis-inducing ligand

UL Unique Long

US Unique Short

VDA viral dissemination assay

Chapter 1

Introduction

1.1 HCMV

1.1.1 General virology and classification

Human cytomegalovirus first came to medical attention when its characteristic "owl's eye inclusions" were seen in histology samples from luetic stillborn foetuses in 1904 [4, 483], and then again in 1964 among patients undergoing organ transplantation [488]. It belongs to the *Herpesviridae* family, which are large, icosahedral, enveloped viruses with double-stranded DNA genomes. The *Herpesviridae* are further subdivided into alpha-, beta-, and gamma-herpesviridae. HCMV belongs to the betaherpesviridae subfamily, of which mammals serve as natural hosts. There are 18 species in this subfamily, among which three are pathogenic to humans : human herpesvirus 5 (cytomegalovirus), human herpesvirus 6 (HHV-6) and human herpesvirus 7 (HHV-7).

1.1.2 Structure and genome

The virion structure consists of a DNA core inside an icosahedral capsid made up of 162 capsomeres surrounded by an envelope derived from host cell membrane containing viral glycoproteins that control attachment and entry into cells [160]. The nucleocapsid is enclosed in a tegument composed of virus-encoded proteins, and the tegument is surround by a lipid bilayer envelope derived from the ER-Golgi intermediate compartment. Five envelope glycoproteins (gB, gH:gL, gM:gN) provide essential attachment functions in fibroblasts and are targets of neutralising antibodies. The HCMV genome consists of two segments, the Unique Long (UL) and Unique Short (US) sequences, both of which are flanked by terminal and internal repeats in a manner that promotes genome isomerisation during replication [403].

1.1.3 Viral life cycle and lytic replication

As with all herpesviruses, HCMV has two life cycle phases: a productive phase where new virions are produced, and a latent phase where there is a restricted gene transcription profile and no new virion production. The HCMV genome is predicted to encode over 50 glycoproteins, of which five are essential for viral entry [396]. These include glycoprotein B (gB; UL55), gM/gN (UL100/UL73), and gH/gL (UL75/UL115) [396].

Lytic HCMV DNA synthesis occurs in the nucleus of infected cells, starting as early as 14 to 16 hours post-infection and reaching to greater than 10,000 viral genome copies per cell [587] at the time progeny virions start to form [18,425]. *In vitro*, skin or lung fibroblasts are the most efficient producer cell lines for HCMV and thus remain the standard cell line for isolation and propagation of HCMV from patient samples [529], while other cell cultures (e.g. monocyte-derived macrophages) are only low-level productive and hardly release sufficient amounts of infectious progeny to maintain the virus during repeated passaging of cell-free supernatant on the respective cell type [532].

HCMV initiates infection via a tethering interaction of virions to cell surface heparan sulphate proteoglycans (HSPG), mediated by gB and gM/gN [110, 287]. Binding to HSPG is thought to help stabilise the virion at the cell surface until other downstream receptors are engaged [110]. Receptor clustering and signaling occurs following engagement of cellular integrins by gB and gH, leading to downstream signaling events necessary for virus entry and/or gene expression. Lastly, gH/gL/gO along with gB mediates fusion of viral and cellular membranes, through gB and gH interactions with cellular integrins [250]. The trimeric gH complex is sufficient for infection of fibroblasts, while the pentameric gH complex, which consists of gH, gL, UL128, UL130 and UL131A is required for infection of endothelial and epithelial cells. [493, 622]

Following entry, three kinetic classes of genes, immediate-early (IE), early (E) and late (L), are expressed sequentially over the course of 48-72 hours. During the IE phase, the most abundant gene transcription occurs from the major immediate early promoter (MIEP), when alternative splicing of UL123 and UL122 regions give rise to the IE72 and IE86 proteins, which remove epigenetic repressors and transactivate further HCMV genes and promoters, allowing progression into early and late phase. Expression of IE gene transcription is controlled by transcription factors binding to upstream viral gene enhancers and the tegument protein pp71. [394].

Following peak expression of MIE regulatory proteins, the E proteins become transcriptionally active. A total of 65 proteins and assorted miRNAs are produced during this period, with some key proteins being UL54 (encoding DNA polymerase) [637], UL34 and various structural and core proteins. Late gene expression initiates capsid assembly in the nucleus, followed by nuclear egress to the cytosol. Capsids associate with tegument proteins in the cytosol and

are trafficked to the viral assembly complex that contains components of the endoplasmic reticulum, Golgi apparatus and endosomal machinery. The capsids further acquire tegument and viral envelope by budding into intracellular vesicles at the viral assembly complex. Eventually, enveloped infectious particles are released along with non-infectious dense bodies [45]. Expression of HCMV late genes is maximal after viral DNA replication has begun. The lytic life cycle of HCMV is summarised in Figure 1.1.

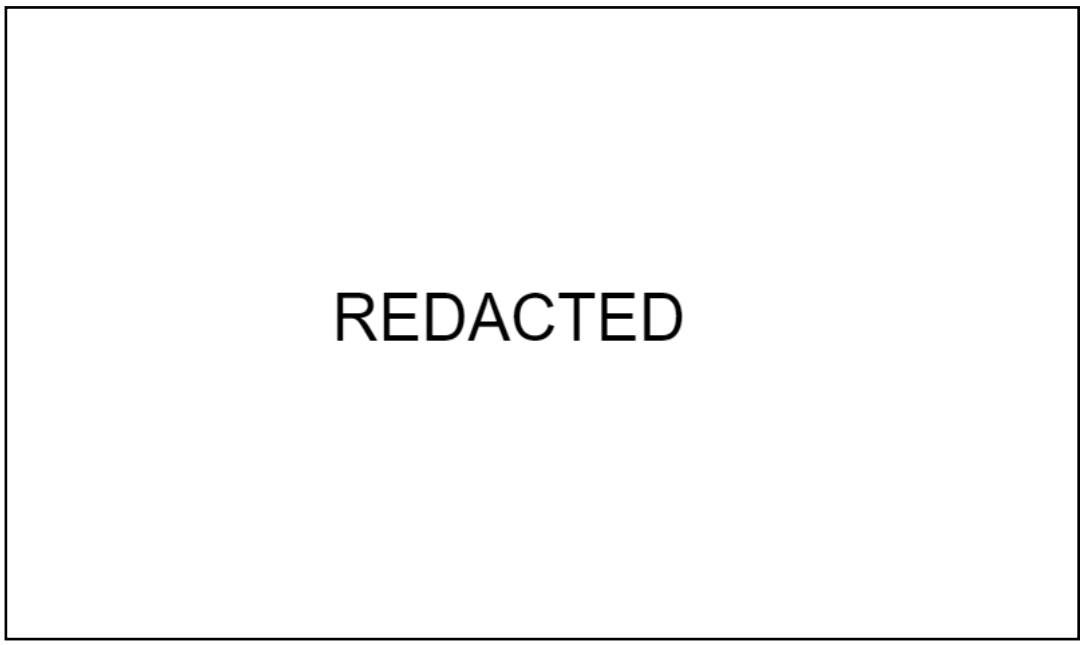

Figure 1.1: Lytic life cycle of HCMV
From Crough and Kanna, 2009 [120]

1.1.4 Viral Latency

Following primary infection, HCMV establishes a latent infection involving the $CD34^+$ haematopoietic stem cell population in the bone marrow [388, 527] and $CD14^+$ monocytes in the peripheral blood [326, 569, 570]. Latent carriage of the virus is defined by the viral genome being maintained in the host cell but no infectious virions being produced, with the virus maintaining an ability to reactivate to a lytic infection. At the molecular level, this is characterised by overall suppression of viral lytic gene expression attributable to epigenetic regulation via histone modification machinery, a limited and specific transcriptional gene profile, and a responsiveness to host-derived cues to exit latency and re-enter the lytic lifecycle [140, 471].

Suppression of the major immediate early promoter (MIEP) is achieved through cellular transcriptional repressors directing histone-modifying enzymes to impart repressive post-translational modifications of MIEP-associated histones [525]: there is tri-methylation of histone H3 and recruitment of heterochromatin protein-1 (HP-1) with a concomitant absence of histone acetylation on histone H4 [404, 472, 473, 490], leading to repression of MIEP and

lytic gene expression in $CD34^+$ progenitor cells. This chromatin phenotype is maintained in the monocytes directly infected by the virus as well as those derived from these progenitors [473,474]. Upon differentiation to terminally differentiated macrophages or dendritic cells, these repressive histone modifications are lost and IE gene expression is observed followed by production of infectious virus [223, 473, 543, 570].

While it would seem ideal to maintain a quiescent state to evade immune detection, it has been found that latency does not equate to transcriptional quiescence. A number of transcripts have now been confirmed to be expressed during natural latency, and some of these transcripts and their functions are as summarised in Table 1.1 below.

Table 1.1: HCMV gene products during latency

Gene products	Function in latency	Refs
UL135	Interacts with Abi-1 and CIN85 to downregulate EGFR, promoting reactivation from latency	[73, 461]
UL136	23- and 19-kDA isoforms suppress replication and promote latency, 33- and 26-kDA isoforms required for efficient reactivation/replication	[90, 593]
UL138	Upregulation of TNFR1 and downregulation of MRP1, repression of MIEP	[329, 628]
UL81-82ast (LUNA)	Promotes UL138 expression	[44, 299]
Splice variant of UL111A (LAcmvIL-10)	Downregulation of MHC Class II Suppression of cellular miRNA hsa-miR-92a, leading to upregulation of CCL8	[265, 266] [449]
lnc4.9	Binds PRC2, silencing the MIEP	[490]
UL84	Genome maintenance	[490]
US28	Attenuates MAP kinase and NF-κB pathways Downregulation of interferon-inducible genes Evasion of neutrophil recruitment and killing	[312] [149] [148]
UL144	Regulated by GATA-2, function unknown	[448]
UL33	Induces cellular CREB1 phosphorylation, promoting reactivation when recruited to MIEP	[313]
lnc2.7	Unknown	[490, 520]
miR-UL112-3p	Targets IE72 expression, limits cytotoxic T cell recognition of infected cells	[390]
miR-UL148D	Inhibits activin A-triggered secretion of IL-6 Maintains CDC25B activity in host cells	[327] [424]
miR-US5-2	Targets NAB1 to increase TGF-β secretion	[220]

Table 1.1 continued from previous page

Gene products	Function in latency	Refs
miR-UL22A, miR-US25-1	Inhibit proliferation of latently infected $CD34^+$ progenitor cells	[220, 267]

Abi-1 = Abelson interactor 1 protein; CDC25B = cell division cycle 25B phosphatase; CIN85 = Cbl (Calcineurin B-like protein)-interacting protein of 85 kDa; CREB1 = cyclic AMP response element binding protein 1; EGFR = epidermal growth factor receptor; GATA-2 = GATA-2 transcription factor; lnc = long non-coding RNA; LUNA = latency unique natural antigen; MAP kinase = mitogen-activation protein kinase; MIEP = major immediate-early promoter; miR = microRNA; MRP1 = Multidrug resistance-associated protein 1; NAB1 = nerve growth factor-induced protein A-binding protein 1; NF-κB = Nuclear factor-κB; PRC2 = polycomb repressor complex 2; TGFβ = transforming growth factor β; TNFR1 = Tumour necrosis factor receptor 1.

Adapted from Sinclair and Reeves, 2013 [526]

1.1.5 Clinical aspects

1.1.5.1 Primary infection

Primary HCMV infection in the immunocompetent host may manifest as a viral syndrome of fever for >10 days, malaise, myalgias, headache and fatigue. Less commonly, hepatomegaly, splenomegaly and lymphadenopathy may also occur, while laboratory findings include lymphocytosis with activated or atypical lymphocytes and elevated hepatic transaminases [160]. In immunocompetent individuals, the innate and adaptive arms of the immune system are capable of limiting lytic viral replication and preventing end-organ disease [120]. This thus results in a largely self-resolving mononucleosis-like illness, although the virus then establishes a lifelong persistent infection through latency with periods of reactivation, during which productive lytic infection and viral shedding occurs [526].

1.1.5.2 In utero

Primary maternal CMV infection during gestation poses a 40-50% risk of intrauterine transmission [71], while reactivation in seropositive mothers rarely causes symptomatic disease [173, 174], suggesting a significant role of maternal antibodies in fetal protection, although superinfection during pregnancy is also a cause of congenital CMV [295]. Congenital disease and placental damage are more severe when primary maternal infection occurs in the first trimester [47, 199, 549]. Up to two-thirds of affected newborns present with central nervous system involvement, manifesting as intracranial calcifications, microcephaly, and mental retardation, while other common abnormalities include hearing loss and chorioretinitis, with

neonatal death occurring in approximately 10% of symptomatic newborns [160]. The level of viraemia at birth or early infancy correlates with severity of congenital disease [65, 67, 321].

1.1.5.3 In immune-compromised and transplant patients

HCMV remains one of the most common complications affecting transplant recipients [203]. Clinical manifestations of infection arise from virus from the donor organ or stem cells, or from latent virus reactivation within the recipient [160]. Common presentations of end-organ disease include pneumonitis, gastrointestinal lesions, hepatitis, retinitis, pancreatitis, myocarditis, and rarely, encephalitis or peripheral neuropathy. Primary HCMV infection in this population has also been linked with dysfunction of the transplanted organ [162, 163]. Section 1.2.7 will consider the situations in both solid organ transplants and haematopoietic stem cell transplants in greater detail.

1.1.5.4 Innate immune response to HCMV

HCMV induces a broad immune response involving the innate and adaptive arms of the immune system in healthy people. The innate response includes intrinsic immunity, which refers to cellular responses, such as DNA sensing mechanisms or apoptosis pathways, and also includes innate cell-mediated responses, such as NK cells, macrophages and the Complement system. Some of the intrinsic cellular responses are discussed in the following section and listed in Table 1.2 below.

Toll-like receptors (TLRs)

The initial stages of CMV infection are subject to innate detection by TLR2, a class of pattern recognition receptors that detect pathogens through recognition of features not seen in human cells, facilitated by CD14 [109]. A possible clinical corollary is the observation that liver transplant recipients carrying an inactivating point mutation in the Toll-IL-1 receptor (TIR) domain of TLR2 were found to have a higher HCMV load [301]. This was subsequently followed by discovery that TLR2, TLR3 and TLR9 were upregulated in THP-1 monocytes infected with HCMV [653]. This also has a possible clinical correlate in the observation that a polymorphism (T-1237C) affecting TLR9 promoter activity was seen to be significantly associated with symptomatic HCMV infection in stem cell transplant recipients [87].

Nucleotide-binding oligomerisation domain (NOD)-like receptors (NLRs)

NLRs induce NF-κB in response to bacterial pathogens. Infection of human fibroblasts with HCMV was found to promote expression of NLRC5 mRNA within 24 hours [316], while ectopic expression of a NOD2 mutant (3020insC) was found to cause increased HCMV replication and

reduced levels of IFN-β in HFFs [286]. The same group also subsequently found that activation of NOD1 (through IKKα and IRF3) resulted in inhibition of HCMV infection in HFFs [155].

cyclic GMP-AMP synthase (cGAS)

cGAS is a DNA sensor that binds HCMV dsDNA. HCMV infection leads to enhanced expression of cGAS in plasmacytoid dendritic cells (pDCs) and monocyte-derived DC (moDCs) [423], leading to activation of the STING/TBK-1/IRF3 pathway [356].

Gamma-inteferon-inducible protein 16 (IFI16)

IFI16 is, as its name suggests, an interferon (IFN)-inducible protein, a member of the PYHIN family of proteins (pyrin and HIN200 domain–containing proteins), a group of proteins that have been fairly recently discovered as receptors mediating the detection of foreign DNA and initiating innate immune responses [118]. In the context of HCMV, IFI16 was found to bind viral DNA and trigger expression of antiviral cytokines including IFN-β via the STING-TBK-IRF3 signaling pathway, while the tegument protein pp65 binds to the pyrin domain of IFI16, hindering its DNA-dependent oligomerisation and promoting IFI16 nuclear delocalisation and inhibition of the immune response [342, 594].

Z-DNA-binding protein 1 (ZBP1)/DNA-dependent activator of IRFs

In experiments performed in human fibroblast cell lines, it was shown that after entry into host cells, HCMV activates ZBP1 transcription. ZBP1 then promotes TANK binding kinase 1 (TBK1)-mediated phophorylation of Dead box protein 3 (DDX3) and IRF3 proteins, leading to transcription of IFN-β and IFN-stimulated genes in a Jak-STAT-dependent manner [130].

Table 1.2: Sensors of HCMV DNA and intrinsic immune response pathways triggered

DNA sensor	Immune pathway triggered	References
TLR2	IFN-β via MyD88	[37]
	IL-6, IL-8 & IL-12 via NF-κB	[109]
TLR3	IFN-β via TRIF	[653]
	IL-6, IL-8 & IL-12 via NF-κB	[653]
TLR9	IFN-β via TRIF	[653]
	IL-6, IL-8 & IL-12 via NF-κB	[653]
NLRC5	IFN-α	[316]
NOD2	IFN-β via IRF-3	[286]
	IL-8 via NF-κB	[286]
NOD1	IFN-β	[155]
cGAS	IFN-α, IFN-β via STING	[356, 423]
IFI16	IFN-β via STING	[594]

Table 1.2 continued from previous page

DNA sensor	Immune pathway triggered	References
ZBP1	IFN-β via DDX3	[130]

cGAS = cyclic GMP-AMP synthase; DDX3 = DEAD box protein 3; IFI16 = gamma-interferon-inducible protein 16; TLR=Toll-like receptor; MyD88 = Myeloid differentiation primary response 88; NF-κB = nuclear factor kappa-light-chain-enhancer of activated B cells; NLRC5 = NOD-like receptor family caspase activation and recruitment domain-containing 5; NOD = Nucleotide-binding oligomerisation domain; STING=stimulator of interferon genes; TRIF = TIR-domain-containing adapter-inducing interferon-β; ZBP1 = Z-DNA-binding protein 1.

Adapted from Biolatti et al, 2018 [56]

NK cells

Natural Killer (NK) cells are cytotoxic innate lymphoid cells that primarily recognise their targets by a lack of major histocompatability complex (MHC) I (MHC Class I) expressed on the cell surface, so-called "missing self" recognition [289, 358]. They primarily exert their cytotoxic effects by release of lytic granules which contain molecules such as perforin, granzyme and granulysin that can induce cell death in stress cells, and also secrete tumour necrosis factor (TNF) superfamily members, such as Fas Ligand and TNF-related apoptosis-inducing ligand (TRAIL), which can induce apoptosis in targeted cells [325]. The regulation of NK cell activity is governed by a balance of activating receptors (such as NKG2D, which recognises ligands on stressed cells, and members of the natural cytotoxic receptor family, such as NKp30,NKp40 and NKp46) and inhibitory receptors, (such as killer immunoglobulin-like receptors, KIRs, which recognise MHC Class I complexes) [627]. NK cells can also be activated by antibody-coated targets which are recognised via FcγRIII, a phenomenon known as antibody-dependent cellular cytotoxicity [324, 464].

There are observations of patients with NK cell defects experiencing severe HCMV (and other herpesvirus) infections [57, 183, 419], and some evidence in transplant patients that show an association of recovery of NK cell function with protection against HCMV viraemia [40]. HCMV-infected individuals exhibit elevated proportions of LIR-1$^+$ and CD94$^+$NKG2C$^+$ NK cells [49, 210], and during acute HCMV infection, the CD94$^+$NKG2C$^+$ NK cells proliferate and acquire expression of CD57 [362], a marker associated with greater cytotoxic potential but reduced responsiveness to cytokines [361]. This expansion may represent an adaptive antiviral NK response with associated characteristics of memory, though the exact function of CD57 has been difficult to discern as CD57 is not a protein but a sulfoglucoronyl carbohydrate moiety found on a range of different glycolipids and glycoproteins [103, 315]. However, multiple *in vitro* studies using low-passage HCMV strains in fibroblasts showed protection against NK cell-mediated cytotoxicity [95, 620, 623], and the only example of NK cells controlling low-

passage HCMV strains was via a non-cytolytic mechanism [252]. Perhaps as a testament to the success of HCMV against NK cell-mediated cytotoxicity, the virus encodes multiple gene products targeting NK cell functions, a summary of which is listed in Table 1.3 below (non-exhaustive list).

Table 1.3: Modulation of NK cells by HCMV

Gene	Activity	Refs
US2	Reduction of MHC-I surface expression by proteasomal degradation	[38, 638]
US3	ER retention of MHC-I	[270]
US6	Blocks TAP-mediated peptide translocation, leading to downregulation of MHC-I	[336]
US9	Proteasomal degradation of MICA *008	[513]
US10	Degradation of HLA-G	[427]
US11	Proteasomal degradation of MHC-I	[38, 269]
US12, US13	Downregulation of ULBPs	[159]
US18	MHC-I homolog Lysosomal degradation of activating receptor NKG2D ligand MICA Downregulation of B7-H6, ligand of activating receptor NKp30	[455] [158] [97]
US20	Lysosomal degradation of activating receptor NKG2D ligand MICA Downregulation of B7-H6, ligand of activating factor NKp30	[158] [97]
pUL11	Inhibition of CD45-mediated signalling through direct binding	[665]
UL16	Intracellular retention of activating receptor NKG2D ligands MICA/B and ULBPs	[144] [633]
UL40, miR376a	Upregulates HLA-E independent of TAP, miR376a blocks HLA-E surface expression	[580]
UL83 (pp65)	Inhibition of NKp30-mediated killing via suppressing activating signal through CD3ζ.	[25]
RL11-13, UL119-118	Fcγ binding and inhibition of FcR signalling, inhibition of ADCC	[112]
UL135	Suppression of immune synapse formation by actin remodeling via relocalisation of WAVE2 complex	[551]
UL141	ER retention of CD155, ligand involved with motility, adhesion, transendothelial migration and endocytosis ER retention of CD112 ligand for activating receptor DNAM-1 (requires US2) ER retention of TRAIL ligands	[581] [456] [541]
UL142	Intracellular retention o activating receptor NKG2D ligand ULBP3 Intracellular retention of activating receptor NKG2D ligands MICA/B	[633] [26]

Table 1.3 continued from previous page

Gene	Activity	Refs
UL148	Lysosomal degradation of LFA-3, ligand for activating receptor CD2	[624]
UL148A	Lysosomal degradation of activating receptor NKG2D ligands MICA/B and ULBPs	[127]
miR-UL112	Downregulation of MICB expression	[554]
miR376a	Blocks HLA-E surface expression	[406]

ER=endoplasmic reticulum; TAP=transporter associated with antigen processing; MICA/B=MHC Class I polypeptide-related sequence A/B (stress-induced ligands for NKG2D); ULBP=UL16 binding protein; ADCC=antibody-dependent cellular cytotoxicity; WAVE2=Wiskott-Aldrich syndrome protein family verprolin-homologous protein 2; DNAM-1=DNAX accessory molecule-1 (CD226); LFA-3=lymphocyte function-associated antigen-3 (CD58); TRAIL=TNF receptor apoptosis-inducing ligand

Adapted from Wilkinson, et al, 2008 [642] and Forrest, et al, 2020 [170]

There have also been corollaries of these modulatory effects seen in murine CMV (MCMV). For instance, the MCMV glycoprotein m157 is an MHC-I homolog which inhibits NK cell activation via inhibitory receptor Ly49I [23, 332]. Murine resistance to MCMV is determined by the *Cmv1*^{r} gene, which encodes the activating NK receptor Ly49H [505, 506]. NK cells which bear the activating receptor Ly49H directly recognise and are activated by virally-infected cells expressing m157 [23, 72, 124], while most strains of MCMV possess forms of m157 which can evade Ly49H-dependent NK cell activation [610].

Although NK cells have classically been described as part of innate immunity, in recent years there has been emerging evidence for NK cell memory and adaptive NK cell responses. NK cells from mice show characteristics of adaptive immunity, such as undergoing expansion and contraction phases following primary infection, and have 'memory' and recall characteristics upon rechallenge with MCMV antigens [559] while those bearing the Ly49H receptor proliferate in response to their recognition of m157 [135]. These adaptive features were also seen in liver-resident NK cells [632]. In humans, NK cells positive for the activating receptor NKG2C$^+$ have been well-described to expand in response to acute HCMV infection [211, 212, 362, 374] and reactivation [167] and are found in higher numbers in HCMV-seropositive individuals [210].

1.1.5.5 Adaptive immune response to HCMV

The adaptive arm of the immune response comprises of cell-mediated immunity, and antibody-mediated, or humoral immunity. Cell-mediated immunity of the adaptive immune response includes responses from CD8$^+$ and CD4$^+$ T cells. The humoral and CD8$^+$ T cell

responses to HCMV are covered in brief in the following paragraphs, and a more in-depth explanation of $CD4^+$ T cell response to HCMV is detailed in Section 1.2.4.

Humoral response

Following primary infection, antibodies specific for structural tegument (pp65, pp150, pp28), envelope glycoproteins (gB, gH) and non-structural proteins such as IE1 and pp52 can be detected in the serum [202,322,602]. Initially, the HCMV envelope glycoproteins gB, gH/gL, and gM/gN were thought to be the major targets of the humoral response, although subsequently antibodies directed against the pentameric complex gH/gL/pUL128L/pUL130/pUL131 were shown to prevent viral entry into epithelial and endothelial cells [493]. Most of the neutralising antibodies detected after natural and experimental infection and in commercial immunoglobulin preparations comprise of antibodies to the pentameric complex [172,275,350]. The presence of antibodies does not provide protection from infection, although in the context of congenital CMV (cCMV) the presence of maternal antibody to CMV before conception prevents severe sequelae of disease [174]. Vaccine trials using recombinant gB have shown partial protection from maternal and congenital infection [428], and solid organ transplant recipients [204], although a fully protective vaccine has yet to be designed (reviewed in [187]), perhaps hampered by the fact that relatively little experimental data exists on the mechanisms of protection of the individual antibodies [3].

$CD8^+$ T cells

$CD8^+$ T cells are cytotoxic lymphoid cells expressing the T cell receptor, and CD3 and CD8 co-receptors [85] that primarily recognise infected cells by antigen presentation via the MHC Class I pathway [476,546]. They exert their cytotoxic effects primarily via secretion of cytokines IFN-γ and TNF-α [294, 429] and release of cytotoxic granules such as perforin and granzymes [231, 442, 443]. They can also kill infected cells via Fas/Fas ligand binding on infected cells, which results in the triggering of apoptosis pathways [219, 364]. Upon exposure to antigen, naïve $CD8^+$ T cells differentiate into a variety of subsets, with the subsets they differentiate into dependent on the specific polarising cytokines present, as detailed in Fig.1.2. Following a primary response to antigen, $CD8^+$ T cells then contract and a population of memory $CD8^+$ T cells remain [393], which are capable of rapid proliferation and conversion to effector cells upon re-encounter with antigen [277, 521] .

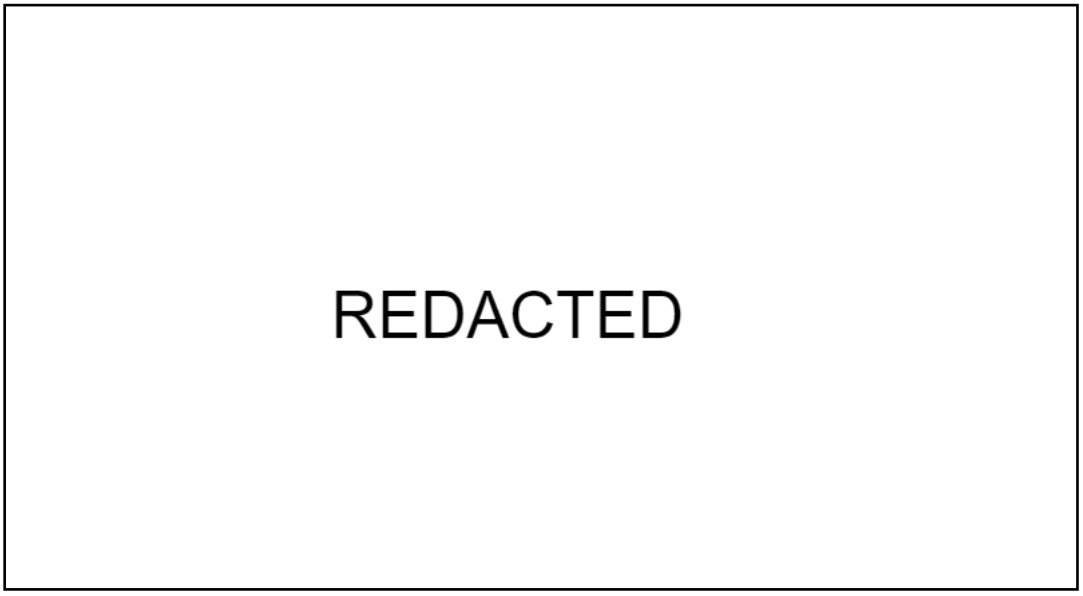

Figure 1.2: CD8$^+$ T cell subsets, and the cytokines which influence their differentiation Upon exposure to antigen, CD8$^+$ T cells differentiate to different subsets, depending on the polarising cytokines present. Following differentiation, each subset produces distinct cytokine profiles. T_c = cytotoxic T cell; IFN = interferon; TNF = tumour necrosis factor; IL = interleukin; TGF = transforming growth factor. Figure from St. Paul and Ohashi, 2020 [548]

Patients with normal antibody levels but profoundly impaired cell-mediated immunity can suffer from CMV disease, and the degree of T-cell impairment parallels the severity of the disease, as reflected clinically in AIDS patients as well as solid organ and stem cell transplant recipients [151, 465]. The T-cell response is broad and persistent, and in adoptive transfer experiments, CD8$^+$ T cells with specificity for HCMV tegument proteins appear protective, although dependent upon the presence of CD4$^+$ T cells in the transfer.

CMV-specific CD8$^+$ T cell populations have been studied extensively and make up a high frequency of CMV-specific memory T cell populations, with epitopes derived from pp65 and IE1 regularly reaching 5-10% of total CD8$^+$ T cells in the blood. In the most comprehensive study to date examining IFN-γ responses to 213 predicted HCMV open reading frames (ORFs), up to 30% of total CD8$^+$ T cells in healthy seropositive adults showed an IFN-γ response, and recognised a median of 8 ORFs [564]. There is, however, a wide variability in the size of T cell responses between individuals and the reasons for this are as yet unclear [254]. These T cells appear to occupy the more mature end of a continuum of memory T cell phenotypes, and are associated with downregulated expression of CD27 and CD28, upregulated CD57, killer cell lectin-like receptor subfamily G member 1 (KLRG1) and the expression of effector molecules such as perforin and granzyme B [22]. In transplant patients, multiple studies have shown that recovery of the CMV-specific CD8$^+$ T cell response is required for successful protection against CMV disease [583–585].

In mouse models, effector and memory CD8$^+$ T cells protected against lethal MCMV disease after adoptive transfer into immunocompromised MCMV-infected recipients [468, 470],

and in a mouse model of experimental CMV-associated interstitial pneumonia after bone marrow transplant, depletion of $CD8^+$ T cells by anti-$CD8^a$ntibodies led to lethal organ disease [444, 445], while adoptive transfer of pulmonary $CD8^+$ T cells prevented viral replication and disease in immunocompromised recipients [16, 445].

1.1.6 HCMV strains used in experimental work of this project

The initial HCMV strain used in most studies worldwide was isolated from adenoid tissue of a 7 year old girl, designated AD169 [491]. Subsequently, attempts to develop an attenuated vaccine by passaging HCMV 125 times *in vitro* led to development of the Towne strain [441]. Characterisation of the genomes of these strains showed that both had deletions at the 3' end of the U_L/b' region, combined with expansion of the long terminal repeat, TR_L/IR_L [98]. A prospective study comparing the genomes of HCMV strains that had been passaged up to 63 times *in vitro* with the original clinical sample showed that mutations occurred in all samples [126]. In particular, defects in UL128L were specifically associated with culture in fibroblasts [126]. Earlier studies using AD169 and Towne strains also showed susceptibility to NK cell-mediated lysis [95,580,623], but following repair of the U_L/b' region, the Towne strain showed resistance to this [581]. Thus, when interpreting studies of HCMV, it is important to consider the strain used and which deletions it may contain. Pertinent to this Introduction, other HCMV strains used in the papers cited include the low-passage clinical strain NEWT, which has been adapted for propragation in human umbilical vein endothelial cells (HUVECs), and the clinical isolate VR1814, from the cervical secretions of a pregnant woman with primary HCMV, which has been shown to be leukotropic and endothelial cell-tropic [201].

The strain used in most of the experiments in this project is a bacterial artificial chromosome (BAC)-cloned version of strain Merlin, which was isolated from neonatal urine samples and chosen on the basis of efficient recovery from frozen stocks and genomic integrity in preliminary sequencing analysis [641]. It contains the complete wildtype HCMV genome, with the exception of point mutations in RL13 and UL128, which were subsequently repaired to match the presumed sequence in the clinical sample, except for three non-protein-coding differences in the *b/b'* region [641]. RL13 encodes a virion glycoprotein which represses HCMV replication in HFFFs and ARPE-19 cell lines [550], while UL128L proteins form part of the pentameric virion envelope glycoprotein complex that promotes infection of endothelial, epithelial and myeloid cells [8, 188, 213, 430, 493, 557, 621] but not in fibroblasts [550].

The other strain used in the experimental work of this project is the TB40/E strain. This strain is derived from the throat wash of a bone marrow transplant recipient by propagation for 5 passages in fibroblasts and 22 passages in endothelial cells [531], and has been used by multiple groups as a highly endotheliotropic and macrophage-tropic strain [14,48,233,239,303, 401,472,475,533] due to its ability to maintain endothelial cell tropism for both fibroblasts and

endothelial cells even after extensive passaging in fibroblasts [531], although genetic sequencing has shown it to be both genetically [136] and phenotypically heterogeneous [497].

1.2 CD4$^+$ T cells

CD4$^+$ T cells comprise the majority of T lymphocytes in healthy individuals. T lymphocytes originate from precursors arising in the foetal liver and adult bone marrow that then enter the thymus. Here, cells whose TCRs bind with low avidity to self peptide-self major histocompatibility complex (MHC) complexes on cortical thymic epithelial cells are stimulated to survive and differentiate into CD4$^+$ or CD8$^+$ T cells (a process known as "positive selection") [19]. This is followed by a further process of elimination (by apoptosis) in the thymic medulla of most T cells that bind to self peptide-MHC complexes with high avidity ("negative selection") [566], although a few of these cells survive to differentiate into regulatory T cells (T_{reg}). This process is also known as central tolerance. These CD4$^+$ T cells then enter the bloodstream and differentiate into CD4$^+$ T cell subsets as described in the subsequent sections.

1.2.1 The MHC class II antigen presentation pathway to CD4$^+$ T cells

The CD4 co-receptor on CD4$^+$ T cells binds to the MHC class II molecule on antigen presenting cells (APCs). The MHC class II molecule is a heterodimeric receptor which consists of an α and β chain and is constitutively found on professional antigen presenting cells, but its expression can also be induced on the surface of non-professional APCs by a variety of immune regulators [236]. MHC class II molecules assemble within the endoplasmic reticulum (ER) and are transported to endosomes with an associated protein, the invariant chain (I_i), which occupies the peptide-binding cleft of these newly synthesised MHC class II molecules and prevents the newly-synthesised MHC class II heterodimer from accepting peptides. These MHC class II-I_i complexes are then transported through the Golgi apparatus to the MHC class II compartment, either directly or via the plasma membrane [411]. The I_i is then released by progressive protelysis in acidic endosomes [626], resulting in a peptide of roughly 20 amino acid residues that is associated with the binding groove in the MHC class II molecule, known as class II-associated invariant chain peptide (CLIP) [62]. The MHC-encoded heterodimeric glycoprotein HLA-DM then interacts with MHC class II-CLIP complexes and promotes a conformational change that induces CLIP dissociation and subsequently allows loading of MHC class II molecules with antigenic peptides, which are then presented to CD4$^+$ T cells in association with co-stimulatory molecules (not shown in diagram). A summary of the MHC class II antigen presentation pathway is shown in Figure 1.3.

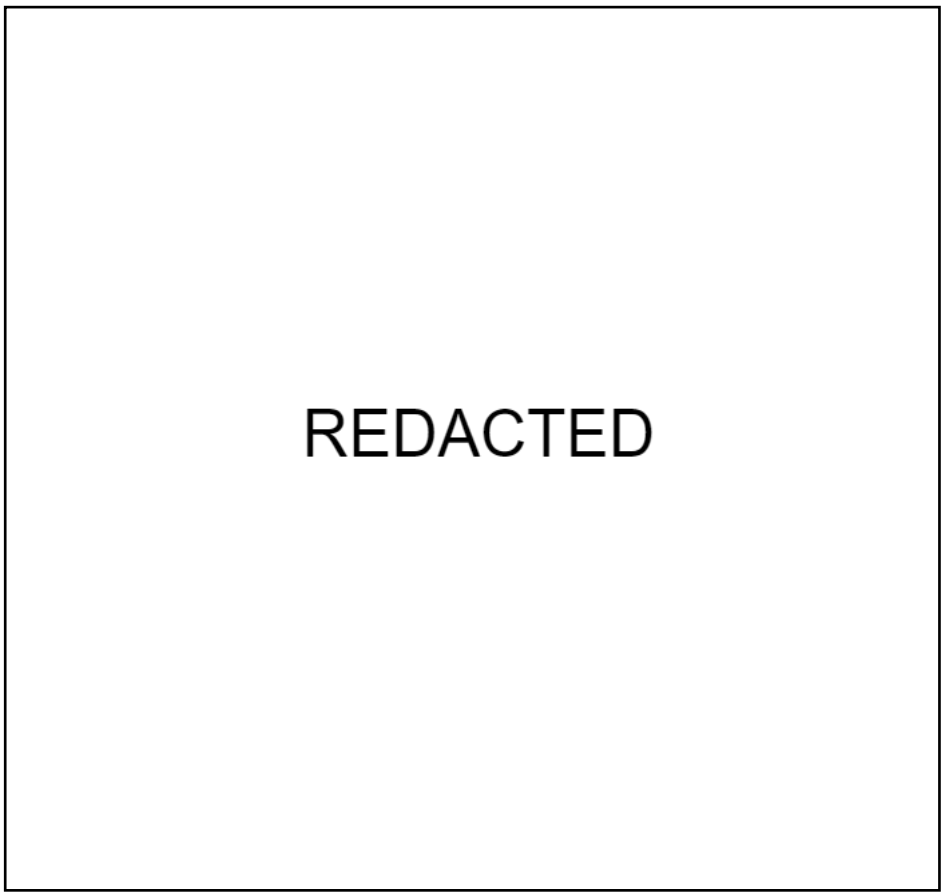

Figure 1.3: Basic MHC class II antigen presentation pathway
APC = antigen presenting cell; CLIP = Class II-associated invariant chain peptide; ER = endoplasmic reticulum; Ii = invariant chain; MIIC = MHC Class II compartment; TCR = T-cell receptor. Figure from Neefjes, et al., 2011 [411]

1.2.2 Activation and their role in adaptive immunity

Binding of the T cell receptor on T cells (with CD4 as a co-receptor) with the MHC class II-antigen complex induces a network of downstream signalling events that trigger $CD4^+$ T cell activation, differentiation and memory cell generation. The subset into which the $CD4^+$ T cell differentiates depends on the cytokine milieu of the microenvironment, concentration of antigens, type of APC, and co-stimulatory molecules involved in the interaction [365], though there has been demonstration of a degree of plasticity between these different subsets [91]. The cytokines that influence the differentiation of the activated $CD4^+$ T cell into the respective $CD4^+$ T cell subset, and the corresponding cytokines secreted by each subset, is summarised in Figure 1.4.

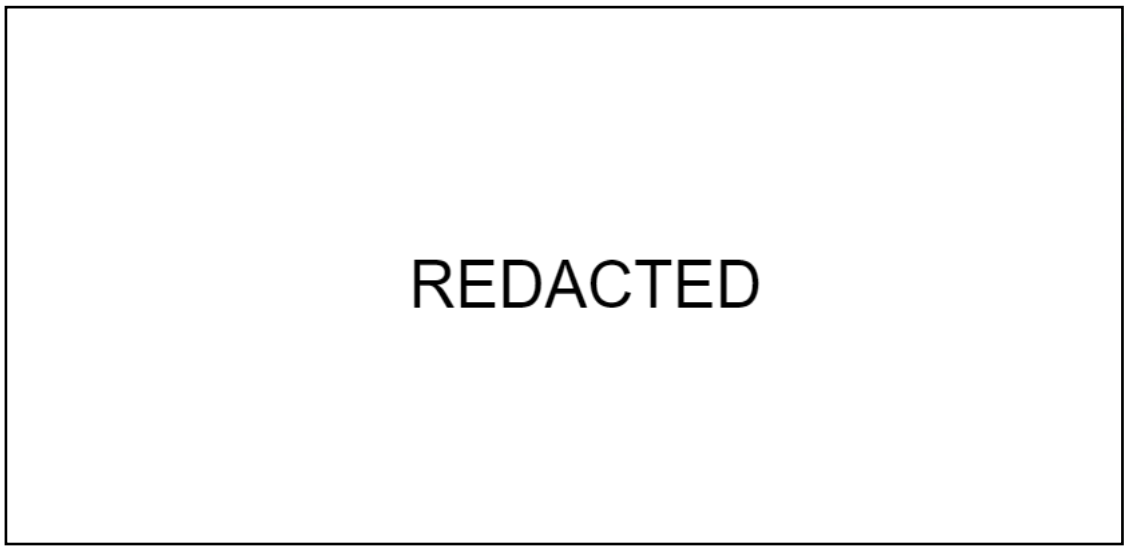

Figure 1.4: CD4$^+$ T cell subsets and associated transcription factors and cytokines Following activation of the CD4$^+$ T cell, cytokines present in the microenvironment (indicated on arrows) trigger expression of various transcription factors (labelled in each cell subset in circles), which then determine the type of effector cell that is induced. The typical cytokines secreted by each CD4$^+$ T cell subset are also shown. Mature T_h1 cells produce IFN-γ which can upregulate MHC Class I and II molecules on cells in the local microenvironment. These cells are antiviral and protective against intracellular bacteria and fungi. T_h2 cells typically secrete IL-4, IL-5, and IL-13 and are active against extracellular parasites and implicated in allergy responses. T follicular helper cells (T_{fh}) are specialized to provide B cell help and assist in germinal center formation. Mature T_h17 cells aid in protection against extracellular bacteria and fungi. Regulatory T cells (T_{reg}) are characterized by the expression of the transcription factor Foxp3 and help to control activation of the immune response. T_h22 cells have been shown to play a role in mediating immune responses in the skin. From Lim et al., 2020 [352]

1.2.3 CD4$^+$ T cells and antiviral immunity

The roles that CD4$^+$ T cells fulfill in antiviral immune responses can broadly be divided into 3 categories: recruitment of lymphoid cells to sites of infection, mediating expansion or function of other effector cells, or providing direct antiviral effects through cytokine production or cell-mediated cytotoxicity [502]. The classic view of CD4$^+$ T cells is as a helper cell. In antiviral responses they help recruit CD8$^+$ T cells to sites of infection by promoting engagement of CD8$^+$ T cells with dendritic cells via chemokines such as CCL3 and CCL4. They can also facilitate entry of naïve CD8$^+$ T and B cells to draining lymph nodes and recruit innate or antigen-specific effectors to sites of viral replication via production of IFN-γ and local chemokine secretion. CD4$^+$ T cells can also mediate expansion and function of both B cells and CD8$^+$ T cells. Binding of antigen on CD4$^+$ T cells initiates expression of CD40 ligand (CD40L), which engages CD40 on B cells and induces proliferation and differentiation of B cells, initially in extra-follicular foci and then in germinal centres of lymph nodes, resulting in production of antibody-producing plasma cells and memory B cells. With CD8$^+$ T cells, CD4$^+$ T cells have been shown to facilitate development of memory CD8$^+$ T cells via various mechanisms, such as through downregulation of TNF-related apoptosis-inducing ligand (TRAIL) expression,

generation of cytokines such as IL-2, or direct ligation of CD40 on naïve $CD8^+$ T cells by CD40L on $CD4^+$ T cells [502, 562]. Finally, there has been increasing evidence of a role of $CD4^+$ T cells in antiviral immunity that is independent of their helper function through two distinct mechanisms: production of cytokines IFN-γ and TNF-α, and through direct cytolytic actions via perforin- and Fas-dependent killing [274]. In particular, these cytotoxic T cells have been described to emerge after CMV infection [417, 600] and have demonstrated a capability to lyse CMV antigen-expressing target cells in vitro [599]. They have also been found to express the transcription factor Homolog of Blimp-1 in T cells (Hobit) [417].

The majority of $CD4^+$ T cells produced in response to viral infection are of the T-helper 1 (T_h1) subtype, producing IFN-γ and expressing the transcription factor T-bet [91]. This has also been observed following primary CMV infection [479]. However, other functional subsets are also involved in antiviral immunity. T follicular helper (T_{fh}) cells, characterized by their expression of the chemokine receptor CXCR5 and transcriptional repressor Bcl6, produce IL-21 which facilitates germinal centre B cell selection and differentiation of activated B cells that provide long-term antibody-mediated protection against viral pathogens [216, 217]. Regulatory T cells (T_{reg}), identified by expression of transcription factor Foxp3 and cell surface marker CD25, limit immunopathology in chronic viral infections [288]. T_{reg}s that develop in the thymus are termed natural T_{reg} (nT_{reg}), while those that develop in peripheral lymphoid organs are termed inducible Tregs (iT_{reg}). In the context of antiviral responses to CMV, CMV-specific iT_{reg} were found to be increased in older women and may attenuate the chronic vascular injury caused by CMV [573].

1.2.4 HCMV antigen specificity of $CD4^+$ T cells

Initially, studies to identify HCMV-specific $CD4^+$ T cells used lysate derived from HCMV infected fibroblast cells to stimulate the antigen-specific response [355, 452, 453, 516]. Subsequently, studies of the $CD8^+$ T cell repertoire identified multiple peptides that were most frequently recognised by HCMV-specific $CD8^+$ T cells [150, 191, 296, 643]. Among the most commonly recognised were pp65 and IE-1, although some structural, early/late antigens, and HCMV-encoded immunomodulators were also identified (such as pp28, pp50, gH, gB, US2, US3, US6 and UL18) [150]. This was thus used to guide studies identifying $CD4^+$ T cells that were HCMV-specific [629]. In the same landmark study that screened 213 ORFs to identify the most common ones recognised by $CD8^+$ T cells, it was also found that $CD4^+$ T cells recognise proteins from up to 125 different ORFs. In particular, $CD4^+$ T cells recognised immediate-early (IE) gene products by 2.3-fold over their representation in the HCMV genome, and there was also preferential recognition of primary immune evasion proteins and viral tegument and glycoproteins [564]. Recognition of HCMV glycoproteins by $CD4^+$ T cells has also been reported in a number of other studies [119, 420, 421]. A summary of HCMV antigens commonly recognised by $CD4^+$ T cells is listed in Table 1.4.

In addition, measurement of the functional capability of these cells has also evolved. Initially, most studies measured intracellular cytokine production, predominantly IFN-γ, to determine specificity of these $CD4^+$ T cells to HCMV (reviewed in [255]). More recently, work in our laboratory has demonstrated a functional capability of these cells *in vitro*, where autologous HCMV-specific $CD4^+$ T cells (identified by upregulation of activation markers CD40L and 4-1BB above the background response) were shown to be able to restrict viral dissemination in monocyte-derived dendritic cells [256].

Table 1.4: Antigens recognised by $CD4^+$ T cells

Antigens	Response test used	References
pp65, gB, gH, IE1, IE2, UL69	Lymphoproliferative assay	[46]
IE1 & total HCMV Ag lysate (AD169)	Proliferation response to transfected astrocytoma cells	[128]
pp65	ICS for IFN-γ response to peptide pools	[297]
gB, pp65, UL86, pp28, IE2, UL36, UL48, pp150 (8 most common)	ICS for IFN-γ response to peptide pools	[564]
UL86	ICS for IFN-γ response to peptide pools	[176]
gB (presented through HLA-DRB*0701)	Chromium release assay of peptide-loaded lymphoblastoid cell lines	[119]
gB, gH, gL (95% of donors have gB response, but only 20% have gH or gL response)	ICS for IFN-γ (gB colocalizes with $CD4^+$ class II loading compartment, but gH does not)	[421]
pp65, gB, IE1, IE2	IFN-γ Fluorospot response to peptide pools	[256, 257]
UL138, LUNA	IFN-γ and IL-10 ELISPOT response to peptide-loaded lymphoblastoid cell lines	[381]
UL138, LUNA, US28, vIL-10, US3, pp71	IL-10 Fluorospot to peptide pools	[258]

ICS=intracellular cytokine staining

1.2.5 Phenotypes and characteristics of HCMV-specific $CD4^+$ T cells

As mentioned in Section 1.1.5, primary HCMV infection in the immunocompetent host may manifest as a viral syndrome, although it is often asymptomatic in healthy hosts as well.

This difficulty in obtaining a cohort of patients with primary HCMV infection at the time of diagnosis has led to studies of the $CD4^+$ T cell response during acute primary infection being conducted mainly on pregnant women cohorts or during primary infection in kidney transplant patients where the recipient is seronegative and donor is seropositive (D^+R^-) [168, 347, 348, 386]. In pregnant women cohorts, at early time points post-infection the dominant $CD4^+$ T cell responses are to gB and pp65 [386]. However, these CMV-specific $CD4^+$ T cells have lower functional avidity [21], and express higher levels of immune checkpoint proteins such as PD-1 as compared to the memory responses of CMV-specific $CD4^+$ T cells in healthy seropositive adults [21, 386, 484]. A summary of these studies is listed in Table 1.5.

Table 1.5: Phenotypes & characteristics of $CD4^+$ T cells in primary HCMV infection

Surface marker	Cohort studied	Refs
$CD45RA^+$ $CD45RO^+$ (Recently activated $T_{naïve}$)	D^+R^- renal transplant recipients	[479]
$CD38^+$ ($CD38^-$ during latency)	D^+R^- renal transplant recipients	[479]
$CD49d(VLA\text{-}4)^+$, $CD62L^-$, $CD11a^{high}$	Both acute and latently infected (data not shown)	[479]
$CD28^-GzmB^+$ (Cytotoxic $CD4^+$)	D^+R^- renal transplant recipients	[599, 600]
$CD28^-$	D^+R^- renal transplant recipients	[599]
$CD45RA^+$	Healthy pregnant women	[348]
$CD45RA^+$ less likely to transmit to foetus	Healthy pregnant women	[168, 169]
$PD\text{-}1^+$ (Only in $CD28^+CD4^+$)	Healthy pregnant women	[21]
$CD28^-$	Primary infection in healthy pregnant women	[21]
$PD\text{-}1^+$, NKG2D, DNAM-1 (CD226), CD57	Severe symptomatic primary infection in healthy adults	[484]
$IL\text{-}7R^{pos}$ (Found in 50% of CMV-specific $CD4^+$, increasing to 70% after 12 months, associated with non-transmitters)	Primary infection in healthy pregnant women	[386]

After the initial proliferative response to primary infection, the $CD4^+$ T cell population then contracts, and the fraction of T_h1 and T_{fh} that survive become long-lived memory cells of central memory (T_{CM}), effector memory (T_{EM}) or T_{fh} phenotypes. Surface markers of some

of these memory T cell subsets are listed in Figure 1.5, although this is a non-exhaustive list, as classification of newer memory T cell subsets is still ongoing and a matter of debate.

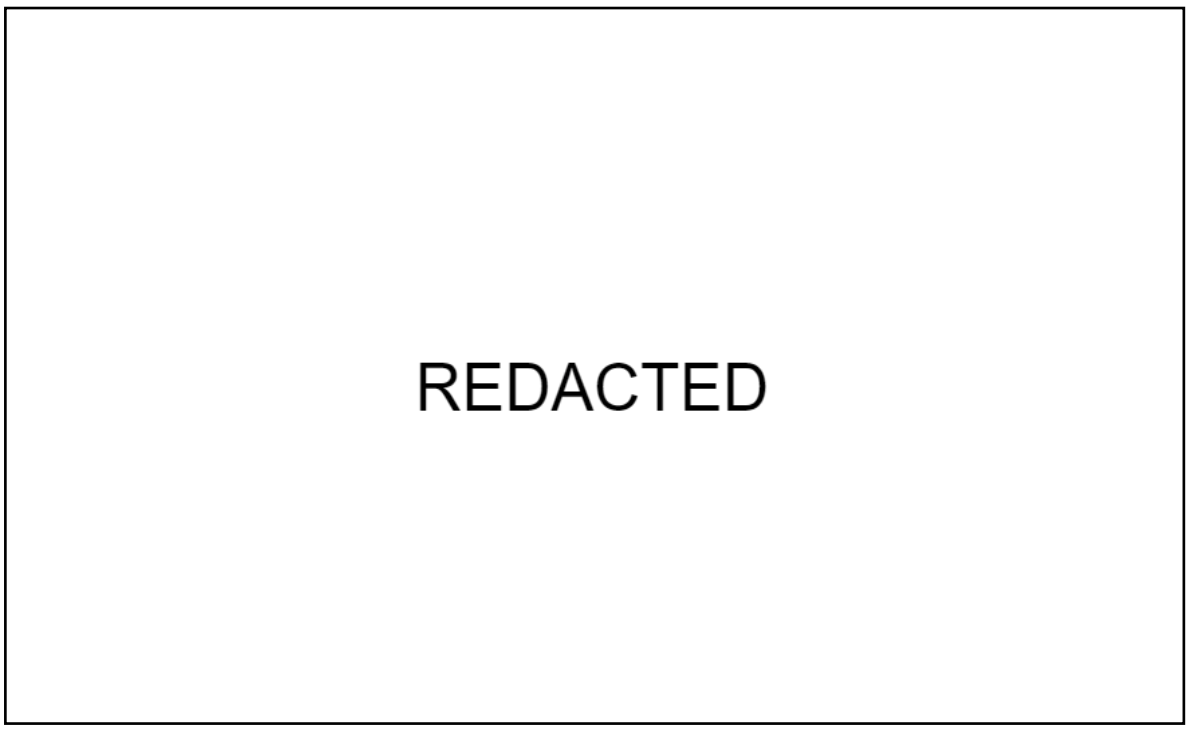

Figure 1.5: Surface markers of memory T cell subsets
Adapted from Golubovskaya et al., 2016 [198]

Examination of the CMV-specific $CD4^+$ T cell population in healthy seropositive adults reveals that these $CD4^+$ T cells can be found in the entire spectrum from naïve to central memory T cells, and that up to 88% of CMV-specific $CD4^+$ T cells can have an effector memory phenotype [420]. In addition, CMV-specific $CD4^+$ T cells that secrete IL-10, a suppressive cytokine, or have a phenotype of a T_{reg} have been identified in other studies [105,511,573,586]. CMV-specific $CD4^+$ T cells have also been shown to have cytotoxic capacity, measured via surrogate markers such as expression of CD107a (a marker of degranulation), detection of intracellular perforin and granzyme molecules or via cytotoxicity assays including chromium release assays [119, 181, 256, 381, 420, 421, 599], suggesting that some CMV-specific $CD4^+$ T cells have the ability to kill CMV infected cells. Table 1.6 lists some phenotypes and characteristics of these $CD4^+$ T cells that have been found in CMV-seropositive adults.

Table 1.6: Surface markers and characteristics of CMV-specific $CD4^+$ T cells in HCMV-seropositive adults

Surface markers/Secreted factors	Cohort studied	Refs
$CD45RO^+$, $CD27^-$, $CD62L^-$, $CCR7^{lo}$ (Mature effector phenotype)	Seropositive healthy adults and renal transplant recipients	[516]

Table 1.6 continued from previous page

Surface marker/Secreted factors	Cohort studied	Refs
$CD27^-$ (but also a small proportion of $CD27^+$)	HCMV-seropositive adults	[61]
$CD45RA^+CD45RO^+$ to $CD45RA^-$ to $CCR7^+CD45RO^+$ (Progression from naïve to central memory)	Healthy HCMV-seropositive adults	[420]
$CCR7^-CD45RA^-$ (Effector memory, found in 88% of CMV-specific $CD4^+$ T cells)	Healthy HCMV-seropositive adults	[420]
$CD27^-CD28^-$ (64% of CMV-specific $CD4^+$ cells)	Healthy HCMV-seropositive adults	[420]
$CD57^+$ (Found almost exclusively on $CD27^-CD28^-$ cells)	Healthy HCMV-seropositive adults	[420]
MIP-1β, TNF-α, and IFN-γ in absence of IL-2	Healthy HCMV-seropositive adults	[88]
CD107a, perforin & Gzm	Healthy HCMV-seropositive adults	[88]
$CX3CR1^+$, PD-1^+, $GzmB^{high}$, perforin	Healthy HCMV-seropositive adults	[420]
$CD45RO^{low}CD45RA^{high}$ & $CD45RO^{high}CD45RA^{low}$	Healthy HCMV-seropositive adults	[629]
$CD27^-CD28^-$, with shortened telomeres (Late-differentiated phenotype)	Healthy elderly HCMV-seropositive adults	[164]

1.2.6 HCMV Immune Evasion of $CD4^+$ T cell responses

The HCMV genome encodes multiple evasion proteins during the course of infection that allows the virus to modulate intrinsic, innate and adaptive immune responses [644], the end result of this being the persistence of active primary infection viraemia even in the immunocompetent host, which is accompanied by virus excretion for months (in adults) or even years (in children). In particular, the lack of a $CD4^+$ T cell response in healthy children has been associated with persistent shedding of virus into the urine and saliva of these hosts [589]. A summary diagram of the mechanisms of immune evasion of $CD4^+$ T cells by HCMV is shown in Figure 1.6, and will be elaborated on in the following sections.

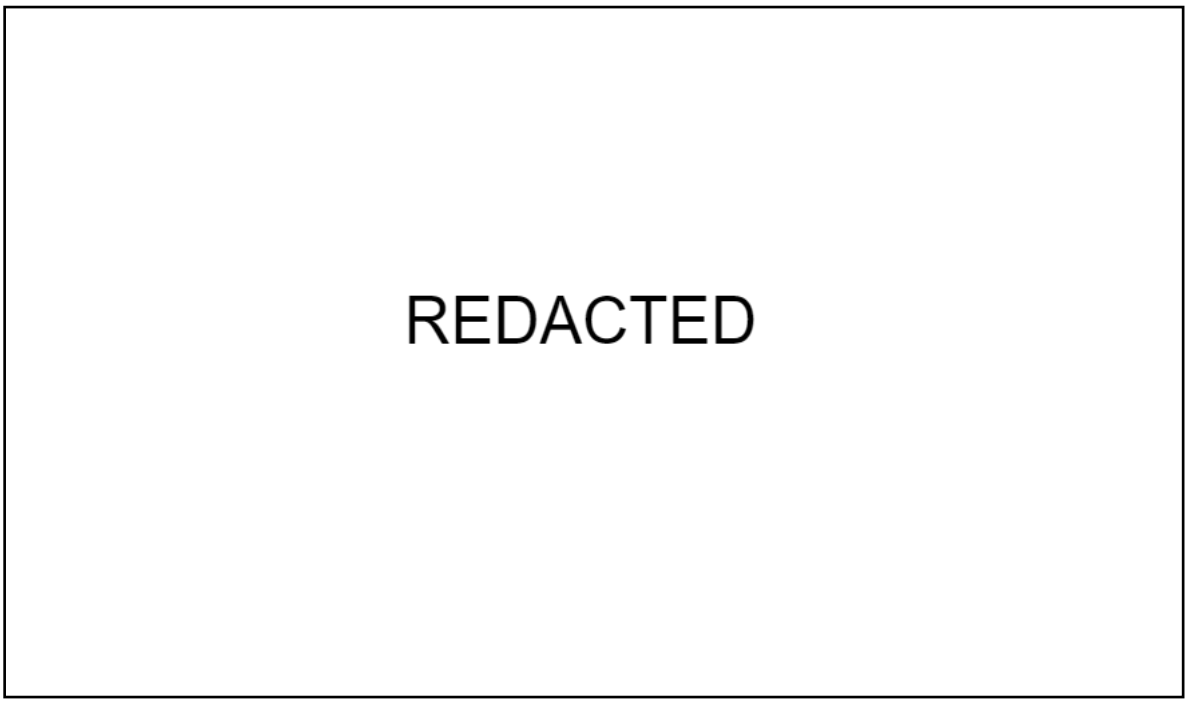

Figure 1.6: Summary of mechanisms of immune evasion of CD4$^+$ T cells by HCMV
CIITA = class II transactivator; CLIP = Class II invariant peptide; cGAMP = cyclic guanosine monophosphate–adenosine monophosphate; cGAS = =cyclic GMP-AMP synthase; ER = endoplasmic reticulum; ISG = interferon-γstimulated gene; Jak = Janus kinase; MHCII = MHC Class II; STAT = signal transducer and activator of transcription proteins; STING = stimulator of interferon genes. From Lim et al., 2020 [352]

1.2.6.1 Evasion via downregulation of MHC class II proteins by US2 and US3

Early work characterising essential and non-essential genes of HCMV found that infection led to downregulation of MHC class I molecules on the surface of infected cells [39,43,131,192, 650]. The US1-US11 region of the HCMV genome encodes at least 4 proteins, US2, US3, US6 and US11 that can independently interfere with the stability, assembly or export of MHC class I molecules [268, 440]. Two of these proteins also interfere with MHC Class II. US2 has been shown to affect the MHC class II processing pathway, specifically by binding to MHC class II-α chains and assembled MHC class II-$\alpha/\beta/\mathrm{I_i}$ complexes, leading to their degradation [582]. US3 alters assembly of MHC class II complexes by binding HLA-DR (but not HLA-DM) proteins before or during assembly of α/β complexes in the ER, preventing the binding of the invariant chain. This leads to mislocalisation of these complexes to other post-Golgi compartments and results in the reduction of antigen presentation in US3-expressing cells [228]. (Seen in Figure 1.6).

1.2.6.2 Evasion via downregulation of Class II transcriptional activator and modulating the effects of interferon-γ

Interferon-γ (IFN-γ) upregulates MHC class II molecules in cells constitutively expressing MHC class II, such as B cells, dendritic cells and professional antigen presenting cells (APCs). However, it is also able to induce MHC class II expression in cells that do not constitutively express MHC class II, such as epithelial cells and fibroblasts, via the MHC class II transactivator gene (CIITA) [553]. The mechanism of how this occurs is not fully elucidated. However, it is known that it involves regulation of a number of signaling pathways and transcription factors in a cell-specific manner. Binding of IFN-γ to its cell-surface receptor activates the protein tyrosine kinases Jak1 and Jak2, and activation of these Jak kinases phosphorylates the tyrosines of the cytoplasmic transcription factor STAT1, and translocates it to the nucleus. STAT1 then binds directly to the IFN-γ-activation site (GAS) element of CIITA. The CIITA promoter region also includes an interferon regulatory factor (IRF)-1 binding site and binding of both these regions are essential for activation by IFN-γ [402]. Activation of CIITA leads to the assembly of a MHC class II enhanceosome, triggering a cascade of events that ends in autophosphorylation of CIITA and allows transcription of MHC class II genes to initiate [528]. The process of induction of MHC Class II complexes by IFN-γ is illustrated in Fig.1.7. In macrophages the transcription factor NFAT5 is required for expression of the CIITA and MHC class II molecules, but this is not the case for dendritic cells and B cells [77].

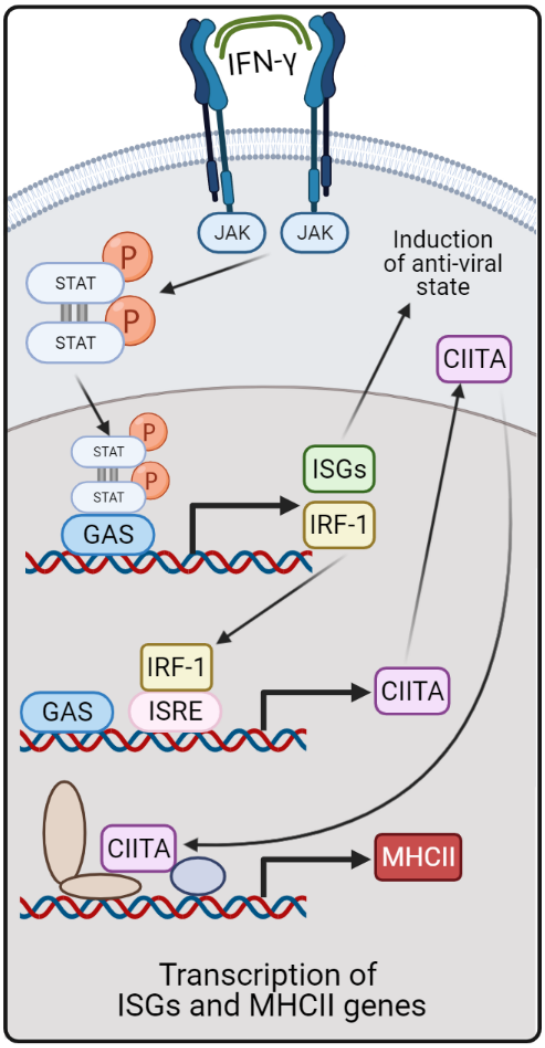

Figure 1.7: Mechanism of induction of MHC Class II by IFN-γ
CIITA = class II transactivator; Jak = Janus kinase; GAS = Gamma-interferon-activation site; STAT = signal transducer and activator of transcription protein; IRF = interferon regulatory factor; ISG = interferon-stimulated gene; ISRE = interferon-stimulated response element. Figure created at BioRender.com

The HCMV genome encodes for a number of proteins that assist in modulation of the effects of IFN-γ [200] and directly modulate CIITA transcription. In Langerhans cells, a

dendritic cell subset, HCMV infection results in a decrease in constitutive expression of CIITA [330]. Further evidence in a transfected cell line model system showed that CMV downregulates MHC class II expression on the cell surface via regulation of CIITA and independently of known CMV Class II modulators US2 and US3 [92]. Recently, it has also been shown in kasumi-3 cells, a myeloid lineage tumour cell line, that reduction in endogenous expression of MHC class II is as a result of decreased CIITA transcription, although as a caveat the study did not define if this occurred in latent or lytic infection [501]. UL23 binds to the STAT effector molecule N-myc, preventing proper activation and translocation of the STAT1 homodimers required for IFN-γ signalling [157], while UL31 preferentially binds the cytosolic DNA sensor cGAS in a manner that results in inhibition of interferon-associated gene transcription [242]. The tegument protein pp71 binds Daxx, a Death-domain associated protein, and targets it for degradation, resulting in an inhibitory effect on induction of downstream antiviral genes [86, 247, 367] (illustrated in Figure 1.8). It has also been demonstrated that pp71 can negatively regulate the signaling role of STING (Stimulator of Interferon Genes) by inhibiting its translocation to the nucleus and preventing recruitment of accessory proteins to the complex [175] (illustrated in Figure 1.6). The end result of all these modulations is a decrease in transcription of downstream interferon-γ-associated genes, which, among other effects, results in decreased expression of MHC class II on the surface of infected cells and a decreased ability to present antigen via the MHC class II antigen presentation pathway.

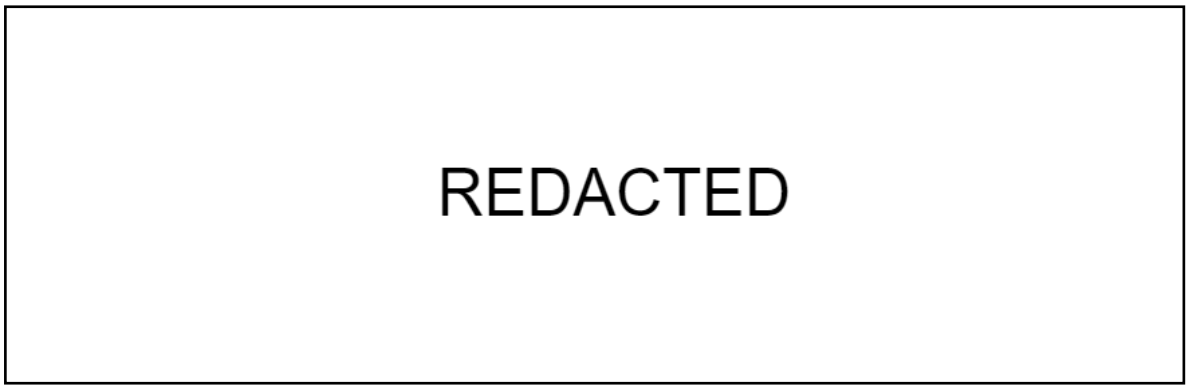

Figure 1.8: pp71 degrades Daxx
In infections with pp71-null virus, Daxx represses viral transcription through its interaction with HDAC and an unknown transcription factor (Panel A). In infections with wildtype virus, pp71 enters the nucleus and degrades Daxx, allowing IE gene expression to occur (Panel B). Adapted from Saffert et al, 2006 [496]

1.2.7 The CD4$^+$ T cell response to HCMV in different clinical settings

1.2.7.1 In solid organ transplant recipients

Cytomegalovirus is the most common viral opportunistic infection in solid organ transplant (SOT) recipients, with the risk of infection or reactivation being stratified according to the CMV sero-status of the donor and recipient. An organ donation from a sero-positive donor to a sero-negative recipient (D^+R^-) carries the highest risk, a sero-positive recipient (R^+) is at intermediate risk, and D^-R^- transplants are at lowest risk [309]. Other factors affecting risk of CMV reactivation or disease include the type of organ transplanted, with lung and small intestine transplant recipients having the highest risk, while liver and heart recipients are at an intermediate risk and kidney recipients are at the lowest risk of CMV infection [243]. The reasons for this stratification are likely related to the amount of immunosuppression required, and the latent viral load present in these organs [385]. In addition, use of anti-lymphocyte antibody induction agents also increase risk of reactivation [454].

There have been multiple studies in solid organ transplant recipients assessing the CD4$^+$ T cell response in solid organ transplant recipients. A summary of these is presented in Table 1.7. The majority of these show that the HCMV-specific CD4$^+$ T cell recovery is associated with lower risk of HCMV viraemia and disease. However, most of these studies have focused on using HCMV-specific CD4$^+$ T cell recovery as a monitoring tool for predicting the risk of developing HCMV disease [75,76,351,498], and have used cytokine production (most commonly IFN-γ or IL-2) in response to CMV lysate, peptide pools, or virally infected dendritic cells as a surrogate marker for the effectiveness of the CMV-specific CD4$^+$ response. However, there are other antiviral mechanisms of CD4$^+$ T cells as described in Section 1.2.3 above, and it must be remembered that such measurements do not reflect the complete spectrum of the CD4$^+$ T cell response to HCMV.

Table 1.7: CD4$^+$ T cell recovery and CMV reactivation in solid organ transplant recipients

Organ	Test used	Findings	Refs
Kidney (76 R^+, 66 R^-)	Staining for CD69 and IFN-γ to CMV antigen	Symptoms of CMV preceded by decrease in CMV-specific CD4$^+$ T cell frequencies	[515]
Kidney (48 R^+, 25 D^+R^-)	Staining for CD69 and IFN-γ to CMV fibroblast lysate/pp71 and pp65 peptide pools	pp65 CD4$^+$ T cell responses above 0.03% associated with lower risk of CMV replication	[145]

Table 1.7 continued from previous page

Organ	Test used	Findings	Refs
Liver (17 D^+R^-)	ICS for IFN-γ to AD169 lysate or pp65/IE1 peptide library	No association between presence of CMV-specific $CD4^+$ T cells and development of CMV viraemia	[319]
Liver (29 D^+R^+ or D^+R^- or $D\text{-}R^+$)	IFN-γ and/or IL-2 and/or CD69 to AD169 lysate or pp65/IE1 peptide pools	Polyfunctional $CD4^+$ T cells occur at lower frequency in those who eventually develop CMV viraemia	[410]
20 heart, 9 lung, 9 kidney	Staining for IFN-γ response on exposure to DC infected with VR1814 HCMV strain	Presence of HCMV-specific $CD4^+$ T cells less likely to require antiviral treatment	[186]
58 heart, 24 lung, 52 kidney	Staining for IFN-γ response on exposure to DC infected with VR1814 HCMV strain	Presence of $CD4^+$ and $CD8^+$ $\geq 0.4/\mu$L protective against HCMV disease	[185]
46 kidney, 39 liver, 10 heart	ICS for CD69+/IFN-γ to pp65/IE-1 peptide pools	Presence of any cell-mediated immunity response protective against CMV disease	[498]
12 heart, 40 kidney (all R^+)	Staining for IFN-γ response on exposure to DC infected with VR1814 HCMV strain	Lower number of HCMV-specific $CD4^+$ T cells in patients with high load of CMV viraemia	[351]
9 heart, 8 lung, 3 kidney (D^+R^-, D^-R^+ or D^+R^+)	Staining for IFN-γ response on exposure to DC infected with VR1814 HCMV strain	Protection from HCMV associated with presence of response against multiple viral proteins, but not pp65 or IE-1 only	[345]
Liver (25 D^+R^-, 24 R^+ controls)	$\geq$2 of IFN-γ, IL-2, TNF-α or CD109a to IE1 or pp65 peptide libraries	$CD4^+$ T cell responses to pp65 or IE1 not predictive for late stage CMV disease	[353]

1.2.7.2 In haematopoietic stem cell transplant recipients

In haematopoietic stem cell transplant (HSCT) recipients, the highest risk of CMV viremia and disease occurs in the reactivation of latent infection in R^+ patients due to the ablation of their existing CMV specific T cell response. In particular, D^-R^+ recipients are at a higher risk than D^+R^+ patients, as reactivation of latent disease in the sero-positive recipient will appear

as a primary CMV infection to the naïve lymphocytes transplanted from the sero-negative donor [227, 597].

Use of CD4$^+$ T Cell response to predict risk of HCMV Viremia or disease, and the relationship to end-organ disease

Similar to that which occurs in solid organ transplant recipients, recovery of HCMV-specific CD4$^+$ T cells in haematopoietic stem cell transplant recipients often heralds the recovery of cell-mediated immunity and improved clinical outcomes. Table 1.8 lists publications of the observations of CD4$^+$ T cell recovery and association with HCMV viraemia or disease. Earlier studies looked at the association of absolute CD4$^+$ T cell recovery, while later ones looked at CMV-specific CD4$^+$ T cell response.

Table 1.8: $CD4^+$ T cell recovery and CMV reactivation in haematopoietic stem cell transplant recipients

Patient characteristics	Test used to detect CMV-specific T cells	Findings	Refs
63 allogeneic BMTs	Not stated	Decrease in $CD4^+$ T cells numbers to $<100/\mu$l 49 days after BMT was 100% predictive for the development of CMV disease	[146]
71 T cell-depleted BMTs	Not stated	Life-threatening opportunistic infections occurred exclusively in patients whose $CD4^+$ counts were <200 cells/μl	[537]
48 allogeneic HSCTs (27 R^+D^+, 6 R^-D^+, 15 R^+D^-)	ICS for IFN-γ response to AD169 antigen	Patients with CMV-specific $CD4^+$ T cells at 4 weeks had lower peak CMV viral loads	[31]
57 paediatric allogeneic HSCTs (28 D^+R^+, 11 D^-R^+, 18 D^+R^-, 4 D^+R^-)	ICS for IFN-γ to VR1814-infected DCs	1 HCMV-specfic $CD4^+$ T cell/μl of blood protective against recurrent HCMV viraemia	[349]
45 adult allogeneic HSCTs (28 D^+R^+, 9 D^-R^+, 8 D^+R^-)	ICS for IFN-γ/IL-2 to VR1814-infected DCs	1 HCMV-specfic $CD4^+$ T cell/μl of blood predictive for spontaneous control of HCMV	[346]
36 allogeneic HSCTs (29 D^+R^-, 6 D^-R^+, 1 D^+R^-)	ICS for IFN-γ to pp65 and IE1	CMV-specific $CD4^+$ (and $CD8^+$) T cell counts higher in those who do not develop CMV viraemia	[544]
32 adult allogeneic HSCTs	ICS for IFN-γ/IL-2 and $CD69^+$ to pp65/IE1/pp50	Lower frequency of CMV-specific $CD4^+$ (and $CD8^+$) T cells associated with >1 CMV reactivation episode	[452]
133 adult HSCTs (77 D^+R^+, 46 D^-R^+, 10 D^+R^-)	ICS for IFN-γ to pp65 and IE1	>1.2 CMV-specific $CD4^+$ T cells/μl of blood protective for CMV reactivation episodes	[584]

Table 1.8 continued from previous page

Patient characteristics	Test used to detect CMV-specific T cells	Findings	Refs
63 allogeneic HSCTs (46 D^+R^+, 17 D^-R^+)	IFN-γ/IL-2/TNF-α response to VR1814-infected iDCs	Recurrent CMV infections and disease associated with persistently low levels of total $CD4^+$ T cells and <1 cell/μl of blood of HCMV-specific $CD4^+$ T cells 6 months post-transplant	[178]

One finding of note is that one study found that levels of HCMV-specific $CD4^+$ T cells above 1 cell/μl was not protective of development for late-stage HCMV gastro-intestinal disease, although all these patients were receiving immunosuppressive treatment at time of diagnosis [178].

Kinetics of recovery of HCMV-Specific $CD4^+$ T cell numbers and the impact of prophylaxis and use of G-CSF on $CD4^+$ T cell recovery

It has been theorized that HCMV reactivation causes activation of T cells, and this leads to an early expansion of T cells and faster reconstitution of T lymphocytes. In a study of 34 pediatric patients who underwent allogeneic BMT, the authors found that children with HCMV reactivation had a higher probability of reaching the 5th percentile of total $CD4^+$ T cells of an age-matched healthy population [129]. This was also seen in a study of 201 adult R^+ allogeneic non-T cell-depleted peripheral blood stem cell or bone marrow transplants [215]. CMV-specific $CD4^+$ T cell responses, as measured by a lymphoproliferative response to CMV lysate, were significantly better in patients who developed breakthrough CMV antigenemia despite ganciclovir prophylaxis, versus those who did not. However, a complicating factor is the use of high-dose steroids for treatment of graft-versus-host disease (GVHD). When the sub-group of patients who developed breakthrough CMV antigenemia were analyzed, 100% of patients without GVHD had better recovery of the CMV-specific $CD4^+$ T cell response compared to patients who received high-dose steroids. They thus concluded that high-dose steroids can override this inducing effect of breakthrough CMV antigenemia on the CMV-specific $CD4^+$ T cell recovery [215].

Emergence of CMV specific $CD4^+$ T cell responses prior to the $CD8^+$ T cell response has been shown, in a primary model of infection in solid organ transplant patients, to be associated with a lack of overt CMV disease [180, 181, 478, 479]. In HSCT patients there is evidence that recovery of $CD4^+$ T cells before $CD8^+$ T cells may assist with priming the $CD8^+$ T cell response via "licensing" of dendritic cells. Dendritic cell licensing refers to the phenomenon of upregulation of MHC class I and costimulators CD80/86 on dendritic cells after antigen presentation to $CD4^+$ T cells via MHC class II and CD40-CD40L interactions have occurred. In this way, dendritic cells are able to present antigen to, and activate, $CD8^+$ T cells, and this allows for tighter regulation of $CD8^+$ T cell activation [575]. In a study of 6 seropositive recipients of cord blood transplants, the appearance of CMV-pp65-specific $CD4^+$ T-helper cells preceded an expansion of CMV-specific $CD8^+$ T cells. When co-cultured with $CD8^+$ T cells alone, these pp65-specific $CD4^+$ T cells did not induce cytokine production by $CD8^+$ memory T cells, but when done so in the presence of dendritic cells loaded with pp65, there was activation of these $CD8^+$ memory T cells [165].

There has also been the suggestion that ganciclovir prophylaxis delays recovery of CMV-

specific $CD4^+$ (and $CD8^+$) T cell responses possibly due to a decrease in viral replication, resulting in late-onset CMV disease [341]. This observation has led to the development of pre-emptive instead of prophylactic use of antiviral drugs in patients. However, in a large study of 201 R^+ allogeneic HSCTs [215], there was no significant difference on CMV-specific $CD4^+$ T cell recovery between patients who received prophylaxis versus pre-emptive treatment with ganciclovir, the authors suggest this may be driven by sub-clinical reactivation of the virus despite ganciclovir treatment. The impact of antiviral treatment resulting in decreased T-cell responses to HCMV stimulation has also been observed in paediatric allogeneic-HSCT patients. A study of 30 allogeneic-HSCT patients showed that the patients who received anti-CMV chemotherapy because of prolonged viremia had lower HCMV-specific $CD4^+$ T cell numbers and delayed and depressed lymphoproliferative responses to HCMV stimulation [206].

The use of peripheral blood stem cells (PBSCs) for transplantation improves survival in patients with high-risk haematological malignancies compared with the use of bone marrow (BM) as a stem cell source, because PBSC products from donors who have received G-CSF contain higher numbers of T cells and monocytes. However, PBSC recipients saw an increased incidence of early HCMV reactivation and delayed recovery of HCMV-specific immune responses, with a corresponding lower number of HCMV-specific $CD4^+$ T cells (as measured by limiting dilution assay and CMV-specific cell lysis) in the stem cell product [208]. This may be as a result of G-CSF administration to the donor, which is given in order to mobilize stem cells to migrate to the peripheral blood, but can also cause the reactivation of HCMV from latency. However, a subsequent study showed that although a reduced diversity of the TCRβ repertoire of $CD4^+$ T cells was significantly correlated with HCMV (and EBV) reactivation, administration of G-CSF did not change this repertoire [486]. A recent study that measured the frequency of $CD4^+$ T cells in recipients of PBSC grafts that produced IL-2, IFN-γ, or TNF-α in response to incubation with a HCMV lysate also did not find a deficiency in these cell responses compared to BM recipients [615]. In fact, these recipients of PBSC grafts had faster T cell reconstitution, including more naïve $CD4^+$ T cells. Therefore, more studies are required to determine if the apparent increased risk of HCMV reactivation with G-CSF use warrants a more cautionary use of this product.

Investigations of the recovery of CMV specific $CD4^+$ T cells in HSCT patients demonstrated that there are different kinetic patterns that result in the recovery of the $CD4^+$ T cell response: (i) rapid expansion of IFN-γ-secreting T cells within the first week after initiation of pre-emptive therapy concomitant with rapid clearance, (ii) early expansion of a lower magnitude than that seen in rapidly cleared episodes, and (iii) an inconsistent or lack of expansion associated with persistent CMV DNAemia [585]. The reconstitution of HCMV-specific $CD4^+$ T cells can also be stratified by donor and recipient serostatus—recovery is fastest in D^+R^+, followed by D^-R^+, and is slowest in D^+R- populations [346]. In fact, in D^+R^+ patients, it appears that the reconstitution kinetics of HCMV-specific $CD4^+$ T cells are the same as

HCMV-specific $CD8^+$ T cells [171]. It is important when interpreting these results to remember that reconstitution of CMV specific $CD4^+$ T cells is not equivalent to recovery of a fully functional CMV specific $CD4^+$ T cell response. Measuring whether there is a lymphoproliferative response to CMV antigens is possibly more reflective of the actual ability of the T cells to prevent HCMV reactivation and disease. Early studies in allogeneic bone marrow transplant patients showed that up to 30% of recipients with a lack of a CMV-specific $CD4^+$ lymphoproliferative responses by day 120 post-transplant develop CMV disease [311]. When HCMV-specific $CD4^+$ T cells in paediatric allogeneic HSCT recipients were examined for both IFN-γ and proliferative responses, there was first a recovery of the IFN-γ response before the proliferative response [206]. This is also seen in primary HCMV infection, where development of the lymphoproliferative response to HCMV is delayed compared to the development of $CD4^+$ and $CD8^+$ IFN-γ-producing T cells [168].

Surface markers of HCMV-Specific $CD4^+$ T cells in transplant recipients

Alongside measuring HCMV T-cell reconstitution in HSCT recipients, some studies have assessed whether the presence of polyfunctional HCMV-specific $CD4^+$ T cells, measured by an ability to produce both IFN-γ and IL-2 in response to HCMV, corresponds with protection from HCMV reactivation [346]. IL-2 is a cytokine which can have multiple effects on $CD4^+$ T cell immune responses, including modulating the development of T cells into memory subsets. It signals to the T cell via binding to the IL-2 receptor, a complex consisting of three chains, termed α (CD25), β (CD122), and γ (CD132) [343]. Other phenotypic markers and characteristics of $CD4^+$ T cells have been found in patients with CMV reactivations, and is presented in Table 1.9.

Table 1.9: Implications of surface markers of $CD4^+$ T cells in transplant recipients

Surface marker/ Secreted cytokines	Type of $CD4^+$ T cell	Association	Refs
Reduced $CD25^{high}$		Independent risk factor for CMV reactivation	[263]
CD107a and CD40L		Found in patients with PCR-positive reactivations, and higher antigen load	[314]
$CD27^-CD28^-$	Cytotoxic T cells	Found in SOTR	[75, 76, 134] [599, 600]

Table 1.9 continued from previous page

Surface marker	Type of $CD4^+$ T cell	Association	Refs
PD-1 and CTLA-4		PD-1 and CTLA-4 expression on $CD27^-CD28^-$ $CD4^+$ T cells associated with viraemia (this study includes dialysis patients with CMV reactivations)	[134]
IL-2	Conversion from effector memory to central memory	Ratio of IL-2 to IFN-γ production increases with time post-transplant	[452]
Progressive loss of CD31	Loss of $T_{naïve}$ cells	Progressive loss of $CD31^+CD4^+$ $T_{naïve}$ cells in those with HCMV reactivation & reversal of CD4:CD8	[558]

1.2.7.3 Lessons learnt from adoptive transfer therapies

Adoptive immunotherapy has been used as a treatment option for transplant recipients with HCMV disease not amenable to antiviral therapy, or for patients unable to tolerate antiviral drugs. It was initially trialled in 1995 in a cohort of bone marrow transplant recipients, [616] and since then there have been multiple other phase 1 and 2 clinical trials performed [194,385, 598]. The method of treatment, in principle, involves generating HCMV-specific T cell clones and infusing them into the transplant recipients. The long lag time and cost of generating these clones has meant that this treatment option is instituted only when other modes of treatment have failed or are unsuitable. In SOT recipients, the challenge of autologous adoptive T cell therapy is to be able to generate a sufficient number of CMV-specific T cells from the immunosuppressed recipients. Multiple case reports performed in mostly lung transplant recipients appear to have shown potential [68,238,438], though there has been just one clinical trial of autologous CMV-specific T-cell therapy in SOT recipients so far [538].

Some lessons have been learnt from these trials of adoptive T cell therapy. In the initial published trial, only clones of CMV-specific $CD8^+$ T cells were infused into the recipients. These $CD8^+$ T cell clones were generated by co-culturing peripheral blood mononuclear cells (PBMCs) from the donors with autologous fibroblasts infected with the AD169 strain of CMV. These PBMCs were then depleted of $CD4^+$ T cells before being grown up in culture and then infused into the recipients. The results showed that patients who had a progressive decline in cytotoxic T cell activity were deficient in CMV-specific $CD4^+$ T cell responses,

which suggested that $CD4^+$ T cells were required to maintain the population of CMV-specific $CD8^+$ T cells [616]. Of note, however, is that this decline in cytotoxic T cell activity was an *in vitro* finding, and no CMV viraemia nor CMV disease developed in any of these patients, although the trial was designed to assess safety as opposed to efficacy of this treatment modality. Following this finding, there was a change of approach in subsequent trials, and preparation of the T-cell infusions involved pulsing donor dendritic cells with CMV antigen, then co-culturing the PBMCs and subsequently selecting for CMV-specific T cells, resulting in infusions containing both $CD8^+$ and $CD4^+$ CMV-specific T cells. Though not all the trials evaluated if the infusions consisted of more $CD8^+$ or $CD4^+$ T cells, in those that did, there appears to be a predominance of $CD4^+$ T cells [13, 147, 337]. One study has assessed the functional and phenotypic characteristics of $CD4^+$ T cells generated this way, and showed that these T cells expressed the T_h1 transcription marker T-bet, and were able to lyse iDCs that had been infected with NEWT-strain HCMV via a perforin-mediated pathway [218]. Another has found that there was a much higher degree of expansion and expression of $T_{naïve}$ stem cell phenotype($CD62L^+CD45RA^+$) when using IE1 (1- to 961-fold) as compared to pp65 (1-to 33-fold) [13].

Of recent interest has also been the use of stored CMV-specific T cells from third-party donors for T cell therapy. This involves generating virus-specific T cell lines (VST) from pre-selected donors and expanding these VSTs ex vivo. These T cells are then cryopreserved, and, when needed for patients with refractory viremia, a VST from a HLA-matched donor can be used "off-the-shelf". The advantage of such an approach over using VSTs from a specific donor is that it eliminates the usual 2–3 week waiting period needed to generate a VST. So far, there have been just 3 prospective trials examining the use of VSTs in patients with intractable CMV disease [333, 412, 646], which have shown that VSTs are a feasible option in these patients. One of these trials [646] examined the phenotypes of $CD8^+$ and $CD4^+$ T cells in these patients post-VST infusion, and demonstrated that $CD4^+$ T cells were predominantly effector memory cells ($CD45RA^-CD62L^-$), whereas $CD8^+$ T cells showed a shift in phenotype from effector memory ($CD45RA^-CD62L^-$) to terminally differentiated effector T cells ($CD45RA^+CD62L^-$). Interestingly, of these 3 studies, the group which showed the poorest rate of complete response to therapy ([412], $\sim$50% compared to $>$70% in [333, 646]) used an expansion of CMV-specific $CD8^+$ T cells, in contrast to the other 2 groups which used an expansion of cytotoxic T lymphocytes. This would appear to suggest that the presence of $CD4^+$ T cells in the VST infusion were crucial to providing to a more robust immune response to CMV in these patients. In addition, a recent retrospective study of allogeneic HSCT recipients who received CMV-specific cytotoxic T lymphocytes for refractory CMV disease showed that patients with a baseline $CD4^+$ T cell count of $\geq 50 \times 10^6$ cells/L were more likely to respond to therapy and had a superior odds of survival [154], which suggested that a baseline $CD4^+$ T cell response was needed to mediate a more durable immune response. However, so far no studies have explored possible explanations for these trends.

1.2.7.4 In congenital HCMV

The risk of transmission of CMV from mother to foetus, resulting in congenital CMV infection, is highest in primary infection in the mother, with reported ranges of approximately 40% [174]. However, transmission of CMV to the foetus can also occur in mothers who are seropositive, albeit at much lower rates [69, 295]. These were initially thought to occur as a result of reactivation of latent virus, although more recent studies have suggested that infection with a serologically distinct strain of HCMV may be a cause as well [489, 649].

The kinetics of the development of an antibody response during primary HCMV infection in pregnant versus non-pregnant women appear to be comparable [481], but pregnant women having a primary infection appear to have a decreased $CD4^+$ lymphoproliferative response to CMV lysate and IL-2 production for at least 9 months after infection [169]. Mothers that do not transmit CMV to the foetus are more likely to have an earlier and higher lymphoproliferative response of $CD4^+$ T cells to HCMV [169,481], with some observations that the $CD4^+$ response develops earlier than the $CD8^+$ lymphoproliferative response [347]. The CMV-specific $CD4^+$ T cells of mothers who did not transmit had higher percentages of IL-$7R^{pos}$ [386], $CD45RA^+$ [169], and IL-2 [168]. When compared with healthy sero-negative pregnant mothers, the $CD4^+$ T cells of seropositive pregnant women had higher levels of IFN-γ and TNF-α production in response to exposure to CMV antigen, but this response was less than in healthy, non-pregnant seropositive females [177].

Decreased cytokine production following stimulation with CMV antigens is also seen in infants with congenital CMV. An analysis of seven infants with congenital CMV infection showed a lack of production of IFN-γ, IL-2, and IL-4 from $CD4^+$ T cells on exposure to pp65-derived peptide [225]. Other early studies made the observation that symptomatic children with congenital CMV had higher percentages of $CD4^+$ T cells that produced IFN-γ and TNF-α in response to CMV antigen, though there was a limitation of small sample sizes [177, 414], and a later study of the response of $CD4^+$ T cells from congenitally infected infants showed they had a reduced polyfunctional response (defined as $\geq$2 out of CD107, MIP1β, IFN-γ, and/or IL-2) to pp65 antigen [190].

A comparison of congenitally infected neonates and their mothers showed that neonatal sera contained significantly higher levels of IL-8 when compared with their mothers, and also had increased levels of IL-2, IL-12, and IFN-γ with a corresponding lack of IL-4, suggesting a predominantly T_h1 response [224]. There may also be extrapolations that can be made from studies of HIV-positive mothers co-infected with HCMV. A maternal $CD4^+$ T cell count of $<$200 cells/μl is associated with higher risk of transmission to the fetus [182]. Retrospective studies of infants born to HIV-positive mothers showed that, if their mothers received full anti-retroviral prophylaxis, they had higher $CD4^+$ T cell counts [377] and were less likely to have congenital CMV [209].

A large Swedish study of infants up to 2 years of age with congenital CMV infection found

that they had CMV-specific $CD4^+$ T cell responses (measured by IFN-γ) that were inferior compared to adults during the first 3 months of age, though this difference was not significant by the age of 24 months [344]. This was in contrast to the $CD4^+$ T cell responses in 8 adults with primary CMV infection, which was high initially and then subsequently decreased. This increase in CMV-specific $CD4^+$ T cells appears to be approximately linear [100]. The slower increase of $CD4^+$ T cell function may explain the longer duration of viral shedding seen in neonates and children [82, 589], and illustrates the important role $CD4^+$ T cells play in controlling CMV disease. In addition to causing a slower increase of fetal $CD4^+$ T cells, CMV infection in utero also appears to cause an oligoclonal expansion of $CD4^+$ T cells in the infected newborn. Higher frequencies of $CD27^-CD28^-CD4^+$ T cells were detected in newborns with congenital CMV, with decreased expression of CCR7, IL-7R and increased expression of CD57 and the transcription factor T-bet and chemokine receptor CCR5, indicating T_h1 and cytotoxic T cell phenotypes. They also had a higher expression of the PD-1 inhibitory receptor, a similar profile to that seen in exhausted T lymphocytes [246].

The importance of $CD4^+$ T cells to generate a sustained and protective response to CMV is also seen in vaccine studies. In the rhesus model of CMV, rhesus macaques that received $CD4^+$ T-cell-depleting antibody had fetal loss or infant rhCMV-associated sequelae [55]. A phase 2 clinical trial for a gB-based vaccine with MF59 adjuvant showed an efficacy of 50% [428], and subsequent analysis of the immune response showed that there was not only an increase in antibody production but there also an increase in gB-specific $CD4^+$ T cell proliferation and IFN-γ production after vaccination [494], suggesting that, just like in primary infection [180], the formation of effector memory $CD4^+$ T cells was needed for an effective and sustained immune response to CMV.

1.2.7.5 Lessons learnt from murine models

Whilst many murine studies have illustrated the essential role $CD4^+$ T cells play in resolving CMV disease, there are limitations to these studies. During acute MCMV infection in mice, the $CD4^+$ T cell response peaks early and then contracts sharply to very low levels, and is dominated by high frequencies of IFN-γ and TNF-α double-producing $CD4^+$ T cells [24, 619]. These MCMV-specific $CD4^+$ T cells accumulate in the spleen and lungs of infected mice and produce multiple cytokines—IFNγ, TNF, IL-2, IL-10, and IL-17 [24]. In the lungs of infected mice, nodular inflammatory foci form around infected cells, which contain $CD8^+$ and $CD4^+$ T cells and exert viral control via IFN-γ and perforin [366]. However, in the context of suppressing viral reactivation, $CD4^+$ T cells appear to be less essential, as experiments in a B cell-deficient mouse model have established a hierarchy of $CD8^+$ T cells being more crucial to suppressing viral reactivation compared to $CD4^+$ T cells [447], with viral control and expansion of these MCMV-specific $CD4^+$ T cells being dependent on CD27-CD70 co-stimulation [634].

There is also evidence for cytolytic activity of $CD4^+$ T cells in the MCMV model. MCMV-

specific $CD4^+$ T cells that had high levels of granzyme B expression were able to lyse infected target cells in the BALB/c mouse liver. In addition, $CD4^+$ T cell epitope vaccination of immunocompetent mice reduced MCMV replication in the same organs where this cytotoxic activity was seen [606].

Approaches to examining the role of $CD4^+$ T cells in MCMV infection

There have been multiple approaches to interrogating the role of $CD4^+$ T cells in the control of MCMV infection. The first approach involved depletion of $CD4^+$ T cells. This was initially achieved through injecting mice with anti-$CD4^+$ (L3T4) antibodies. Early studies using anti-$CD4^+$ monoclonal antibodies to deplete $CD4^+$ T cells showed that the BALB/c strain of mice had delayed clearance of replicating virus, but were still able to generate protective $CD8^+$ effector T cells and restrict viral replication to the acinar cells of the salivary glands [272]. This finding was repeated in a later experiment using a different mouse strain, C57BL/6, where mice depleted of $CD4^+$ T cells were unable to control chronic viral replication in the liver and salivary glands [619]. Subsequently, it was demonstrated that MHC class I and II expression was detectable only at low levels in salivary gland cells and that antigen-presenting cells in the salivary gland were deficient in cross-presentation to $CD8^+$ T cells, thus control of MCMV replication in the salivary gland was likely to be due to $CD4^+$ T cells that had been selectively induced by antigen-presenting cells in the salivary glands [617]. These MCMV-specific $CD4^+$ T cells produce IL-10, which in turn is induced by IL-27, and these cytokines promote persistence of MCMV in the salivary glands [244, 630].

Another approach involved generating knockout mouse models—$CD4^-/^-$ and MHC $II^-/^-$. One major difference between these two lines is that $CD4^-/^-$ mice are able to generate isotype-switched antibody responses. This is achieved via a population of $CD8^-CD4^-$ T cells that are capable of adopting some of the function of T-helper cells, such as mediating antibody class switching [359, 460] and supporting somatic hypermutation and affinity maturation of germinal center B cells [659]. There also exists a population of MHC class II-restricted T cells that are misdirected into the CD8 lineage [382, 590]. In contrast to the mice depleted with anti-$CD4^+$ T cell antibodies, when $CD4^-/^-$ mice were infected with MCMV, these mice were able to clear viral infection in all organs, albeit at a slower rate (of 200 to 400 days post-infection) than wildtype controls [617]. A possible reason for this difference is that the viral loads in the organs of the $CD4^-/^-$ mice were observed for much longer periods than the earlier studies. When MHC $II^-/^-$ mice were infected with MCMV, they were not able to eliminate viral replication. As MCMV-specific antibodies were previously shown to inhibit viral dissemination during MCMV infection, the authors surmised that the inability to generate isotype-switched antibody responses was the likely reason that $CD4^-/^-$ but not MHC $II^-/^-$ mice were able to halt active MCMV replication [273, 645].

It thus appears that $CD4^+$ T cells are not essential to elimination of actively replicating MCMV. To examine if $CD4^+$ T cells provide assistance to $CD8^+$ T cells in clearance of replicating virus, $CD4^{-/-}$ mice were infected with MCMV, and the percentage of $CD8^+$ T cells that recognized various MCMV epitopes were measured at multiple time points post-infection. The results showed that only accumulation of the late-appearing IE3-specific $CD8^+$ T cells was substantially impaired, suggesting that the help that $CD4^+$ T cells provide to $CD8^+$ T cells is limited to assisting in the expansion of only a limited subset of MCMV-specific $CD8^+$ T cells [542]. A caveat of interpreting this result was that only very limited epitopes (M45, M38, m139, and IE3) were tested, and with the knowledge that a large repertoire of epitopes are recognized by T cells, perhaps more extensive testing needs to occur.

$CD4^+$ T cell help provided via MHC class II expression is also needed to maintain a stable $CD8^+$ T cell memory pool, although ongoing lytic viral replication is partially able to provide this assistance as well. When splenic $CD8^+$ T cells from CD4-deficient MHC $II^{-/-}$ mice that had been chronically infected with MCMV were transferred into mice that were then infected with MCMV, the $CD8^+$ T cells from MHC $II^{-/-}$ mice proliferated much less vigorously than $CD8^+$ T cells from wildtype mice [618].

A third approach involved using adoptive transfer techniques, which can help to inform the equivalent adoptive transfer T cell therapies employed in transplant patients. Early studies of transfer of $CD4^+$ T cells into irradiated BALB/c mice that were subsequently infected with MCMV showed that $CD4^+$ T cells were not able to prevent viral replication in the lungs [469, 470], spleen or adrenal glands [468]. Later studies using the same murine system also demonstrated that controlling CMV-mediated lung disease in treated mice required $CD8^+$ T cells rather than $CD4^+$ T cells [445, 552]. However, when adoptive transfer was performed in severe combined immunodeficiency (SCID) mice, $CD4^+$ T cells were able to prevent viral dissemination in the brain [480]. Overall, therefore, $CD4^+$ T cells appear to be essential only for control of viral replication in the specific organs in the mouse model.

Caveats to interpreting MCMV models

Limitations exist in extrapolating the findings in murine models of cytomegalovirus infection, due to the underlying differences between murine CMV infection and HCMV [338]. In an early mouse model of adoptive immunotherapy, transfer of $CD4^+$ T cells into irradiated and MCMV-infected mice did not reduce viral titers in the lungs, spleen nor adrenal glands of these mice. In contrast, transfer of $CD8^+$ T cells had significant reductions in viral titers [468]. When graded numbers of $CD4^+$ T cells were transferred with a constant number of $CD8^+$ T cells, there was no difference to viral titers either (suggesting no helper effect). However, as already discussed it is clear that in the case of HCMV infection $CD4^+$ T cells are a necessary component of CMV T cell therapy.

There have thus been attempts to create a "humanized" mouse model of CMV infection, by generating an immune-deficient mouse with a mutation in IL-2 receptor γ-chain locus (IL-2γc $^{-}/^{-}$) that is severely impaired in generating mouse B, T and NK cell lines (reviewed in [116, 522]). When these mice were engrafted with human haematopoietic progenitor cells, they were able to reconstitute monocytes, macrophages and limited T-cells. This model was further refined by reconstituting these mice with human foetal bone marrow, liver and thymus tissue [115]. Latent infection of these mice was able to induce generation of central and effector memory HCMV-specific T-cells and produce HCMV-specific IgM and IgG neutralizing antibodies [117]. Adoptive transfer of $CD4^+$ T cells in such a model has shown that these $CD4^+$ T cells did not have an antiviral effect on their own, but when co-administered with $CD8^+$ T cells, they appeared to enhance the antiviral efficacy of $CD8^+$ T cells and significantly decreased viral titers in the spleen and lungs [579].

1.3 Plasmacytoid dendritic cells (pDCs)

Plasmacytoid dendritic cells (pDCs) were first described in the 1950s as a cell type found in T cell zones of human lymphoid tissue that were similar to plasma cells but lacking B cell and plasma cell markers [339]. They were subsequently identified in human peripheral blood [415] and tonsils as a subset of $CD11c^-$ dendritic cells that were able to differentiate into DCs with mature morphology [205], and eventually discerned to be the cells responsible for type I interferon production in peripheral blood in response to most viral infections [94, 261, 523].

1.3.1 Surface markers to identify pDCs

Dendritic cells are identified by being HLA-DR^+ with a lack of "lineage" markers, (i.e. negative for lineage markers of T cells, $CD3^-$; B cells, $CD19^-CD20^-$; NK cells, $CD16^-CD56^-$; and monocytes, $CD14^-$) [104], and plasmacytoid dendritic cells are further identified from dendritic cells by being $CD11c^-$, $CD123^+$, $CD303^+$ and $CD304^+$ [142, 260, 371]. CD303 (also known as blood dendritic cell antigen 2, BDCA-2) and CD304 (neuropilin-1) were initially described to be specific for plasmacytoid dendritic cells (pDCs) [142], but a recent single-cell RNA sequencing analysis found that there was an overlap in expression of CD303 and CD304 between the myeloid cDC precursor component and pDCs, although only pDCs were found to be the cells that expressed those markers in the highest amounts [107, 608].

1.3.2 Roles in antiviral immunity

pDCs utilise multiple pathways to detect viral infection: the endosomal toll-like receptor (TLR)7/9-MyD88, a pathway which is exclusively used by pDCs [193, 276]; TLR9 coupled to interferon-regulatory factor 7 (IRF7) [240, 291, 519]; and TLR9 coupled to nuclear factor

κ-light-chain-enhancer of activated B cells (NF-κB) leading to tumour necrosis factor (TNF) and IL-6 production (reviewed in [193]). These culminate, ultimately, in cytokine production—primarily type I interferons, but also IL-6, IL-12, IL-18 and various other chemokines [563].

Cytokine production by pDCs have wide-ranging effects on innate and adaptive immunity [108, 563]. On NK cells, type I interferons from pDCs activate NK cell cytolytic activity [588], protect uninfected cells from NK-mediated lysis [36], and induce IFN-γ production in NK cells. On T cells, type I interferons from pDCs induce activation markers, long-term T cell survival, IFN-γ production and T_H1 differentiation (reviewed in [9]), while on DCs, they promote differentiation, maturation and immunostimulatory functions [503]. They also induce B cell differentiation into plasma cells and stimulate production of immunoglobulin, particularly IgG [264, 446]. A summary of pDC functions is shown in Fig.1.9.

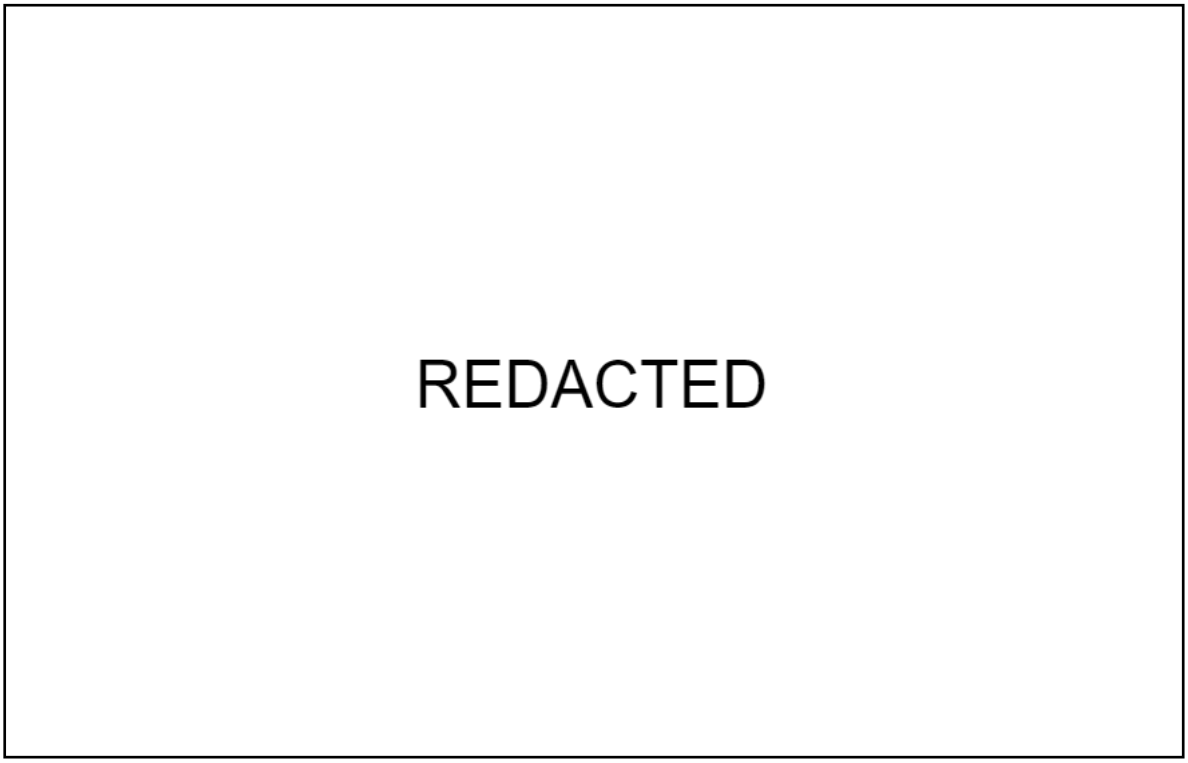

Figure 1.9: Summary of functions of pDCs
APRIL = A proliferation-inducing ligand; BAFF = B-cell activating factor; CCL = C-C motif chemokine ligand; ICOSL = inducible T-cell co-stimulator ligand; IDO = indoleamine 2,3-dioxygenase; iNKT = invariant natural killer T cells; OX40L = OX40 ligand; PDL1 = programmed death-ligand 1; TRAIL = TNF-related apoptosis-inducing ligand. Figure from Swiecki, et al. [563]

1.3.3 Plasmacytoid dendritic cells and HCMV

Plasmacytoid DCs do not appear to support direct HCMV infection as compared to conventional DCs [96, 604], but consistent with their role as the major producer of type I interferons in response to viral infections, pDCs respond to HCMV-infected cells by secretion of large amounts of IFN-α [318, 657], a process which is inhibited by cmvIL-10 [96]. Supernatants from pDCs co-cultured with TB40/E HCMV appear to be able to activate and induce B cell proliferation [604], and co-cultures of NK cells with pDCs exposed to CMV-infected MRC5 fibroblasts led to activation of NK cells [657]. Given their roles in antigen presentation and production of type I interferons, it would be expected that type I pDCs would prime and induce $CD4^+$ and $CD8^+$ T cell proliferation. Indeed, they have been shown to do so in influenza [93, 133], HIV ([235], reviewed in [477]), and also in a graft-versus-host model of disease [310], although this was not the case in one example of HCMV-infected pDCs co-cultured with PBMCs [604].

1.4 Aims of the project

While there has been a large amount of work published on the association of the recovery of HCMV-specific $CD4^+$ T cells with improved clinical outcomes and decreased risks of HCMV reactivation and disease, much less has been done on examining the mechanisms of how this occurs. It has also been shown that $CD4^+$ T cells recognise a wide range of HCMV peptides, and they can mount a cytokine response to this. However, less is known about the effects of these cytokines on the target cells, and how these effects contribute to the overall immune response to HCMV. The work presented in thesis aims to answer these questions:

1. Elucidate the mechanisms by which HCMV-specific $CD4^+$ T cells exert control over viral dissemination, expanding on the preliminary observation that $CD4^+$ cells can prevent viral dissemination in fibroblast co-cultures.
2. Examine how the $CD4^+$ T cells of an immunocompetent host overcome immune evasion strategies of the virus to control viraemia
3. Examine how the viral genes US2-11 contribute to immune evasion of $CD4^+$ T cells
4. Examine the antiviral capability of $CD4^+$ T cells from a cohort of kidney and liver transplant recipients using the *in vitro* viral dissemination assay developed in our laboratory
5. Determine if this antiviral capability is correlated with clinical viraemia or CMV disease in these transplant recipients
6. Examine the kinetics of this HCMV-specific $CD4^+$ T cell response, using serial results obtained from these kidney transplant recipients

Chapter 2

Materials & Methods

2.1 Cell culture

2.1.1 Human foetal foreskin fibroblasts, primary dermal fibroblasts and adult retinal pigment epithelium cells

Human foetal foreskin fibroblasts (HFFFs) (ATCC, U.K.), adult retinal pigmented epithelium-19 (ARPE-19) (ATCC, U.K.) and primary dermal fibroblasts were from laboratory stocks stored in liquid nitrogen . Primary dermal fibroblasts from healthy HCMV-seropositive and HCMV-seronegative donors were previously grown from 2mm skin punch biopsies by Georgina Okecha and Dr Sarah Jackson using a protocol published in [451].

Human foetal foreskin fibroblasts, primary dermal fibroblasts and ARPE-19 cells were grown in 175cm^2 tissue culture flasks (Corning, U.K.) and maintained in Dulbecco's Modified Eagle Medium (DMEM) (high glucose) (Sigma-Aldrich, U.K.) supplemented with 10% foetal calf serum (FCS) and 100 units/ml of penicillin/streptomycin. All further experiments involving any of these cell lines used the same media to propagate and maintain the cells throughout the experiment duration.

2.1.2 Human umbilical vein epithelial cells

Human umbilical vein epithelial cells (HUVECs) were a gift from Jing Garland and grown in 75cm^2 tissue culture flasks (Corning, U.K.) and maintained with Endothelial Cell Growth Medium 2 supplemented with Endothelial Cell Growth Medium 2 Supplement Pack (PromoCell, Germany).

2.1.3 Human primary dermal fibroblasts from clinical samples

To obtain the primary dermal fibroblasts from transplant recipients, a 2mm punch biopsy of the skin was taken from these recipients and grown out in DMEM-10 to obtain primary

dermal fibroblast cell lines following a protocol published in [450]. These were performed by Dr Claire Atkinson from University College London, and aliquots of fibroblast lines kept in liquid nitrogen storage until needed. When required, cells were defrosted as described in Section 2.11 below and maintained in DMEM supplemented with 20% foetal calf serum, 100 units/ml of penicillin/streptomycin and 1mM sodium pyruvate (ThermoFisher Scientific, U.S.A.). When in use, cells were maintained with DMEM-10 (Sigma-Aldrich, U.K.) supplemented with 10% FCS and 100 units/ml of penicillin/streptomycin in 175cm^2 tissue culture flasks (Corning, U.K.).

2.2 Virus propagation

The virus used in most of the experiments in this thesis is a bacterial artificial chromosome (BAC)-cloned Merlin strain of HCMV. Strain Merlin was originally isolated on fibroblast cell culture from congenitally infected neonatal urine samples from Public Health Laboratories, Cardiff [136]. The initial prototype Merlin clone was sequenced at passage 3 and contained a nucleotide substitution in UL128 and mutations in RL13 [12, 136], the presence of which was found to be inhibitory to growth in fibroblasts [550], but was otherwise found to match the presumed sequence in the clinical sample, except for three non-protein-coding differences in the *b/b'* region [641]. For use in laboratory work, this Merlin strain was then edited to contain mCherry fused to a UL36-peptide 2A sequence which is subsequently cleaved to give mCherry fluorescence when UL36 is expressed, and an enhanced green fluorescent protein (eGFP) fused to the C-terminus of pUL32. This virus was a gift from Dr Richard Stanton of Cardiff University.

The other virus strain used in this thesis is the endotheliotropic and fibroblast-tropic strain TB40/E-UL32-GFP, a gift from Dr Christian Sinzger, University of Ulm [497].

The viruses were propagated by seeding virus stock at 0.1 MOI into confluent HFFFs in 175cm^2 tissue culture flasks (Corning, U.K.) and rocked for 20 minutes at room temperature before incubation at 37°C, 5% CO_2. The cells were maintained with DMEM supplemented with 10% FCS and penicillin/streptomycin. When there was >90% infection of the cell sheet, observed either by cytopathic effect or fluorescence microscopy, media was removed and fresh media was applied every 2-3 days until the cellular layer was destroyed. The harvested media at each time point was centrifuged at 1600 G (ALC PK120 centrifuge, O-E24 rotor) for 25 minutes to remove cellular debris, then supernatant was stored at -80°C until all harvests were complete. When all harvests were complete, the supernatants were pooled and centrifuged at 15000 G for 2 hours at 4°C (12000RPM, Beckman-Coulter Avanti J-25 centrifuge, JLA-16.250 rotor) to obtain the virus pellets. These were resuspended with DMEM into 100μL aliquots and stored at -80°C until needed.

The viruses were titrated in HFFFs by the Reed & Muench method adapted by BD Lin-

denbach [354]. Viruses were grown with the assistance of Georgina Okecha.

2.3 Viral growth and dissemination assays

For the viral growth and dissemination assays, fibroblasts were seeded in 96-well full-area plates (Corning, U.K.) at 20,000 cells per well, or 96-well half-area plates (Greiner Bio-One, USA) at a density of 10,000 cells per well and grown to confluency overnight in DMEM as described in Section 2.1.1. When cells were confluent, infections were performed by adding virus at the required multiplicity of infection (MOI), given by the following equation:

$$\mathrm{MOI} = \frac{\text{number of plaque forming units per ml} \times \text{volume of virus used (in ml)}}{\text{number of cells}}$$

2.3.1 Addition of immune cells to viral dissemination assays

For viral dissemination assays, PBMCs, $CD4^+$ cells, $CD8^+$ T cells or NK cells were added at 1 day post-infection. When using stocks from liquid nitrogen, cells were washed in DMEM at 4°C at 757G (1800RPM on ThermoScientific Megafuge 40 centrifuge with TX1000 rotor) for 10 minutes, incubated with Benzonase® Nuclease (Sigma-Aldrich, U.K.) for 1 hour, then washed again and rested for 3 hours at 37°C before trypan blue staining and counting, followed by addition of the cells at the required E:T ratios.

On the day of analysis, the cells were harvested by removing the media in the wells, followed by washing with PBS and incubating with 0.25% trypsin for 15 minutes. Trypsin was inactivated by adding 4% paraformaldehyde to the wells. Wells were then analysed by flow cytometry.

The data was then plotted as graphs showing amount of infection on the y-axis, which was either expressed as a percentage of total cells ("% $mCherry^+GFP^-$") or as a percentage of the amount of cells in the same phase of CMV gene expression in the infected controls of the experiment, i.e. "normalised to infected controls" ("% $mCherry^+GFP^-$ (normalised)" or "% $mCherry^+GFP^+$ (normalised)"). The equation below gives an example of the calculation for % $mCherry^+GFP^-$ (normalised).

$$\%\,\mathrm{mCherry^+GFP^-}\ (\text{normalised}) = \frac{\%\ \mathrm{mCherry^+GFP^-}\ \text{cells in well}}{\text{Mean }\%\ \mathrm{mCherry^+GFP^-}\ \text{cells in infected controls}} \times 100$$

2.4 Cell surface staining and phenotyping analysis

Staining of cellular surface markers were performed as such: cells to be stained were trypsinised (if they were adherent cells) before centrifugation in 3ml tubes or V-bottom plates. Excess trypsin and media was aspirated. Normal mouse serum was added at a dilution of

1:50 and incubated at room temperature for 10 minutes, followed by addition of cell surface staining antibodies and incubation at room temperature in the dark for 45 minutes. Excess antibody was washed off with PBS by centrifugation at 935G (1800RPM on ThermoScientific Megafuge 40 centrifuge with TX1000 rotor) for 5 minutes and tipping off supernatant, followed by fixation of cells with 4% paraformaldehyde before flow cytometry analysis.

The antibody-fluorochrome combinations used for purity analysis of $CD4^+$, $CD8^+$ and NK cell populations obtained from MACS and used in the VDAs in Chapters 3, 5 & 6 are listed in Table 2.1, and those used for purity analysis of $CD4^+$ and $CD14^+$ populations used in VDAs in Chapter 5 are listed in Table 2.2. Purity analysis of these populations was performed with the BD Accuri™ C6 (BD Biosciences, USA) flow cytometer. Antibody-fluorochrome combinations used for HLA-DR staining (Chapters 4 & 5) and phenotyping cell populations isolated with CD4 MicroBeads (Section 5.5) are listed in Table 2.3.

Table 2.1: Antibody panel for post-separation analysis of purity for viral dissemination assays with $CD4^+$ cells, $CD8^+$ T cells and NK cells

Cell surface marker	Species/ Isotype	Clone	Fluorochrome	Manufacturer	Volume per stain (μL)
CD3	Mouse IgG1, κ	UCHT1	FITC	BioLegend	2.0
CD4	Mouse IgG1, κ	RPA-T4	PE	BioLegend	2.0
CD56	Mouse IgG1, κ	HCD56	PE	BioLegend	2.5
CD8a	Mouse IgG1, κ	HIT8a	PerCP/Cy5.5	BioLegend	2.0
Live-Dead	-	-	Far Red	ThermoFisher	2.0 (of a 1:10 dilution in PBS)

Table 2.2: Antibody panel for post-separation analysis of purity for viral dissemination assays with $CD4^+$ and $CD14^+$ cells

Cell surface marker	Species/ Isotype	Clone	Fluorochrome	Manufacturer	Volume per stain (μL)
CD3	Mouse IgG2a, κ	HIT3a	AF647	BioLegend	2.0
CD4	Mouse IgG1, κ	RPA-T4	PE	BioLegend	2.0
CD14	Mouse IgG1, κ	61D3	FITC	eBioScience	5.0
CD8a	Mouse IgG1, κ	HIT8a	PerCP/Cy5.5	BioLegend	2.0

Table 2.3: Antibody panel for HLA-DR staining and phenotyping cells

Cell surface marker	Species/ Isotype	Clone	Fluorochrome	Manufacturer	Volume per stain (μL)
CD3	Mouse IgG2a, κ	BW264/56	VioGreen	Miltenyi Biotec	10
CD4	Mouse IgG2b, κ	OKT4	BV 605	BioLegend	2.5
CD11c	Mouse IgG1, κ	3.9	APC	BioLegend	2.0
CD14	Mouse IgG2a, κ	M5E2	BV 570	BioLegend	4.0
CD16	Mouse IgG1, κ	3G8	BV 650	BioLegend	2.0
CD19	Mouse IgG1, κ	SJ25C1	BUV 395	BD BioSciences	3.0
CD45	Mouse IgG2a, κ	5B1	VioBlue	Miltenyi Biotec	5.0
CD123	Mouse IgG2a, κ	6H6	PerCP/Cy5.5	BioLegend	4.0
CD303	Mouse IgG2a, κ	201A	FITC	BioLegend	2.0
HLA-DR	Mouse IgG2a, κ	L243	PE-Cy5	BioLegend	3.0
HLA-DR	Mouse IgG2a, κ	L243	BV 421	BioLegend	2.0

2.5 Immunofluorescence staining and image analysis

Cells were fixed with 1% paraformaldehyde for 15 minutes and permeabilised with 70% ethanol at -20°C for 20 minutes. Cells were then incubated with 5% milk for 1 hour at 22–26°C, then milk was removed and E13 antibody (bioMérieux, U.S.A.) was added at 1:1000 dilution for 1 hour. This was followed by 3 washings with TBS Tween, then cells were incubated for 1 hour with secondary antibody (goat anti-mouse IgG1 conjugated to AlexaFluor 788) at 1:500 dilution with 5% milk. This was followed by two washings with TBS Tween. PBS was then added to cells and fluorescence microscopy carried out with a wide-field Nikon TE200 microscope with CoolLED pE-4000 as UV light source, and digital images taken with Image-Pro Premier 9.3 software. Images were processed using ImageJ (available at https://imagej.nih.gov/ij/).

2.6 Interferon-γ treatment

Addition of recombinant interferon-γ to human foetal foreskin fibroblasts (HFFFs), primary dermal fibroblasts, ARPE-19 or human umbilical vein endothelial cells (HUVECs) was performed with recombinant interferon-γ1b (Miltenyi, U.K.) at concentrations 500-6000pg/ml added at 24 hours after seeding the cell lines in 96-well plates or 24 hours after viral infections. On the day of addition, media was aspirated from wells and IFN-γ was added to fresh media to achieve required concentrations before addition to wells.

2.7 Neutralisation protocols

Table 2.4 lists the antibodies used for neutralisation experiments. Concentrations used are as stated in the text, in accordance with the manufacturer's recommendations:

Table 2.4: Neutralisation & associated isotype antibodies

Neutralisation/ Isotype antibody	Species	Clone	Manufacturer	Range of concentrations used
IFN-γ	Goat IgG	Polyclonal	R&D Systems, USA	4-33.3μg/ml
Normal Goat IgG Control	Goat IgG	Polyclonal	R&D Systems, USA	4-33.3μg/ml
HLA-DR, DP, DQ	Mouse IgG2a, κ	Tu39	BD Biosciences, U.K.	10-50μg/ml
Purified NA/LE Mouse IgG2a, κ	Mouse (BALB/c)	G155-178	BD Biosciences, U.K.	10-50μg/ml

2.8 Flow cytometry analysis

Flow cytometry analysis of post-separation purities was performed with the BD Accuri C6 (BD Biosciences, USA) flow cytometer. Flow cytometry analysis of VDAs and phenotyping analysis was performed with Attune NxT4 (Thermo Fisher Scientific, USA) and BD LSRFortessa™ (BD Biosciences, USA) with assistance from NIHR Cambridge BRC Cell Phenotyping Hub. Analysis of results was performed with FlowJo version 10. In order to allow comparison between viral dissemination assays from different donors, the number of cells in each phase of CMV gene expression was expressed as a percentage of the number of cells in the same phase of CMV gene expression in infected controls in the same assay (i.e. "normalised to infected controls"). The equation to calculate this is given in Section 2.3.1 above.

2.9 Isolation of PBMC from whole blood

Fresh whole blood was obtained from HCMV-seropositive and HCMV-seronegative donors by venepuncture and collected into 50ml centrifuge tubes containing heparin 100U/ml at a blood:heparin ratio of 5:1. Blood was then diluted 1:2 in PBS before isolating PBMC via Lymphoprep (Axis-shield, Oslo, Norway) density gradient centrifugation. 25ml of blood was overlaid onto 12.5ml of Lymphoprep then centrifuged at 395G (1300RPM on ThermoScientific Heraeus Megafuge 40 with TX-1000 Rotor) for 25 minutes with the brake off. The PBMC layer was extracted using a Pasteur pipette and resuspended in 50ml PBS before being centrifuged at 935G (2000RPM on ThermoScientific Heraeus Megafuge 40 with TX-1000 Rotor) for 10 minutes with the brake on. Finally, the supernatant was poured off, and the PBMC resuspended in 50ml PBS and centrifuged at 395G (1300RPM on ThermoScientific Heraeus Megafuge 40 with TX-1000 Rotor) for 10 minutes. PBMC numbers were then enumerated by

haemocytometer counting of cells stained with trypan blue.

2.10 Cryopreservation of cells for storage

When PBMCs obtained from whole blood or dermal cell lines were not required for immediate use, the cells were frozen for storage in liquid nitrogen by the following process: cells were first centrifuged at 935G for 5 minutes to form a pellet. The supernatant was decanted off and the cell pellet resuspended in freezing media (90% DMSO, 10% DMEM-10) at a concentration of $1 - 2 \times 10^7$ cells/ml. They were then cooled to $-80°$C at a rate of $1°$C per minute, and transferred to storage in liquid nitrogen after 24 hours.

2.11 Defrosting of cells for use

When cells in liquid nitrogen storage were required for use, the vials were defrosted by warming rapidly to room temperature, either in a water bath or in the hands of the experimenter. The freezing media was washed off by adding the vial of cells to 10mls of media (DMEM-10, ThermoFisher Scientific, U.K.) and centrifuging at 757G (1800RPM on ThermoScientific Heraeus Megafuge 40 with TX-1000 Rotor) for 10 minutes. The supernatant was then decanted off and cells resuspended in the appropriate media for use. If these cells were PBMCs or immune cells, the cell pellet was resuspended in 10mls of RPMI-1640 or TexMACS (Miltenyi, U.K.) with 10 IU/ml of RNase-free DNase Benzonase® Nuclease (Sigma-Aldrich, U.K.) for 1 hour at $37°$C, before washing off the DNase by centrifuging for 5 minutes at 300G and resuspending in the appropriate media. This was to minimise non-specific activation of the immune cells due to cellular debris in the media from the defrosting process. The defrosted PBMCs or immune cells used in the viral dissemination assays were rested overnight at $37°$C before addition to the assays. This was to ensure that any immune cells that would have died overnight would not be added to the assays.

2.12 Cell separation using Magnetic Associated Cell Sorting (MACS)

T cell, NK cell, and $CD14^+$ monocytes were obtained from PBMCs using magnetic-activated cell sorting by autoMACS Pro Separator® (Miltenyi, U.K.). Cells were selected either by positive selection or negative selection, as elaborated in the following sections.

2.12.1 Positive selection

Positive selection involves selection of target population by adding magnetic beads ("Microbeads") conjugated to antibodies to cellular surface marker of interest. The input cell population is washed in MACS buffer (PBS without calcium and magnesium, supplemented with 2nM EDTA and 0.5% FCS) then resuspended in MACS buffer at concentrations as per manufacturer's instructions. MicroBeads are then added and incubated at 4°C for 15 minutes, following which cells are washed again in MACS buffer before resuspension at required concentrations in MACS buffer and cell separation using either LS columns (Miltenyi) or autoMACS (Miltenyi) is performed. The target population of cells is initially retained by magnetic action of the columns and subsequent washing of the columns after release from magnetic action allows collection of the target population.

2.12.2 Negative selection/Depletion

In negative selection, the input cells are depleted of unwanted cell populations by adding magnetic beads ("Isolation Kits") conjugated to antibodies to cellular surface markers that are not present on the surface of the target cell population. The input cell population is washed in MACS buffer, then resuspended at concentrations as per manufacturer's instructions. A two-step incubation is then performed according to the manufacturer's instructions, involving, firstly, addition of a biotin-antibody cocktail followed by addition of microbead cocktail. The cells are then resuspended in MACS buffer at a required concentration and cell separation using either LD columns (Miltenyi) or autoMACS (Miltenyi) is performed. The magnetic action of the columns retains cellular populations to be depleted, and the target cell population is allowed to pass through the column to be collected.

2.12.3 Selections of multiple populations of cells from a sample of PBMC

For work involving transplant donors and healthy seropositive and seronegative donors, it was necessary to obtain $CD4^+$ cells, $CD8^+$ T cells and NK cells from a single sample of PBMCs. Therefore, the sequence of isolation of the various cell populations were performed as illustrated below in Fig.2.1: after defrosting from liquid nitrogen, PBMCs were added at the required E:T ratios to the infected wells. $CD4^+$ cells were then isolated from the remaining PBMCs using positive selection MicroBead kits. This allowed the resultant CD4-depleted PBMC to remain unlabelled and thus able to undergo another cell separation process. The CD4-depleted PBMCs were then split into 2 populations in an approximate proportion of $\frac{1}{3}$ and $\frac{2}{3}$, and depletion of unwanted cell populations with isolation kits was performed to obtain $CD8^+$ T cells from the $\frac{1}{3}$ population, and NK cells from the $\frac{2}{3}$ population. The rationale for splitting the cells in a $\frac{1}{3}$:$\frac{2}{3}$ manner is due to the fact that there is usually a higher frequency

of CD8$^+$ T cells than NK cells in a population of PBMCs, and doing so minimises the risk of having insufficient NK cells from the separation process. This sequence of events is illustrated in Fig.2.1 below.

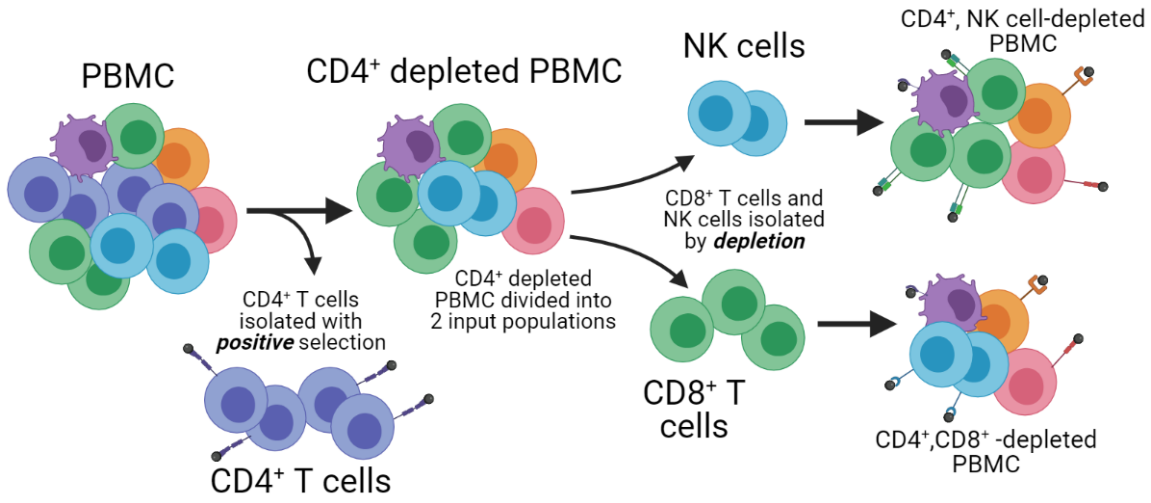

Figure 2.1: Sequence of cell isolations to obtain CD4$^+$ T cells, CD8$^+$ T cells and NK cells from a PBMC sample
After defrosting from liquid nitrogen, PBMCs were added at the required E:T ratios to the infected wells. CD4$^+$ cells were then isolated from the remaining PBMCs by MACS positive selection with CD4 MicroBead kits. This allowed the resultant CD4-depleted PBMC to remain unlabelled and thus able to undergo another cell separation process. The CD4-depleted PBMCs were then split into 2 populations in an approximate proportion of $\frac{1}{3}$ and $\frac{2}{3}$, and depletion of unwanted cell populations with isolation kits was performed to obtain CD8$^+$ T cells from the $\frac{1}{3}$ population, and NK cells from the $\frac{2}{3}$ population. Image created at BioRender.com.

2.13 Secretome preparation

To generate the PBMC or CD4$^+$ cell secretomes, CD4$^+$ cells were isolated from PBMCs by automated magnetic activated cells sorting (autoMACS, Miltenyi, U.K.) using CD4 MicroBeads (Miltenyi, U.K.) in accordance with the manufacturer's instructions. The purity of the resulting CD4$^+$ cell fraction was then assessed by cell surface staining of CD4 followed by analysis using flow cytometry.

The PBMC and CD4$^+$ cell fractions were then added to either HCMV-infected (at high MOI) or uninfected autologous primary dermal fibroblasts at E:T ratios of 10:1 or 20:1 in 24-well plates in RPMI media supplemented with 10% FCS and 100 units/ml of penicillin/streptomycin. After one week, media was harvested from the wells and supernatant from the wells obtained by centrifugation at 935G (2000RPM) for 10 minutes. These supernatants were then stored at -80°C until needed.

2.14 DNA extraction and PCR protocol

HFFFs were plated in 24-well plates at 100,000 cells/well and grown to confluency overnight before infection with either Merlin wildtype virus or Merlin ΔUS2-11 virus at MOI = 0.5. Viral DNA was extracted using QIAgen DNeasy Blood and Tissue Kit (QIAgen, U.K.) as per manufacturer's instructions. Briefly, cells were trypsinised (with 0.25% trypsin) and centrifuged to a maximum of 5×10^6 cells for 5 minutes at 300G before resuspension in 200μL of PBS. 20μL of proteinase K was added before addition of 200μL of Buffer AL, followed by vortexing to ensure thorough mixing and then incubation at 56°C for 10 minutes in a heat block. Then, 200μL of (96–100%) ethanol was added and mixed in by vortexing before pipetting into a DNeasy Mini spin column (QIAgen, U.K.), placing in a 2ml collection tube and centrifugation at 6000G for 1 minute. The flow-through was discarded and the spin column placed in a new 2ml collection tube before addition of 500μL of Buffer AW1 and centrifugation at 6000G for 1 minute. The flow-through was discarded and spin column placed in another new 2ml collection tube before addition of Buffer AW2 and centrifugation at 20,000G for 3 minutes. The spin column was then transferred to a new microcentrifuge tube and DNA eluted by adding 200μL of Buffer AE to the centre of the membrane, incubation for 1 minute at 15–25°C and centrifugation at 6000G for 1 minute.

The DNA extracted was then amplified using polymerase chain reactions (BioRad S1000 Thermal Cycler). The PCR cycles were as detailed in Table 2.5. Total PCR volume was 25μL per sample, consisting of 12.5μL Biomix red (Bioline, U.K.), 6μL nuclease-free water, 0.5μL each of forward and reverse primer and magnesium chloride (Bioline, U.K.), and 5μL of sample. The PCR products were then run on a 1.5% agarose gel. The sequences of the primers used are as listed in Table 2.6. DNA Hyperladder IV (100-1000bp) (Bioline, U.K.) was used as the DNA ladder in the electrophoresis gels.

Stage	Temperature (°C)	Duration
1	94	1 minute
2	94	1 minute
3	Tm	30 seconds
4	72	40 seconds
5	Repeat stages 2-4	For 40 cycles
6	72	5 minutes

Table 2.5: PCR cycles
T_m = 60°C for US2, 3, 6 and 11 and 55°C for GAPDH

Primer name	Direction	Sequence
US2	Forward	AGCACACGAAAAACCGCATC
US2	Reverse	TGCAAGGGGATGTGATCTGG
US3	Forward	ACCGTGGATATGGTGGACAT
US3	Reverse	AACAGCAGACCCCAATTGTC
US6	Forward	ACAACCAGCAGGGTAATCCC
US6	Reverse	ACAAATCCCGTCCGAACGAT
US11	Forward	GGCATTGATGACAGGGGGAA
US11	Reverse	GTCGACTGGAGGCTCTGTG
IE1 (exon 4)	Forward	CAAGAACTCAGCCTTCCCTAAGAC
IE1 (exon 4)	Reverse	TGAGGCAAGTTCTGCAATGC
GAPDH	Forward	CCACCATGGAGAAGGCTGGG
GAPDH	Reverse	ATCACGCCACAGTTTCCCGG

Table 2.6: Sequences of PCR primers
Expected sizes of PCR products: US2 = 270 bp, US3 = 155 bp , US6 = 226 bp, US11 = 221 bp, IE1 (exon 4) = 72bp, GAPDH = 287 bp

2.15 Real Time-quantitative PCR protocol

A two-step qPCR reaction was used. RNA extraction from samples was performed with RNEasy Kit using RNEasy spin columns (both from QIAgen, U.K.) according to manufacturer's instructions. Cells were trypsinised with 0.25% trypsin in PBS followed by addition of media before transferring to a polypropylene centrifuge tube and centrifugation at 300G for 5 minutes. Supernatant was aspirated before addition of RLT buffer and thorough mixing. The lysate was homogenised by vigorous pipetting followed by 1 volume of 70% ethanol and mixing. Up to 700μL of the sample was transferred to an RNeasy spin column and placed in a 2ml collection tube followed by centrifugation for 15 seconds at 8000G. Flow-through was discarded before addition of 700μL of Buffer RW1 and centrifugation for 15 seconds at 8000G to wash the spin column membrane. Following this, 500μL Buffer RPE was added to the RNeasy spin column and the columns centrifuged at 8000G for 15 seconds to wash the spin column membrane. The RNeasy spin column was then placed in a new 1.5ml collection tube and 30–50μL of RNase-free water was added directly to the spin column membrane before centrifugation for 1 minute at 8000G to elute the RNA.

Removal of genomic DNA and subsequent complementary DNA was made using QuantiTect Reverse Transcription Kit (QIAgen, U.K.) as per manufacturer's instructions. Briefly, 2μL of gDNA Wipeout Buffer was added to up to 1μg of sample RNA and made up to 14μL volume with RNase-free water. This was incubated for 2 minutes at 42°C followed by placing on ice. The reverse transcription master mix was made from 1μL of Quantiscript Reverse

Transcriptase, 4μL Quantiscript RT Buffer 5x, and 1μL RT primer mix before addition of 14μL of the cleaned-up RNA sample. This was incubated for 15 minutes at 42°C followed by incubation for 3 minutes at 95°C to inactivate the reverse transcriptase before proceeding to RT-qPCR.

RT-qPCR analysis was performed using New England Biotech LUNA SYBR Green qPCR reagents (New England Biolabs, U.K.). Glyceraldehyde phosphate dehydrogenase (GAPDH) was used as reference genes and relative gene expression was analysed using 2^ΔCt values (cycle threshold values). The ΔCt value was calculated using the equation below:

$$\Delta\text{Ct} = \text{Ct value of gene of interest} - \text{GAPDH Ct value}$$

Primer sequences are given in Table 2.7.

Primer Name	Direction	Sequence
UL44	Forward	TACAACAGCGTGTCGTGCTCCG
UL44	Reverse	GGCGTAAAAAACATGCGTATCAAC
pp28/UL99	Forward	TTCACAACGTCCACCCACC
pp28/UL99	Reverse	GTGTCCCATTCCCGACTCG

Table 2.7: Sequences of primers for RT-qPCR
Primer sequences obtained from Omoto, et al. [418]

2.16 Cytokine quantification by flow cytometry

Quantification of absolute amounts of cytokines present in supernatants from co-cultures was performed using the LEGENDplex™ Human Anti-Virus Response Panel (BioLegend), in accordance with the manufacturer's instructions. This assay utilises bead populations of varying sizes and levels of APC fluorescence ("capture beads") to detect amounts of analytes in the sample. Subsequently, biotinylated detection antibodies are added which bind to the capture beads, followed by addition of Streptavidin-PE, which binds to the detection antibodies. The resultant fluorescent signal thus intensifies in proportion to the amount of analytes present in the sample. This signal is measured by flow cytometry and the specific quantities of each analyte are determined by comparison with a standard curve. Concentrations of IFN-γ, IFN-α, IFN-β, IFN-λ1, IFN-λ2/3, IL-1β, IL-8, IL-10, GM-CSF and TNF-α were determined using this assay.

2.17 Relative quantification of cytokines by cytokine array

For detection of relative amounts of cytokines in various supernatants, a Proteome Profiler™ Human XL Cytokine Array Kit (R&D Systems) was used. This assay uses a nitrocellulose membrane containing capture antibodies which bind to 105 different cytokines. Supernatants are incubated overnight with the membranes and then biotinylated detection antibodies followed by streptavidin-HRP and chemiluminescent detection reagents are added. This was done in accordance with the manufacturer's instructions. The chemiluminescent signal produced by each capture antibody is measured on x-ray film and average mean gray values from the duplicate of each analyte was obtained using using ImageJ. Then, the mean intensity of each analyte is calculated using the formula:

$$\text{Mean Intensity} = 255 - \text{mean gray value}$$

This is followed by subtraction of background mean intensity and then normalised by expressing it as a percentage of the mean intensity of standard reference spots provided on each membrane.

2.18 Statistical analysis and presentation

Data was analysed and graphs were plotted using GraphPad Prism 9.0.2. For statistical analysis, the populations to be compared were first tested to see if they followed a Gaussian distribution. If so, a parametric test (such as Student's *t*-test or one-way ANOVA) was performed. If not, a non-parametric test (such as Mann-Whitney or Kruskal-Wallis) was performed. Statistical significance was indicated by values of p, where * symbolises $p \leq 0.05$, ** symbolises $p \leq 0.01$, *** symbolises $p \leq 0.001$, **** symbolises $p \leq 0.0001$ and ns symbolises $p > 0.05$.

2.19 Gene Ontology terms enrichment analysis

To look for enrichment of specific Gene Ontology (GO) terms in the datasets generated from the Proteome Profiler™ Human XL Cytokine Array, the fold changes of the differences in mean intensity of chemiluminescent signal for each cytokine analysed with the cytokine array was calculated, and those which had a value of <1 and p value of ≥ 0.05 were eliminated. The resultant list was then input into the Database for Annotation, Visualisation and Integrated Discovery (DAVID) analysis tool (available at https://david.ncifcrf.gov/home.jsp) to generate the list of enriched GO terms.

2.20 FluoroSpot™ analysis

The FluoroSpot™ assay is an enzyme-linked immune absorbent spot (ELISpot)-based assay that allows quantitative measurement of frequencies of cytokine secretion of single cells. First, the polyvinylidene fluoride (PVDF) membrane-lined 96-well plates were activated by 35% ethanol and washed 5 times with 200μl of sterile water as per manufacturer's instructions before coating with detection antibodies to IFN-γ overnight. On the evening of the same day, PBMCs of the donors to be analysed were defrosted, treated with DNase for 1 hour before washing off (procedure as described in Section 2.11 above) and resting overnight at 37°C, 5% CO_2 in TexMACS™ media (Miltenyi, U.K.). The next day, the PBMCs were centrifuged at 935G for 5 minutes and resuspended in fresh TexMACS™ for enumeration with trypan blue staining. If required, the PBMCs then underwent CD4- or CD8-cells depletion by addition of CD4 or CD8 MicroBeads (described in Section 2.12.1) to obtain the non-labelled CD4-depleted ("CD8-enriched") or CD8-depleted ("CD4-enriched") cell fractions. The immune cells were then resuspended in the appropriate volume of media to achieve a target of as close to 250,000 cells per 90μl of media as possible. 90μl of immune cells were then added to the wells, followed by the relevant peptides, mitogens (for positive control wells) or media (for negative control wells). 90μl of cells was also stained with an antibody mix containing antibodies to LiveDead FarRed, CD3, CD4 and CD8 before analysis with Accuri C6 flow cytometer to obtain an accurate count of the number of $CD3^+$ cells that had been added to the wells.

The FluoroSpot™ plates were then incubated for 48 hoursat 37°C, 5% CO_2 before removal of media, washing and addition of tag-labelled secondary detection antibodies followed by fluorescently-labelled anti-tag antibodies, as per manufacturer's instructions. The amount of IFN-γ secreted is then quantified by enumerating the number of fluorescence "spots" per well with a fluorescence reader, and given as the number of "spot-forming units" (sfu) per 10^6 $CD3^+$ cells added to the well. The number of "spot-forming units" per 10^6 $CD3^+$ cells is then calculated using the following formula:

$$\text{sfu per } 10^6 \text{ CD3}^+ \text{ cells} = \frac{\text{number of sfu per well}}{\text{number of live CD3}^+ \text{ cells added to well}} \times 10^6$$

Chapter 3

$CD4^+$ cells control cytomegalovirus dissemination *in vitro*

3.1 Introduction

As discussed in the Introduction, most early studies on the cell-mediated response to HCMV have focused on $CD8^+$ T cells. In recent years, the importance of the contribution of $CD4^+$ T cells to this response has become more evident. However, most prior studies of $CD4^+$ T cells in the context of HCMV have utilised lysate from HCMV-infected fibroblasts [355,452,453,516] or peptide pools [119,420,421] as stimulation to identify HCMV-specific $CD4^+$ T cells, followed by measurement of cytokine production or staining for activation markers to determine specificity and activity of these cells (summarised in Table 1.4). While these studies inform us on the frequency of HCMV-specific $CD4^+$ T cells found in various patient populations and the peptides they respond to, they fail to reveal the reasons for the many clinical observations of transplant patients with poorer $CD4^+$ T cell recovery or counts experiencing more frequent episodes of HCMV viraemia, reactivation and disease (summarised in Tables 1.7 and 1.8). Apropos to this, few studies have examined the capability of $CD4^+$ T cells to control viral dissemination *in vitro*. A few prior studies from our laboratory have demonstrated the use of a viral dissemination assay to assess the capacity of $CD8^+$ T cells [241, 254], NK cells [99], or PBMCs [241] to control HCMV replication, while another published study from our laboratory has used fibroblasts overlaid onto HCMV-infected dendritic cells co-cultured with $CD4^+$ T cells to quantify viral spread [256]. This study found that when $CD4^+$ T cells were co-cultured with HCMV-infected monocyte-derived dendritic cells (moDCs), fibroblasts that were subsequently overlaid showed almost nil viral growth as opposed to those overlaid on moDCs that were not co-cultured with $CD4^+$ T cells. In another series of preliminary experiments performed by a postgraduate student on attachment with our group, (Gabriel Marsères, unpublished data) $CD4^+$ T cells added to HCMV-infected fibroblasts were able to limit viral growth when compared to infected controls. These results suggest that $CD4^+$ T cells had direct antiviral

and cytotoxic responses to HCMV.

I thus sought to utilise the assay to further examine the direct $CD4^+$ T cell responses to HCMV. How do $CD4^+$ T cells recognise CMV-infected cells, and how do they then exert their antiviral effects? In this section, I first introduce the dual-tagged HCMV used in my experiments and its growth characteristics. I then introduce the viral dissemination assay and demonstrate the differences in ability between PBMC and lymphocyte populations from healthy HCMV-seronegative and HCMV-seropositive individuals to control viral dissemination in this assay.

3.2 A Merlin HCMV that allows quantification of immediate-early and late CMV gene expression

The HCMV used in the following experiments is the clinical isolate Merlin that has mCherry fused to a UL36-peptide 2A sequence that is subsequently cleaved to give mCherry fluorescence when UL36 is expressed, and an enhanced green fluorescent protein (eGFP) fused to the C-terminus of pUL32. Peptide 2As are small (18-22 amino acids) peptide sequences that are used for stoichiometric production of discrete protein products through inducing ribosomal skipping during translation, causing apparent "cleavage" of the protein downstream of the peptide 2A sequence [565]. Unless otherwise stated, this virus was used in all the experiments in this thesis, and is henceforth referred to as "Merlin WT" or "WT".

The HCMV UL36 gene encodes the viral inhibitor of caspase-8 activation (vICA), which binds procaspase 8 to prevent proteolytic activation and caspase 8-dependent apoptosis [535]. It is expressed at immediate-early (IE) times of infection with the ability to regulate nuclear gene expression [17], and then persists throughout infection [431, 571].

HCMV UL32 gene encodes a betaherpesvirus-conserved virion tegument protein, pp150, a 149-kDa protein that, together with two other major phosphoproteins, ppUL83 and ppUL82 and several minor structural proteins, form the tegument around the viral nucleocapsid [232]. Upon infection, these accumulate within a cytoplasmic inclusion adjacent to the nucleus at late times during infection [29, 561] and are involved in stabilisation of nucleocapsids through secondary envelopment at the assembly component [123, 391, 568]. It is a substrate for cyclin A2-dependent phosphorylation, the product of which blocks IE gene expression in undifferentiated cells [64].

As with other herpesviruses, HCMV late genes are divided into two categories : leaky late (γ_1) genes, which are expressed independent of viral DNA synthesis; and true late (γ_2) genes, expression of which is dependent on active viral DNA synthesis [160, 394]. pp150 expression occurs with true late kinetics [568] and deletion of the UL32 ORF leads to loss of infectious virus production [139, 656, 664]. The implication, therefore, is that when this double-taggled

Merlin WT virus is added to cells, the appearance of mCherry (i.e. an mCherry^{+}GFP^{-} cell) suggests that viral entry into the cell has occurred and the cell is in the IE phase of infection, while the presence of both mCherry and GFP (i.e. an mCherry^{+}GFP^{+} cell) suggests that infection has progressed to late phase and viral DNA replication has occurred.

3.2.1 mCherry is expressed at the same time as IE72 immediate-early protein in infected fibroblasts

The use of this double-tagged virus allows discrimination between cells that are in IE phase of infection, and cells that have progressed to true late phase infection. During the IE phase of infection, infected cells express mCherry only (i.e. they are mCherry^{+}GFP^{-} on flow cytometry). To show these cells are expressing IE genes, I infected HFFFs with HCMV (MOI = 0.027) and stained for IE72 at 20 hours post-infection. HCMV IE72 is a 491-amino acid nuclear phosphoprotein that is the initial and most abundant spliced mRNA transcript that arises from the major IE promoter. It is present within 1 hour after virus adsorption, reaches a maximum at 4 to 5 hours after infection [556], and is associated with multiple proteins involved with modulating the cell cycle (reviewed in [89]). Fig.3.1 shows that a majority of the cells that express mCherry are also positive for IE72.

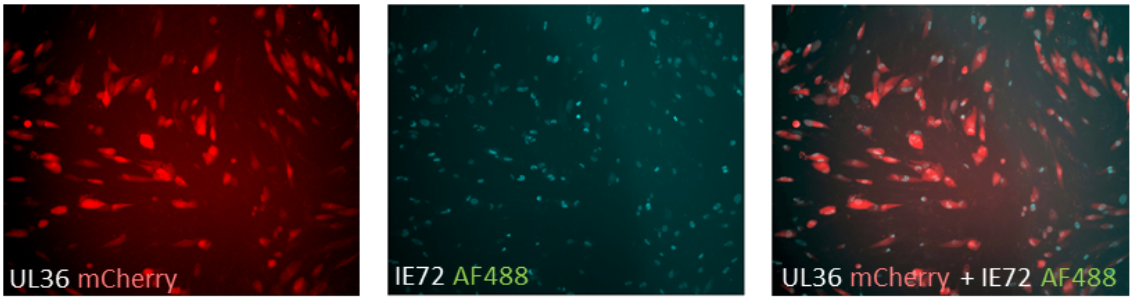

Figure 3.1: mCherry is expressed at immediate-early phase of infection
HFFFs were infected with HCMV (MOI = 0.027). At 20 hours post-infection, staining for IE72 with Alexa Fluor 788 secondary antibody was carried out, and cells examined by fluorescence microscopy. Left image shows microscopy images of cells expressing mCherry, middle image shows same cells stained for IE72. Right image shows superimposed images of both stains.

3.2.2 mCherry^{+}GFP^{+} infected fibroblasts express mRNA to late CMV genes

Following the above immunofluorescence stain to show that mCherry^{+} cells are in the IE phase of infection, I next sought to substantiate the presumption that mCherry^{+}GFP^{+} cells have entered the late phase of infection. To do this, HFFFs were grown to confluency in a T25 flask before infection with Merlin WT (MOI = 0.3) and incubated for 7 days. At 7 dpi, these cells were harvested and sorted into mCherry^{+}GFP^{-} and mCherry^{+}GFP^{+} populations

with the assistance of the NIHR Cambridge BRC Cell Phenotyping Hub. Fig.3.2A shows the gating strategy used to obtain singlets, and Fig.3.2B shows the gating strategy used to obtain the mCherry^{+}GFP^{-} and mCherry^{+}GFP^{+} populations. Real-time quantitative PCR (RT-qPCR) was then performed on these cell populations for levels of expression of UL44 and pp28.

The UL44 protein (pUL44) is an accessory subunit of DNA polymerasae encoded by UL54 [426,485] that increases processivity of the polymerase along the viral DNA template [153,631]. It accumulates to very high levels at late times after infection [184, 556] and is required for efficient viral gene expression [251].

The pp28 protein is a product of the UL99 gene. It localizes to the cytoplasmic assembly complex, a structure that consists of redistributed components of the cellular secretory apparatus [499, 500, 539]. It is essential for viral assembly [514] and is involved in secondary envelopment of the virion in the cytoplasm [70,524]. It is expressed after the initiation of viral DNA synthesis, and viral DNA replication is absolutely required for pp28 expression, thereby defining it as a true late gene [132, 298].

Figs.3.2C shows levels of expression of each of these true late genes in 2 replicates of this experiment, relative to the levels of GAPDH present in the samples.

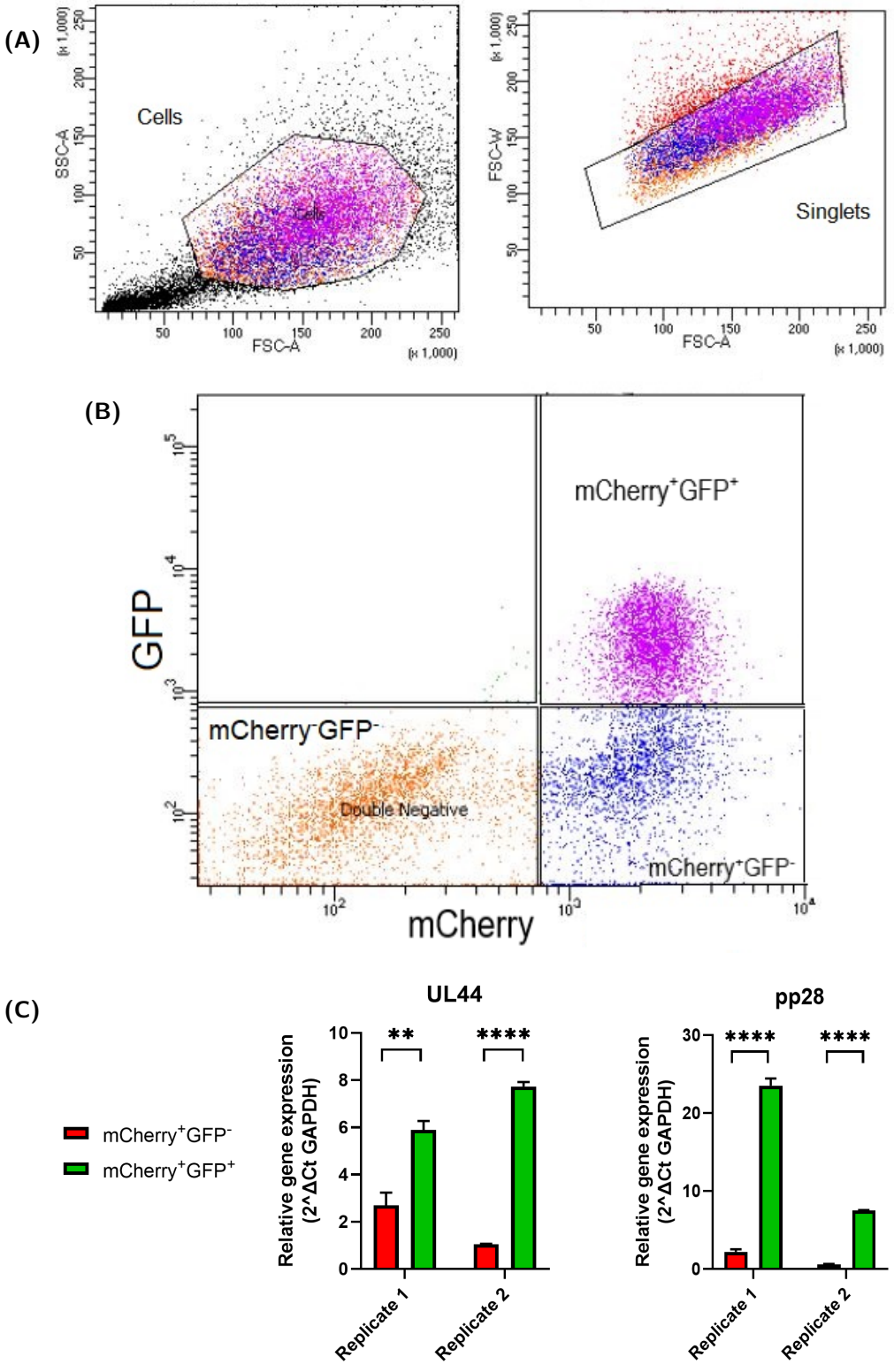
(A)
Cells
SSC-A
FSC-A
(x 1,000)
Singlets
FSC-W
(B)
mCherry+GFP+
mCherry-GFP-
Double Negative
mCherry+GFP-
GFP
mCherry
(C)
mCherry+GFP-
mCherry+GFP+
UL44
pp28
Relative gene expression (2^ΔCt GAPDH)
**
****
Replicate 1
Replicate 2

Figure 3.2: mCherry$^+$GFP$^+$ cells express late proteins
T25 flasks were seeded with HFFFs and grown to confluency overnight before infection with Merlin WT (MOI = 0.3) and incubated for 7 days. At 7 dpi, these cells were harvested and sorted into mCherry$^+$GFP$^-$ and mCherry$^+$GFP$^+$ populations with the assistance of the NIHR Cambridge BRC Cell Phenotyping Hub. Fig.3.2A shows the gating strategy used to obtain singlets, and Fig.3.2B shows the gating strategy used to obtain the mCherry$^+$GFP$^+$ population. RT-qPCR was then performed on mCherry$^+$GFP$^+$ for levels of expression of UL44 and pp28. Fig.3.2C shows levels of expression of each of these genes in 2 replicates of this experiment, relative to the levels of GAPDH present in the respective samples. Statistics performed using Students' *t* tests, mean of triplicate wells with error bars representing SD are shown. (*$p \leq 0.05$; **$p \leq 0.01$; ***$p \leq 0.001$; ****$p \leq 0.0001$; ns = not significant)

3.2.3 *In vitro* growth characteristics of Merlin wildtype HCMV

In order to use this virus in an assay to compare the functional capacity of various immune cell populations to control IE and late gene expression, I first needed to establish its growth characteristics on fibroblasts *in vitro*. HFFFs were plated in 96-well plates at 20,000 cells/well and grown to confluency overnight. The next day, they were infected with Merlin WT virus at an MOI of 0.017. Harvests (as described in Section 2.3) were performed at 1, 4, 7, and 10 days post-infection and then analysed by flow cytometry. Fig.3.3A shows a sample flow cytometry plot of the gating strategy to obtain the populations of interest, and the percentages of amount of cells in each population: mCherry$^-$GFP$^-$, mCherry$^+$GFP$^-$, and mCherry$^+$GFP$^+$. Fig.3.3B shows a representative FACS plot at each time point. Figs.3.3C and 3.3D show a representative fluorescence microscopy picture of mCherry and GFP expression at each day of harvest, and superimposed images are seen in Fig.3.3E. Fig.3.3F shows the graphical representation of the percentage of total cells with IE and late gene expression, and the total amount of infected cells (obtained by adding the percentages of cells that are mCherry$^+$GFP$^-$ and mCherry$^+$GFP$^+$), expressed as a percentage of the total cells in each well.

As can be seen in Fig.3.3B, at 1 dpi, only mCherry$^+$GFP$^-$ cells can be seen. At 4 dpi, cells that were initially mCherry$^+$GFP$^-$ had progressed to being mCherry$^+$GFP$^+$, and more cells had become infected and begun to express mCherry, as seen by the new population of cells that were now mCherry$^+$GFP$^-$. This is repeated on days 7 and 10 post-infection, as reflected by the progressive accumulation of cells that were mCherry$^+$GFP$^-$ and mCherry$^+$GFP$^+$. This progression of infection is also seen on the fluorescence microscopy images in Figs.3.3C–3.3E, and on the graph in Fig.3.3F.

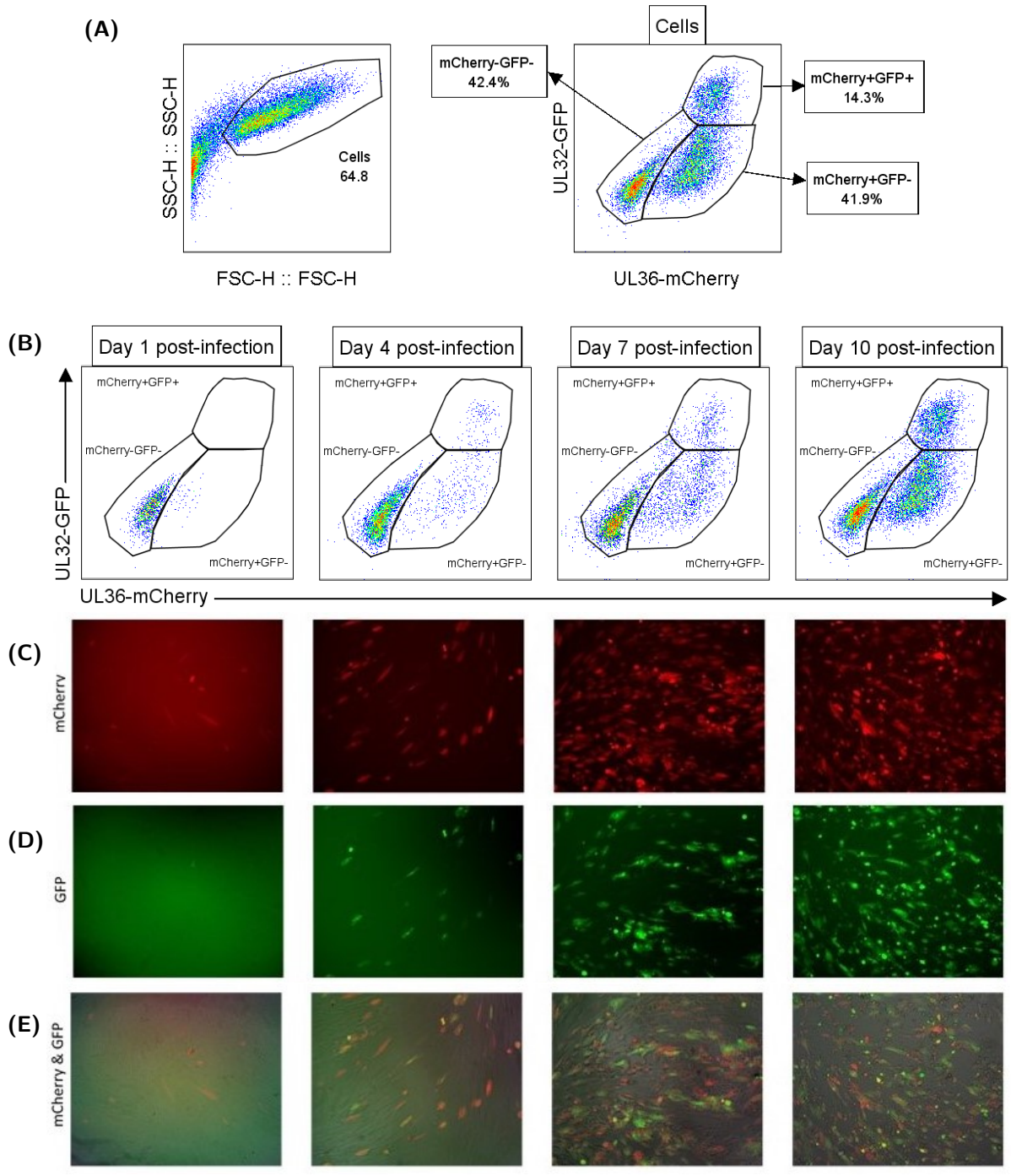
(A)
SSC-H :: SSC-H
Cells
64.8
FSC-H :: FSC-H
Cells
mCherry-GFP-
42.4%
mCherry+GFP+
14.3%
mCherry+GFP-
41.9%
UL32-GFP
UL36-mCherry
(B)
Day 1 post-infection
Day 4 post-infection
Day 7 post-infection
Day 10 post-infection
mCherry+GFP+
mCherry-GFP-
mCherry+GFP-
UL32-GFP
UL36-mCherry
(C)
mCherry
(D)
GFP
(E)
mCherry & GFP

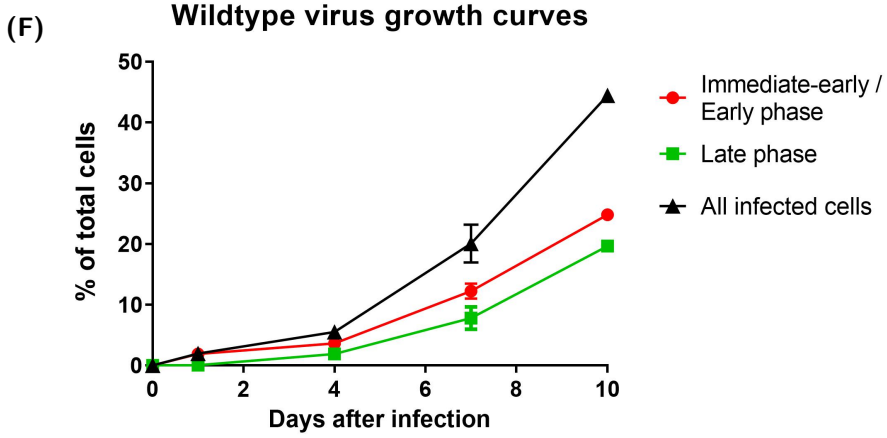
(F)
Wildtype virus growth curves
% of total cells
Days after infection
Immediate-early / Early phase
Late phase
All infected cells

Figure 3.3: FACS plots, fluorescence microscopy images and growth curves of Merlin WT virus
96-well plates were seeded with HFFFs and infected with Merlin WT virus at an multiplicity of infection (MOI) of 0.017. At 1, 4, 7 and 10 days post-infection, HFFFs were harvested and the mCherry and GFP expression was measured by flow cytometry. Fig.3.3A shows a sample flow cytometry plot of the gating strategy to obtain the populations of interest, and the percentages of amount of cells in each population: $mCherry^{-}GFP^{-}$, $mCherry^{+}GFP^{-}$, and $mCherry^{+}GFP^{+}$. Fig.3.3B shows a representative FACS plot at each time point. Figs.3.3C and 3.3D show a representative fluorescence microscopy picture of mCherry and GFP expression at each day of harvest, and superimposed images are seen in Fig.3.3E. Fig.3.3F shows the graphical representation of the percentage of total cells with immediate-early or late gene expression, and the total amount of infected cells (obtained by adding the percentages of cells that are $mCherry^{+}GFP^{-}$ and $mCherry^{+}GFP^{+}$), expressed as a percentage of the total cells in each well. Error bars represent SD of triplicate wells.

3.3 $CD4^+$, $CD8^+$ T and NK cells from HCMV-seropositive and HCMV-seronegative donors show different capabilities in controlling HCMV dissemination *in vitro*

The abovementioned figures showed that the Merlin WT virus is able to infect primary dermal fibroblasts and undergo multiple cycles of viral replication over the time course of the assay. As mentioned in the introduction to this chapter, a few prior studies from our laboratory have demonstrated the use of this viral dissemination assay to assess the direct antiviral responses of PBMCs [241], $CD8^+$ T cells [241, 254], NK cells [99] and $CD4^+$ T cells (unpublished data). A sample of the results of some of these experiments is shown in Fig.3.4. The experiments were conducted as such: dermal fibroblasts from a HCMV-seropositive donor were infected with HCMV Merlin UL32-GFP at a MOI of 1.06 (Fig.3.4A) or 0.33 (Figs.3.4B-F), or left uninfected, and co-cultured with immune cells at different E:T ratios (10:1 in Fig.3.4A). At seven days post-infection, the percentages of GFP^+ fibroblasts were measured by flow cytometry and expressed as a proportion of the positive control (infected fibroblasts alone).

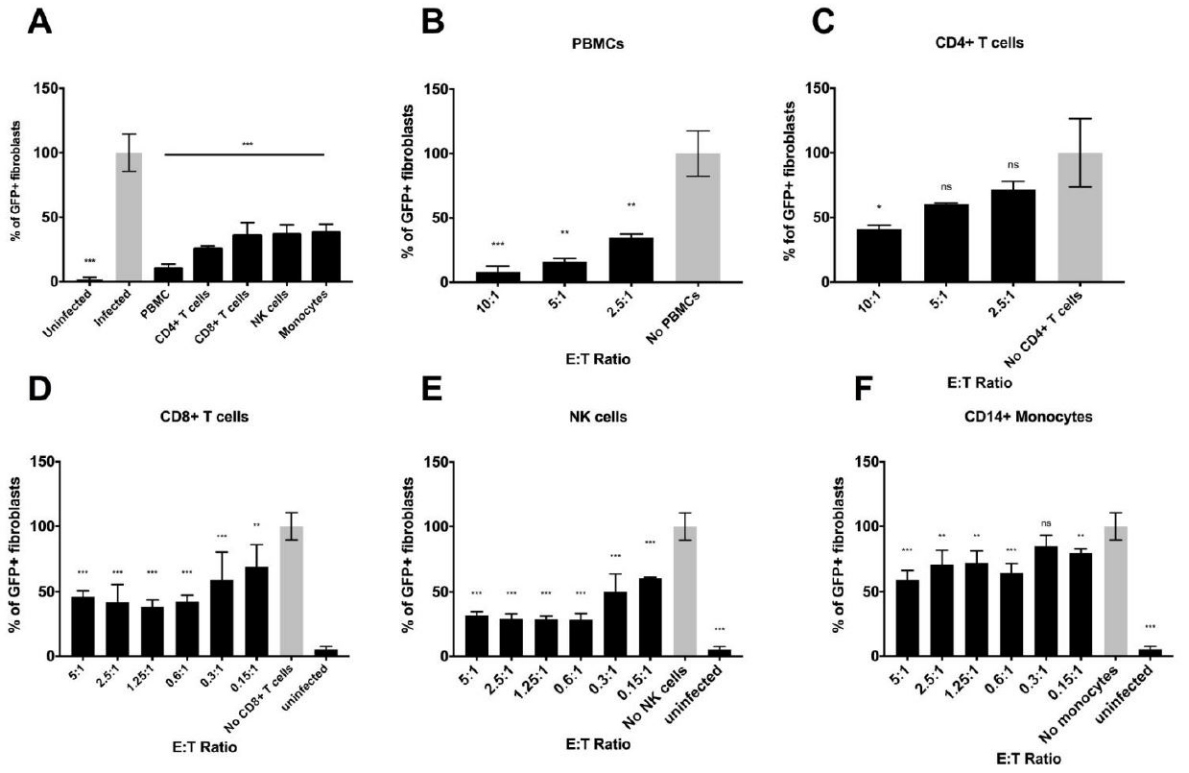

Figure 3.4: Results of preliminary experiments with viral dissemination assay
Dermal fibroblasts from a HCMV-seropositive donor were infected with HCMV Merlin UL32-GFP at a MOI of 1.06 (A) or 0.33 (B-F), or left uninfected, and co-cultured with immune cells at different E:T ratios (10:1 in A). At seven days post-infection, the percentages of GFP^+ fibroblasts were measured by flow cytometry and expressed as a proportion of the positive control (infected fibroblasts alone). Results presented in Fig.3.4A correspond to the means of two separate experiments. Statistics performed using Students' t tests, mean of triplicate wells with error bars representing SD are shown. (*$p \leq 0.05$; **$p \leq 0.01$; ***$p \leq 0.001$; ns = not significant) Data from Gabriel Marsères, a previous postgraduate student in the group.

The results show that PBMCs, $CD4^+$ and $CD8^+$ T cells, NK cells and, to a lesser extent, $CD14^+$ monocytes from a HCMV-seropositive donor all showed an ability to limit expression of GFP (i.e. late gene expression) when added to HCMV-infected fibroblasts. As discussed in the Introduction (Sections 1.1.5.4 & 1.1.5.5), $CD8^+$ T cells and NK cells are capable of direct cytotoxic effects on CMV-infected cells—$CD8^+$ T cells recognise a wide range of CMV epitopes and exhibit a polyfunctional profile [102, 256, 320], while NK cells respond to CMV infection by expansion of an activated NKG2C phenotype [167, 211, 362] that demonstrates enhanced cytotoxic responses in the presence of HCMV-specific antibodies [113, 648]. PBMCs by definition consist of blood cells with round nuclei, and include monocytes, lymphocytes (mainly $CD4^+$ and $CD8^+$ T cells and NK cells), $\gamma\delta$ T cells, B cells and monocytes. In addition, these experiments were mostly performed in HCMV-seropositive donors, where it has been shown that up to 30% of total $CD8^+$ T cells can respond to CMV peptide pools [564], albeit there being an extensive variability in these responses [254, 304]. It is interesting to observe that despite HCMV-mediated immune evasion function directed at avoiding $CD8^+$

T cell and NK cell recognition, when $CD8^+$ T cells, NK cells and PBMCs from a HCMV-seropositive donor were added to HCMV-infected fibroblasts, they were capable of limiting viral dissemination. In addition, the main route of antigen recognition by $CD4^+$ T cells is via the MHC Class II pathway, and in the absence of cells that constitutively express MHC Class II, such as macrophages or dendritic cells, it is also somewhat surprising that $CD4^+$ cells added to the assay in isolation are able to demonstrate inhibition of viral dissemination.

These studies showed that this assay can be used to compare the direct antiviral responses of the different lymphocyte populations from a single donor, and also compare lymphocyte populations from different donors. I thus wanted to use this system to determine direct antiviral responses of PBMCs, $CD8^+$ T cells, NK cells and $CD4^+$ cells to HCMV in a cohort of healthy HCMV-seropositive and HCMV-seronegative adults. By characterising the overall control by PBMCs from each serostatus group, followed by doing so with the individual lymphocyte populations, this would allow me to dissect out the cell populations that were responsible for the control (or lack thereof) of HCMV in the PBMCs of this cohort and determine the level of control mediated by adaptive immunity from HCMV-seropositive individuals as compared to innate responses, and how these then compare to responses mediated by HCMV-seronegative individuals. Characterising the dynamic range of this assay would be important if this approach were to be used to determine failure of immune responses to HCMV during transplantation.

3.3.1 Using the viral dissemination assay to assess antiviral capabilities of various immune cell populations from HCMV-seropositive and seronegative individuals

Due to limited amounts of frozen donor PBMCs available, it was necessary to obtain the $CD4^+$ and $CD8^+$ T cells and NK cells from a single vial of frozen PBMCs. The process of obtaining different populations of lymphocytes from a single defrosted vial of PBMCs and then adding them to the autologous HCMV-infected dermal fibroblasts is illustrated in Fig.3.5, and also detailed in Sections 2.3 and 2.12.3. Primary dermal fibroblasts were seeded at a density of 10,000 cells per well in 96-well half-area plates and grown to confluency overnight before infection with Merlin WT virus. 96-well half-area plates were used in order to reduce the number of immune cells needed to achieve the required E:T ratios. On the day of infection, PBMCs from the autologous donor were defrosted and treated with DNase for 1 hour before washing and resting in media overnight. Following overnight incubation, the PBMCs were washed and counted before addition to the 1 day post-infected fibroblasts at a starting E:T ratio of 2.5:1, followed by halving dilutions. $CD4^+$ cells were then selected from the remaining PBMCs by MACS using positive selection with CD4 MicroBeads (methods detailed in Section 2.12.1) and CD4-selected cells were added to the infected fibroblasts at a starting E:T ratio of 5:1, followed by halving dilutions. The remaining CD4-depleted PBMCs were then divided in

an approximate proportion of $\frac{1}{3}$ and $\frac{2}{3}$, and depletion of unwanted cell populations with $CD8^+$ T cell and NK cell Isolation Kits was performed to obtain $CD8^+$ T cells from the $\frac{1}{3}$ population, and NK cells from the $\frac{2}{3}$ population (detailed in Section 2.12.2). The $CD8^+$ T cells and NK cells were then added at starting E:T ratios of 5:1 or 2.5:1 (depending on number of cells obtained) followed by halving dilutions.

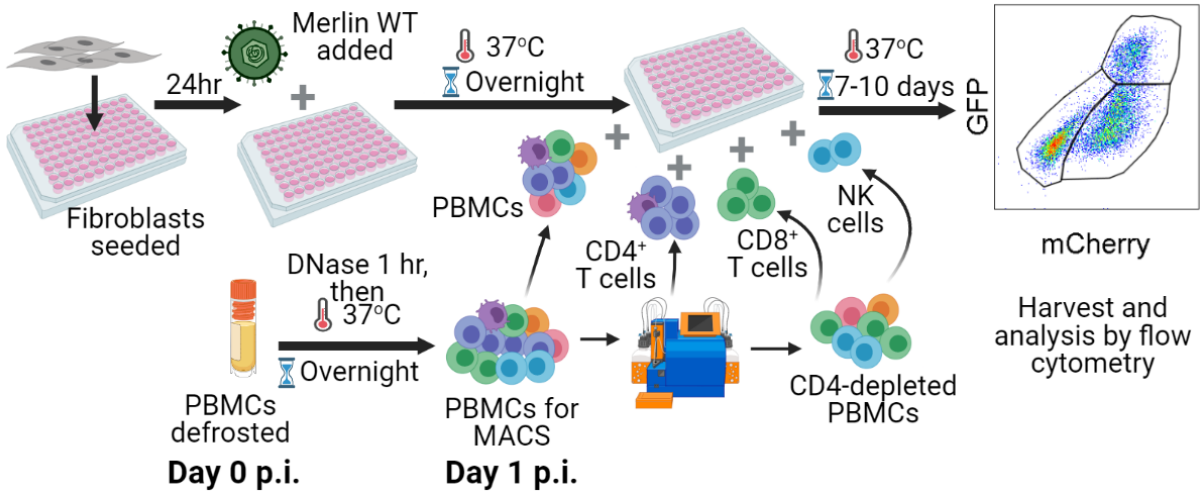

Figure 3.5: Process of setting up the viral dissemination assay to assess antiviral capabilities of PBMCs, CD4$^+$ and CD8$^+$ T cells, and NK cells
Primary dermal fibroblasts were seeded at a density of 10,000 cells per well in 96-well half-area plates and grown to confluency overnight before infection with Merlin WT virus. On the day of infection, PBMCs from the autologous donor were defrosted and treated with DNase for 1 hour before washing and resting in media overnight. At 1 dpi, the PBMCs were washed and counted before addition to the infected fibroblasts at a starting E:T ratio of 2.5:1, followed by halving dilutions. The CD4$^+$ cells were then selected from the remaining PBMCs by MACS using positive selection with CD4 MicroBeads (methods detailed in Section 2.12.1) and CD4-selected cells were added to the infected fibroblasts at a starting E:T ratio of 5:1, followed by halving dilutions. The remaining CD4-depleted PBMCs were then divided in an approximate proportion of $\frac{1}{3}$ and $\frac{2}{3}$, and depletion of unwanted cell populations with Isolation Kits was performed to obtain CD8$^+$ T cells from the $\frac{1}{3}$ population, and NK cells from the $\frac{2}{3}$ population. The CD8$^+$ T cells and NK cells were then added at starting E:T ratios of 5:1 or 2.5:1 (depending on number of cells obtained) followed by halving dilutions. After 7–10 days' incubation, the fibroblasts were harvested by trypsinisation and fixed with 2% paraformaldehyde before measurement of mCherry and GFP expression by flow cytometry. Figure created at BioRender.com

3.3.2 Determination of post separation purity for each lymphocyte population

Following isolation of the various lymphocyte populations as described in Section 3.3.1 above, post-separation purities of the $CD8^+$ T cell and $CD4^+$ populations were assessed by staining with the following antibody cocktail:

Antibody/Stain	Fluorophore
CD3	FITC
CD4	PE
CD8	PerCP-Cy5.5
Live/Dead	FarRed

Table 3.1: Antibody panel to assess post-separation purity of $CD8^+$ T cell and $CD4^+$ cells

Following this, the cells were analysed by flow cytometry, and the gating strategy used to obtain the percentage purities of each $CD8^+$ T cell and $CD4^+$ cell population is shown in Fig.3.6. First, PBMCs were analysed to determine the appropriate gates to identify live cells, $CD3^+$ cells in the "Live cells" gate, and $CD4^+$ and $CD8^+$ cells in the "$CD3^+$" gate (Fig.3.6A). Then, the post-separation $CD4^+$ and $CD8^+$ T cell populations were analysed through the same gates, and post-separation purities of $CD4^+$ cells was given by percentage of $CD4^+$ T cells in the $CD3^+$ gate (Fig.3.6B), while post-separation purities of $CD8^+$ T cells was given by the percentage of $CD8^+$ T cells in the $CD3^+$ gate (Fig.3.6C). Post-separation purities of separations performed on the cohort of healthy donors presented in this chapter ranged from 85.8 – 99.7 % for $CD4^+$ cells (full list in Appendix C) and 73.9 – 99.4% for $CD8^+$ T cells (full list in Appendix E).

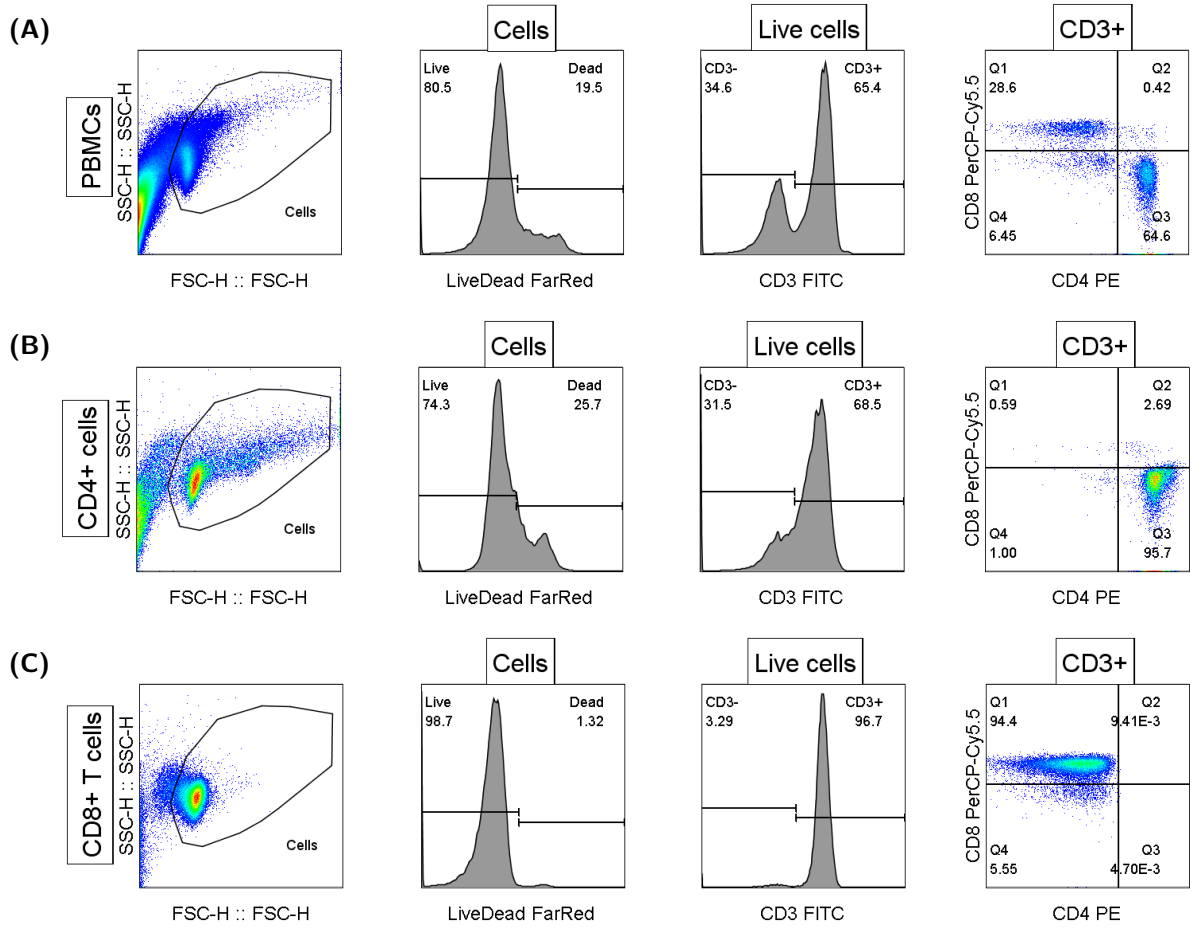

Figure 3.6: Gating strategy to assess post-separation purity of CD8$^+$ T cell and CD4$^+$ cells Cell populations were assessed for purity following isolation by MACS using the following antibodies: FarRed live/dead stain to identify live cells, FITC to identify CD3$^+$ cells, PE to identify CD4$^+$ cells, and PerCP-Cy5.5 to identify CD8$^+$ cells. The first column shows the gate to identify cells from forward and side scatter, the second column shows the gate to identify live cells from the Cells gate, the third column shows gate to identify the CD3$^+$ cells from the Live gate and the fourth column shows gates to identify CD4$^+$ and CD8$^+$ T cells from the CD3$^+$ gate. Fig.3.6A shows total PBMCs from one representative donor, Fig.3.6B shows cells obtained following CD4 selection, and Fig.3.6C shows cells obtained following CD8 selection from the same donor.

To assess the purities of NK cell populations, the PBMCs and NK cells from each donor were stained with the following antibody cocktail:

Antibody/Stain	Fluorophore
CD3	FITC
CD56	PE
CD8	PerCP-Cy5.5
Live/Dead	FarRed

Table 3.2: Antibody panel to assess post-separation purity of NK cells

Following this, the cells were analysed by flow cytometry, and the gating strategy used to obtain the percentage purities of each NK cell population is shown in Fig.3.7. First, PBMCs were analysed to determine the appropriate gates to identify live cells, $CD3^-$ cells in the "Live cells" gate, and the $CD56^{bright}$ and $CD56^{dim}$ populations (Fig.3.7A). Then, the post-separation NK cell populations were analysed through the same gates, and post-separation purities of NK cells was given by percentage of $CD3^-$ cells in the "Live cells" gate (Fig.3.7B). This $CD3^-$ gate was used as a surrogate for NK cell purity as the majority of NK cells are $CD56^{dim}$ [398] and the delineation of the true $CD56^+$ population of NK cells is not as clear without additional staining for other cell surface markers. The post-separation purities of NK cells obtained from the cohort of healthy donors presented in this chapter ranged from 92.5 – 100% (full list in Appendix G).

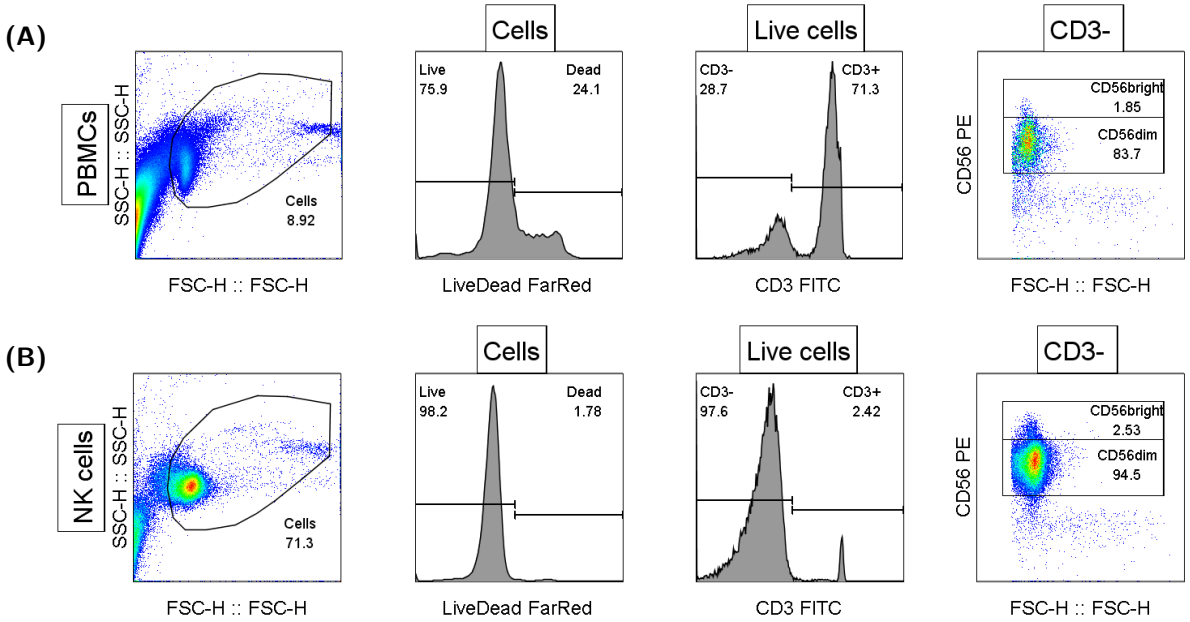

Figure 3.7: Gating strategy to assess post-separation purity for NK cells
Cell populations were assessed for purity following isolation by MACS using the following antibodies: FarRed stain to identify live cells, FITC to identify $CD3^+$ cells, PE to identify $CD56^+$ cells, and PerCP-Cy5.5 to identify $CD8^+$ cells. The first column shows the gate to identify cells from forward and side scatter, the second column shows the gate to identify live cells from the Cells gate, the third column shows gate to identify the $CD3^-$ cells from the Live gate and the fourth column shows gates to identify NK cells from the $CD3^-$ gate. Fig.3.7A shows total PBMCs from one representative donor and Fig.3.7B shows cells obtained following NK selection from the same donor.

3.3.3 Control of *in vitro* HCMV dissemination by PBMCs from a healthy seropositive and seronegative donor

I wanted to first examine the differences in control of IE and late gene expression between PBMCs from a healthy HCMV-seropositive versus a healthy HCMV-seronegative donor. After setting up the viral dissemination assay as described in the preceding sections, the results from a representative HCMV-seropositive and a representative HCMV-seronegative donor are shown below. Figs.3.8A & 3.8C show fluorescence microscopy images at day of harvest (8 dpi) of a representative well from a HCMV-seropositive donor with PBMCs added at E:T of 2.5:1 and 0.3:1, respectively, and Figs.3.8B & 3.8D show fluorescence microscopy images of a representative well from a HCMV-seronegative donor with PBMCs added at E:T of 10:1 and 0.5:1, respectively. These images show that when PBMCs from a HCMV-seropositive donor are added to the viral dissemination assay at an E:T of 2.5:1, there is almost no IE and late viral gene expression; when they are added at an E:T of 0.3:1, there is a slight increase of IE and late viral gene expression, but overall there is still a large suppression of viral gene expression. In contrast, with the HCMV-seronegative donor, at the E:T ratio of 10:1, there is some suppression of late gene expression, but not much suppression of IE CMV gene expression; at the E:T of 0.5:1, there is poor suppression of both IE and late gene expression.

(A) Seropositive donor, PBMCs, 2.5:1

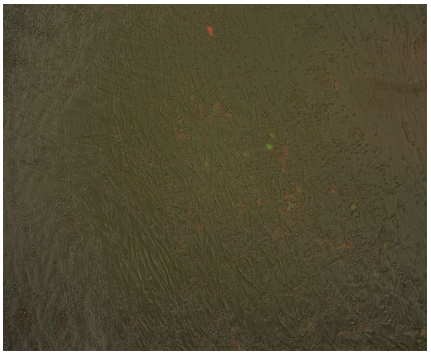

(B) Seronegative donor, PBMCs, 10:1

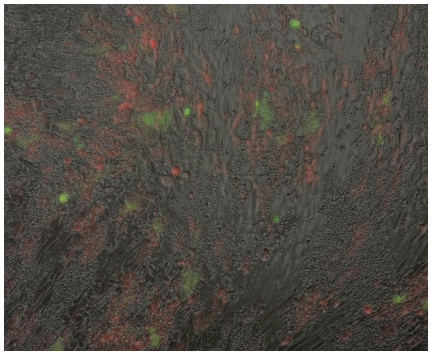

(C) Seropositive donor, PBMCs, 0.3:1

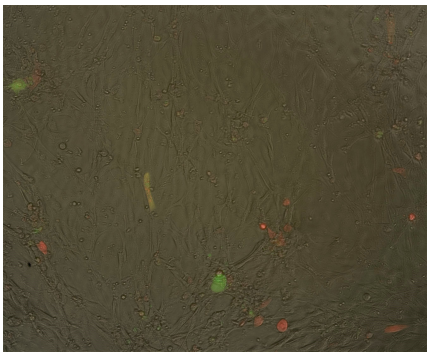

(D) Seronegative donor, PBMCs, 0.6:1

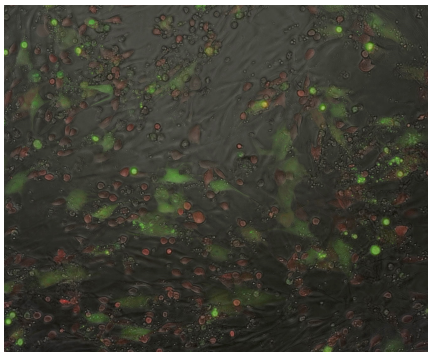

Figure 3.8: Fluorescence microscopy images of viral dissemination assay from one representative HCMV-seropositive and one HCMV-seronegative donor
Primary dermal fibroblasts from an HCMV-seropositive and an HCMV-seronegative donor were seeded in 96-well half-area plates and grown to confluency overnight before infection with Merlin WT virus (MOI = 0.03). On the day of infection, PBMCs from both donors were defrosted, treated with DNase and rested overnight. These PBMCs were then added to the infected primary dermal fibroblasts at 1 dpi at a starting E:T ratio of 2.5:1 (HCMV-seropositive donor) or 10:1 (HCMV-seronegative donor), followed by halving dilutions. The plates were incubated for 7 days before harvest and analysis by flow cytometry. Figs.3.8A & 3.8C show fluorescence microscopy images at day of harvest (8 dpi) of a representative well from the HCMV-seropositive donor with PBMCs added at E:T of 2.5:1 and 0.3:1, respectively, and Figs.3.8B & 3.8D show fluorescence microscopy images of a representative well from a HCMV-seronegative donor with PBMCs added at E:T of 10:1 and 0.5:1, respectively. Images acquired by Dr Charlotte Houldcroft and processed by myself.

To quantify the amount of $mCherry^{+}GFP^{-}$ and $mCherry^{+}GFP^{+}$ cells in the assay at the end of the incubation period, the cells were harvested by trypsinisation, fixed with 2% paraformaldehyde, and analysed by flow cytometry. Figs.3.9A, 3.9B and 3.9C show flow cytometry plots from an HCMV-seropositive donor of infected controls (with no PBMCs added), PBMCs added at E:T of 0.15:1, and PBMCs added at E:T of 2.5:1 respectively; Figs.3.9D, 3.9E and 3.9F show the same plots from an HCMV-seronegative donor. One representative well out of a triplicate for each E:T is shown. These plots show that at the low E:T ratio of 0.15:1,

there is little difference in amount of mCherry^{+}GFP^{-} and mCherry^{+}GFP^{+} cells between the HCMV-seropositive and HCMV-seronegative donor, but at the high E:T ratio of 2.5:1, there is a near-complete absence of any mCherry^{+}GFP^{-} and mCherry^{+}GFP^{+} cells in the wells from the HCMV-seropositive donor, whereas there is still a significant amount of mCherry^{+}GFP^{-} and mCherry^{+}GFP^{+} cells in the wells from the HCMV-seronegative donor.

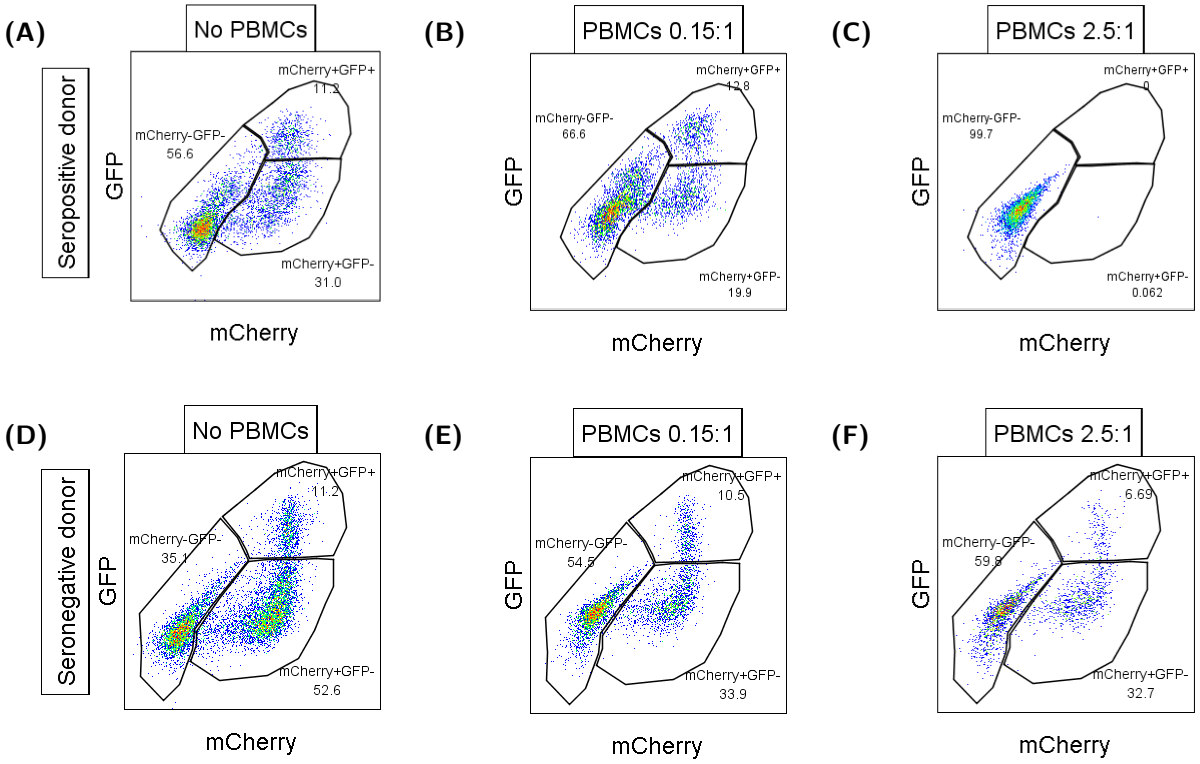

Figure 3.9: Sample flow cytometry plots of viral dissemination assay from one representative HCMV-seropositive and one HCMV-seronegative donor
To quantify the amount of mCherry^{+}GFP^{-} and mCherry^{+}GFP^{+} cells in the plates from Fig.3.8 at the end of the incubation period, these plates were harvested by trypsinisation, fixed with 2% paraformaldehyde, and analysed by flow cytometry. Figs.3.9A, 3.9B and 3.9C show sample flow cytometry plots from the HCMV-seropositive donor of infected controls (with no PBMCs added), PBMCs added at E:T of 0.15:1, and PBMCs added at E:T of 2.5:1 respectively; Figs.3.9D, 3.9E and 3.9F show the same plots from the HCMV-seronegative donor. One representative well out of a triplicate for each E:T is shown.

Fig.3.10 shows the complete results from the flow cytometry analysis from Fig.3.9. Fig.3.10A shows average amount of mCherry^{+}GFP^{-} (red bars) and mCherry^{+}GFP^{+} (green bars) cells at each E:T ratio performed in the HCMV-seropositive donor, expressed as a percentage of the amount of cells in the same phase of viral gene expression in infected control wells (i.e."normalised" to infected controls); Fig.3.10C shows the same for the HCMV-seronegative donor. As can be seen in Fig.3.10A, PBMCs from the healthy seropositive donor show almost complete control of IE viral gene expression at higher E:T ratios (2.5:1, 1.25:1 and 0.6:1), an effect which then dilutes out with decreasing E:T ratios, with loss of control of IE viral gene expression occurring to a greater degree than loss of control of late gene expression.

This dilution eventually leads to a near-complete absence of any control of IE or late viral gene expression at the lowest E:T ratio of 0.08:1. In contrast, PBMCs from the seronegative donor show approximately 75% control of IE and late CMV gene expression at the highest E:T ratio of 5:1, an effect which then rapidly dilutes out from the next E:T ratio of 2.5:1 onwards (Fig.3.10C).

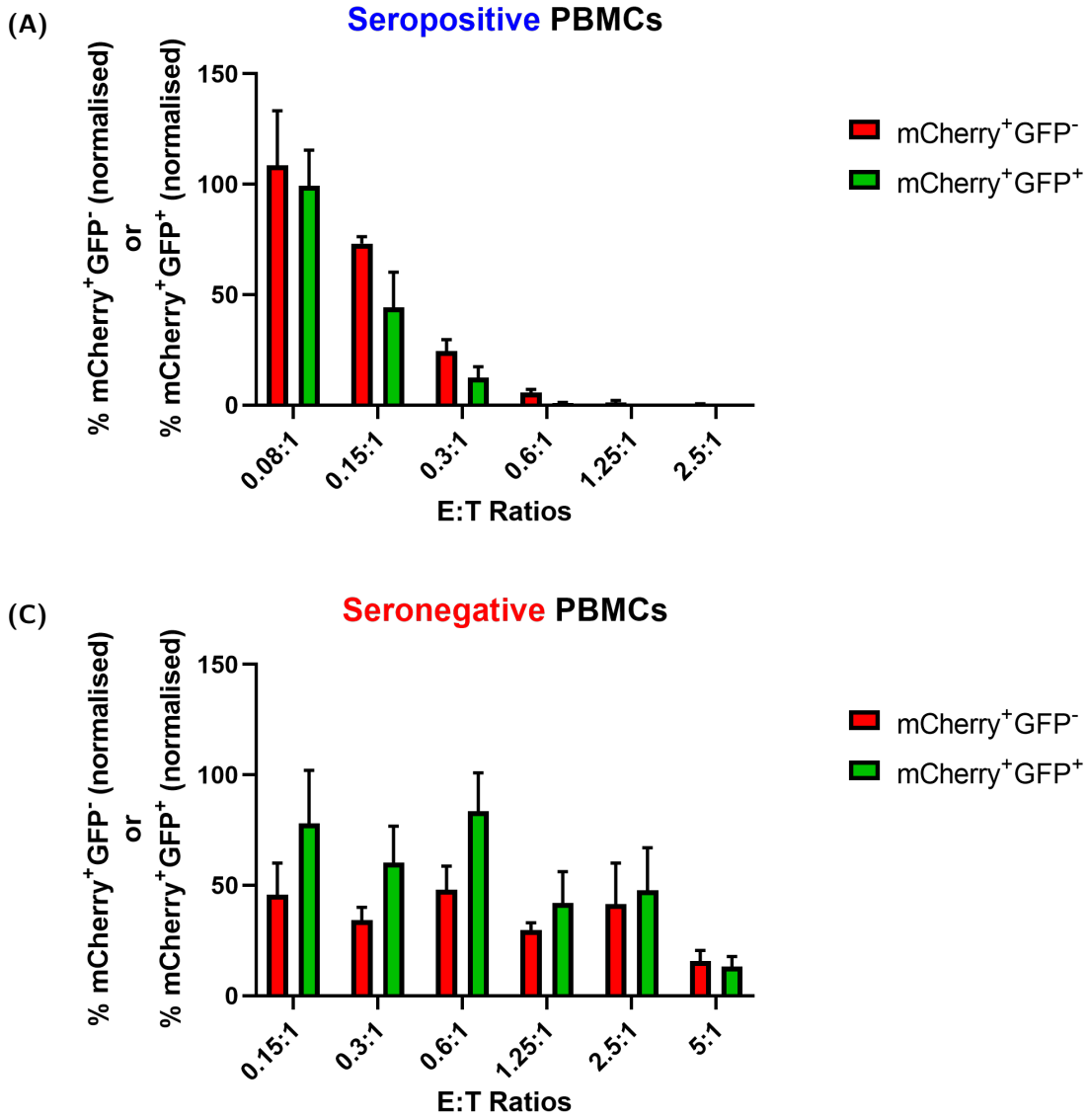

Figure 3.10: Control of viral dissemination by PBMCs from one seropositive and one seronegative donor

The complete results of the flow cytometry analysis from Fig.3.9 is shown here. Fig.3.10A shows average amount of mCherry$^+$GFP$^-$ (red bars) and mCherry$^+$GFP$^+$ (green bars) cells at each E:T ratio performed in the HCMV-seropositive donor, expressed as a percentage of the amount of cells in the same phase of CMV gene expression in infected control wells (i.e."normalised" to infected controls); Fig.3.10C shows the same for the HCMV-seronegative donor. Error bars reprsent SD of triplicate wells.

3.3.4 Control of *in vitro* HCMV dissemination by CD4$^+$ cells from a healthy HCMV-seropositive and HCMV-seronegative donor

After the addition of PBMCs to the viral dissemination assay, CD4$^+$ cells were isolated by MACS positive selection using the CD4 MicroBead Kit and added to autologous HCMV-infected primary dermal fibroblasts at starting E:T ratios of 5:1, followed by halving dilutions. After a further 7 days of incubation, the cells were harvested and analysed by flow cytometry. Figs.3.11A & 3.11C show fluorescence microscopy images taken just before harvest of a representative well with CD4$^+$ cells from the HCMV-seropositive donor added at E:T ratios of 5:1 and 0.3:1; Figs.3.11B & 3.11D show the same from a HCMV-seronegative donor. Figs.3.11E and 3.11F show the results of the flow cytometry analysis from the HCMV-seropositive donor and HCMV-seronegative donor respectively. Red bars show average amount of mCherry$^+$GFP$^-$ cells at each E:T ratio "normalised" to infected controls; green bars show the same for mCherry$^+$GFP$^+$ cells. Figs.3.11E, 3.11A & 3.11C show that CD4$^+$ cells from an HCMV-seropositive donor are able to control IE and late viral gene expression in an E:T-dependent manner, with loss of control beginning to be seen only at the E:T ratio of 0.3:1; whereas CD4$^+$ cells from an HCMV-seronegative donor show an approximate level of control of 25% for IE and 50% for late CMV gene expression at the highest E:T ratio tested of 5:1, an effect which then rapidly dilutes out with decreasing E:T ratios.

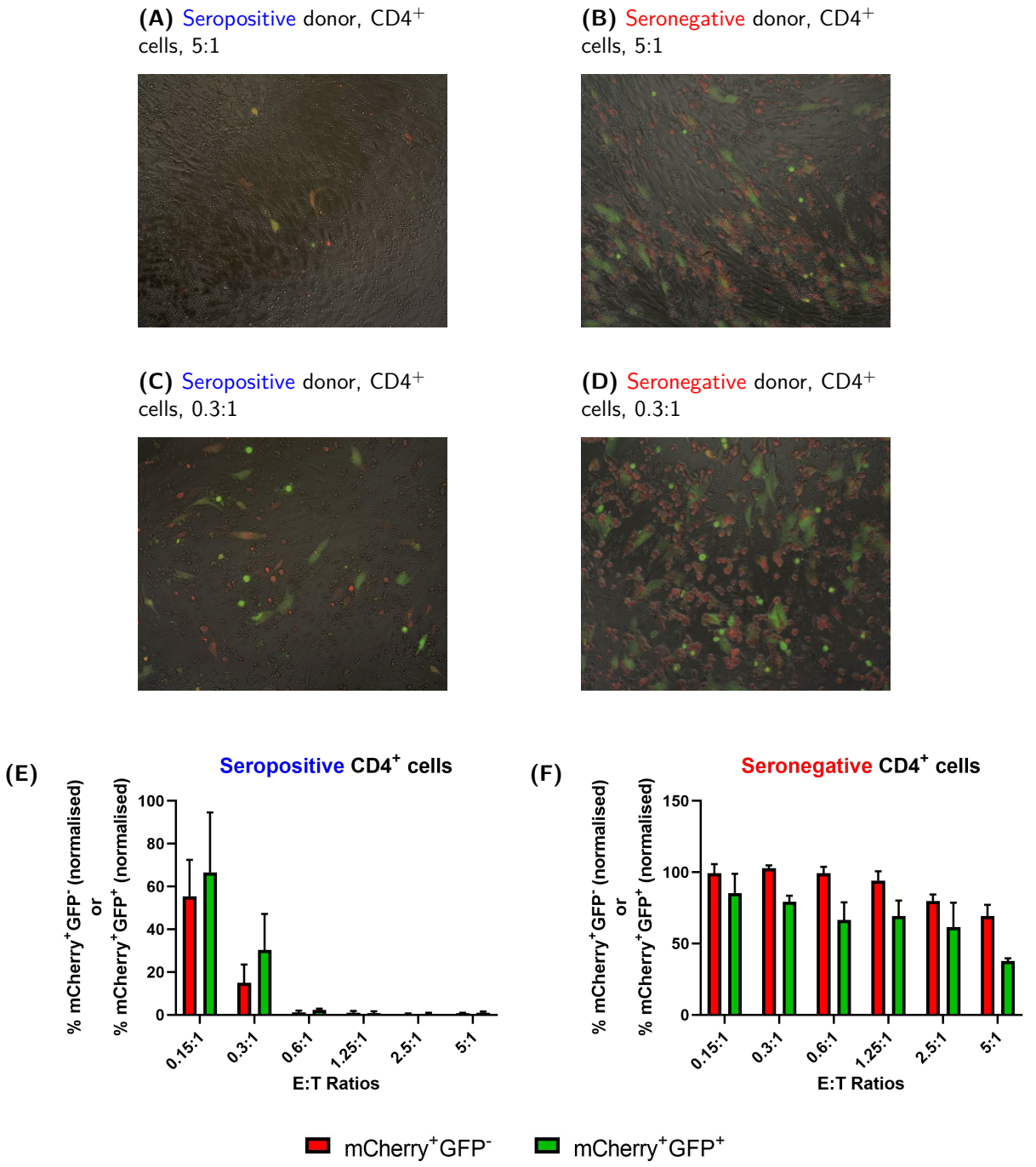

Figure 3.11: Control of viral dissemination by CD4$^+$ cells from one seropositive and one seronegative donor

After the addition of PBMCs to the viral dissemination assay, CD4$^+$ cells were isolated by MACS positive selection using the CD4 MicroBead Kit and added to autologous HCMV-infected primary dermal fibroblasts at starting E:T ratios of 5:1, followed by halving dilutions. After a further 7 days of incubation, the cells were harvested and analysed by flow cytometry. Figs.3.11A & 3.11C show fluorescence microscopy images taken just before harvest of a representative well with CD4$^+$ cells from the HCMV-seropositive donor added at E:T ratios of 5:1 and 0.3:1; Figs.3.11B & 3.11D show the same from the HCMV-seronegative donor. The complete results from the flow cytometry analysis is summarised in Figs.3.11E (HCMV-seropositive donor) and 3.11F (HCMV-seronegative donor). Red bars show average amount of mCherry$^+$GFP$^-$ cells at each E:T ratio "normalised" to infected controls; green bars show the same for mCherry$^+$GFP$^+$ cells. Error bars reprsent SD of triplicate wells. Images (A–D) acquired by Dr Charlotte Houldcroft and processed by myself.

3.3.5 Control of *in vitro* HCMV dissemination by CD8$^+$ T cells in a healthy HCMV-seropositive and HCMV-seronegative donor

After the addition of PBMCs and CD4$^+$ cells to the viral dissemination assay, CD8$^+$ T cells were isolated by MACS depletion using the CD8$^+$ T cell Isolation Kit and added to autologous HCMV-infected primary dermal fibroblasts at starting E:T ratios of 5:1 (for the HCMV-seropositive donor) and 2.5:1 (for the seronegative donor), followed by halving dilutions. After a further 7 days of incubation, the cells were harvested and analysed by flow cytometry. Figs.3.12A & 3.12C show fluorescence microscopy images taken just before harvest of a representative well with CD8$^+$ T cells from the HCMV-seropositive donor added at E:T ratios of 2.5:1 and 0.3:1; Figs.3.12B & 3.12D show the same from the HCMV-seronegative donor. The complete results from the flow cytometry analysis is summarised in Figs.3.12E (HCMV-seropositive donor) and 3.12F (HCMV-seronegative donor). These results show that CD8$^+$ T cells from an HCMV-seropositive donor are able to control IE and late viral gene expression at the higher E:T ratios of 0.6–2.5:1, an effect which then is diluted out at the lower E:T ratios of 0.3 and 0.15:1. In contrast, CD8$^+$ T cells from a HCMV-seronegative donor show a very poor to almost nil ability to control IE and late gene expression at all E:T ratios tested.

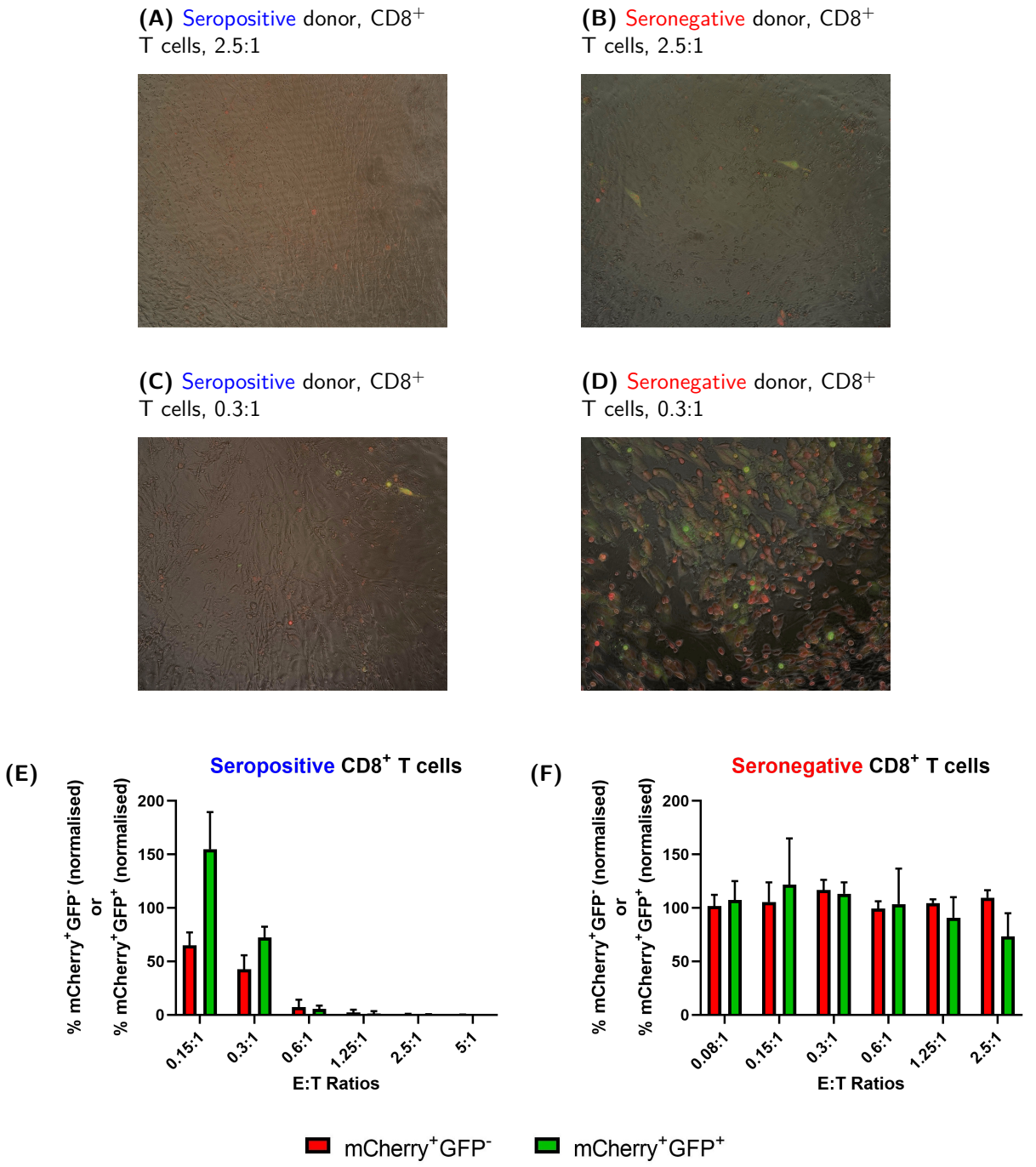

Figure 3.12: Control of viral dissemination by CD8$^+$ T cells from one seropositive and one seronegative donor

After the addition of PBMCs and CD4$^+$ cells to the viral dissemination assay, CD8$^+$ T cells were isolated by MACS depletion using the CD8$^+$ T cell Isolation Kit and added to autologous HCMV-infected primary dermal fibroblasts at starting E:T ratios of 2.5:1, followed by halving dilutions. After a further 7 days of incubation, the cells were harvested and analysed by flow cytometry. Figs.3.12A & 3.12C show fluorescence microscopy images taken just before harvest of a representative well with CD8$^+$ T cells from the HCMV-seropositive donor added at E:T ratios of 2.5:1 and 0.3:1; Figs.3.12B & 3.12D show the same from the HCMV-seronegative donor. The complete results from the flow cytometry analysis is summarised in Figs.3.12E (HCMV-seropositive donor) and 3.12F (HCMV-seronegative donor). Red bars show average amount of mCherry$^+$GFP$^-$ cells at each E:T ratio "normalised" to infected controls; green bars show the same for mCherry$^+$GFP$^+$ cells. Error bars represent SD of triplicate wells. Images (A–D) acquired by Dr Charlotte Houldcroft and processed by myself.

3.3.6 Control of *in vitro* HCMV dissemination by NK cells from a healthy HCMV-seropositive and HCMV-seronegative donor

After the addition of PBMCs, $CD4^+$ cells and $CD8^+$ T cells to the viral dissemination assay, NK cells were isolated by MACS depletion using the NK cell Isolation Kit and added to autologous HCMV-infected primary dermal fibroblasts at starting E:T ratios of 5:1 (for the HCMV-seropositive donor) and 2.5:1 (for the HCMV-seronegative donor), followed by halving dilutions. After a further 7 days of incubation, the cells were harvested and analysed by flow cytometry. Figs.3.13A & 3.13C show fluorescence microscopy images taken just before harvest of a representative well with NK cells from the HCMV-seropositive donor added at E:T ratios of 5:1 and 0.3:1; Figs.3.13A & 3.13C show fluorescence microscopy images taken just before harvest of a representative well with NK cells from the HCMV-seropositive donor added at E:T ratios of 2.5:1 and 0.3:1. The results from the flow cytometry analysis in Figs.3.13E (HCMV-seropositive donor) and 3.13F (HCMV-seronegative donor) show that NK cells from a seropositive donor show poor control of IE gene expression at all E:T ratios tested, and moderate control of late gene expression only at the highest E:T ratio of 5:1. In the seronegative donor, there is also poor control of IE gene expression at all E:T ratios tested, but moderate control of late gene expression at all E:T ratios except the lowest E:T ratio of 0.3:1. It is worth noting that of all the different lymphocyte populations tested, NK cells show the least difference in ability to control IE and late gene expression between an HCMV-seropositive and HCMV-seronegative donor—in fact, the NK cells from the HCMV-seronegative donor in this example show a marginally better ability to control late gene expression as compared to NK cells from the HCMV-seropositive donor.

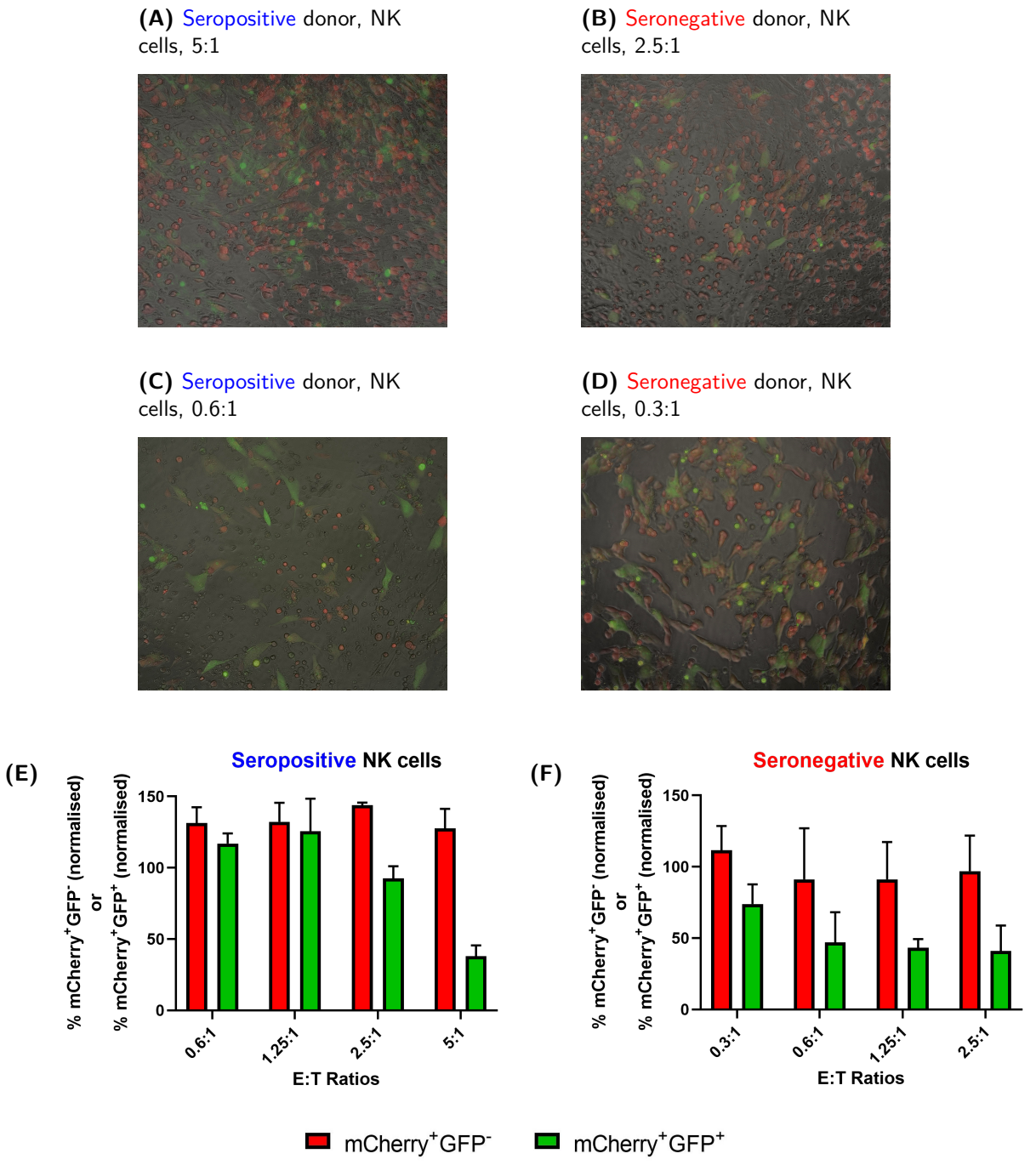

Figure 3.13: Control of viral dissemination by NK cells from a seropositive and a seronegative donor

After the addition of PBMCs and $CD4^+$ cells to the viral dissemination assay, NK cells were isolated by MACS depletion using the NK cell Isolation Kit and added to autologous HCMV-infected primary dermal fibroblasts at starting E:T ratios of 5:1 (for the HCMV-seropositive donor) and 2.5:1 (for the HCMV-seronegative donor). After a further 7 days of incubation, the cells were harvested and analysed by flow cytometry. Figs.3.13A & 3.13C show fluorescence microscopy images taken just before harvest of a representative well with NK cells from the HCMV-seropositive donor added at E:T ratios of 5:1 and 0.3:1; Figs.3.13B & 3.13D show fluorescence microscopy images taken just before harvest of a representative well with NK cells from the HCMV-seropositive donor added at E:T ratios of 2.5:1 and 0.3:1. The complete results from the flow cytometry analysis is summarised in Figs.3.13E (HCMV-seropositive donor) and 3.13F (HCMV-seronegative donor). Red bars show average amount of $mCherry^+GFP^-$ cells at each E:T ratio "normalised" to infected controls; green bars show the same for $mCherry^+GFP^+$ cells. Error bars reprsent SD of triplicate wells. Images (A–D) acquired by Dr Charlotte Houldcroft and processed by myself.

3.4 Control of *in vitro* HCMV dissemination by a cohort of healthy HCMV-seropositive and HCMV-seronegative donors

3.4.1 PBMCs

The preceding sections(3.3.3–3.3.6) show a sample of the differences in control of IE and late viral gene expression by PBMCs, $CD4^+$ cells, $CD8^+$ T cells and NK cells from a single healthy HCMV-seropositive and a single healthy HCMV-seronegative donor. However, there are wide variabilities in ability of immune cells to recognise CMV antigens, even amongst HCMV-seropositive individuals [564]. Therefore, I wanted to examine the range of abilities of the various immune cell populations to control IE and late viral gene expression in a cohort of healthy HCMV-seropositive and HCMV-seronegative donors. Characteristics of these donors (age, gender and HCMV serostatus) are given in Appendix A.

PBMCs, $CD4^+$ cells, $CD8^+$ T cells and NK cells from a cohort of 8 healthy HCMV-seropositive and 8 healthy HCMV-seronegative donors were added to the viral dissemination assay as previously described. After flow cytometry analysis, the mean of the amount of % $mCherry^+GFP^-$ and % $mCherry^+GFP^+$ cells from each triplicate of wells at the same E:T ratio from one donor is represented as one data point on the violin plots. Fig.3.14A shows the comparison of amount of $mCherry^+GFP^-$ cells between PBMCs from HCMV-seropositive and HCMV-seronegative donors. When compared to healthy seronegative donors, all PBMCs from healthy seropositive donors showed good control of IE viral gene expression at high E:T ratio of 2.5:1; as E:T ratio decreases, the PBMCs from HCMV-seropositive donors then begin to lose this control, with PBMCs from some HCMV-seropositive individuals losing control earlier than others. In comparison, PBMCs from HCMV-seronegative donors show a wide range of ability to control IE CMV gene expression at the highest E:T raio of 2.5:1. This is manifested as a much larger standard deviation of % $mCherry^+GFP^-$ cells in the violin plot of HCMV-seronegatives versus HCMV-seropositives (34.613 (seronegative) vs 7.230 (seropositive) for E:T of 2.5:1; 32.778 (seronegative) vs 19.426 (seropositive) for E:T of 1.25:1; calculations not shown). This suggests that PBMCs from some HCMV-negative individuals are able to control IE viral gene expression at high E:T ratio to a much better degree than others; whereas all the PBMCs from HCMV-seropositive individuals are able to control IE gene expression at high E:T ratios.

For $mCherry^+GFP^+$ cells (Fig.3.14B), only the E:T ratio of 2.5:1 showed a statistically significant difference between healthy seropositives and healthy seronegatives, and overall the difference in ability to control late gene expression between PBMCs from HCMV-seropositive and HCMV-seronegative donors is much smaller than the difference seen in ability to control IE viral gene expression. This suggests that even PBMCs from HCMV-seronegative donors

showed a good ability to control late gene expression, even at the lower E:T ratios of 1.25:1 or less.

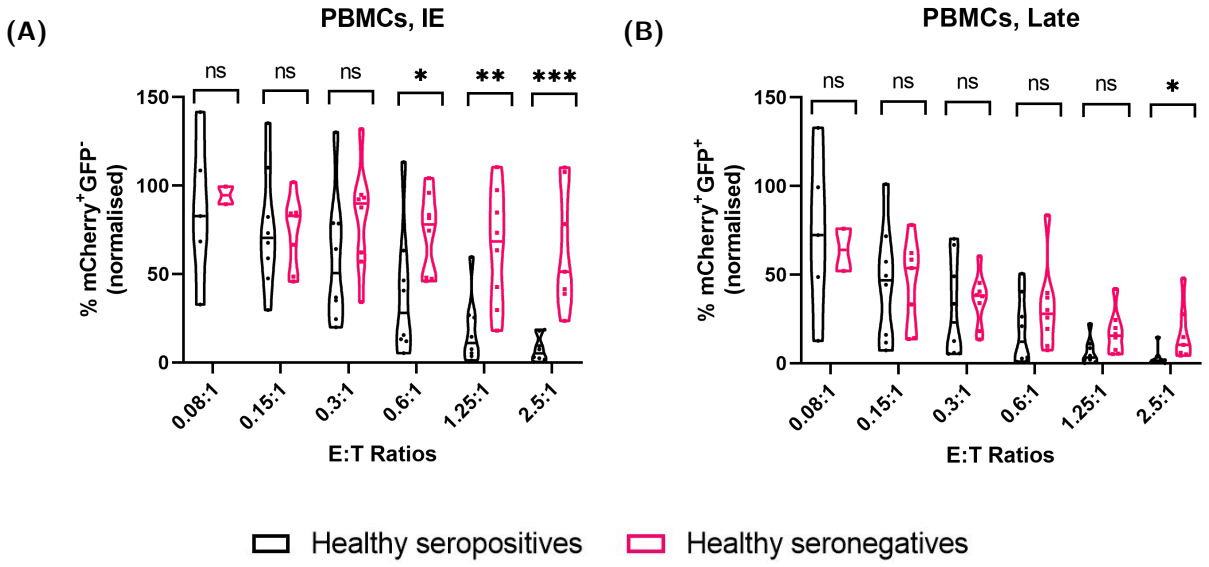

Figure 3.14: Comparison of control of viral dissemination by PBMCs from healthy HCMV-seropositive and HCMV-seronegative donors
PBMCs from 8 healthy HCMV-seropositive and 8 healthy HCMV-seronegative donors were added to autologous dermal fibroblasts infected with WT virus at 1 d.p.i. at E:T ratios of 2.5, 1.25, 0.6, 0.3, 0.15 and 0.08, and incubated for 7 to 10 days, followed by harvest and analysis by flow cytometry. Fig.3.14A shows violin plots of cells that are $mCherry^{+}GFP^{-}$, expressed as a % of $mCherry^{+}GFP^{-}$ cells in infected wells from the same donor that did not have PBMCs added (i.e. "normalised" to infected controls). Fig.3.14B shows the same for $mCherry^{+}GFP^{+}$ cells. Statistics performed using Student's *t*-test. (*$p \leq 0.05$; **$p \leq 0.01$; ***$p \leq 0.001$; ****$p \leq 0.0001$; ns = not significant)

3.4.2 $CD8^+$ T cells from healthy HCMV-seropositive donors control viral dissemination at lower E:T ratios

$CD8^+$ T cells were isolated from defrosted PBMC populations by MACS (as detailed in Section 2.12.2), and based on the number of $CD8^+$ T cells obtained, added to infected autologous fibroblasts at starting a E:T ratio of either 5, 2.5 or 1.25:1, followed by halving dilutions. As with the PBMCs, after flow cytometry analysis, the mean of the amount of % $mCherry^+GFP^-$ and % $mCherry^+GFP^+$ cells from each triplicate of wells at the same E:T ratio from one donor is represented as one data point on the violin plots in Figs.3.15A and 3.15B respectively. Fig.3.15A shows that there is much less CMV IE gene expression when $CD8^+$ T cells from HCMV-seropositive donors are added to HCMV-infected fibrobalsts as compared to when $CD8^+$ T cells from HCMV-seronegative donors are added to HCMV-infected fibroblasts. This difference is largest at E:T ratios of 1.25 and 2.5:1 and then decreases with decreasing E:T ratios, but is still statistically significant up to the fairly low E:T ratio of 0.3:1.

For $mCherry^+GFP^+$ expression, $CD8^+$ T cells from HCMV-seropositive donors also show a strong ability to limit late gene expression, but $CD8^+$ T cells from HCMV-seronegative donors do also show a moderate ability to limit this, especially at the higher E:T ratios of 1.25 – 5:1. The smaller difference in abilities between $CD8^+$ T cells from HCMV-seropositive versus HCMV-seronegative donors is seen as higher p values (i.e. lower number of *) on the Student's t-tests performed between the groups.

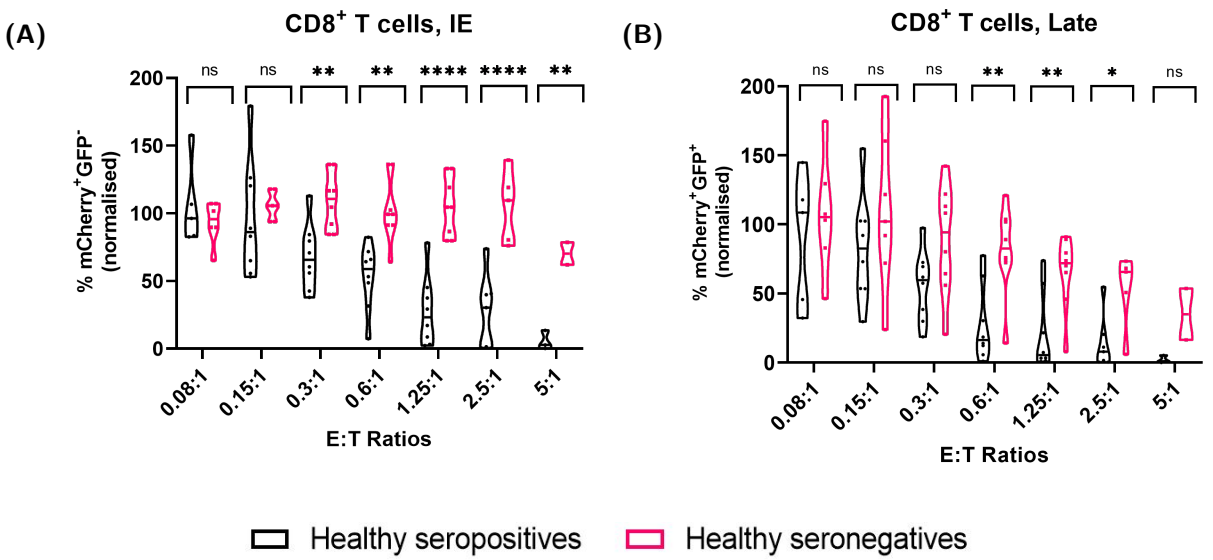

Figure 3.15: Comparison of control of viral dissemination by CD8$^+$ T cells from healthy HCMV-seropositive and HCMV-seronegative donors
CD8$^+$ T cells from 8 healthy HCMV-seropositive and 8 healthy HCMV-seronegative donors were added to autologous dermal fibroblasts infected with WT virus at 1 d.p.i. at starting E:T ratios of 5, 2.5, or 1.25:1, followed by halving dilutions, then incubated for 7 to 10 days, before harvest and analysis. Fig.3.15A shows violin plots of cells that are mCherry$^+$GFP$^-$, expressed as a % of mCherry$^+$GFP$^-$ cells in infected wells from the same donor that did not have CD8$^+$ T cells added (i.e. "normalised" to infected controls). Fig.3.15B shows the same for mCherry$^+$GFP$^+$ cells. Statistics performed using Student's *t*-test. (*$p \leq 0.05$; **$p \leq 0.01$; ***$p \leq 0.001$; ****$p \leq 0.0001$; ns = not significant)

CD8$^+$ T cells recognise antigen via MHC Class I antigen presentation pathway [222]. It would thus be expected that CD8$^+$ T cells from the donors used in this study are recognising infected cells by antigen presentation via MHC Class I complexes on the surface of infected fibroblasts. To confirm that the primary dermal fibroblasts used in this study constitutively expressed MHC Class I complexes on their cell surface, primary dermal fibroblasts from 3 different donors (2 HCMV-seropositive, 1 HCMV-seronegative) were stained for expression of HLA-A,B,C. The results in Fig.3.16 validate this.

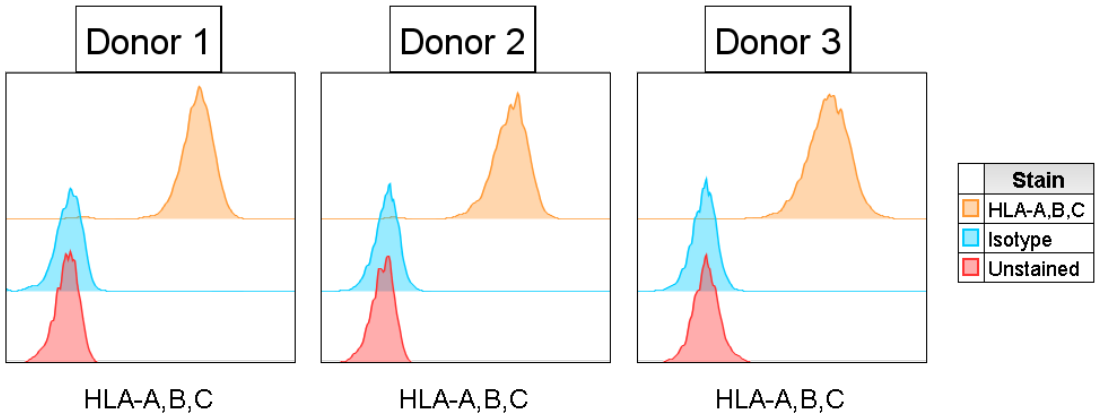

Figure 3.16: Primary dermal fibroblasts constitutively express MHC Class I complexes on their cell surface
Primary dermal fibroblasts from 3 healthy donors (2 HCMV-seropositive, 1 HCMV-seronegative) were stained for expression of HLA-A,B,C on the cell surface. Red histograms show unstained controls, blue histograms show isotype controls, and orange histograms show amount of HLA-A,B,C on the cell surface.

3.4.3 NK cells from HCMV-seropositive donors do not show better control of viral dissemination

NK cell populations were obtained from defrosted PBMCs by methods (detailed in Section 2.12.2) and added to infected autologous fibroblasts at E:T ratios of 5:1, followed by halving dilutions. Unlike PBMCs and $CD8^+$ T cells, NK cells from HCMV-seropositive donors do not appear to control $mCherry^+GFP^-$ (Fig.3.17A) or $mCherry^+GFP^+$ (Fig.3.17B) expression better than NK cells from HCMV-seronegative donors at the E:T ratios tested. NK cells from either HCMV-seropositive or HCMV-seronegative donors were poor at controlling early gene expression but better at controlling late gene expression. In addition, the data appears to show that there is a sub-population of donors whose NK cells consistently perform poorly in controlling $mCherry^+GFP^-$ and $mCherry^+GFP^+$ expression. These have been highlighted by the orange and green data points in Figs.3.17A and 3.17B, where each colour represents a particular donor. There are also some donors in either the HCMV-seropositive or HCMV-seronegative cohorts that do control $mCherry^+GFP^-$ or $mCherry^+GFP^+$ expression. These observations appear to suggest that HCMV serostatus (and, therefore, by implication, a prior exposure to HCMV antigens) appear to have no impact on the ability of NK cells to recognise and kill CMV-infected cells, although this is a small sample size and more observations are required before conclusions can be drawn.

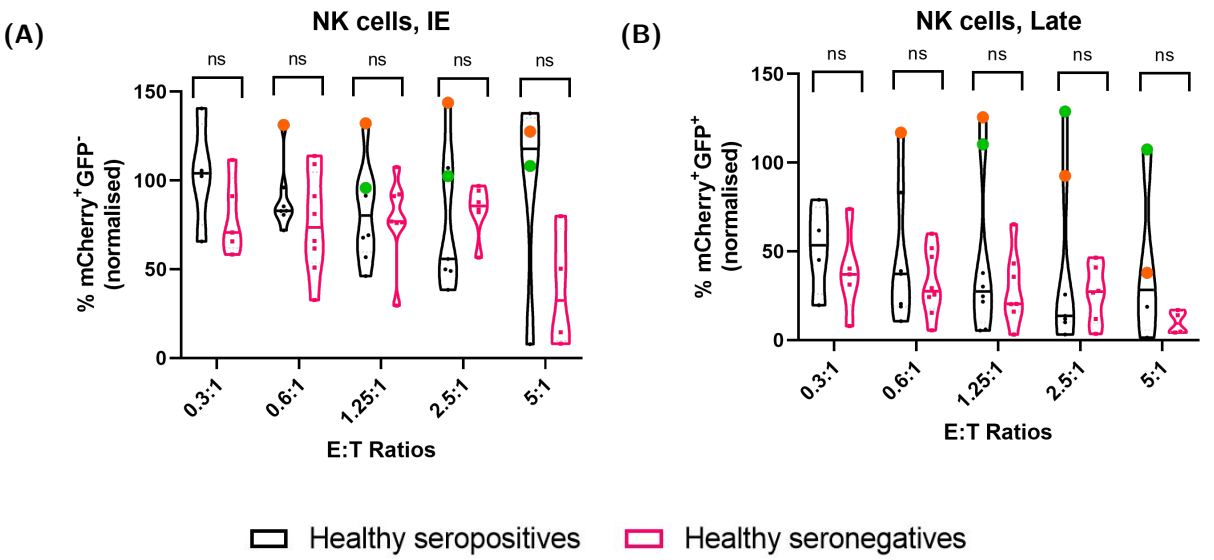

Figure 3.17: Comparison of control of viral dissemination by NK cells from healthy HCMV-seropositive and HCMV-seronegative donors

NK cells from 8 healthy HCMV-seropositive and 8 healthy HCMV-seronegative donors were added to autologous dermal fibroblasts infected with WT virus at 1 d.p.i. at starting E:T ratios of 5, 2.5, or 1.25:1, followed by halving dilutions, then incubated for 7 to 10 days, before harvest and analysis. Fig.3.17A shows violin plots of cells that are $mCherry^{+}GFP^{-}$, expressed as a % of $mCherry^{+}GFP^{-}$ cells in infected wells from the same donor that did not have NK cells added (i.e. "normalised" to infected controls). Fig.3.17B shows the same for $mCherry^{+}GFP^{+}$ cells. Statistics performed using Student's *t*-test. (*$p \leq 0.05$; **$p \leq 0.01$; ***$p \leq 0.001$; ****$p \leq 0.0001$; ns = not significant)

3.4.4 $CD4^+$ cells from healthy HCMV-seropositive donors control viral dissemination at high E:T ratios

$CD4^+$ cells from 13 healthy HCMV-seropositive and 10 healthy HCMV-seronegative donors were isolated from defrosted PBMC populations by MACS using positive selection with CD4 MicroBeads (detailed in Section 2.12.1) and added to Merlin WT-infected autologous fibroblasts at 1 dpi at E:T ratios of 5:1 followed by halving dilutions, then incubated for 7-10 days before harvest. Following flow cytometry analysis, the mean of the amount of % $mCherry^+GFP^-$ and % $mCherry^+GFP^+$ cells from each triplicate of wells at the same E:T ratio from one donor is represented as one data point on the violin plots in Figs.3.18A and 3.18B respectively.

As can be seen in Fig.3.18A, $CD4^+$ cells from healthy seropositive donors can limit $mCherry^+GFP^-$ expression to a greater extent as compared to $CD4^+$ cells from HCMV-seronegative donors, particularly at E:T ratios of 5:1 and 2.5:1. This difference then gradually dilutes out with decreasing E:T ratios, and by E:T ratio of 0.3:1, there is no apparent difference between the 2 groups. There is a similar pattern for late CMV gene expression (Fig.3.18B), although the difference is lost at a higher E:T ratio of 0.6:1.

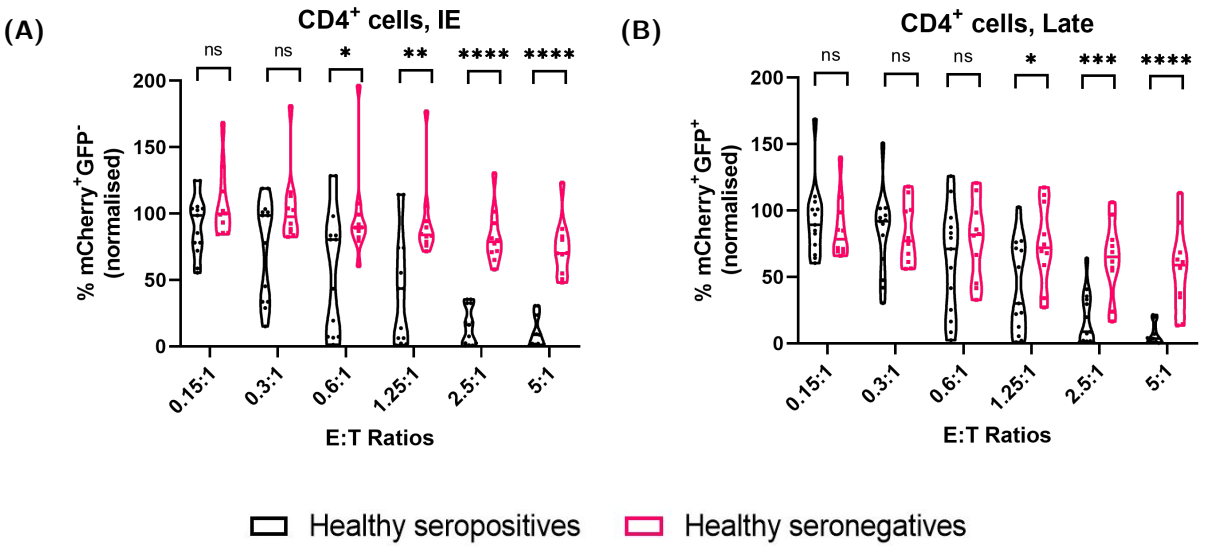

Figure 3.18: Comparison of control of viral dissemination by CD4$^+$ T cells from healthy HCMV-seropositive and HCMV-seronegative donors
CD4$^+$ T cells from 13 healthy HCMV-seropositive and 10 healthy HCMV-seronegative donors were added to autologous dermal fibroblasts infected with WT virus at 1 d.p.i. at E:T ratios of 5, 2.5, 1.25, 0.6, 0.3 and 0.15:1, and incubated for 7 to 10 days, followed by harvest and analysis by flow cytometry. Fig.3.18A shows violin plots of percentage of cells (normalised to infected control) in with IE CMV gene expression at each E:T ratio for healthy HCMV seropositive and seronegative donors, and Fig.3.18B shows percentage of cells with late CMV gene expression for the same donors. Statistics performed using Student's *t*-test. (*$p \leq 0.05$; **$p \leq 0.01$; ***$p \leq 0.001$; ****$p \leq 0.0001$; ns = not significant)

These results confirm in a much larger cohort of donors that CD4$^+$ T cells from HCMV-seropositive donors are able to control HCMV gene expression *in vitro* and that this is related to previous infection with HCMV, suggesting that antigen-specific memory CD4$^+$ T cells are responsible. It is well known that CD4$^+$ T cells recognise antigen via the MHC Class II antigen presentation pathway. However, MHC Class II is not expected to be constitutively expressed on primary dermal fibroblasts. This was confirmed by staining for HLA-DR on the surface of primary dermal fibroblasts from 3 of the donors used in this study (results in Fig.3.19). It is therefore surprising that CD4$^+$ cells added to the viral dissemination assay in isolation can recognise CMV-infected cells.

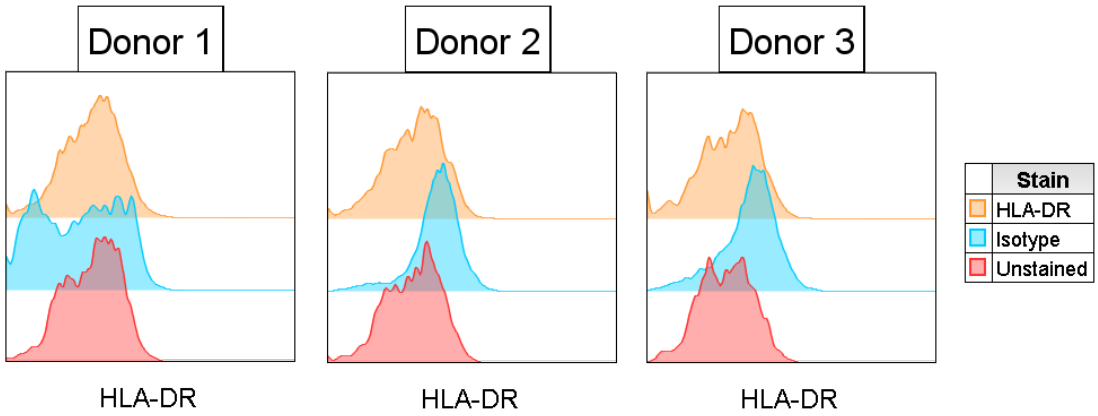

Figure 3.19: Primary dermal fibroblasts do not constitutively express MHC Class II on their cell surface
Primary dermal fibroblasts from 3 healthy donors (2 HCMV-seropositive, 1 HCMV-seronegative) were stained for expression of HLA-DR on the cell surface. Red histograms show unstained controls, blue histograms show isotype controls, and orange histograms show amount of HLA-DR on the cell surface.

3.5 Discussion

3.5.1 Viral dissemination assay as a tool to assess functional capacity of various immune cell lineages *in vitro*

As discussed in the Introduction, most studies involving $CD4^+$ T cells and HCMV in non-immunocompromised persons have focused on investigating their antigen specificity (Section 1.2.4) or phenotypes, characteristics and surface markers (Section 1.2.5), while those in immunocompromised or transplant patients have focused on looking for associations with eventual development (or not) of viraemia or CMV disease (Section 1.2.7).

One of the more commonly employed techniques to detect HCMV-specific $CD4^+$ T cells involves intra-cellular staining for cytokines such as IFN-γ, IL-2 or TNF-α, or looking for activation markers such as CD69 or CD107a (summarised in Tables 1.7 & 1.8). While these methods are able to identify HCMV-specific $CD4^+$ T cells, they do not accurately reflect if or how these $CD4^+$ T cells then exert their antiviral effect, nor does it explain the dissonance between why some of these patients with HCMV-specific $CD4^+$ T cell responses still go on to develop viraemia, but others do not.

The viral dissemination assay described in this chapter thus offers 2 advantages over conventional intra-cellular staining techniques:

1. **Use of the "double-tagged" UL36-peptide 2A-mCherry, UL32-GFP virus allows one to discriminate between cells that are in the stages of immediate-early CMV gene expression from those that have entered late CMV gene expression.** Presence of UL36 would suggest that viral entry into the cell has occurred, while the appearance of GFP suggests that viral replication has occurred, given its role in nucleocapsid stabilisation [123, 568] and in experiments where expression of UL32 antisense mRNA led to much reduced levels of virus yield [391]. The fact that there are more $mCherry^-GFP^-$ fibroblasts that become $mCherry^+$ *after* GFP expression is seen suggests that the virus is spreading to uninfected cells. As such, measuring $mCherry^+GFP^-$ cells is a marker of dissemination of the virus through the fibroblast cell culture. For example, PBMCs were shown to limit both mCherry and GFP expression. This could be interpreted as inhibiting viral dissemination and preventing late gene expression. Likewise, it can be seen that individual lymphocyte populations (most evidently, NK cells) cannot inhibit viral spread (little or no control of mCherry expression) but do inhibit GFP expression. This suggests that fibroblasts can become infected and express IE genes but that the viral life cycle is being prevented from achieving completion (seen as an accumulation of $mCherry^+GFP^-$ cells that do not subsequently become $mCherry^+GFP^+$).

2. **Adding immune cell populations directly to infected autologous fibroblasts allows for direct observation of the antiviral effects of each of these cell lines on**

infected cells, and provides a more holistic picture of the interaction of these various immune cell populations with HCMV-infected cells beyond production of cytokines or markers of activation.

In addition, by using whole PBMCs in addition to the individual immune cell populations derived from them, it allows for a dissection of the response to HCMV and how each of these cellular subsets contribute (or not) to the overall antiviral effect of the PBMCs—as will be elaborated on in the section below and in Chapter 6.

3.5.2 Differing abilities of various immune cell populations to control viral dissemination

PBMCs

Figs.3.14A–3.14B show that PBMCs from HCMV-seropositive donors are able to limit *both* IE and late CMV gene expression, whereas PBMCs from HCMV-seronegative donors are only able to limit late CMV gene expression. These findings are not entirely surprising—as discussed earlier in Section 3.3, PBMCs consist of all cells with round nuclei in the blood, and this includes cells from both the innate and adaptive arms of the immune system. HCMV infection elicits a broad immune response that involves both the innate and adaptive arms of immunity [255]. While HCMV-seropositivity would allow priming of the immune response and a more directed adaptive response, in HCMV-seronegative individuals the innate response mediated by cytokine release, monocytes and NK cells would still allow PBMCs from HCMV-seronegative individuals to recognise HCMV-infected cells and therefore exhibit some antiviral effect. The results from Fig.3.14A however, would suggest that this innate response is not able to prevent IE CMV gene expression, whereas the combination of an innate and adaptive response in HCMV-seropositive individuals appear to be able to allow PBMCs from HCMV-seropositive individuals to recognise and kill cells with IE CMV gene expression. In the large screening study of ORFs recognised by HCMV-seropositive adults [564], genes expressed in the IE phase of infection, such as IE1, IE2, and UL36, were among the ORFs that were most-frequently recognised by $CD4^+$ and $CD8^+$ T cells from HCMV-seropositive adults, whereas this was not seen in HCMV-seronegative subjects. This could explain why PBMCs from HCMV-seropositive adults, which contain effector memory $CD4^+$ and $CD8^+$ T cells, are able to recognise and kill cells expressing CMV IE genes.

$CD8^+$ T cells

$CD8^+$ T cells from HCMV-seropositive individuals are able to limit both IE and late CMV gene expression when added to HCMV-infected fibroblasts, but $CD8^+$ T cells from HCMV-seronegative individuals are unable to control either, except at the highest E:T ratio of 5:1. The results in Fig.3.16 show that primary dermal fibroblasts express MHC Class I on their

cell surface, and it would be assumed that $CD8^+$ T cells are able to recognise IE and late CMV gene-expressing cells via the MHC Class I antigen presentation pathway. In an immunocompetent HCMV-seropositive individual, up to 20% and 27% of the total $CD8^+$ T cells can be directed against the immediate-early antigen pUL122/123 and structural tegument protein pp65 (pUL83) respectively [300], so it is therefore not surprising that $CD8^+$ T cells from HCMV-seropositive individuals are able to recognise both IE and late CMV gene-expressing cells.

It is also perhaps worth nothing that HCMV possesses a number of genes that downregulate MHC Class I complexes—US3 prevents intracellular transport of MHC class I molecules to the cell surface [10, 270]; US2 and US11 dislocate newly synthesised MHC Class I molecules from the ER to the cytoplasm, where they are targeted for degradation by the proteasome [269, 270, 639]; and US6 blocks translocation of peptides to the ER via the transporter associated with antigen presentation (TAP), preventing peptide loading onto MHC Class I molecules [11, 229, 230, 335]. The combined effect of these viral immune evasion genes would be to disrupt antigen presentation via MHC Class I to $CD8^+$ T cells. US3 is expressed immediately after viral entry into the host cell, and US2 and US11 are expressed at early phase of viral replication. Yet clearly Figs.3.15A–3.15B suggest that there is a lag between infection and complete downregulation, as $CD8^+$ T cells from HCMV-seropositive individuals are still able to recognise HCMV-infected cells. This observation is also supported by *in vivo* evidence: a recent immunohistochemical analysis of tissue sections from HCMV-infected organs showed reduced MHC class I signals on infected cells, but infiltration of sites of infection by predominantly $CD8^+$ T cells [179].

A number of immunodominant HCMV targets for $CD8^+$ T cells are tegument proteins and as these are delivered to cells during viral infection they are immediately available to potentially enter the MHC Class processing pathway and be presented to T cells before immune evasion genes are able to shut down *de novo* processing and presentation of viral antigens. It is interesting to speculate that the VDA, which uses a low MOI with contiguous co-culture of immune cells that spread through the culture, might model *in vivo* conditions more accurately than many other assays that have examined immune evasion gene functions, which use high MOI and extended periods of observation post-infection.

NK cells

As mentioned briefly in Section 1.1.5.4, HCMV also encodes multiple gene products targeting normal NK cell functions, and multiple *in vitro* studies have shown that HCMV-infected fibroblasts are protected against NK cell-mediated cytotoxicity [95, 620, 623]. Again, these studies frequently used high MOI and were examined for extended periods post-infection. Yet, clinically, individuals with NK cell defects can experience severe HCMV infections [57,183,419]. This would appear to suggest that the presence of an intact and functioning NK cell population

does not guarantee protection against HCMV, but the lack of one could lead to severe HCMV infection. The data from adding NK cells to HCMV-infected fibroblasts also appear to support this (Figs.3.17A & 3.17B)—HCMV seropositivity did not appear to confer any advantage to the ability of NK cells to control IE or late CMV gene expression, and crucially, there appears to be a sub-population of donors that had NK cells that were poor controllers of both IE and late CMV gene expression in infected fibroblasts.

NK cell function is regulated by a balance of multiple activating and inhibitory factors (reviewed in [534]), such as the NKG2C activating receptor, which has been frequently reported to be over-represented in HCMV-seropositive populations [54, 362, 508, 540] and is associated with cytolysis [399]. The numbers, subtypes, receptor expression and cytolytic activity of NK cells have been shown to vary greatly even within healthy populations [81, 226, 248, 375, 437]. That there are differences between NK cells from individual donors in controlling HCMV *in vitro* that appear to be independent of their HCMV serostatus would suggest that it is possibly the variations in these different subtypes or receptor expression among individuals that dictate the ability of their NK cells to control HCMV. There is, nonetheless, the caveat that this is a small sample size, as this study was not designed primarily to examine the NK cell response to HCMV, and so more observations are needed before conclusions can be drawn.

$CD4^+$ cells

It would be expected that $CD4^+$ cells from healthy HCMV-seropositive donors would be able to control viral dissemination *in vivo* (i.e. in the presence of other cell populations, such as antigen presenting cells or $CD8^+$ T cells). This allows recognition and presentation of viral antigen via the MHC class II pathway and activation of $CD4^+$ T cells, as discussed in Section 1.2.1. When $CD4^+$ T cells are added to the viral dissemination assay in the presence of other cells that constitutively express MHC Class II on their cell surface, such as dendritic cells and monocytes, it might be expected that $CD4^+$ T cells can recognise CMV antigens via antigen presentation by these cells. This is supported by the results showing that PBMCs from HCMV-seropositive donors can control IE and late CMV gene expression (Figs.3.14A & 3.14B). However, Figs.3.18A & 3.18B show that $CD4^+$ cells from HCMV-seropositive donors can control IE and late CMV gene expression *in isolation* (i.e. without the presence of other cell populations), despite primary dermal fibroblasts not constitutively expressing MHC Class II complexes on their cell surface (as seen in Fig.3.19). This is interesting and raises a number of questions:

1. How are these $CD4^+$ T cells able to recognise HCMV-infected cells? Arguably, there may be professional MHC Class II-positive antigen-presenting cells that have come through the isolation process and remained in the population of $CD4^+$ T cells that were added to the viral dissemination assay. However, all cell populations were checked for purity post-separation, and most post-separation purities (as defined by % of $CD3^+$ cells in the

population) were >95%.

2. If professional antigen-presenting cells are present and presenting HCMV antigen to activate HCMV-specific memory $CD4^+$ T cells, how are these $CD4^+$ T cells then recognising MHC Class II-negative fibroblasts in order to exert their antiviral effector functions?

I will attempt to address these questions in the subsequent results chapters.

Immune cell populations responsible for control of CMV gene expression in HCMV-seronegative individuals

When examining the violin plots for CMV IE gene expression, PBMCs from HCMV-seronegative donors have a large distribution of ability to limit IE CMV gene expression, even at the relatively high E:T ratios of 1.25:1 and 2.5:1 (Fig.3.14A), and similarly for $CD4^+$ and $CD8^+$ T cells, both immune cell populations from HCMV-seronegative donors have lost control of IE CMV gene expression and have normalised % infection of close to 100% even at the highest E:T ratios tested of 5:1 and 2.5:1 respectively (Figs.3.18A & 3.15A). However, when looking at the corresponding violin plots for late CMV gene expression, PBMCs from HCMV-seronegative donors only show a statistically significant difference in ability to limit late CMV gene expression from PBMCs from HCMV-seropositive donors at the highest E:T ratio tested (Fig.3.14B). When ability to control CMV late gene expression is examined by each immune cell population, $CD4^+$ cells from HCMV-seronegative donors lose their ability to limit late CMV gene expression at a much higher E:T ratio than $CD8^+$ T cells from HCMV-seronegative donors (Figs.3.18B & 3.15B). This suggests 2 points: (1) PBMCs from HCMV-seronegative individuals are unable to recognise and target CMV IE gene-expressing cells, but (2) $CD8^+$ T cells from HCMV-seronegative donors are likely to be the immune cell population responsible for the ability of PBMCs from HCMV-seronegative donors to control late CMV gene expression at higher E:T ratios. Indeed, in the expansive study of HCMV ORFs which $CD4^+$ and $CD8^+$ T cells respond to [564], of the few HCMV-seronegative individuals that showed a response to HCMV ORFs, all responses came from $CD8^+$ T cells, and to only 3 different ORF mixes: US32, US29 and UL116. US32 and UL116 are both expressed late in the viral replication cycle [29, 80, 561], while US29 is inferred to be a membrane protein [576] but remains poorly characterised [74]. The authors suggestive that this likely arose from cross-reactive recognition of HCMV epitopes by memory T cells originating from non-HCMV antigenic exposures (i.e. molecular mimicry).

There have also been reports of discordant T cell and antibody responses in cohorts of healthy individuals [572,661], transplant recipients [357,596] and cancer patients [459], where IFN-γ T cell responses to CMV antigens were present in the absence CMV IgG. These suggest that using CMV serology alone may not be the most reliable indicator of prior exposure to

CMV, and may also help to explain why some HCMV-seronegative PBMCs, and in particular $CD8^+$ T cells, show a degree of ability to limit late CMV gene expression.

The above observations also helped to inform the starting E:T ratios chosen when adding the various immune cell populations to the VDA in my subsequent experiments, particularly those carried out on transplant recipients in Chapter 6—at the highest E:T ratios, even the immune cell populations from HCMV-seronegative donors were also able to exert an antiviral effect, and it would have been difficult to differentiate between the levels of control shown by the various patients.

Chapter 4

$CD4^+$ cells can exert control of cytomegalovirus dissemination via their secreted factors

4.1 Introduction

In the context of HCMV, the majority of studies on the $CD4^+$ T cell response have examined the antigen specificity of $CD4^+$ T cells (summarised in Table 1.4) or have focused on identifying surface markers and characteristics of $CD4^+$ T cells present in primary HCMV infection (summarised in Table 1.5). However, to my knowledge, few studies have explored possible mechanisms of how $CD4^+$ T cells exert control over HCMV-infected cells.

The *modus operandi* by which most T cells use to communicate with other cells to execute their functions is via soluble secreted factors such as cytokines and chemokines [245], although some $CD4^+$ T cell subsets can mediate cytotoxicity in an MHC Class II-restricted fashion [274, 417]. In particular, this has been described for many HCMV-specific $CD4^+$ T cells [274]. This milieu of secreted factors in response to HCMV-infected cells is known as the secretome [591]. In order to deconstruct how $CD4^+$ T cells could limit viral dissemination, I first addressed the following questions: does the secretome produced by $CD4^+$ T cells co-cultured with HCMV-infected cells prevent HCMV dissemination, and what cytokines are secreted by $CD4^+$ T cells in the presence of HCMV-infected cells?

To address these questions, I proceeded to examine the secretomes of $CD4^+$ cells that had been incubated with autologous dermal fibroblasts infected with wildtype and ΔUS2-11 Merlin strain of HCMV. As mentioned in Section 1.2.6, the US2-11 region of the HCMV genome encodes multiple proteins that allow the virus to modulate host immune defences and facilitate viral persistence. US6 binds to the transporter associated with antigen processing (TAP), which inhibits MHC Class I assembly [11, 229, 234, 335], and US11 dislocates MHC Class I heavy chains from the endoplasmic reticulum for proteasomal degradation in the cytosol [331, 639],

while US2 and US3 code for proteins that not only interfere with MHC Class I processing but also alter MHC Class II assembly and transport [228, 582]. Infection with recombinant HCMV where the US2-11 region has been deleted should therefore, theoretically, allow greater amounts of antigen presentation due to reduced downregulation of MHC Class II complexes on the surface of infected cells. Whether this results in a secretome that is more antiviral than that from infection with "wildtype" HCMV is another question I attempt to address in this Chapter.

4.2 Secretome of PBMCs and CD4$^+$ cells co-cultured with HCMV-infected cells inhibits viral dissemination

4.2.1 Making PBMC and CD4$^+$ cell secretomes

To examine the secretome of PBMCs and CD4$^+$ cells that had been co-cultured with HCMV-infected cells, autologous primary dermal fibroblasts were plated in 24-well plates and grown to confluency overnight. The next day, the fibroblasts were infected with Merlin WT at high MOI (MOI $= 1$). The following day, PBMCs from the autologous donor (obtained either by venepuncture or defrosting from liquid nitrogen) were added at E:T ratios of 10:1 or 20:1. If CD4$^+$ cell secretomes were required, then CD4$^+$ cells were obtained from the PBMCs by MACS positive selection using CD4 MicroBeads, post-separation purity was performed by flow cytometry, and CD4$^+$ cells were added at E:T ratios of 20:1 or 10:1. To generate a "negative control" secretome, PBMCs or CD4$^+$ cells were added to uninfected autologous fibroblasts at the same E:T ratios at the same time. The plates were then incubated for 7 days. After 7 days, media was aspirated from the wells and centrifuged to pellet any cellular debris in the media. The supernatant from the centrifuged media was then aspirated at stored at -80°C until needed. Fig.4.1 illustrates this process.

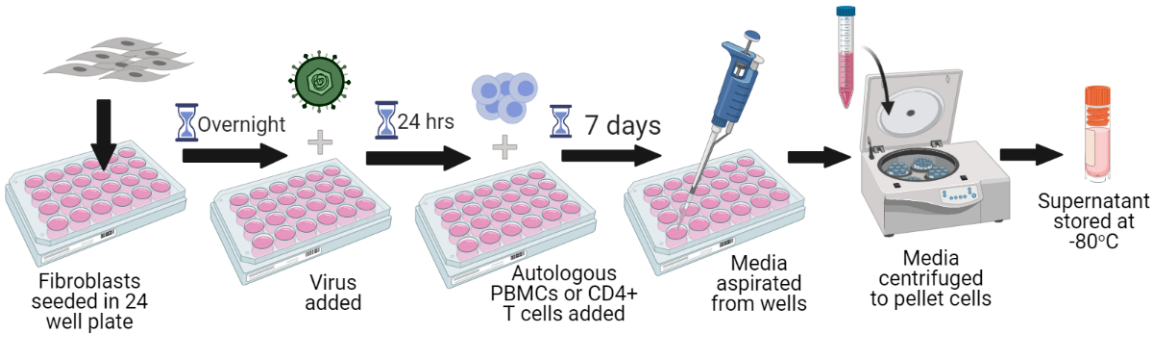

Figure 4.1: Obtaining secretomes of PBMCs and CD4$^+$ cells co-cultured with HCMV-infected autologous fibroblasts
Primary dermal fibroblasts were plated in 24-well plates and grown to confluency overnight. The next day, the fibroblasts were infected with Merlin WT at high MOI. The next day, PBMCs from the autologous donor (obtained either by venepuncture or defrosting from liquid nitrogen) were added at E:T ratios of 10:1 or 20:1. If CD4$^+$ cell secretomes were required, then CD4$^+$ cells were selected from the PBMCs by MACS positive selection using CD4 MicroBeads, post-separation purity was performed by flow cytometry, and CD4$^+$ cells were added at E:T ratios of 20:1 or 10:1. To generate a "negative control" secretome, PBMCs or CD4$^+$ cells were added to uninfected autologous fibroblasts at the same time. The plates were then incubated for 7 days. After 7 days, media was aspirated from the wells and centrifuged to pellet any cellular debris in the media. The supernatant from the centrifuged media was then aspirated at stored at $-80°$C until needed. Figure created at BioRender.com.

4.2.2 Secretomes from PBMCs and CD4$^+$ cells co-cultured with Merlin WT-infected autologous fibroblasts can restrict HCMV gene expression

The results presented in Chapter 3 showed that PBMCs and CD4$^+$ cells from HCMV-seropositive donors are able to limit viral gene expression when added to HCMV-infected fibroblasts. To investigate if this antiviral effect was mediated by their secretome, I proceeded to add these secretomes by themselves (i.e. without immune cells) to HCMV-infected fibroblasts. Secretomes of PBMCs or CD4$^+$ cells co-cultured with Merlin WT-infected fibroblasts ("PBMC + WT" or "CD4 + WT"), or PBMCs co-cultured with uninfected fibroblasts ("PBMC + uninf"), were added to Merlin-WT infected fibroblasts (MOI = 0.03) at 1 dpi at serial two-fold dilutions starting at 1:4 and incubated for 7 days before harvest and analysis by flow cytometry. The experiment timeline is shown in Fig.4.2A. Fig.4.2B shows the amount of mCherry$^+$GFP$^-$ cells, expressed as a % of cells that were mCherry$^+$GFP$^-$ in wells with no secretome added (i.e. "normalised" to infected controls). Fig.4.2C shows the same for mCherry$^+$GFP$^+$ cells.

The results in Fig.4.2 showed that the secretomes of PBMCs and CD4$^+$ cells co-cultured with Merlin WT-infected fibroblasts were able to limit both IE and late viral gene expression. This effect was dose-dependent, with eventual complete loss of the antiviral effect at approximately 1:32 dilution. In contrast, the secretomes of PBMCs co-cultured with uninfected fibroblasts showed no antiviral effect, even at the lowest dilution ratio of 1:4.

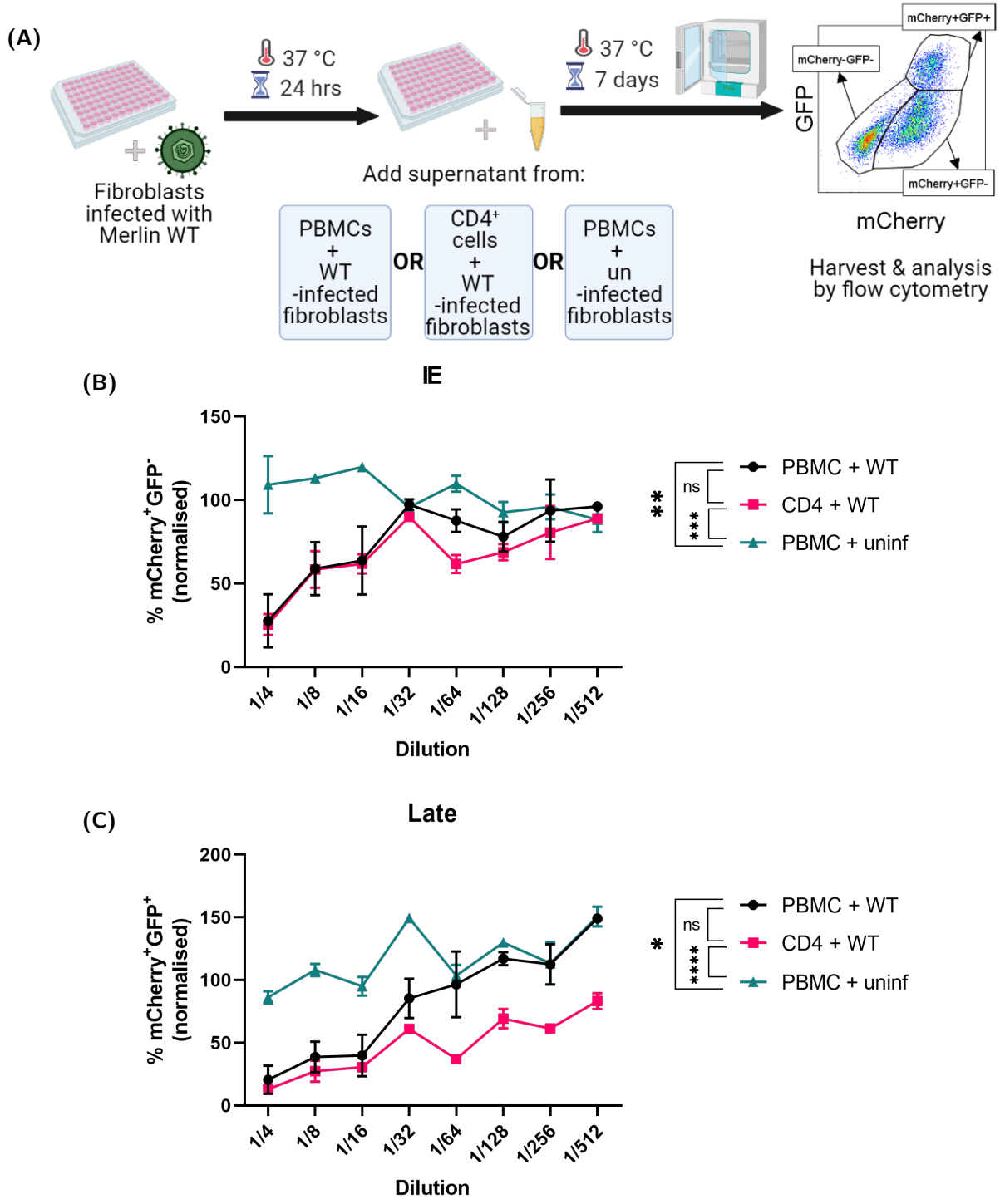

Figure 4.2: Secretome of PBMCs and CD4$^+$ cells co-cultured with HCMV-infected cells inhibits viral dissemination

Secretomes of PBMCs or CD4$^+$ cells co-cultured with Merlin WT-infected fibroblasts ("PBMC + WT" or "CD4 + WT"), or PBMCs co-cultured with uninfected fibroblasts ("PBMC + uninf"), were added to Merlin-WT infected fibroblasts (MOI = 0.03) at 1 dpi at a starting dilution of 1:4 followed by halving dilutions followed by incubation for 7 days before harvest and analysis by flow cytometry. Experiment timeline is shown in Fig.4.2A. Fig.4.2B shows amount of mCherry$^+$GFP$^-$ cells, expressed as a % of amount of mCherry$^+$GFP$^-$ cells in wells with no secretome added (i.e. "normalised" to infected controls). Fig.4.2C shows the same for mCherry$^+$GFP$^+$ cells. Mean ± SD of triplicate wells is shown. Statistics performed using Student's *t*-test. (*$p \leq 0.05$; **$p \leq 0.01$; ****$p \leq 0.0001$; ns = not significant) Fig.4.2A created at BioRender.com.

4.3 Characterisation of the Merlin $\triangle$US2-11 virus

As mentioned in the introduction to this chapter, the US2-11 region of the HCMV genome contains genes that interfere with antigen processing and presentation to T cells by encoding for multiple proteins that downregulate MHC Class I and II complexes on the cell surface. Using an HCMV strain with deletions of the US2-11 region would allow me to examine the effect of the absence of these viral genes on the ability of various immune cell populations to limit viral dissemination. To do this, I first needed to show that the ΔUS2-11 virus used in my experiments contains deletions of the relevant genes, and that it shows growth characteristics similar to that of Merlin WT virus. The virus used in these following sections is the HCMV clinical isolate Merlin, also tagged with UL36-peptide 2A-mCherry and UL32-GFP, but with deletion of US2-11 regions of the genome, and is henceforth referred to as "Merlin ΔUS2-11" or "ΔUS2-11" virus. $CD4^+$ cells were then added to Merlin WT- and Merlin ΔUS2-11-infected autologous fibroblasts to generate the relevant secretomes. I then examined the effects of these secretomes on viral dissemination, and then proceeded to investigate the effects they had on target cells and the cytokines they contained.

4.3.1 PCR analysis of US2-11 deletion

To confirm that the ΔUS2-11 virus has deletions of the genes of interest (US2-11), HFFFs were infected with either Merlin WT or Merlin ΔUS2-11 virus, or left uninfected. At 6 dpi, after expression of mCherry and GFP was seen on fluorescence microscopy, the cells were trypsinised and cellular and viral DNA extracted, followed by amplification with polymerase chain reaction (PCR) and gel electrophoresis for presence (or absence) of genes of interest (Details of methods given in Section 2.14). Fig.4.3 shows that, in samples from Merlin WT-infected cells, a band can be seen for US2, US3, US6 and US11 as expected, whereas in the Merlin ΔUS2-11-infected cells, these bands are absent. IE1 is present in samples from Merlin WT- and Merlin ΔUS2-11-infected fibroblasts, but absent in the sample from uninfected fibroblasts.

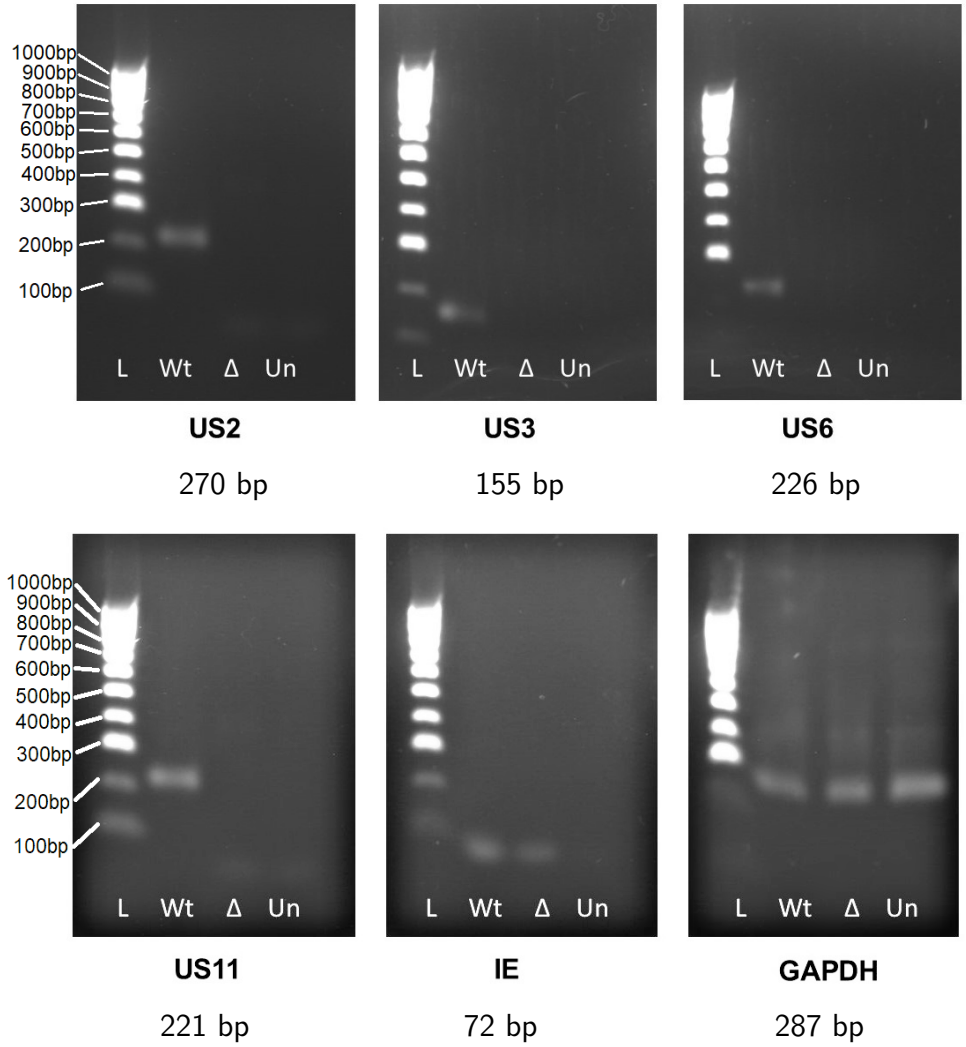

Figure 4.3: PCR for US2,3,6,11 DNA of Merlin wildtype and ΔUS2-11 virus
HFFFs were infected with wildtype or ΔUS2-11 virus or left uninfected. After 6 days, cells were harvested, DNA was extracted and PCR followed by gel electrophoresis was performed. L = DNA ladder (100-1000bp), Wt = Merlin wildtype virus, Δ = Merlin ΔUS2-11 virus, Un = uninfected HFFFs. Expected sizes of PCR products is given below gene name.

4.3.2 Growth curves of Merlin wildtype and ΔUS2-11 virus are similar

After confirmation by PCR of deletion of viral genes in the region of interest, I compared the *in vitro* growth characteristics of both viruses to ensure that deletion of US2-11 did not cause a growth defect. Merlin WT or ΔUS2-11 virus was added to primary dermal fibroblasts that had been plated and grown to confluency overnight (Merlin WT MOI = 0.03, Merlin ΔUS2-11 MOI = 0.045), and then harvested at 2, 5 and 10 days post-infection and analysed by flow cytometry for amount of $mCherry^{+}GFP^{-}$ and $mCherry^{+}GFP^{+}$ expression. Fig.4.4A shows the amount of $mCherry^{+}GFP^{-}$ cells and Fig.4.4B shows the amount of $mCherry^{+}GFP^{+}$ cells, expressed as a percentage of total number of cells in the well. Fig.4.4C shows total amount of infected cells, obtained by adding the percentages of $mCherry^{+}GFP^{-}$ and $mCherry^{+}GFP^{+}$ cells. The growth curves of the Merlin WT and ΔUS2-11 viruses can be seen to overlap for amounts of $mCherry^{+}GFP^{-}$ and $mCherry^{+}GFP^{+}$ cells, and *t*-tests performed on each of these groups did not show any statistically significant difference.

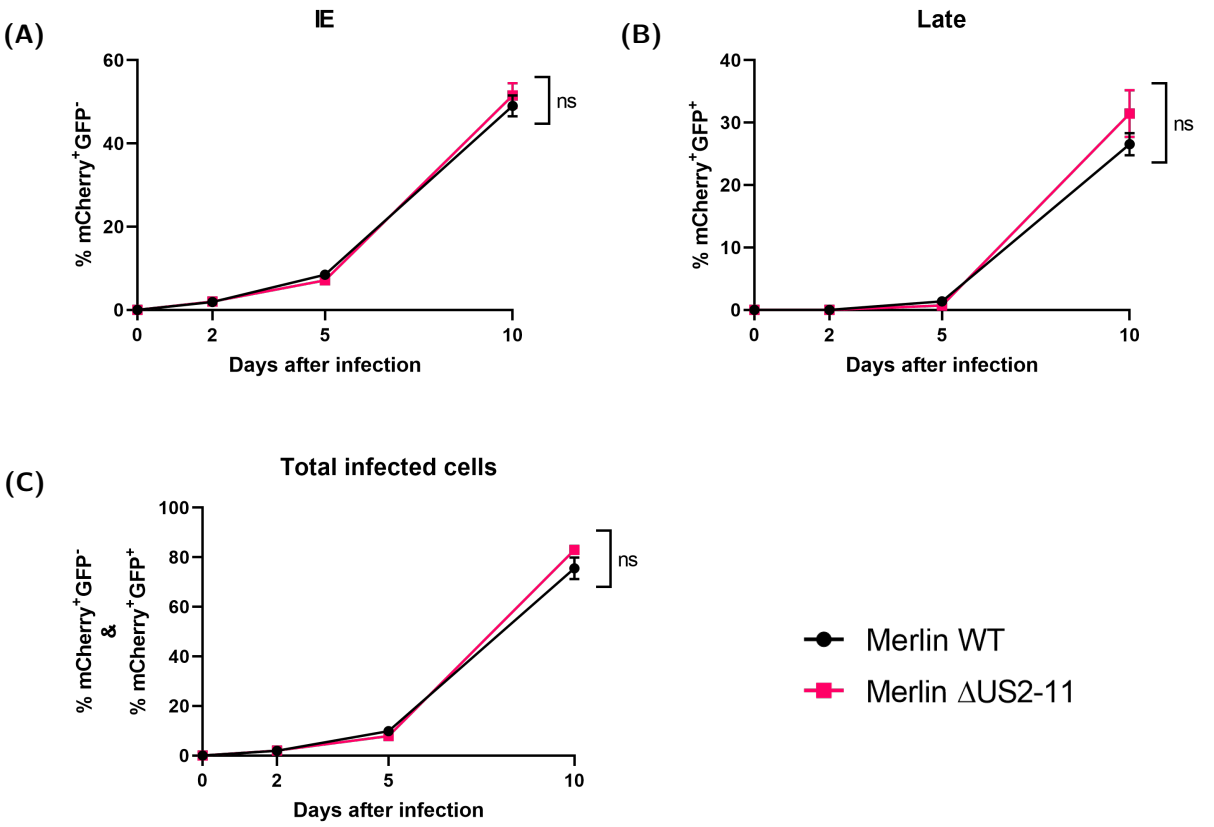

Figure 4.4: Growth curves of Merlin wildtype vs ΔUS2-11 virus
Merlin WT or ΔUS2-11 virus was added to primary dermal fibroblasts that had been plated and grown to confluency overnight, and then harvested at 2, 5 and 10 days post-infection and analysed by flow cytometry. Fig.4.4A shows the amount of mCherry^{+}GFP^{-} cells and Fig.4.4B shows the amount of mCherry^{+}GFP^{+} cells, expressed as a percentage of total number of cells in the well. Fig.4.4C shows total amount of infected cells, obtained by adding the percentages of mCherry^{+}GFP^{-} and mCherry^{+}GFP^{+} cells. Error bars represent SD of triplicate wells, statistics performed using Student's *t*-test. (ns = not significant)

4.4 Deletion of US2-11 results in a secretome that is more antiviral than secretomes from CD4$^+$ cells co-cultured with Merlin WT-infected autologous fibroblasts

Having shown that the secretomes from PBMCs and CD4$^+$ cells co-cultured with Merlin WT-infected autologous fibroblasts were able to limit IE and late viral gene expression, I proceeded to investigate if secretomes from CD4$^+$ cells co-cultured with Merlin ΔUS2-11-infected fibroblasts would produce a similarly, if not more, antiviral secretome. Secretomes of CD4$^+$ cells co-cultured with Merlin WT-infected ("CD4 + WT"), Merlin ΔUS2-11-infected ("CD4 + ΔUS2-11") and uninfected autologous fibroblasts ("CD4 + uninfected") were generated in the same manner as illustrated in Fig.4.1. CD4$^+$ cells were once again obtained from PBMCs by MACS positive selection using CD4 MicroBeads.

Primary dermal fibroblasts from an HCMV-seropositive donor were seeded in 96-well half-area plates overnight, then infected with Merlin WT virus (MOI of 0.087). At 1 dpi, the secretomes were added to the Merlin WT-infected fibroblasts at serial two-fold dilutions starting at 1:5 and incubated for 7 days before harvest and analysis by flow cytometry. This experiment timeline is illustrated in Fig.4.5A. The results of this experiment are shown in Figs.4.5B (mCherry$^+$GFP$^-$ expression) and 4.5C (mCherry$^+$GFP$^+$ expression).

These results show a consistent pattern: secretomes from CD4$^+$ cells co-cultured with uninfected autologous fibroblasts show no control of mCherry$^+$GFP$^-$ expression, and nearly no control of mCherry$^+$GFP$^+$ expression. Secretomes from CD4$^+$ cells co-cultured with Merlin WT virus show an approximate 50% decrease in expression of IE and late viral gene expression as compared to those incubated with secretomes from CD4$^+$ cells co-cultured with uninfected fibroblasts. Secretomes from CD4$^+$ cells co-cultured with Merlin ΔUS2-11 virus show an even greater ability to limit IE and late viral gene expression as compared to secretomes from CD4$^+$ cells co-cultured with Merlin WT virus, a difference that is more pronounced (as seen by greater statistical significance) at dilutions of 1:10 and 1:20. This initial result supports the hypothesis mentioned in the introduction to this section—that absence of immune evasion gene US2-11 appears to generate a more antiviral secretome, possibly as a result of decreased downregulation of MHC Class II complexes on the cell surface and therefore increased antigen presentation to lymphocytes.

This experiment was repeated with secretomes from the same donor (Figs.4.5D & 4.5E), and with "CD4 + WT" and "CD4 + uninfected" secretomes from another HCMV-seropositive donor, at serial four-fold dilutions starting at 1:4 (Figs.4.5F & 4.5G). The results were consistent with the initial observations: "CD4 + uninfected" secretomes show poor control of IE and late CMV gene expression, even at the lowest dilution of 1:4 or 1:5; there is a decrease of

at least 50% or more of viral gene expression with the "CD4 + WT" secretomes; and "CD4 + ΔUS2-11" secretomes show marginally more inhibition than "CD4 + WT" secretomes.

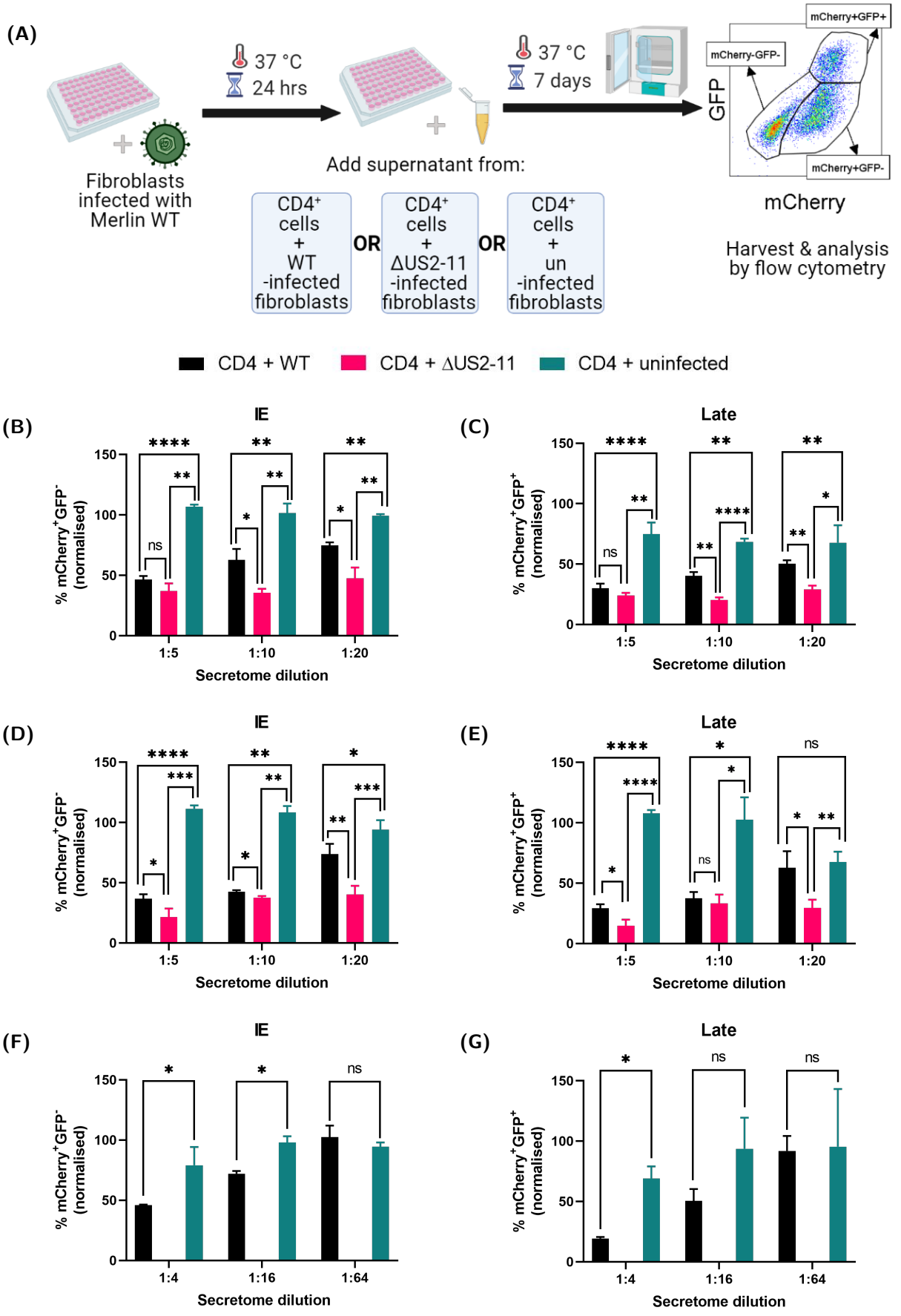
(A)
37 °C
24 hrs
37 °C
7 days
Fibroblasts infected with Merlin WT
Add supernatant from:
CD4+ cells + WT -infected fibroblasts
OR
CD4+ cells + ΔUS2-11 -infected fibroblasts
OR
CD4+ cells + un -infected fibroblasts
mCherry+GFP+
mCherry-GFP-
mCherry+GFP-
GFP
mCherry
Harvest & analysis by flow cytometry
CD4 + WT
CD4 + ΔUS2-11
CD4 + uninfected
(B)
IE
(C)
Late
(D)
IE
(E)
Late
(F)
IE
(G)
Late
% mCherry+GFP- (normalised)
% mCherry+GFP+ (normalised)
Secretome dilution
1:5
1:10
1:20
1:4
1:16
1:64
ns

Figure 4.5: Secretomes from CD4$^+$ cells co-cultured with HCMV-infected autologous fibroblasts limit viral dissemination in an *in vitro* viral dissemination assay
Secretomes from CD4$^+$ cells co-cultured with WT virus-infected (black bars), ΔUS2-11 virus-infected (pink bars) or uninfected autologous fibroblasts (green bars) were added to primary dermal fibroblasts infected with Merlin WT at 1 dpi, and incubated for a further 7 days before analysis with flow cytometry. Fig.4.5A shows experiment timeline. Fig.4.5B shows amount of mCherry$^+$GFP$^-$ cells, expressed as a percentage of the amount of mCherry$^+$GFP$^-$ cells in infected controls (i.e. no secretome added), for each of these 3 different secretomes at dilutions of 1:5, 1:10 and 1:20; Fig.4.5C shows the same for mCherry$^+$GFP$^+$ cells. Figs.4.5D–4.5E show a replicate experiment with secretomes from the same donor, and Figs.4.5F–4.5G show replicate experiment with secretomes from another donor (without "CD4 + ΔUS2-11" secretome). Error bars represent SD of triplicate wells, statistics performed using Student's *t*-test. (*$p \leq 0.05$; **$p \leq 0.01$; ***$p \leq 0.001$; ****$p \leq 0.0001$; ns = not significant) Fig.4.5A created at BioRender.com.

4.5 Cytokine array analysis of the CD4$^+$ cell secretome following co-culture with HCMV-infected fibroblasts

Having shown that the secretome from CD4$^+$ cells incubated with infected cells is antiviral, I then proceeded to identify the cytokines present in the secretomes that could be responsible for this effect. The Proteome Profiler^{TM} Human XL Cytokine Array Kit (R&D Systems) is a multi-analyte cytokine array which contains nitrocellulose membranes impregnated with antibodies to 105 different cytokines. These membranes are incubated overnight with samples of interest before washing and addition of biotinylated detection antibodies, followed by Streptavidin-HRP and chemiluminescent detection reagents. The chemiluminescent signal from each analyte is then measured by imaging onto X-ray film. Multiple exposures are taken of the X-ray films to capture the wide range of signals, and an appropriate exposure time for each analyte is chosen (i.e. an exposure time where the signal from that analyte is seen on all 4 membranes). Analysis using ImageJ software is performed to measure the intensity of signal from each analyte at the chosen exposure time, with correction for background luminescence. The list of cytokines that were analysed is listed in Table 4.1. An example of the X-ray film images of the membranes is given in Fig.4.6A (2 min exposure) & 4.6C (10 min exposure), and the transparency overlay used to identify the position of each analyte in Fig.4.6B. (Details of the methods are given in Section 2.16.) Due to some cytokines having chemiluminescent signals less than that of the background on some of the membranes, these signals were left out and only 94 cytokines were analysed.

Table 4.1: List of cytokines tested in array

Adiponectin	Angiogenin	Angiopoietin-1	Angiopoietin-2
Apolipoprotein A-I	BAFF	BDNF	C5/C5a
CCL17	CCL2	CCL7	CD105
CD14	CD147	CD31	CD40 ligand
CD71	Chitinase 3-like 1	Complement Factor D	C-Reactive Protein
Cripto-1	CSF1	CXCL1	CXCL10
CXCL11	CXCL12	CXCL4	CXCL5
Cystatin C	Dipeptidyl-peptidase IV	Dkk-1	FGF Basic
FGF-19	Flt-3 Ligand	G-CSF	GDF-15
GM-CSF	Growth Hormone	HGF	ICAM-1
IFN-γ	IGFBP-3	IL-1 R4	IL-10
IL-11	IL-12 p70	IL-16	IL-17A
IL-18 Bpa	IL-1ra	IL-2	IL-22
IL-23	IL-24	IL-27	IL-3
IL-31	IL-34	IL-4	IL-5
IL-6	IL-8	Kallikrein 3	Leptin
LIF	Lipocalin-2	MIF	MIG
MIP-1α/MIP-1β	MIP-3α	MIP-3β	MMP-9
Myeloperoxidase	Osteopontin	PDGF-AA	PDGF-AB/BB
Pentraxin 3	RAGE	RANTES	RBP-4
Relaxin-2	Resistin	Serpin E1	SHBG
TFF3	TGF-α	Thrombospondin-1	TIM-3
TNF-α	uPAR	VCAM-1	VEGF
Vitamin D BP			

BAFF = B-cell activating factor, BDNF = brain-derived neurotrophic factor, C5/C5a = Complement5/5a, Dkk-1 = Dickkopf-related protein 1, FGF = fibroblast growth factor, GDF = growth differentiation factor, HGF = hepatocyte growth factor, ICAM = intercellular adhesion molecule, IGFBP = insulin-like growth-factor-binding protein, LIF = leukaemia inhibitory factor, MIF = macrophage migration inhibitory factor, MIG = monokine induced by IFN-γ, MIP = macrophage inflammatory protein, MMP = matrix metalloproteinase, PDGF = platelet-derived growth factor, RAGE = Receptor for Advanced Glycation Endproducts, RANTES = Regulated upon Activation, Normal T cell Expressed and Presumably Secreted, RBP = retinol-binding protein, SHBP = steroid hormone binding protein, TFF = trefoil factor family, TIM = T-cell Immunoglobulin domain and Mucin domain, uPAR = urokinase plasminogen activator surface receptor, VCAM = vascular cell adhesion molecule, VEGF = vascular endothelial growth factor

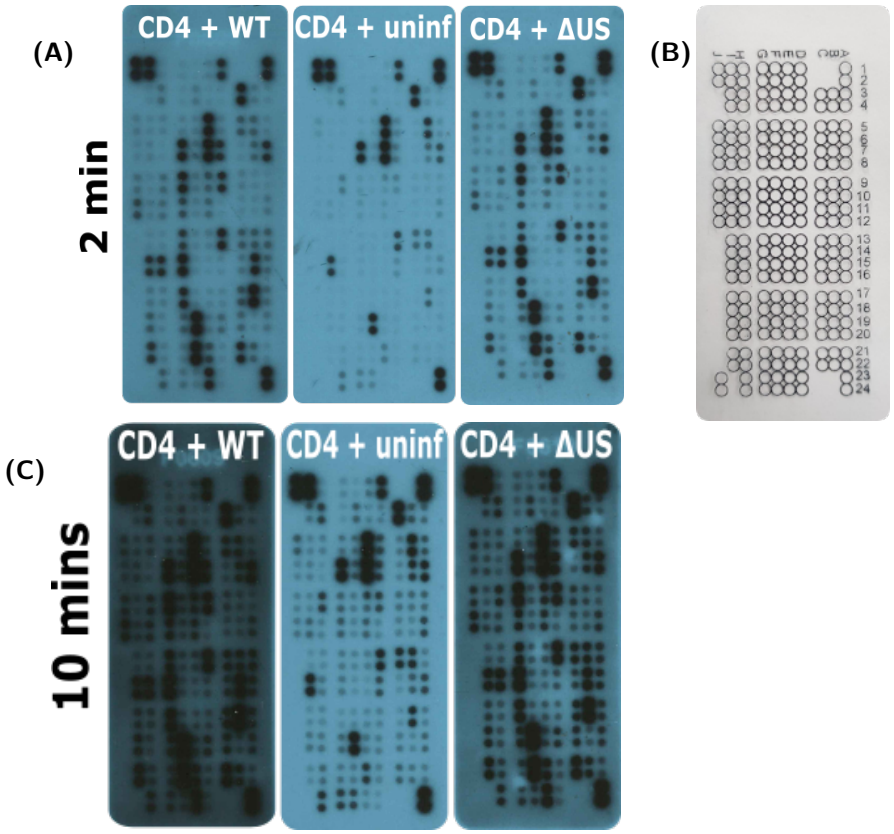

Figure 4.6: Membranes from cytokine array
Fig.4.6A: Sample of X-ray film images at 2 minutes exposure time of membranes with antibodies to 105 different analytes impregnated within which were incubated with secretomes. From left to right, membrane which was incubated with secretome from $CD4^+$ cells co-cultured with Merlin WT-infected fibroblasts ("CD4 + WT"); $CD4^+$ cells co-cultured with uninfected fibroblasts ("CD4 + uninf"); and $CD4^+$ cells co-cultured with Merlin ΔUS2-11-infected fibroblasts ("CD4 + ΔUS2-11"). Fig.4.6C shows the same for an exposure time of 10 minutes. Fig.4.6B shows the overlay used to identify the positions of each of the 105 cytokines in the membranes.

4.5.1 Relative quantification of cytokines present in secretome of $CD4^+$ cells co-cultured with HCMV-infected fibroblasts

This assay does not provide absolute quantities of the cytokines present in the secretomes, but it is able to compare the relative amounts of cytokines between the different secretomes. This is done by calculating the mean luminescent signal from the duplicate readings of each analyte at the chosen exposure time, subtracting background luminescent signal, and comparing with the mean amount of luminescent signal from the duplicate readings of the same analyte from a different membrane. The difference between the two is then plotted as $\log_2(\text{fold change})$ on the x-axis. (So, any value >0 corresponds to an increase in the amount of cytokine, while a value <0 corresponds to a decrease in the amount of cytokine.) Student's *t*-test was performed on the duplicate readings from each sample and the *p* values of the comparison is plotted on the y-axis. 3 comparisons were made: secretome from $CD4^+$ cells co-cultured with Merlin WT-infected fibroblasts ("CD4 + WT") compared with secretome

from CD4$^+$ cells co-cultured with uninfected fibroblasts ("CD4 + uninf", results in Fig.4.7A); secretome from CD4$^+$ cells co-cultured with Merlin ΔUS2-11-infected fibroblasts ("CD4 + ΔUS2-11") compared with "CD4 uninf" secretome (Fig.4.7B); and "CD4 + ΔUS2-11" secretome compared with "CD4 + WT" secretome (Fig.4.7C), to see which cytokines were upregulated in the "CD4 + ΔUS2-11" secretome in relation to the "CD4 + WT" secretome.

Fig.4.7A shows the comparison of secretome from CD4$^+$ cells co-cultured with Merlin WT-infected fibroblasts with that from co-cultures with uninfected fibroblasts ("CD4 WT vs CD4 uninf"). The cytokines that were most significantly upregulated included chemokines induced by IFN-γ, such as CXCL11 (also known as interferon-γ-inducible protein 9) and CXCL9 (monokine induced by IFN-γ), while other highly upregulated cytokines included Complement 5/5a, colony stimulating factors (G-CSF, GM-CSF, IL-3, CSF1), and members of the CC chemokine family (CCL3/CCL4, CCL5, CCL7, CCL20). IFN-γ and TNF-α are also upregulated in the "CD4 + WT" secretome, although not as highly as these other cytokines. Other cytokines that were highly upregulated include colony stimulating factors (granulocyte and granulocyte-macrophage colony stimulating factors, G-CSF and GM-CSF; IL-3, also known as colony stimulating factor) and cytokines involved with macrophage regulation, such as macrophage migration inhibitory factor (MIF), an important regulator of innate immunity [79], and macrophage inflammatory protein (MIP-3β), which is produced by dendritic cells [651].

A similar trend of the types of cytokines upregulated is seen when comparing the secretome from CD4$^+$ cells co-cultured with ΔUS2-11 Merlin HCMV-infected fibroblasts with secretome from CD4$^+$ cells co-cultured with uninfected fibroblasts (Fig.4.7B). TNF-α and IFN-γ are both upregulated, as well as the various colony-stimulating factors, CC chemokines (CCL5, CCL7, CCL20), CXC chemokines (CXCL11).

Comparing the secretomes from CD4$^+$ cells co-cultured with Merlin ΔUS2-11-infected fibroblasts with those co-cultured with Merlin WT-infected fibroblasts directly (Fig.4.7C), most cytokines were expressed in similar amounts (values around 0 on the x-axis). The cytokines that showed the most significant decrease in the "CD4 + ΔUS2-11" compared to the "CD4 + WT" secretome include IL-5, IL-19 and CSF1 ($\log_2(\text{fold change})$ values of 1.5 – 3.5, with p values $<$0.01), while the most significant increases in amounts are seen with CXC chemokines (CXCL1, CXCL9/MIG, CXCL10), protease inhibitor Serpin E1, angiogenin and IL-8 ($\log_2(\text{fold change})$ values of -1.5 to -4, p values $<$0.01).

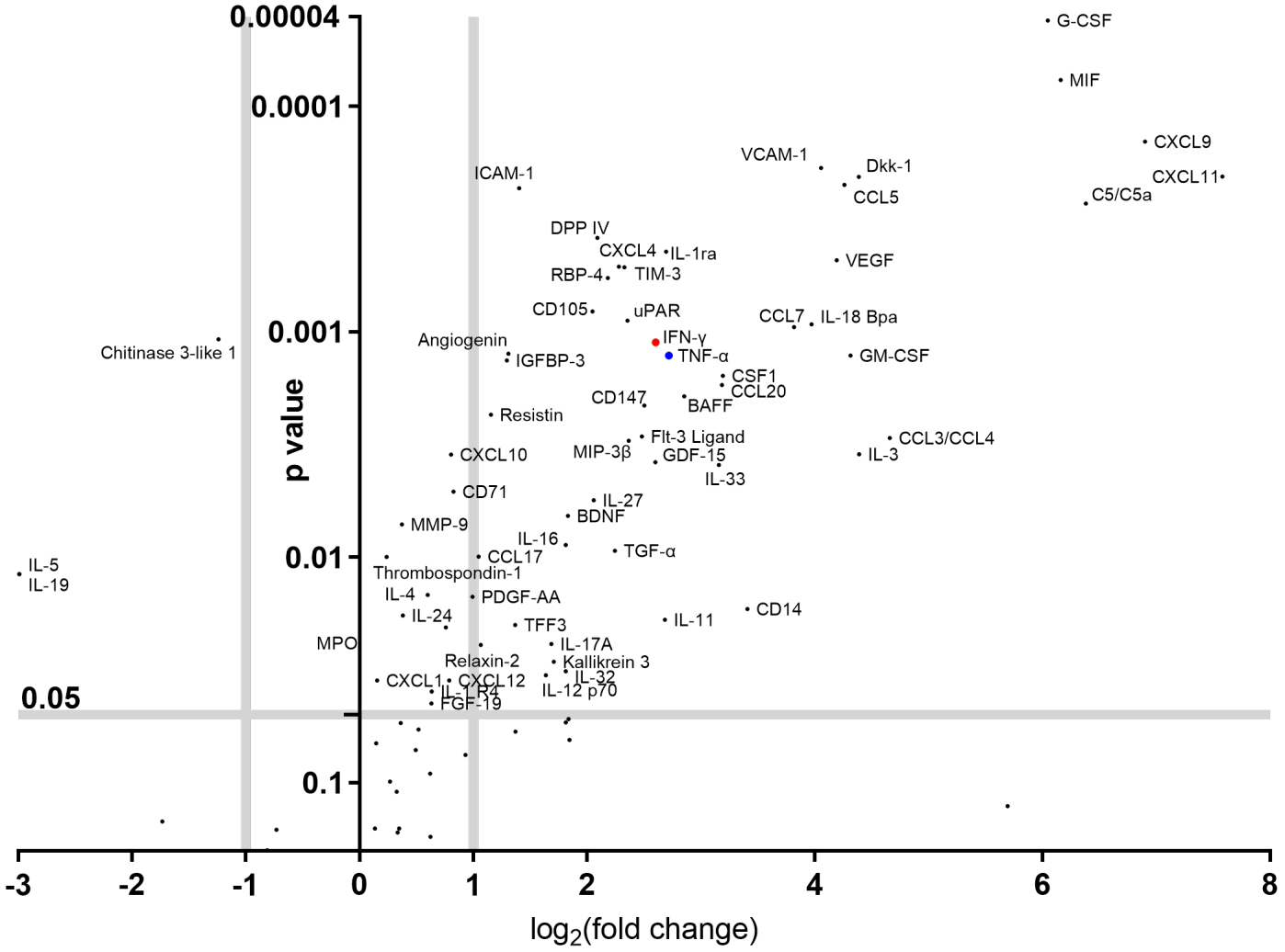

(A) "CD4 + WT" vs "CD4 + uninf" secretomes

Figure 4.7: Quantification of relative levels of cytokines in CD4$^+$ cell secretomes
Supernatants from CD4$^+$ cells co-cultured with wildtype Merlin HCMV-infected ("CD4 + WT"), ΔUS2-11 Merlin HCMV-infected ("CD4 + ΔUS2-11") or uninfected autologous fibroblasts ("CD4 + uninf") were assayed with a multi-cytokine array as described in Section 2.17. Fig.4.7A shows volcano plots of relative values of cytokines between "CD4 + WT" and "CD4 + uninf" secretome, Fig.4.7B shows comparison of "CD4 + WT" and "CD4 + uninf" secretome, and Fig.4.7C shows comparison of "CD4 + ΔUS2-11" and "CD4 + WT" secretome. Statistics performed using Student's *t*-test on duplicate readings from each cytokine.

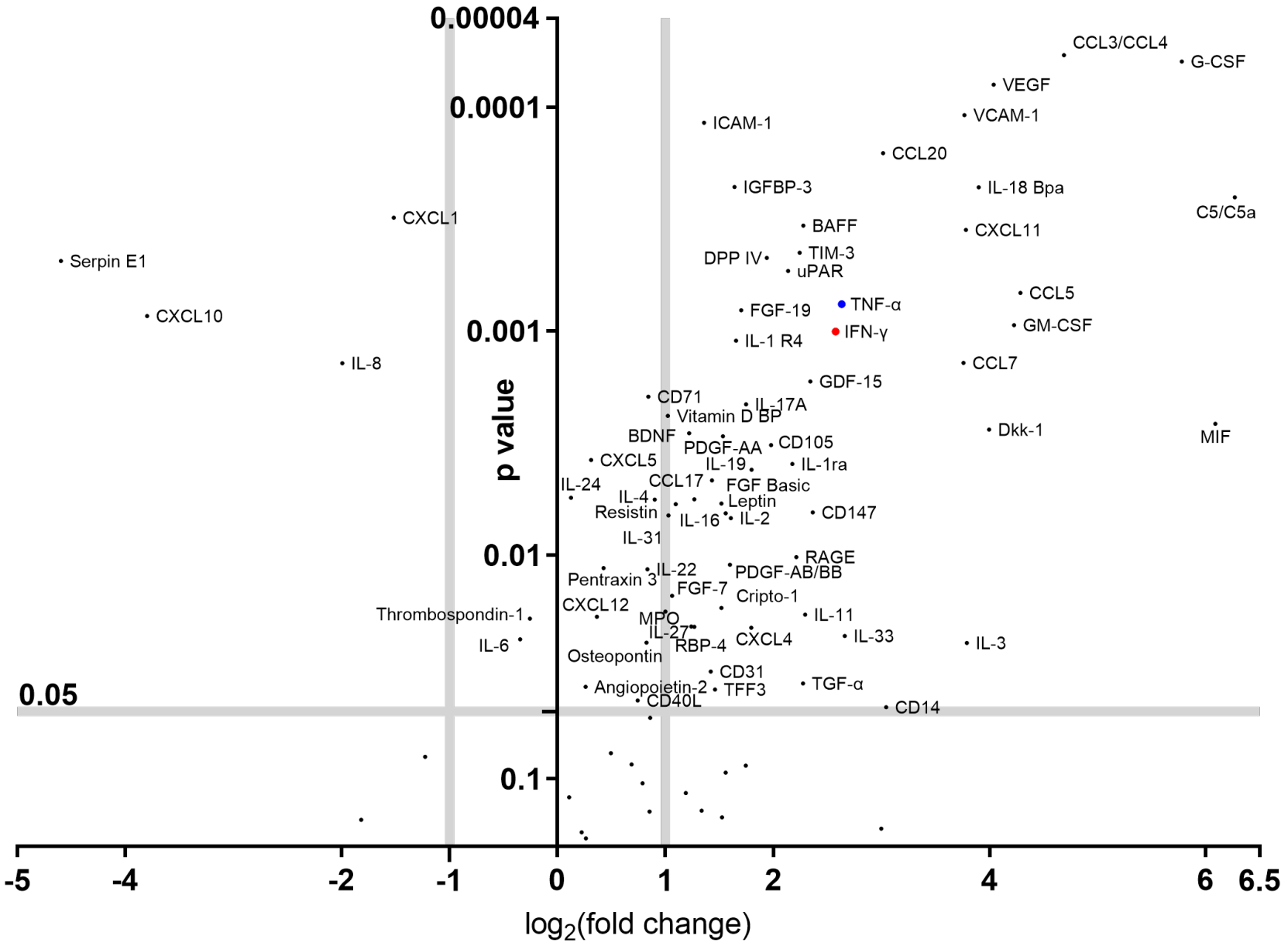

(B) "CD4 + ΔUS2-11" vs "CD4 + uninf" secretomes

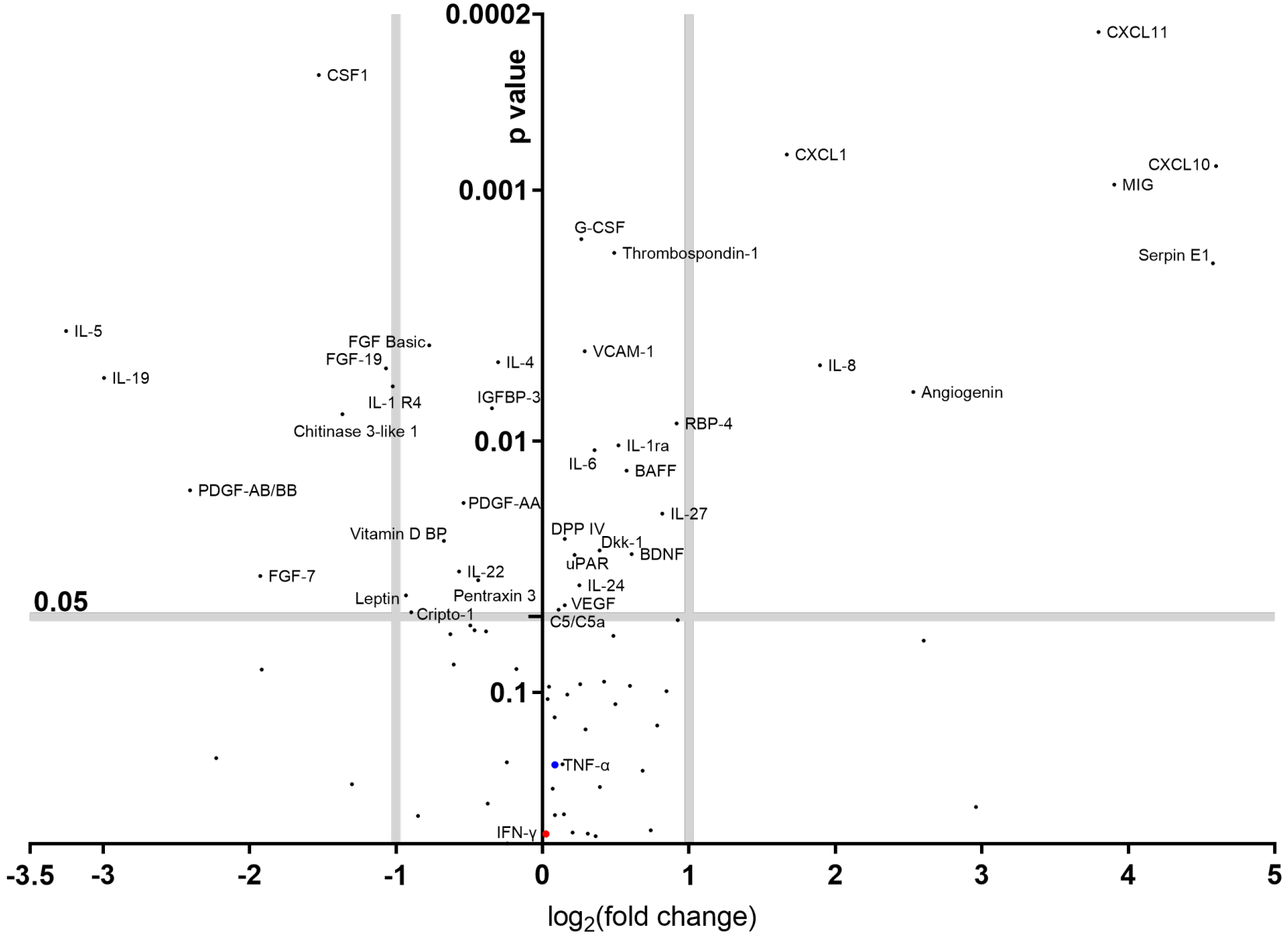

(C) "CD4 + ΔUS2-11" vs "CD4 + WT" secretomes

Gene Ontology (GO) terms are key phrases annotated to genes and proteins in public databases which describe the biological processes, molecular functions and cellular components associated with them. The Database for Annotation, Visualisation and Integrated Discovery (DAVID) analysis tool (available at https://david.ncifcrf.gov/home.jsp) is a method of analysis to identify GO terms which have been enriched (i.e. are more commonly found) in a list of submitted genes. To look for commonalities in the cytokines that had been found to be upregulated in the cytokine array, I performed a DAVID analysis on each of the sets of data, after eliminating those that had a p value of $\geq$0.05 and a $\log_2(\text{fold change})$ value of $<$1. The GO terms that have been enriched are then classified into clusters based on their similarities. Fig.4.8A shows a list of representative GO terms of the top-enriched clusters of genes from the list of genes that had been upregulated in Fig.4.7A; Fig.4.8B shows the same for upregulated genes from Fig.4.7B and Fig.4.8C for genes from Fig.4.7C.

Figs.4.8A & 4.8B show that the cytokines upregulated in the "CD4 + WT" and "CD4 + ΔUS2-11" secretomes come from largely similar groups—they are both strongly associated with chemokine-mediated signaling pathways, cellular responses to IFN-γ, positive regulation of NK cell chemotaxis and liposaccharide-mediated signaling pathways. When comparing the "CD4 + ΔUS2-11" against "CD4 + WT" secretomes, fewer cytokines are found to be upregulated and this resulted in only a few clusters of GO terms found to be enriched, belonging to the broad classes of belonging to the cytokine activity and signaling pathways, such as mitogen-activated protein kinase (MAPK) cascade and regulation of phosphatidylinositol 3-kinase pathways, which would suggest that these secretomes are largely similar.

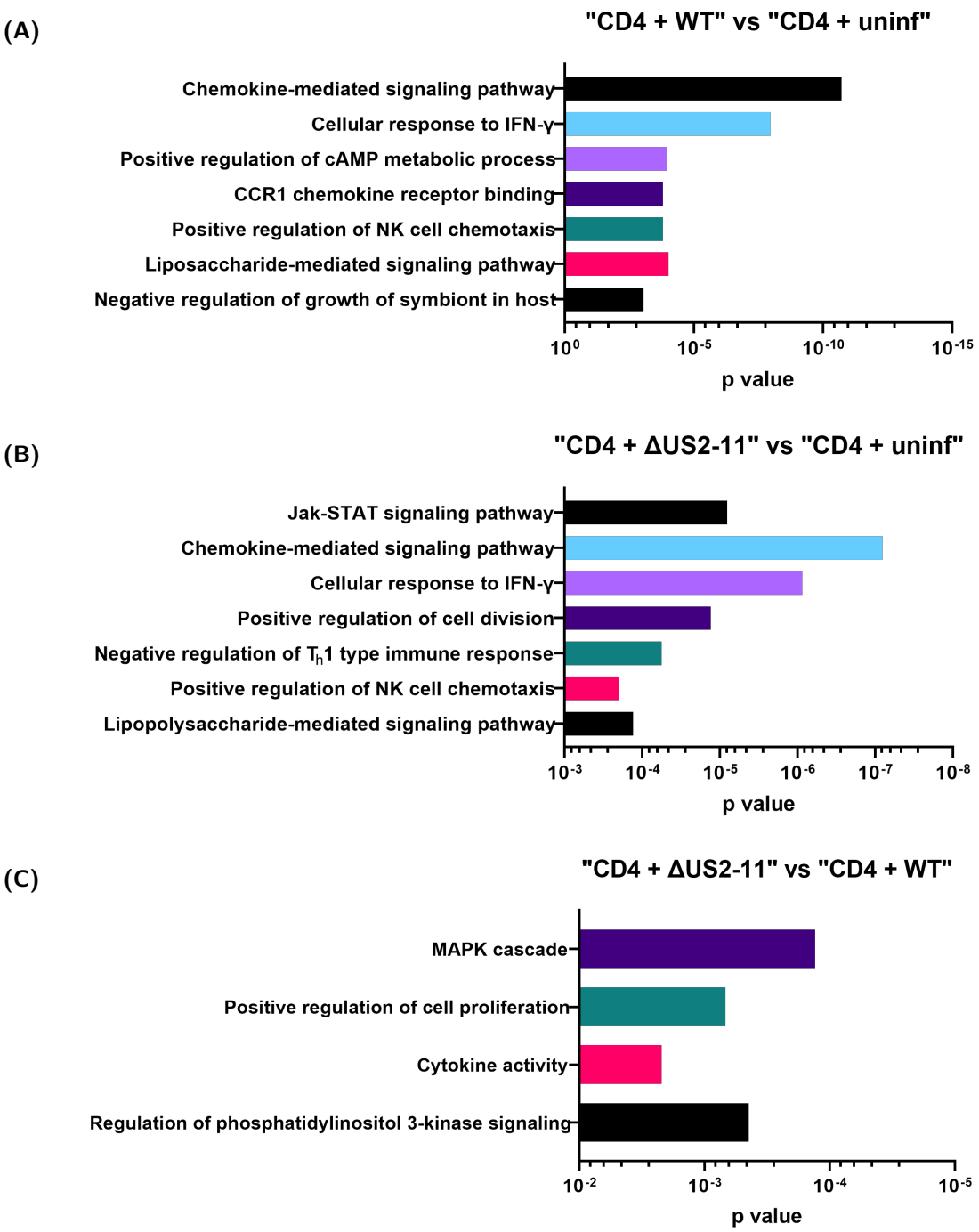

Figure 4.8: DAVID analysis of CD4$^+$ secretomes
DAVID analysis was performed on the results of the cytokine array performed in Fig.4.7 to find the GO terms most commonly associated with the cytokines that had been upregulated in each comparison in the assay, after elimination of cytokines that had a p value of $\geq$0.05 and a $\log_2(\text{fold change})$ value of $<$1. Fig.4.8A shows a list of representative GO terms of the top-enriched clusters of genes from the list of genes that had been upregulated in Fig.4.7A; Fig.4.8B shows the same for upregulated genes from Fig.4.7B and Fig.4.8C for genes from Fig.4.7C.

4.5.2 Quantification of cytokines present in the secretome of CD4$^+$ cells co-cultured with HCMV-infected fibroblasts

The cytokine array allowed me to identify cytokines that had been upregulated relative to other cytokines in the array. To quantify amounts of specific cytokines in these secretomes, I next performed a LegendPlex^{TM} assay of the supernatants from CD4$^+$ cells that had been co-cultured with either wildtype ("CD4 + WT") or ΔUS2-11 Merlin strain HCMV-infected ("CD4 + ΔUS2-11"), or uninfected ("CD4 + uninf"), autologous fibroblasts. I also performed this assay on supernatants from PBMCs that had been co-cultured with either wildtype Merlin strain HCMV ("PBMC + WT") or uninfected autologous fibroblasts ("PBMC + uninf"). This assay utilises a bead-based sandwich immunoassay method to quantify amounts of cytokines by flow cytometry. These beads are differentiated by size (Fig.4.9A, leftmost plot, P1 and P2 gates) and allophycocyanin; antigen presenting cell (APC) fluorescence intensities (Fig.4.9A, middle and right plots), and are conjugated with antibodies to the analytes of interest. First, these capture beads are incubated with the sample, followed by washing and addition of biotinylated detection antibodies. Subsequently streptavidin-phycoerythrin (SA-PE) is added, which binds to the biotinylated detection antibodies and provides a phycoerythrin fluorescence signal in proportion to the amount of bound analytes in the sample. The amount of each analyte present is quantified by comparing mean fluorescence intensity (MFI) of the PE signal from each bead to standard curves generated from samples made with known concentrations of each analyte. Figs.4.9A and 4.9B show the flow cytometry plots from the bottom and top standard samples and demonstrate the gating strategy used to identify each analyte. Fig.4.9C shows an example of a standard curve generated from the samples with known concentrations of each analyte (generated from software provided by the manufacturer), and Fig.4.9D shows the results from one test sample, with varying amounts of the different analytes. Due to a technical error, only 10 analytes were able to be measured.

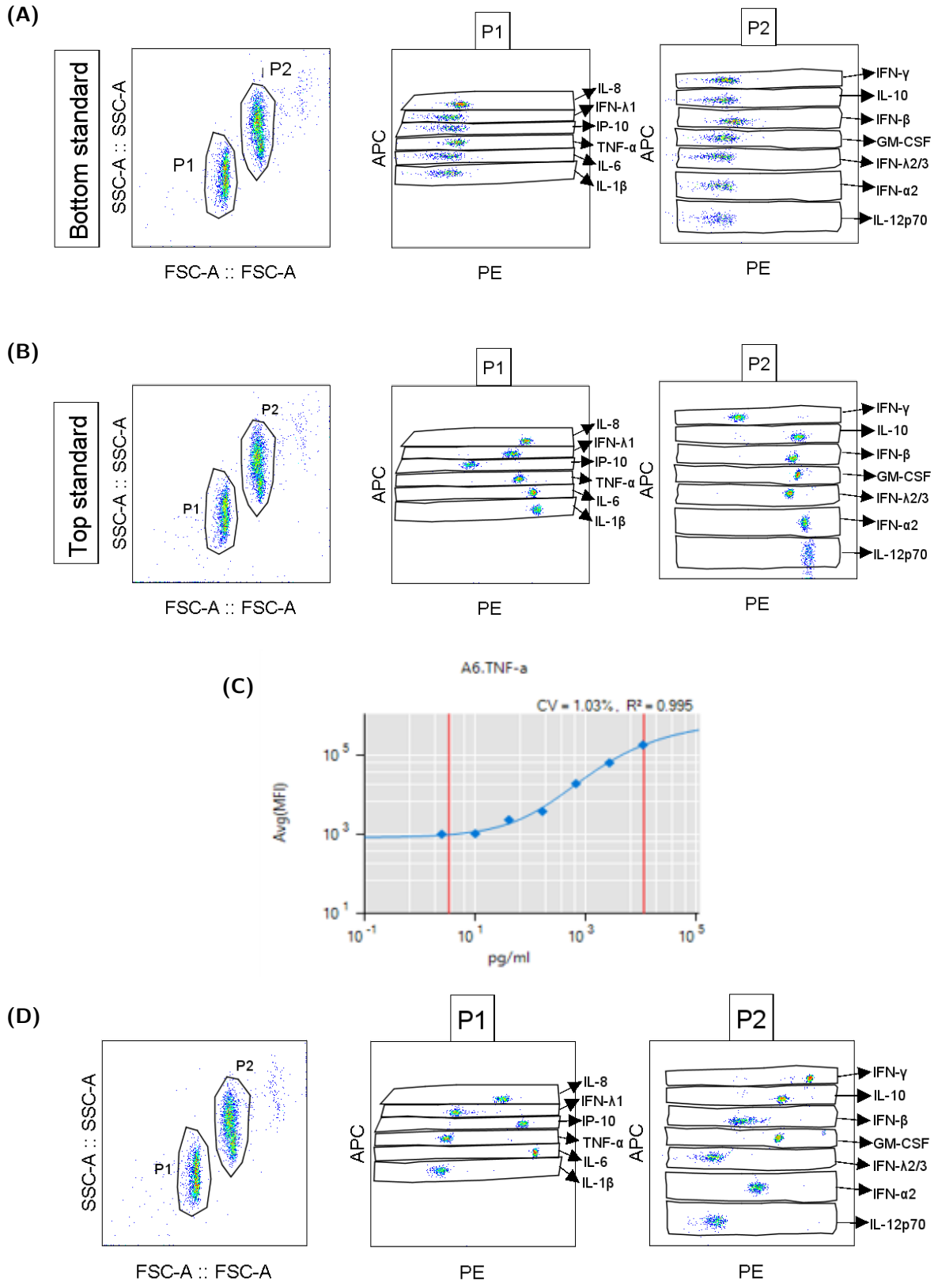
(A)
Bottom standard
SSC-A :: SSC-A
FSC-A :: FSC-A
P1
P2
APC
PE
IL-8
IFN-λ1
IP-10
TNF-α
IL-6
IL-1β
IFN-γ
IL-10
IFN-β
GM-CSF
IFN-λ2/3
IFN-α2
IL-12p70
(B)
Top standard
(C)
A6.TNF-a
CV = 1.03%, R² = 0.995
Avg(MFI)
pg/ml
(D)

Figure 4.9: Gating strategy to analyse LegendPlex^{TM} data
The LegendPlex^{TM} assay utilises a bead-based sandwich immunoassay method to quantify amounts of cytokines by flow cytometry. These beads are differentiated by size and APC fluorescence intensities, and are conjugated with antibodies to the analytes of interest. First, these capture beads are incubated with the sample, followed by washing and addition of biotinylated detection antibodies. Subsequently streptavidin-phycoerythrin (SA-PE) is added, which binds to the biotinylated detection antibodies and provides a phycoerythrin fluorescence signal in proportion to the amount of bound analytes in the sample. The amounts of each analyte present is quantified by comparing mean fluorescence intensities (MFI) of PE signal from each bead to standard curves generated from samples made with known concentrations of each analyte. Figs.4.9A and 4.9B show the flow cytometry plots from the bottom and top standard samples and demonstrate the gating strategy to identify each analyte. Fig.4.9C shows an example of a curve generated from the standard samples with known concentrations, and Fig.4.9D shows the results from one test sample, with varying amounts of the different analytes.

Figs.4.10A–4.10J show a comparison of the amounts of IFN-γ, IFN-α2, IFN-β, TNF-α, IFN-λ1, IFN-λ2/3, IL-1β, IL-8, IL-10 and GM-CSF in supernatants from PBMCs or CD4^{+} cells that had been co-cultured with wildtype Merlin HCMV, ΔUS2-11 Merlin HCMV, or uninfected autologous fibroblasts. The E:T ratio at which the immune cell population was added to the fibroblasts is shown in parentheses in the sample name.

The cytokine that was found in the highest concentration in the "CD4 + WT", "PBMC + WT" and "CD4 + ΔUS2-11" secretomes was IFN-γ. Other cytokines found in high concentrations in these secretomes were the type I interferons, IFN-α2 and IFN-β; TNF-α, IL-10 and GM-CSF. These results showed similar trends as the results from the cytokine array in Fig.4.7.

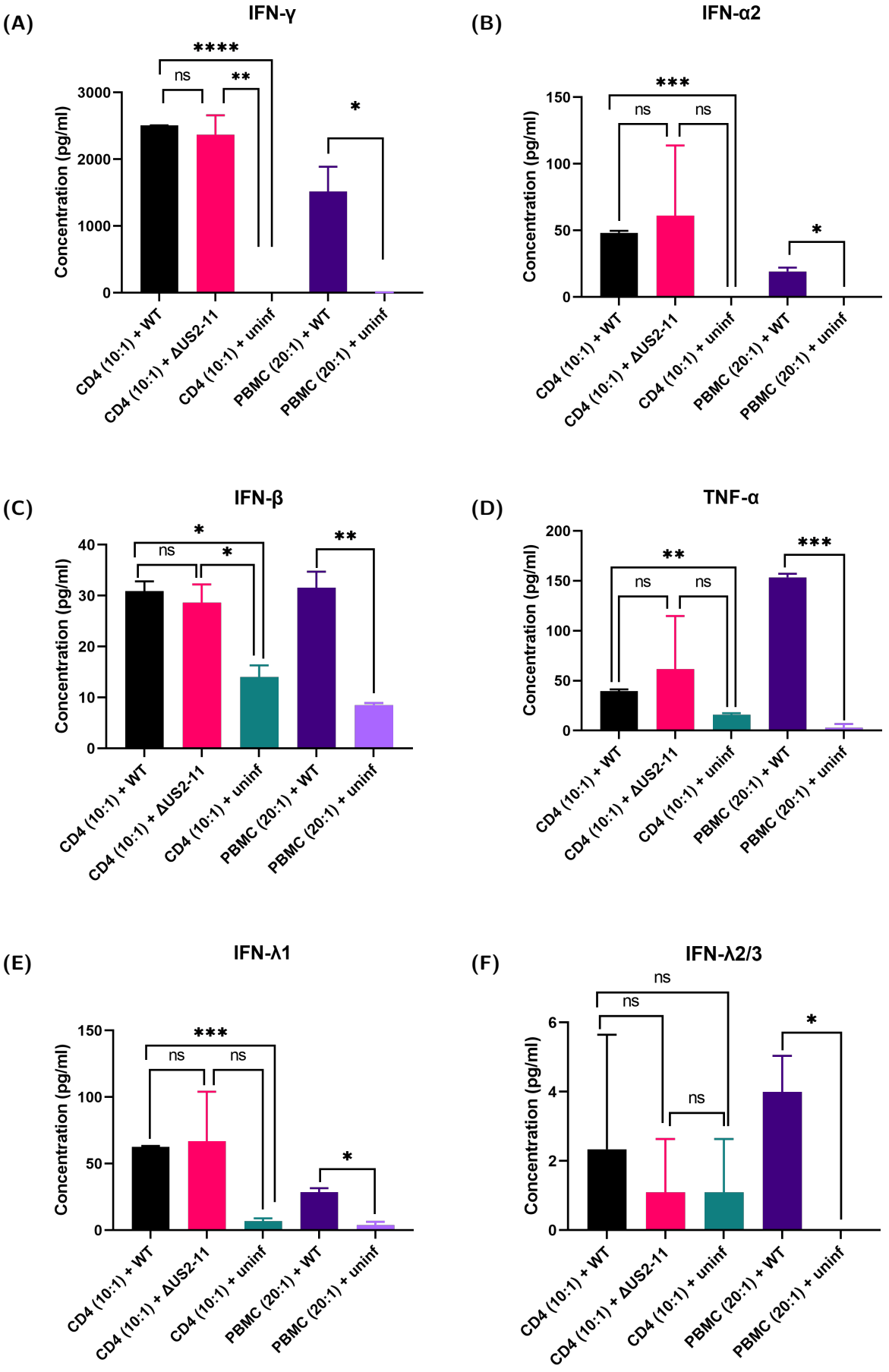
(A)
IFN-γ
Concentration (pg/ml)
3000
2000
1000
0
****
ns
**
*
CD4 (10:1) + WT
CD4 (10:1) + ΔUS2-11
CD4 (10:1) + uninf
PBMC (20:1) + WT
PBMC (20:1) + uninf
(B)
IFN-α2
Concentration (pg/ml)
150
100
50
0
***
ns
ns
*
CD4 (10:1) + WT
CD4 (10:1) + ΔUS2-11
CD4 (10:1) + uninf
PBMC (20:1) + WT
PBMC (20:1) + uninf
(C)
IFN-β
Concentration (pg/ml)
40
30
20
10
0
*
ns
*
**
CD4 (10:1) + WT
CD4 (10:1) + ΔUS2-11
CD4 (10:1) + uninf
PBMC (20:1) + WT
PBMC (20:1) + uninf
(D)
TNF-α
Concentration (pg/ml)
200
150
100
50
0
**
ns
ns
***
CD4 (10:1) + WT
CD4 (10:1) + ΔUS2-11
CD4 (10:1) + uninf
PBMC (20:1) + WT
PBMC (20:1) + uninf
(E)
IFN-λ1
Concentration (pg/ml)
150
100
50
0
***
ns
ns
*
CD4 (10:1) + WT
CD4 (10:1) + ΔUS2-11
CD4 (10:1) + uninf
PBMC (20:1) + WT
PBMC (20:1) + uninf
(F)
IFN-λ2/3
Concentration (pg/ml)
6
4
2
0
ns
ns
ns
*
CD4 (10:1) + WT
CD4 (10:1) + ΔUS2-11
CD4 (10:1) + uninf
PBMC (20:1) + WT
PBMC (20:1) + uninf

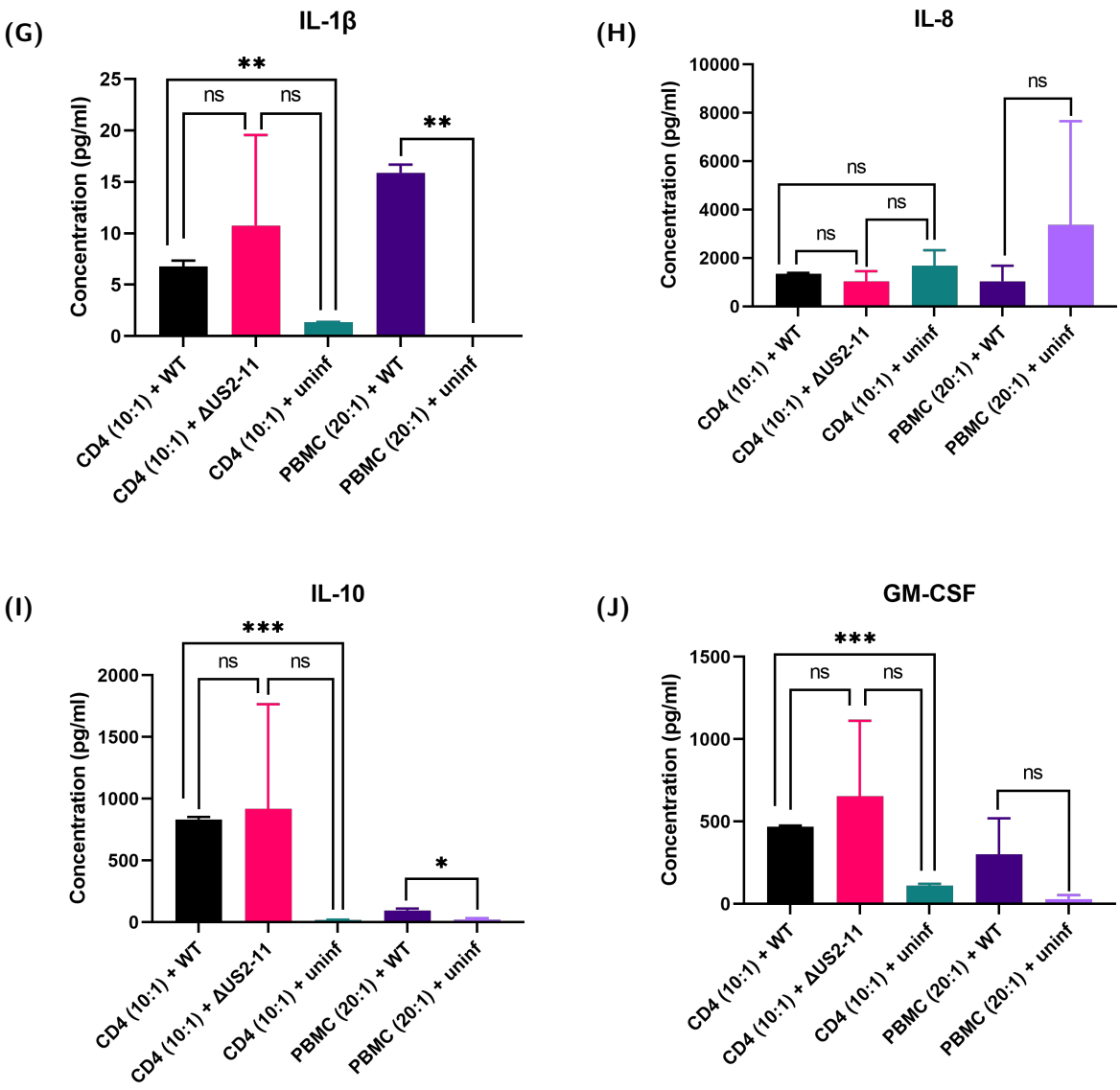

Figure 4.10: Quantification of amounts of various cytokines in secretomes of CD4$^+$ cells or PBMCs incubated with HCMV-infected autologous fibroblasts
Secretomes of PBMCs or CD4$^+$ cells co-cultured with Merlin WT- or ΔUS2-11-infected autologous fibroblasts were assayed using the LegendPlex^{TM} assay as described in Fig.4.10. Secretomes from one representative donor out of 2 is shown. Figs.4.10A–4.10J show amounts of IFN-γ, IFN-α2, IFN-β, TNF-α, IFN-λ1, IFN-λ2/3, IL-1β, IL-8, IL-10 and GM-CSF in these secretomes. Error bars represent SD of duplicate readings, statistics performed with Student's *t*-test. (*$p\leq0.05$; **$p\leq0.01$; ****$p\leq0.0001$; ns = not significant)

4.6 Effects of IFN-γ on HCMV gene expression in the viral dissemination assay

The results from Section 4.5 show that IFN-γ was the cytokine that was found in the highest concentration in the secretomes that had been obtained from co-cultures with infected fibroblasts. IFN-γ is a type II interferon, a non-covalently linked 34 kDa homodimer that was initially identified by its antiviral activity in nonimmune cells [636]. It was subsequently found to regulate a wide range of immune responses and is a master regulator of the T_h1 response. Classically thought to only be produced by $CD4^+$ T_h1 cells, cytotoxic $CD8^+$ and NK cells, it was subsequently found that B cells, NKT cells and professional antigen-presenting cells also secrete IFN-γ [510]. IFN-γ production is controlled by cytokines secreted by APCs, most notably IL-12 and IL-18. It has been shown to upregulate MHC Class I and II expression, activate macrophages/microglia, act as a cytostatic agent on numerous normal and oncogenic cell lines, and induce several interferon-inducible antiviral mechanisms [156, 510].

Other cytokines which had antiviral effects that were found to be upregulated in the secretomes by LegendPlex™ assay were the type I interferons (IFN-α2 and IFN-β) and TNF-α. However, as IFN-γ was found in much higher concentrations than these other cytokines, I decided to focus first on examining the effects of IFN-γ on HCMV-infected cells.

4.6.1 IFN-γ limits late viral gene expression at lower concentrations

To determine the extent to which IFN-γ was responsible for the antiviral effects of the secretome when it was added to the viral dissemination assay, I first needed to investigate its effects when added to HCMV-infected cells. It would be expected that addition of IFN-γ to a well of HCMV-infected fibroblasts (in the absence of any effector immune cells) would result in reduced amounts of infected cells via induction of an antiviral state in fibroblasts that had yet to be infected, though the degree to which this would occur is unknown.

Primary dermal fibroblasts from 4 different donors were infected with Merlin WT virus (MOI = 0.023). At 1 dpi, IFN-γ (500pg/ml) was added to half the wells and further incubation was carried out before harvests at 3, 5 and 8 dpi. Fig.4.11 shows amount of $mCherry^+GFP^-$ (left column) and $mCherry^+GFP^+$ (right column) cells at each of these timepoints. It can clearly be seen that addition of IFN-γ at 1 dpi does not inhibit spread of $mCherry^+GFP^-$ (IE viral gene expression), but it significantly inhibits amount of $mCherry^+GFP^+$ (late gene expression) at 8 dpi. However, it does not eliminate late CMV gene expression fully, as there was still a small percentage of cells at 8 dpi that were $mCherry^+GFP^+$. These $mCherry^+GFP^+$ cells were most likely to be the initial population of cells that were $mCherry^+GFP^-$ at 1 dpi. The implication, therefore, is that IFN-γ is not able to prevent viral entry into uninfected cells, nor can it prevent a cell from progressing to late CMV gene expression if it is added after

the cell has undergone viral entry, but it can arrest progression to late CMV gene expression if it is added before the virus has entered the cell. In addition, it is also unable to prevent production of new virions in cells that have progressed to late CMV gene expression, as there was an increase in the amount of $mCherry^{+}GFP^{-}$ cells even in wells that had IFN-γ added, which meant that there was new virion production and viral entry.

There was also a decrease in amount of $mCherry^{+}GFP^{-}$ cells from days 5 to 8 post-infection in 2 donors (CMV 342 and 307). This was probably because there was a high percentage of $mCherry^{+}GFP^{-}$ cells at 5 days post-infection in these 2 donors, which meant that there was a high number of cells that had viral entry in the initial replicative cycle, likely leading to cell death by day 8 post-infection, and an apparent decrease in the proportion of $mCherry^{+}GFP^{-}$ cells.

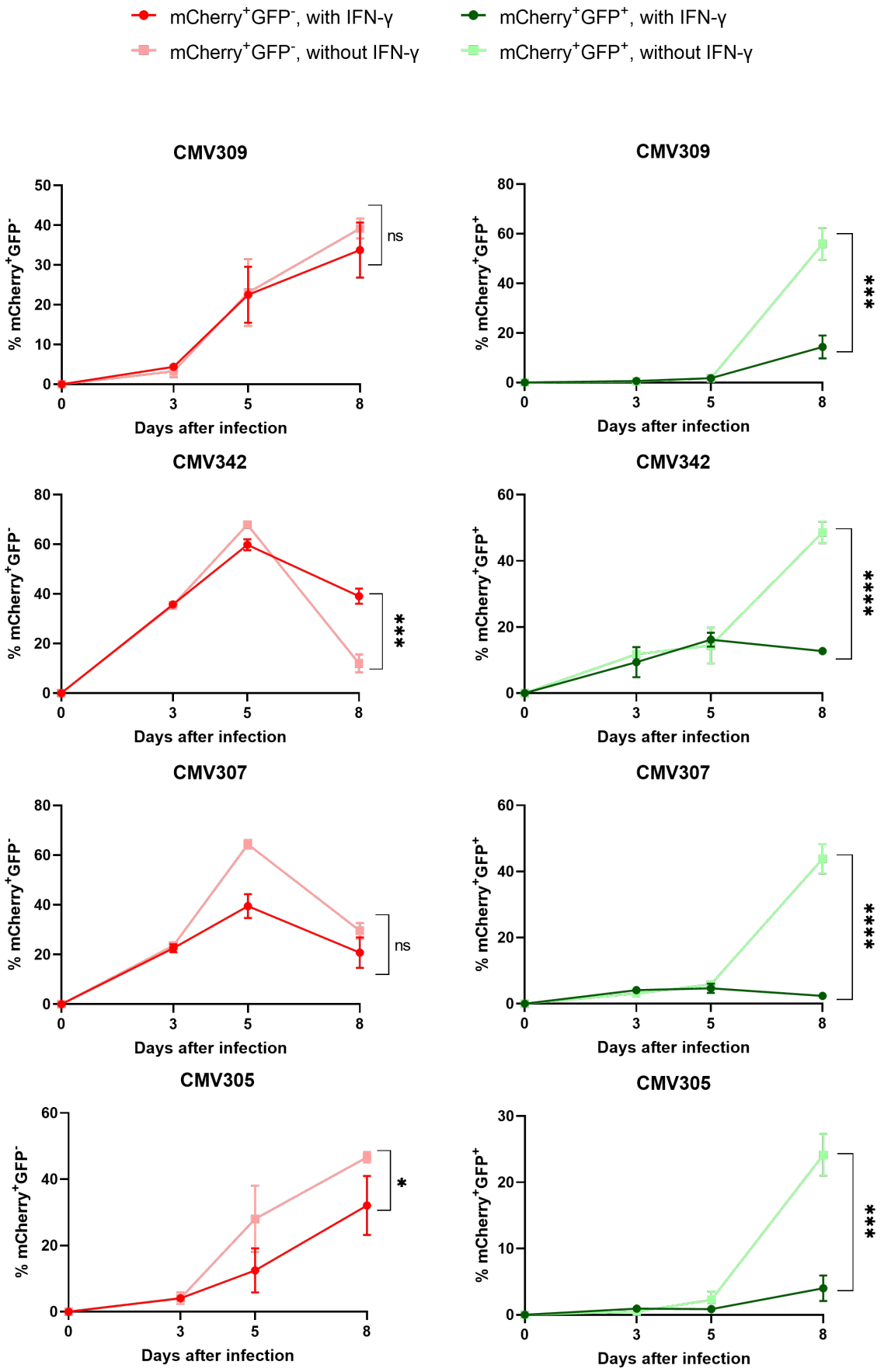
mCherry+GFP-, with IFN-γ
mCherry+GFP-, without IFN-γ
mCherry+GFP+, with IFN-γ
mCherry+GFP+, without IFN-γ
CMV309
% mCherry+GFP-
Days after infection
ns
CMV309
% mCherry+GFP+
Days after infection
***
CMV342
% mCherry+GFP-
Days after infection
***
CMV342
% mCherry+GFP+
Days after infection
****
CMV307
% mCherry+GFP-
Days after infection
ns
CMV307
% mCherry+GFP+
Days after infection
****
CMV305
% mCherry+GFP-
Days after infection
*
CMV305
% mCherry+GFP+
Days after infection
***

Figure 4.11: Addition of IFN-γ limits late viral gene expression in HCMV-infected fibroblasts
Primary dermal fibroblasts from 4 healthy donors were seeded in 96-well plates and grown to confluency overnight before infection with Merlin WT (MOI = 0.023). At 1 dpi, IFN-γ (500pg/ml) was added to half of the infected wells, the remaining wells had a change of media. Cells were harvested at 3, 5 and 8 dpi and analysed by flow cytometry. The mean amount of $mCherry^{+}GFP^{-}$ cells at each timepoint, expressed as a % of total cells in the well, is shown on the left column; right column shows the same for $mCherry^{+}GFP^{+}$ cells. Error bars represent SD of triplicate wells. Statistics performed using Student's *t*-test. (*$p \leq 0.05$; **$p \leq 0.01$; ***$p \leq 0.001$; ****$p \leq 0.0001$; ns = not significant)

4.6.2 Inhibition of IE gene expression by IFN-γ is dose-dependent

The previous experiment showed that, at concentrations of 500pg/ml, IFN-γ was able to limit late CMV gene expression, but had much less effect on IE CMV gene expression. To investigate if IFN-γ could inhibit IE gene expression at higher concentrations, the experiment was repeated with different concentrations of IFN-γ. Primary dermal fibroblasts were infected with Merlin WT (MOI = 0.03) after seeding in a 96-well plate and grown to confluency overnight. At 1 dpi, IFN-γ was added at 500, 1000, 3000 or 6000 pg/ml, or media was changed (infected controls). Wells were harvested at 4, 8 and 11 dpi and analysed by flow cytometry. Fig.4.12A shows that there is a dose-dependent inhibition of mCherry$^+$GFP$^-$ while Fig.4.12B shows that, even at low doses, there is inhibition of mCherry$^+$GFP$^+$ expression.

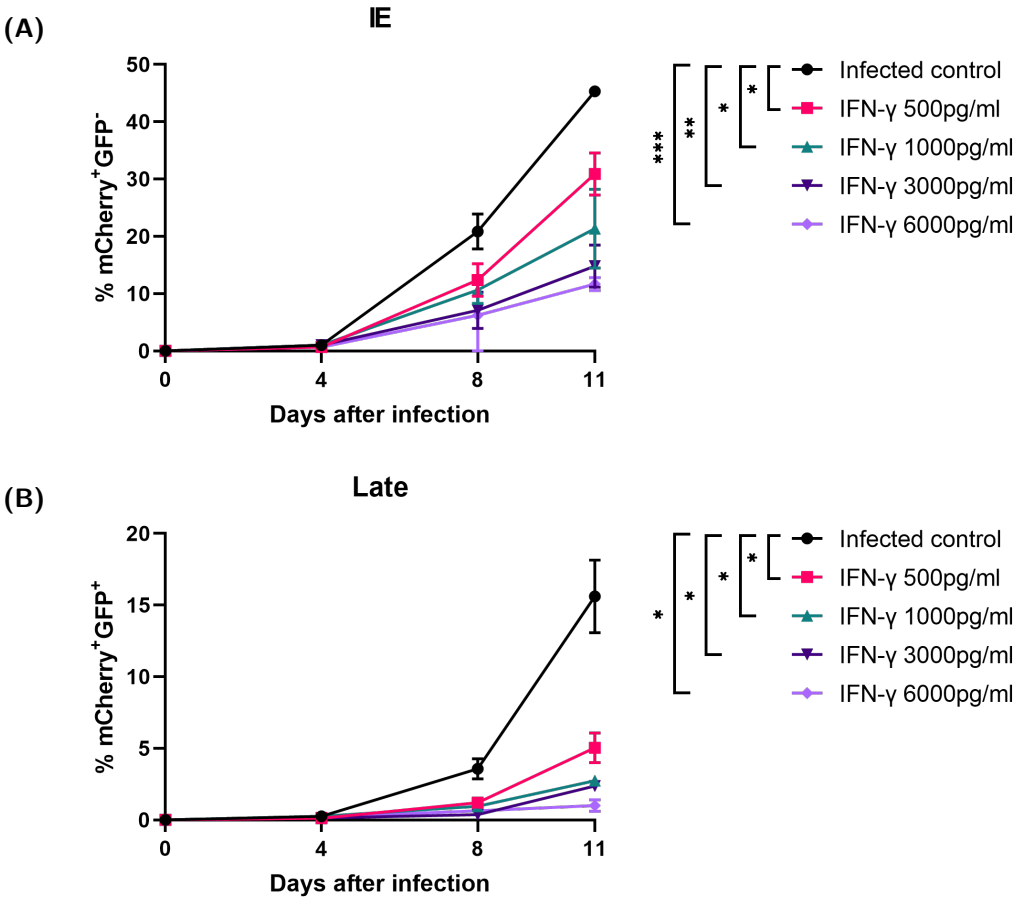

Figure 4.12: Interferon-γ limits late viral gene expression in a dose-dependent manner Primary dermal fibroblasts were infected with Merlin WT (MOI = 0.03) after seeding in a 96-well plate and grown to confluency overnight. At 1 dpi, IFN-γ was added at 500, 1000, 3000 or 6000 pg/ml, or media was changed (infected controls). Wells were harvested at 4, 8 and 11 dpi and analysed by flow cytometry. Mean amounts of mCherry$^+$GFP$^-$(Fig.4.12A) and mCherry$^+$GFP$^+$(Fig.4.12B) is shown, expressed as a % of total cells in the well. Error bars represent SD of triplicate wells. Statistics performed using Student's *t*-test. (*$p \leq 0.05$; **$p \leq 0.01$; ***$p \leq 0.001$; ****$p \leq 0.0001$; ns = not significant)

4.6.3 IFN-γ induces HLA-DR on fibroblasts in a time- & concentration-dependent manner

IFN-γ has been shown to induce MHC Class II expression on somatic cells that do not constitutively express this molecule [553]. To further understand the effects of IFN-γ-mediated upregulation of HLA-DR on fibroblasts, IFN-γ was added to primary dermal fibroblasts at concentrations of 625, 1250, 2500 and 5000 pg/ml. These fibroblasts were then harvested and stained for HLA-DR at 24, 48 and 72 hours post-addition of IFN-γ. Fig.4.13A shows that the effects of IFN-γ-mediated upregulation of HLA-DR increases with increasing dose of IFN-γ, up to a maximum of approximately 1250 pg/ml. Between the 24, 48 and 72 hour timepoints, HLA-DR was maximally upregulated at 72 hours. This was repeated with IFN-γ dose of 1000 pg/ml for timepoints of 24, 48, 72 and 144 hours. Fig.4.13B shows that maximal upregulation occurred at 72 hours, and by 144 hours, the amount of HLA-DR on the cell surface had reduced. This was likely to be due to uptake of IFN-γ by the cells leading to exhaustion of the amount of IFN-γ present in the media.

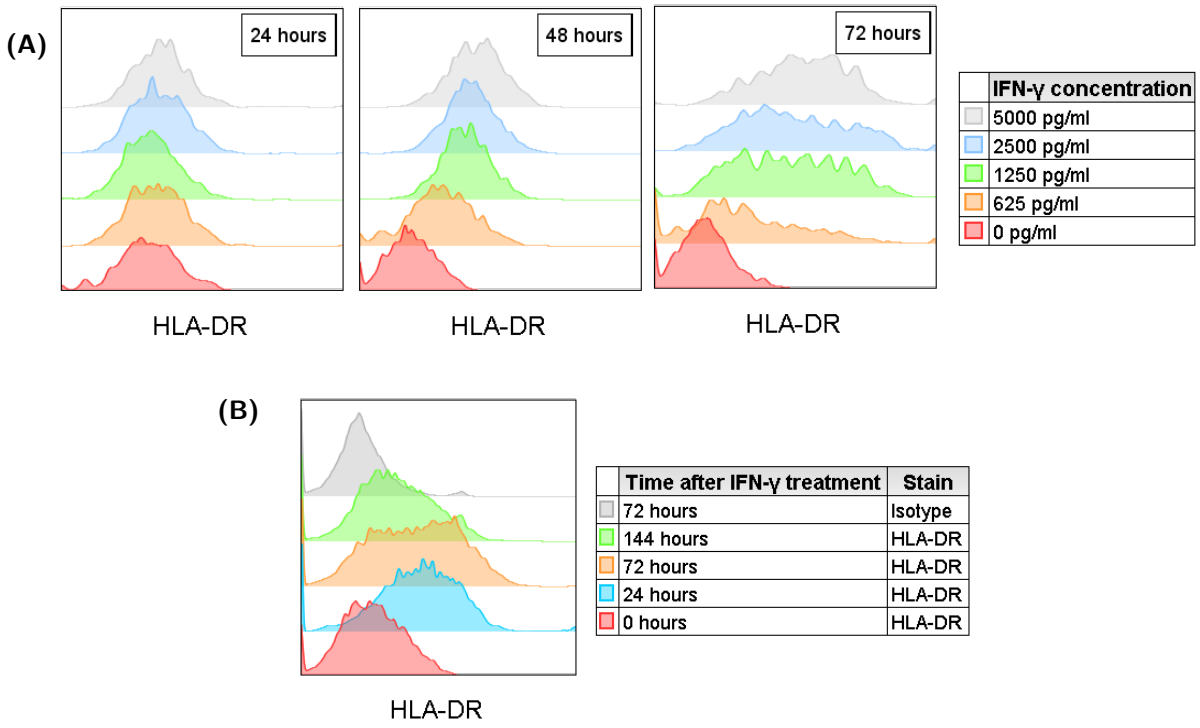

Figure 4.13: IFN-γ induces expression of HLA-DR on fibroblasts in a time- and concentration-dependent manner
IFN-γ was added to dermal fibroblasts at concentrations of 625, 1250, 2500 and 5000 pg/ml, then harvested and stained for HLA-DR at 24, 48 and 72 hours post-addition of IFN-γ. Fig.4.13A shows the histograms of amount of HLA-DR at the various concentrations at each timepoints. IFN-γ was then added to fibroblasts at 1000 pg/ml and stained for HLA-DR at 24, 48, 72 and 144 hours post-addition of IFN-γ. Fig.4.13B shows the histograms of the amount of HLA-DR at each of these timepoints. One representative replicate out of two is shown.

4.6.4 The CD4$^+$ cell secretome induces MHC Class II on fibroblasts via IFN-γ

Having shown that the secretome of CD4$^+$ cells co-cultured with Merlin WT or ΔUS2-11 virus is able to inhibit both IE and late phase viral gene expression, and by extension can limit both viral dissemination and the full lytic viral life cycle, I next examined the effect this secretome had on these cells. CD4$^+$ cells recognise virus-infected cells by antigen presentation via the MHC Class II antigen presentation pathway. As discussed in Section 1.2.6.2, IFN-γ is able to induce expression of MHC Class II on cells that do not constitutively express it, such as fibroblasts [553]. I investigated if the secretome from CD4$^+$ cells co-cultured with Merlin WT-infected autologous fibroblasts was able to induce MHC Class II on uninfected fibroblasts, and whether this could be blocked by an anti-IFN-γ antibody.

Primary dermal fibroblasts were seeded in 96-well plates and incubated for 3 days under one of the following conditions: IFN-γ 2000pg/ml (Fig.4.14A), "PBMC + WT" secretome with or without anti-IFN-γ antibody (Fig.4.14B), "CD4 + WT secretome" with or without anti-IFN-γ antibody (Fig.4.14C), or "CD4 + uninf" secretome (Fig.4.14D). They were then stained for HLA-DR and analysed by flow cytometry. Fig.4.14A shows that HLA-DR is upregulated when fibroblasts were incubated with IFN-γ, Figs.4.14B & 4.14C show that "PBMC + WT" and "CD4 + WT" secretome induces HLA-DR expression on fibroblasts, which is abrogated by addition of anti-IFN-γ antibody, and Fig.4.14D shows that "CD4 + uninf" secretome does not induce HLA-DR expression on fibroblasts.

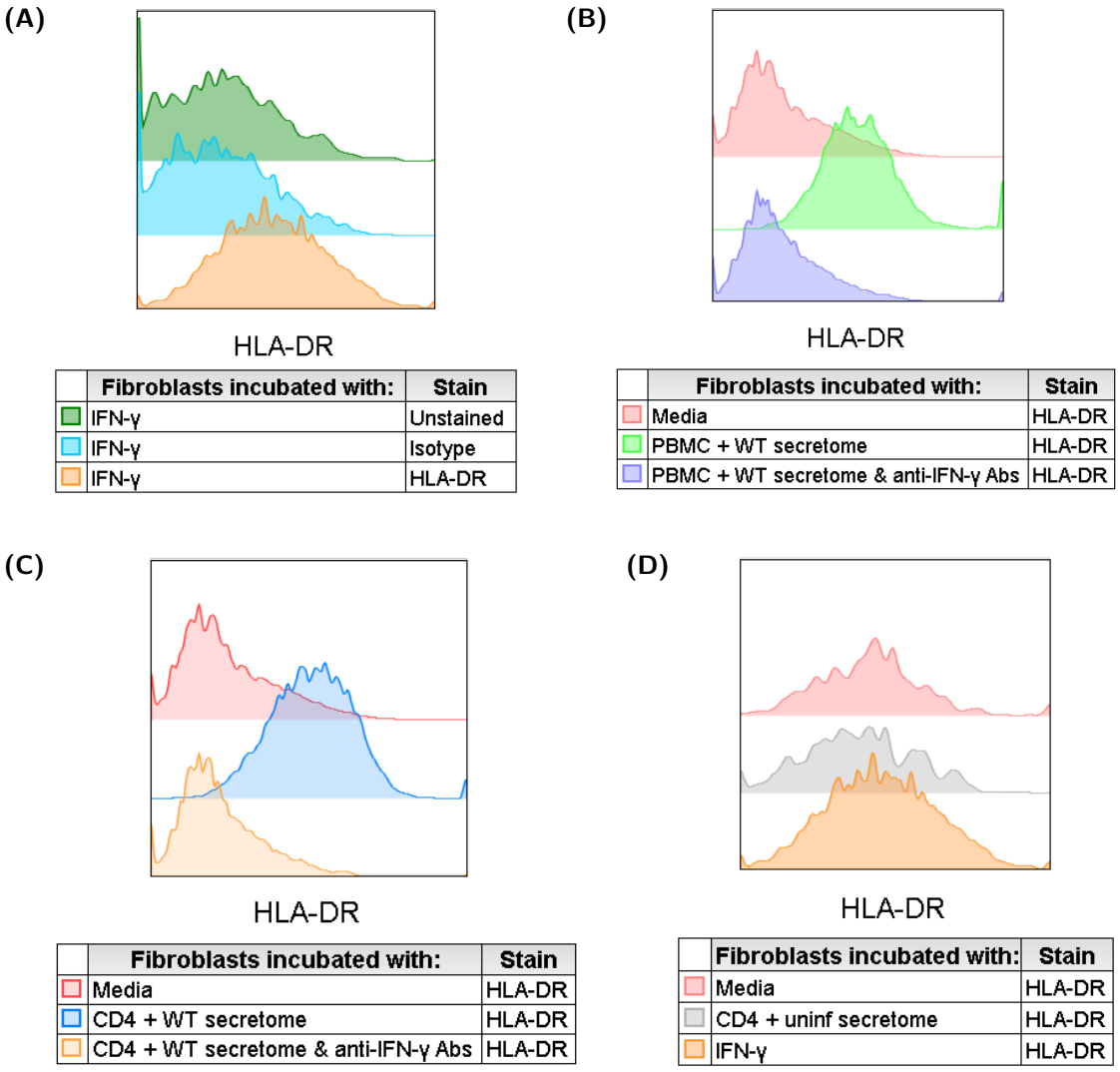

Figure 4.14: "CD4 + WT" secretome induces HLA-DR expression in fibroblasts via IFN-γ Primary dermal fibroblasts were incubated under the following conditions for 3 days before staining for HLA-DR: incubation with IFN-γ (2ng/ml) (Fig.4.14A), "PBMC + WT" secretome with or without anti-IFN-γ antibody (Fig.4.14B), "CD4 + WT secretome" with or without anti-IFN-γ antibody (Fig.4.14C), or "CD4 + uninf" secretome (Fig.4.14D).

4.7 Control of viral dissemination in other cell types

Clinical HCMV infection has protean manifestations, due to the ability of HCMV to infect multiple cell types *in vivo*. In episodes of disseminated disease, HCMV can be found in multiple organs, including the lung, kidney, pancreas, spleen, adrenals, bowels, liver, brain, bone marrow, eyes and heart [125, 196, 262, 405, 467, 529]. In cases of congenital disease, it is also known to infect the placenta [59]. Histopathological examination of infected organs reveal that fibroblasts are a major target of HCMV infection *in vivo* but endothelial cells, epithelial cells and smooth muscle cells are also frequently found to harbour HCMV [530]. It would thus be relevant to investigate if the $CD4^+$ cell secretome has effects on these other cell types as well.

4.7.1 $CD4^+$ cell secretome induces HLA-DR on retinal pigmented epithelial cells in a concentration-dependent manner

ARPE-19 is a spontaneously arising human retinal pigmented epithelium cell line with structural and functional properties characteristic of retinal pigmented epithelium cells *in vivo* [138]. In histopathological examinations of eyes with CMV retinitis, viral presence was found within retinal pigment epithelial cells [467], though it is hypothesised that entry of the virus into the retina is likely due to infection of the blood vessels entering the retina accompanied by local inflammation [195, 434, 463]. An interesting observation is that CMV retinitis is frequent in congenital CMV infection and in late stage AIDS, but not in transplant patients. This is likely because periods of prolonged HCMV replication and presumably viraemia are required to develop the pathological changes that lead to viral entry into the retina, and in the setting of post-transplant patients with close monitoring for CMV viraemia, this is less likely to occur.

In addition, epithelial cells are also a target for HCMV infection [63, 530]. During acute infection, late-stage infected epithelial cells have been detected in salivary glands, kidneys and in the gastrointestinal tract [59, 530, 605] and are likely to be the source of viral shedding into saliva, urine and stools [529]. Thus, I proceeded to examine the effects of the $CD4^+$ cell secretome on ARPE-19 cells.

Firstly, to show that HLA-DR can be induced by IFN-γ on ARPE-19 cells, IFN-γ was added at a concentration of 2000pg/ml and incubated for 48 hours, then stained for HLA-DR and analysed by flow cytometry. Fig.4.15A shows that expression of HLA-DR on the surface of ARPE-19 cells can be upregulated by IFN-γ. Next, secretomes from $CD4^+$ cells co-cultured with Merlin WT ("CD4 + WT") or uninfected autologous fibroblasts ("CD4 + uninf") were made as described in Section 2.13 and were added to ARPE-19 cells at dilutions of 1:2, 1:4 or 1:8 and incubated for 48 hours before staining for HLA-DR. Fig.4.15B shows that the secretome of $CD4^+$ cells co-cultured with Merlin WT-infected fibroblasts is able to induce expression of HLA-DR on ARPE-19 cells. This effect is concentration-dependent, as seen in

Fig.4.15C, where the amount of HLA-DR induced decreases with increasing dilution of the secretome.

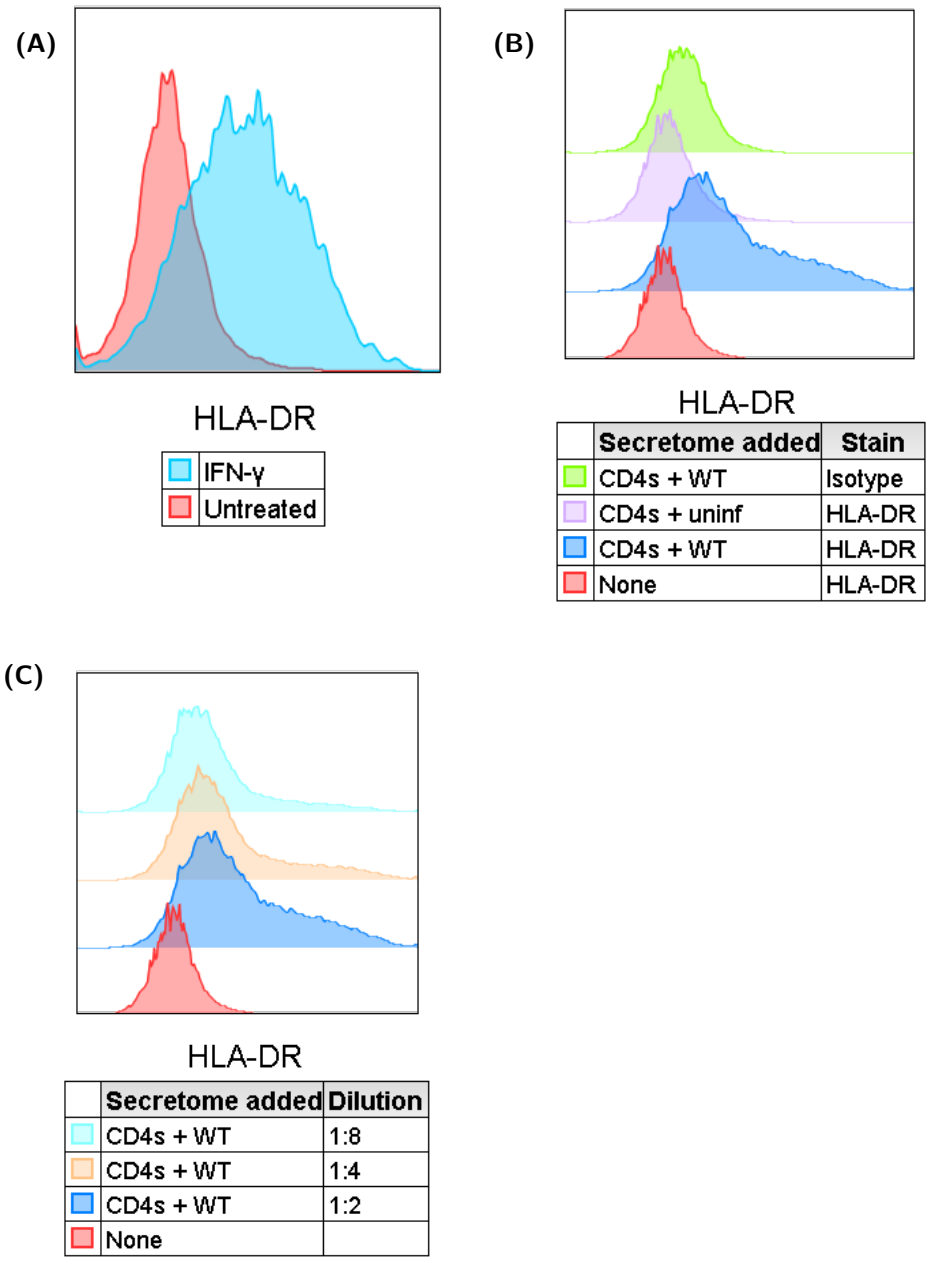

Figure 4.15: Secretomes from CD4$^+$ cells co-cultured with HCMV-infected autologous fibroblasts can induce HLA-DR expression on adult retinal pigmented epithelial cells in a concentration-dependent manner
IFN-γ (2000pg/ml) was added to ARPE-19 cells and incubated for 48 hours, then stained for HLA-DR. Fig.4.15A shows histograms of amount of HLA-DR on ARPE-19 cells with and without IFN-γ added. Subsequently, secretomes from CD4$^+$ cells co-cultured with Merlin wildtype HCMV-infected autologous fibroblasts ("CD4s + WT"), or co-cultured with uninfected fibroblasts ("CD4s + uninf") were added to ARPE-19 cells at dilutions of 1:2, 1:4 or 1:8 and incubated for 48 hours, before staining for HLA-DR. Fig.4.15B shows a comparison of the amount of HLA-DR induced by the different secretomes at 1:2 dilution, and Fig.4.15C shows a comparison of the amount of HLA-DR induced by 1:2, 1:4 and 1:8 dilutions of secretome from CD4$^+$ cells co-cultured with Merlin WT strain of HCMV-infected autologous fibroblasts.

4.7.2 $CD4^+$ cell secretome induces HLA-DR on human umbilical vein endothelial cells

HUVECs, as their name suggests, are endothelial cells obtained from the vein of the human umbilical cord and used as a laboratory model for endothelial cells. There is marked HCMV tropism for endothelial cells *in vivo* [529] and HCMV-infected endothelial cells can be detected in the microvasculature of multiple organs that HCMV infects, including but not limited to the brain [640], liver [58], gastrointestinal tract [487, 530], kidneys, heart [405] and lungs [530]. There has been some conflicting evidence in the ability of endothelial cells of arterial origin to support productive lytic infection [161, 278], but HUVECs have been shown to be supportive of productive lytic HCMV infection [613, 614].

To examine if the $CD4^+$ cell secretome induces HLA-DR on HUVECs, secretomes from $CD4^+$ cells co-cultured with wildtype Merlin ("CD4s + WT") or ΔUS2-11 Merlin ("CD4s + ΔUS2-11") strain of HCMV-infected autologous fibroblasts, or co-cultured with uninfected fibroblasts ("CD4s + uninf"), were made as described in Section 2.13. These secretomes were added to HUVECs at dilutions of 1:2, 1:4 or 1:8 and incubated for 48 hours before staining for HLA-DR. As a positive control, IFN-γ at 1000pg/ml and 2000pg/ml were also added to HUVECs over the same time period. The results demonstrate that IFN-γ shows a dose-dependent ability to induce HLA-DR on HUVECs (green and blue histograms, Fig.4.16A), and that both "CD4s + WT" and "CD4s + ΔUS2-11" secretomes are also able to do so to approximately the same degree (purple and green histograms, Fig.4.16B) but not the "CD4s + uninf" secretome (grey histogram, Fig.4.16B). Dilution of the "CD4 + WT" secretome to 1:4 and 1:8 reduces the amount of HLA-DR induced to a small degree (orange and cyan histograms, Fig.4.16C). However, dilution of the "CD4 + ΔUS2-11" to 1:8 does not appear to decrease the amount of HLA-DR induced on HUVECs (Fig.4.16D).

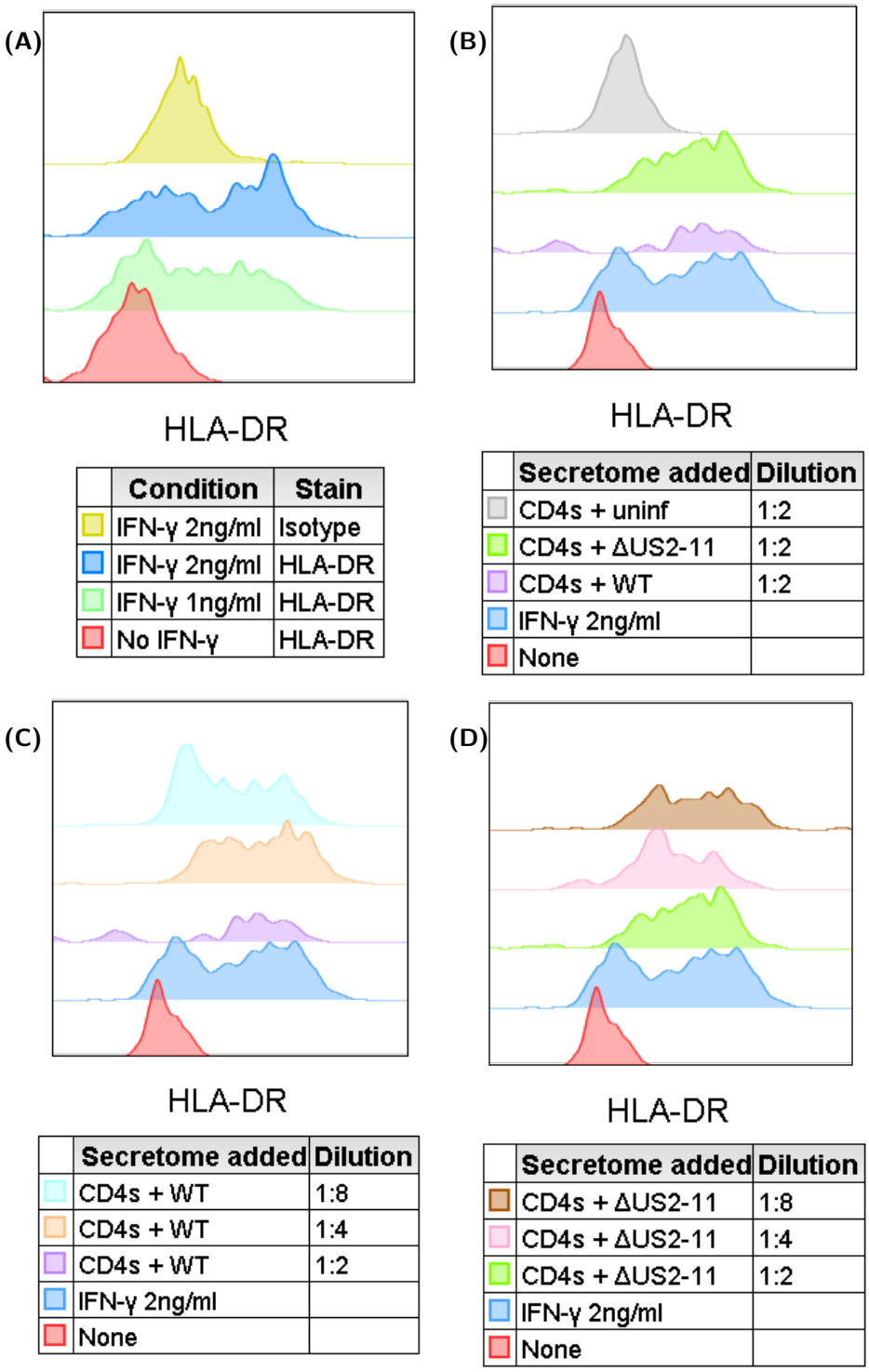

	Condition	Stain
	IFN-γ 2ng/ml	Isotype
	IFN-γ 2ng/ml	HLA-DR
	IFN-γ 1ng/ml	HLA-DR
	No IFN-γ	HLA-DR

	Secretome added	Dilution
	CD4s + uninf	1:2
	CD4s + ΔUS2-11	1:2
	CD4s + WT	1:2
	IFN-γ 2ng/ml	
	None	

	Secretome added	Dilution
	CD4s + WT	1:8
	CD4s + WT	1:4
	CD4s + WT	1:2
	IFN-γ 2ng/ml	
	None	

	Secretome added	Dilution
	CD4s + ΔUS2-11	1:8
	CD4s + ΔUS2-11	1:4
	CD4s + ΔUS2-11	1:2
	IFN-γ 2ng/ml	
	None	

Figure 4.16: Secretomes from CD4$^+$ cells co-cultured with HCMV-infected autologous fibroblasts can induce HLA-DR expression on human umbilical vein endothelial cells
Secretomes from CD4$^+$ cells co-cultured with wildtype Merlin ("CD4s + WT") or ΔUS2-11 Merlin ("CD4s + ΔUS2-11") HCMV-infected autologous fibroblasts, or co-cultured with uninfected fibroblasts ("CD4s + uninf"), were added to HUVECs at dilutions of 1:2, 1:4 or 1:8 and incubated for 48 hours before staining for HLA-DR. Incubation of HUVECs with IFN-γ (2ng/ml) for 48 hours was used as positive control. Fig.4.16A shows the amount of HLA-DR induced on HUVECs by IFN-γ (2ng/ml) after 48 hours, Fig.4.16B shows a comparison of the amount of HLA-DR induced by the different secretomes in comparison to IFN-γ (2ng/ml), Fig.4.16C shows the amount of HLA-DR induced by 1:2, 1:4 and 1:8 dilutions of "CD4 + WT" secretome, and Fig.4.16D shows the amount of HLA-DR induced by 1:2, 1:4 and 1:8 dilutions of "CD4 + ΔUS2-11" secretome.

4.7.3 IFN-γ inhibits viral dissemination in human umbilical vein endothelial cells

The results in Section 4.7.2 appear to suggest that HUVECs are fairly sensitive to the effects of IFN-γ, although a dose-dependent response of upregulating MHC Class II in response to IFN-γ was not done in ARPE-19 cells.

HUVECs were used in a viral dissemination assay to determine the effect of IFN-γ treatment on viral dissemination and viral gene expression. HUVECs were infected with TB40/E UL32-GFP virus at MOIs of 0.05, 0.1, 0.2 and 0.4. At 1 dpi, 2000pg/ml of IFN-γ was added. At 6 dpi, IFN-γ was topped up by removing media in the wells and adding fresh media with IFN-γ (2000pg/ml) or media was changed in the untreated controls. At 12 dpi, cells were harvested and stained for expression of HLA-DR and analysed by flow cytometry.

The reason for using the TB40/E instead of the Merlin strain of HCMV in this experiment is because the Merlin strain is a BAC-cloned version of a clinical isolate with point mutations in RL13 and UL128 [550] that allows it to propagate well in fibroblasts but shows poor infection of endothelial cells, monocytes and dendritic cells [122, 189, 609]. The TB40/E strain of HCMV is a strain that retains tropism for endothelial cells despite propagation and purification in fibroblasts [531] and thus was used for this experiment. The TB40/E strain used in this experiment has GFP tagged to UL32.

Fig.4.17B shows that addition of IFN-γ (2000pg/ml) at 1 dpi inhibits late gene expression in HUVECs at most MOIs tested. Fig.4.17C shows that in the wells without IFN-γ added, there were GFP^+ cells but no obvious upregulation of HLA-DR. However, in the wells that had IFN-γ added, there were cells that had HLA-DR upregulated on their cell surface which did not have virus that had reached the phase of late gene expression, while there cells that had late viral gene expression which did not have upregulation of HLA-DR. The use of a single-tagged GFP virus (as opposed to the mCherry-GFP double-tagged virus) meant that I was unable to comment on whether there was viral entry in the cells that had upregulated HLA-DR.

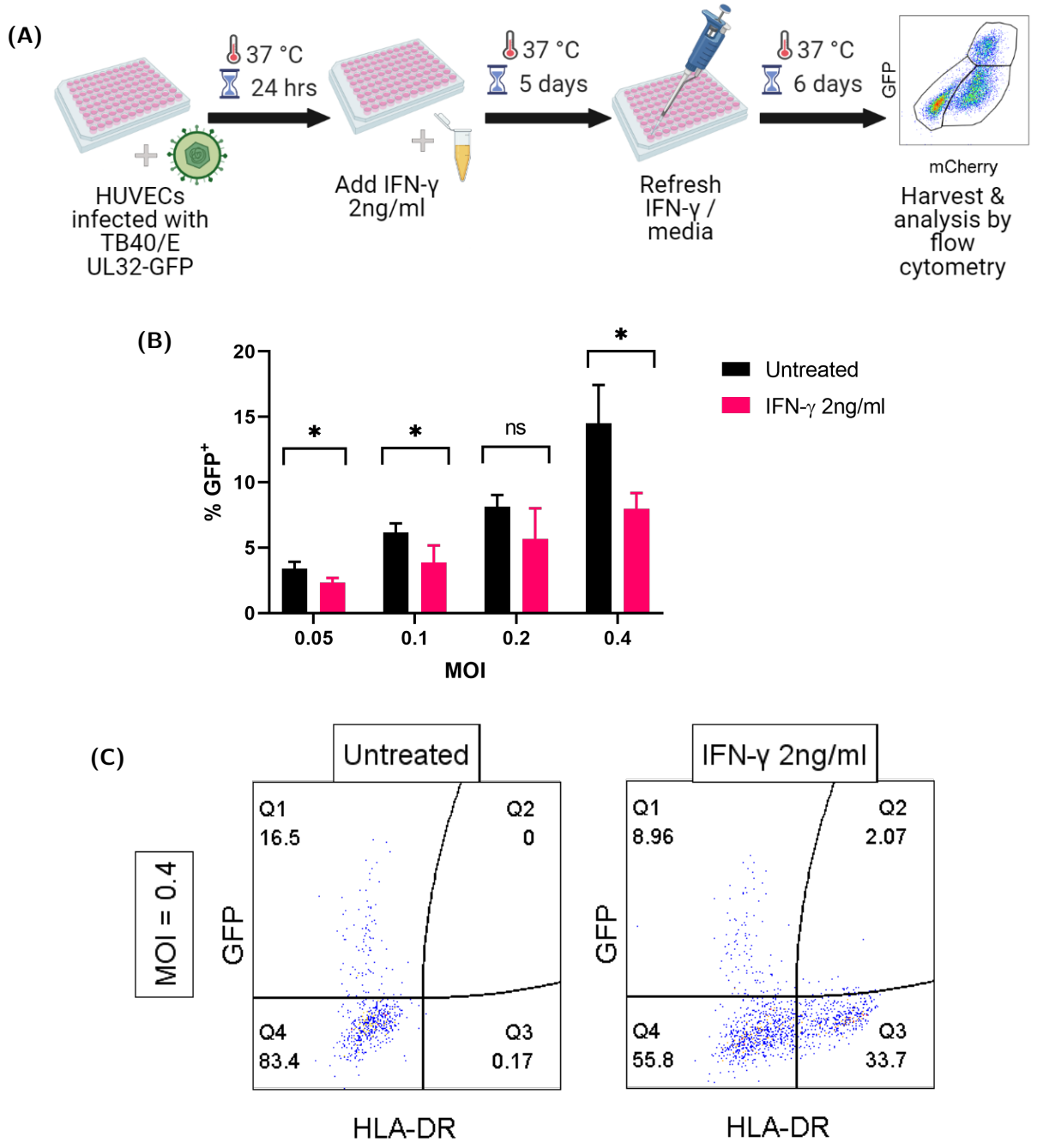

Figure 4.17: IFN-γ inhibits viral dissemination in human umbilical vein epithelial cells HUVECs were infected with TB40/E UL32-GFP virus at various MOIs as shown. 24 hours after infection, IFN-γ (2ng/ml) was added. At 6 dpi, IFN-γ was topped up by removing media in the wells and adding fresh media with IFN-γ (2ng/ml) or media was changed in the untreated controls. At 12 dpi, cells were harvested and stained for expression of HLA-DR and analysed by flow cytometry. Fig.4.17A shows experiment timeline, Fig.4.17B shows amount of GFP-expressing cells at the various MOIs at 12 dpi, and Fig.4.17C shows amount of HLA-DR and GFP expression in a flow cytometry plot of one representative MOI. Error bars represent SD of triplicate wells, statistics performed using Student's *t*-test. (*$p \leq 0.05$; ns = not significant) Fig.4.17A created at BioRender.com.

4.8 Control of viral dissemination by secretome is virustatic and not virucidal

Having shown that the "CD4 + WT" secretome is able to limit viral replication and dissemination, I next proceeded to examine if removal of the secretome restores this i.e. if the secretome was virustatic or virucidal. Primary dermal fibroblasts were infected with Merlin WT (at MOI 0.08) after seeding in 96-well plates overnight, and secretome from $CD4^+$ cells co-cultured with Merlin WT-infected autologous fibroblasts was added (at 1:4 dilution) at 1 dpi. After 6 further days of incubation, some wells with and without secretome were harvested and analysed by flow cytometry, and half of the remaining wells that were treated with secretome had a change of media, while the remaining half did not. After another 7 days' incubation, the plate was harvested and remaining wells analysed by flow cytometry.

Figs.4.18B, 4.18D and 4.18G show that at 7 dpi, wells that had secretome added had fewer cells with IE gene expression than wells that did not have secretome added. At 14 dpi, the wells that had the secretome washed off (at 7 dpi) had only a small (6.1%) increase in the amount of cells with IE CMV gene expression compared to those that did not have secretome washed off (Fig.4.18G, blue vs red lines; microscopy images in Figs.4.18C & 4.18F). However, they had a large (23%) increase in late CMV gene expression (Fig.4.18H, blue vs red lines), nearly to the same level as control wells that did not have the secretome added at all (Fig.4.18H, black line; microscopy image in Fig.4.18E). The reason for the apparent decrease in amount of IE CMV gene expression at 14 dpi in wells that did not have any secretome added (Fig.4.18G, black line) is likely because most of the cells in these wells had become infected and already progressed to late CMV gene expression by 14 dpi (Fig.4.18H, black line).

These results show that the cells that had viral entry *prior* to addition of secretome at 1 dpi are unaffected by this and continue to progress to late CMV gene expression and new virion production (Fig.4.18G & 4.18H, blue lines, 7 dpi). This explains why there is a continued increase of IE CMV gene-expressing cells (i.e. there is continued viral entry and progression to IE CMV gene expression), even in those wells that had secretome added. If the secretome is left on, the continued presence of secretome still does not prevent progression to late CMV gene expression in cells that had viral entry *prior* to addition of secretome, but prevents progression to late CMV gene expression in most of those cells that had viral entry *after* addition of the secretome. This explains why there was a continued increase in $mCherry^+GFP^-$ cells, but very little increase in $mCherry^+GFP^+$ cells in those wells that had secretome left on (Fig.4.18 & 4.18H, red lines, 14 dpi).

When the secretome was washed off, the cells that had expression of IE CMV genes were then able to progress to late CMV gene expression, leading to resumption of the viral life cycle, new virion production and continuation of viral spread. This explains the increase in both $mCherry^+GFP^-$ and $mCherry^+GFP^+$ cells at 14 dpi (Fig.4.18G & 4.18H, blue lines, 14

dpi). Taken together, these results support the conclusion that the inhibitory effect of the secretome is virustatic, but not virucidal, as washing off the secretome leads to a resumption of both IE and late CMV gene-expressing cells.

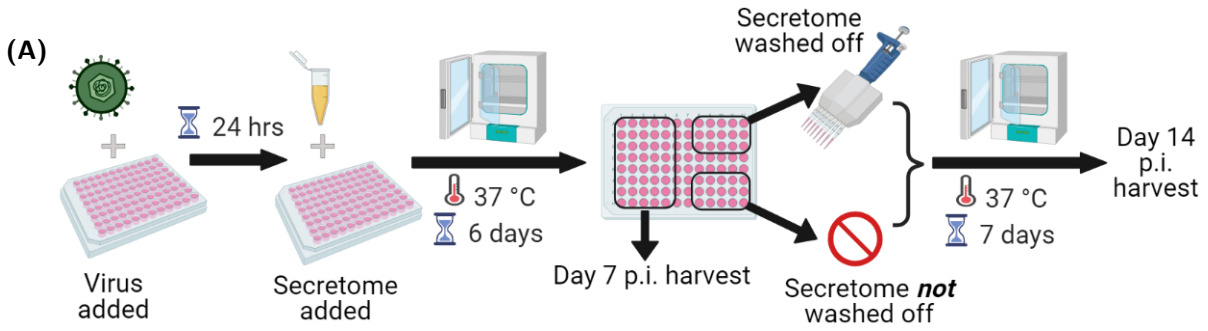

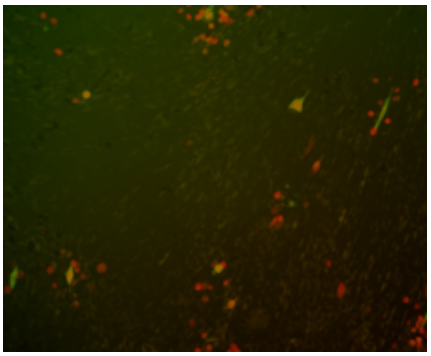

(B) At **7 dpi**, cells with secretome added

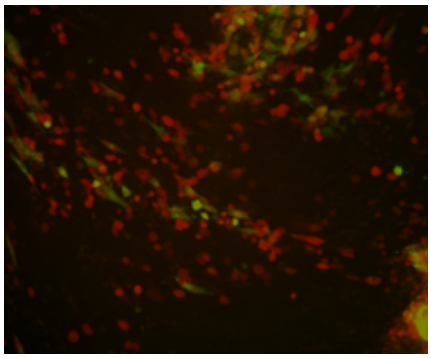

(C) At **14 dpi**, cells with secretome *not* washed off

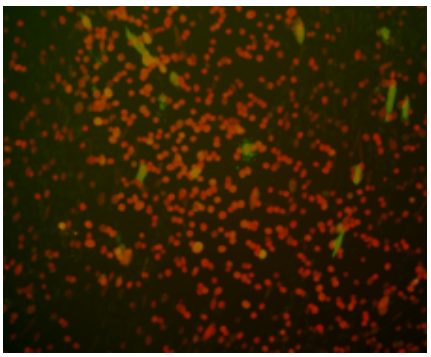

(D) At **7 dpi**, cells *without* secretome added

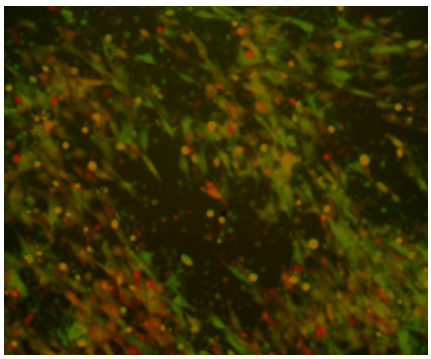

(E) At **14 dpi**, cells *without* secretome added

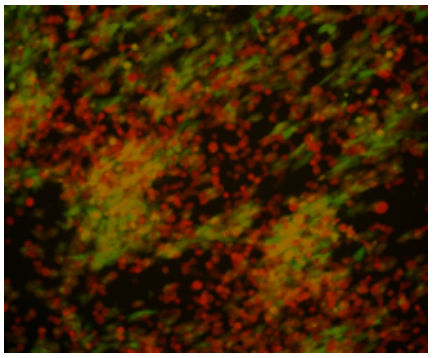

(F) At **14 dpi**, cells with secretome washed off

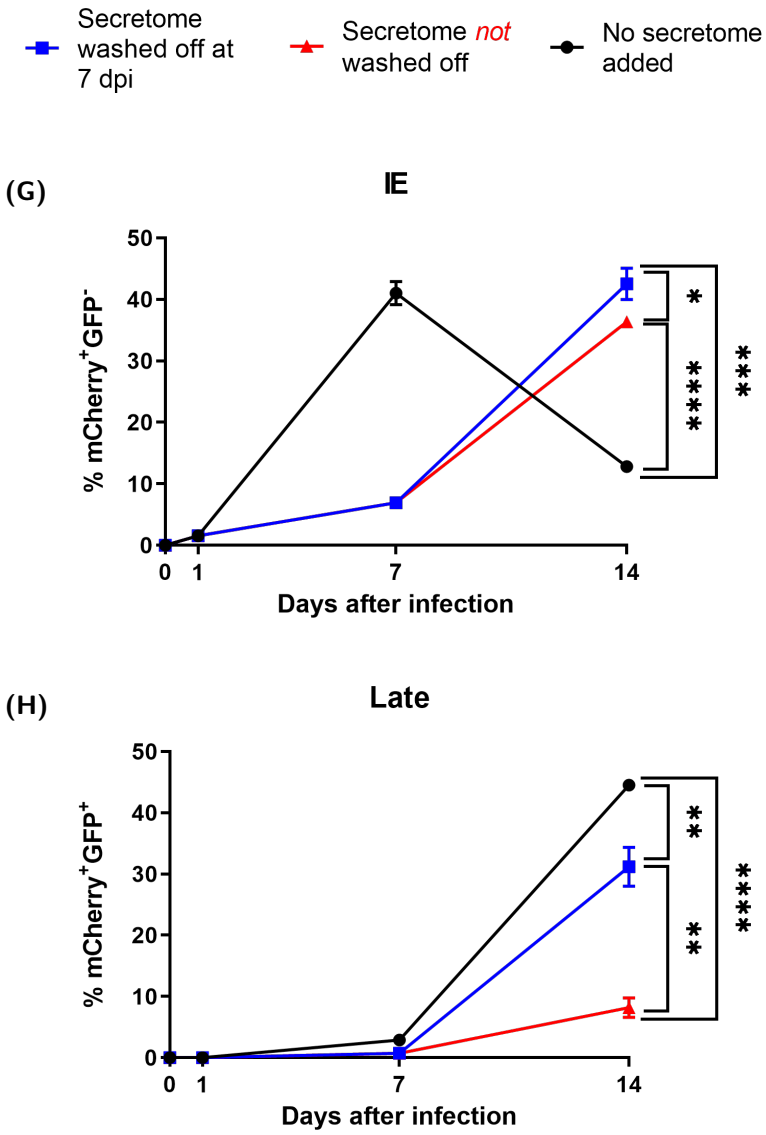

Figure 4.18: Washing off secretome allows progression of infection
Secretomes from $CD4^+$ cells co-cultured with Merlin WT-infected autologous fibroblasts are added to Merlin WT-infected fibroblasts at 1 dpi. After 6 days of incubation, some wells with and without secretome were harvested, and half of the remaining wells that had secretome added had a change of media, while the remaining half did not. After another 7 days' incubation, the remaining wells were harvested and analysed by flow cytometry. Fig.4.18A shows experiment timeline, Figs.4.18B and 4.18D show fluorescence microscopy images at 7 dpi and Figs.4.18C, 4.18E and 4.18F show images at 14 dpi of one representative replicate out of 3. Fig.4.18G shows amount of $mCherry^+GFP^-$ cells at each of the timepoints, expressed as a percentage of total cells in the well, and Fig.4.18H shows the same for $mCherry^+GFP^+$ cells. Error bars represent SD of triplicate wells, statistics performed using Student's *t*-test. (*$p \leq 0.05$; **$p \leq 0.01$; ***$p \leq 0.001$; ****$p \leq 0.0001$; ns = not significant) Fig.4.18A created at BioRender.com.

4.9 Discussion

4.9.1 Co-culture of CD4$^+$ T cells with HCMV-infected fibroblasts generates a virustatic secretome

The results presented in Chapter 3 showed that CD4$^+$ cells (isolated by positive MACS with CD4 MicroBeads) from healthy HCMV-seropositive donors were able to control IE and late CMV gene expression *in vitro*. In this chapter, I sought to determine if this means of control was exerted by secreted factors (i.e. the secretome) of these CD4$^+$ cells.

Antiviral effect of the secretome in the VDA

In the work presented in Section 4.2.2, I showed that the supernatants of PBMCs and CD4$^+$ cells that had been co-cultured with HCMV-infected fibroblasts were able to limit both IE and late CMV gene expression. It might not be surprising that the supernatants from PBMCs of HCMV-seropositive donors that had been co-cultured with HCMV-infected fibroblasts were antiviral when tested in a viral dissemination assay. These PBMCs contain CD8$^+$ and CD4$^+$ HCMV-specific memory T cells, as well as NK cells and monocytes that likely interact to provide professional antigen presentation, driving T cell responses and limiting immune evasion strategies of the virus. The observation that the supernatants of CD4$^+$ cells alone added to HCMV-infected fibroblasts is antiviral suggests that these CD4$^+$ cells have the ability to recognise HCMV-infected cells. This is able to occur despite the presence of immune evasion genes present in the "wildtype" virus used in the experiments. Given that fibroblasts do not usually express MHC Class II, which would be required to present antigen to CD4$^+$ T cells, this result along with the original observation that CD4$^+$ cells from HCMV-seropositive donors have antiviral activity is an unexpected observation.

I then showed that co-culture of immune cells with fibroblasts infected with HCMV which had deletion of US2-11 genes results in a secretome that was more antiviral than that generated by co-culture with "wildtype" virus. This would suggest that removal of the ability to downregulate MHC Class II complexes by the virus allows more antigen presentation and recognition by CD4$^+$ cells to occur, and therefore generation of a more antiviral secretome. However, it is worth noting that the increase in antiviral activity of the secretome is only marginal. A possible explanation for this observation is that the abrogation of downregulation of MHC Class II is incomplete, and the virus still retains some other MHC Class II downregulation functions. Another possibility is that, when the secretomes were made, the immune cells were added at a high E:T ratio (10 or 20:1). This would mean that co-culture with wildtype virus-infected fibroblasts would probably already lead to maximal amounts of antiviral cytokines produced, and it might have been difficult to produce any higher amounts of cytokines, even with co-cultures with ΔUS2-11 virus-infected fibroblasts. A further possibility

is that there may have been immune cells other than $CD4^+$ T cells in the cells selected by positive selection MACS with CD4 MicroBeads, which might allow antigen presentation to the $CD4^+$ T cells to occur.

Analysis of cytokines in the secretomes

The results of the multi-cytokine array and LegendPlex™ analysis of the secretomes support the observations made in the preceding section. The LegendPlex™ assay validated some of the results from the cytokine array. The LegendPlex™ assay showed that the antiviral cytokines that were found at the highest concentrations in the secretomes were IFN-γ, followed by TNF-α. These two cytokines were also found to be upregulated in the "CD4 + WT" and "CD4 + ΔUS2-11" secretomes by the cytokine array. The other antiviral cytokines found to be upregulated on the LegendPlex™ array were the type I interferons (IFN-α2 and IFN-β), and type III interferons (IFN-λ1). Unfortunately, the type I and III interferons were not on the list of cytokines that were tested by the cytokine array. However, TNF-α, IFN-α and IFN-β are all known antiviral cytokines [328, 373, 433, 510, 654], and were all shown to be able to inhibit late CMV gene expression in a viral dissemination assay done at low concentrations of approximately 50–100pg/ml in experiments done by a colleague in the group, while IFN-λ1 did not show any inhibition of viral spread on fibroblasts (Martin Potts, personal communication). The IFN-λ receptor is found mainly only on cells of epithelial origin [307, 328, 517], which would explain why no antiviral effect on fibroblasts was seen. However, the presence of IFN-γ, IFN-α2, IFN-β and TNF-α at sufficiently inhibitory concentrations in the secretome could explain the antiviral effect seen when the secretome was added to HCMV-infected fibroblasts.

Interestingly, another cytokine that was found to be upregulated on the LegendPlex™ assay was the cytokine IL-10, which has been shown to be associated with inducing immunologic tolerance and suppression of the immune response [33, 492, 560, 611]. In support of this observation, earlier publications by our group and others have also shown that HCMV-specific $CD4^+$ T cells produce IL-10 responses to HCMV peptides [105, 256, 257], and it is well-known that HCMV encodes a viral ortholog of IL-10 [306], cmvIL-10, which suppresses immune cell activation [265, 545] and induces expression of cellular IL-10 [30, 449].

The LegendPlex™ assay also showed that GM-CSF and IL-1β were upregulated in the secretome. IL-1β has been shown to inhibit HCMV growth in stromal cells [253] and HCMV has been shown to be able to activate IL-1β gene transcription [625], both of which would add to the antiviral effects of the secretome, while IL-1β is known to stimulate GM-CSF production [7, 50]. The presence of GM-CSF in the secretome could also lead to differentiation of any monocytes present into dendritic cells [249, 370], which are professional antigen-presenting cells that could activate $CD4^+$ T cells.

When the results of these earlier sections are considered together with the results in Section

4.8, it would appear that, overall, the cytokines in the secretome are not able to prevent viral entry into the cell, nor are they able to prevent progression to IE CMV gene expression. However, they are able to put the cell into an antiviral state, such that there is decreased progression to late CMV gene expression. Removal of the secretome by washing then removes these antiviral effects and allows progression of these IE CMV gene-expressing cells to late CMV gene expression.

4.9.2 Effect of deletion of US2-11 on the secretome

The US2-US11 region of the HCMV genome encodes for 4 proteins that contribute to immune evasion mechanisms of $CD4^+$ T cells by HCMV, by disruption of either MHC Class I or II assembly or transport [268, 440]. Therefore, we would expect that cells that had been infected with HCMV containing a deletion of US2-11 would not downregulate MHC Class I or II on the cell surface and should thus be able to present antigen despite infection. We would hypothesise that, in the presence of larger amounts of antigen presentation, there would be larger amounts of IFN-γ and other antiviral cytokines produced. The results in Fig.4.5 appear to support this, as the secretome from $CD4^+$ cells co-cultured with Merlin ΔUS2-11 virus appear to be able to suppress both IE and late viral gene expression to a slightly greater degree than those from $CD4^+$ cells co-cultured with Merlin WT virus. When examined for ability to induce HLA-DR, the secretome from $CD4^+$ cells co-cultured with Merlin ΔUS2-11 virus also appears to be able to induce HLA-DR expression in HUVECs to a similar degree as secretome from $CD4^+$ cells co-cultured with Merlin WT virus (Fig.4.16B). The result from the multi-analyte cytokine array also appears to support this—IFN-γ was highly upregulated in the "CD4 + ΔUS2-11" secretome compared to the "CD4 + uninf" secretome (Fig.4.7B). When quantified by the flow cytometry-based assay, Fig.4.10 shows that the amount of IFN-γ in the "CD4 + ΔUS2-11" secretome was similar to that found in the "CD4 + WT" secretome, although it is worth noting that the amounts of IFN-γ detected approached the upper limits of the assay and thus differences in the amount of IFN-γ between the secretomes may not have been able to be detected.

4.9.3 The role of IFN-γ in the secretome

IFN-γ was found to be one of the most upregulated cytokines in the secretomes of $CD4^+$ cells co-cultured with HCMV-infected fibroblasts. In this chapter, I have also investigated the effects of adding IFN-γ to HCMV-infected fibroblasts. IFN-γ was added at 1 dpi post-infection, but the amount of IE CMV gene-expressing cells was only marginally different to the amount of IE CMV gene-expressing cells in HCMV-infected fibroblasts that did not have IFN-γ added. This suggests that IFN-γ is unable to prevent viral entry into cells and that viral gene expression could take place, at least for IE and UL36 genes.

The continued increase in amount of IE CMV gene-expressing cells at each timepoint would suggest that there is a persistent source of viral replication producing fresh virions that infect the cells. However, wells that had IFN-γ added did not have an increase in the amount of late CMV gene-expressing cells (and therefore, by implication, infected cells producing new virions) beyond the initial amount that was seen at the 3 days post-infection timepoint. The source of this persistent viral replication is therefore likely to be these late CMV gene-expressing cells that had been infected during the initial 24 hours pre-addition of IFN-γ. This would suggest that IFN-γ is unable to arrest progression to late CMV gene expression and productive infection once viral entry and progression to IE CMV gene expression has occurred. Thus, IFN-γ is not able to prevent viral entry to an uninfected cell, nor progression to late gene expression in a cell that has undergone viral entry, but it is able to prevent progression to late CMV gene expression in a cell that has not yet had viral entry.

Interferon-γ mediates its effects via the IFN-γ receptor, which leads to IFN-γ-stimulated gene (ISG) transcription and CIITA gene transcription [279,510]. Transcription of ISGs leads to myriad downstream antiviral effects of IFN-γ, which include (but are not limited to) expression of antiviral mediators such as PKR (IFN-induced, RNA-activated protein kinase) which can interfere with protein translation [283,495], ISG15 (interferon-stimulated gene 15 kDa protein) which can be conjugated to target viral proteins [141,536], and Viperin, which interferes with viral assembly and egress [372]. Viperin was initially identified in human primary macrophages stimulated with IFN-γ and in fibroblasts infected with HCMV [101,660]. The overall effect of addition of IFN-γ on a cell that has not yet had CMV entry in the VDA appears to be insufficient to completely prevent expression of IE genes, but sufficient to prevent progression to late CMV gene expression. This is supported by the data in Fig.4.12, where even at supra-physiologic doses of IFN-γ (6000pg/ml), there was still the presence of mCherry^{+}GFP^{-} cells, but the amount of mCherry^{+}GFP^{-} did decrease with increasing doses of IFN-γ.

That IFN-γ is unable to prevent viral entry into an uninfected cell is perhaps unsurprising, as viral entry occurs via attachments of the pentamer complex to heparan sulphate proteoglycans on the cell surface [110,287], which IFN-γ would be unable to interfere with. After viral entry, however, HCMV encodes multiple immune evasion genes that can counteract the effects of IFN-γ: UL23, which binds to the STAT effector protein N-myc [157]; UL31, which binds cGAS and results in inhibition of interferon-associated gene transcription [242]; and UL82 (pp71), which can inhibit Stimulator of Interferon Genes (STING) [175]. The kinetics of pUL23 are not fully determined but it arises from the pUL22 family, which is expressed at early times (24h) post-infection [395]. UL31 was previously reported to be a late protein of HCMV [635], but the presence of pUL31 has also been detected as early as 6 hours post-infection [242], while pp71 is a tegument protein which activates viral immediate-early transcription and has a role in initiating lytic infection [280]. In a fibroblast that had been induced into an antiviral state by IFN-γ *prior* to CMV entry, it is unclear which of these genes had been expressed.

Ultimately, however, the action of these IFN-γ-evasion genes and their products are still unable to overcome the effects of IFN-γ in the secretome, if at least only temporarily. Nonetheless, upon washing off the secretome (and therefore removal of IFN-γ), HCMV in these cells are then able to express these genes and progress to late CMV gene expression.

Following on from this, an additional experiment could have been to sort for mCherry^{+}GFP^{-} fibroblasts, from conditions with and without IFN-γ added, and possibly perform PCR analyses or RNA sequencing analysis, in order to determine if these IFN-γ genes had been expressed and were ineffective, and also to find out specifically where in the viral life cycle these mCherry^{+}GFP^{-} cells had been "halted" while in the presence of extracellular IFN-γ or secretome.

4.9.4 Questions that remain

It still remains unexplained how CD4^{+} cells are able to recognise virus-infected fibroblasts. IFN-γ is produced as a result of activation of CD4^{+} T cells, which occurs with antigen presentation, but IFN-γ is required to induce MHC Class II complexes in the first place, so it is still unclear where the source of this initial IFN-γ is. The presence of other types of interferons (i.e. type I and type III interferons) would suggest that there were other immune cell types in the CD4^{+} cell population, as these cytokines are not typically produced by antigen-specific T cells. A known cell type which produces large amounts of type I interferons in response to viral infections is pDCs [563], which have been shown to respond to HCMV-infected cells by secretion of large amounts of IFN-α [318, 657]. Other possible antigen presenting cells are monocytes [259], which, in the presence of GM-CSF and IL-4 in the secretome, could differentiate into monocyte-derived dendritic cells, which have also been shown to be able to present antigen via MHC Class II pathways [166, 305, 612].

Chapter 5

How do CD4$^+$ T cells recognise HCMV-infected fibroblasts and exert their antiviral effect?

5.1 Introduction

The data presented in Chapter 3 demonstrated that PBMCs, CD4$^+$ cells, and CD8$^+$ T cells from HCMV-seropositive donors are able to limit IE and late CMV gene expression to varying degrees. As discussed in the Introduction, (Sections 1.2.1–1.2.2), antigen presentation to CD4$^+$ T cells via the MHC Class II pathway induces CD4$^+$ T cell activation, and cytokines present in the microenvironment then influence differentiation into the various CD4$^+$ T cell subsets. This mechanism explains how CD4$^+$ T cells could contribute to limiting viral dissemination when PBMCs are added to the viral dissemination assay—the presence of antigen-presenting cells in the PBMCs added to the assay, such as CD14$^+$ monocytes and dendritic cells, can process and present antigens to CD4$^+$ T cells, while the presence of IFN-γ-producing cells in PBMCs, such as CD8$^+$ T cells and NK cells, can induce MHC Class II on fibroblasts in order that they may process and present HCMV antigens to HCMV-specific CD4$^+$ T cells. However, it fails to explain how isolated CD4$^+$ cells co-cultured with HCMV-infected fibroblasts can recognise the infected cells in order to mediate their effector function, as there is no obvious mechanism for MHC Class II presentation and thus MHC Class II upregulation in order to drive this control over viral spread, such as was observed in Fig.3.18.

In Chapter 4, I showed that the secretome generated by these CD4$^+$ cells was virustatic, and that IFN-γ in the secretome was at least partly responsible for this effect. IFN-γ is the canonical cytokine produced by CD4$^+$ T_h1 cells in response to activation following antigen presentation [5,290,400,562]. This demonstrates one mechanism of how the CD4$^+$ cells added to the assay could have exerted their antiviral effects, but it still did not explain how IFN-γ production was initiated in the absence of antigen presenting cells when CD4$^+$ cells were added

to the VDA.

In order to obtain optimal numbers of $CD4^+$ and $CD8^+$ T cells and NK cells from a single defrosted sample of PBMCs, positive selection with MACS columns by CD4 MicroBeads was used to isolate $CD4^+$ cells when performing the viral dissemination assays on healthy HCMV-seropositive and HCMV-seronegative donors in Chapter 3. CD4 MicroBeads (Miltenyi) consist of MicroBeads conjugated to monoclonal anti-human CD4 antibodies. However, the CD4 marker is not only found on $CD4^+$ T cells, but also on $CD4^+CD8^+$ T cells, monocytes [292], dendritic cells [260, 432] (both plasmacytoid DCs and conventional/myeloid DCs), and a small number of neutrophils [60], $CD34^+$ progenitor cells [363, 658], and NK cells [51]. The $CD4^+$ T cell Isolation Kit (Miltenyi) utilises a cocktail of biotin-conjugated monoclonal antibodies against CD8a, CD14, CD15, CD16, CD19, CD36, CD56, CD123, TcRγ/δ and CD235a and secondary anti-biotin and anti-CD61 antibodies conjugated to MicroBeads to remove these cell populations to leave behind a "pure" $CD4^+$ T cell population.

In this chapter, I first examined if the antiviral effect of adding $CD4^+$ cells to HCMV-infected cells was mediated by IFN-γ and the resultant MHC Class II expression. Then, to investigate the differences between cell populations obtained using CD4 MicroBeads and those obtained using the $CD4^+$ T cell Isolation Kit, I performed phenotyping analyses on these populations. To investigate if there were functional differences between these two populations, I then added the cell populations obtained using these two different methods to the viral dissemination assay.

5.2 Effects of $CD4^+$ cells on HCMV-infected fibroblasts are at least partially mediated by IFN-γ

5.2.1 MHC Class II is induced on uninfected cells exposed to $CD4^+$ cells, which is abrogated by blocking IFN-γ

In the previous chapter I showed that IFN-γ in the secretome of $CD4^+$ co-cultured with HCMV-infected fibroblasts was at least partially responsible for the antiviral effects of the secretome. I also showed that addition of IFN-γ to uninfected fibroblasts led to upregulation of MHC Class II on the cell surface, while addition of IFN-γ to HCMV-infected fibroblasts did not prevent viral entry, but could prevent progression to late CMV gene expression in cells that had not been prior-infected. I next wanted to examine if addition of $CD4^+$ cells would also lead to upregulation of MHC Class II, and whether addition of anti-IFN-γ antibody would neutralise this effect. To address this, primary dermal fibroblasts from an HCMV-seropositive donor were infected with Merlin WT virus (MOI = 0.04) after seeding overnight in a 96-well plate. At 1 dpi, $CD4^+$ cells were isolated by positive selection on MACS with anti-CD4 MicroBeads and were added to the virus-infected autologous fibroblast cultures at E:T ratios of 3, 1.5 or

0.75:1, with or without anti-IFN-γ antibody (at 10μg/ml). The plate was then incubated for a further 7 days before harvest, staining for HLA-DR expression and analysis by flow cytometry.

Fig.5.1A shows a representative FACS plot of a well with $CD4^+$ cells added at E:T ratio of 1.5:1, and the gating strategy used to obtain $mCherry^-GFP^-$, $mCherry^+GFP^-$ and $mCherry^+GFP^+$ sub-populations. The amount of surface HLA-DR expression is highest on the $mCherry^-GFP^-$ (uninfected) sub-population of cells (blue histogram), but this is downregulated following CMV infection and expression of $mCherry^+GFP^-$ (red histogram), and eventually as late phase gene expression is reached (green histogram), surface expression of HLA-DR is almost completely absent, as evidenced by this sub-population showing amounts of fluorescence similar to that seen in unstained samples (grey histogram).

Figs.5.1C, 5.1D & 5.1E show the amounts of IE and late CMV gene-expressing cells when $CD4^+$ cells were added to HCMV-infected cells at E:T ratios of 0.75:1, 1.5:1 and 3:1 (solid red and green bars), and when $CD4^+$ cells and anti-IFN-γ antibody were added to the wells (outlined pink and pale green bars). Fig.5.1F shows the amounts of surface HLA-DR expression on the uninfected (i.e. $mCherry^-GFP^-$) population of cells from the same wells.

These results show that $CD4^+$ cells were able to limit IE CMV gene expression in an E:T-dependent manner when added to HCMV-infected cells (solid red bars). When anti-IFN-γ antibody was added to the wells, this effect was completely abrogated at the E:T ratios of 0.75:1 and 1.5:1, and was partially abrogated (to approximately 50%) at the higher E:T ratio of 3:1 (pink outlined bars). For late CMV gene expression, there was also an E:T-dependent limitation of late CMV gene expression (solid green bars), and addition of anti-IFN-γ antibody tended to increase the frequency of cells expressing the late CMV gene UL32, particularly at E:T ratios of 1.5:1 and 0.75:1, although the differences were not statistically significant (outlined pink bars). When these fibroblasts were stained for HLA-DR expression (Fig.5.1F), the results show that the amount of surface HLA-DR on the $mCherry^-GFP^-$ populations in these wells increases with increasing E:T ratio (red histograms). When anti-IFN-γ antibody was added to the wells, this upregulation was removed (blue histograms).

Three conclusions can be drawn from this experiment: (1) addition of $CD4^+$ cells to autologous HCMV-infected fibroblasts can induce MHC Class II expression on the uninfected sub-population of fibroblasts in the same well; (2) the greatest downregulation of MHC Class II complexes occurs on cells that have progressed to late CMV gene expression—i.e. cells that have been infected for the longest duration; (3) addition of anti-IFN-γ antibodies abrogates the control of IE and late CMV gene expression that $CD4^+$ cells exert on HCMV-infected cells, and also prevents MHC Class II upregulation induced by these $CD4^+$ cells.

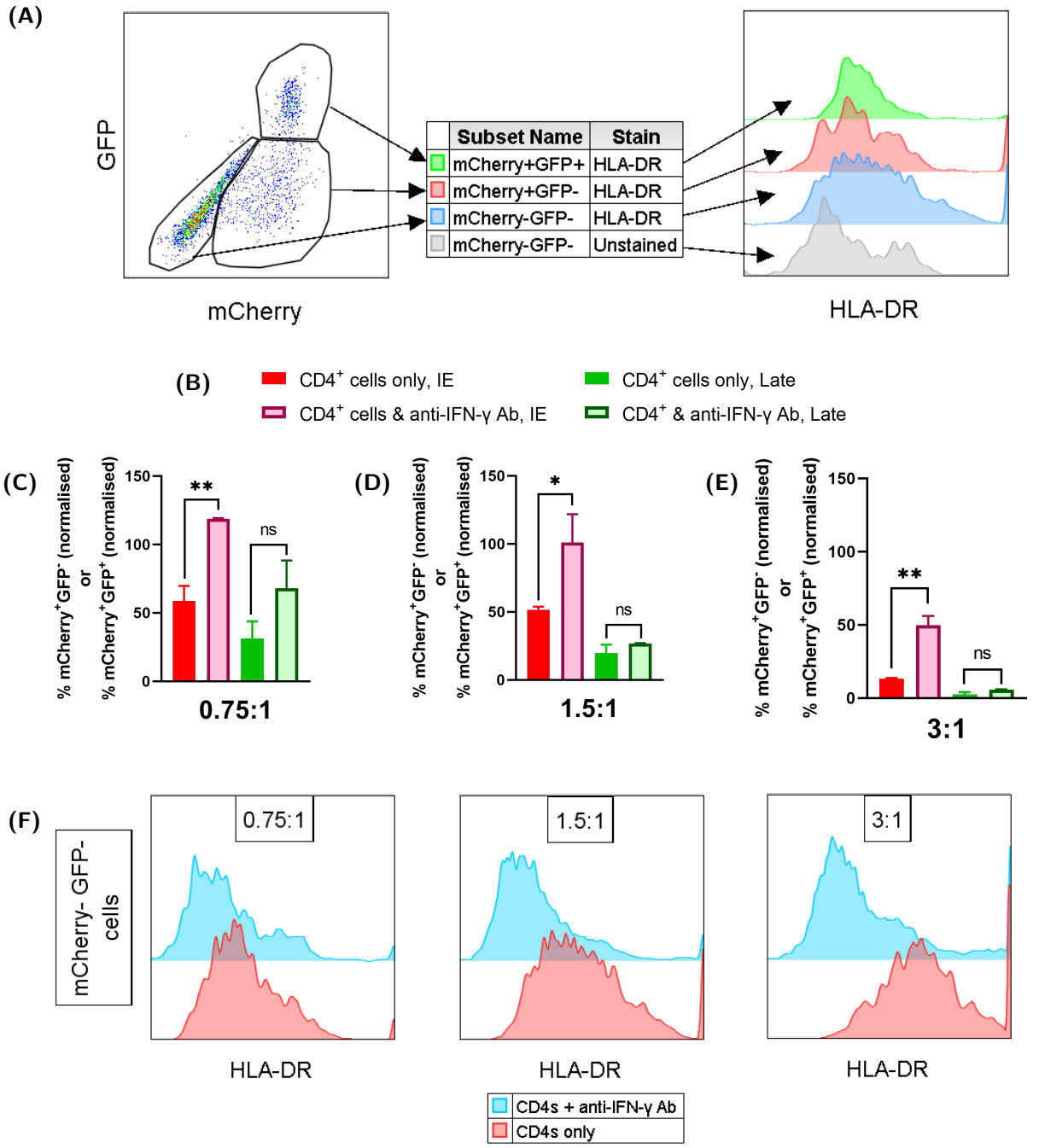
(A)
GFP
mCherry
Subset Name
Stain
mCherry+GFP+
HLA-DR
mCherry+GFP-
HLA-DR
mCherry-GFP-
HLA-DR
mCherry-GFP-
Unstained
HLA-DR
(B)
CD4+ cells only, IE
CD4+ cells & anti-IFN-γ Ab, IE
CD4+ cells only, Late
CD4+ & anti-IFN-γ Ab, Late
(C)
% mCherry+GFP- (normalised) or % mCherry+GFP+ (normalised)
150
100
50
0
**
ns
0.75:1
(D)
% mCherry+GFP- (normalised) or % mCherry+GFP+ (normalised)
150
100
50
0
*
ns
1.5:1
(E)
% mCherry+GFP- (normalised) or % mCherry+GFP+ (normalised)
150
100
50
0
**
ns
3:1
(F)
mCherry- GFP- cells
0.75:1
1.5:1
3:1
HLA-DR
HLA-DR
HLA-DR
CD4s + anti-IFN-γ Ab
CD4s only

Figure 5.1: Surface expression of HLA-DR is upregulated by addition of autologous CD4$^+$ cells to autologous infected fibroblasts, which is blocked by addition of anti-IFN-γ antibody
Primary dermal fibroblasts were infected with Merlin WT (MOI = 0.04). At 1 dpi, autologous CD4$^+$ cells were obtained from defrosted PBMCs by MACS positive selection and added at E:T ratios of 3, 1.5, and 0.75:1, either with or without anti-IFN-γ antibody (10μg/ml), then incubated for a further 7 days before harvest and staining for HLA-DR. Fig.5.1A shows the gating strategy to obtain mCherry$^-$GFP$^-$, mCherry$^+$GFP$^-$ and mCherry$^+$GFP$^+$ sub-populations from a sample well with CD4$^+$ cells added to infected fibroblasts at an E:T ratio of 1.5:1, and histograms of the amount of HLA-DR expressed on mCherry$^-$GFP$^-$ (blue histogram), mCherry$^+$GFP$^-$ (red histogram) and mCherry$^+$GFP$^+$ (green histogram) sub-populations in the same well, with histogram of an mCherry$^-$GFP$^-$ sub-population from an unstained well with CD4$^+$ cells added at 1.5:1 for comparison (grey histogram). Figs.5.1C–5.1E show amount of IE and late CMV gene expression in wells with or without anti-IFN-γ antibodies added, at E:T ratios of 0.75, 1.5 and 3:1 respectively, expressed as a percentage of cells in same phase of CMV gene expression in infected controls. Legend for these graphs is given in Fig.5.1B. Fig.5.1F shows the amount of HLA-DR in the uninfected (mCherry$^-$GFP$^-$) sub-populations of cells in the same wells as those in Figs.5.1C–5.1E. Error bars represent SD of triplicate wells, statistics performed using Student's *t*-test. (*$p\leq0.05$; **$p\leq0.01$; ***$p\leq0.001$; ****$p\leq0.0001$; ns = not significant)

5.2.2 Blocking of MHC class II and interferon-γ limits the antiviral effects of CD4$^+$ cells on HCMV-infected fibroblasts

IFN-γ exerts its antiviral effects via a number of mechanisms [279], which includes induction and upregulation of MHC Class II expression. Having shown that addition of anti-IFN-γ antibodies abrogated the effect of MHC Class II upregulation on uninfected cells and increased the frequency of IE and late CMV gene-expressing cells, I wanted to examine if blocking of MHC Class II would also lead to an increase in the frequency of cells expression IE and late CMV genes. Blocking of MHC Class II should, in theory, prevent antigen presentation to CD4$^+$ cells and the downstream effects of this, but it would still allow the other pathways by which IFN-γ exerts its antiviral effects to occur.

Primary dermal fibroblasts were seeded overnight in 96-well plates at 20,000 cells per well, then infected with Merlin WT virus (MOI $= 0.04$). At 1 dpi, autologous PBMCs were defrosted and CD4$^+$ cells were isolated by MACS using positive selection beads. They were then added to the HCMV-infected fibroblasts alone, or with anti-MHC class II antibody (50μg/ml), anti-IFN-γ antibody (2μg/ml), or isotype control antibody (10μg/ml) at E:T ratios of 2.5:1, 1.25:1, 0.6:1 and 0.3:1. After a further incubation of 7 days, harvest and analysis by flow cytometry was performed. The results show that blocking of MHC class II (Fig.5.2B, pink bars) or IFN-γ (Fig.5.2B, teal bars) by blocking antibodies reduces the amount of inhibition of both IE and late CMV gene expression by CD4$^+$ cells (Fig.5.2B, black bars) at almost all E:T ratios tested, while addition of isotype control antibody (Fig.5.2B, purple bars) did not reduce the amount of inhibition of both IE and late CMV gene expression by CD4$^+$ cells. However, as the E:T ratio increases, the percentage of inhibition by the blocking antibodies decreases.

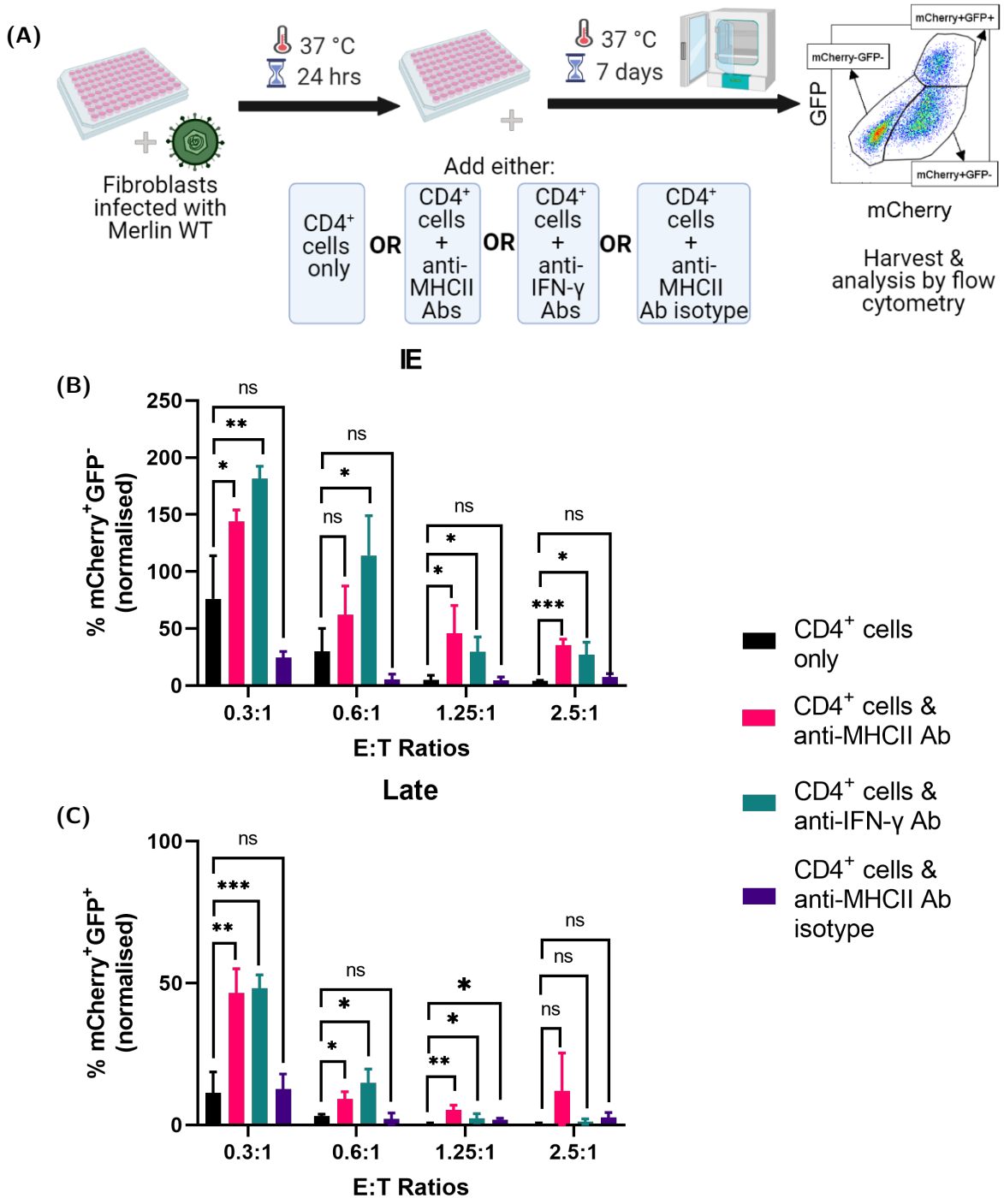

Figure 5.2: Blocking of MHC Class II and interferon-γ limits antiviral effects of CD4$^+$ cells on HCMV-infected fibroblasts

Primary dermal fibroblasts from a HCMV-seropositive donor were infected with Merlin WT HCMV. At 1 dpi, CD4$^+$ cells from the autologous donor's PBMCs were obtained by positive selection MACS. These CD4$^+$ cells were then either added alone, or with anti-MHC class II antibody, or anti-IFN-γ antibody, or isotype to anti-MHC class II antibody. At 8 dpi, cells were harvested and analysed by flow cytometry. Fig.5.2A shows experiment timelines, Fig.5.2B shows amount of cells in IE CMV gene expression, and Fig.5.2C shows amount of cells in late CMV gene expression, expressed as a percentage of the amount of cells in the same phase of CMV gene expression in infected controls. Error bars represent SD of triplicate wells, statistics performed using Student's *t*-test. (*$p \leq 0.05$; **$p \leq 0.01$; ***$p \leq 0.001$; ****$p \leq 0.0001$; ns = not significant) Fig.5.2A created at BioRender.com.

5.3 $CD4^+$ cell populations isolated by magnetic-activated cell sorting using positive selection contain a population of $CD4^+CD3^-$ cells, which are not found in $CD4^+$ T cell populations isolated by depletion

As mentioned in the introduction to this chapter, the CD4 molecule is expressed by other cell types in PBMCs besides $CD4^+$ T cells. I thus wanted to see if $CD4^+$ cell populations isolated by positive selection MACS using CD4 MicroBeads contained any of these immune cells. Cell separations by positive selection MACS with CD4 MicroBeads and by depletion MACS with a $CD4^+$ T cell Isolation Kit were performed on PBMCs obtained from a healthy donor as described in Section 2.12. The cell populations obtained were then stained with an antibody mix containing fluorophore-conjugated antibodies to CD45, CD3 and CD4. (Methods detailed in Section 2.4.) The top row of Fig.5.3A shows flow cytometry plots of the cell populations obtained using MACS positive selection with CD4 MicroBeads, and the bottom row shows the flow cytometry plots of the cell populations obtained using MACS depletion with $CD4^+$ T cell Isolation Kit on the same donor. Comparing the rightmost plots in these 2 rows, it can be seen that cells isolated by positive selection using CD4 MicroBeads contained a population of cells that were $CD3^-CD4^+$ (outlined in red), whereas this was absent in cells isolated using the $CD4^+$ T cell Isolation Kit (outlined in green). Fig.5.3B shows a repeat of this experiment performed on another donor, where the same population of cells was seen, albeit to a smaller degree, likely because fewer cells had been used for staining. In addition, there were also smaller populations of cells that were $CD4^-$ (Fig.5.3A, rightmost plot, lower two quadrants). Some of these were $CD3^+$ and a smaller proportion were $CD3^-$. The $CD3^+$ population could possibly be $CD8^+$ T cells that had come through the selection. It is worth noting that these populations were also present in the second donor, and thus is likely related to efficiency of magneting cell sorting by the MACS columns.

(A) Donor 1

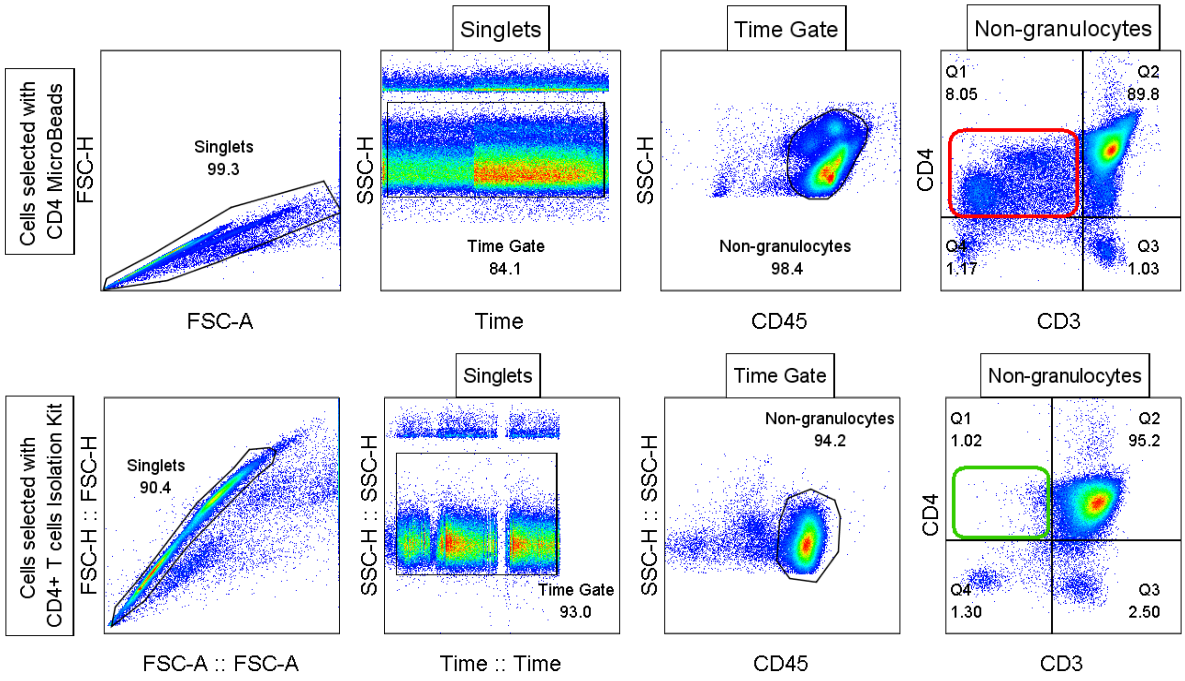

(B) Donor 2

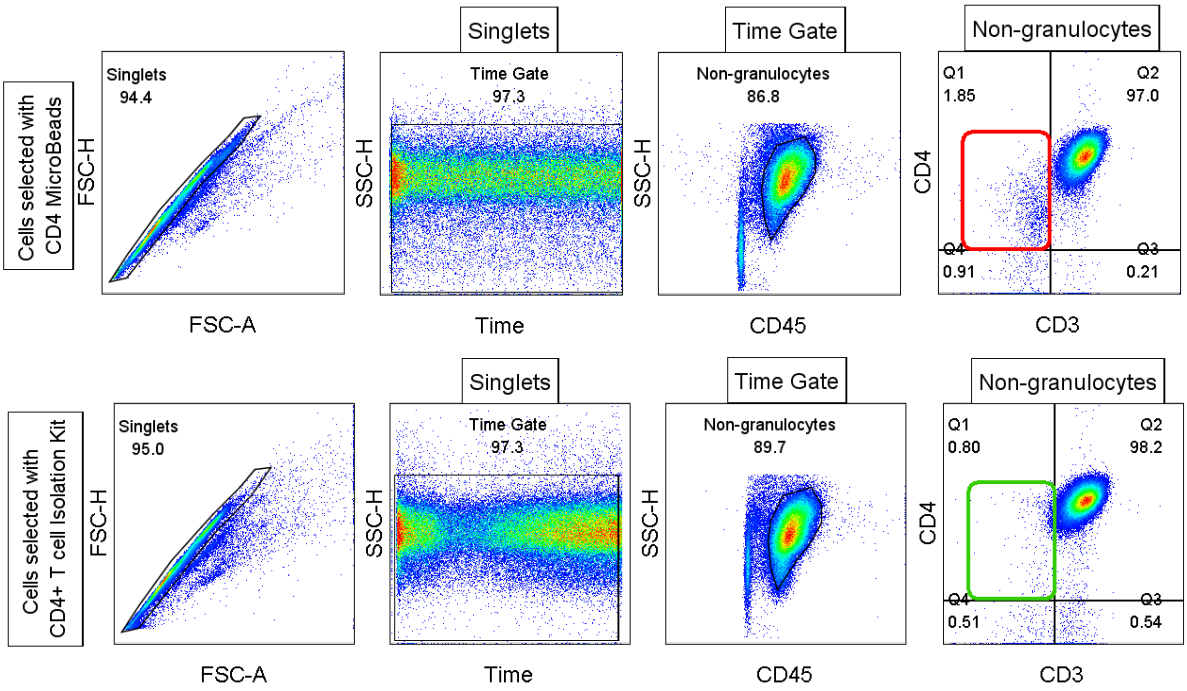

Figure 5.3: Comparing immune cell populations isolated by magnetic-activated cell sorting using positive selection with CD4 MicroBeads to those isolated by depletion with CD4$^+$ T cell Isolation Kit

Fig.5.3A: Cell populations obtained from PBMCs of a healthy donor by MACS using positive selection with CD4 MicroBeads (top row) and by MACS using depletion with the CD4$^+$ T cell Isolation Kit (bottom row) were stained with antibodies to CD45, CD3, CD4, CD14 and CD16. From left to right, first column shows gating strategy to identify singlets, second column shows time gate to eliminate readings from poor flow, third column shows gate to identify non-granulocytes, and fourth column shows non-granulocyte population stained for amount of CD3 and CD4 expression. Fig.5.3B shows the same from another donor.

5.4 Cells selected by depletion MACS with CD4$^+$ T cell Isolation Kit show poor control of IE and late CMV gene expression

Section 5.3 showed that there was a population of CD4$^+$CD3$^-$ cells present in cells selected by positive selection MACS with CD4 MicroBeads that was not present in cells selected by depletion MACS with CD4$^+$ T cell Isolation Kit. I therefore wondered if this population of cells was responsible for the ability of CD4$^+$ cells to recognise HCMV-infected cells in the viral dissemination assay. First, I needed to examine if CD4$^+$ T cells selected by MACS depletion were able to limit IE and late CMV gene expression in the VDA.

Primary dermal fibroblasts from a healthy HCMV-seropositive donor were seeded on 96-well half-area plates and grown to confluency overnight before infection with Merlin WT (MOI = 0.27) virus. At 1 dpi, PBMCs from the autologous donor were defrosted, treated with DNase and rested before being split into 2 aliquots. One aliquot underwent MACS by positive selection with CD4 MicroBeads, and the other aliquot underwent MACS depletion with CD4$^+$ T cell Isolation Kit. Fig.5.4A shows the gating strategy to determine the post-separation purities of each of these populations. Consistent with the data seen in Section 5.3, cells selected by positive selection MACS with CD4 MicroBeads contained a population of CD3$^-$ cells (middle row, middle column, solid red arrow) that was absent in the cells selection by depletion MACS with the CD4$^+$ T cell Isolation Kit (bottom row, middle column, broken green arrow). The CD4$^+$ cells and CD4$^+$ T cells were then added to the Merlin WT-infected fibroblasts at a starting E:T ratio of 10:1, followed by halving dilutions. Plates were incubated for 7 days before harvest and analysis by flow cytometry. The results in Fig.5.4 show that cells selected with CD4$^+$ T cell Isolation Kit had much worse control of both IE (Fig.5.4B) and late (Fig.5.4C) CMV gene expression than cells isolated with CD4 MicroBeads at most E:T ratios tested.

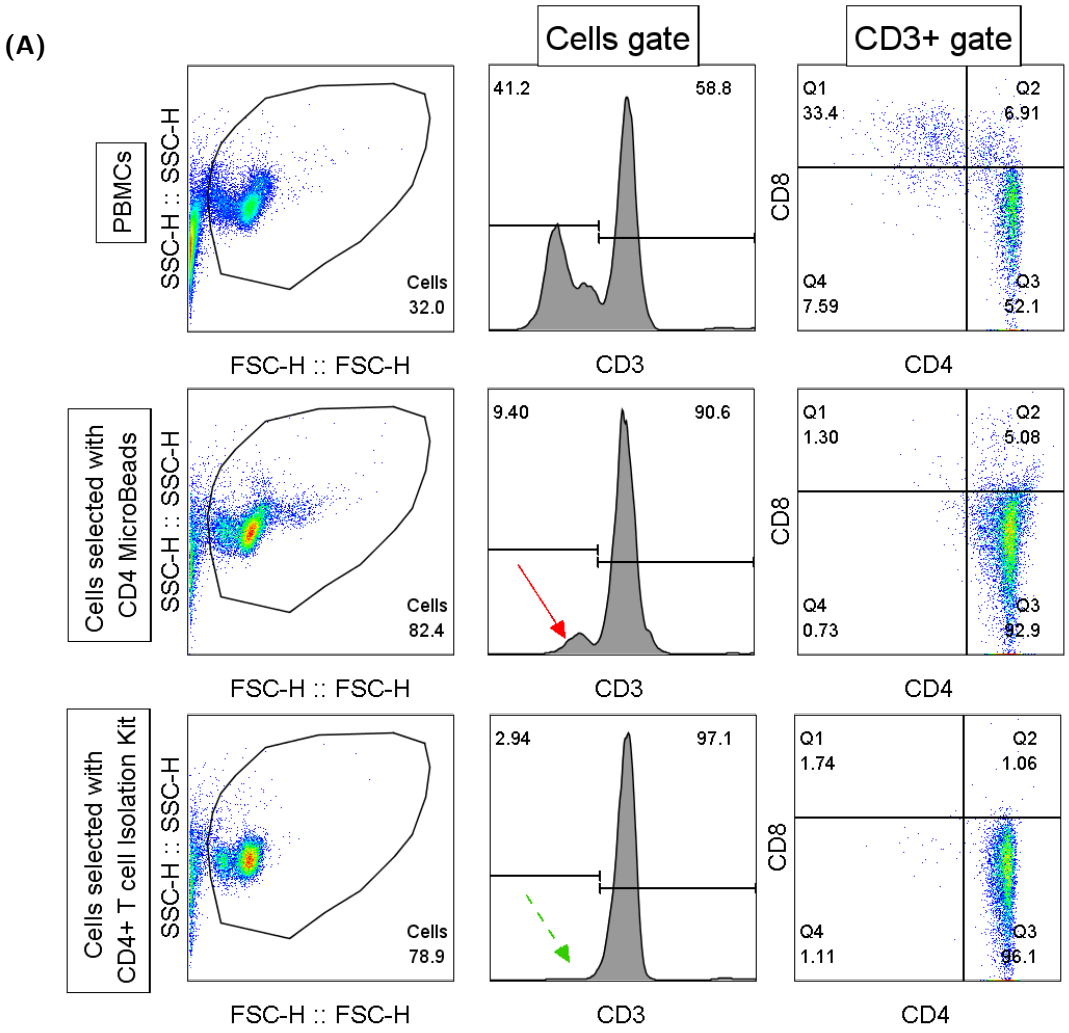
(A)
Cells gate
CD3+ gate
PBMCs
SSC-H :: SSC-H
FSC-H :: FSC-H
Cells
32.0
41.2
58.8
CD3
CD8
CD4
Q1
33.4
Q2
6.91
Q4
7.59
Q3
52.1
Cells selected with CD4 MicroBeads
Cells
82.4
9.40
90.6
Q1
1.30
Q2
5.08
Q4
0.73
Q3
92.9
Cells selected with CD4+ T cell Isolation Kit
Cells
78.9
2.94
97.1
Q1
1.74
Q2
1.06
Q4
1.11
Q3
96.1

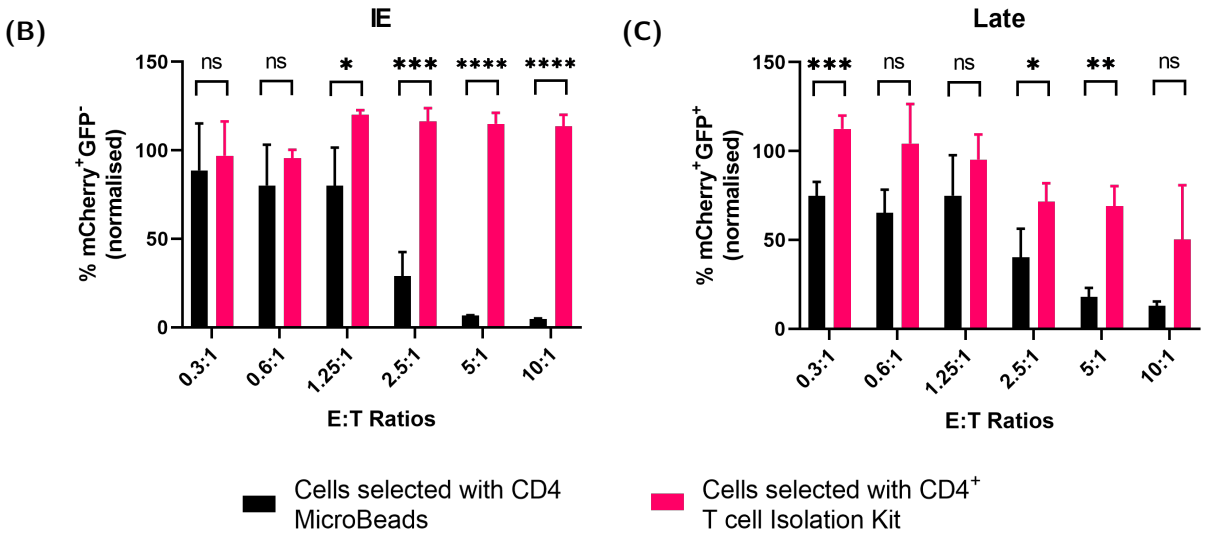
(B)
IE
(C)
Late
% mCherry+GFP- (normalised)
150
100
50
0
ns
ns
*
***
****
****
***
ns
ns
*
**
ns
0.3:1
0.6:1
1.25:1
2.5:1
5:1
10:1
E:T Ratios
Cells selected with CD4 MicroBeads
Cells selected with CD4+ T cell Isolation Kit

Figure 5.4: Cells selected by depletion MACS with CD4$^+$ T cell Isolation Kit show poor control of IE and late CMV gene expression
Primary dermal fibroblasts from a healthy HCMV-seropositive donor were seeded on 96-well half-area plates and grown to confluency overnight before infection with Merlin WT (MOI = 0.27) virus. At 1 dpi, PBMCs from the autologous donor were defrosted, treated with DNase and rested before being split into 2 aliquots. One aliquot underwent MACS by positive selection with CD4 MicroBeads, and the other aliquot underwent MACS depletion with CD4$^+$ T cell Isolation Kit. Fig.5.4A shows the gating strategy to determine the post-separation purities of each of these populations. Each of these populations were then added to the Merlin WT-infected fibroblasts at a starting E:T ratio of 10:1, followed by halving dilutions. Plates were incubated for 7 days before harvest and analysis by flow cytometry. Fig.5.4B shows amount of IE CMV gene expression and Fig.5.4C shows amount of late CMV gene expression in the wells. Error bars represent SD of triplicate wells, statistics performed using Student's *t*-test. (*$p \leq 0.05$; **$p \leq 0.01$; ***$p \leq 0.001$; ****$p \leq 0.0001$; ns = not significant)

5.5 Identification of immune cell populations isolated by positive selection on MACS with CD4 Microbeads

The difference in ability to control IE and late CMV gene expression between CD4$^+$ cells selected with CD4 MicroBeads and CD4$^+$ T cells selected with the CD4$^+$ T cell Isolation Kit led me to question what the CD3$^-$CD4$^+$ cells found in the former population are. As noted in the introduction to this chapter, besides CD4$^+$ T cells, the CD4 molecule is also expressed on multiple other peripheral blood cells, such as monocytes [292], dendritic cell subsets [260, 432], neutrophils [60], CD34$^+$ progenitor cells [363, 658], and NK cells [51]. However, of note, after CD4$^+$ T cells, the type of immune cells that most highly express the CD4 molecule are plasmacytoid dendritic cells and monocytes [592]. I therefore decided to perform phenotyping analyses on CD4$^+$ cells selected with CD4 MicroBeads with a panel of antibodies specific for CD3, CD4, CD45, CD14, CD16, CD11c, CD303, CD123, and HLA-DR. Details of the antibody-fluorophore combinations are given in Methods Section 2.4.

CD45 (also known as protein tyrosine phosphatase receptor type C (PTPRC) or leucocyte common antigen) is a type I transmembrane protein found on all differentiated haematopoietic cells except erythrocytes and plasma cells [237], and is widely used to identify non-granulocytes from whole blood specimens [509]. Human monocytes can be segregated into classical, non-classical and intermediate sub-populations. Classical monocytes account for approximately 80–90% of peripheral blood monocytes [66] and are phenotypically identified as being CD14^{hi}CD16$^-$, while intermediate and non-classical monocytes are identified by being CD14^{dim}CD16$^+$ and CD14$^-$CD16$^+$ respectively [66]. CD14 is a glycoprotein expressed on cells of the myelomonocyte lineage including monocytes, macrophages and some granulocytes [20, 662], with functions of activating innate immunity [41, 647], while CD16 (FcγRIII) is a low affinity Fc receptor for IgG [555] found on the surface of NK cells, monocytes,

macrophages, and neutrophils [407] and is responsible for antibody-dependent cellular cytotoxicity on NK cells [376].

Human dendritic cells are defined as HLA-DR$^+$ but negative for lineage markers of T cells (CD3), B cells (CD19 or CD20), NK cells (CD16 then CD56) and monocytes (CD14) (i.e. Lin$^-$HLA-DR$^+$) [104]. They are distinguished from monocytes by their lack of CD14, and can be segregated into CD11c$^+$ conventional dendritic cells (cDCs) and CD11c$^-$ plasmacytoid dendritic cells (pDCs) [104, 371]. CD11c is a type I transmembrane protein (also known as Integrin, alpha X (ITGAX)) that is involved in adherence of neutrophils and monocytes to stimulated endothelium cells [1] and is abundantly expressed on monocytes, granulocytes, tissue macrophages, CD11c$^+$ dendritic cells, and at low levels on neutrophils [281]. It is also expressed on a subset of B cells, T cells, and NK cells, with expression levels varying from dim to bright [197]. Additionally, pDCs can also be identified by the presence of CD123 [260], CD303 and CD304 [142]. CD123 is the interleukin-3 receptor alpha chain (IL-3Rα) that is also found on myeloid cDCs precursors, macrophages, mast cells, basophils, megakaryocytes, and some B cells (reviewed in [574]), while CD303 (also known as blood dendritic cell antigen (BDCA)-2 / C-type lectin domain family 4 member C (CLEC4C)) is a type II C-type lectin involved in ligand internalisation, processing and presentation as well as inhibition of IFN-α/β synthesis in pDCs [143]. CD303 and CD304 overlap in expression between the myeloid cDC precursor component and pDCs and cannot be used to separate the two populations completely, although the highest expressing cells will include only pDCs [107, 608].

On the basis of the above phenotypes, the antibody panel was designed to identify the subsets of monocytes, and to determine if plasmacytoid dendritic cells were present in the CD3$^-$CD4$^+$ population of cells. Table 5.1 lists the expected results of the phenotyping panel to identify monocyte subsets and pDCs.

	CD14	CD16	CD11c	CD303	CD123	HLA-DR
Classical monocytes	++	-	+	-	+ (some)	+
Intermediate monocytes	dim	+	+	-	+ (some)	++
Non-classical monocytes	-	++	+	-	+ (some)	++
pDCs	-	-	-	++	++	+
cDCs*	-	+ (subset)	+	-	int/+	+/++
preDCs	-	-	lo	+	+	+

Table 5.1: Expected results of phenotyping panel
*Consisting of cDC1, cDC2, $CD16^+$ DC, Axl^+ DC. lo = low; int = intermediate; preDC = DC precursors.
Summarised from : [142, 284, 482, 512, 578, 592, 663]

PBMCs from 2 healthy HCMV-seropositive donors were defrosted and treated with DNase before undergoing separations by MACS positive selection with CD4 MicroBeads, followed by staining with the phenotyping panel described above. Figs.5.5A–5.5B shows the results from one donor, and Figs.5.5C–5.5D shows the results from a second donor. In Figs.5.5A & 5.5C, the top row shows the gating strategy to obtain the $CD3^-CD4^+$ population (outlined in red). In both donors, when these $CD3^-CD4^+$ cells were examined for CD14 and CD16 expression, there were populations of cells that were $CD14^+CD16^-$, $CD14^+CD16^+$, and $CD14^{dim}CD16^+$ (second row, blue, pink and yellow labels). These cells were likely to be classical, intermediate and non-classical monocytes respectively [379]. In addition, there was also a population of cells that were $CD4^+$, but $CD3^-$, $CD14^-$ and $CD16^-$ (second row, purple label).

Figs.5.5B & 5.5D show the $CD11c^-CD303^+$ (green outline), $CD11c^+CD303^-$ (cyan outline) and $CD11c^-CD303^-$ (orange outline) cells from the $CD14^-CD16^-$ population of each donor examined for HLA-DR and CD123 expression. On the basis of being $CD14^-CD16^-$**$CD11c^-$ $CD303^{++}CD123^+$** and $HLA\text{-}DR^+$, it is likely that the populations outlined in green were plasmacytoid DCs, while the populations outlined in cyan were $CD14^-CD16^-$**$CD11c^+CD303^-$** and had intermediate to high amounts of CD123 and HLA-DR, and thus were likely to be conventional DCs [104, 107].

In addition, there was also a population of cells that were $CD3^-CD4^+$ but $CD14^-CD16^-$ $CD11c^-CD303^-$, with low amounts of HLA-DR and CD123 (orange outline). It would be difficult to speculate what these cells could be without further staining, but a possibility could be that they were a subset of NK cells, dendritic cells or $CD34^+$ progenitor cells.

(A) Donor 1

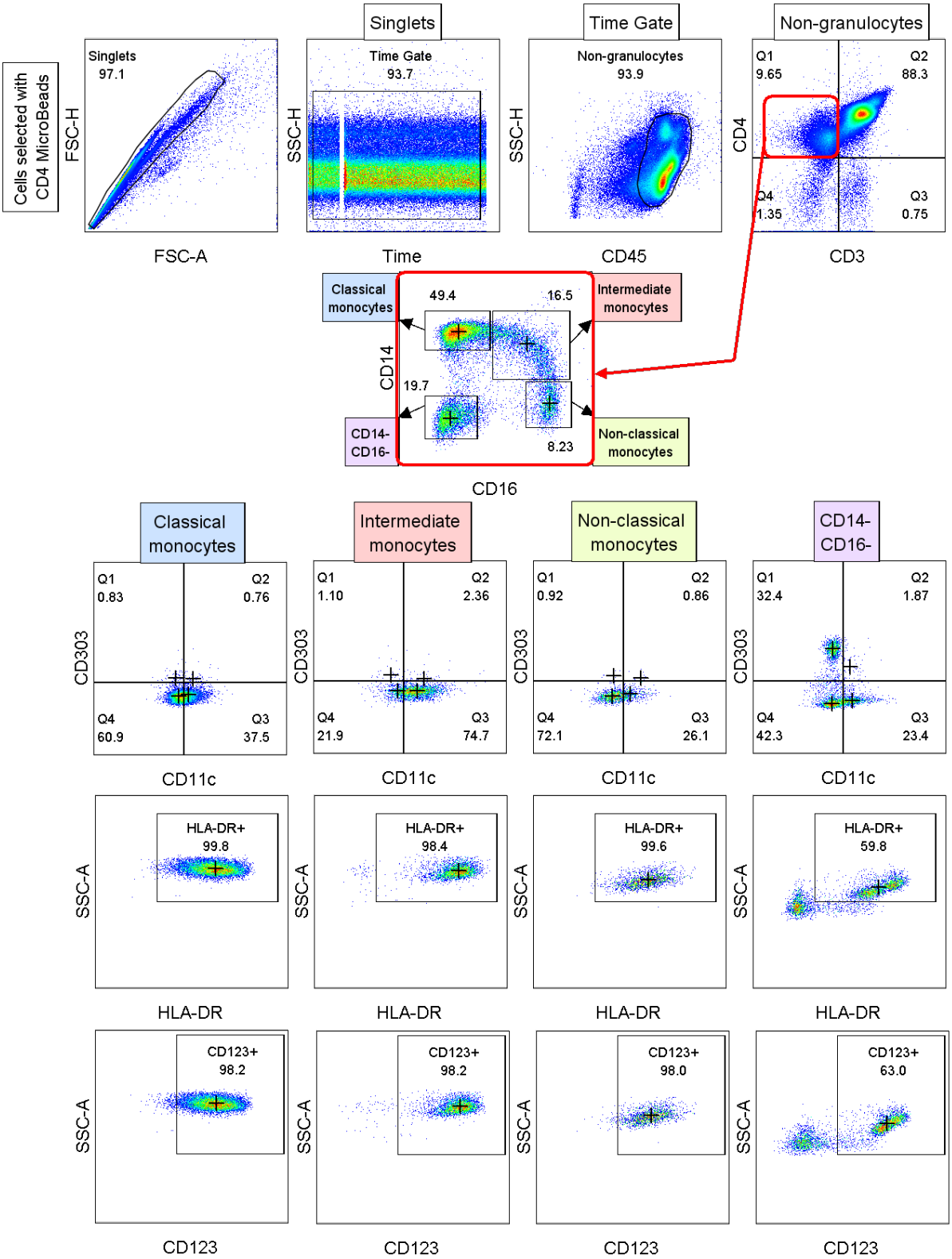
Cells selected with CD4 MicroBeads
FSC-H
FSC-A
Singlets
97.1
Singlets
SSC-H
Time
Time Gate
93.7
Time Gate
SSC-H
CD45
Non-granulocytes
93.9
Non-granulocytes
CD4
CD3
Q1
9.65
Q2
88.3
Q4
1.35
Q3
0.75
CD14
CD16
Classical monocytes
49.4
Intermediate monocytes
16.5
19.7
CD14-
CD16-
8.23
Non-classical monocytes
Classical monocytes
Intermediate monocytes
Non-classical monocytes
CD14-
CD16-
CD303
CD11c
Q1
0.83
Q2
0.76
Q4
60.9
Q3
37.5
Q1
1.10
Q2
2.36
Q4
21.9
Q3
74.7
Q1
0.92
Q2
0.86
Q4
72.1
Q3
26.1
Q1
32.4
Q2
1.87
Q4
42.3
Q3
23.4
SSC-A
HLA-DR
HLA-DR+
99.8
HLA-DR+
98.4
HLA-DR+
99.6
HLA-DR+
59.8
CD123
CD123+
98.2
CD123+
98.2
CD123+
98.0
CD123+
63.0

(B) Donor 1

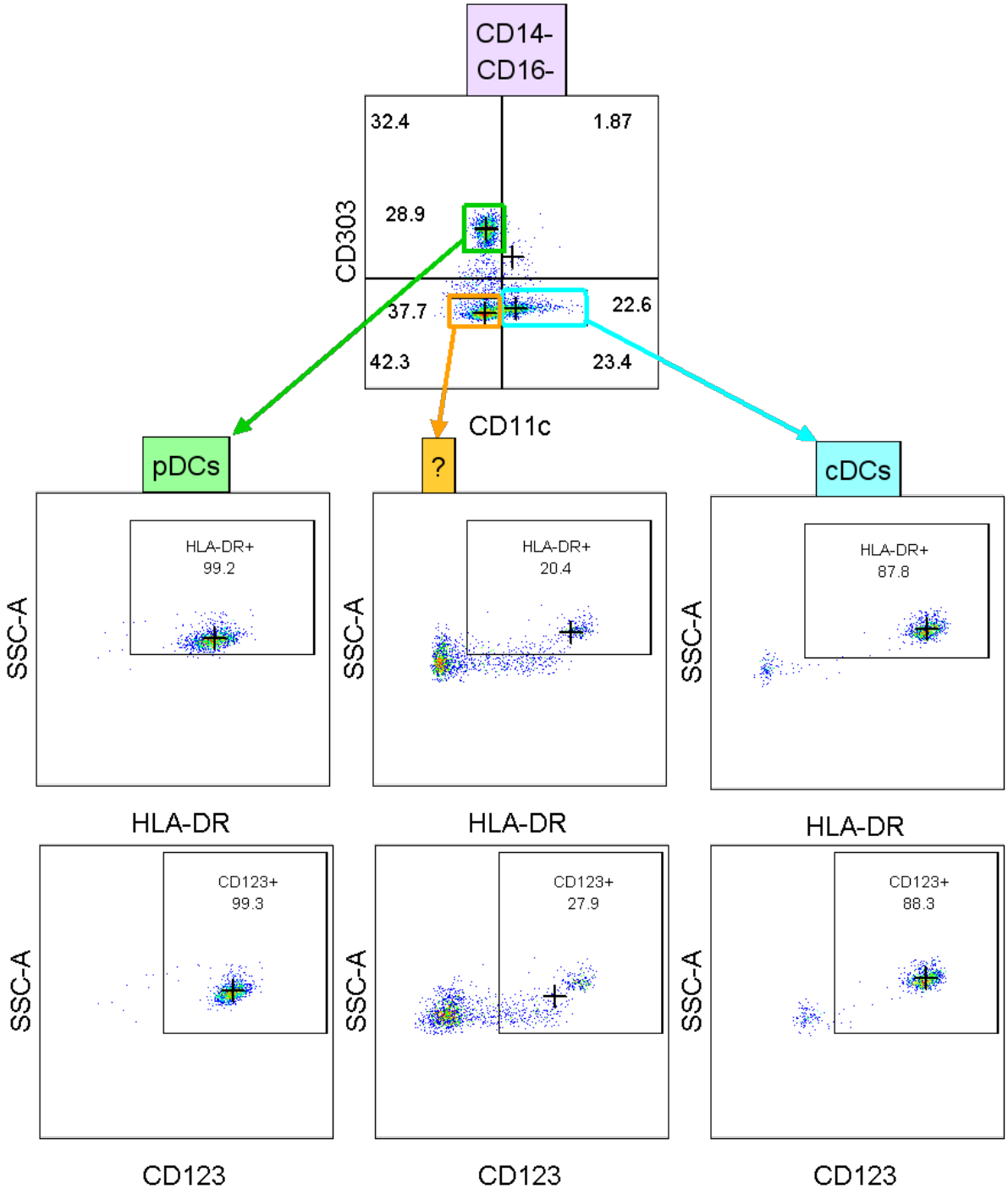
CD14-
CD16-
32.4
1.87
28.9
CD303
37.7
22.6
42.3
23.4
CD11c
pDCs
?
cDCs
HLA-DR+
99.2
HLA-DR+
20.4
HLA-DR+
87.8
SSC-A
HLA-DR
CD123+
99.3
CD123+
27.9
CD123+
88.3
CD123

(C) Donor 2

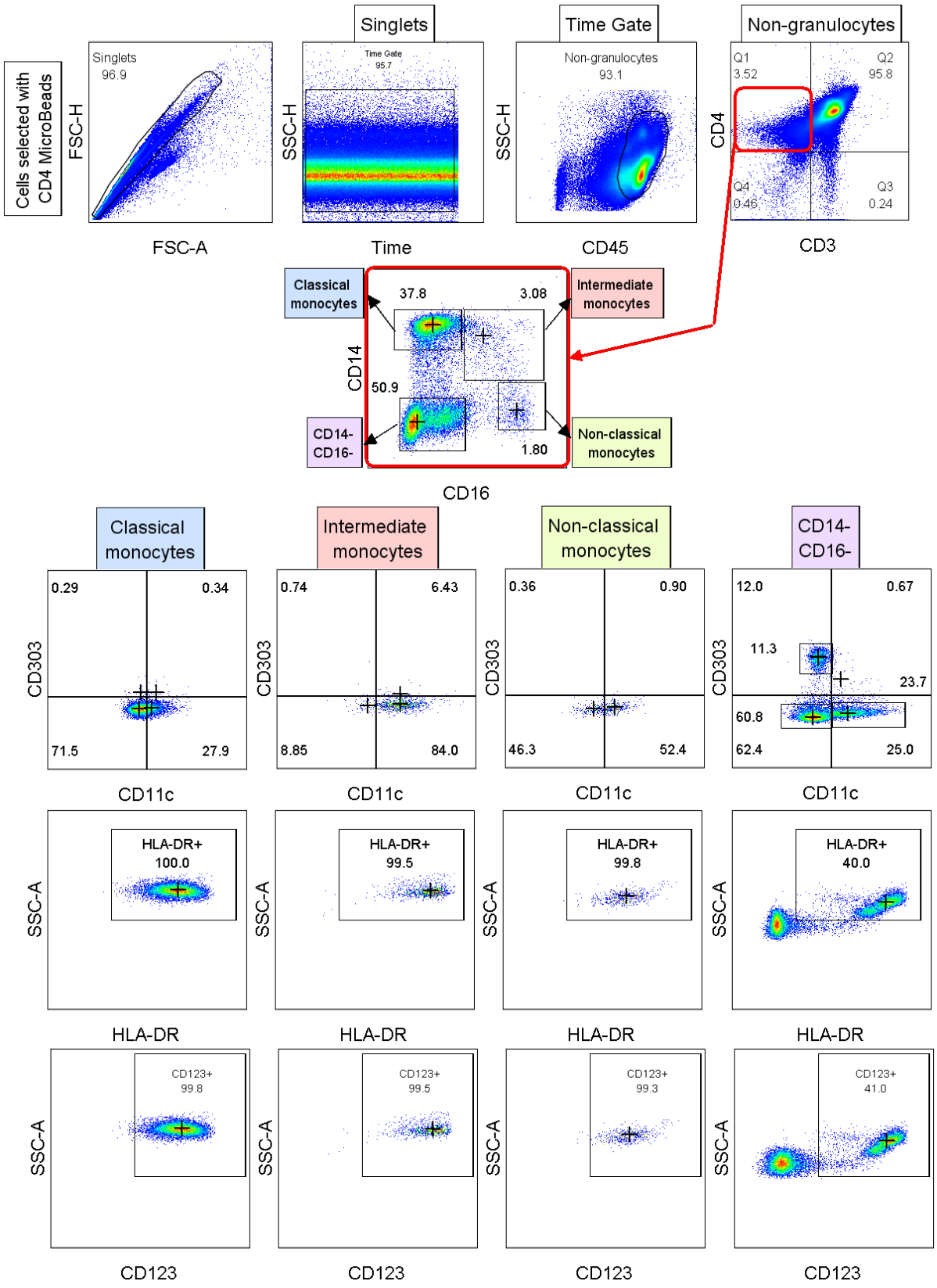
Cells selected with CD4 MicroBeads
FSC-H
FSC-A
Singlets
96.9
SSC-H
Time
Time Gate
95.7
Time Gate
Non-granulocytes
93.1
SSC-H
CD45
Non-granulocytes
CD4
CD3
Q1
3.52
Q2
95.8
Q4
0.46
Q3
0.24
Classical monocytes
Intermediate monocytes
Non-classical monocytes
CD14-CD16-
37.8
3.08
50.9
1.80
CD14
CD16
Classical monocytes
Intermediate monocytes
Non-classical monocytes
CD14-CD16-
CD303
CD11c
0.29
0.34
71.5
27.9
0.74
6.43
8.85
84.0
0.36
0.90
46.3
52.4
12.0
0.67
11.3
23.7
60.8
62.4
25.0
SSC-A
HLA-DR
HLA-DR+
100.0
HLA-DR+
99.5
HLA-DR+
99.8
HLA-DR+
40.0
CD123
CD123+
99.8
CD123+
99.5
CD123+
99.3
CD123+
41.0

(D) Donor 2

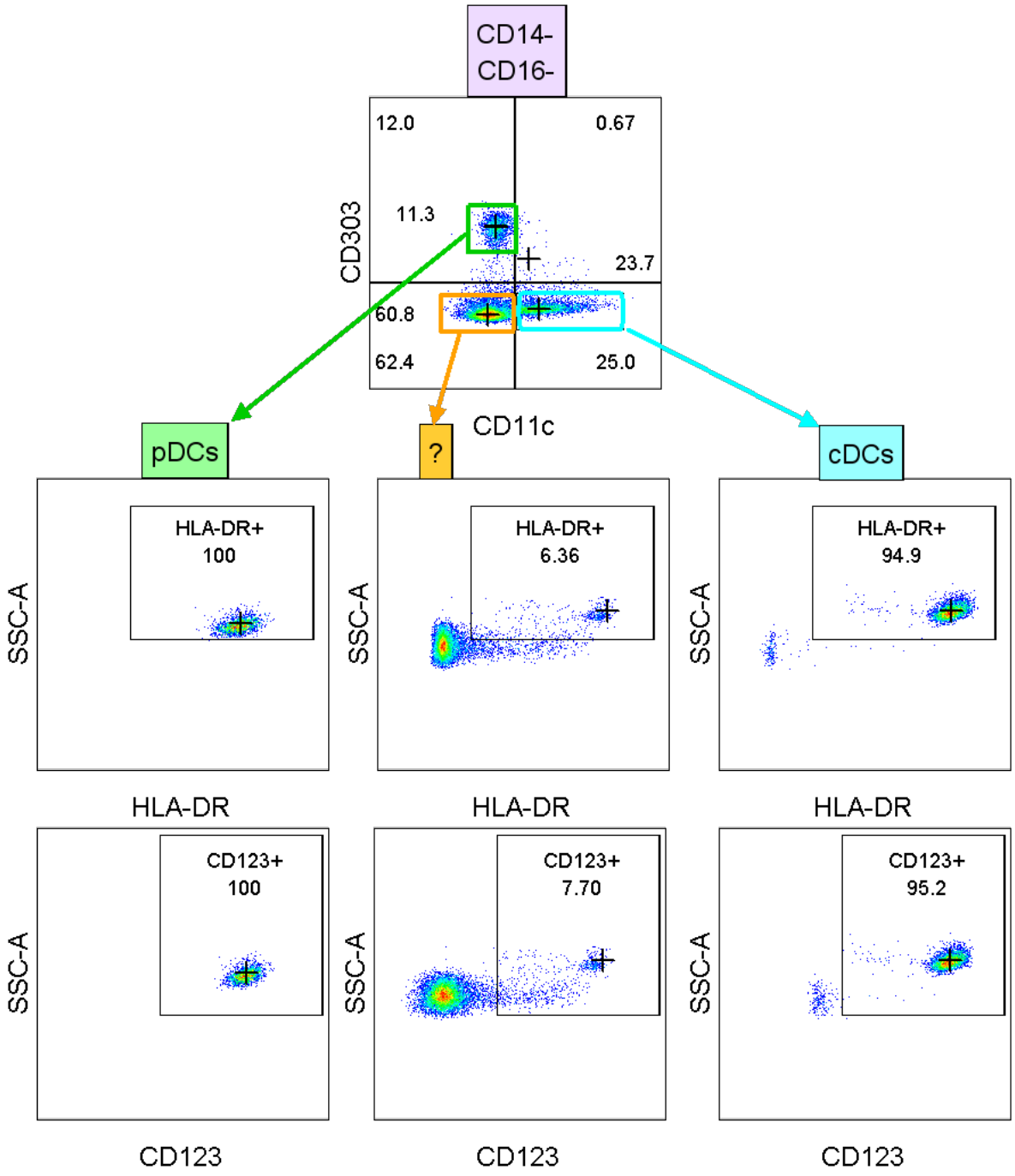

Figure 5.5: Phenotyping $CD3^{-}CD4^{+}$ population obtained from MACS by positive selection using CD4 MicroBeads

Seperation by MACS was performed on PBMCs from 2 donors using positive selection by CD4 MicroBeads followed by staining with antibodies to CD3, CD4, CD45, CD14, CD16, CD11c, CD303, CD123, and HLA-DR. Fig.5.5A: top row shows the gating strategy to obtain the $CD3^{-}CD4^{+}$ population, second row shows the identification of classical, intermediate and non-classical monocytes, and $CD14^{-}CD16^{-}$ population from the $CD3^{-}CD4^{+}$ population, and subsequent rows show staining for CD11c, CD303, HLA-DR and CD123 on the classical, intermediate, non-classical monocyte populations and the $CD14^{-}CD16^{-}$ population. Fig.5.5B shows the $CD11c^{-}CD303^{+}$ (pDCs), $CD11c^{+}CD303^{-}$ (cDCs) and $CD11c^{-}CD303^{-}$ populations examined for expression of HLA-DR and CD123. Figs.5.5C–5.5D shows the same from another donor.

5.6 Co-culture of $CD4^+$ T cells with $CD14^+$ monocytes potentiates control of IE and late CMV gene expression, which is abrogated by blocking MHC Class II

The experiments so far in this chapter have shown that blocking MHC Class II or IFN-γ results in abrogation of control of IE and late CMV gene expression in the viral dissemination assay. They have also shown that immune cells isolated by positive selection on MACS with CD4 MicroBeads are able to limit IE and late CMV gene expression in the VDA to a greater degree than immune cells isolated by depletion on MACS with the $CD4^+$ T cell Isolation Kit. Purity analyses and phenotyping of the cells isolated by these 2 different methods show that in addition to $CD3^+CD4^+$ cells, the former also contains a population of $CD3^-CD4^+$ cells, which are made up of monocytes, plasmacytoid dendritic cells, conventional dendritic cells, and other cells of uncertain aetiology.

It would appear that these $CD3^-CD4^+$ cells were responsible for the difference in ability to control IE and late CMV gene expression *in vitro*. This led to the question of whether the antiviral activity seen was due to effector functions of CMV-specific $CD4^+$ T cells, or the functions of monocytes, conventional dendritic cells of pDCs. The results in Figs.5.3, 5.4A, 5.5A & 5.5C showed that between 1.9–9.7% of the CD4 MicroBead-selected cells were $CD3^-CD4^+$.

I thus asked the question of whether monocytes or plasmacytoid dendritic cells alone were antiviral in the VDA, or if $CD4^+$ T cells were also required. I first investigated the function of $CD14^+$ monocytes in isolation and in combination with $CD4^+$ T cells. To create an approximate simulation of this, $CD14^+$ monocytes were added to $CD4^+$ T cell Isolation Kit-selected cells in a ratio of 1:9 (i.e. 10% of total cells added), which represents the highest proportion of monocytes present in the cell populations isolated by positive selection with CD4 MicroBeads.

Primary dermal fibroblasts from 2 healthy donors (1 HCMV-seropositive, 1 HCMV-seronegative) were seeded in 96-well half-area plates and grown to confluency overnight before infection with Merlin WT. At 1 dpi, PBMCs from the autologous donor were split into 2 aliquots in an approximate $\frac{1}{4}$:$\frac{3}{4}$ ratio: $\frac{1}{4}$ of the PBMCs underwent MACS positive selection using CD4 MicroBeads, and $\frac{3}{4}$ of the PBMCs underwent MACS positive selection using CD14 MicroBeads to obtain $CD14^+$ monocytes before isolation of $CD4^+$ T cells using the $CD4^+$ T cell Isolation Kit. This cell separation strategy is illustrated in Fig.5.6A. The post-separation purities of each of these populations from one representative donor is shown in Fig.5.6B. The first column shows the gate to identify cells, the second column shows histograms of CD3 expression on the cells, the third column shows amount of CD4 and CD8 expression on the $CD3^+$ population, and the fourth column shows histograms of CD14 expression on $CD3^-$ population. The parent

cell populations are labelled on the left of each row. The rightmost plot on the second row shows that, in the $CD3^-$ population from cells selected by MACS positive selection with CD4 MicroBeads, 32.3% are $CD14^+$ (outlined in red), whereas this is largely absent (only 1.24%) in the cells selected by MACS depletion with $CD4^+$ T cells Isolation Kit (rightmost plot on third row, green outline).

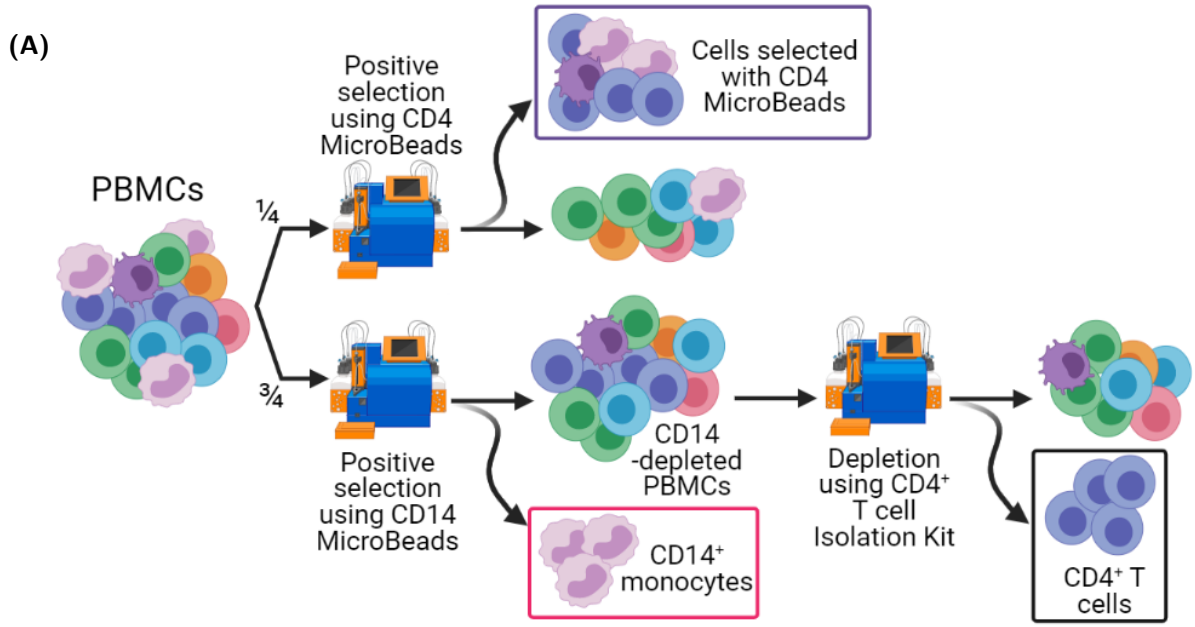

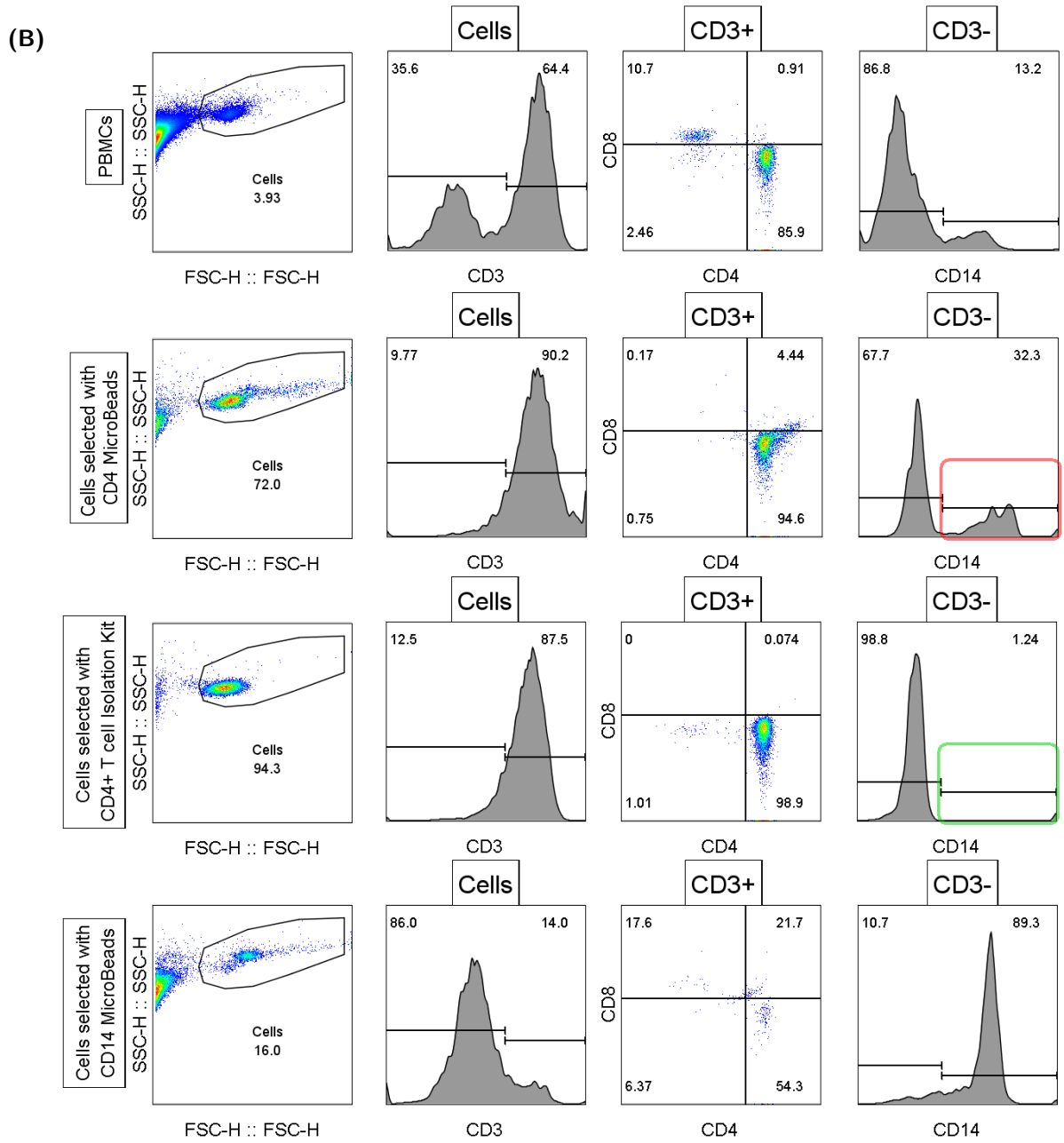

Figure 5.6: Isolation of immune cell populations from PBMCs using anti-CD4 MicroBeads, CD4$^+$ T cell Isolation Kit, and anti-CD14 MicroBeads, and post-separation purities
Primary dermal fibroblasts were seeded in 96-well plates and grown to confluency overnight. PBMCs were obtained from the autologous donor either by arm bleed or by defrosting from liquid nitrogen storage. The PBMCs were then split into 2 aliquots in an approximate $\frac{1}{4}$:$\frac{3}{4}$ ratio: $\frac{1}{4}$ of the PBMCs underwent MACS positive selection using CD4 MicroBeads, and $\frac{3}{4}$ of the PBMCs underwent MACS positive selection using CD14 MicroBeads to obtain CD14$^+$ monocytes before depletion using CD4$^+$ T cell Isolation Kit to obtain CD4$^+$ T cells. The cell separation process is illustrated in Fig.5.6A. Fig.5.6B shows the gating strategy to check for post-separation purities of these populations. The first column shows the gate to identify cells, the second column shows histograms of CD3 expression on the cells, the third column shows amount of CD4 and CD8 expression on the CD3$^+$ population, and the fourth column shows histograms of CD14 expression on CD3$^-$ population. The parent cell populations are labelled on the left of each row. Fig.5.6A created at BioRender.com.

The various immune cell populations were then added to the infected fibroblasts in the E:T ratios as shown in Table 5.2 as shown below. A higher E:T ratio was chosen for the HCMV-seronegative donor as a degree of control of IE and late CMV gene expression in the VDA was only seen at higher E:T ratios in HCMV-seronegative donors, as shown in Chapter 3.

	Seropositive	**Seronegative**
$CD4^+$ T cells only	1.125	9
$CD14^+$ cells only	0.125	1
Cells selected with CD4 MicroBeads	1.25	10
$CD4^+$ T cells & $CD14^+$ cells	1.125 + 0.125	9 + 1

Table 5.2: E:T ratios of each immune cell population added to the VDA

Cells were then incubated for a further 7 days before harvest and analysis by flow cytometry. Fig.5.7B shows the results from the HCMV-seropositive donor, and Fig.5.7C shows the results from the HCMV-seronegative donor, with the frequency of cells with IE and late CMV gene expression shown as a percentage of the amount of cells in the same phase of CMV gene expression in infected controls (i.e. "normalised" to infected controls).

For the HCMV-seropositive donor, cells selected by MACS depletion with $CD4^+$ T cells Isolation Kit ("$CD4^+$ T cells") and those selected by positive selection with CD14 MicroBeads ("$CD14^+$ monocytes") showed poor control of IE and late CMV gene expression when added separately (Fig.5.7B, black and pink bars). However, when they were mixed together ("$CD4^+$ T cells & $CD14^+$ monocytes", teal bars), they showed levels of control of IE and late CMV gene expression similar to that seen in cells selected by MACS positive selection with anti-CD4 MicroBeads ("Cells selected with CD4 MicroBeads", dark purple bars). This suggests that $CD14^+$ monocytes in isolation could not inhibit IE and late CMV gene expression, as this only occurred when $CD4^+$ T cells were present. For the HCMV-seronegative donor, $CD14^+$ monocytes and $CD4^+$ T cells in isolation did not control IE and late CMV gene expression (as expected). When $CD4^+$ T cells and $CD14^+$ monocytes were added together, there was a slight increase in antiviral activity, although the differences were not statistically significant.

Fluorescence microscopy images were also taken of wells with $CD4^+$ T cells (Fig.5.7E) and $CD14^+$ monocytes (Fig.5.7F) added in isolation, and together (Fig.5.7G). In Fig.5.7E, it appears that the $CD4^+$ T cells (orange arrowheads) adhere to some infected cells, but do not take up the mCherry or GFP fluorescence. In Fig.5.7F, monocytes (purple arrowheads) can be seen adhering to the infected cells and taking up the mCherry fluorescence. In Fig.5.7G, what are likely to be monocytes (purple arrowheads) and $CD4^+$ T cells (orange arrowhead) can be seen adhering to the infected cells, with monocytes taking up the mCherry fluorescence,

and also what is likely to be the presence of other monocytes that had not yet taken up any fluorescence can be seen (cyan arrowhead).

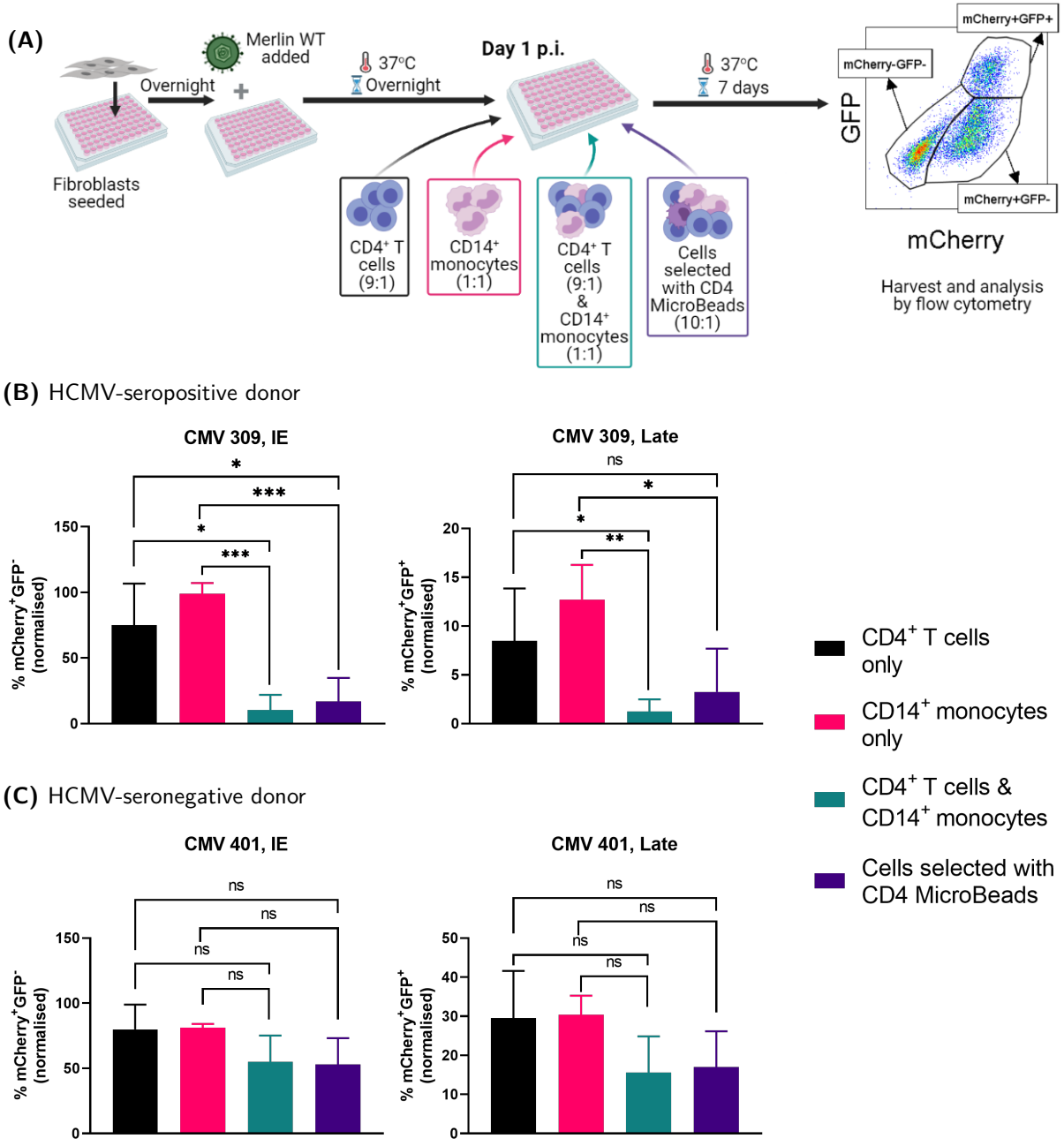

Figure 5.7: Co-culture of CD4$^+$ T cells with CD14$^+$ monocytes potentiates control of IE and late CMV gene expression

Primary dermal fibroblasts from an HCMV-seropositive and an HCMV-seronegative donor were seeded in 96-well plates and grown to confluency overnight. At 1 dpi, the immune cell populations obtained as illustrated in Fig.5.6A were then added to the infected fibroblasts in the following combinations: CD4$^+$ T cells only, CD14$^+$ monocytes only, CD4$^+$ T cells and CD14$^+$ monocytes or cells selected with CD4 MicroBeads. The E:T ratios at which these cells were added at is shown in Table 5.2. The experimental set-up is illustrated in Fig.5.7A. Cells were harvested at 8 dpi and analysed by flow cytometry and amount of cells in IE and late CMV gene expression is shown in Fig.5.7B for the HCMV-seropositive donor and Fig.5.7C for the HCMV-seronegative donor, expressed as a percentage of the amount of cells in the same phase of gene expression in infected controls. Error bars represent SD of triplicate wells, statistics performed using Student's *t*-test. (*$p \leq 0.05$; **$p \leq 0.01$; ***$p \leq 0.001$; ns = not significant) Fig.5.7A created at BioRender.com.

(E) $CD4^+$ T cells only

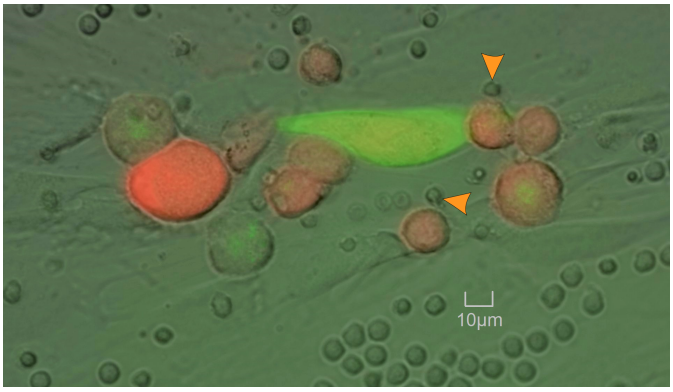

(F) $CD14^+$ monocytes only

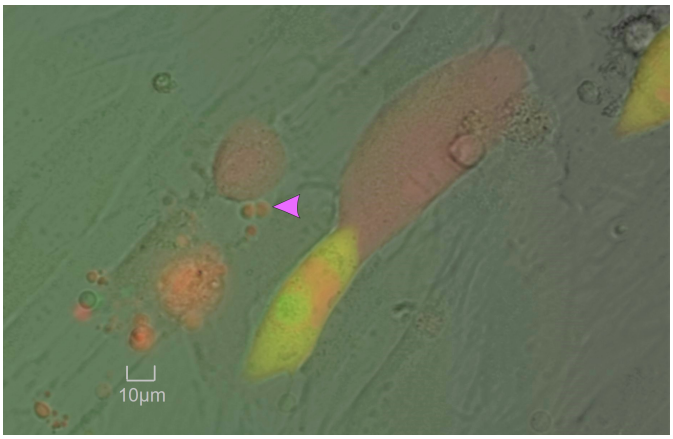

(G) $CD4^+$ T cells & $CD14^+$ monocytes

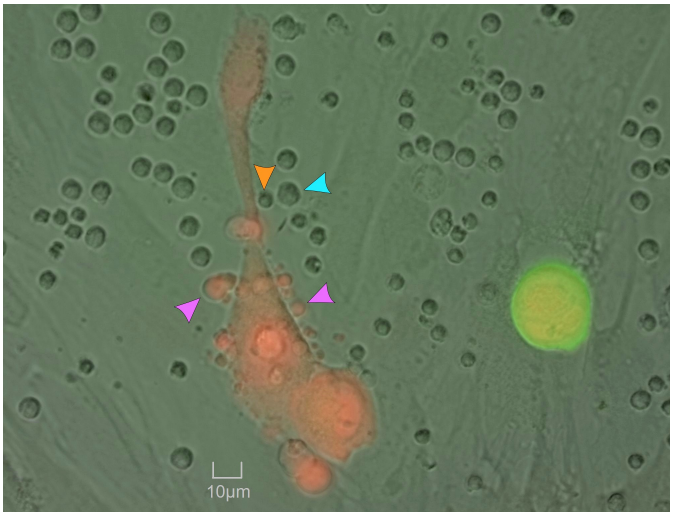

Figure 5.7: Co-culture of $CD4^+$ T cells with $CD14^+$ monocytes potentiates control of IE and late CMV gene expression (Continued)
Figs.5.7E, 5.7F & 5.7G show fluorescence microscopy images of wells with $CD4^+$ T cells only, $CD14^+$ monocytes only, and $CD4^+$ T cells with $CD14^+$ monocytes added together. (Orange arrowheads = monocytes that have taken up fluorescence, purple arrowheads = $CD4^+$ T cells, cyan arrowhead = monocytes that have not taken up fluorescence.)

To investigate if the potentiation of control seen in the HCMV-seropositive donor was mediated by antigen presentation via the MHC Class II pathway, the experiment was repeated on 2 HCMV-seropositive donors, with the immune cell populations added at the E:T ratios as stated in Table 5.3 below.

	E:T ratio
$CD4^+$ T cells only	9
$CD14^+$ cells only	1
Cells selected with CD4 MicroBeads	10
$CD4^+$ T cells & $CD14^+$ cells	9 + 1

Table 5.3: E:T ratios of each immune cell population added to the VDA with anti-MHC Class II antibodies

In addition, anti-MHC Class II antibodies (15μg/ml) were added to half of the wells that had the mixture of $CD4^+$ T cells and $CD14^+$ monocytes. The results are seen in Fig.5.8. For donor CMV 314 (Fig.5.8A), co-culture of $CD4^+$ T cells and $CD14^+$ monocytes leads to control of both IE and late CMV gene expression, seen as a near-90% decrease in the amount of both IE and late CMV gene expression, while addition of anti-MHC Class II antibodies decreases this control to approximately 50% for IE CMV gene expression, and completely abrogates it for late CMV gene expression. For donor CMV 320 (Fig.5.8B), a similar trend (but to a smaller degree) was seen for IE CMV gene expression, but addition of anti-MHC Class II antibodies was not able to abrogate control of late CMV gene expression.

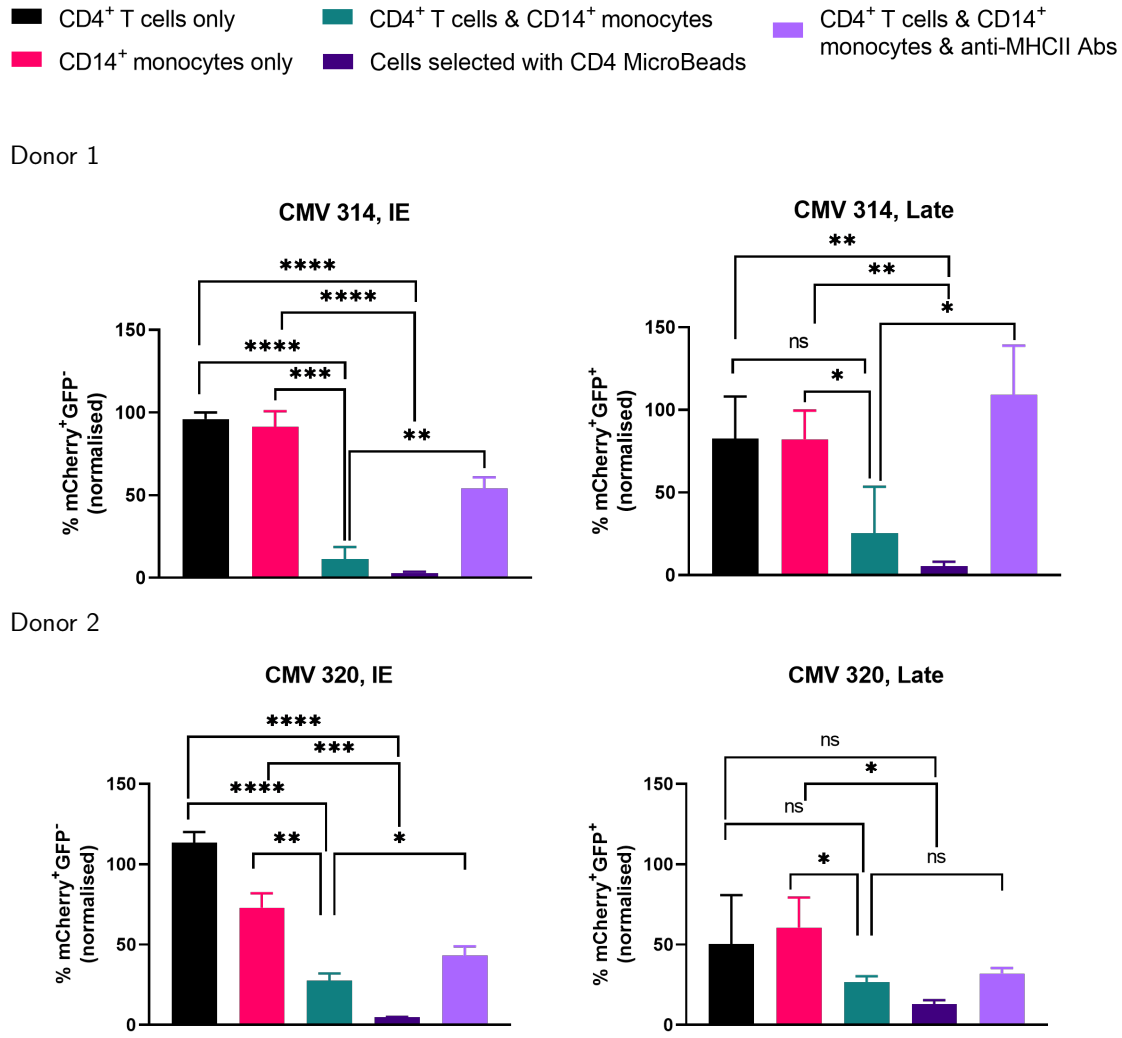

Figure 5.8: Addition of anti-MHC Class II antibody abrogates potentiation of control of CMV gene expression seen when CD14$^+$ cells are added with CD4$^+$ T cells to the viral dissemination assay

Primary dermal fibroblasts from 2 HCMV-seropositive donors were seeded in 96-well half-area plates and grown to confluency overnight. At 1 dpi, PBMCs from the autologous donors were defrosted and CD4$^+$ cells selected by CD4 MicroBeads, CD14$^+$ monocytes, and CD4$^+$ T cell populations were obtained from them in the manner as illustrated in Fig.5.6A. They were then added to the infected fibroblasts in the following combinations: CD4$^+$ T cells (at an E:T of 9:1), CD14$^+$ monocytes (E:T 1:1), CD4$^+$ T cells and CD14$^+$ monocytes (E:T 9 + 1 : 1) or cells selected with CD4 MicroBeads (E:T 10:1). Half of the wells with CD4$^+$ T cells and CD14$^+$ monocytes added had anti-MHC Class II antibodies (15μg/ml) added at the same time as the immune cells were added. Cells were incubated for a further 7 days before harvest and analysis by flow cytometry. The amount of cells in IE and late CMV gene expression in each of the conditions is shown, expressed as a percentage of the amount of cells in the same phase of gene expression in infected controls. Error bars represent SD of triplicate wells, statistics performed using Student's *t*-test. (*$p \leq 0.05$; **$p \leq 0.01$; ***$p \leq 0.001$; ns = not significant)

5.7 Plasmacytoid dendritic cells in isolation control viral dissemination, but do not potentiate the effects of $CD4^+$ T cells

The results of the phenotyping analyses in Fig.5.5 showed that, besides $CD14^+$ monocytes, the $CD3^-CD4^+$ population of cells selected by MACS positive selection with anti-CD4 MicroBeads also contained a population of cells that were likely to be pDCs. pDCs are capable of antigen presentation via MHC Class I and II on their cell surface (reviewed in [563, 607]), and have roles in activation of T cells (reviewed in [477]). In the context of HCMV, they have been shown to produce IFN-α in response to HCMV-infected cells, although there appears to be some dispute over whether pDCs are able to be infected directly by HCMV [42, 423] or produce cytokines only in response to recognition of HCMV-infected cells [657].

5.7.1 pDCs show a direct antiviral effect with HCMV-infected fibroblasts

The question thus arose: do the plasmacytoid dendritic cells also contribute to the antiviral effect seen in cells selected by MACS positive selection with anti-CD4 MicroBeads at the frequencies found in the $CD4^+$ selected population? To investigate this, I first had to determine if pDCs on their own showed an antiviral effect in the viral dissemination assay. Primary dermal fibroblasts from a healthy HCMV-seronegative donor were seeded in 96-well half-area plates and grown to confluency overnight before infection with Merlin WT (MOI = 0.03). At 1 dpi, pDCs were isolated from autologous PBMCs by depletion using the Plasmacytoid Dendritic Cell Isolation Kit II (Miltenyi, U.K.) and added to the infected fibroblasts at a starting E:T ratio of 0.75:1 followed by halving dilutions. In order to obtain an estimate of the E:T ratio at which pDCs would start to show an antiviral effect, the highest possible starting E:T ratio (based on number of pDCs isolated from the PBMCs) was used. Fig.5.9A shows the gating strategies to check post-separation purities of the pDCs. The first column shows PBMCs, middle column shows post-separation pDCs and third column shows pDC-depleted PBMCs. Top row shows gate to identify cells, and second row shows amount of CD123 and CD303 on the populations. Harvest and analysis was carried out after 7 days of incubation, and results in Fig.5.9B show that pDCs are able to control IE and late CMV gene expression at higher E:T ratios of 0.75:1 and 0.38:1, an effect which then dilutes out at the lower E:T ratios.

These results show that pDCs have a direct antiviral effect on HCMV-infected fibroblasts at these E:T ratios. In Fig.5.5, the percentage of pDCs ranged from 11.3%–28.9% of $CD14^-CD16^-$ cells, the percentage of $CD14^-CD16^-$ cells ranged from 19.7%–50.9% of $CD3^-CD4^+$ cells, and the percentage of $CD3^-CD4^+$ cells in the population which was selected by anti-CD4 MicroBeads ranged from 3.5%–9.7%. Therefore, pDCs would probably comprise only a maximum

of $\sim$1.5–2% of cells selected by anti-CD4 MicroBeads (28.9% $\times$ 50.9% $\times$ 9.7% $\approx$ 1.5%). In an E:T ratio of anti-CD4 MicroBead-selected cells of 10:1, this is an E:T ratio of $\sim$ 0.15–0.2:1 of pDCs. Therefore, the E:T ratios used in this experiment were likely to be higher than what was likely to have been the E:T ratios of pDCs present in the anti-CD4 MicroBead-selected populations added to earlier VDAs.

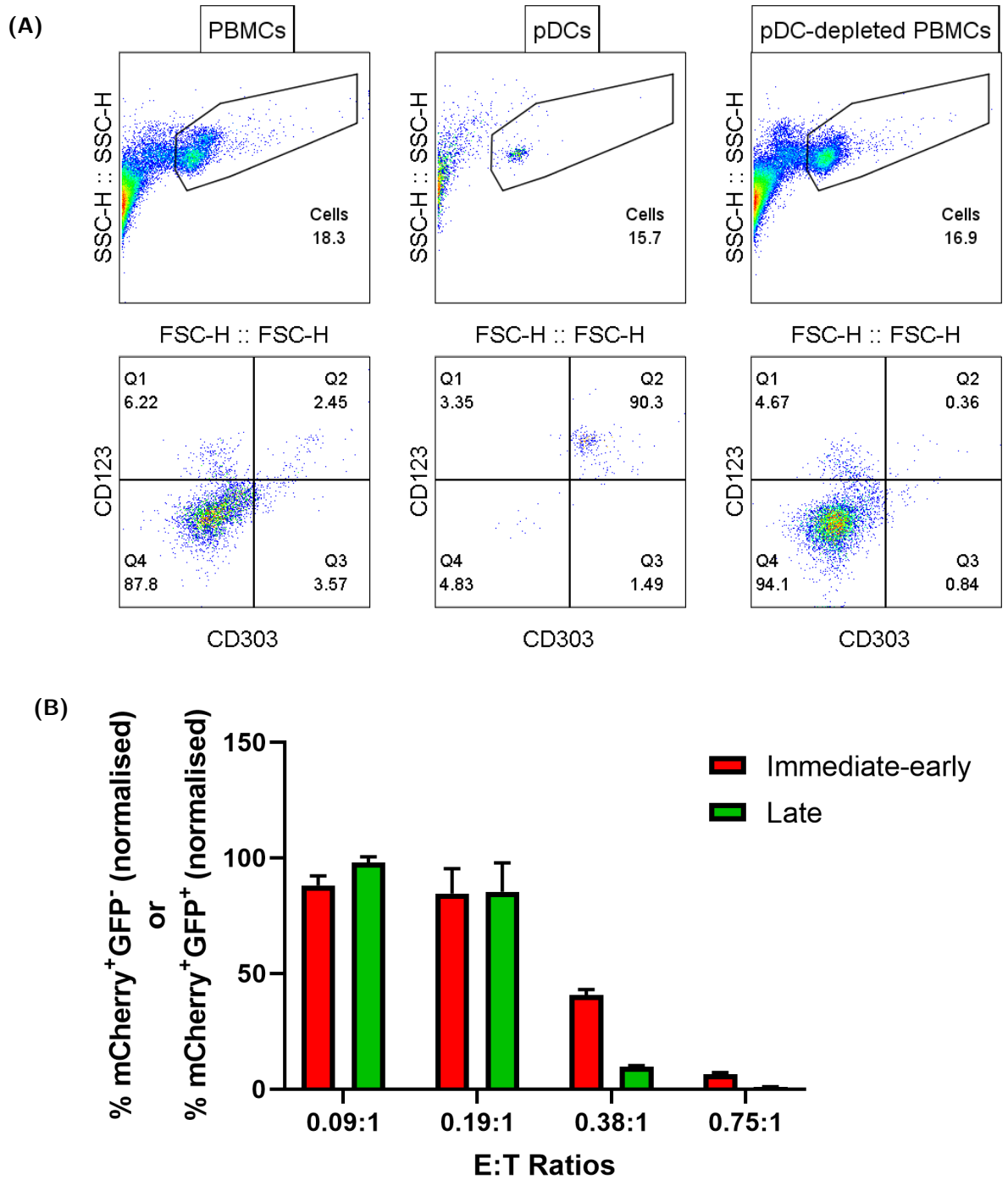

Figure 5.9: Viral dissemination assay with plasmacytoid DCs
Primary dermal fibroblasts from a healthy HCMV-seronegative donor were seeded in 96-well half-area plates and grown to confluency overnight before infection with Merlin WT (MOI = 0.03). At 1 dpi, pDCs were obtained from autologous PBMCs by depletion using the Plasmacytoid Dendritic Cell Isolation Kit II (Miltenyi, U.K.) and added to the infected fibroblasts at a starting E:T ratio of 0.75:1 followed by halving dilutions. Fig.5.9A shows the gating strategies to check post-separation purities of the pDCs. The first column shows PBMCs, middle column shows post-separation pDCs and third column shows pDC-depleted PBMCs. Top row shows gate to identify cells, and second row show amount of CD123 and CD303 on the populations. Harvest and analysis was carried out after 7 days of incubation. Fig.5.9B shows the amount of cells in IE and late CMV gene expression, expressed as a percentage of the amount of cells in the same phase of CMV gene expression in the infected controls. Error bars represent SD of triplicate wells.

5.7.2 pDCs do not appear to potentiate the antiviral effects of CD4$^+$ T cells

As pDCs appeared to be able to control IE and late CMV gene expression in the viral dissemination assay, I then wanted to see if they contributed to CD4$^+$ T cell recognition of infected cells. I proceeded to add pDCs to a viral dissemination assay with CD4$^+$ T cells in the same manner as I had done with CD14$^+$ in Fig.5.7. Primary dermal fibroblasts from an HCMV-seronegative donor were seeded in 96-well half-area plates and grown to confluency overnight before infection with Merlin WT (MOI = 0.03). At 1 dpi, PBMCs from the autologous donor were obtained and divided into 3 populations in an approximate ratio of 1:7:2, whereupon 3 populations of cells were obtained: cells selected by MACS positive selection with CD4 MicroBeads; pDCs selected by MACS depletion with Plasmacytoid Dendritic Cell Isolation Kit II; and CD4$^+$ T cells selected by MACS depletion with CD4$^+$ T cell Isolation Kit. Fig.5.10A illustrates the cell separation process. The cells were then added in the following manner: cells selected with CD4 MicroBeads (at a starting E:T ratio of 10:1); CD4$^+$ T cells (at a starting E:T ratio of 9.5:1); pDCs only (at a starting E:T ratio of 0.5:1); and pDCs with CD4$^+$ T cells (at a starting E:T ratio of 0.5 + 9.5:1). As stated earlier, the maximum likely percentage of pDCs present in an anti-CD4 MicroBead-selection population was estimated to be $\sim$2%. As it was unlikely that it would exceed 5%, pDCs were added to the mixture of pDCs + CD4$^+$ T cells in the proportion of 0.5:9.5 (i.e. 5% of total cells). After 7 days incubation, harvest and analysis by flow cytometry was performed.

The results in Figs.5.10B (IE CMV gene expression) and 5.10C (late CMV gene expression) show that pDCs were able to demonstrate a direct antiviral effect on their own at the high E:T ratio of 0.5:1, but this rapidly diluted out, with no antiviral activity at E:T of 0.25:1 and below (black bars). Cells selected by anti-CD4 MicroBeads had a high degree of antiviral activity at all E:T ratios tested for both IE and late CMV gene expression (dark purple bars). The results for the CD4$^+$ T cells obtained using the Isolation Kit (pink bars) did show substantial antiviral activity at the high E:T ratios of 9.5, 4.75 and 2.37:1, which was greater than previous experiments. This is likely due to the post-separation purity of this population, which contained $\sim$6% of CD3$^-$ cells (flow cytometry plots given in Appendix I). However, at the CD4$^+$ T cell ratio of 1.19 and 0.57:1 there was only minimal antiviral effect, which was not increased by addition of pDCs (teal bars). In contrast, the cells selected with direct anti-CD4 MicroBeads were still able to mediate substantial antiviral control. When this experiment was repeated on an HCMV-seronegative donor, addition of pDCs also did not appear to allow CD4$^+$ T cells to better control IE and late CMV gene expression (Figs.5.10D & 5.10E).

Taking these results together, while pDCs themselves can exert antiviral activity, adding them to CD4$^+$ T cells at lower E:T ratios in line with the frequencies found in anti-CD4 MicroBead preparations showed no substantial increase in control of IE and late CMV gene expression the way that CD14$^+$ monocytes were able to, vis-à-vis Figs.5.7 & 5.8.

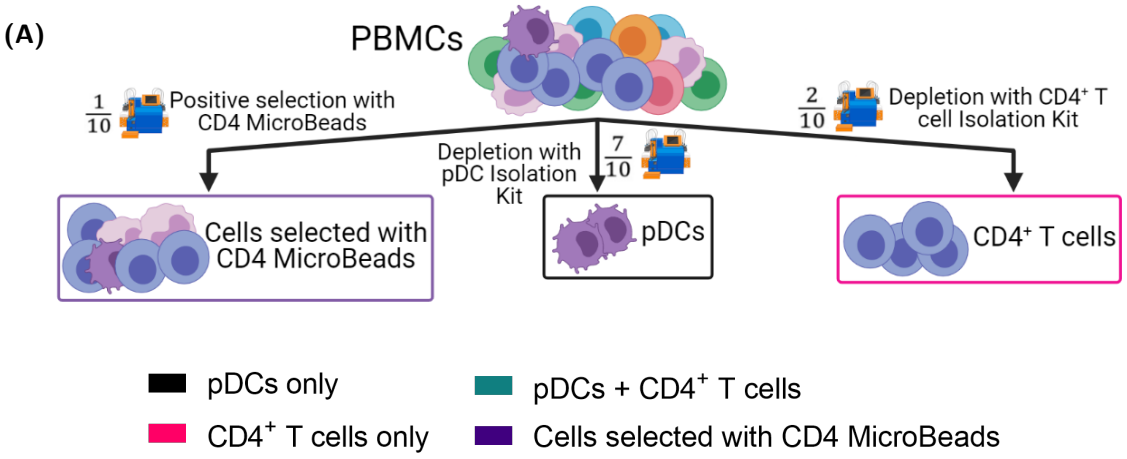

(B)

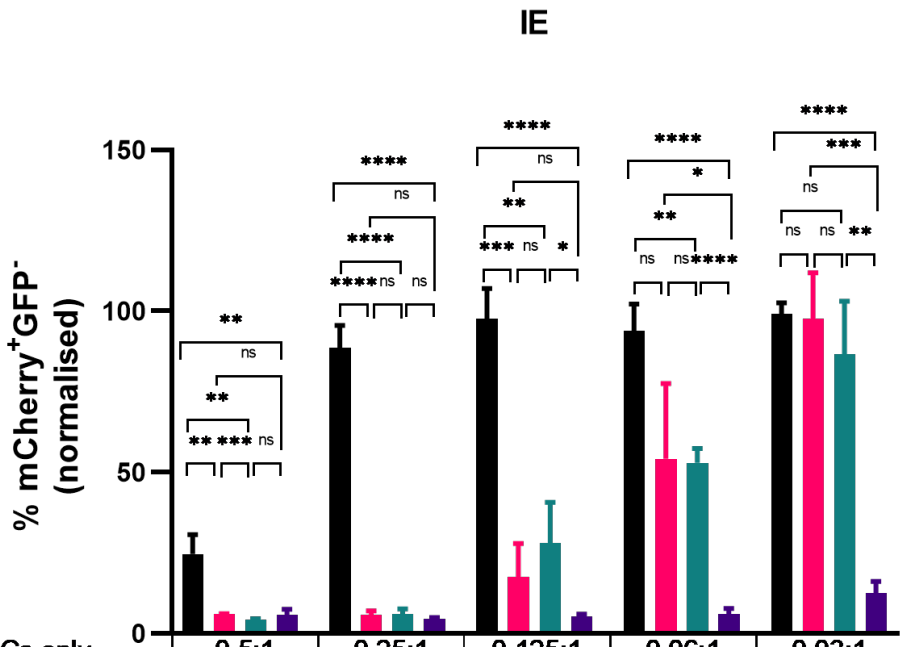

pDCs only	0.5:1	0.25:1	0.125:1	0.06:1	0.03:1
CD4+ T cells only	9.5:1	4.75:1	2.375:1	1.19:1	0.57:1
pDCs + CD4+ T cells	0.5:1 + 9.5:1	0.25:1 + 4.75:1	0.125:1 + 2.375:1	0.06:1 + 1.19:1	0.03:1 + 0.57:1
Cells selected by CD4 MicroBeads	10:1	5:1	2.5:1	1.25:1	0.6:1

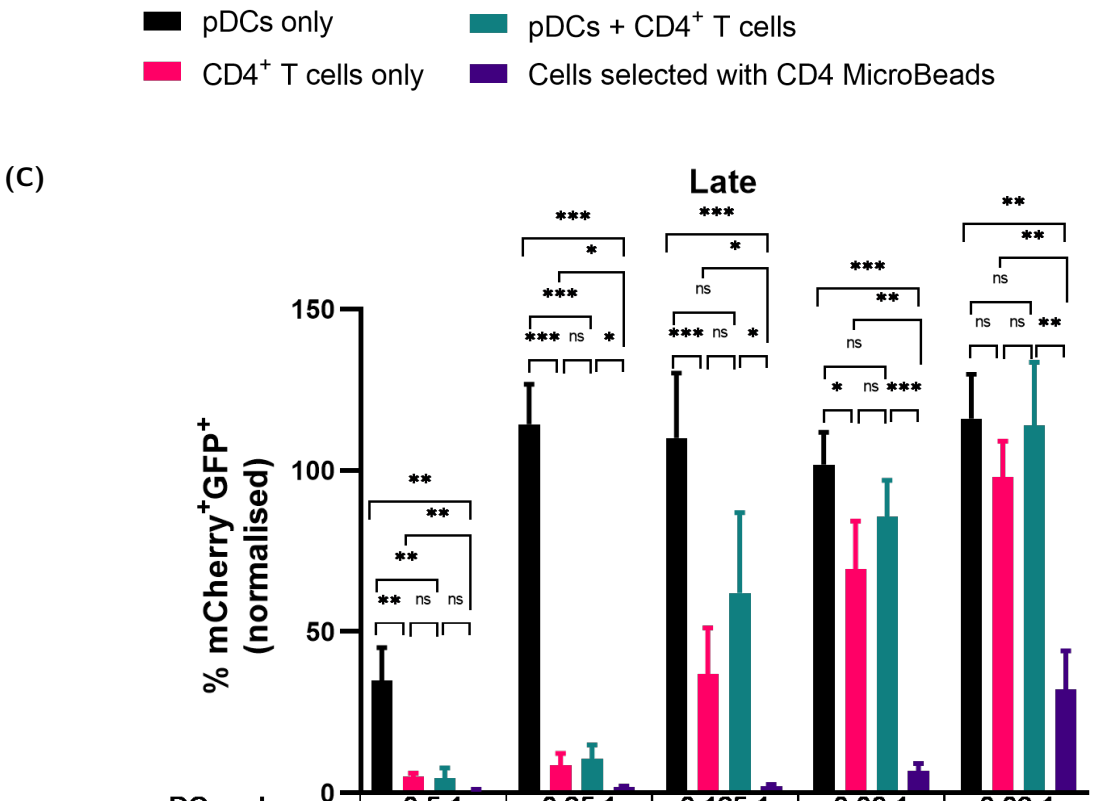

pDCs only	0.5:1	0.25:1	0.125:1	0.06:1	0.03:1
CD4+ T cells only	9.5:1	4.75:1	2.375:1	1.19:1	0.57:1
pDCs + CD4+ T cells	0.5:1 + 9.5:1	0.25:1 + 4.75:1	0.125:1 + 2.375:1	0.06:1 + 1.19:1	0.03:1 + 0.57:1
Cells selected by CD4 MicroBeads	10:1	5:1	2.5:1	1.25:1	0.6:1

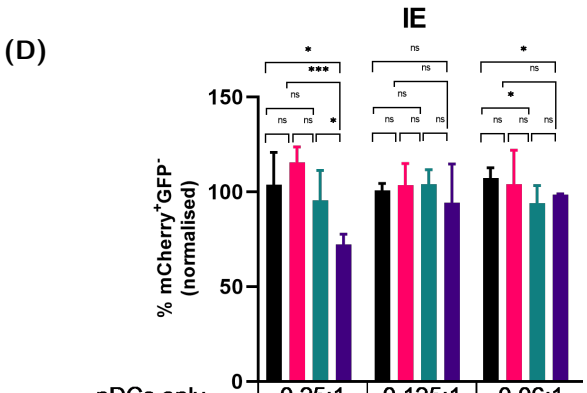

pDCs only	0.25:1	0.125:1	0.06:1
CD4+ T cells only	4.75:1	2.375:1	1.19:1
pDCs + CD4+ T cells	0.25:1 + 4.75:1	0.125:1 + 2.375:1	0.06:1 + 1.19:1
Cells selected by CD4 MicroBeads	5:1	2.5:1	1.25:1

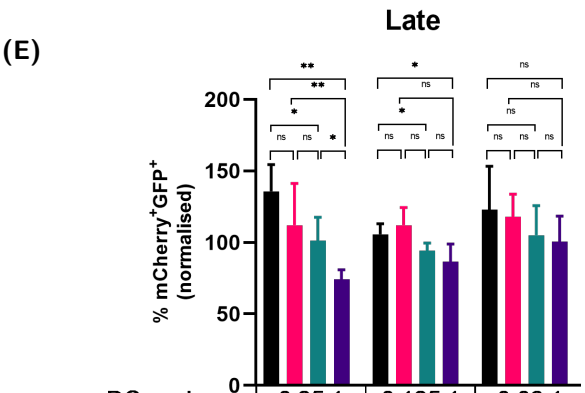

pDCs only	0.25:1	0.125:1	0.06:1
CD4+ T cells only	4.75:1	2.375:1	1.19:1
pDCs + CD4+ T cells	0.25:1 + 4.75:1	0.125:1 + 2.375:1	0.06:1 + 1.19:1
Cells selected by CD4 MicroBeads	5:1	2.5:1	1.25:1

Figure 5.10: Viral dissemination assays with plasmacytoid DCs and CD4$^+$ T cells
Primary dermal fibroblasts from an HCMV-seropositive donor were seeded in 96-well half-area plates and grown to confluency overnight before infection with Merlin WT (MOI = 0.03). At 1 dpi, PBMCs from the autologous donor were obtained and divided into 3 populations in an approximate ratio of 1:7:2, whereupon 3 populations of cells were obtained: cells selected by MACS positive selection with CD4 MicroBeads; pDCs selected by MACS depletion with Plasmacytoid Dendritic Cell Isolation Kit II; and CD4$^+$ T cells selected by MACS depletion with CD4$^+$ T cell Isolation Kit. Fig.5.10A illustrates the cell separation process. The cells were then added in the following manner: cells selected with CD4 MicroBeads (at a starting E:T ratio of 10:1); CD4$^+$ T cells (at a starting E:T ratio of 9.5:1); pDCs only (at a starting E:T ratio of 0.5:1); and pDCs with CD4$^+$ T cells (at a starting E:T ratio of 0.5 + 9.5:1). The E:T ratios at which each cell population is added is listed in Fig.5.10B. Plates were incubated for 7 days before harvest and analysis by flow cytometry. Fig.5.10B shows amount of cells with IE CMV gene expression, and Fig.5.10C shows amount of cells with late CMV gene expression, expressed as a percentage of the amount of cells in the same phase of gene expression in the infected controls. This experiment was repeated with cells from an HCMV-seronegative donor, and the results are seen in Figs.5.10D–5.10E. Error bars represent SD of triplicate wells, statistics performed using Student's *t*-test. (*$p \leq 0.05$; **$p \leq 0.01$; ***$p \leq 0.001$; ****$p \leq 0.0001$; ns = not significant)

5.8 Blocking of MHC Class II and IFN-γ abrogates the ability of CD4$^+$ cells to control viral dissemination

The results in Section 5.6 showed that co-culturing of CD14$^+$ monocytes with CD4$^+$ T cells allowed control of viral dissemination to occur. As discussed in the Introduction (Section 1.2.1), CD4$^+$ T cells recognise antigen via the MHC Class II antigen presentation pathway, and CD14$^+$ monocytes are known to be able to recognise and present antigen via MHC Class II on their cell surface (reviewed in [259]). In my earlier experiments in Chapter 4 I showed that IFN-γ can upregulate HLA-DR on the cell surface, and that blocking IFN-γ by anti-IFN-γ antibody leads to reversal or prevention of this upregulation.

CD14$^+$ monocytes constitutively express MHC Class II and are a professional antigen-presenting cell. I hypothesised that CD14$^+$ monocytes in the co-cultures might take up HCMV antigens which are then processed and presented to HCMV-specific T cells, activating these T cells and causing IFN-γ production and subsequent MHC Class II upregulation by fibroblasts.

In trying to determine the mechanism of how addition of these CD14$^+$ monocytes assist the CD4$^+$ T cells to control HCMV IE and late CMV gene expression, I thus investigated if blocking MHC Class II and IFN-γ would similarly lead to a decrease in ability to control viral dissemination.

Primary dermal fibroblasts were seeded in 96-well half-area plates and grown to confluency overnight before infection with Merlin WT (MOI = 0.27). At 1 dpi, cell separations were performed on PBMCs from the autologous donor. First, CD14$^+$ monocytes were selected by MACS positive selection using CD14 MicroBeads. Next, CD4$^+$ T cells were selected by MACS depletion using CD4$^+$ T cell Isolation Kit. The cell separation process is illustrated in Fig.5.11A. The CD4$^+$ T cells and CD14$^+$ monocytes were then added in isolation, or together (in a proportion of 9:1) at an E:T ratio of 1.25:1 (i.e. CD4$^+$ T cells added at E:T of 1.125:1 and CD14$^+$ monocytes added at E:T ratio of 0.125:1). Where they were added together, blocking antibodies to MHC Class II and IFN-γ were added, either singly or in combination, and either at high doses (50μg/ml for anti-MHCII; 10μg/ml for anti-IFN-γ) or low doses (10μg/ml for anti-MHCII; 30μg/ml for anti-IFN-γ). Incubation was carried out for 8 days before harvest and analysis by flow cytometry.

Fig.5.11B shows percentage of total cells in the well with IE CMV gene expression when CD4 T$^+$ cells and CD14$^+$ monocytes were added in isolation or co-cultured together, and Fig.5.11C shows the same for late CMV gene expression. These results recapitulate those seen in earlier experiments: CD4$^+$ T cells and CD14$^+$ monocytes added in isolation show poor control of CMV infection, but when added together, they are able to control both IE and late CMV gene expression.

Figs.5.11D & 5.11E show percentage of cells with IE and late CMV gene expression when blocking antibodies were added. Addition of MHC Class II and IFN-γ-blocking antibodies at

the higher concentrations individually (Figs.5.11D & 5.11E, light purple and green bars) leads to an approximate 50% reduction in antiviral effect, while adding them in combination leads to a near-complete abrogation of antiviral effect (grey bars). This effect is dose-dependent, as a similar trend is seen at low doses of blocking antibody, but is less effective (light blue, dark blue and coral bars).

This experiment was repeated with 2 other HCMV-seropositive donors (CMV 309 and CMV 320), and the results are shown in Figs.5.11F–5.11I. The results show that addition of anti-MHC Class II antibodies at 50μg/ml showed a reduction of control of IE and late CMV gene expression in both donors (Figs.Figs.5.11F–5.11I, light purple bars), although this was only statistically significant in one donor (CMV 320), while addition of anti-IFN-γ antibodies at 10μg/ml (Figs.5.11F–5.11I, green bars) showed a statistically significant reduction of control of IE and late CMV gene expression in one donor (CMV 309).

Addition of both anti-MHC Class II (50μg/ml) and anti-IFN-γ (10μg/ml) antibodies together only showed an additive effect in control of IE CMV gene expression in one donor (Fig.5.11H, grey bar). It is unclear why this was so and may have been as a result of an insufficient concentration of anti-IFN-γ antibodies used.

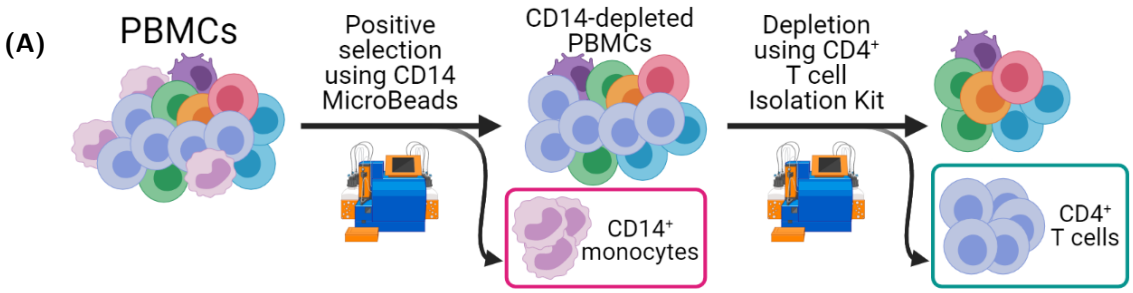
(A)
PBMCs
Positive selection using CD14 MicroBeads
CD14-depleted PBMCs
CD14⁺ monocytes
Depletion using CD4⁺ T cell Isolation Kit
CD4⁺ T cells

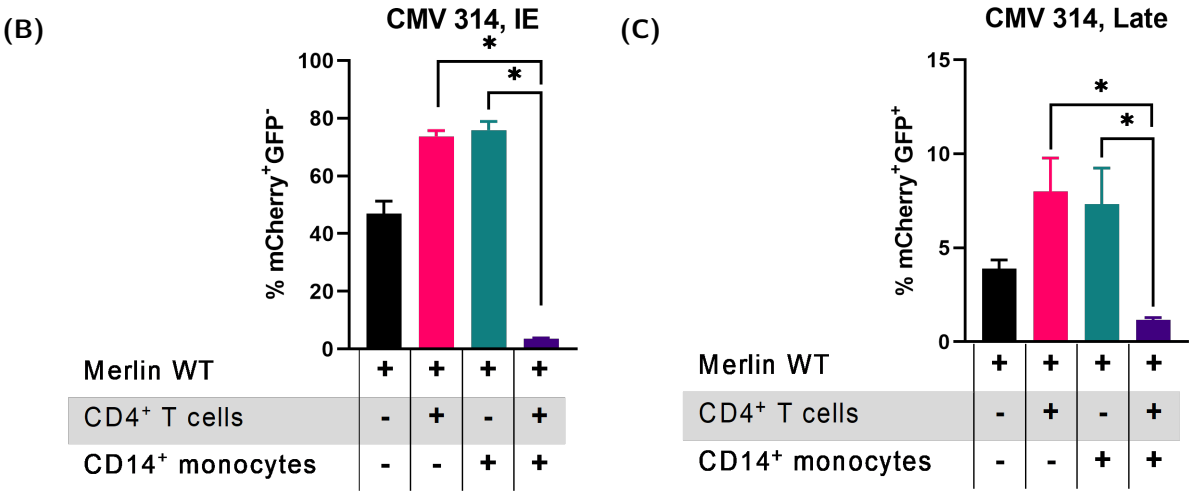
(B)
CMV 314, IE
% mCherry⁺GFP⁻
Merlin WT + + + +
CD4⁺ T cells - + - +
CD14⁺ monocytes - - + +
(C)
CMV 314, Late
% mCherry⁺GFP⁺
Merlin WT + + + +
CD4⁺ T cells - + - +
CD14⁺ monocytes - - + +

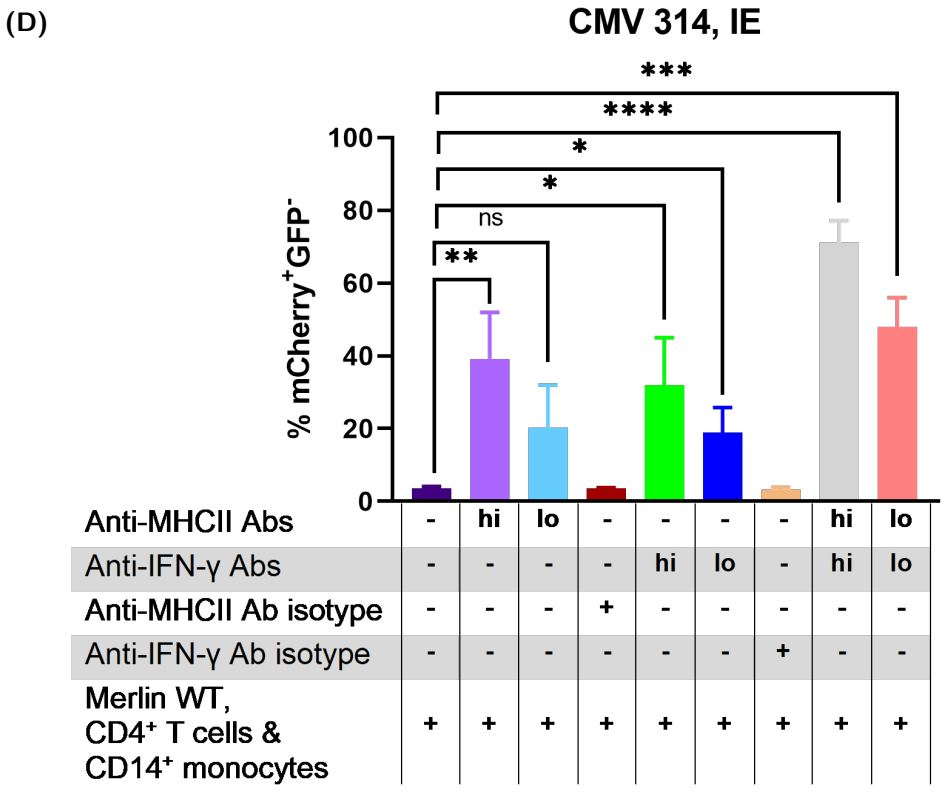
(D)
CMV 314, IE
% mCherry⁺GFP⁻
Anti-MHCII Abs - hi lo - - - - hi lo
Anti-IFN-γ Abs - - - - hi lo - hi lo
Anti-MHCII Ab isotype - - - + - - - - -
Anti-IFN-γ Ab isotype - - - - - - + - -
Merlin WT, CD4⁺ T cells & CD14⁺ monocytes + + + + + + + + +

(E)

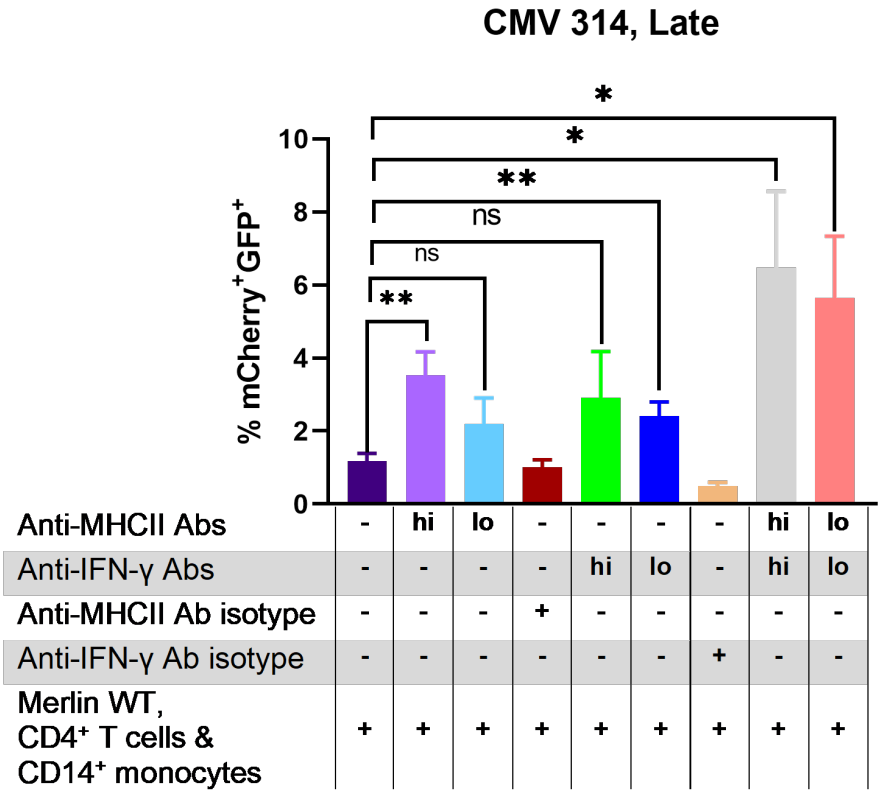
CMV 314, Late
% mCherry+GFP+
0
2
4
6
8
10
*
*
**
ns
ns
**
Anti-MHCII Abs - hi lo - - - - hi lo
Anti-IFN-γ Abs - - - - hi lo - hi lo
Anti-MHCII Ab isotype - - - + - - - - -
Anti-IFN-γ Ab isotype - - - - - - + - -
Merlin WT, CD4+ T cells & CD14+ monocytes + + + + + + + + +

(F)

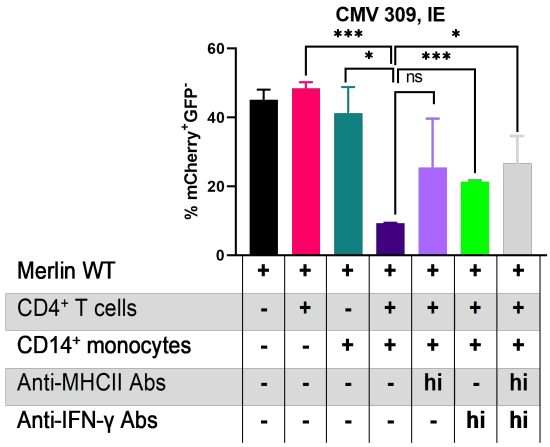
CMV 309, IE
% mCherry+GFP-
0
20
40
60
***
*
*
***
ns
Merlin WT + + + + + + +
CD4+ T cells - + - + + + +
CD14+ monocytes - - + + + + +
Anti-MHCII Abs - - - - hi - hi
Anti-IFN-γ Abs - - - - - hi hi

(G)

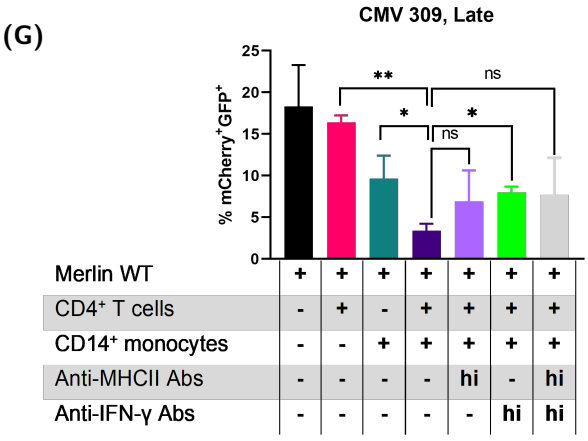
CMV 309, Late
% mCherry+GFP+
0
5
10
15
20
25
**
ns
*
*
ns
Merlin WT + + + + + + +
CD4+ T cells - + - + + + +
CD14+ monocytes - - + + + + +
Anti-MHCII Abs - - - - hi - hi
Anti-IFN-γ Abs - - - - - hi hi

(H)

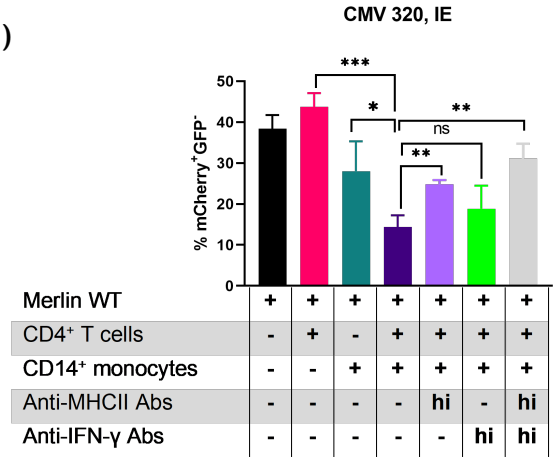
CMV 320, IE
% mCherry+GFP-
0
10
20
30
40
50
***
*
**
ns
**
Merlin WT + + + + + + +
CD4+ T cells - + - + + + +
CD14+ monocytes - - + + + + +
Anti-MHCII Abs - - - - hi - hi
Anti-IFN-γ Abs - - - - - hi hi

(I)

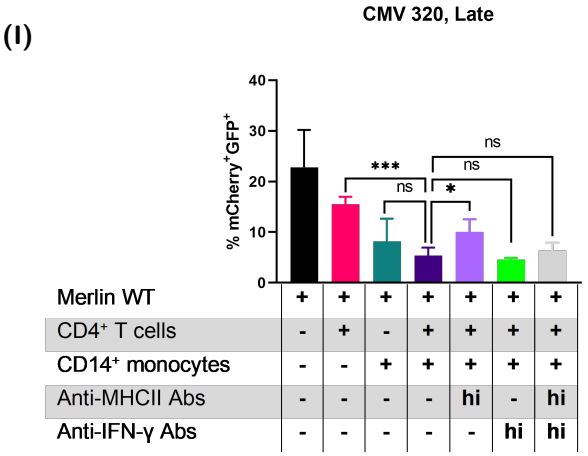
CMV 320, Late
% mCherry+GFP+
0
10
20
30
40
***
ns
ns
ns
*
Merlin WT + + + + + + +
CD4+ T cells - + - + + + +
CD14+ monocytes - - + + + + +
Anti-MHCII Abs - - - - hi - hi
Anti-IFN-γ Abs - - - - - hi hi

Figure 5.11: Blocking of MHC Class II and IFN-γ abrogates ability of CD4$^+$ cells to control viral dissemination
Primary dermal fibroblasts from an HCMV-seropositive donor (CMV 314) were seeded in 96-well half-area plates and grown to confluency overnight before infection with Merlin WT (MOI = 0.27). At 1 dpi, cell separations were performed on PBMCs from the same donor. First, CD14$^+$ monocytes were selected by MACS positive selection using CD14 MicroBeads. Next, CD4$^+$ T cells were selected from the remaining cells by MACS depletion using CD4$^+$ T cell Isolation Kit. The cell separation process is illustrated in Fig.5.11A. The CD4$^+$ T cells and CD14$^+$ monocytes were then added in isolation, or together (in a proportion of 9:1) at an E:T ratio of 1.25:1. Incubation was carried out for 8 days before harvest and analysis by flow cytometry. Fig.5.11B shows percentage of cells with IE CMV gene expression when CD4 T$^+$ cells and CD14$^+$ monocytes were added in isolation or together, and Fig.5.11C shows the same for late CMV gene expression. In addition, in wells with both CD4$^+$ T cells and CD14$^+$ monocytes, blocking antibodies to MHC Class II and IFN-γ were also added, either singly or in combination, and either at high doses (50μg/ml for anti-MHCII; 10μg/ml for anti-IFN-γ; indicated by "hi") or low doses (10μg/ml for anti-MHCII; 3μg/ml for anti-IFN-γ; indicated by "lo"). Fig.5.11D shows percentage of cells with IE CMV gene expression when blocking antibodies were added, and Fig.5.11E shows the same for late CMV gene expression. This experiment was repeated with 2 other HCMV-seropositive donors (CMV 309 and CMV 320), and the results are shown in Figs.5.11F–5.11I. Error bars represent SD of triplicate wells, statistics performed using Student's *t*-test. (*$p \leq 0.05$; **$p \leq 0.01$; ***$p \leq 0.001$; ****$p \leq 0.0001$; ns = not significant) Fig.5.11A created at BioRender.com.

5.9 Discussion

5.9.1 A potential mechanism of how CD4$^+$ cells can recognise infected cells that do not constitutively express MHC Class II in the viral dissemination assay

The results in this chapter have provided a possible explanation for how the CD4$^+$ populations in Chapter 3 were able to recognise HCMV-infected fibroblasts. As shown by phenotyping analyses in Figs.5.3 and 5.5, CD4$^+$ populations selected by MACS positive selection using CD4 MicroBeads contain a population of cells that were likely to be classical, intermediate and non-classical monocytes, characterised by CD14$^+$CD16$^-$, CD14$^+$CD16$^+$, and CD14^{dim}CD16$^+$. During viral infections, monocytes are able to induce T_H1 responses [302, 408], and in a adjuvant-induced model of inflammation, monocytes played a substantial role in antigen presentation to CD4$^+$ T cells [323]. During inflammation, monocytes are also capable of differentiation into dendritic cells, antigen presentation and driving the consequent proliferation of other relevant T cell subsets (reviewed in [462]). Therefore, the presence of a population of monocytes in the CD4 MicroBead-selected cells would allow for antigen presentation to the CD4$^+$ T cells in the same well, triggering the cascade of downstream signalling events that lead to IFN-γ production and T_H1 differentiation.

Fig.5.7 showed that when a population of "pure" CD4$^+$ T cells, obtained by MACS depletion using the CD4$^+$ T cell Isolation Kit, was added to the viral dissemination assay, these cells were much less able to control viral dissemination as compared to the cells selected by MACS positive selection using CD4 MicroBeads. However, when CD14$^+$ cells were added to the CD4$^+$ T cells, they reached levels of control similar to that seen in CD4$^+$ cells isolated by positive selection. When anti-MHC Class II or anti-IFN-γ antibody was added in isolation at high doses, these levels of control were reduced partially, and when they were added in combination, antiviral control was removed (Fig.5.11).

The anti-IFN-γ antibody neutralises human IFN-γ. Addition of this antibody would prevent binding of IFN-γ to its receptor on the cell surface and thus limit its myriad downstream actions with antiviral effects. In the context of these experiments, these could be broadly divided into 2 categories: (1) activation of IFN-γ-stimulated gene transcription leading to induction of an antiviral state via transcription of antiviral genes (summarised in [510]); and (2) induction of MHC Class II proteins on the cell surface via Class II transactivator (CIITA) gene transcription.

However, CD14$^+$ monocytes constitutively express MHC Class II and do not require IFN-γ to induce expression of MHC Class II for antigen presentation. Therefore, while addition of IFN-γ-blocking antibodies would inhibit induction of MHC Class II on fibroblasts which had not yet undergone viral entry and thereby its downstream antiviral effects on these cells, it

would not prevent antigen presentation to $CD4^+$ T cells via MHC Class II on $CD14^+$. In addition, in Chapter 4 I have shown that the secretome also contains other antiviral cytokines at effective concentrations (such as TNF-α and type I interferons). The presence of these other cytokines would therefore also have an antiviral effect on the fibroblasts.

The anti-MHC Class II antibody used recognises MHC Class II HLA-DR, DP and most DQ antigens. Addition of this antibody would inhibit antigen presentation via MHC Class II by competitive inhibition. However, surface expression of MHC Class II is controlled by regulated ubiquitination and recycling of MHC Class II complexes from the cell surface [397,416,518,601]. As such, a possible reason that addition of MHC Class II blocking antibodies did not result in complete abrogation of the antiviral effect could be that there was sufficient recycling of MHC Class II complexes to allow antigen presentation to occur, albeit to a less efficient degree. Even so, the addition of *both* IFN-γ and MHC Class II-blocking antibodies concurrently does frequently result in a substantial decrease of the antiviral effect, although to a greater degree in some donors than others.

Further to this, future experiments from this work could be to attempt to differentiate between MHC Class II on the fibroblasts and the $CD14^+$ monocytes, to tease apart how each of these contribute to $CD4^+$ cell control of HCMV. This could possibly be done by using CRISPR to remove CIITA genes, which would prevent the upregulation of MHC Class II complexes on the surface of these fibroblasts, thus leaving only antigen presentation via MHC Class II on the monocytes. Another possible method of showing that antigen presentation by monocytes and subsequent activation of $CD4^+$ occurs could be to incubate $CD14^+$ monocytes with infected fibroblasts, following by subsequent sorting of these monocytes and adding them to autologous $CD4^+$ T cells, followed by staining for activation markers, which would imply antigen presentation. Other experiments could also include further characterising the monocytes in the assay at the end of the incubation period by phenotyping analysis to elucidate the monocyte subsets that were present, and possibly the extent of differentiation into other immune cell subtypes, such as dendritic cells or macrophages.

5.9.2 Plasmacytoid dendritic cells have direct antiviral effect at sufficiently high E:T ratios, but do not appear to potentiate $CD4^+$ T cell responses

When added to the viral dissemination assay, pDCs appeared to have a direct antiviral effect (Fig.5.9B), limiting the amount of IE and late CMV gene-expression HCMV-infected fibroblasts, up to an E:T ratio of 0.38:1. As discussed in the Introduction (Section 1.3), pDCs have wide-ranging effects on innate and adaptive immune responses to viral infection, primarily through driving responses of T cells, NK cells and plasma cells by cytokine production, but also by inducing an antiviral state by production of type I interferon. This could explain the

control of IE and late CMV gene expression seen when pDCs were added to HCMV-infected fibroblasts.

These results are also corroborated by the results of the flow cytometry-based cytokine array (LegendPlex™) in Chapter 4 (Fig.4.10). After interferon-γ, the cytokines that were found in the next-highest quantities were IFN-α, IFN-λ1 and IFN-β. The secretomes were made with $CD4^+$ cells that had been selected by MACS positive selection with CD4 MicroBeads. They would thus be expected to contain pDCs, which would account for the significant amounts of IFN-α and IFN-β in the secretome.

There did not appear to be an additional antiviral effect when pDCs were added to $CD4^+$ T cells (Fig.5.10). Plasmacytoid dendritic cells contain MHC Class II on their cell surface and have been shown to be able to present antigen via MHC Class II complexes and activate T cell responses, although they appear to be poorer presenters of exogenous antigens than cDCs (reviewed in [607]). The reason for this may be because MHC Class II ubiquitination and turnover is not downregulated in activated pDCs [655]. This would mean that despite having antigens "loaded" onto their MHC Class II complexes, these complexes still get removed from the cell surface, and therefore there is a shorter duration for $CD4^+$ T cells to recognise the antigen-loaded MHC Class II complexes on the surface of pDCs, making pDCs less efficient antigen-presenting cells than other dendritic cell subsets. Thus, the addition of pDCs to $CD4^+$ T cells in the viral dissemination assay did not result in increased control of viral dissemination.

However, the $CD4^+$ T cells selected with the $CD4^+$ T cell Isolation Kit showed an antiviral effect that was greater than expected in this experiment, likely due to suboptimal post-separation purity. At the E:T ratio that these $CD4^+$ T cells began to lose this effect (2.375:1), the addition of pDCs (at E:T of 0.125:1) may have been at an E:T ratio that was too low to see an effect.

Hence, more repeats of this experiment are required before conclusions can be drawn. Additionally, the repeat of this experiment with CRISPR-edited fibroblasts with deletion of CIITA would also be a useful tool to allow me to examine the effects of the pDCs without upregulation of MHC Class II on the fibroblasts.

5.9.3 Presence of conventional DCs in the $CD3^-CD4^+$ cell populations

Besides monocytes and plasmacytoid dendritic cells, there was also a population of what was likely to be conventional/classical DCs (cDCs), in the $CD3^-CD4^+$ cells selected by CD4 MicroBeads.

cDCs are professional antigen-presenting cells of the innate immune system that comprise approximately one-tenth of steady-state blood leucocytes in humans [78]. They are

Lineage$^-$HLA-DR$^+$ cells derived from haematopoietic stem cells and segregated from pDCs by the presence of CD11c [371] and expression of transcription factor zBTB46 [389, 504]. They can broadly be divided into 2 subsets, cDC1 (identified by canonical markers XCR1 [34], DNGR-1 [121] and additionally by CD141 and CADM1 [104]) and cDC2 (identified by expression of CD1c and SIRPα/CD172A and absence of cDC1 markers XCR1 and DNGR-1 [608]), although cDC2s are a heterogeneous population and classification and characterisation are still ongoing [78].

cDC1s are more efficient at cross-presentation of exogenously acquired antigens [35, 221, 271] while cDC2s are more likely to induce Th17 and Th2 responses [207,435,507]. cDC2s were shown to have superior MHC Class II antigen presentation of soluble ovalbumin or ovalbumin coupled to antibodies targeted to Fc or other surface receptors [137, 334], an observation that is also supported by transcriptional studies [603], although some studies have reported lower MHC Class II processing by cDC2 than cDC1 for cell-associated antigens [577,595]. Regardless of this, the presence of these CD11c$^+$ cDCs in the CD3$^-$CD4$^+$CD14$^-$CD16$^-$ population provide another pathway by which the CD4$^+$ T cells present in the well can recognise HCMV-infected fibroblasts.

The results of the cytokine array and LegendPlex^{TM} assay in Chapter 4 also showed that GM-CSF and IL-4 was present in the secretome. Both of these cytokines would lead to differentiation of monocytes into dendritic cells [111, 380] and further enhance their antigen-presenting capabilities [106].

Chapter 6

Using the viral dissemination assay to assess *in vitro* antiviral capabilities of PBMCs, $CD8^+$ T cells, NK cells and $CD4^+$ cells from kidney and liver transplant recipients

6.1 Introduction

Multiple studies of CMV disease in transplant recipients have shown that the presence of HCMV-specific $CD4^+$ T cells is associated with a lower risk of CMV disease [75, 76, 145, 186, 351]. These studies primarily identify HCMV-specific T cell responses using cytokine (IFN-γ, IL-2 or TNF-α) responses to CMV peptides, or activation markers (CD69 or CD107a) (summarised in Table 1.7). However, measurement of cytokine responses and activation markers may not necessarily reflect the *in vivo* functionality of these cells. This may perhaps explain the results of other studies [319, 353] that have not shown a protective effect of HCMV-specific $CD4^+$ T cells against CMV disease in this group of patients. To my knowledge, besides an earlier study published by our group [241], no other groups have developed an assay to examine the functional response of PBMCs or T cells in transplant patients. I thus used this viral dissemination assay to assess the capability of these cells to control HCMV in an *in vitro* setting.

As the data presented in Sections 3.4.1–3.4.4 from Chapter 3 show, PBMCs, $CD8^+$ T cells, NK cells and $CD4^+$ cells from a cohort of healthy HCMV-seropositive and HCMV-seronegative donors show differing abilities to limit IE and late viral gene expression when added to the viral dissemination assay. In particular, $CD8^+$ T cells and $CD4^+$ cells from healthy HCMV-seronegative donors show a significantly poorer ability to limit viral gene expression than $CD8^+$

T cells and $CD4^+$ cells from healthy HCMV-seropositive donors. This would be expected, as $CD8^+$ and $CD4^+$ T cells from HCMV-seronegative donors do not have memory T cell responses to HCMV. The viral dissemination assay is thus capable of demonstrating functional differences of various immune cell populations between individuals who do or do not have an adaptive immune response to HCMV. I therefore hypothesised that this assay could also be used to demonstrate functional differences between transplant recipients, and wanted to use this assay to find out if there were deficiencies in particular subsets of immune cells in transplant recipients who experienced episodes of HCMV reactivation.

Risk factors for HCMV reactivation and disease in this cohort of kidney and liver transplant recipients

As discussed in the Introduction (Section 1.2.7.1), the HCMV serostatus of the organ donor and recipient influences the risk of CMV reactivation and disease in these patients. Seronegative recipients of an organ from a seropositive donor (D^+R^-) are at the highest risk, as the CMV-immunonaïve recipient is required to mount a primary immune response to reactivation of latent CMV in the donor organ, and the lack of a pre-existing CMV-specific humoral and cell-mediated response means that the initial ability to suppress viral reactivation would rely initially purely on innate immune responses, against which CMV has numerous immune evasion genes, allowing for very rapid CMV replication [466]. The risk of CMV viraemia usually begins 3-4 weeks after transplant, peaks at 6-16 weeks, and tends to become uncommon after 6 months [32], although there has been an incident of transmission of HCMV from a seropositive liver to a seronegative donor after only 28 hours *in situ* [369]. Seropositive recipients are at intermediate risk of reactivation. In D^-R^+ patients, the seropositive recipient faces the risk of reactivation of endogeneous latent virus during periods of immunosuppression post-transplantation, while D^+R^+ patients face the risk of reactivation of both endogeneous latent virus and virus from the donor organ, which may be of different strains [282, 378]. These HCMV-seropositive recipients possess a pre-existing immune response to HCMV but post-transplantation immunosuppression may impair this response.

However, the transmission dynamics of HCMV in solid organ transplant recipients is complex, as evidenced by the fact that not all transplant recipients which are HCMV-seropositive, or those which are HCMV-seronegative but receive an organ donated from a HCMV-seropositive donor, experience CMV reactivation or disease. Other contributory factors to an increased risk of CMV disease are a higher CMV viral load at first positive post-transplant screening and a high rate of increase in CMV viral load during subsequent screening PCR tests [152, 340, 385, 466].

Another possible contributing factor could be that there are inherent differences in the ability to control HCMV replication between the various immune cell populations in these patients. The viral dissemination assay introduced in the earlier chapters allowed me to in-

vestigate this. It would be expected that PBMCs, $CD8^+$ T cells, NK cells and $CD4^+$ cells from patients that did not have episodes of cytomegaloviraemia would exhibit levels of control of CMV gene expression similar to that seen in healthy HCMV-seropositive controls, while those that did have episodes of viraemia would demonstrate a functional defect in one or more lymphocyte subsets, manifested by increased levels of CMV gene expression, implicating an impaired immune response to HCMV. The experiments in this chapter attempt to address this hypothesis, by looking for differences in ability to control IE and late CMV gene expression in the *in vitro* viral dissemination assay by the various immune cell populations from a cohort of kidney and liver transplant recipients, and comparing them to the same immune cell populations in a cohort of healthy individuals.

Obtaining multiple immune cell populations from a single sample of PBMCs

As explained in Section 2.12.3, it was required to obtain $CD4^+$ cells, $CD8^+$ T cells and NK cells from a single sample of PBMCs. As such, in the cell separations for viral dissemination assays described in this chapter, after removal of the required number of total PBMCs, $CD4^+$ cells were first isolated by positive selection using MACS. The remaining CD4-depleted PBMCs were then split into 2 aliquots, with one being used for undergoing $CD8^+$ T cell isolation and the other for NK cell isolation. This was done using specific Isolation Kits to deplete all cells that were not $CD8^+$ T cells or NK cells. The use of depletion methods was necessary for $CD8^+$ T cells and NK cells as the CD8 molecule is expressed on up to 40% of NK cells [6,547] while the common NK cell molecule, CD56, is also expressed on other T cells, such as $\gamma\delta$T cells [293].

Contributions

The work in this chapter was undertaken in collaboration with a team from University College London (headed by Dr Matthew Reeves), funded by a Wellcome Trust collaborative grant and Medical Research Council grants, and with a post-doctoral colleague from Dr Mark Wills' group (Dr Charlotte Houldcroft). Skin biopsy samples, initial growing of primary dermal fibroblast cell lines and collection of patient blood samples were carried out by the team from University College London. The cellular separations and assay set-ups were performed by myself. Dr Houldcroft performed the viral infections and added the cellular subsets post-separation, and performed the FluoroSpot™ assays. Flow cytometry to obtain VDA results was performed in equal shares by Dr Houldcroft and myself. All subsequent data analysis and statistical analysis was performed by myself.

6.2 Characteristics of transplant recipients in the study

The transplant patients included in this study were a cohort of kidney and liver transplant recipients ranging from ages 20-68 who were recruited by Royal Free Hospital, London and had either kidney or liver transplants from October 2018 to September 2019. These patients had monitoring for CMV viral load as per clinical protocols [28, 383], during which PBMCs were also taken for the purposes of this study pre-transplant and at regular intervals post-transplant. As part of the post-transplant protocol to prevent organ rejection, the kidney transplant patients in this study received an immunosuppressive regimen based on basiliximab (monoclonal antibody to IL2 receptor [285]), mycophenolate mofetil (inhibitor of inosine monophosphate dehydrogenase and inducible nitric oxide synthase inhibitor [15]) and tacrolimus (a calcineurin inhibitor [436], immunosuppression guidelines found in [2]); while the liver transplant patients received a regimen based on tacrolimus, azathioprine (a purine analogue [457]) or mycophenolate mofetil and steroids (guidelines in [392]).

2-mm punch biopsy of the skin was also taken from each of these patients and grown out to obtain primary dermal fibroblast cell lines (protocol published in [451], modified in [450]). This enabled me to use autologous dermal fibroblasts when the various immune cell populations from these transplant recipients were added to the viral dissemination assay, thus allowing for appropriate MHC Class I and II antigen presentation to occur without generating *in vitro* allogeneic reactions. Table 6.1 lists the characteristics of the patients included in this study, and Table 6.2 lists the number of donors with and without viraemia in each serostatus group. A viraemic episode was defined as presence of CMV viral load $>$200 genome copies/ml of blood for 2 consecutive tests during routine post-transplant CMV PCR screening, and patients that experienced episodes of viraemia were classified as "viraemic donors". This classification applies to all subsequent analyses in this chapter. Details of each of these patients is given in Appendix J.

	Organ transplanted		*p* value*
	Kidney (n=7)	Liver (n=8)	
Age			0.9691
<55 years	4	4	
≥55 years	3	4	
Serostatus			0.1737
D^+R^+	6	4	
D^+R^-	1	2	
D^-R^+	0	2	
Episodes of viraemia?**			0.0127
Yes	1	5	
No	6	3	
Viraemia >1000 copies/ml?			0.4795
Yes	1	2	
No	6	6	

Table 6.1: Characteristics of transplant recipients
*Statistics performed using Chi-square test.
**Defined as presence of CMV viral load >200 copies/ml of blood for 2 consecutive tests during routine post-transplant CMV PCR screening.

Serostatus	Viraemic donors	Non-viraemic donors	*p* value*
D^+R^+	4	7	0.3174
D^+R^-	2	1	
D^-R^+	0	2	

Table 6.2: Number of viraemic and non-viraemic donors in each serostatus group
*Statistics performed using Chi-square test.

6.3 Viral dissemination assay provides a more nuanced analysis of immune cell response to HCMV

6.3.1 Viraemic patients are not always lymphopaenic

Patients with recurrent CMV infections are more likely to have lower lymphocyte counts [308, 409], and in a multi-variate analysis of 276 liver transplant recipients, pre-transplant lymphopenia was found to be an independent predictor for CMV disease [413]. To examine if lymphopenia or low total PBMC counts was associated with episodes of viraemia in our cohort of patients, lymphocyte, monocyte and total PBMC counts, calculated by addition of lymphocyte and monocyte counts, were plotted against a time course of CMV viral load levels of all patients in the study. Fig.6.1A shows the counts for patients who experienced episodes of viraemia, defined as detection of $>$200 CMV genome copies/ml of blood on two consecutive post-transplant PCR screening tests, while Fig.6.1B shows the counts for patients who did not experience viraemia (note that the left y-axis is different between Figs.6.1A & 6.1B).

The results in Fig.6.1A show that there were patients who experienced episodes of viraemia even though they had lymphocyte and PBMC counts above threshold levels (R01-079, R01-081 and R02-011, pink and teal dotted lines). Conversely, Fig.6.1B shows that there were also patients who did not experience episodes of viraemia despite low PBMC and lymphocyte counts (R02-005, R02-015, and R02-058). In addition, two of the patients that experienced viraemic episodes despite PBMC and lymphocyte counts above threshold were the "high-risk" D^+R^- (R01-079 and R01-081). These figures suggest that absolute PBMC or lymphocyte numbers do not completely describe the functional capability of these cells to prevent HCMV replication, particularly in D^+R^- patients.

(A) Viraemic patients

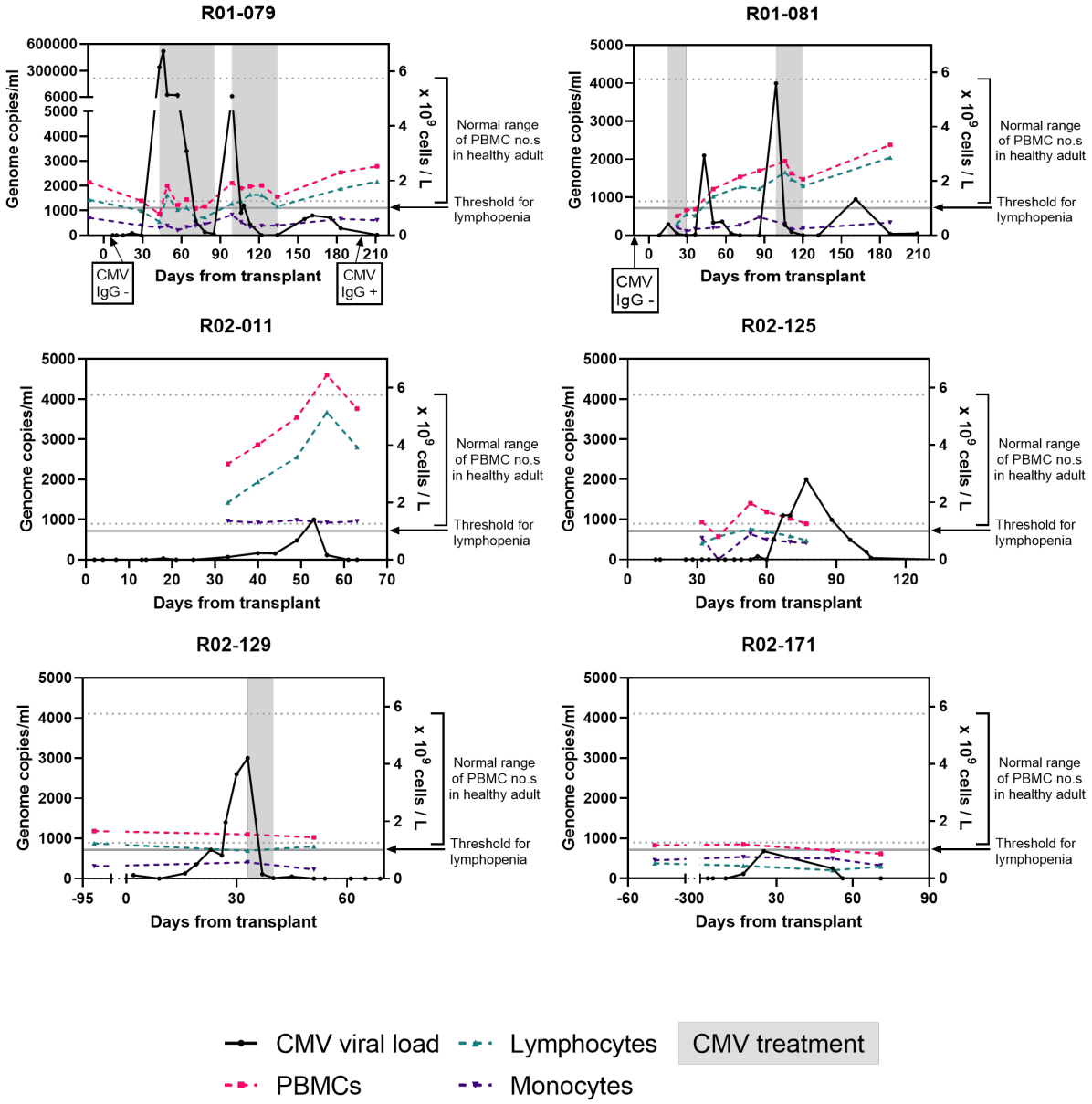

(B) Non-viraemic patients

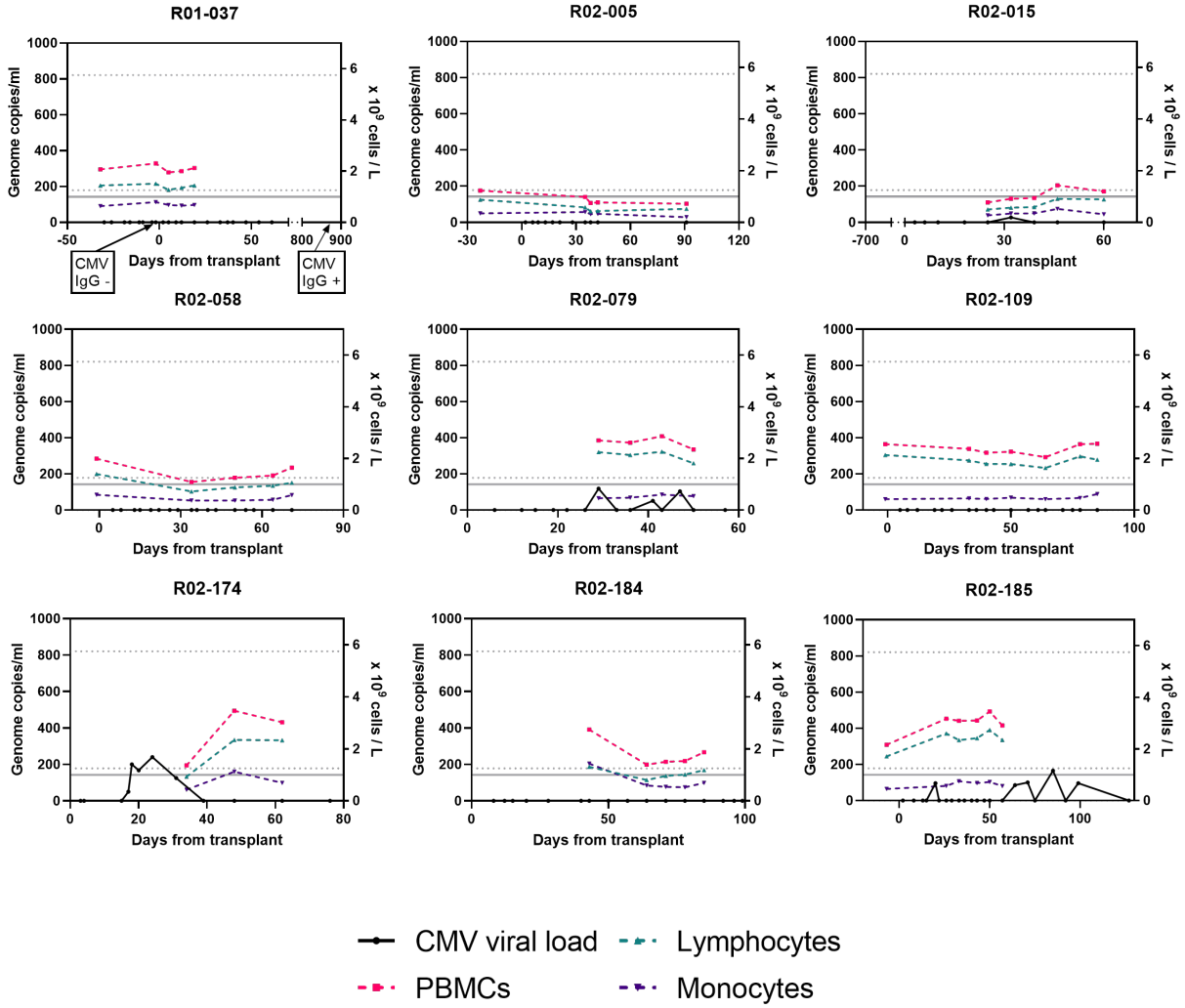

Figure 6.1: Time course of CMV viral load, total PBMCs, lymphocyte and monocyte counts in transplant recipients
Time course of CMV viral load, lymphocyte counts, monocyte counts and total PBMC counts, obtained by addition of lymphocyte and monocyte counts, were plotted for the 6 patients with episodes of viraemia (Fig.6.1A), defined as detection of CMV viral load >200 genome copies/ml of blood for 2 consecutive tests during routine post-transplant CMV PCR screening of blood, and 9 patients without episodes of viraemia (Fig.6.1B). Shaded grey areas indicate time periods when CMV treatment was given, dotted grey lines indicate range of expected numbers of PBMCs in healthy adults, and solid grey line indicates threshold for defining lymphopenia (1×10^9 cells/L). Note that the left y-axis is different between Figs.6.1A & 6.1B

6.3.2 Fluorospot^{TM} analysis of IFN-γ responses to CMV peptides

From whole PBMCs

Monitoring for CMV-specific T-cell responses, usually by detecting an IFN-γ response to stimulation of whole blood or PBMCs with CMV-specific antigens, can predict individuals at

risk of CMV disease post-transplant [308], although the largest study to date of using CMV-specific immune monitoring to predict CMV infection suggested that its highest clinical utility lay in risk-stratifying R^+ patients, as opposed to "high-risk" D^+R^- patients [317]. However, lack of routine availability, high costs and slow turnaround time limit its incorporation into routine clinical monitoring [214].

To examine the CMV-specific immunity of the cohort of patients in this study, IFN-γ responses of PBMCs from transplant recipients to HCMV peptide pools were measured and subsequently stratified according to donor and recipient serostatus, and whether they experienced episodes of viraemia. The peptide pools consisted of peptides from IE, gB, pp65, pp71, US28 and latency-associated antigens (such as Latency Unique Nuclear Antigen, LUNA). The IFN-γ responses of these PBMCs were measured using the FluoroSpot^{TM} assay. This assay involves coating monoclonal antibodies to specific analytes (in this case, IFN-γ) onto a polyvinylidene fluoride (PVDF) membrane in a 96-well plate. Subsequently, PBMCs and the relevant peptides are added and the plates incubated for 48 hours to allow T cell recognition of antigens and production of the cytokine response. Biotinylated or tag-labelled secondary detection antibodies to the analyte(s) are then added before final addition of fluorescently-labelled anti-tag antibodies or streptavidin. The amount of IFN-γ is then quantified by enumerating the number of fluorescence "spots" per well with a fluorescence reader, and given as the number of "spot-forming units" (sfu) per 10^6 cells added to the well. The number of $CD3^+$ cells per well was measured by staining an equivalent amount of PBMCs added to the well with antibodies to CD3/CD4/CD8 and analysing by flow cytometry to obtain the number of $CD3^+$ cells in the PBMC population. The number of "spot-forming units" is then corrected for the number of $CD3^+$ cells per well, to obtain number of "spot-forming units per 10^6 $CD3^+$ cells". These FluoroSpot^{TM} assays were performed by Dr Charlotte Houldcroft, and data and statistical analysis was performed by me.

The results are seen in Fig.6.2A. Two patients in the study experienced recurrent episodes of viraemia (R01-079 and R01-081). As such, PBMCs were sampled from multiple timepoints throughout the post-transplant monitoring period for both donors (4 timepoints for R01-079 and 3 timepoints for R01-081) and were analysed as part of the "D^+R^- Viraemics" group in Fig.6.2A. Mann-Whitney *U* tests were then performed to look for statistically significant differences between the groups.

Fig.6.2A shows that PBMCs from D^-R^+ patients who did not experience any episodes of viraemia had the lowest median IFN-γ response to HCMV peptide pools, while the PBMCs from the D^+R^- patients who experienced multiple episodes of viraemia showed the highest median IFN-γ responses to HCMV peptide pools overall. However, I was unable to find any statistically significant difference between the IFN-γ responses from any of the groups. We would expect that patients that did not experience episodes of viraemia (i.e. they had sufficient CMV-specific immunity to prevent viraemia) would demonstrate higher IFN-γ responses to

HCMV-peptide pools as a reflection of their CMV-specific immunity *in vivo*. However, this is clearly not the case. This data suggests that examining the summed IFN-γ response of PBMCs as a whole to HCMV peptide pools may not be sufficient to give a complete picture of the CMV-specific immunity of these patients.

Furthermore, when these data points were re-analysed purely by whether they experienced viraemic episodes or not, Fig.6.2B shows that the viraemic patients actually had a higher median IFN-γ response to HCMV peptide pools than patients who did not. This would suggest that using a poor IFN-γ response to HCMV peptides as a predictor of viraemic episodes could possibly be misleading.

There is, however, a caveat to this data, which is that these PBMCs were taken at various timepoints pre- and post-transplant, ranging from 22 days pre-transplant to up to 211 days post-transplant (with most data falling between 22 and 85 days post-transplant), and, particularly for the viraemic patients, most samples were taken from timepoints *after* the onset of viraemia. It would thus be impossible to comment if the IFN-γ responses were predictive of viraemic episodes.

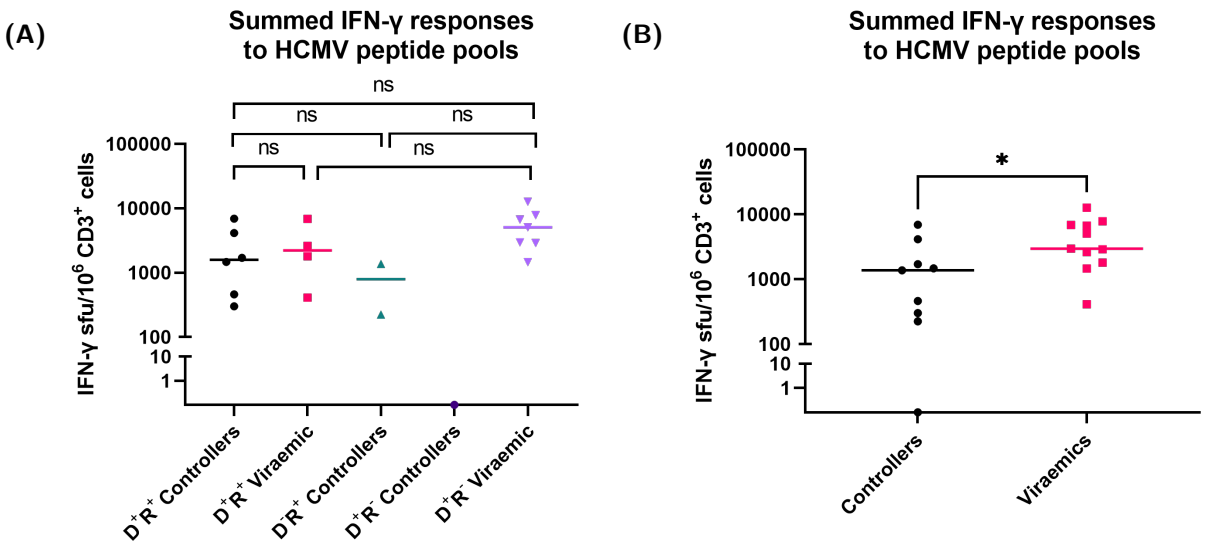

Figure 6.2: Summed IFN-γ responses of PBMCs from transplant recipients to HCMV peptide pools
FluoroSpot^{TM} assays were performed on PBMCs from transplant recipients and IFN-γ responses to HCMV peptide pools containing IE, gB, pp65, pp71, US28 and latency-associated HCMV antigens were measured and added together. Fig.6.2A: These responses were then stratified by donor and recipient HCMV serostatus and whether the recipient experienced episodes of viraemia ("Viraemics") or not ("Controllers"). Two D^+R^- transplant recipients (R01-079 and R01-081) had PBMC samples taken from 4 and 3 different timepoints post-transplant, respectively, which were added to the "D^+R^- Viraemics" group. Fig.6.2B shows these same data points re-organised into whether they had viraemic episodes ("Viraemics") or not ("Controllers"). Medians of each group are shown and statistical analysis performed using Mann-Whitney *U* tests. FluoroSpot^{TM} data obtained from Dr Charlotte Houldcroft, statistical analysis performed by myself.

From CD4- and CD8-enriched cell populations

The association of a functioning $CD8^+$ T cell response with a lower risk of HCMV reactivation and disease in solid organ transplant recipients is well-documented [83, 84, 360, 384, 387, 422, 439], although there is a growing body of evidence that an adequately-functioning $CD4^+$ T cell response is also necessary (reviewed in [352]).

To examine if there was an association between the magnitude of $CD4^+$ and $CD8^+$ T cell responses with the development of CMV viraemia in our cohort of patients, the FluoroSpot™ IFN-γ responses of the CD4-enriched and CD8-enriched immune cell populations from our cohort of transplant recipients was studied. These CD4- and CD8-enriched immune cell populations were obtained by using CD8 or CD4 MicroBeads to label $CD8^+$ or $CD4^+$ cells on whole PBMC populations, followed by removal of these labelled cells with MACS columns. FluoroSpot™ assays were then performed on these immune cell populations in the same manner as for the data shown in Fig.6.2 above. The FluoroSpot™ assays were performed by Dr Charlotte Houldcroft.

The results in Fig.6.3A show that, for patients with episodes of viraemia, CD8-enriched immune cell populations tended to generate a stronger IFN-γ response to HCMV peptide pools than CD4-enriched population (pink squares vs light purple inverted triangles), but this difference was not statistically significant. When the CD4-enriched and CD8-enriched populations were analysed by serostatus group (Fig.6.3B), there was no statistically significant differences between the groups.

These graphs therefore show that :

1. Both CD4- and CD8-enriched populations from this cohort of transplant recipients were able to generate an IFN-γ response to HCMV peptide pools, regardless of whether they were viraemic and their serostatus groups.

2. Their serostatus groups and viraemic status appeared to have no impact on the magnitude of these IFN-γ responses.

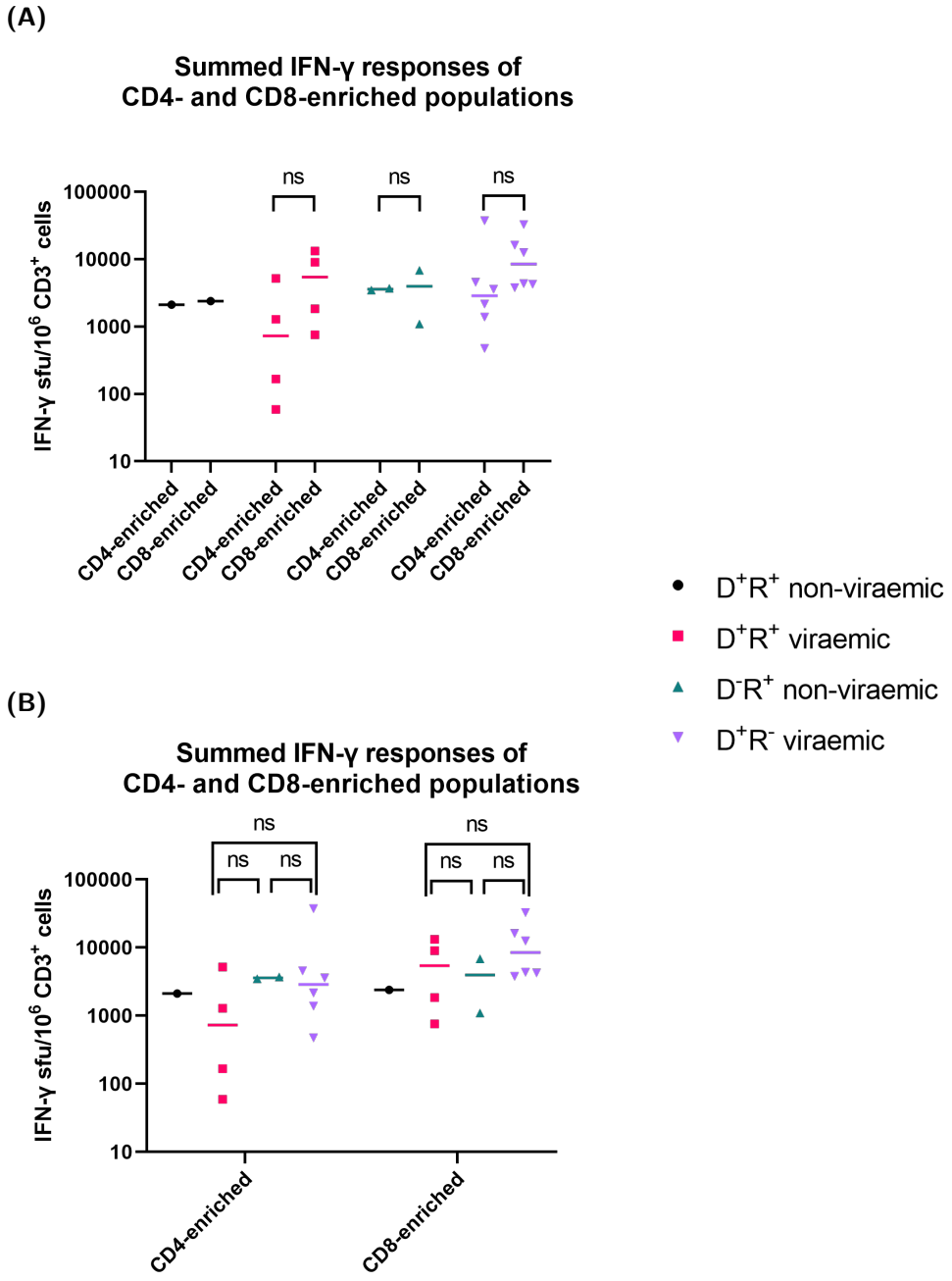

Figure 6.3: Summed IFN-γ responses of CD4- and CD8-enriched immune cell populations from transplant recipients to HCMV peptide pools
FluoroSpot^{TM} assays were performed on CD4- and CD8-enriched immune cell populations from transplant recipients and IFN-γ responses to HCMV peptide pools containing IE, gB, pp65, pp71, US28 and latency-associated HCMV antigens were measured and added together. Fig.6.3B: These responses were then stratified by donor and recipient HCMV serostatus and whether the recipient experienced episodes of viraemia ("Viraemics") or not ("Non-viraemics"). Two D^+R^- transplant recipients (R01-079 and R01-081) had PBMC samples taken from 4 and 2 different timepoints post-transplant, respectively, which were added to the "D^+R^- Viraemics" group. Fig.6.3B shows the comparisons between the different serostatus groups for the CD4- and CD8-enriched populations. Medians of each group are shown and statistical analysis performed using Mann-Whitney *U* tests. FluoroSpot^{TM} data obtained from Dr Charlotte Houldcroft, statistical analysis performed by myself.

Comparison of FluoroSpot™ IFN-γ responses with results from viral dissemination assays

There were two patients in this cohort who experienced recurrent episodes of viraemia (R01-079 & R01-081), both of whom belonged to the "high-reactivation-risk" D^+R^- group. Figs.6.2A & 6.3B showed that the patient groups that experienced viraemic episodes appeared to have CMV-specific T cell responses, measured by summed IFN-γ responses, which were not dissimilar to those from patients who remained non-viraemic. We thus wanted to examine if the recurrent episodes of viraemia in these patients was due to the lack of a CMV-specific T cell response at a particular timepoint during transplantation, or if it was due to the lack of a CMV-specific $CD4^+$ or $CD8^+$ T cell response at a particular timepoint. FluoroSpot™ assays were performed on whole PBMCs, $CD8^+$ cell-depleted PBMCs ("CD4-enriched"), or $CD4^+$ cell-depleted PBMCs ("CD8-enriched") from various timepoints post-transplant. The results in Figs.6.4A–6.4D show that this is not the case. Figs.6.4A & 6.4B show that whole PBMCs are able to produce an IFN-γ response to HCMV peptide pools at multiple timepoints post-transplant, even when taken during periods of viraemia. In particular, Fig.6.4A shows that for one donor (R01-079), the highest IFN-γ response to HCMV-peptides arose from PBMCs taken during a viraemic episode. When $CD8^+$ cells or $CD4^+$ cells were depleted from the PBMCs of these patients, Fig.6.4C shows that for patient R01-079, there is a CMV-specific IFN-γ response from $CD8^+$ T cells, while Fig.6.4D shows that there is a CMV-specific IFN-γ response from both $CD4^+$ and $CD8^+$ T cells.

Figs.6.4A–6.4D thus tell us that these 2 patients possessed a CMV-specific T cell response. Yet, this did not prevent either patient from experiencing recurrent episodes of viraemia, which suggests that the CMV-specific T cell response was insufficient to prevent CMV replication *in vivo*. Figs.6.4E & 6.4G show the results of the viral dissemination assay performed on PBMCs, $CD4^+$ cells, $CD8^+$ T cells and NK cells from multiple timepoints for patient R01-079, and Figs.6.4F & 6.4H show the same for patient R01-081. The E:T ratios at which these immune cells were added is specified in brackets in each figure legend. Fig.6.4E shows that, overall, the different immune cell populations show a fairly poor ability in limiting the amount of IE CMV gene expression in the VDAs, while Fig.6.4G shows that $CD4^+$ cells and $CD8^+$ T cells showed a poor ability to limit late CMV gene expression at all timepoints tested after 60 days post-transplantation. For patient R01-081, Fig.6.4H shows that all immune cell populations showed a poor ability to limit late CMV gene expression at 100-110 days post-transplantation. These results show that the CMV-specific IFN-γ response as measured by FluoroSpot™ assay does not provide a complete picture of the true functional ability of these immune cell populations to limit CMV replication, and demonstrate that the VDA may provide a better means of dissecting the antiviral responses of each of these immune cell populations.

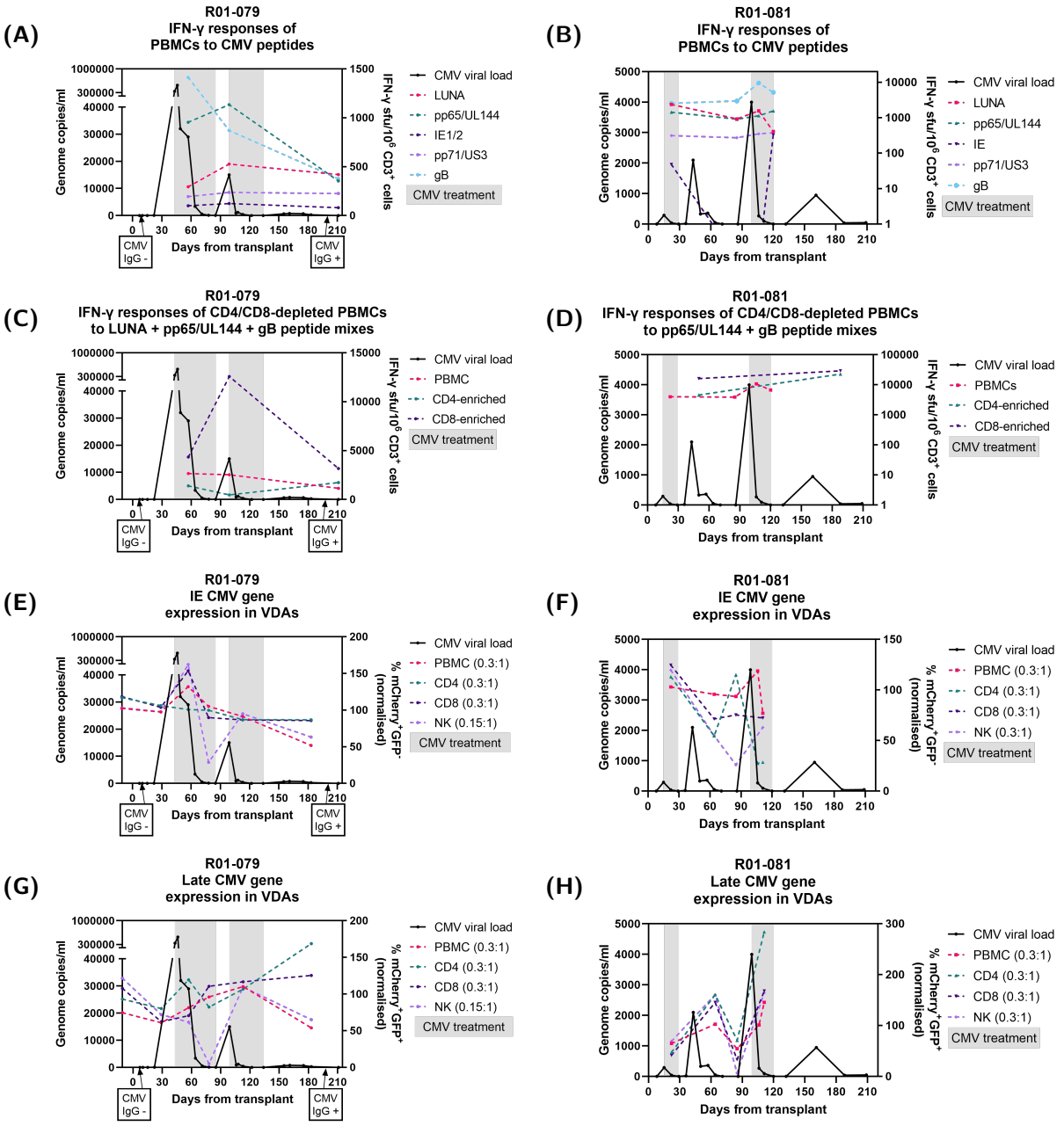
(A)
R01-079
IFN-γ responses of PBMCs to CMV peptides
Genome copies/ml
IFN-γ sfu/10^6 CD3+ cells
Days from transplant
CMV IgG -
CMV IgG +
CMV viral load
LUNA
pp65/UL144
IE1/2
pp71/US3
gB
CMV treatment
(B)
R01-081
IFN-γ responses of PBMCs to CMV peptides
IE
(C)
R01-079
IFN-γ responses of CD4/CD8-depleted PBMCs to LUNA + pp65/UL144 + gB peptide mixes
PBMC
CD4-enriched
CD8-enriched
(D)
R01-081
IFN-γ responses of CD4/CD8-depleted PBMCs to pp65/UL144 + gB peptide mixes
PBMCs
(E)
R01-079
IE CMV gene expression in VDAs
% mCherry+GFP- (normalised)
PBMC (0.3:1)
CD4 (0.3:1)
CD8 (0.3:1)
NK (0.15:1)
(F)
R01-081
IE CMV gene expression in VDAs
(G)
R01-079
Late CMV gene expression in VDAs
% mCherry+GFP+ (normalised)
(H)
R01-081
Late CMV gene expression in VDAs

Figure 6.4: Time course of CMV viral load, IFN-γ response of total PBMCs and CD4-enriched or CD8-enriched PBMCs to HCMV peptide pools on FluoroSpot^{TM} assay, and amount of IE and late CMV gene expression on viral dissemination assays for 2 D$^+$R$^-$ patients with recurrent episodes of viraemia
Figs.6.4A, 6.4B: IFN-γ responses to various HCMV peptide pools of PBMCs from various timepoints post-transplantation from 2 D$^-$R$^+$ patients measured by FluoroSpot^{TM} assay, plotted against time course of CMV viral load. Figs.6.4C, 6.4D: Sum of all IFN-γ responses to pp65/UL144 and gB peptide pools, from PBMCs, PBMCs that had CD8$^+$ cells removed ("CD4-enriched"), and PBMCs that had CD4$^+$ cells removed ("CD8-enriched") at various timepoints post-transplantation from the same 2 patients. Figs.6.4E, 6.4F: Mean amount of mCherry$^+$GFP$^-$ cells from triplicate wells, expressed as a percentage of mCherry$^+$GFP$^-$ cells in infected controls, when PBMCs, CD4$^+$ cells, CD8$^+$ T cells and NK cells from each patient was added to the viral dissemination assay. E:T ratios at which immune cells were added is given in brackets in figure legends. Figs.6.4G, 6.4H: Mean amount of mCherry$^+$GFP$^+$ cells from the same wells as Figs.6.4G & 6.4H. Grey areas indicate time periods when CMV treatment was given. LUNA = Latency Unique Natural Antigen, Tx = time of transplantation. FluoroSpot^{TM} data obtained from Dr Charlotte Houldcroft.

6.4 Comparing ability of different immune cell populations from transplant recipients to control immediate-early and late CMV gene expression using the viral dissemination assay

To compare the capability of each cell type to limit viral dissemination *in vitro*, a viral dissemination assay was set up for samples from each transplant recipient. As with the viral dissemination assays described in Chapters 3 and 5, primary dermal fibroblasts from the transplant recipient were seeded in 96-well half-area plates at 10,000 cells/well and grown to confluency overnight. Half-area plates were used as this allowed me to use fewer immune cells to achieve the required E:T ratios when adding the immune cells. The next day, these fibroblasts were infected with Merlin WT virus. Also on the same day, frozen PBMCs from multiple timepoints (typically, three): one pre-transplant (if available) and two post-transplant were chosen. For patients that had detectable viraemia, PBMCs from timepoints before and after episodes of viraemia were chosen if available. The post-separation purities of each immune cell population and results of the viral dissemination assays on all 4 immune cell populations from each individual patient is given in Appendices K–Q.

The PBMCs, CD4$^+$ cells, CD8$^+$ T cells and NK cells were obtained in the same manner as for the healthy donors (as described in Methods Section 2.11 and Chapter 3) and added to Merlin WT-infected fibroblasts at the following starting E:T ratios, followed by halving dilutions: 1.25:1 for PBMCs, 5:1 for CD4$^+$ cells, and 0.3–2.5:1 for CD8$^+$ and NK cells, depending on the number of cells obtained post-separation. These assays were then harvested at 7-10 dpi and analysed by flow cytometry. The results are then graphed as such: the amount

of cells expressing mCherry^{+}GFP^{-}, expressed as a percentage of the amount of cells expressing the same in infected controls of the respective transplant recipient, is calculated for each E:T ratio and the mean of triplicate wells is plotted. This is repeated for the amount of cells expressing mCherry^{+}GFP^{+}.

The results from two representative transplant recipients in comparison to a healthy HCMV-seropositive control are shown in Fig.6.5: left column shows the healthy HCMV-seropositive control, middle column shows a D^{-}R^{+} recipient that did not experience episodes of viraemia (R02-015), and right column shows a D^{+}R^{+} recipient that did (R02-125). The number of days pre- or post-transplant from which the sample is obtained is shown in brackets next to the respective timepoint.

PBMCs from the non-viraemic recipient (R02-015) at 60 days post-transplant showed a good ability to limit IE and late CMV gene expression even at lower E:T ratios (Fig.6.5A, middle column, teal lines), similar to that seen in a healthy HCMV-seropositive individual (Fig.6.5A, left column), while PBMCs from the pre-transplant timepoint and at 25 days post-transplant lost this ability at a much higher E:T ratio (Fig.6.5A, middle column, black and pink lines). In contrast, for PBMCs from the donor who experienced viraemic episodes, PBMCs from all 3 timepoints post-tranplant lost the ability to limit IE and late CMV gene expression at a comparatively higher E:T ratio (Fig.6.5A, right column).

In Fig.6.5B, CD8^{+} T cells from pre-transplant and 60 days post-transplant timepoints from the non-viraemic patient lost the ability to limit IE CMV gene expression only at the relatively low E:T ratio of 0.08:1 (middle column, upper graph, black and teal lines), and those from 25 days post-transplant lost it at the slightly higher E:T ratio of 0.15:1 (middle column, lower graph, pink line). For late gene expression, CD8^{+} T cells from all 3 timepoints showed a good ability of control at nearly at E:T ratios tested (middle column, lower graph). The degree of control seen at these timepoints is similar or even better than that seen in the healthy HCMV-seropositive control (left column, upper and lower graphs). In contrast, for the viraemic patient, CD8^{+} T cells from all 3 timepoints had lost ability to limit IE CMV gene expression at the higher E:T ratio of 0.6:1 (right column, upper graph), while for late CMV gene expression, CD8^{+} T cells showed a moderate ability to limit late CMV gene expression at 21 days post-transplant (right column, lower graph, black line), but this worsened at 60 and 70 days post-transplant, as they lost this ability at the higher E:T ratios of 0.3:1 and 1.25:1 respectively (right column, lower graph, pink and teal lines).

In Fig.6.5C, CD4^{+} cells from the non-viraemic patient showed a poorer ability to limit IE CMV gene expression at the pre-transplant and 25 days post-transplant timepoint (middle column, upper graph, black and pink lines), losing this ability at the E:T ratio of approximately 1.25:1, but this had improved by 60 days post-transplant (middle column, upper graph, teal line). For late gene expression, CD4^{+} cells from all timepoints only completely lost ability to limit late CMV gene expression at the lowest E:T ratios of 0.15–0.3:1 (Fig.6.5C, middle

column, lower graph). In contrast, for the viraemic patient, $CD4^+$ cells from 21 and 70 days post-transplant (right column, upper and lower graphs, black and teal lines) lost ability to limit IE and late CMV gene expression at the higher E:T ratios of 0.6–1.25:1, while those from 60 days post-transplant overall only lost this ability at the lower E:T ratio of 0.3:1 (right column, upper and lower graphs, pink lines). In comparison, $CD4^+$ cells from the healthy HCMV-seropositive donor showed a sharp drop in ability to control both IE and late CMV gene expression at the E:T ratio of 0.6:1 (Fig.6.5C, left column).

For NK cells (Fig.6.5D), those from all 3 timepoints of the non-viraemic donor showed no ability to limit IE CMV gene expression at all E:T ratios tested (middle column, upper graph, all lines), while those from the viraemic donor showed no ability at 21 and 70 days post-transplant (right column, upper graph, black and teal lines) and a marginally better ability at 60 days post-transplant (pink line). This is similar to that seen in the healthy HCMV-seropositive donor, which also showed no ability to control at the same E:T ratios (left column, upper graph). For late CMV gene expression, NK cells from the healthy donor showed a good ability to control at E:T ratios of 0.3:1 and above, only beginning to lose this ability at the lowest E:T ratio of 0.15:1 (left column, lower graph), whereas those from the non-viraemic donor showed a nearly no ability at the pre-transplant and initial post-transplant timepoint (middle column, lower graph, black and pink lines), and only showed some control at the higher E:T ratios from the last timepoint tested (middle column, lower graph, teal line), an effect that tails off fairly quickly. For the viraemic donor, NK cells from 60 days post-transplant showed a good ability to control late CMV gene expression (right column, lower graph, pink line), but those from the first 2 timepoints post-transplant had nearly no ability to control late CMV gene expression (right column, lower graph, black and teal lines).

As discussed in Chapter 3, cells that express $mCherry^+GFP^+$ also express UL32, a late gene. Infected cells that have reached late gene expression would also be expected to have active viral replication occurring. These results suggest that a loss of ability of $CD4^+$ cells from a viraemic transplant recipient to control late gene expression *in vitro* could account for loss of control of viral replication *in vivo*, and therefore result in episodes of CMV viraemia.

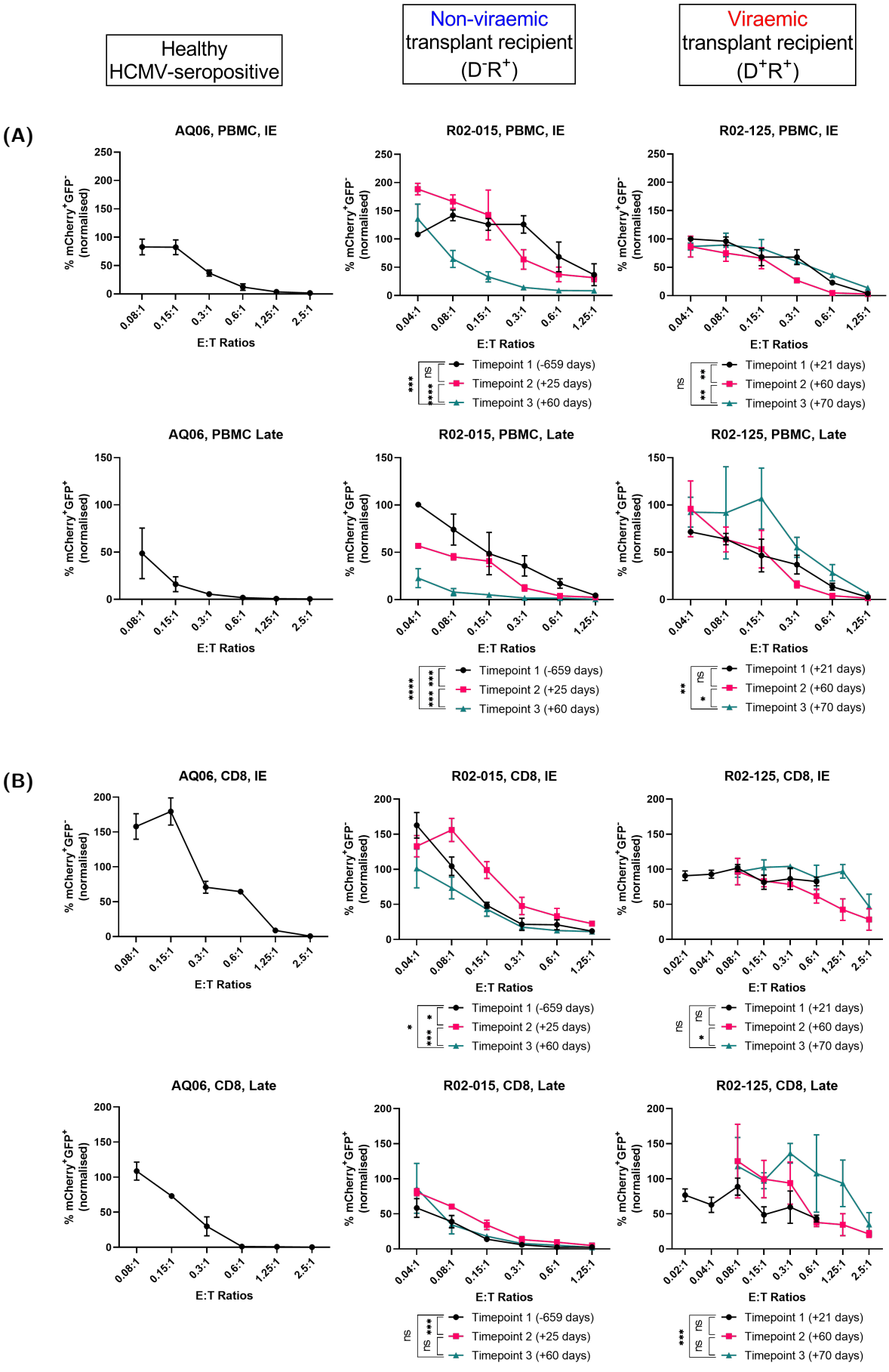
Healthy HCMV-seropositive
Non-viraemic transplant recipient (D-R+)
Viraemic transplant recipient (D+R+)
(A)
AQ06, PBMC, IE
R02-015, PBMC, IE
R02-125, PBMC, IE
AQ06, PBMC Late
R02-015, PBMC, Late
R02-125, PBMC, Late
(B)
AQ06, CD8, IE
R02-015, CD8, IE
R02-125, CD8, IE
AQ06, CD8, Late
R02-015, CD8, Late
R02-125, CD8, Late
% mCherry+GFP- (normalised)
% mCherry+GFP+ (normalised)
E:T Ratios
Timepoint 1 (-659 days)
Timepoint 2 (+25 days)
Timepoint 3 (+60 days)
Timepoint 1 (+21 days)
Timepoint 2 (+60 days)
Timepoint 3 (+70 days)

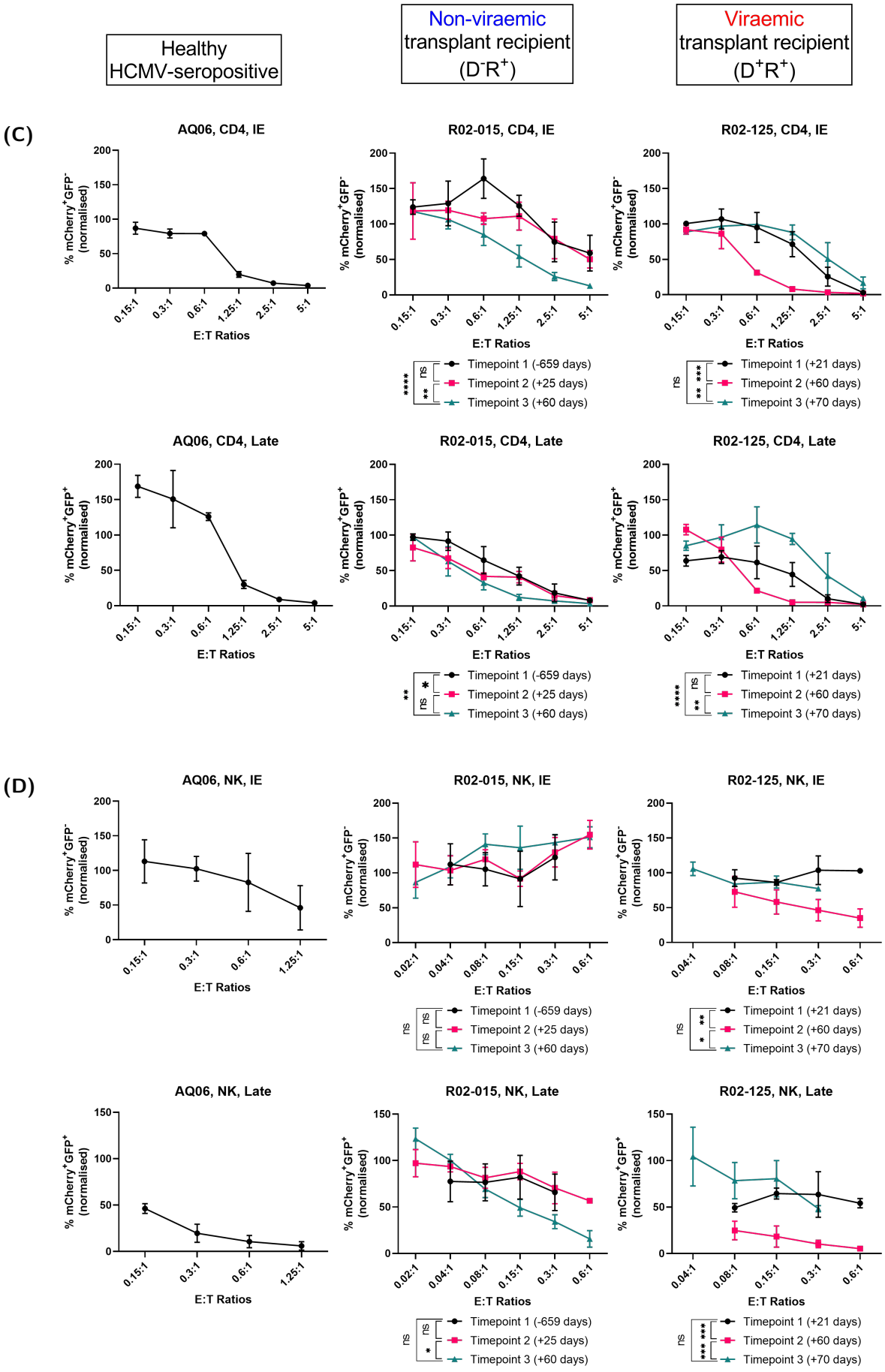
Healthy HCMV-seropositive
Non-viraemic transplant recipient (D^-R^+)
Viraemic transplant recipient (D^+R^+)
(C)
AQ06, CD4, IE
R02-015, CD4, IE
R02-125, CD4, IE
AQ06, CD4, Late
R02-015, CD4, Late
R02-125, CD4, Late
(D)
AQ06, NK, IE
R02-015, NK, IE
R02-125, NK, IE
AQ06, NK, Late
R02-015, NK, Late
R02-125, NK, Late
% mCherry+GFP- (normalised)
% mCherry+GFP+ (normalised)
E:T Ratios
Timepoint 1 (-659 days)
Timepoint 2 (+25 days)
Timepoint 3 (+60 days)
Timepoint 1 (+21 days)
Timepoint 2 (+60 days)
Timepoint 3 (+70 days)

Figure 6.5: Comparing control of IE and late CMV gene expression by PBMCs, $CD8^+$ T cells, NK cells and $CD4^+$ cells in a non-viraemic and viraemic donor
Primary dermal fibroblasts from a transplant recipient were seeded in 96-well half-area plates at 10,000 cells/well and grown to confluency overnight. The next day, these fibroblasts were infected with Merlin WT virus. Also on the same day, frozen PBMCs from multiple timepoints (typically, three): one pre-transplant (if available) and two post-transplant were chosen. For patients that had detectable viraemia, PBMCs from timepoints before and after episodes of viraemia were chosen if available. The PBMCs were defrosted from liquid nitrogen (methods described in Section 2.11) and treated with DNase for one hour before washing and resting in media at 37°C overnight. At 1 dpi, the PBMCs were washed and counted before addition to the infected fibroblasts at starting a E:T ratio of 1.25:1 in triplicate wells, followed by halving dilutions. Subsequently, the $CD4^+$ cells, $CD8^+$ T cell and NK cell populations were obtained from the PBMCs in the same manner as described in Chapter 3 (illustrated in Fig.3.5)—$CD4^+$ cells were obtained first by MACS positive selection with CD4 MicroBeads, followed by splitting the remaining CD4-depleted PBMCs into 2 populations and obtaining the $CD8^+$ T cell and NK cell populations by MACS depletion using the respective Isolation Kits. The $CD4^+$ cells were added at a starting E:T ratio of 5:1. For $CD8^+$ T cells and NK cells, the starting E:T ratio was dependent on the number of cells obtained after separation. This ranged from 0.3–2.5:1. These assays were then harvested at 7-10 dpi and analysed by flow cytometry. The results are then graphed as such: the amount of cells expressing $mCherry^+GFP^-$, expressed as a percentage of the amount of cells expressing the same in infected controls of the respective transplant recipient, is calculated for each E:T ratio and the mean of triplicate wells is plotted. This is repeated for amount of cells expressing $mCherry^+GFP^+$. Middle column shows graphs from one patient that did not experience episodes of viraemia (R02-015) and right column shows graphs from one patient that had an episode of viraemia (R02-125). Left column shows corresponding graphs from a healthy HCMV-seropositive donor for comparison. The number of days pre- or post-transplant from which the sample is obtained is shown in brackets next to the respective timepoint. Error bars represent SD of triplicate wells. Statistics performed using two-way ANOVA with Tukey's multiple comparisons test. (*$p \leq 0.05$; **$p \leq 0.01$; ***$p \leq 0.001$; ****$p \leq 0.0001$; ns = not significant)

The results in Fig.6.5 demonstrate how the viral dissemination assay was used to compare the functional ability of the various immune cell populations from different timepoints of the same patient, and also between different patients. It also shows the challenges I faced when attempting to analyse the data. Firstly, I needed a method to analyse the data that would include examining the function of these immune cell populations at all the E:T ratios tested, and also at all the different timepoints tested. Secondly, due to limited amounts of PBMC samples available, it was not always possible to obtain sufficient $CD8^+$ T cells and NK cells to have a consistent starting E:T ratio at every timepoint. This made it challenging to attempt to examine the $CD8^+$ T cell and NK cell function across the entire cohort in a consistent manner. It was also crucial to examine the function of all these immune cell populations in relation to their performance *in vivo*—i.e. whether the patient ultimately experienced viraemic episodes post-transplantation, and also *when* these blood samples were taken in relation to the periods of viraemia. The graphs in the following sections attempt to stratify the data in a way that would allow me to examine these correlations.

In addition, there was the observation in some VDA results where, after "normalisation" to

infected controls, some of these data points showed a %mCherry^{+}GFP^{-} or %mCherry^{+}GFP^{+} of $>$100%. This occurred when the infected controls (i.e. wells that had *no* immune cells added) had a lower percentage of mCherry^{+}GFP^{-} or mCherry^{+}GFP^{+} than wells that had had immune cells added. This was likely due to the "edge effect" in these plates, where wells at the edge of the plate (where the infected control wells usually were) had more evaporation of media than those closer to the middle of the plate, possibly leading to greater cell death and lower infection rates of surviving cells.

6.5 Comparing PBMCs, $CD8^+$ T cells, NK cells and $CD4^+$ cells taken during periods with and without viraemia

The results shown in Fig.6.5 from viral dissemination assays suggest that immune cell populations from transplant recipients show varying abilities to limit IE and late CMV gene expression, and that this could correlate with episodes of CMV viraemia. In particular, $CD8^+$ T cells and $CD4^+$ cells from the non-viraemic recipient were able to control late CMV gene expression to a better degree than the $CD8^+$ T cell and $CD4^+$ cells from the viraemic recipient at the same E:T ratio. I thus wondered if this lack of ability to control virus in the VDA is more generally associated with episodes of viraemia in transplant recipients. In order to determine this, I examined a total of 50 timepoints from the cohort of 15 transplant recipients in the same manner as described in Section 6.4, and stratified the results by whether these recipients were viraemic or not at that timepoint. The results of all 50 timepoints are shown in the violin plots in Fig.6.6. The mean of triplicate wells for each E:T ratio was calculated and is represented as one data point in the violin plot. As part of post-transplant protocol, regular monitoring for the occurrence of CMV viraemia was performed. As such, if the CMV viral load was above the detection threshold at the timepoints the samples were obtained, these samples were classified as being from a "Viraemic timepoint" and those that did not have viraemia were classified as being from a "Non-viraemic timepoint". There was a total of 37 non-viraemic timepoints and 13 viraemic timepoints. As the data points in each group were found to be normally distributed using the Shapiro-Wilk test, the Student's *t*-test was then performed between these groups at each E:T ratio to determine if there were any differences between the immune cell population from viraemic timepoints versus non-viraemic timpoints. The left column of graphs in Fig.6.5 shows the amount of IE CMV gene expression at each of these timepoints and E:T ratios, expressed as a percentage of the amount of IE CMV gene expression in infected control wells of the respective recipient and timepoint; the right column shows the same for late CMV gene expression.

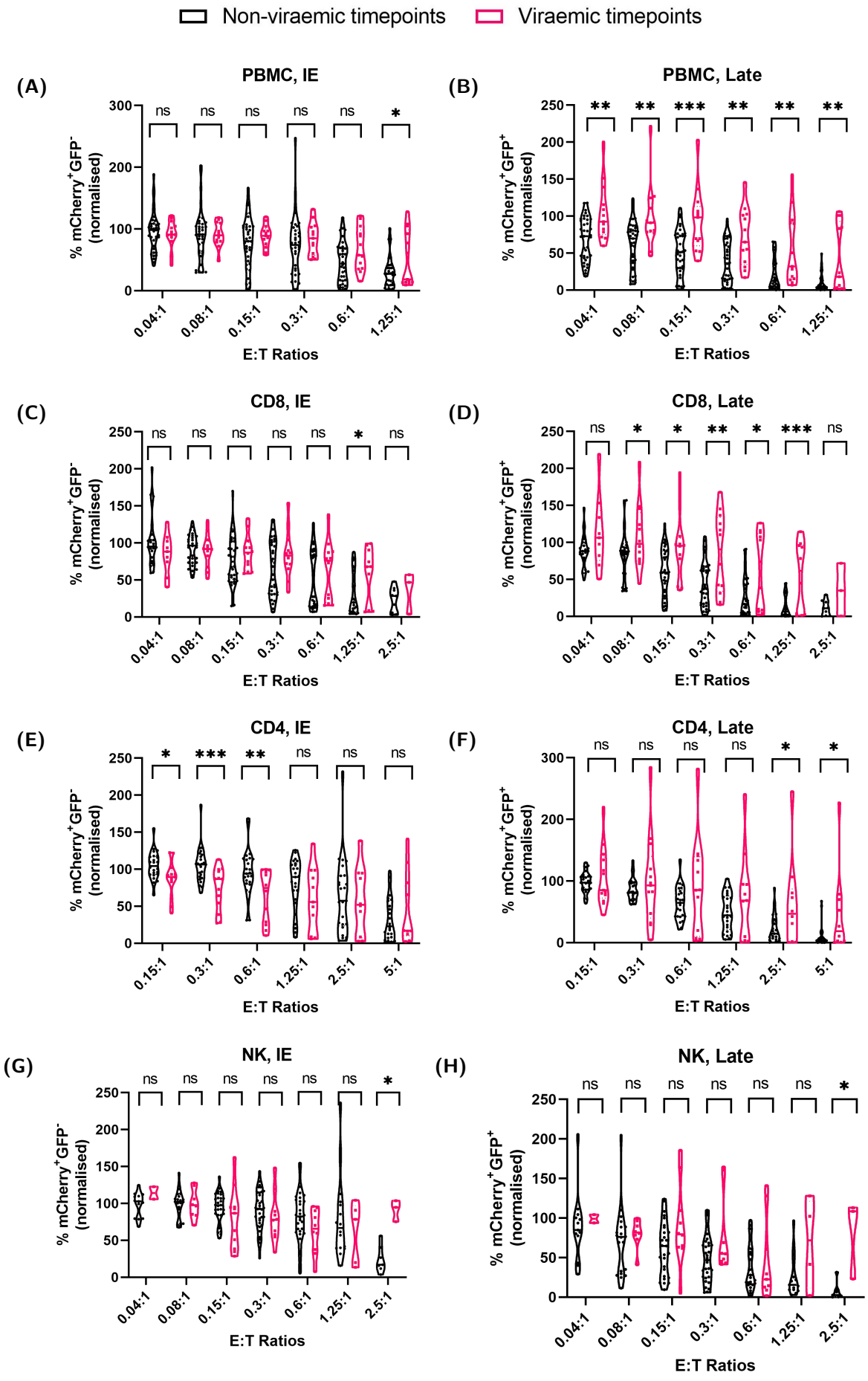
Non-viraemic timepoints
Viraemic timepoints
(A)
PBMC, IE
(B)
PBMC, Late
(C)
CD8, IE
(D)
CD8, Late
(E)
CD4, IE
(F)
CD4, Late
(G)
NK, IE
(H)
NK, Late
% mCherry+GFP- (normalised)
% mCherry+GFP+ (normalised)
E:T Ratios
0.04:1
0.08:1
0.15:1
0.3:1
0.6:1
1.25:1
2.5:1
5:1
ns
*
**
***

Figure 6.6: Comparison of control of viral dissemination by PBMCs, $CD8^+$ T cells, NK cells and $CD4^+$ cells from timepoints with or without viraemia
A total of 50 timepoints from the cohort of 15 transplant recipients was examined in the same manner as described in Section 6.4. PBMCs, $CD4^+$ cells, $CD8^+$ T cells and NK cells were added to the viral dissemination assay, and the mean of triplicate wells for each E:T ratio was calculated and is represented as one data point in the violin plot. If there was presence of CMV viral load above detection threshold at the timepoints the samples were obtained, these samples were classified as being from a "Viraemic timepoint" and those that did not have viraemia were classified as being from a "Non-viraemic timepoint". Student's *t*-test was then performed between these groups at each E:T ratio to determine if there were any differences between the 2 groups. The left column of graphs in Fig.6.5 shows amount of IE CMV gene expression at each of these timepoints and E:T ratios, expressed as a percentage of the mean amount of IE CMV gene expression in infected control triplicate wells of the respective recipient and timepoint; the right column shows the same for late CMV gene expression. (*$p \leq 0.05$; **$p \leq 0.01$; ***$p \leq 0.001$; ****$p \leq 0.0001$; ns = not significant)

PBMCs from viraemic timepoints do not control late CMV gene expression at all E:T ratios tested

The violin plots in Figs.6.6A and 6.6B show that there is no statistically significant difference between PBMCs from viraemic timepoints and non-viraemic timepoints in limiting IE CMV gene expression, except at the highest E:T ratio tested of 1.25:1 (Fig.6.6A). The results show that at the higher E:T ratios PBMCs from some donors are more effective at suppression of IE CMV gene expression than others and that as the E:T ratio is decreased this suppressive effect is diluted. However, when comparing late CMV gene expression, PBMCs from non-viraemic timepoints are more able to limit late CMV gene expression at all E:T ratios tested (Fig.6.6B). These results would suggest that episodes of clinical viraemia can be reflected *in vitro* by a loss of ability of PBMCs to control late CMV gene expression at some points, but importantly, there are still PBMC samples from viraemic timepoints that exert good control.

$CD8^+$ T cells from non-viraemic timepoints are able to control late viral dissemination at a wide range of E:T ratios

Comparing $CD8^+$ T cells from viraemic and non-viraemic timepoints, there was no statistically significant difference between either group in the ability of $CD8^+$ T cells to control IE CMV gene expression at nearly all E:T ratios tested (Fig.6.6C), similar to the results with whole PBMCs. For late CMV gene expression (Fig.6.6D), at the highest E:T ratio of 2.5:1, $CD8^+$ T cells from both groups showed an ability to control progression to late phase infection. This is likely because $CD8^+$ T cells have direct cytotoxicity against CMV-infected cells, and at high E:T ratios, the number of $CD8^+$ T cells in the well is sufficient for direct cytotoxic effects to limit late CMV gene expression and viral replication, regardless of whether these $CD8^+$ T cells were from viraemic or non-viraemic timepoints. However, at the lower E:T ratios, $CD8^+$ T cells from non-viraemic timepoints showed a much better capability to limit late CMV gene expression at a wide range of E:T ratios (from 0.08:1 to 1.25:1) as compared to $CD8^+$ T cells

from viraemic timepoints.

$CD4^+$ cells from viraemic timepoints do not control late CMV gene expression at higher E:T ratios

For $CD4^+$ cells, the difference in ability to control late CMV gene expression between non-viraemic and viraemic timepoints is only statistically significant at the higher E:T ratios of 5:1 and 2.5:1 (Fig.6.6F), although $CD4^+$ cells from viraemic timepoints show a much wider variation in ability to control late CMV gene expression as compared to $CD4^+$ cells from non-viraemic timepoints. This suggests that $CD4^+$ cells may vary widely with regards to contribution to overall control of HCMV replication *in vivo*, as some $CD4^+$ cells from viraemic timepoints show a good ability to limit late CMV gene expression *in vitro*, yet these transplant recipients still experience episodes of CMV viraemia. In Fig.6.6E, at E:Ts of 0.15:1, 0.3:1 and 0.6:1, $CD4^+$ cells from non-viraemic timepoints show an apparent poorer ability to control IE CMV gene expression as compared to $CD4^+$ cells from viraemic timepoints. This is likely due to fewer cells progressing to late phase infection in the non-viraemic group, leading to an accumulation of cells expressing only IE CMV genes. This is reflected by the narrower distribution of data points at E:Ts of 0.15:1, 0.3:1 and 0.6:1 in the non-viraemic group in Fig.6.6F. Thus Fig.6.6E does not represent a poorer ability of $CD4^+$ T cells from non-viraemic timepoints to control viral dissemination.

NK cells from viraemic timepoints show poor ability to control late CMV gene expression even at a high E:T ratio

Fig.6.6G shows that there was no difference in the ability to control IE CMV gene expression between NK cells from viraemic and non-viraemic timepoints, except in the highest E:T ratio tested of 2.5:1, and Fig.6.6H shows the same for late gene expression, except for the highest E:T ratios of 2.5:1 and 1.25:1. As with $CD8^+$ T cells, NK cells have cytotoxic effects against CMV-infected cells, and the ability of NK cells from viraemic timepoints but not those from non-viraemic timepoints to limit IE CMV and late CMV gene expression at high E:T ratios suggests that a loss of NK cell-mediated cytotoxicity may contribute to overall loss of control of viral replication *in vivo*, and thus lead to episodes of viraemia.

6.6 Examining impact of donor and recipient serostatus, type of organ transplanted, and viral load on ability of PBMCs, $CD8^+$ T cells, NK cells and $CD4^+$ cells to control *in vitro* viral gene expression

The results in Section 6.5 show that PBMCs from some viraemic timepoints were not able to control late CMV gene expression *in vitro*. The data would also suggest that this loss of control could predominantly be attributed to $CD8^+$ T cells, but NK cells and $CD4^+$ cells also contribute to this loss. In Chapter 3, PBMCs from healthy HCMV-seropositive donors were able to control IE CMV gene expression at E:T ratios of 2.5:1, 1.25:1 and 0.6:1, while those from healthy HCMV-seronegative donors were not (Fig.3.14); for late CMV gene expression, PBMCs from both HCMV-seropositive and HCMV-seronegative donors were able to limit late CMV gene expression up to E:T ratios of approximately 0.3:1, although PBMCs from healthy HCMV-seropositive donors were able to do so better than those from HCMV-seronegative donors. I thus wanted to examine how the level of IE and late CMV gene expression by PBMCs from viraemic and non-viraemic timepoints compared to PBMCs from healthy HCMV-seropositive and seronegative donors. The hypothesis was that PBMCs from non-viraemic timepoints would have a similar level of control as those from HCMV-seropositive donors, while those from viraemic timepoints would likely suppress viral gene expression to a similar level (or possibly worse) than that seen in HCMV-seronegative donors. I also wanted to examine if there were other factors that contributed to loss of control of viral replication *in vivo*—such as the donor and recipient serostatus or type of organ transplanted—that would lead to episodes of viraemia.

To do these comparisons, I first produced violin plots of mean amounts of IE and late CMV gene expression seen when PBMCs from healthy HCMV-seropositive and HCMV-seronegative donors were added to the viral dissemination assay (previously shown in Fig.3.14). Three E:T ratios of 1.25:1, 0.6:1 and 0.3:1 were plotted—these E:T ratios were chosen as these were the E:T ratios at which there was a statistically significant difference in ability to control IE and late CMV gene expression between HCMV-seropositive and HCMV-seronegative healthy controls, as well as between cells from viraemic and non-viraemic timepoints. Next, I added the violin plots (from Fig.6.5) of mean amounts of IE and late CMV gene expression seen when PBMCs from non-viraemic and viraemic timepoints were added to the viral dissemination assay for the respective E:T ratios. The data points from the transplant recipients were then stratified according to their donor and recipient serostatus (D^+R^+, D^+R^-, or D^-R^+), whether they were kidney or liver transplants, and, where the information was available, whether they had viral loads of $\geq$1000 or $<$1000 genome copies/ml at the time of sampling ("high viraemics" or "low viraemics"). Statistical analysis was also performed using Mann-Whitney *U* tests to look for

statistically significant differences between the groups. The results of this analysis is shown in Fig.6.7.

6.6.1 PBMCs

On comparing the PBMCs from transplant recipients with healthy donors (Fig.6.7), it can be seen that PBMCs from non-viraemic timepoints are similar to PBMCs from healthy HCMV-seropositive donors in their ability to limit IE and late CMV gene expression at E:T ratios of 1.25:1 and 0.6:1 (Figs.6.7A–6.7D, black vs teal violin plots). When comparing PBMCs from viraemic timepoints with those from HCMV-seronegative donors, those from viraemic timepoints appear to show a poorer control of late CMV gene expression, although this difference was not statistically significant (Figs.6.7B, 6.7D & 6.7F, pink vs dark purple violin plots). On examining the impact of donor and recipient serostatus, PBMCs from D^+R^- transplants showed the poorest ability overall to control late CMV gene expression (light purple, light blue and brown violin plots, Figs.6.7B, 6.7D, 6.7F). Figs.6.7B, 6.7D, & 6.7F also show that most of the viraemic timepoints occurred in D^+R^- transplants (light blue vs dark purple violin plots) and that PBMCs from liver transplant recipients were also more likely to have poorer control of late CMV gene expression than PBMCs from kidney transplant recipients (navy vs green violin plots). However, PBMCs from patients with high viral loads at the time when the blood sample was taken ($\geq$1000 copies/ml) did not show a poorer ability to control late CMV gene expression *in vitro* than PBMCs from patients with low viral loads of $<$1000 copies/ml (grey vs beige violin plots).

Overall, the conclusions that can be drawn from these graphs are:

1. PBMCs from viraemic timepoints are *not* better able to decrease amount of CMV entry and IE gene expression than those from non-viraemic timepoints, but they are better able to limit progression to late gene expression.

2. PBMCs from D^+R^- patients consistently show the worst ability to limit IE and late CMV gene expression among the three different serostatus groups present in this cohort of patients. This is in line with prior observations that D^+R^- patients are at the highest risk of CMV reactivation and disease. D^+R^- patients have no memory T cell responses to HCMV and therefore need to produce a primary immune response to replicating HCMV, whereas D^+R^+ and D^-R^+ patients should, theoretically, have primed immune responses which are able to rapidly produce a secondary immune response to replicating HCMV.

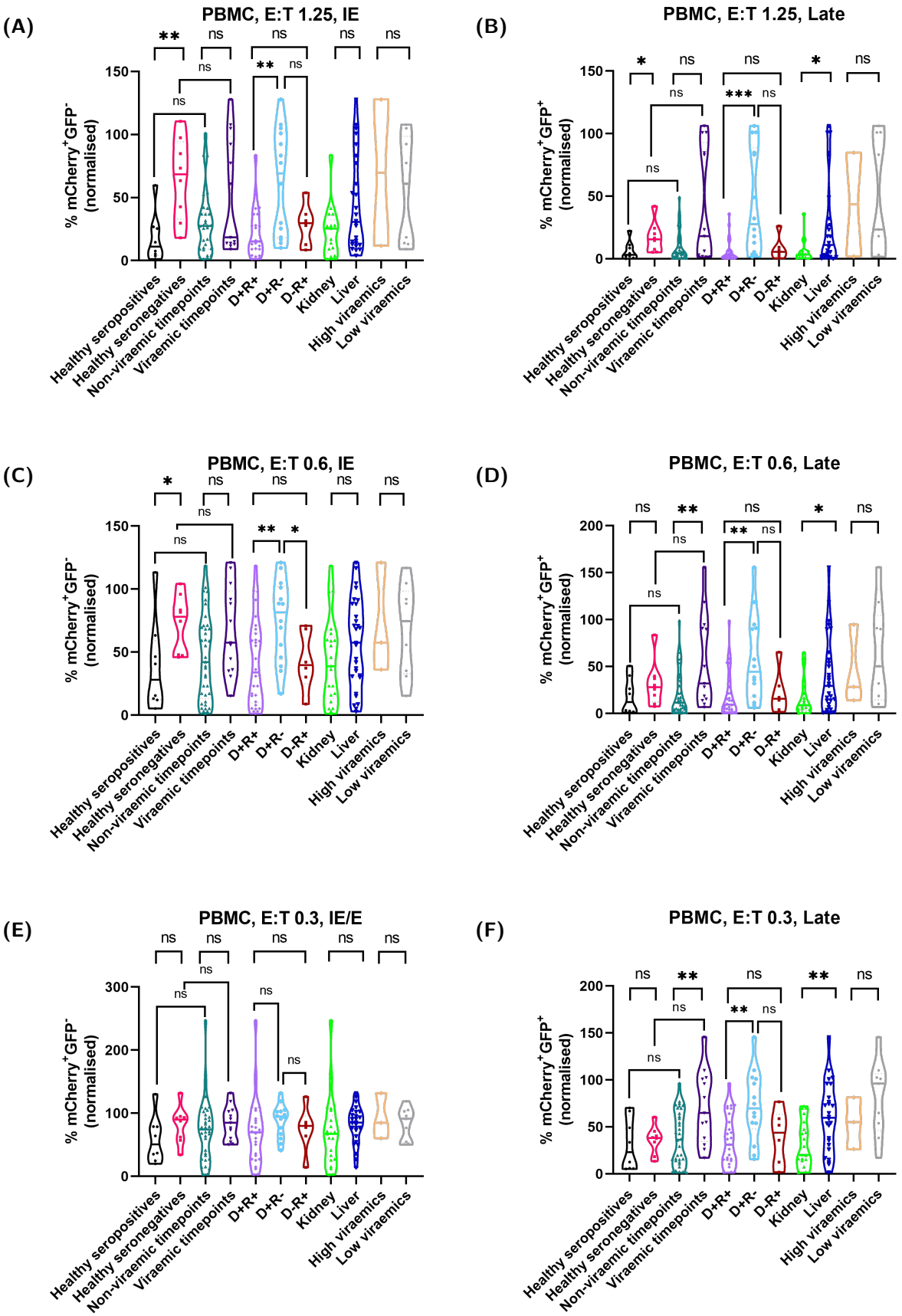
(A)
PBMC, E:T 1.25, IE
(B)
PBMC, E:T 1.25, Late
(C)
PBMC, E:T 0.6, IE
(D)
PBMC, E:T 0.6, Late
(E)
PBMC, E:T 0.3, IE/E
(F)
PBMC, E:T 0.3, Late
% mCherry+GFP- (normalised)
% mCherry+GFP+ (normalised)
Healthy seropositives
Healthy seronegatives
Non-viraemic timepoints
Viraemic timepoints
D+R+
D+R-
D-R+
Kidney
Liver
High viraemics
Low viraemics

Figure 6.7: Comparison of control of viral gene expression by PBMCs from viraemic and non-viraemic timepoints with healthy HCMV-seropositive and HCMV-seronegative controls

Violin plots of mean amounts of IE and late CMV gene expression for PBMCs from healthy HCMV-seropositive and HCMV-seronegative donors that were added to the viral dissemination assay at E:T ratios of 1.25:1, 0.6:1 and 0.3:1 were plotted (black and pink violin plots, previously shown in Fig.3.14). Next, violin plots showing mean amounts of IE and late CMV gene expression for PBMCs from viraemic and non-viraemic timepoints that had been added to the viral dissemination assay at E:T ratios of 1.25:1, 0.6:1 and 0.3:1 were added (teal and dark purple violin plots). The data points from the transplant recipients (i.e. the teal and dark purple violin plots) were then re-categorised by the following criteria and re-plotted onto the same graphs: donor and recipient serostatus (light purple, light blue, and brown violin plots); whether they were kidney or liver transplants (green and navy violin plots); and whether they had viral loads of $\geq$1000 ("high viraemics", beige violin plots) or $<$1000 genome copies/ml ("low viraemics", grey violin plots) at the time when the blood sample was drawn. Titles above each graph state the E:T ratio and phase of gene expression shown by the respective graph. Statistics were performed using a Mann-Whitney U test. (IE = immediate-early CMV gene expression, Late = late CMV gene expression; *$p\leq$0.05; **$p\leq$0.01; ***$p\leq$0.001; ****$p\leq$0.0001; ns = not significant)

6.6.2 CD8$^+$ T cells

The results presented in Fig.6.5 show that the viral dissemination assay can be used as a tool to dissect how CD8$^+$ T cells, NK cells and CD4$^+$ contribute (or not) to overall PBMC control of HCMV-infected cells. Having shown that PBMCs from non-viraemic timepoints performed similarly to PBMCs from healthy HCMV-seropositive donors while PBMCs from viraemic timepoints behaved similarly to PBMCs from HCMV-seronegative donors, I next wanted to examine if this observation also applied to the different immune cell populations as well. In the same manner as with the PBMCs, violin plots of mean amounts of IE and late CMV gene expression seen when CD8$^+$ T cells from healthy HCMV-seropositive and HCMV-seronegative donors were added to the viral dissemination assay at E:T ratios of 1.25:1, 0.6:1 and 0.3:1 were plotted (Fig.6.8, black and pink violin plots; data originally presented in Fig.3.15). Then, violin plots (from Fig.6.6) of mean amount of IE and late CMV gene expression seen when CD8$^+$ T cells from non-viraemic and viraemic timepoints were added to the viral dissemination assay were plotted for each respective E:T ratio (Fig.6.8, teal and purple violin plots). Similarly to the PBMCs, the data points from the transplant recipients were then stratified according to their donor and recipient serostatus (D$^+$R$^+$, light purple violin plots; D$^+$R$^-$, light blue violin plots; or D$^-$R$^+$, brown violin plots), whether they were kidney (green violin plots) or liver transplants (navy violin plots), and, where the information was available, whether they had viral loads of $\geq$1000 or $<$1000 genome copies/ml ("high viraemics", beige violin plots; or "low viraemics", grey violin plots) when the blood sample was taken. These data points were then re-plotted as violin plots on the same graph. I then performed statistical analysis using Mann-Whitney *U* tests to look for statistically significant differences between the groups.

Similar to PBMCs, CD8$^+$ T cells from non-viraemic timepoints showed similar levels of ability to limit IE and late CMV gene expression when compared to CD8$^+$ T cells from healthy HCMV-seropositive donors (Fig.6.8, black vs teal violin plots), while CD8$^+$ T cells from viraemic timepoints showed a similar lack of ability to control late CMV gene expression when compared to CD8$^+$ T cells from healthy HCMV-seronegative donors (Figs.6.8B, 6.8D $\&$ 6.8F, pink vs dark purple violin plots). When the data points from viraemic and non-viraemic timepoints were stratified according to donor and recipient status, CD8$^+$ T cells from D$^+$R$^-$ transplants showed the poorest ability to limit IE and late CMV gene expression (Fig.6.8, light blue violin plots), while there appeared to be no statistically significant difference between the ability of CD8$^+$ T cells from D$^+$R$^+$ and D$^-$R$^+$ transplants to limit IE or late CMV gene expression (light purple and brown violin plots). There was no statistically significant difference in ability to control IE or late CMV gene expression between CD8$^+$ T cells from kidney or liver transplant recipients (green and navy violin plots), nor did the amount of viral load present at time of sampling appear to affect whether CD8$^+$ T cells were able to control IE or late CMV gene expression (beige and grey violin plots).

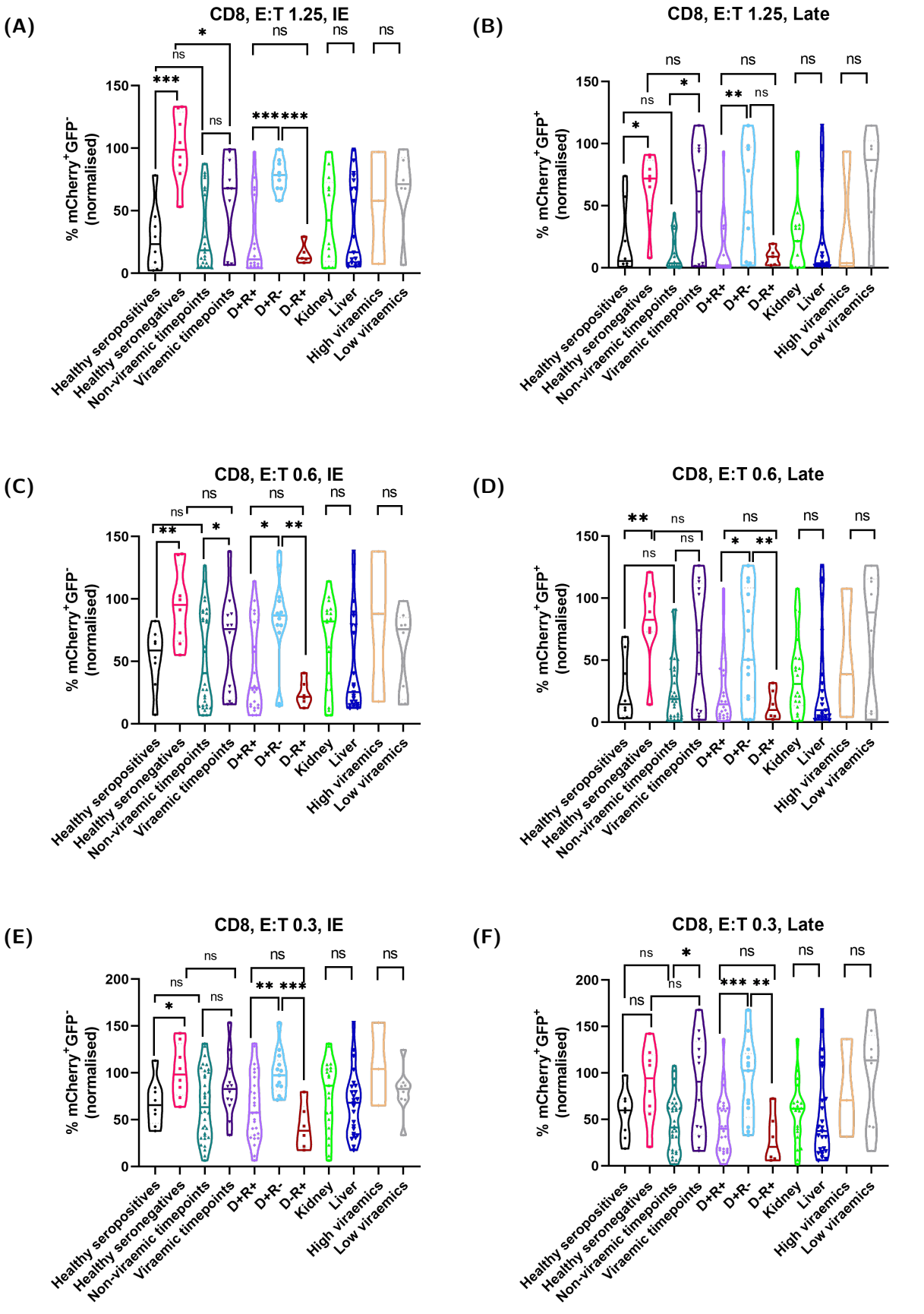
(A)
CD8, E:T 1.25, IE
(B)
CD8, E:T 1.25, Late
(C)
CD8, E:T 0.6, IE
(D)
CD8, E:T 0.6, Late
(E)
CD8, E:T 0.3, IE
(F)
CD8, E:T 0.3, Late
% mCherry+GFP- (normalised)
% mCherry+GFP+ (normalised)
Healthy seropositives
Healthy seronegatives
Non-viraemic timepoints
Viraemic timepoints
D+R+
D+R-
D-R+
Kidney
Liver
High viraemics
Low viraemics

Figure 6.8: Comparison of control of viral gene expression by CD8$^+$ T cells from viraemic and non-viraemic timepoints with healthy HCMV-seropositive and HCMV-seronegative controls

Violin plots of mean amounts of IE and late CMV gene expression for CD8$^+$ T cells from healthy HCMV-seropositive and HCMV-seronegative donors that were added to the viral dissemination assay at E:T ratios of 1.25:1, 0.6:1 and 0.3:1 were plotted (black and pink violin plots, previously shown in Fig.3.15). Next, violin plots showing mean amounts of IE and late CMV gene expression for CD8$^+$ T cells from viraemic and non-viraemic timepoints that had been added to the viral dissemination assay at E:T ratios of 1.25:1, 0.6:1 and 0.3:1 were added (teal and dark purple violin plots). The data points from the transplant recipients (i.e. the teal and dark purple violin plots) were then re-categorised by the following criteria and re-plotted onto the same graphs: donor and recipient serostatus (light purple, light blue, and brown violin plots); whether they were kidney or liver transplants (green and navy violin plots); and whether they had viral loads of $\geq$1000 ("high viraemics", yellow violin plots) or $<$1000 genome copies/ml ("low viraemics", grey violin plots) when the blood sample was taken. Titles above each graph state the E:T ratio and phase of gene expression shown by the respective graph. Statistics performed using Mann-Whitney *U* test. (IE = immediate-early CMV gene expression, Late = late CMV gene expression; *$p\leq0.05$; **$p\leq0.01$; ***$p\leq0.001$; ****$p\leq0.0001$; ns = not significant)

6.6.3 NK cells

I next examined whether NK cells from viraemic and non-viraemic timepoints showed similar levels of control of IE and late CMV gene expression to NK cells from healthy HCMV-seropositive and HCMV-seronegative donors in the viral dissemination assay. The violin plots and statistical analysis as calculated for PBMCs and $CD8^+$ T cells in Sections 6.6.1 and 6.6.2 were performed on NK cells in the same manner as for PBMCs and $CD8^+$ T cells. Only one E:T ratio (of 2.5:1) was plotted as this was the only E:T ratio that showed a statistically significant difference between NK cells from viraemic and non-viraemic timepoints in controlling IE and late CMV gene expression. There were insufficient samples to compare whether NK cells from patients with high or low viral loads had any difference in ability to control IE or late CMV gene expression. The results are shown in Fig.6.9.

NK cells from non-viraemic timepoints were better able to limit IE and late CMV gene expression as compared to NK cells from healthy HCMV-seropositive controls (Fig.6.9, black vs teal violin plots), whereas NK cells from viraemic timepoints showed a poorer ability to limit late CMV gene expression, although this was not statistically significant (Fig.6.9B, pink and dark purple violin plots). There were no differences in ability to limit IE and late CMV gene expression between NK cells from D^+R^+, D^+R^-, and D^-R^+ transplants (light purple, light blue and brown violin plots). However, NK cells from liver transplant recipients showed a poorer ability to limit IE and late CMV gene expression than those from kidney transplant recipients (green and navy violin plots).

NK cells form part of the innate immune response, and therefore, theoretically, do not require a prior exposure to pathogens in order to carry out their cytotoxic functions, although $NKG2C^+$ $CD57^+$ "adaptive" NK cells have been described in HCMV-seropositive individuals [53, 210, 508]. The observation that there were no differences between NK cells from the D^+R^+, D^+R^- and D^-R^+ serostatus groups in controlling IE and late CMV gene expression is in support of this, and would seem to suggest that the factors that determine if a patient can mount an effective NK cell response to HCMV are not dependent on the presence of memory T cell responses. There is, however, the caveat that there were few NK cell samples that had adequate E:T ratios available, and therefore more samples are needed before conclusions can be drawn.

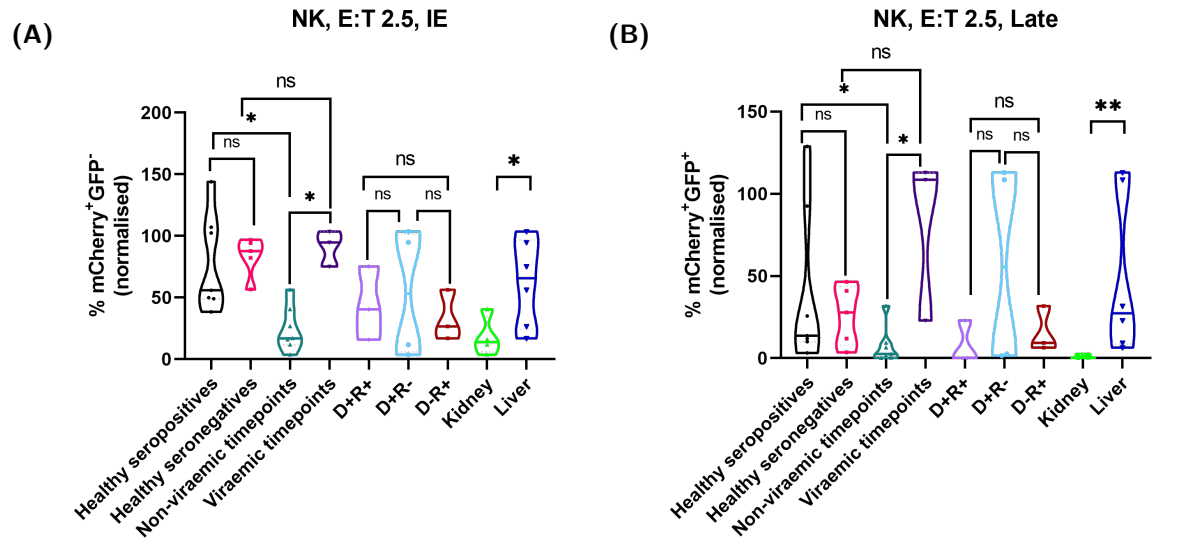

Figure 6.9: Comparison of control of viral gene expression by NK cells from viraemic and non-viraemic timepoints with healthy HCMV-seropositive and HCMV-seronegative controls

Violin plots of mean amounts of IE and late CMV gene expression for NK cells from healthy HCMV-seropositive and HCMV-seronegative donors that were added to the viral dissemination assay at E:T ratios of 2.5:1 were plotted (black and pink violin plots, previously shown in Fig.3.17). Next, violin plots showing mean amounts of IE and late CMV gene expression for NK cells from viraemic and non-viraemic timepoints that had been added to the viral dissemination assay at E:T ratios of 2.5:1 were added (teal and dark purple violin plots). The data points from the transplant recipients (i.e. the teal and dark purple violin plots) were then re-categorised by the following criteria and re-plotted onto the same graphs: donor and recipient serostatus (light purple, light blue, and brown violin plots); and whether they were kidney or liver transplants (green and navy violin plots). Titles above each graph state the E:T ratio and phase of gene expression shown by the respective graph. Statistics performed using Mann-Whitney U tests. (IE = immediate-early CMV gene expression, Late = late CMV gene expression; *$p \leq 0.05$; **$p \leq 0.01$; ***$p \leq 0.001$; ****$p \leq 0.0001$; ns = not significant)

6.6.4 $CD4^+$ cells

Fig.3.18 in Chapter 3 showed that $CD4^+$ cells from a cohort of healthy HCMV-seropositive donors were able to control late CMV gene expression at higher E:T ratios of 1.25:1, 2.5:1 and 5:1. The experiments in Chapter 4 showed that cytokines in the secretome of $CD4^+$ cells co-cultured with HCMV-infected fibroblasts were a component of this control. The results in Chapter 5 suggested that it was a monocyte population that was present in cells selected with CD4 MicroBeads that was responsible for this. It also showed that the mechanism of how this occurred was by antigen presentation via the MHC Class II pathway to $CD4^+$ T cells, such that the $CD4^+$ T cells could produce IFN-γ that could then induce MHC Class II on uninfected fibroblasts. This then allowed the $CD4^+$ T cells to recognise these fibroblasts when they became infected with HCMV. The results in Fig.6.5C showed that $CD4^+$ cells from non-viraemic timepoints were able to limit late CMV gene expression at higher E:T ratios of 2.5:1 and 5:1. It would thus be expected that the control of viral gene expression by $CD4^+$ cells from non-viraemic timepoints would be similar to that from healthy HCMV-seropositive controls.

To test this hypothesis, violin plots and statistical analysis as calculated for PBMCs, $CD8^+$ T cells and NK cells in the preceding Sections 6.6.1–6.6.3 were performed on $CD4^+$ cells. Violin plots of mean amounts of IE and late CMV gene expression for $CD4^+$ cells from healthy HCMV-seropositive and HCMV-seronegative donors that were added to the viral dissemination assay at E:T ratios of 5:1 and 2.5:1 were plotted (Fig.6.5C, black and pink violin plots, previously shown in Fig.3.18). Next, violin plots showing mean amounts of IE and late CMV gene expression for NK cells from viraemic and non-viraemic timepoints that had been added to the viral dissemination assay at E:T ratios of 5:1 and 2.5:1 were added (Fig.6.5C, teal and dark purple violin plots). The data points from the transplant recipients (i.e. the teal and dark purple violin plots) were then re-categorised by the following criteria and re-plotted onto the same graphs: donor and recipient serostatus (light purple, light blue, and brown violin plots); whether they were kidney or liver transplants (green and navy violin plots); and whether they had viral loads of $\geq$1000 or $<$1000 genome copies/ml ("high viraemics", beige violin plots; or "low viraemics", grey violin plots) at the time when the sample was taken.

Fig.6.10 shows that $CD4^+$ cells from non-viraemic timepoints show poorer control of IE CMV gene expression than $CD4^+$ cells from healthy HCMV-seropositive controls (Figs.6.10A & 6.10C, black vs teal violin plots). However, for late CMV gene expression, $CD4^+$ cells from non-viraemic timepoints showed similar amounts of control as $CD4^+$ cells from healthy HCMV-seropositive controls (Figs.6.10B & 6.10D, black vs teal violin plots). $CD4^+$ cells from viraemic timepoints demonstrated a wide range of ability to control IE and late CMV gene expression, a result that was similar to the wide range of ability seen in healthy HCMV-seronegative controls (Figs.6.10A–6.10D, pink vs dark purple violin plots). When stratified by donor and recipient serostatus, D^+R^- transplants again showed the poorest ability to control

late IE CMV gene expression (Figs.6.10B & 6.10D, light blue violin plots), a result that was also seen in PBMCs and $CD8^+$ T cells. $CD4^+$ cells from liver transplant recipients showed a poorer ability to limit late CMV gene expression when compared to kidney transplant recipients (Figs.6.10B & 6.10D, navy vs green violin plots), although this difference was only statistically significant at the E:T ratio of 5:1. A high or low viral load at the time of blood sampling was not associated with a difference in the ability of $CD4^+$ cells to limit IE or late CMV gene expression (beige vs grey violin plots).

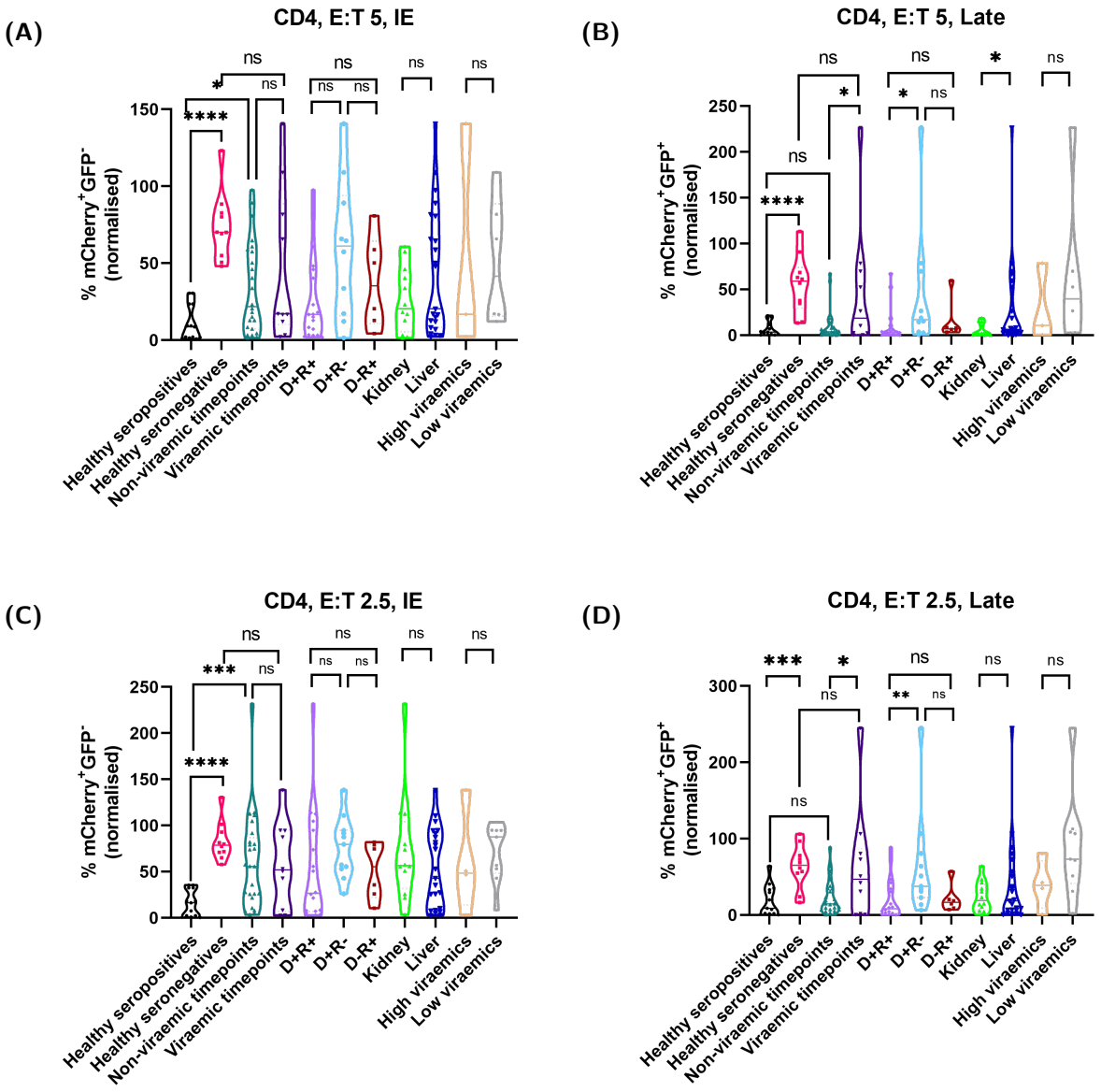

Figure 6.10: Comparison of control of viral gene expression by CD4$^+$ cells from viraemic and non-viraemic timepoints with healthy HCMV-seropositive and HCMV-seronegative controls

Violin plots of mean amounts of IE and late CMV gene expression for CD4$^+$ cells from healthy HCMV-seropositive and HCMV-seronegative donors that were added to the viral dissemination assay at E:T ratios of 5:1 and 2.5:1 were plotted (black and pink violin plots, previously shown in Fig.3.18). Next, violin plots showing mean amounts of IE and late CMV gene expression for CD4$^+$ cells from viraemic and non-viraemic timepoints that had been added to the viral dissemination assay at E:T ratios of 5:1 and 2.5:1 were added (teal and dark purple violin plots). The data points from the transplant recipients (i.e. the teal and dark purple violin plots) were then re-categorised by the following criteria and re-plotted onto the same graphs: donor and recipient serostatus (light purple, light blue, and brown violin plots); whether they were kidney or liver transplants (green and navy violin plots); and whether they had viral loads of $\geq$1000 ("high viraemics", yellow violin plots) or $<$1000 genome copies/ml ("low viraemics", grey violin plots) when the blood sample was taken. Titles above each graph state the E:T ratio and phase of gene expression shown by the respective graph. Statistics performed using Mann-Whitney *U* test. (IE = immediate-early CMV gene expression, Late = late CMV gene expression; *$p\leq0.05$; **$p\leq0.01$; ***$p\leq0.001$; ****$p\leq0.0001$; ns = not significant)

6.7 Using the viral dissemination assay to compare PBMCs, $CD8^+$ T cells, NK cells and $CD4^+$ cells over the transplant time course

The previous section allowed me to examine how PBMCs, $CD8^+$ T cells, NK cells and $CD4^+$ cells from viraemic and non-viraemic timepoints, different serostatus groups, and 2 different types of solid organ transplants differed in their ability to limit IE and late CMV gene expression in the viral dissemination assay. However, this did not allow me to examine how these immune cell populations from the same patient contributed to overall control of CMV *in vivo*, or whether the control seen in the VDAs showed a relation to *when* they had their viraemic episodes. To do this, I plotted the mean %mCherry$^+$GFP$^-$ and %mCherry$^+$GFP$^+$ cells in the viral dissemination assay of each immune cell population for each patient in a graph with their transplant time course and CMV viral load as measured on regular post-transplant screening. As it was not possible to plot all the E:T ratios from the same immune cell population on the graph, one E:T ratio that was thought to show the greatest difference between the timepoints was chosen. These graphs are shown in Fig.6.11 below and grouped according to their transplant serostatus group, and whether they were viraemic or not. Left column shows %mCherry$^+$GFP$^-$, right column shows %mCherry$^+$GFP$^+$. For ease of comparison, graphs from the 2 donors (R01-079 & R01-081) shown earlier in Fig.6.4E–6.4H are shown here as well.

Fig.6.11 demonstrates the difficulty of interpreting the large dataset with multiple variables to consider. However, it would appear that there were a few trends that were noted:

1. **Control of late CMV gene expression was a better discriminator of functional ability between viraemic and non-viraemic patients.**
   The amount of IE CMV gene expression (%mCherry$^+$GFP$^-$) was between 50 to 100% or more for most of the immune cell populations in most of the patients, with only a few exceptions in some PBMC (pink dotted lines in graphs) and $CD8^+$ T cell populations (dark purple dotted lines in graphs) from a few donors (e.g. R02-109, R02-015). As such, it was difficult to use suppression of IE CMV gene expression to differentiate between the control exerted by the different immune cell populations.

2. **Post-transplant PBMCs almost always controlled late CMV gene expression to $<$50%mCherry$^+$GFP$^+$ by the final timepoint in non-viraemic patients.**
   With the exception of patient R02-174, PBMC (pink dotted lines) control of late CMV gene expression was either always to a degree of $<$50%mCherry$^+$GFP$^+$ at all post-transplant timepoints, or had improved to $<$50%mCherry$^+$GFP$^+$ by the final timepoint. In one patient that had approximately 50%mCherry$^+$GFP$^+$ at the final timepoint tested (R02-185), this was followed by small blips of CMV viral load detected by routine screening, although it was not sufficient to be classified as a viraemic episode or warrant CMV

treatment.

3. **There was frequently a deterioration of control of late CMV gene expression, or baseline poor control, from at least 3 immune cell populations preceding episodes of viraemia. Conversely, there was often an improvement in control, or baseline good control, of at least 2 immune cell populations by the last timepoint post-transplant in non-viraemic patients.**
   With the exception of R02-185, who continued to have small blips of detectable CMV viral load after the last timepoint tested, nearly all the other non-viraemic patients showed an improvement in late CMV gene control (seen as a downward sloping line) of at least 2 immune cell populations by the last timepoint post-transplant. The exceptions were R02-079, who showed a worsening of $CD4^+$ and $CD8^+$ function but an improvement in PBMC function, and R02-184, who showed a worsening of $CD8^+$ T cell function and NK function but had overall good PBMC function. Conversely, in 4 of the 6 viraemic patients (R02-011, R02-125, R01-079 and R01-081), there was a worsening of control of late gene expression (seen as an upward sloping line) of at least 3 of the immune cell populations just before onset or during the episode of viraemia. For the remaining 2 viraemic patients (R02-129 and R02-171), there were no samples just before the onset of viraemia to observe this trend, although R02-171 did have a worsening of control in PBMCs, $CD4^+$ cells and NK cells at the last timepoint post-transplant.

(A) D^+R^+ Non-viraemic

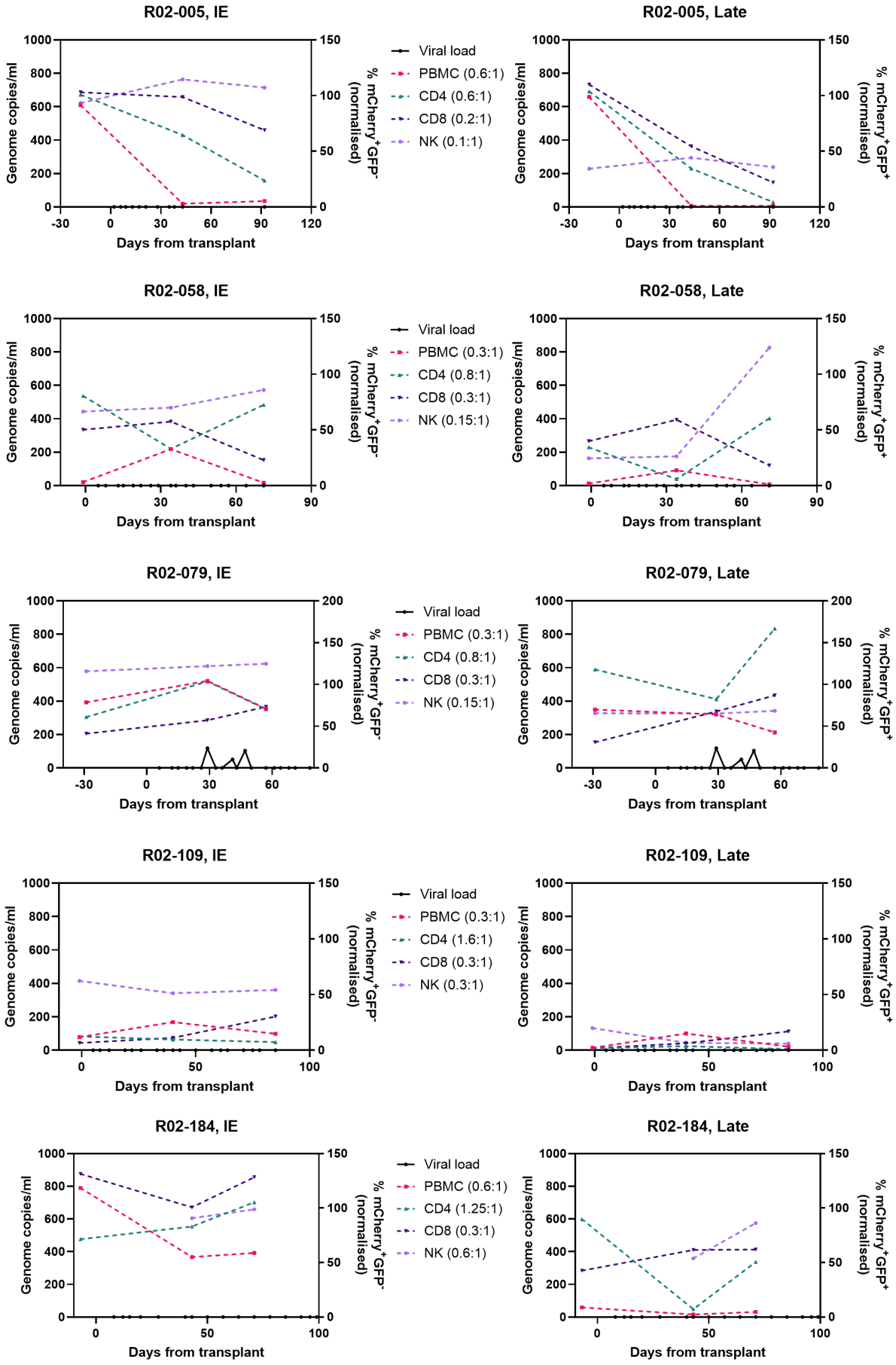

(B) D^+R^+ Non-viraemic continued

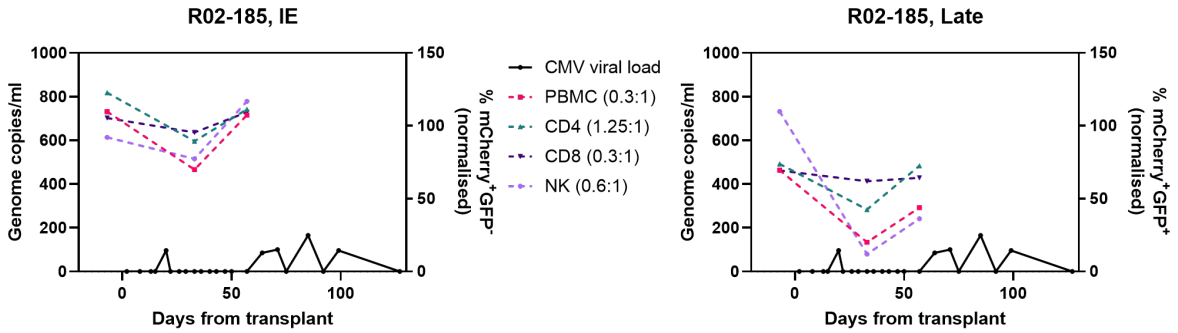

(C) D^-R^+ Non-viraemic

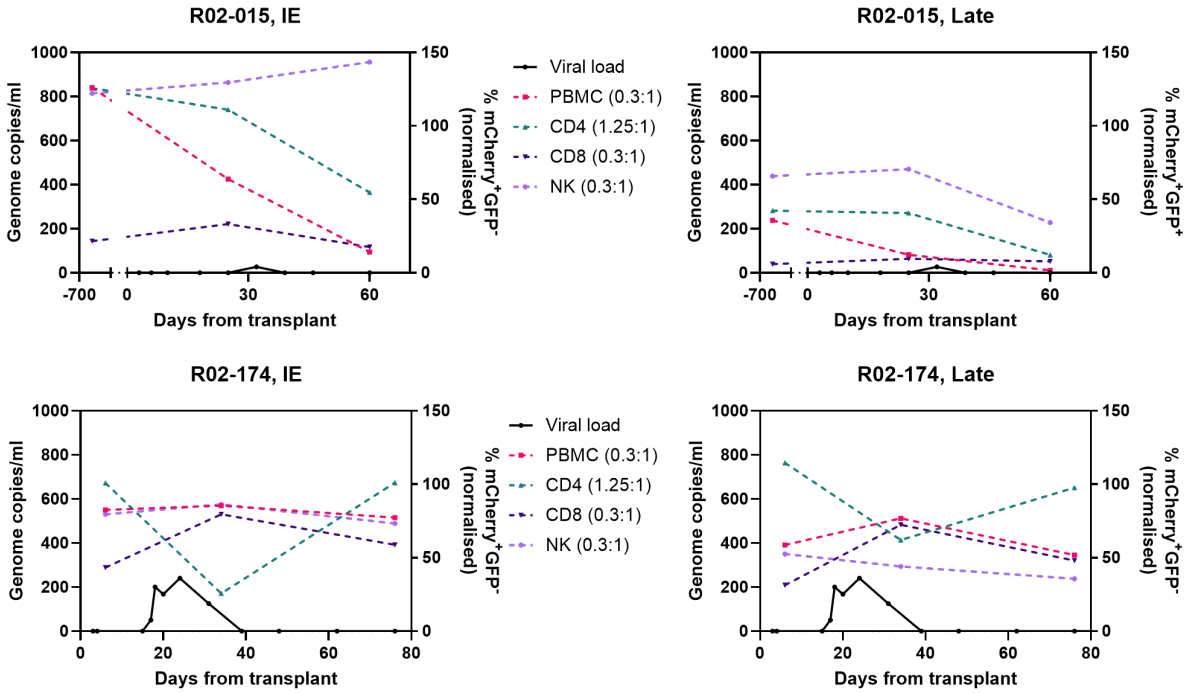

(D) D^+R^- Non-viraemic

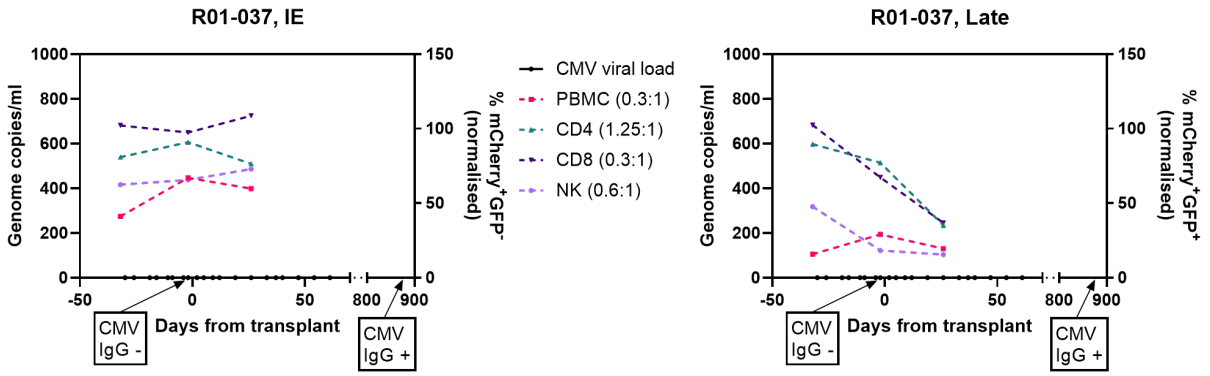

(E) D^+R^+ Viraemic

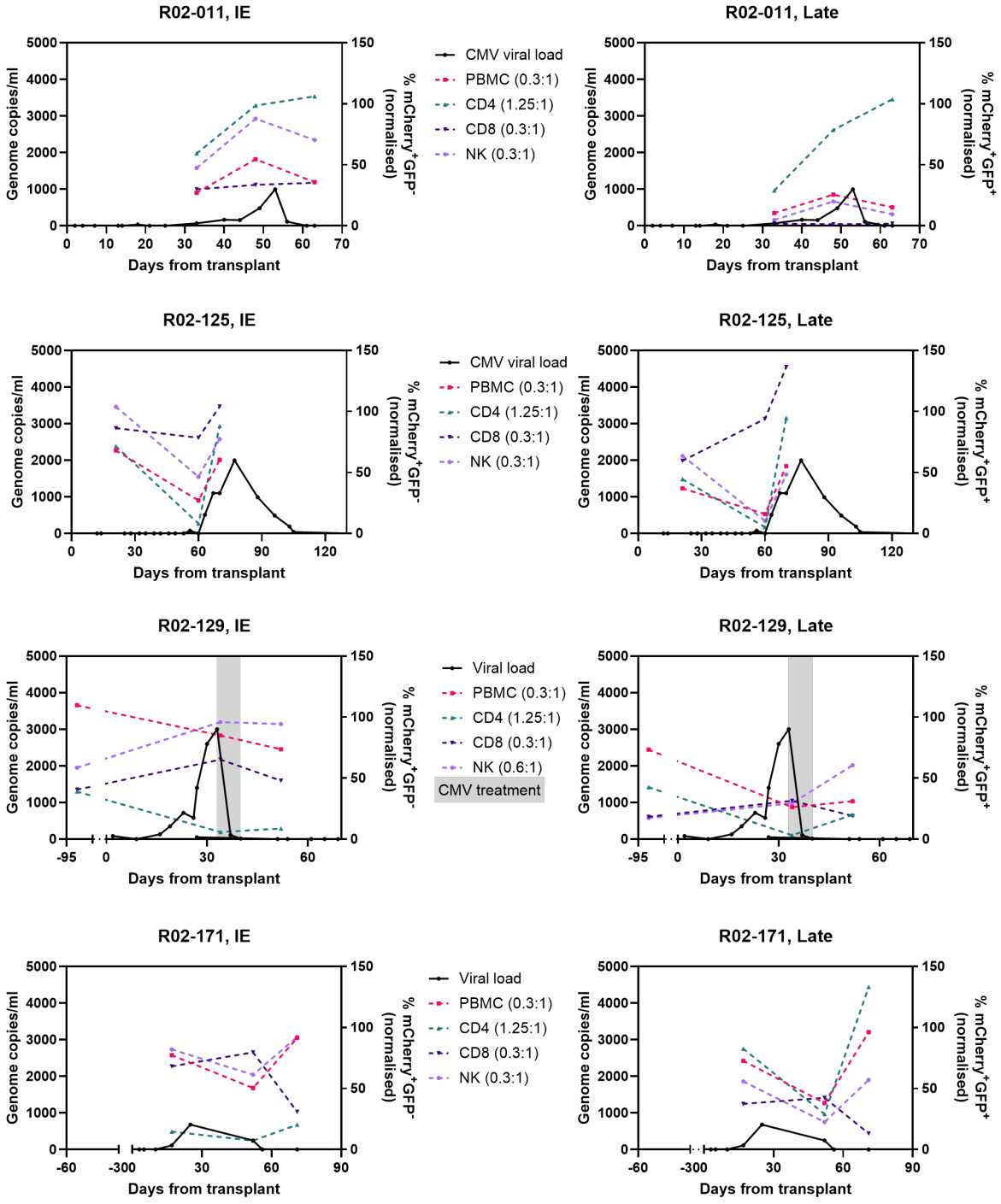

(F) D^+R^- Viraemic

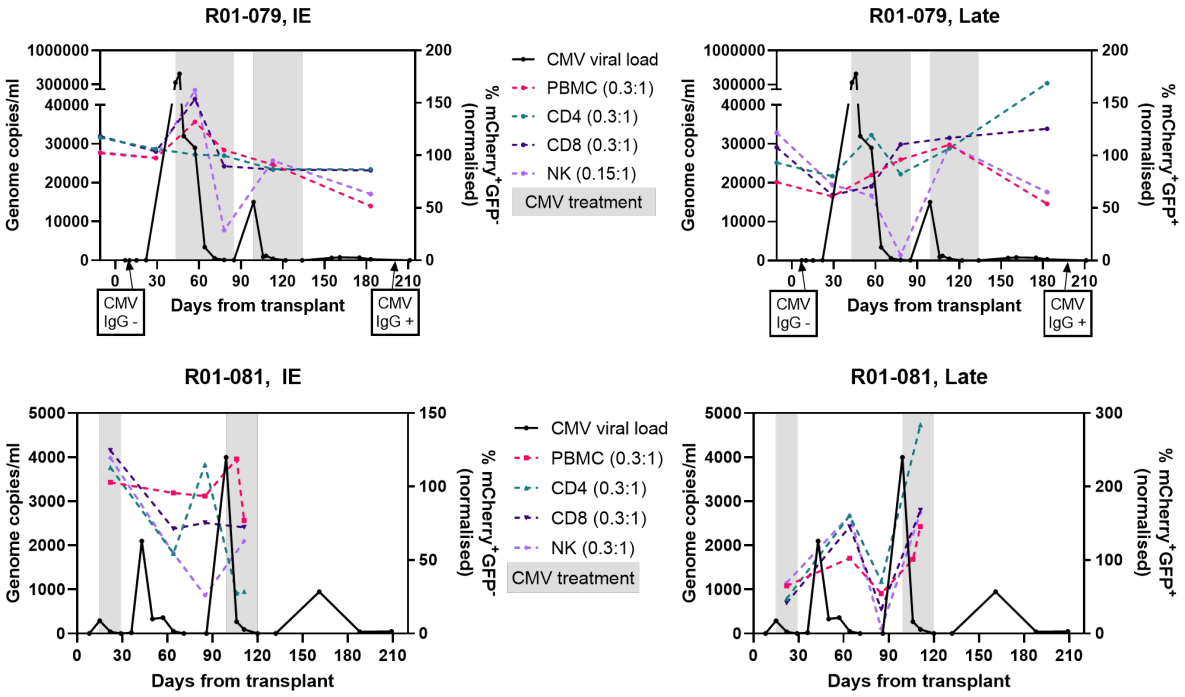

Figure 6.11: Using the viral dissemination assay to compare PBMCs, $CD8^+$ T cells, NK cells and $CD4^+$ cells over the transplant time course
%mCherry$^+$GFP$^-$ and %mCherry$^+$GFP$^+$ cells in the viral dissemination assay with PBMCs, $CD8^+$ T cells, NK cells and $CD4^+$ cells for each transplant patient was plotted in a graph with the transplant time course and CMV viral load as measured on regular post-transplant screening. Figs.6.11A & 6.11B show the D^+R^+ non-viraemic patients, Fig.6.11C shows the D^-R^+ non-viraemic patients, Fig.6.11D shows the D^+R^- non-viraemic patient, Fig.6.11E shows the D^+R^+ viraemic patients, and Fig.6.11F shows the D^+R^- viraemic patients. Left column shows %mCherry$^+$GFP$^-$, right column shows %mCherry$^+$GFP$^+$. Note different y-axis scales between viraemic and non-viraemic patients. Mean of triplicate wells is shown. The E:T ratio at which the immune cell population was added is shown in brackets in the legend of each graph. Grey areas represent duration of CMV treatment, and points at which CMV IgG was tested for the R^- patient is shown on the graph.

Fig.6.11 therefore shows how the VDA can be used to dissect the contributions of the different immune cell populations to overall control of IE and late CMV gene expression, and how this is reflected clinically by episodes of viraemia. However, there are clearly some caveats to mention. Firstly, there were exceptions to the trends seen. Some of these exceptions could be due to a lack of samples tested (for example, R02-185, who did not have samples tested during the multiple small blips of detectable CMV viral load) after the last timepoint. There were also patients that did not have samples tested at a timepoint clearly before the onset of viraemia (e.g. R02-171, R02-129), which made it difficult to comment on whether the immune cell function had shown a deterioration before the onset of viraemia. There were also patients who showed fairly poor control of late CMV gene expression in at least two immune cell populations (i.e. R02-079 and R02-184) but did not have episodes of viraemia. This may have been due to inconsistent sample preparation, leading to poorer cell recovery and therefore poorer function in the VDA.

6.8 Discussion

6.8.1 Comparing the ability to control CMV gene expression between PBMCs, CD8$^+$ T cells, CD4$^+$ and NK cells from transplant recipients with healthy individuals

PBMCs from viraemic timepoints control *in vitro* CMV replication less efficiently than PBMCs from healthy HCMV-seronegative controls

The results presented in Section 6.5 showed that PBMCs from viraemic timepoints show a statistically significant poorer ability to control late CMV gene expression than PBMCs from non-viraemic timepoints at all E:T ratios tested. Given that PBMCs at these timepoints were taken during episodes of viraemia, this *in vitro* observation corresponds to the clinical picture and reflects a similar loss of control of viral replication *in vivo*. When the PBMCs from these viraemic timepoints were compared to those from healthy controls in Section 6.6.1, it can be seen that these PBMCs showed an even poorer ability in controlling late CMV gene expression than those from healthy HCMV-seronegative donors.

PBMCs consist of all mononuclear cells in the peripheral blood, which includes monocytes, T lymphocytes (including CD4$^+$, CD8$^+$ and $\gamma\delta$ T cells), NK cells and B cells. Monocytes and NK cells are part of the innate immune response which does not require memory T cells to function. In HCMV-seronegative individuals with no memory T cell responses, the PBMC response should therefore consist mostly of the innate immune responses of these individuals. The observation that PBMCs from viraemic timepoints showed worse control than PBMCs from healthy HCMV-seronegative donors would therefore suggest that there were deficiencies in the innate immune responses of these PBMCs.

Hence, in order to examine how each of these immune cell populations from viraemic and non-viraemic timepoints contributed (or not) to limit CMV replication, I added each of these populations to the VDA and compared the amount of IE and late CMV gene expression present. Clearly, the CD8$^+$ and CD4$^+$ T cell populations from HCMV-seropositive recipients ought to have memory T responses present, and would be expected to exert better control of IE and late CMV gene expression than those from HCMV-seronegative recipients, while HCMV serostatus ought to have no impact on the ability of NK cells to control CMV gene expression, as seen in the data from Chapter 3.

CD8$^+$ T cells from viraemic timepoints show poor control of CMV gene expression

In the data presented in Section 6.5 (Figs.6.6C–6.6D), it is clearly seen that other than at the highest E:T ratio of 2.5:1, CD8$^+$ T cells from viraemic timepoints show a distinctly poorer ability to control late CMV gene expression *in vitro* as compared to CD8$^+$ T cells from non-viraemic timepoints. CD8$^+$ T cells from non-viraemic timepoints, on the other hand, showed

a similar level of control to $CD8^+$ T cells from HCMV-seropositive patients. The requirement of a successful recovery of the HCMV-specific $CD8^+$ T cell response for adequate protection against CMV viraemia and disease in post-transplant patients is well-documented [583–585]. While numerous studies have also shown the importance of an intact HCMV-specific $CD4^+$ T cell response (summarised in Table 1.7), protection from CMV disease is ultimately still dependent upon recovery of a robust CMV-specific $CD8^+$ T cell response, particularly in solid organ transplant recipients. The observation in Fig.6.6 is therefore in keeping with these prior clinical studies, where $CD8^+$ T cells from viraemic timepoints are unable to control viral gene expression *in vitro*. In addition, it would also suggest that it is a functioning memory T cell response that allows for this adequate control to happen.

$CD4^+$ and NK cells from viraemic timepoints show worse control of CMV gene expression than $CD4^+$ and NK cells from healthy HCMV-seronegative controls

During primary infection, CMV-specific $CD4^+$ T cells are only detected at approximately 1-2 weeks post-infection [479]. $CD4^+$ cells from HCMV-seronegative individuals exposed to HCMV-infected cells *in vitro* would therefore not be expected to control viral gene expression, and the results from $CD4^+$ cells from the cohort of healthy individuals presented earlier in Fig.3.18 are consistent with this, where there is only a small amount of control at the highest E:T ratio, which is possibly due to non-specific effects of adding higher numbers of $CD4^+$ cells into the VDA. These non-specific effects may be as a result of small numbers of cytotoxic $CD4^+$ T cells in the CD4 MicroBead-selected population, which could have direct cytotoxicity on infected cells [567]. Another possibility is that, as shown in Chapter 5, the $CD4^+$ cells selected by CD4 MicroBeads also contain a population of monocytes and dendritic cells that can exert a degree of control of viral gene expression.

As shown in Chapter 5, the presence of a monocyte population in the $CD4^+$ cell population potentiated control by $CD4^+$ T cells, an effect that was largely eliminated when MHC Class II and IFN-γ-blocking antibodies were added. The observation that $CD4^+$ cells from viraemic timepoints showed even worse control than $CD4^+$ cells from HCMV-seronegative donors would suggest that there was a small degree of control by the innate immune cells in the $CD4^+$ cells from HCMV-seronegative donors, and also from primary immune responses of the $CD4^+$ T cells, which was not present in the $CD4^+$ cells from viraemic timepoints.

Moreover, a deep phenotyping analysis of the PBMCs or $CD4^+$ cells from these patients was not done. Given sufficient samples, performing such an analysis may have uncovered deficiencies in these immune cell subsets in these patients, which could have affected their $CD4^+$ T cell functions.

6.8.2 Control of viral dissemination by PBMCs, CD4$^+$ cells, and CD8$^+$ T cells from non-viraemic timepoints approximate that seen in healthy HCMV-seropositive controls

HCMV infection in the immunocompetent host is marked by periods of reactivation, during which productive lytic infection [526] and viral shedding into saliva and urine occurs [82, 589]. However, an intact immune response usually precludes this from progressing into a persistent CMV viraemia and end-organ disease. The results in Sections 3.4.1–3.4.4 characterising the *in vitro* response of PBMCs, CD8$^+$ T cells and CD4$^+$ cells from a cohort of healthy controls to HCMV-infected cells are consistent with the *in vivo* observations—PBMCs, CD8$^+$ and CD4$^+$ cells from healthy HCMV-seropositive individuals are able to control IE and late CMV gene expression in the viral dissemination assay, albeit to varying degrees. The data in Figs.6.7–6.10 show that there were no statistically significant differences in control of viral gene expression by PBMCs, CD8$^+$ T cells and CD4$^+$ cells from non-viraemic timepoints with those from healthy HCMV-seropositive controls, while the absence of viraemia in at these timepoints suggests that these immune cell populations are still able to exhibit a degree of normal function despite these recipients receiving immunosuppression. That these immune cells from healthy HCMV-seropositive individuals can exhibit control of CMV gene expression in the VDA despite the presence of multiple immune evasion genes to both innate and adaptive responses (briefly summarised in [652]) would suggest that, ultimately, in a fully-functioning immune system, these immune evasion genes do not succeed in complete evasion of the immune response.

NK cells from non-viraemic timepoints appeared to show a greater degree of control of IE and late CMV gene expression than NK cells from healthy seropositive individuals, and a possible reason for this may be that, as discussed in Section 3.4.3, even among HCMV-seropositive individuals, there appears to be a sub-population of individuals with NK cells that are able to control viral gene expression, and a sub-population that do not. This observation is interesting. Previous publications have reported that NK cells isolated from blood appear to be unable to control wild-type HCMV replication *in vitro* [57, 100], although patients with NK cell defects have been associated with HCMV disease [57, 114, 458]. This would suggest that the artificial *in vitro* methods of assessment of NK cell function do not appear to fully reflect the *in vivo* capabilities of NK cell function [170]. HCMV encodes multiple immune evasion genes against NK cells (reviewed in [52,170]), such as downregulation of stress-induced NK-activating ligands on infected cells and the corresponding activating receptors on NK cells [25, 52]. That there appears to be sub-populations of individuals with NK cells with an inherent ability to control viral gene expression *in vitro* would suggest that there may be individuals who have greater resistance to these immune evasion mechanisms.

6.8.3 D^+R^- transplant recipients

The findings presented in Section 6.6 show that, among the 3 different donor/recipient serostatus combinations present in this cohort, PBMCs, $CD8^+$ T cells, NK cells and $CD4^+$ cells from D^+R^- consistently performed the worst in limiting IE and late CMV gene expression. Among recipients of solid organ transplants, D^+R^- transplants carry the highest risk of CMV viraemia and disease [309]. This is in contrast to HSCTs, where D^-R^+ transplants carry the highest risk of reactivation and disease. The reason for this is because CMV infection in solid organ transplant recipients arises from reactivation of latent CMV from within the donated organ encountering CMV-naïve immune cells in the recipient [385], whereas in HSCTs, pre-transplant conditioning regimens lead to ablation of the existing CMV-specific T cell response of the recipient, and reactivation of latent disease in the recipient then manifests as a primary CMV infection to CMV-naïve lymphocytes from the seronegative donor [227, 597]. The levels of control of viral gene expression seen in these cell populations from D^+R^- transplant recipients approximate that seen in healthy HCMV-seronegative controls, and are also consistent with the observation of D^+R^- transplant recipients having the highest risk of CMV reactivation and disease.

Unfortunately, we did not have sufficient data to determine with specificity when these R^- patients in our cohort seroconverted. Seroconversion would suggest that these individuals had had sufficient exposure to the virus to develop a secondary immune response, and, as evidenced by the data from the healthy cohort in Chapter 3, the presence of a secondary immune response allowed greater control of viral gene expression in the VDA.

That the presence of an IFN-γ T cell response on FluoroSpot^{TM} does not correspond to an ability to control HCMV gene expression in the VDA is, in the face of prior studies done by our group, surprising. In an analysis of the IFN-γ T cell responses from a large cohort of healthy HCMV-seropositive and HCMV-seronegative individuals [257], the IFN-γ response to various lytic- and latency-associated HCMV peptides was consistently higher in healthy HCMV-seropositive individuals, often in an order of magnitude of 10 times or more. This is also in contrast to multiple other studies in post-transplant patients which suggest that the appearance of CMV-specific T cells, measured by the presence of an IFN-γ response, is associated with protection from HCMV viraemia and disease (as discussed in Section 1.2.7.1). This would suggest that, although able to produce IFN-γ, the T cells from these transplant patients still exhibited a functional defect in not being able to prevent HCMV replication.

6.8.4 Liver transplant recipients

Among solid organ transplant recipients, lung and small intestine transplant recipients have the highest risk of CMV reactivation and disease, while liver and heart recipients are at an intermediate risk and kidney recipients are at the lowest risk of CMV infection [243, 368]. In

the results shown in Fig.6.7, PBMCs from liver transplant recipients were consistently poorer at control of late CMV gene expression than PBMCs from kidney transplant recipients. When this is examined by the respective lymphocyte populations, this trend is also present in NK cells (Fig.6.9B) and $CD4^+$ cells (Figs.6.10B,6.10D), but not in $CD8^+$ T cells. The poorer control of late CMV gene expression *in vitro* by PBMCs from liver transplant as compared to kidney transplant recipients is consistent with the clinical trends of liver transplant recipients having a higher risk of CMV reactivation and disease. The results from the NK cell and $CD4^+$ cell graphs suggest that this is likely due to a defect in NK cell or $CD4^+$ function, although the reason for this defect is unclear—some possibilities may be that the post-liver transplant immunosuppression regime more strongly suppresses $CD4^+$ or NK cell responses, or that livers from HCMV-seropositive donors harbour higher latent CMV viral loads than kidneys from HCMV-seropositive donors.

6.8.5 It is not always clear if a specific defect of either $CD4^+$ cells, $CD8^+$ T cells or NK cells leads to viraemic episodes, but an absence of improvement of function of $CD4^+$ cells, $CD8^+$ T cells and NK cells frequently precedes episodes of viraemia

Section 6.7 bears out the complexity of analysing the various immune cell responses to HCMV. The data seemed to suggest that it was often a defect in function of more than one cell population that led to episodes of viraemia, although it was not always clear if one particular immune cell population contributed to a greater degree than others. While the VDA examined the functional ability of the majority of the various immune cell populations present, it did not examine the contribution of a few smaller populations, such as monocytes, macrophages, pDCs or $CD4^-CD8^-\gamma\delta$ T cells. An additional complication was the occasional insufficient numbers of some of the immune cell populations obtained, specifically $CD8^+$ T cells and NK cells. This led to the uncertainty of whether the inability of the $CD8^+$ or NK cell population to control viral gene expression at that particular E:T ratio was simply due to an inadequate E:T ratio used. All in all, assuming adequacy of available samples, further use of this VDA could be modified to include monocyte cell populations among the immune cell populations studied, especially given the findings shown in Chapter 5 which imply an important role of their antigen-presenting function and type I IFN from pDCs in the control of HCMV gene expression.

6.8.6 Limitations and challenges of this study

There were also other challenges in carrying out the experiments on this cohort of samples. Due to the COVID-19 pandemic, sample collection was interrupted, including samples of skin

biopsy collection to obtain the primary dermal cell lines. This led to limitations on the number of patients on which this VDA could be performed on. In addition, there were fewer viraemic patients than expected, which led to challenges in interpreting trends in data from a smaller sample group. Serology data for the three R^- patients in this study was also sporadic, which leads to uncertainties of when these patients developed a primary immune response to HCMV. The $CD4^+$ cell population in this study was also selected by positive selection MACS with CD4 MicroBeads, which likely led to "contamination" of the $CD4^+$ cell population with a small population of monocytes and pDCs, although one could argue that without the presence of these antigen-presenting cells in the VDA it may have been problematic to discriminate between the variations in control shown by the different groups, as a "pure" $CD4^+$ T cell population would likely show overall poor control, even in the healthy HCMV-seropositive population.

Chapter 7

General Discussion

7.1 A model for CD4$^+$ T cell control of HCMV

7.1.1 The effects of IFN-γ

In the work presented in this thesis, I have further developed a viral dissemination assay which was first utilised by our group to characterise the PBMC, CD8$^+$ T cell, CD4$^+$ T cell, and NK cell responses to HCMV in a cohort of healthy HCMV-seropositive and HCMV-seronegative individuals. The results showed that there are inherent differences in ability to control *in vitro* IE and late CMV gene expression between the various immune cell populations from HCMV-seronegative and HCMV-seropositive donors, and also led to surprising findings that CD4$^+$ cells from healthy HCMV-seropositive donors were able to exert control over IE and late CMV gene expression to a significant degree in cells that support lytic infection but do not constitutively express MHC Class II.

I then proceeded to investigate how these CD4$^+$ cells were able to recognise CMV-infected cells which did not constitutively express MHC Class II on their cell surface. The results showed that CD4$^+$ cells exerted control of CMV dissemination in part via their secreted factors ("secretome") and that IFN-γ was a key component of this secretome. IFN-γ was shown to be able to induce MHC Class II expression on uninfected fibroblasts, and severely limit late CMV gene expression. Be that as it may, it was still not able to prevent viral entry, nor progression to IE CMV gene expression, suggesting that the IFN-γ immune evasion mechanisms of the virus, while ultimately unable to completely overcome IFN-γ-mediated host defences, is still able to sufficiently evade them, such that the continuous presence of IFN-γ is required, and that once this immune pressure was released, progression to late CMV gene expression and viral replication took place. An illustration of the effects of IFN-γ to HCMV-infected cells in the viral dissemination assay is shown in Fig.7.1.

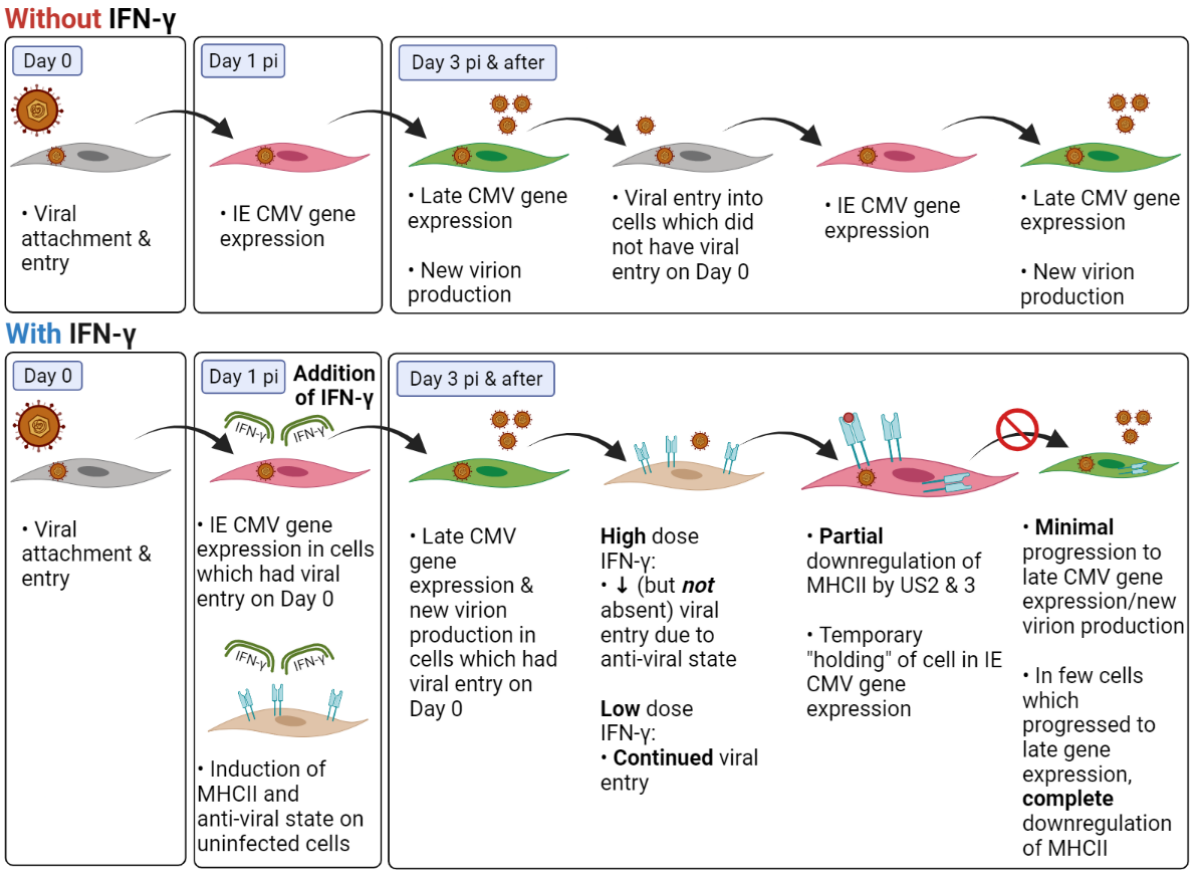

Figure 7.1: The effects of adding IFN-γ to the viral dissemination assay
Figure created at BioRender.com

Given these observations, future work could be to further investigate the HCMV genes which were expressed in mCherry^{+}GFP^{-} cells, by sorting for these cells and performing single-cell mRNA sequencing on them. This could allow further characterisation of the effects of IFN-γ on HCMV gene expression and replication. Another method of examining the effects of IFN-γ could be to use CRISPR gene editing to knock out the IFN-γ receptor, preventing the cells from responding to IFN-γ. Such an approach could delineate more clearly the contribution of the other cytokines in the secretome to control of HCMV gene expression and replication.

7.1.2 The role of antigen presenting cells

The data presented in the next section of this thesis revealed the role of antigen presenting cells in the $CD4^+$ cell response to HCMV, and elucidated how these cells allowed $CD4^+$ T cells to recognise HCMV-infected fibroblasts such that they could exert their antiviral effects. Specifically, the presence of $CD14^+$ monocytes added to $CD4^+$ T cells at a ratio of 1:9 (10% of cells added) was found to enable $CD4^+$ T cells to limit IE CMV gene expression to a small degree and late CMV gene expression to a large degree. In contrast, addition of either monocytes or $CD4^+$ T cells in isolation led to poor control of IE and late CMV gene expression. Therefore, these monocytes were likely able to take up CMV antigen and present them to $CD4^+$ T cells, which allowed the production of a cytokine milieu that included multiple antiviral cytokines such as IFN-α, IFN-β, TNF-α and IFN-γ. An illustration of the sequence of events that follow addition of these immune cell populations in isolation or together to HCMV-infected fibroblasts is shown in Fig.7.2.

When *either* MHC Class II or IFN-γ was inhibited with blocking antibody, the $CD4^+$ cell control of HCMV was inhibited *partially*. When *both* MHC Class II and IFN-γ were inhibited with blocking antibody, this control was completely inhibited in one donor, and inhibited partially in 2 other donors. This suggested that a large part of the control of HCMV-infected cells by $CD4^+$ T cells was mediated by antigen presentation via the MHC Class II pathway and the resultant IFN-γ-related antiviral effects. An illustration of the likely sequence of events following blocking of IFN-γ and MHC Class II in the viral dissemination assay is shown in Fig.7.3.

A recurrent issue I faced was that it did not seem possible to completely block MHC Class II despite high doses of blocking antibody. A possible solution to this could be to use CRISPR gene editing to remove the Class II transactivator (CIITA) gene in the fibroblasts. This would prevent the fibroblasts from being able to upregulate MHC Class II to IFN-γ, and if used in conjunction with the IFN-γ-receptor CRISPR knock-out fibroblast lines, could distinguish between the downstream effects of MHC Class II-mediated events (where the fibroblasts could still respond to IFN-γ produced via MHC Class II antigen presentation pathway-independent mechanisms), versus the downstream effects of IFN-γ (where the fibroblasts would, in theory, not be able to respond to IFN-γ and therefore not be able to upregulate MHC Class II as well). In this scenario, the fibroblasts would only be able to respond to cytokines other than IFN-γ and ought to show a high degree of HCMV entry and progression to IE and late CMV gene expression, although there are other intrinsic cellular defences, such as IFN-independent ISG expression (reviewed in [27]), which could lead to a small degree of inhibition.

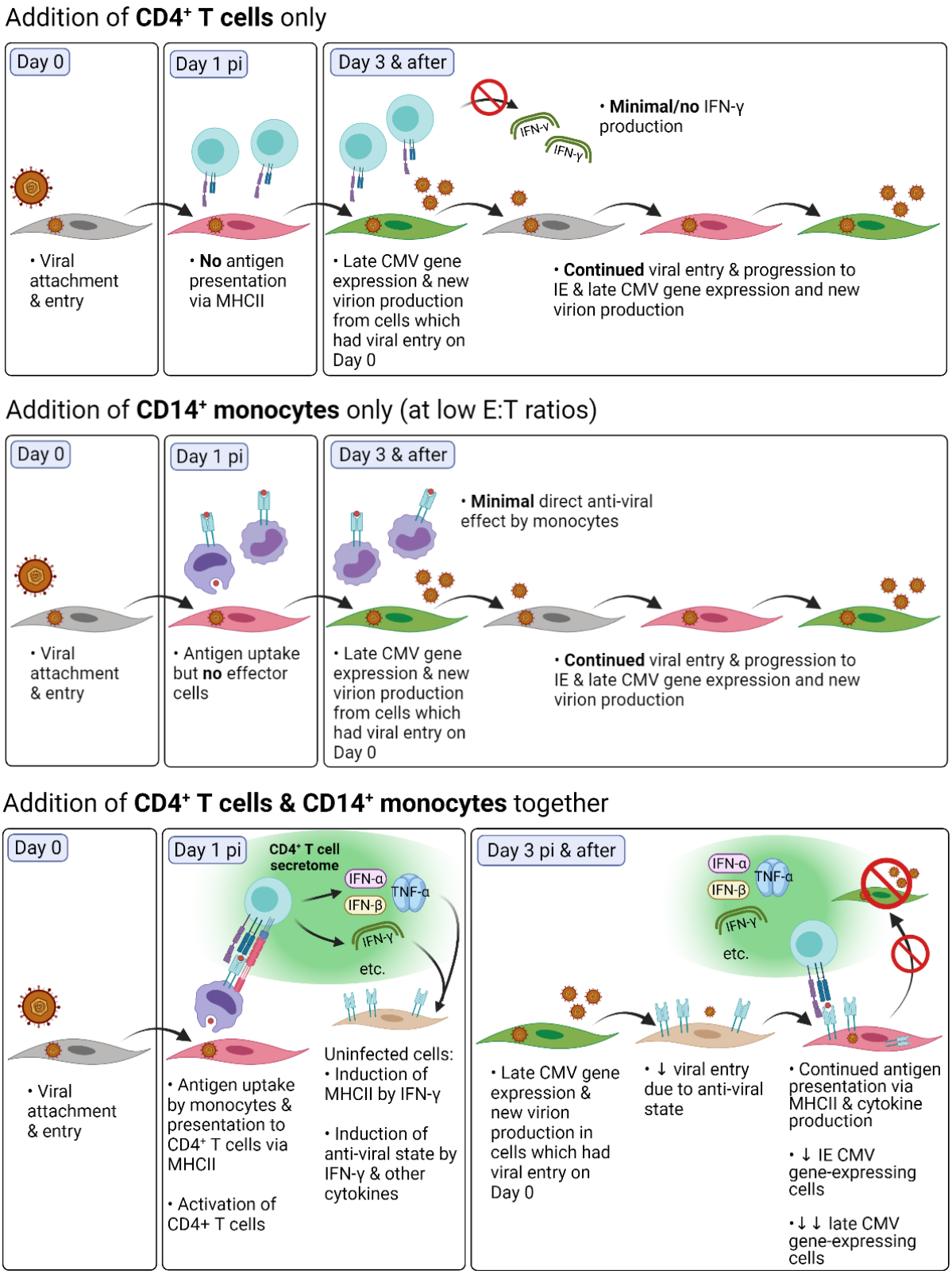

Figure 7.2: Adding CD4$^+$ T cells or CD14$^+$ monocytes in isolation, or together
Figure created at BioRender.com

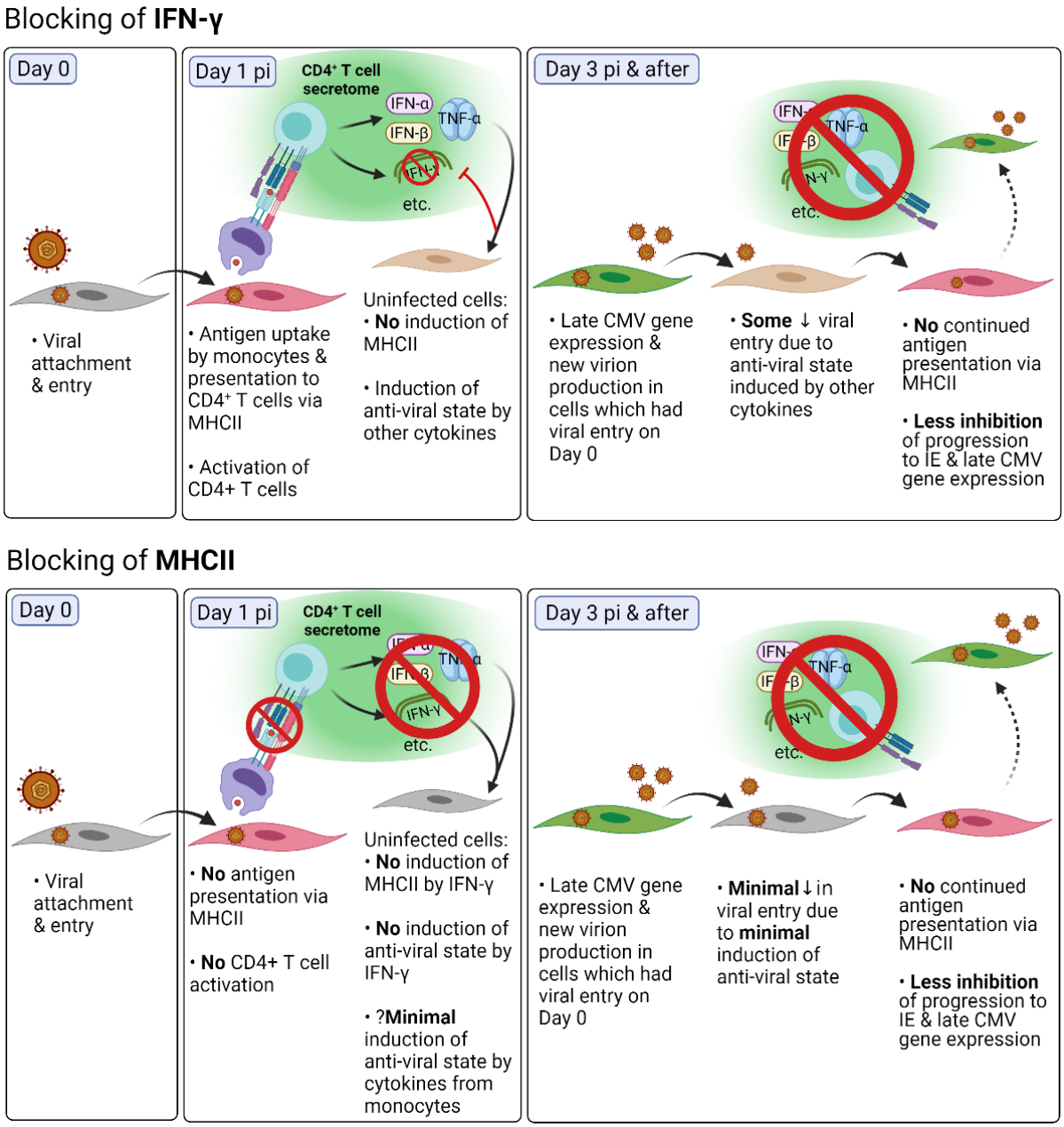

Figure 7.3: The effects of blocking IFN-γ or MHC Class II
Figure created at BioRender.com

7.2 Viral dissemination assay as a better tool to assess HCMV-specific responses in transplant patients

In the final results chapter of this thesis, I have used the viral dissemination assay to assess the responses of PBMCs, $CD4^+$ T cells, $CD8^+$ T cells, and NK cells from kidney and liver transplant patients, and shown that this assay may provide a more comprehensive assessment of the immune response to HCMV than previously commonly used methods in such patient groups, such as IFN-γ T cell responses measured by EliSpor or FluoroSpot^{TM} assay, flow cytometry monitoring by MHC multimers, peptide-pulsed intracellular staining, or the clinically available CMV QuantiFERON^{TM} system. A recent publication from our group has introduced the use of this viral dissemination assay as a more detailed means of evaluating CMV-specific cell-mediated immunity in transplant recipients [241]. I have also compared the responses from these patients to those from healthy adults, and shown that, during periods of viraemia, patients frequently have responses similar to or worse than those from HCMV-seronegative adults (which one would expect to have some innate responses but no CMV-specific T cells), regardless of their HCMV serostatus.

These results appeared to show some potential for the use of this assay in research settings, but more patient samples, specifically patients who experienced episodes of CMV reactivation and disease, would be needed. In addition, only kidney and liver transplant patients were included in this study. Given that, out of all solid organ transplants, kidney transplant recipients face the lowest risk of reactivation of CMV, it would have been ideal to include other types of transplant recipients as well, such as lung and heart transplant recipients and haematopoietic stem cell transplant recipients, although I do note that lung and heart transplants are carried out on a less frequent basis than liver and kidney transplants.

From the data available, it appears that the reasons for why some patients experience viraemic episodes despite the presence of CMV-specific T cells while others do not are likely to be complex and multi-factorial. One possible reason is that there are multiple viral strains during the episodes of viraemia, and the CMV-specific immunity in those patients did not recognise epitopes from all strains. There is also the argument that these patients were under immunosuppression when the viraemic episodes occurred, although all patients were treated with a standard regimen, so it is unclear why some patients are more likely to experience reactivation than others. Overall, however, the observations that: (1) it was not a single immune cell population that was consistently deficient in control; but yet (2) PBMCs from viraemic episodes almost always showed poor control, would suggest that it would be an interruption of the interplay between these immune cell subsets that led to an overall loss of control and the resultant viraemia.

Challenges as a result of the COVID-19 pandemic

The COVID-19 pandemic led to a 6-month suspension of collection of skin biopsy and blood samples from the transplant patients. This led to a subsequent delay in processing and running the samples, and also fewer patient samples available for study. This was particularly an issue with viraemic patients, as there were fewer than expected episodes of viraemia. In addition, under University and NHS Hospitals guidelines, there was much reduced capacity in the laboratories and stricter guidelines regarding hospital visits from non-essential staff, leading to difficulties in obtaining blood samples from healthy volunteers for repeat experiments.

Chapter 8

References

[1] ITGAX integrin subunit alpha X [Homo sapiens (human)] - Gene - NCBI. https://www.ncbi.nlm.nih.gov/gene?Db=gene&Cmd=ShowDetailView&TermToSearch=3687.

[2] Special Issue: KDIGO Clinical Practice Guideline for the Care of Kidney Transplant Recipients. *American Journal of Transplantation*, 9(s3):S1–S155, 2009.

[3] Cytomegaloviruses: From Moleular Pathogenesis to Intervention. volume II.10 Protective Humoral Immunity. Caister Academic Press, UK, 2013.

[4] B Kiolemenoglou A Jesionek. Ueber einen Befund von protozoenartigen Gebilden in den Organen eines hereditar-luetischen Foetus. *Muenchner Med Wochenschr*, (51):1905–1907, 1904.

[5] Abul K. Abbas, Kenneth M. Murphy, and Alan Sher. Functional diversity of helper T lymphocytes. *Nature*, 383(6603):787–793, October 1996.

[6] Elena G. Addison, Janet North, Ismail Bakhsh, Chloe Marden, Sumaira Haq, Samia Al-Sarraj, Reza Malayeri, R. Gitendra Wickremasinghe, Jeffrey K. Davies, and Mark W. Lowdell. Ligation of CD8α on human natural killer cells prevents activation-induced apoptosis and enhances cytolytic activity. *Immunology*, 116(3):354–361, 2005.

[7] K. K. Adkins, T. D. Levan, R. L. Miesfeld, and J. W. Bloom. Glucocorticoid regulation of GM-CSF: Evidence for transcriptional mechanisms in airway epithelial cells. *The American Journal of Physiology*, 275(2):L372–378, August 1998.

[8] Barbara Adler, Laura Scrivano, Zsolt Ruzcics, Brigitte Rupp, Christian Sinzger, and Ulrich Koszinowski. Role of human cytomegalovirus UL131A in cell type-specific virus entry and release. *Journal of General Virology,*, 87(9):2451–2460, 2006.

[9] Davide Agnello, Carla S. R. Lankford, Jay Bream, Akio Morinobu, Massimo Gadina, John J. O'Shea, and David M. Frucht. Cytokines and Transcription Factors That Reg-

ulate T Helper Cell Differentiation: New Players and New Insights. *Journal of Clinical Immunology*, 23(3):147–161, May 2003.

[10] K Ahn, A Angulo, P Ghazal, P A Peterson, Y Yang, and K Früh. Human cytomegalovirus inhibits antigen presentation by a sequential multistep process. *Proceedings of the National Academy of Sciences of the United States of America*, 93(20):10990–10995, October 1996.

[11] Kwangseog Ahn, Albrecht Gruhler, Begona Galocha, Thomas R. Jones, Emmanuel J.H.J. Wiertz, Hidde L. Ploegh, Per A. Peterson, Young Yang, and Klaus Früh. The ER-luminal domain of the HCMV glypcoprotein US6 inhibits peptide translocation by TAP. *Immunity*, 1997.

[12] Parvis Akter, Charles Cunningham, Brian P. McSharry, Aidan Dolan, Clare Addison, Derrick J. Dargan, Aycan F. Hassan-Walker, Vincent C. Emery, Paul D. Griffiths, Gavin W. G. Wilkinson, and Andrew J.YR 2003 Davison. Two novel spliced genes in human cytomegalovirus. *Journal of General Virology*, 84(5):1117–1122, May 2003.

[13] Elena Albiero, Eliana Amati, Elke Baumeister, Hermann Einsele, Götz U. Grigoleit, and Francesco Rodeghiero. Heterogeneity of Specific CD4+ and CD8+ T Cells Stimulated by CMV pp65 and IE1 Antigens. *Journal of Immunotherapy*, 39(9):329, November/December 2016.

[14] Cuider Allal, Claire Buisson-Brenac, Vincent Marion, Clotilde Claudel-Renard, Thomas Faraut, Paola Dal Monte, Daniel Streblow, Michel Record, and Jean-Luc Davignon. Human Cytomegalovirus Carries a Cell-Derived Phospholipase A2 Required for Infectivity. *Journal of Virology*, 78(14):7717–7726, July 2004.

[15] Anthony C Allison and Elsie M Eugui. Mycophenolate mofetil and its mechanisms of action. *Immunopharmacology*, 47(2):85–118, May 2000.

[16] Mariagabriela Alterio de Goss, Rafaela Holtappels, Hans-Peter Steffens, Jürgen Podlech, Peter Angele, Liane Dreher, Doris Thomas, and Matthias J. Reddehase. Control of Cytomegalovirus in Bone Marrow Transplantation Chimeras Lacking the Prevailing Antigen-Presenting Molecule in Recipient Tissues Rests Primarily on Recipient-Derived CD8 T Cells. *Journal of Virology*, 72(10):7733–7744, October 1998.

[17] Colberg-Poley A.M. Functional roles of immediate early proteins encoded by the human cytomegalovirus UL36-38, UL115-119, TRS1/IRS1 and US3 loci. *Intervirology*, (39):350–360, 1996.

[18] Pari GS Anders DG, Kerry JA. CMV DNA synthesis and late viral gene expression. In et al. Arvin AM, Campadelli-Fiume G, Mocarski ES, editor, *Human Herpesviruses: Bi-*

ology, Therapy and Immunoprophylaxis, pages 295–310. Cambridge: Cambridge Press, 2007.

[19] Graham Anderson and Yousuke Takahama. Thymic epithelial cells: Working class heroes for T cell development and repertoire selection. *Trends in Immunology*, 33(6):256–263, June 2012.

[20] Peter Antal-Szalmas, Jos A. G. van Strijp, Annemarie J. L. Weersink, Jan Verhoef, and Kok P. M. van Kessel. Quantitation of surface CD14 on human monocytes and neutrophils. *Journal of Leukocyte Biology*, 61(6):721–728, 1997.

[21] Pierre Antoine, Véronique Olislagers, Ariane Huygens, Sandra Lecomte, Corinne Liesnard, Catherine Donner, and Arnaud Marchant. Functional Exhaustion of CD4+ T Lymphocytes during Primary Cytomegalovirus Infection. *The Journal of Immunology*, 189(5):2665–2672, September 2012.

[22] Victor Appay, P. Rod Dunbar, Margaret Callan, Paul Klenerman, Geraldine M.A. Gillespie, Laura Papagno, Graham S. Ogg, Abigail King, Franziska Lechner, Celsa A. Spina, Susan Little, Diane V. Havlir, Douglas D. Richman, Norbert Gruener, Gerd Pape, Anele Waters, Philippa Easterbrook, Mariolina Salio, Vincenzo Cerundolo, Andrew J. McMichael, and Sarah L. Rowland-Jones. Memory CD8+T cells vary in differentiation phenotype in different persistent virus infections. *Nature Medicine*, 2002.

[23] Hisashi Arase, Edward S. Mocarski, Ann E. Campbell, Ann B. Hill, and Lewis L. Lanier. Direct Recognition of Cytomegalovirus by Activating and Inhibitory NK Cell Receptors. *Science*, 296(5571):1323–1326, May 2002.

[24] Ramon Arens, Peng Wang, John Sidney, Andrea Loewendorf, Alessandro Sette, Stephen P. Schoenberger, Bjoern Peters, and Chris A. Benedict. Cutting Edge: Murine Cytomegalovirus Induces a Polyfunctional CD4 T Cell Response. *The Journal of Immunology*, 180(10):6472–6476, May 2008.

[25] Tal I. Arnon, Hagit Achdout, Ofer Levi, Gal Markel, Nivin Saleh, Gil Katz, Roi Gazit, Tsufit Gonen-Gross, Jacob Hanna, Efrat Nahari, Angel Porgador, Alik Honigman, Bodo Plachter, Dror Mevorach, Dana G. Wolf, and Ofer Mandelboim. Inhibition of the NKp30 activating receptor by pp65 of human cytomegalovirus. *Nature Immunology*, 6(5):515–523, May 2005.

[26] Omodele Ashiru, Neil J. Bennett, Louise H. Boyle, Mair Thomas, John Trowsdale, and Mark R. Wills. NKG2D Ligand MICA Is Retained in the cis-Golgi Apparatus by Human Cytomegalovirus Protein UL142. *Journal of Virology*, 83(23):12345–12354, December 2009.

[27] Caroline L. Ashley, Allison Abendroth, Brian P. McSharry, and Barry Slobedman. Interferon-Independent Innate Responses to Cytomegalovirus. *Frontiers in Immunology*, 10, 2019.

[28] S. F. Atabani, C. Smith, C. Atkinson, R. W. Aldridge, M. Rodriguez-Perálvarez, N. Rolando, M. Harber, G. Jones, A. O'Riordan, A. K. Burroughs, D. Thorburn, J. O'Beirne, R. S. B. Milne, V. C. Emery, and P. D. Griffiths. Cytomegalovirus Replication Kinetics in Solid Organ Transplant Recipients Managed by Preemptive Therapy. *American Journal of Transplantation*, 12(9):2457–2464, 2012.

[29] D. P. AuCoin, G. B. Smith, C. D. Meiering, and E. S. Mocarski. Betaherpesvirus-conserved cytomegalovirus tegument protein ppUL32 (pp150) controls cytoplasmic events during virion maturation. *Journal of Virology*, 2006.

[30] Selmir Avdic, Brian P. McSharry, Megan Steain, Emma Poole, John Sinclair, Allison Abendroth, and Barry Slobedman. Human Cytomegalovirus-Encoded Human Interleukin-10 (IL-10) Homolog Amplifies Its Immunomodulatory Potential by Upregulating Human IL-10 in Monocytes. *Journal of Virology*, 90(8):3819–3827, April 2016.

[31] G. Avetisyan, K. Larsson, J. Aschan, C. Nilsson, M. Hassan, and P. Ljungman. Impact on the cytomegalovirus (CMV) viral load by CMV-specific T-cell immunity in recipients of allogeneic stem cell transplantation. *Bone Marrow Transplantation*, 38(10):687–692, November 2006.

[32] Luiz Sergio Azevedo*, Lígia Camera Pierrotti, Edson Abdala, Silvia Figueiredo Costa, Tânia Mara Varejão Strabelli, Silvia Vidal Campos, Jéssica Fernandes Ramos, Acram Zahredine Abdul Latif, Nadia Litvinov, Natalya Zaidan Maluf, Helio Hehl Caiaffa Filho, Claudio Sergio Pannuti, Marta Heloisa Lopes, Vera Aparecida dos Santos, Camila da Cruz Gouveia Linardi, Maria Aparecida Shikanai Yasuda, and Heloisa Helena de Sousa Marques. Cytomegalovirus infection in transplant recipients. *Clinics*, 70(7):515–523, July 2015.

[33] R Bacchetta, M Bigler, J L Touraine, R Parkman, P A Tovo, J Abrams, R de Waal Malefyt, J E de Vries, and M G Roncarolo. High levels of interleukin 10 production in vivo are associated with tolerance in SCID patients transplanted with HLA mismatched hematopoietic stem cells. *Journal of Experimental Medicine*, 179(2):493–502, February 1994.

[34] Annabell Bachem, Steffen Güttler, Evelyn Hartung, Frédéric Ebstein, Michael Schaefer, Astrid Tannert, Abdulgabar Salama, Kamran Movassaghi, Corinna Opitz, Hans W. Mages, Volker Henn, Peter-Michael Kloetzel, Stephanie Gurka, and Richard A. Kroczek. Superior antigen cross-presentation and XCR1 expression define human

CD11c+CD141+ cells as homologues of mouse CD8+ dendritic cells. *Journal of Experimental Medicine*, 207(6):1273–1281, May 2010.

[35] Sreekumar Balan, Vincent Ollion, Nicholas Colletti, Rabie Chelbi, Frédéric Montanana-Sanchis, Hong Liu, Thien-Phong Vu Manh, Cindy Sanchez, Juliette Savoret, Ivan Perrot, Anne-Claire Doffin, Even Fossum, Didier Bechlian, Christian Chabannon, Bjarne Bogen, Carine Asselin-Paturel, Michael Shaw, Timothy Soos, Christophe Caux, Jenny Valladeau-Guilemond, and Marc Dalod. Human XCR1+ Dendritic Cells Derived In Vitro from CD34+ Progenitors Closely Resemble Blood Dendritic Cells, Including Their Adjuvant Responsiveness, Contrary to Monocyte-Derived Dendritic Cells. *The Journal of Immunology*, 193(4):1622–1635, August 2014.

[36] S Bandyopadhyay, B Perussia, G Trinchieri, D S Miller, and S E Starr. Requirement for HLA-DR+ accessory cells in natural killing of cytomegalovirus-infected fibroblasts. *Journal of Experimental Medicine*, 164(1):180–195, July 1986.

[37] Roman Barbalat, Laura Lau, Richard M. Locksley, and Gregory M. Barton. Toll-like receptor 2 on inflammatory monocytes induces type I interferon in response to viral but not bacterial ligands. *Nature Immunology*, 10(11):1200–1207, November 2009.

[38] Martine T. Barel, Gerco C. Hassink, Sjaak van Voorden, and Emmanuel J. H. J Wiertz. Human cytomegalovirus-encoded US2 and US11 target unassembled MHC class I heavy chains for degradation. *Molecular Immunology*, 43(8):1258–1266, March 2006.

[39] P. D. Barnes and J. E. Grundy. Down-regulation of the class I HLA heterodimer and beta 2-microglobulin on the surface of cells infected with cytomegalovirus. *The Journal of General Virology*, 73 (Pt 9):2395–2403, September 1992.

[40] Michelle A Barron, Dexiang Gao, Kathryn L Springer, Julie A Patterson, Mark W Brunvand, Peter A McSweeney, Zeng Chang, Anna E Barón, and Adriana Weinberg. Relationship of reconstituted adaptive and innate cytomegalovirus (CMV)-Specific immune responses with CMV viremia in hematopoietic stem cell transplant recipients. *Clinical Infectious Diseases*, 49(12):1777–1783, 2009.

[41] Christoph L. Baumann, Irene M. Aspalter, Omar Sharif, Andreas Pichlmair, Stephan Blüml, Florian Grebien, Manuela Bruckner, Pawel Pasierbek, Karin Aumayr, Melanie Planyavsky, Keiryn L. Bennett, Jacques Colinge, Sylvia Knapp, and Giulio Superti-Furga. CD14 is a coreceptor of Toll-like receptors 7 and 9. *Journal of Experimental Medicine*, 207(12):2689–2701, November 2010.

[42] Jennifer Becker, Volker Kinast, Marius Döring, Christoph Lipps, Veronica Duran, Julia Spanier, Pia-Katharina Tegtmeyer, Dagmar Wirth, Luka Cicin-Sain, Antonio Alcamí,

and Ulrich Kalinke. Human monocyte-derived macrophages inhibit HCMV spread independent of classical antiviral cytokines. *Virulence*, 9(1):1669–1684, December 2018.

[43] M. F. Beersma, M. J. Bijlmakers, and H. L. Ploegh. Human cytomegalovirus downregulates HLA class I expression by reducing the stability of class I H chains. *Journal of Immunology (Baltimore, Md.: 1950)*, 151(9):4455–4464, November 1993.

[44] M. Bego, J. Maciejewski, S. Khaiboullina, G. Pari, and S. St. Jeor. Characterization of an antisense transcript spanning the UL81-82 locus of human cytomegalovirus. *Journal of Virology*, 2005.

[45] Pierre M. Jean Beltran and Ileana M. Cristea. The life cycle and pathogenesis of human cytomegalovirus infection: Lessons from proteomics. *Expert Review of Proteomics*, 11(6):697–711, December 2014.

[46] J. Beninga, B. Kropff, and M. Mach. Comparative analysis of fourteen individual human cytomegalovirus proteins for helper T cell response. *Journal of General Virology,*, 76(1):153–160, 1995.

[47] K Benirschke, G J Burton, and R N Baergen. Pathology of the human placenta, sixth edition. In *Pathology of the Human Placenta*. Springer-Verlag, New York, NY, sixth edition, 2012.

[48] Gretchen L. Bentz, Marta Jarquin-Pardo, Gary Chan, M. Shane Smith, Christian Sinzger, and Andrew D. Yurochko. Human Cytomegalovirus (HCMV) Infection of Endothelial Cells Promotes Naïve Monocyte Extravasation and Transfer of Productive Virus To Enhance Hematogenous Dissemination of HCMV. *Journal of Virology*, 80(23):11539–11555, December 2006.

[49] Louise Berg, Gerdt C. Riise, David Cosman, Tomas Bergström, Sigvard Olofsson, Klas Kärre, and Ennio Carbone. LIR-1 expression on lymphocytes, and cytomegalovirus disease in lung-transplant recipients. *Lancet*, 2003.

[50] M. Bergmann, P. J. Barnes, and R. Newton. Molecular regulation of granulocyte macrophage colony-stimulating factor in human lung epithelial cells by interleukin (IL)-1beta, IL-4, and IL-13 involves both transcriptional and post-transcriptional mechanisms. *American Journal of Respiratory Cell and Molecular Biology*, 22(5):582–589, May 2000.

[51] Helene B. Bernstein, Mary C. Plasterer, Sherrie E. Schiff, Christina M. R. Kitchen, Scott Kitchen, and Jerome A. Zack. CD4 Expression on Activated NK Cells: Ligation of CD4 Induces Cytokine Expression and Cell Migration. *The Journal of Immunology*, 177(6):3669–3676, September 2006.

[52] Richard Berry, Gabrielle M. Watson, Stipan Jonjic, Mariapia A. Degli-Esposti, and Jamie Rossjohn. Modulation of innate and adaptive immunity by cytomegaloviruses. *Nature Reviews Immunology*, 20(2):113–127, February 2020.

[53] Vivien Béziat, Olav Dalgard, Tarik Asselah, Philippe Halfon, Pierre Bedossa, Ali Boudifa, Baptiste Hervier, Ioannis Theodorou, Michelle Martinot, Patrice Debré, Niklas K. Björkström, Karl-Johan Malmberg, Patrick Marcellin, and Vincent Vieillard. CMV drives clonal expansion of NKG2C+ NK cells expressing self-specific KIRs in chronic hepatitis patients. *European Journal of Immunology*, 42(2):447–457, 2012.

[54] Vivien Béziat, Lisa L. Liu, Jenny-Ann Malmberg, Martin A. Ivarsson, Ebba Sohlberg, Andreas T. Björklund, Christelle Retière, Eva Sverremark-Ekström, James Traherne, Per Ljungman, Marie Schaffer, David A. Price, John Trowsdale, Jakob Michaëlsson, Hans-Gustaf Ljunggren, and Karl-Johan Malmberg. NK cell responses to cytomegalovirus infection lead to stable imprints in the human KIR repertoire and involve activating KIRs. *Blood*, 121(14):2678–2688, April 2013.

[55] Kristy M. Bialas, Takayuki Tanaka, Dollnovan Tran, Valerie Varner, Eduardo Cisneros De La Rosa, Flavia Chiuppesi, Felix Wussow, Lisa Kattenhorn, Sheila Macri, Erika L. Kunz, Judy A. Estroff, Jennifer Kirchherr, Yujuan Yue, Qihua Fan, Michael Lauck, David H. O'Connor, Allison H. S. Hall, Alvarez Xavier, Don J. Diamond, Peter A. Barry, Amitinder Kaur, and Sallie R. Permar. Maternal CD4+ T cells protect against severe congenital cytomegalovirus disease in a novel nonhuman primate model of placental cytomegalovirus transmission. *Proceedings of the National Academy of Sciences of the United States of America*, 112(44):13645–13650, November 2015.

[56] Matteo Biolatti, Francesca Gugliesi, Valentina Dell'Oste, and Santo Landolfo. Modulation of the innate immune response by human cytomegalovirus. *Infection, Genetics and Evolution*, 64:105–114, October 2018.

[57] Christine A. Biron, Kevin S. Byron, and John L. Sullivan. Severe Herpesvirus Infections in an Adolescent without Natural Killer Cells. *New England Journal of Medicine*, 320(26):1731–1735, June 1989.

[58] A. L. Bissinger, H. Oettle, G. Jahn, P. Neuhaus, and C. Sinzger. Cytomegalovirus infection after orthotopic liver transplantation is restricted by a pre-existing antiviral immune response of the recipient. *Journal of Medical Virology*, 73(1):45–53, 2004.

[59] A. L. Bissinger, C. Sinzger, E. Kaiserling, and G. Jahn. Human cytomegalovirus as a direct pathogen: Correlation of multiorgan involvement and cell distribution with clinical and pathological findings in a case of congenital inclusion disease. *Journal of Medical Virology*, 67(2):200–206, 2002.

[60] Priscilla Biswas, Barbara Mantelli, Antonio Sica, Mauro Malnati, Carla Panzeri, Alessandra Saccani, Hamid Hasson, Andrea Vecchi, Abby Saniabadi, Paolo Lusso, Adriano Lazzarin, and Alberto Beretta. Expression of CD4 on human peripheral blood neutrophils. *Blood*, 101(11):4452–4456, June 2003.

[61] Arlene D. Bitmansour, Daniel C. Douek, Vernon C. Maino, and Louis J. Picker. Direct Ex Vivo Analysis of Human CD4+ Memory T Cell Activation Requirements at the Single Clonotype Level. *The Journal of Immunology*, 169(3):1207–1218, August 2002.

[62] Janice S. Blum, Pamela A. Wearsch, and Peter Cresswell. Pathways of Antigen Processing. *Annual review of immunology*, 31:443–473, 2013.

[63] Bahram Bodaghi, Marlea E. P. Slobbe–vanDrunen, Andrzei Topilko, Emmanuelle Perret, Renée C. R. M. Vossen, Maria C. E. van Dam–Mieras, Donato Zipeto, Jean-Louis Virelizier, Phuc LeHoang, Cathrien A. Bruggeman, and Susan Michelson. Entry of Human Cytomegalovirus into Retinal Pigment Epithelial and Endothelial Cells by Endocytosis. *Investigative Ophthalmology & Visual Science*, 40(11):2598–2607, October 1999.

[64] Boris Bogdanow, Henry Weisbach, Jens von Einem, Sarah Straschewski, Sebastian Voigt, Michael Winkler, Christian Hagemeier, and Lüder Wiebusch. Human cytomegalovirus tegument protein pp150 acts as a cyclin A2–CDK-dependent sensor of the host cell cycle and differentiation state. *Proceedings of the National Academy of Sciences*, 110(43):17510–17515, October 2013.

[65] Suresh B. Boppana, Karen B. Fowler, Robert F. Pass, Lisa B. Rivera, Russell D. Bradford, Fred D. Lakeman, and William J. Britt. Congenital cytomegalovirus infection: Association between virus burden in infancy and hearing loss. *Journal of Pediatrics*, 2005.

[66] Lisa B. Boyette, Camila Macedo, Kevin Hadi, Beth D. Elinoff, John T. Walters, Bala Ramaswami, Geetha Chalasani, Juan M. Taboas, Fadi G. Lakkis, and Diana M. Metes. Phenotype, function, and differentiation potential of human monocyte subsets. *PLOS ONE*, 12(4):e0176460, April 2017.

[67] Russell D Bradford, Gretchen Cloud, Alfred D Lakeman, Suresh Boppana, David W Kimberlin, Richard Jacobs, Gail Demmler, Pablo Sanchez, William Britt, Seng-jaw Soong, Richard J Whitley, National Institute of Allergy Group, and Infectious Diseases Collaborative Antiviral Study. Detection of cytomegalovirus (CMV) DNA by polymerase chain reaction is associated with hearing loss in newborns with symptomatic congenital CMV infection involving the central nervous system. *The Journal of Infectious Diseases*, 2005.

[68] G. Brestrich, S. Zwinger, A. Fischer, M. Schmück, A. Röhmhild, M. H. Hammer, A. Kurtz, L. Uharek, C. Knosalla, H. Lehmkuhl, H.-D. Volk, and P. Reinke. Adop-

tive T-Cell Therapy of a Lung Transplanted Patient with Severe CMV Disease and Resistance to Antiviral Therapy. *American Journal of Transplantation*, 9(7):1679–1684, 2009.

[69] William Britt. Controversies in the natural history of congenital human cytomegalovirus infection: The paradox of infection and disease in offspring of women with immunity prior to pregnancy. *Medical Microbiology and Immunology*, 204(3):263–271, June 2015.

[70] William J. Britt, Michael Jarvis, Jun-Young Seo, Derek Drummond, and Jay Nelson. Rapid genetic engineering of human cytomegalovirus by using a lambda phage linear recombination system: Demonstration that pp28 (UL99) is essential for production of infectious virus. *Journal of Virology*, 78(1):539–543, January 2004.

[71] Britt WJ. Congenital cytomegalovirus infection. In Wasserheit JN Hitchcock PJ, MacKay HT, editor, *Sexually Transmitted Diseases and Adverse Outcomes of Pregnancy*, pages 269–281. ASM Press, Washington, DC, 1999.

[72] Michael G. Brown, Ayotunde O. Dokun, Jonathan W. Heusel, Hamish R. C. Smith, Diana L. Beckman, Erika A. Blattenberger, Chad E. Dubbelde, Laurie R. Stone, Anthony A. Scalzo, and Wayne M. Yokoyama. Vital Involvement of a Natural Killer Cell Activation Receptor in Resistance to Viral Infection. *Science*, 292(5518):934–937, May 2001.

[73] Jason Buehler, Sebastian Zeltzer, Justin Reitsma, Alex Petrucelli, Mahadevaiah Umashankar, Mike Rak, Patricia Zagallo, Joyce Schroeder, Scott Terhune, and Felicia Goodrum. Opposing Regulation of the EGF Receptor: A Molecular Switch Controlling Cytomegalovirus Latency and Replication. *PLoS Pathogens*, 12(5), May 2016.

[74] Sarah W. Burgdorf, Charles L. Clark, James R. Burgdorf, and Deborah H. Spector. Mutation of Glutamine to Arginine at Position 548 of IE2 86 in Human Cytomegalovirus Leads to Decreased Expression of IE2 40, IE2 60, UL83, and UL84 and Increased Transcription of US8-9 and US29-32. *Journal of Virology*, 85(21):11098–11110, November 2011.

[75] Catherine E. Burton, Martina Sester, Joan L. Robinson, Dean T. Eurich, Jutta K. Preiksaitis, and Simon Urschel. Assigning Cytomegalovirus Status in Children Awaiting Organ Transplant: Viral Shedding, CMV-Specific T Cells, and CD27-CD28-CD4+ T Cells. *The Journal of Infectious Diseases*, 218(8):1205–1209, September 2018.

[76] Catherine E. Burton, Martina Sester, Joan L. Robinson, Dean T. Eurich, Simon Urschel, and Jutta K. Preiksaitis. CMV-specific T-cells and CD27-CD28-CD4+ T-cells for assignment of cytomegalovirus (CMV) status in adults awaiting organ transplant. *Journal*

of Clinical Virology: The Official Publication of the Pan American Society for Clinical Virology, 115:37–42, June 2019.

[77] Maria Buxadé, Hector Huerga Encabo, Marta Riera-Borrull, Lucía Quintana-Gallardo, Pilar López-Cotarelo, Mónica Tellechea, Sara Martínez-Martínez, Juan Miguel Redondo, Juan Martín-Caballero, Juana María Flores, Elena Bosch, José Luis Rodríguez-Fernández, Jose Aramburu, and Cristina López-Rodríguez. Macrophage-specific MHCII expression is regulated by a remote Ciita enhancer controlled by NFAT5. *Journal of Experimental Medicine*, 215(11):2901–2918, November 2018.

[78] Mar Cabeza-Cabrerizo, Ana Cardoso, Carlos M. Minutti, Mariana Pereira da Costa, and Caetano Reis e Sousa. Dendritic Cells Revisited. *Annual Review of Immunology*, 39(1):131–166, April 2021.

[79] Thierry Calandra and Thierry Roger. Macrophage migration inhibitory factor: A regulator of innate immunity. *Nature Reviews. Immunology*, 3(10):791–800, 2003.

[80] Stefano Caló, Mirko Cortese, Claudio Ciferri, Luca Bruno, Rachel Gerrein, Barbara Benucci, Giuseppina Monda, Michela Gentile, Tobias Kessler, Yasushi Uematsu, Domenico Maione, Anders E. Lilja, Andrea Carfí, and Marcello Merola. The Human Cytomegalovirus UL116 Gene Encodes an Envelope Glycoprotein Forming a Complex with gH Independently from gL. *Journal of Virology*, 90(10):4926–4938, April 2016.

[81] Xavier Camous, Alejandra Pera, Rafael Solana, and Anis Larbi. NK Cells in Healthy Aging and Age-Associated Diseases. *Journal of Biomedicine and Biotechnology*, 2012:e195956, November 2012.

[82] Michael J. Cannon, Terri B. Hyde, and D. Scott Schmid. Review of cytomegalovirus shedding in bodily fluids and relevance to congenital cytomegalovirus infection. *Reviews in Medical Virology*, 21(4):240–255, 2011.

[83] S. Cantisán, R. Lara, M. Montejo, J. Redel, A. Rodríguez-Benot, J. Gutiérrez-Aroca, M. González-Padilla, L. Bueno, A. Rivero, R. Solana, and J. Torre-Cisneros. Pretransplant Interferon-γ Secretion by CMV-Specific CD8+ T Cells Informs the Risk of CMV Replication After Transplantation. *American Journal of Transplantation*, 13(3):738–745, 2013.

[84] S. Cantisán, C. Rodelo-Haad, A. Páez-Vega, A. Nieto, J. M. Vaquero, A. Poyato, M. Montejo, M. C. Fariñas, A. Rivero, R. Solana, A. Martín-Malo, and J. Torre-Cisneros. Factors related to the development of CMV-specific CD8+ T cell response in CMV-seropositive solid organ transplant candidates. *American Journal of Transplantation: Official Journal of the American Society of Transplantation and the American Society of Transplant Surgeons*, 15(3):715–722, March 2015.

[85] H. Cantor and E. A. Boyse. Regulation of cellular and humoral immune responses by T-cell subclasses. *Cold Spring Harbor Symposia on Quantitative Biology*, 41 Pt 1:23–32, 1977.

[86] Stacy R. Cantrell and Wade A. Bresnahan. Human Cytomegalovirus (HCMV) UL82 Gene Product (pp71) Relieves hDaxx-Mediated Repression of HCMV Replication. *Journal of Virology*, 80(12):6188–6191, June 2006.

[87] Agostinho Carvalho, Cristina Cunha, Alessandra Carotti, Teresa Aloisi, Ornella Guarrera, Mauro Di Ianni, Franca Falzetti, Francesco Bistoni, Franco Aversa, Lucia Pitzurra, Fernando Rodrigues, and Luigina Romani. Polymorphisms in Toll-like receptor genes and susceptibility to infections in allogeneic stem cell transplantation. *Experimental Hematology*, 37(9):1022–1029, September 2009.

[88] Joseph P. Casazza, Michael R. Betts, David A. Price, Melissa L. Precopio, Laura E. Ruff, Jason M. Brenchley, Brenna J. Hill, Mario Roederer, Daniel C. Douek, and Richard A. Koup. Acquisition of direct antiviral effector functions by CMV-specific CD4+ T lymphocytes with cellular maturation. *The Journal of Experimental Medicine*, 203(13):2865–2877, December 2006.

[89] Jonathan P Castillo and Timothy F Kowalik. Human cytomegalovirus immediate early proteins and cell growth control. *Gene*, 290(1):19–34, May 2002.

[90] Katie Caviness, Farah Bughio, Lindsey B. Crawford, Daniel N. Streblow, Jay A. Nelson, Patrizia Caposio, and Felicia Goodrum. Complex Interplay of the UL136 Isoforms Balances Cytomegalovirus Replication and Latency. *mBio*, 7(2), March 2016.

[91] Tiffany Caza and Steve Landas. Functional and Phenotypic Plasticity of CD4+ T Cell Subsets. https://www.hindawi.com/journals/bmri/2015/521957/, 2015.

[92] Colleen Cebulla. Human cytomegalovirus disrupts constitutive MHC class II expression. *Journal of Clinical Virology*, 12(2):117, April 1999.

[93] M. Cella, F. Facchetti, A. Lanzavecchia, and M. Colonna. Plasmacytoid dendritic cells activated by influenza virus and CD40L drive a potent TH1 polarization. *Nature Immunology*, 1(4):305–310, October 2000.

[94] Marina Cella, David Jarrossay, Fabio Facchetti, Olga Alebardi, Hideo Nakajima, Antonio Lanzavecchia, and Marco Colonna. Plasmacytoid monocytes migrate to inflamed lymph nodes and produce large amounts of type I interferon. *Nature Medicine*, 5(8):919–923, August 1999.

[95] Cristina Cerboni, Mehrdad Mousavi-Jazi, Annika Linde, Kalle Söderström, Maria Brytting, Britta Wahren, Klas Kärre, and Ennio Carbone. Human Cytomegalovirus Strain-Dependent Changes in NK Cell Recognition of Infected Fibroblasts. *The Journal of Immunology*, 164(9):4775–4782, May 2000.

[96] W. L. William Chang, Peter A. Barry, Richard Szubin, Dai Wang, and Nicole Baumgarth. Human cytomegalovirus suppresses type I interferon secretion by plasmacytoid dendritic cells through its interleukin 10 homolog. *Virology*, 390(2):330–337, August 2009.

[97] Yoav Charpak-Amikam, Tobias Kubsch, Einat Seidel, Esther Oiknine-Djian, Noemi Cavaletto, Rachel Yamin, Dominik Schmiedel, Dana Wolf, Giorgio Gribaudo, Martin Messerle, Luka Cicin-Sain, and Ofer Mandelboim. Human cytomegalovirus escapes immune recognition by NK cells through the downregulation of B7-H6 by the viral genes US18 and US20. *Scientific Reports*, 7(1):8661, August 2017.

[98] M. S. Chee, A. T. Bankier, S. Beck, R. Bohni, C. M. Brown, R. Cerny, T. Horsnell, C. A. Hutchison, T. Kouzarides, J. A. Martignetti, E. Preddie, S. C. Satchwell, P. Tomlinson, K. M. Weston, and B. G. Barrell. Analysis of the Protein-Coding Content of the Sequence of Human Cytomegalovirus Strain AD169. In James K. McDougall, editor, *Cytomegaloviruses*, Current Topics in Microbiology and Immunology, pages 125–169, Berlin, Heidelberg, 1990. Springer.

[99] Kevin C. Chen, Richard J. Stanton, Jareer J. Banat, and Mark R. Wills. Leukocyte immunoglobulin-like receptor 1-Expressing human natural killer cell subsets differentially recognize isolates of human cytomegalovirus through the viral major histocompatibility complex class I homolog UL18. *Journal of Virology*, 2016.

[100] Sharon F. Chen, Tyson H. Holmes, Teri Slifer, Vasavi Ramachandran, Sally Mackey, Cathleen Hebson, Ann M. Arvin, David B. Lewis, and Cornelia L. Dekker. Longitudinal Kinetics of Cytomegalovirus-Specific T-Cell Immunity and Viral Replication in Infants With Congenital Cytomegalovirus Infection. *Journal of the Pediatric Infectious Diseases Society*, 5(1):14–20, March 2016.

[101] Keh-Chuang Chin and Peter Cresswell. Viperin (cig5), an IFN-inducible antiviral protein directly induced by human cytomegalovirus. *Proceedings of the National Academy of Sciences*, 98(26):15125–15130, December 2001.

[102] Yen-Ling Chiu, Chung-Hao Lin, Bo-Yi Sung, Yi-Fang Chuang, Jonathan P. Schneck, Florian Kern, Graham Pawelec, and George C. Wang. Cytotoxic polyfunctionality maturation of cytomegalovirus-pp65-specific CD4 + and CD8 + T-cell responses in older adults positively correlates with response size. *Scientific Reports*, 6, January 2016.

[103] D. K H Chou, A. A. Ilyas, J. E. Evans, C. Costello, R. H. Quarles, and F. B. Jungalwala. Structure of sulfated glucuronyl glycolipids in the nervous system reacting with HNK-1 antibody and some IgM paraproteins in neuropathy. *Journal of Biological Chemistry*, 1986.

[104] Georgina J. Clark, Pablo A. Silveira, P. Mark Hogarth, and Derek N. J. Hart. The cell surface phenotype of human dendritic cells. *Seminars in Cell & Developmental Biology*, 86:3–14, February 2019.

[105] Mathew Clement, Morgan Marsden, Maria A. Stacey, Juneid Abdul-Karim, Silvia Gimeno Brias, Diana Costa Bento, Martin J. Scurr, Peter Ghazal, Casey T. Weaver, Gianluca Carlesso, Simon Clare, Simon A. Jones, Andrew Godkin, Gareth W. Jones, and Ian R. Humphreys. Cytomegalovirus-Specific IL-10-Producing CD4+ T Cells Are Governed by Type-I IFN-Induced IL-27 and Promote Virus Persistence. *PLOS Pathogens*, 12(12):e1006050, December 2016.

[106] Alice Coillard and Elodie Segura. Antigen presentation by mouse monocyte-derived cells: Re-evaluating the concept of monocyte-derived dendritic cells. *Molecular Immunology*, 135:165–169, July 2021.

[107] Matthew Collin and Venetia Bigley. Human dendritic cell subsets: An update. *Immunology*, 154(1):3–20, May 2018.

[108] Marco Colonna, Giorgio Trinchieri, and Yong-Jun Liu. Plasmacytoid dendritic cells in immunity. *Nature Immunology*, 5(12):1219–1226, December 2004.

[109] Teresa Compton, Evelyn A. Kurt-Jones, Karl W. Boehme, John Belko, Eicke Latz, Douglas T. Golenbock, and Robert W. Finberg. Human Cytomegalovirus Activates Inflammatory Cytokine Responses via CD14 and Toll-Like Receptor 2. *Journal of Virology*, 77(8):4588–4596, April 2003.

[110] Teresa Compton, Dawn M. Nowlin, and Neil R. Cooper. Initiation of human cytomegalovirus infection requires initial interaction with cell surface heparan sulfate. *Virology*, 1993.

[111] Lucia Conti, Marco Cardone, Barbara Varano, Patrizia Puddu, Filippo Belardelli, and Sandra Gessani. Role of the cytokine environment and cytokine receptor expression on the generation of functionally distinct dendritic cells from human monocytes. *European Journal of Immunology*, 38(3):750–762, 2008.

[112] Eugenia Corrales-Aguilar, Mirko Trilling, Katja Hunold, Manuela Fiedler, Vu Thuy Khanh Le, Henrike Reinhard, Katrin Ehrhardt, Eva Mercé-Maldonado, Enver Aliyev, Albert Zimmermann, David C. Johnson, and Hartmut Hengel. Human

Cytomegalovirus Fcγ Binding Proteins gp34 and gp68 Antagonize Fcγ Receptors I, II and III. *PLOS Pathogens*, 10(5):e1004131, May 2014.

[113] Marcel Costa-Garcia, Andrea Vera, Manuela Moraru, Carlos Vilches, Miguel López-Botet, and Aura Muntasell. Antibody-Mediated Response of NKG2Cbright NK Cells against Human Cytomegalovirus. *The Journal of Immunology*, 194(6):2715–2724, March 2015.

[114] Julien Cottineau, Molly C. Kottemann, Francis P. Lach, Young-Hoon Kang, Frédéric Vély, Elissa K. Deenick, Tomi Lazarov, Laure Gineau, Yi Wang, Andrea Farina, Marie Chansel, Lazaro Lorenzo, Christelle Piperoglou, Cindy S. Ma, Patrick Nitschke, Aziz Belkadi, Yuval Itan, Bertrand Boisson, Fabienne Jabot-Hanin, Capucine Picard, Jacinta Bustamante, Céline Eidenschenk, Soraya Boucherit, Nathalie Aladjidi, Didier Lacombe, Pascal Barat, Waseem Qasim, Jane A. Hurst, Andrew J. Pollard, Holm H. Uhlig, Claire Fieschi, Jean Michon, Vladimir P. Bermudez, Laurent Abel, Jean-Pierre de Villartay, Frédéric Geissmann, Stuart G. Tangye, Jerard Hurwitz, Eric Vivier, Jean-Laurent Casanova, Agata Smogorzewska, and Emmanuelle Jouanguy. Inherited GINS1 deficiency underlies growth retardation along with neutropenia and NK cell deficiency. *The Journal of Clinical Investigation*, 127(5):1991–2006, May 2017.

[115] L. Covassin, S. Jangalwe, N. Jouvet, J. Laning, L. Burzenski, L. D. Shultz, and M. A. Brehm. Human immune system development and survival of non-obese diabetic (NOD)-scid IL2rγnull (NSG) mice engrafted with human thymus and autologous haematopoietic stem cells. *Clinical & Experimental Immunology*, 174(3):372–388, 2013.

[116] Lindsey B. Crawford, Daniel A. Streblow, Morgan Hakki, Jay A. Nelson, and Patrizia Caposio. Humanized Mouse Models of Human Cytomegalovirus Infection. *Current opinion in virology*, 13:86–92, August 2015.

[117] Lindsey B. Crawford, Rebecca Tempel, Daniel N. Streblow, Craig Kreklywich, Patricia Smith, Louis J. Picker, Jay A. Nelson, and Patrizia Caposio. Human Cytomegalovirus Induces Cellular and Humoral Virus-specific Immune Responses in Humanized BLT Mice. *Scientific Reports*, 7(1):1–14, April 2017.

[118] Jasmyn A Cridland, Eva Z Curley, Michelle N Wykes, Kate Schroder, Matthew J Sweet, Tara L Roberts, Mark A Ragan, Karin S Kassahn, and Katryn J Stacey. The mammalian PYHIN gene family: Phylogeny, evolution and expression. *BMC Evolutionary Biology*, 12:140, August 2012.

[119] Laura Crompton, Naeem Khan, Rajiv Khanna, Laxman Nayak, and Paul A. H. Moss. CD4+ T cells specific for glycoprotein B from cytomegalovirus exhibit extreme conservation of T-cell receptor usage between different individuals. *Blood*, 111(4):2053–2061, February 2008.

[120] T. Crough and R. Khanna. Immunobiology of human cytomegalovirus: From bench to bedside. *Clinical Microbiology Reviews*, 2009.

[121] Francisco J. Cueto, Carlos del Fresno, and David Sancho. DNGR-1, a Dendritic Cell-Specific Sensor of Tissue Damage That Dually Modulates Immunity and Inflammation. *Frontiers in Immunology*, 10, 2020.

[122] Xiaohong Cui, Daniel C. Freed, Dai Wang, Ping Qiu, Fengsheng Li, Tong-Ming Fu, Lawrence M. Kauvar, and Michael A. McVoy. Impact of Antibodies and Strain Polymorphisms on Cytomegalovirus Entry and Spread in Fibroblasts and Epithelial Cells. *Journal of Virology*, 91(13), July 2017.

[123] Xinghong Dai, Xuekui Yu, Hao Gong, Xiaohong Jiang, Gerrado Abenes, Hongrong Liu, Sakar Shivakoti, William J. Britt, Hua Zhu, Fenyong Liu, and Z. Hong Zhou. The Smallest Capsid Protein Mediates Binding of the Essential Tegument Protein pp150 to Stabilize DNA-Containing Capsids in Human Cytomegalovirus. *PLOS Pathogens*, 9(8):e1003525, August 2013.

[124] Keith A. Daniels, Gene Devora, Wayne C. Lai, Carey L. O'Donnell, Michael Bennett, and Raymond M. Welsh. Murine Cytomegalovirus Is Regulated by a Discrete Subset of Natural Killer Cells Reactive with Monoclonal Antibody to Ly49h. *Journal of Experimental Medicine*, 194(1):29–44, June 2001.

[125] W. M. Dankner, J. A. McCutchan, D. D. Richman, K. Hirata, and S. A. Spector. Localization of human cytomegalovirus in peripheral blood leukocytes by in situ hybridization. *The Journal of Infectious Diseases*, 161(1):31–36, January 1990.

[126] Derrick J. Dargan, Elaine Douglas, Charles Cunningham, Fiona Jamieson, Richard J. Stanton, Katarina Baluchova, Brian P. McSharry, Peter Tomasec, Vincent C. Emery, Elena Percivalle, Antonella Sarasini, Giuseppe Gerna, Gavin W. G. Wilkinson, and Andrew J. Davison. Sequential mutations associated with adaptation of human cytomegalovirus to growth in cell culture. *The Journal of General Virology*, 91(Pt 6):1535–1546, June 2010.

[127] Liat Dassa, Einat Seidel, Esther Oiknine-Djian, Rachel Yamin, Dana G. Wolf, Vu Thuy Khanh Le-Trilling, and Ofer Mandelboim. The Human Cytomegalovirus Protein UL148A Downregulates the NK Cell-Activating Ligand MICA To Avoid NK Cell Attack. *Journal of Virology*, 92(17), September 2018.

[128] J.-L. Davignon, D. Clement, J. Alriquet, S. Michelson, and C. Davrinche. Analysis of the Proliferative T Cell Response to Human Cytomegalovirus Major Immediate-Early Protein (IEI): Phenotype, Frequeney and Variability*. *Scandinavian Journal of Immunology*, 41(3):247–255, March 1995.

[129] E. de Vries, MJD van Tol, RLanglois van den Bergh, J. L. M. Waaijer, MMten Dam, J. Hermans, and J. M. Vossen. Reconstitution of lymphocyte subpopulations after paediatric bone marrow transplantation. *Bone Marrow Transplantation*, 25(3):267–275, February 2000.

[130] Victor R. DeFilippis, David Alvarado, Tina Sali, Stefan Rothenburg, and Klaus Früh. Human Cytomegalovirus Induces the Interferon Response via the DNA Sensor ZBP1. *Journal of Virology*, 84(1):585–598, January 2010.

[131] M. del Val, H. Hengel, H. Häcker, U. Hartlaub, T. Ruppert, P. Lucin, and U. H. Koszinowski. Cytomegalovirus prevents antigen presentation by blocking the transport of peptide-loaded major histocompatibility complex class I molecules into the medial-Golgi compartment. *The Journal of Experimental Medicine*, 176(3):729–738, September 1992.

[132] A S Depto and R M Stenberg. Functional analysis of the true late human cytomegalovirus pp28 upstream promoter: Cis-acting elements and viral trans-acting proteins necessary for promoter activation. *Journal of Virology*, 66(5):3241–3246, 1992.

[133] Tiziana Di Pucchio, Bithi Chatterjee, Anna Smed-Sörensen, Sandra Clayton, Adam Palazzo, Monica Montes, Yaming Xue, Ira Mellman, Jacques Banchereau, and John E. Connolly. Direct proteasome-independent cross-presentation of viral antigen by plasmacytoid dendritic cells on major histocompatibility complex class I. *Nature Immunology*, 9(5):551–557, May 2008.

[134] J. Dirks, H. Tas, T. Schmidt, S. Kirsch, B. C. Gärtner, U. Sester, and M. Sester. PD-1 analysis on CD28(-) CD27(-) CD4 T cells allows stimulation-independent assessment of CMV viremic episodes in transplant recipients. *American Journal of Transplantation: Official Journal of the American Society of Transplantation and the American Society of Transplant Surgeons*, 13(12):3132–3141, December 2013.

[135] Ayotunde O. Dokun, Sungjin Kim, Hamish R. C. Smith, Hyun-Seok P. Kang, Dortha T. Chu, and Wayne M. Yokoyama. Specific and nonspecific NK cell activation during virus infection. *Nature Immunology*, 2(10):951–956, October 2001.

[136] Aidan Dolan, Charles Cunningham, Ralph D. Hector, Aycan F. Hassan-Walker, Lydia Lee, Clare Addison, Derrick J. Dargan, Duncan J. McGeoch, Derek Gatherer, Vincent C. Emery, Paul D. Griffiths, Christian Sinzger, Brian P. McSharry, Gavin W. G. Wilkinson, and Andrew J.YR 2004 Davison. Genetic content of wild-type human cytomegalovirus. *Journal of General Virology*, 85(5):1301–1312, May 2004.

[137] Diana Dudziak, Alice O. Kamphorst, Gordon F. Heidkamp, Veit R. Buchholz, Christine Trumpfheller, Sayuri Yamazaki, Cheolho Cheong, Kang Liu, Han-Woong Lee, Chae Gyu Park, Ralph M. Steinman, and Michel C. Nussenzweig. Differential antigen processing

by dendritic cell subsets in vivo. *Science (New York, N.Y.)*, 315(5808):107–111, January 2007.

[138] K. C. Dunn, A. E. Aotaki-keen, F. R. Putkey, and L. M. Hjelmeland. ARPE-19, A Human Retinal Pigment Epithelial Cell Line with Differentiated Properties. *Experimental Eye Research*, 62(2):155–170, February 1996.

[139] W. Dunn, C. Chou, H. Li, R. Hai, D. Patterson, V. Stolc, H. Zhu, and F. Liu. Functional profiling of a human cytomegalovirus genome. *Proceedings of the National Academy of Sciences*, 100(24):14223–14228, 2003.

[140] Liane Dupont and Matthew B. Reeves. Cytomegalovirus latency and reactivation: Recent insights into an age old problem. *Reviews in Medical Virology*, 26(2):75–89, 2016.

[141] Larissa A. Durfee, Nancy Lyon, Kyungwoon Seo, and Jon M. Huibregtse. The ISG15 conjugation system broadly targets newly synthesized proteins: Implications for the antiviral function of ISG15. *Molecular Cell*, 38(5):722–732, June 2010.

[142] A. Dzionek, A. Fuchs, P. Schmidt, S. Cremer, M. Zysk, S. Miltenyi, D. W. Buck, and J. Schmitz. BDCA-2, BDCA-3, and BDCA-4: Three markers for distinct subsets of dendritic cells in human peripheral blood. *Journal of Immunology (Baltimore, Md.: 1950)*, 165(11):6037–6046, December 2000.

[143] Andrzej Dzionek, Yoshiaki Sohma, Jun Nagafune, Marina Cella, Marco Colonna, Fabio Facchetti, Gritt Günther, Ian Johnston, Antonio Lanzavecchia, Tomoko Nagasaka, Tsutomu Okada, William Vermi, Gregor Winkels, Terumi Yamamoto, Monika Zysk, Yasunori Yamaguchi, and Jürgen Schmitz. BDCA-2, a Novel Plasmacytoid Dendritic Cell–specific Type II C-type Lectin, Mediates Antigen Capture and Is a Potent Inhibitor of Interferon α/β Induction. *Journal of Experimental Medicine*, 194(12):1823–1834, December 2001.

[144] Robert A. Eagle, James A. Traherne, James R. Hair, Insiya Jafferji, and John Trowsdale. ULBP6/RAET1L is an additional human NKG2D ligand. *European Journal of Immunology*, 39(11):3207–3216, 2009.

[145] Adrian Egli, Isabelle Binet, Simone Binggeli, Clemens Jäger, Alexis Dumoulin, Stefan Schaub, Juerg Steiger, Urban Sester, Martina Sester, and Hans H. Hirsch. Cytomegalovirus-specific T-cell responses and viral replication in kidney transplant recipients. *Journal of Translational Medicine*, 6(1):29, June 2008.

[146] H. Einsele, G. Ehninger, M. Steidle, I. Fischer, S. Bihler, F. Gerneth, A. Vallbracht, H. Schmidt, H. D. Waller, and C. A. Müller. Lymphocytopenia as an unfavorable prognostic factor in patients with cytomegalovirus infection after bone marrow transplantation. *Blood*, 82(5):1672–1678, September 1993.

[147] Hermann Einsele, Eddy Roosnek, Nathalie Rufer, Christian Sinzger, Susanne Riegler, Jürgen Löffler, Ulrich Grigoleit, Arnaud Moris, Hans-Georg Rammensee, Lothar Kanz, Annette Kleihauer, Friederike Frank, Gerhard Jahn, and Holger Hebart. Infusion of cytomegalovirus (CMV)–specific T cells for the treatment of CMV infection not responding to antiviral chemotherapy. *Blood*, 99(11):3916–3922, June 2002.

[148] Elizabeth Elder, Benjamin Krishna, James Williamson, Yusuf Aslam, Neda Farahi, Alexander Wood, Veronika Romashova, Kate Roche, Eain Murphy, Edwin Chilvers, Paul J. Lehner, John Sinclair, and Emma Poole. Monocytes Latently Infected with Human Cytomegalovirus Evade Neutrophil Killing. *iScience*, 12:13–26, February 2019.

[149] Elizabeth G. Elder, Benjamin A. Krishna, James Williamson, Eleanor Y. Lim, Emma Poole, George X. Sedikides, Mark Wills, Christine M. O'Connor, Paul J. Lehner, and John Sinclair. Interferon-Responsive Genes Are Targeted during the Establishment of Human Cytomegalovirus Latency. *mBio*, 10(6), December 2019.

[150] Rebecca Elkington, Susan Walker, Tania Crough, Moira Menzies, Judy Tellam, Mandvi Bharadwaj, and Rajiv Khanna. Ex Vivo Profiling of CD8+-T-Cell Responses to Human Cytomegalovirus Reveals Broad and Multispecific Reactivities in Healthy Virus Carriers. *Journal of Virology*, 77(9):5226–5240, May 2003.

[151] Vincent C. Emery, Hermann Einsele, Sowsan Atabani, and Tanzina Haque. Immunotherapy and vaccination after transplant: The present, the future. *Hematology/Oncology Clinics of North America*, 2011.

[152] Vincent C Emery, Caroline A Sabin, Alethea V Cope, Dehila Gor, Aycan F Hassan-Walker, and Paul D Griffiths. Application of viral-load kinetics to identify patients who develop cytomegalovirus disease after transplantation. *The Lancet*, 355(9220):2032–2036, June 2000.

[153] P. F. Ertl and K. L. Powell. Physical and functional interaction of human cytomegalovirus DNA polymerase and its accessory protein (ICP36) expressed in insect cells. *Journal of Virology*, 66(7):4126–4133, July 1992.

[154] Vanessa A. Fabrizio, M. Irene Rodriguez-Sanchez, Audrey Mauguen, Parastoo B. Dahi, Ekaterina Doubrovina, Richard J. O'Reilly, and Susan E. Prockop. Adoptive therapy with CMV-specific cytotoxic T lymphocytes depends on baseline CD4+ immunity to mediate durable responses. *Blood Advances*, 5(2):496–503, January 2021.

[155] Yi-Hsin Fan, Sujayita Roy, Rupkatha Mukhopadhyay, Arun Kapoor, Priya Duggal, Genevieve L. Wojcik, Robert F. Pass, and Ravit Arav-Boger. Role of nucleotide-binding oligomerization domain 1 (NOD1) and its variants in human cytomegalovirus control in

vitro and in vivo. *Proceedings of the National Academy of Sciences*, 113(48):E7818–E7827, November 2016.

[156] M A Farrar and R D Schreiber. The molecular cell biology of interferon-gamma and its receptor. *Annual Review of Immunology*, 1993.

[157] Linyuan Feng, Jingxue Sheng, Gia-Phong Vu, Yujun Liu, Chingman Foo, Songbin Wu, Phong Trang, Marco Paliza-Carre, Yanhong Ran, Xiaoping Yang, Xu Sun, Zemin Deng, Tianhong Zhou, Sangwei Lu, Hongjian Li, and Fenyong Liu. Human cytomegalovirus UL23 inhibits transcription of interferon-γ stimulated genes and blocks antiviral interferon-γ responses by interacting with human N-myc interactor protein. *PLOS Pathogens*, 14(1):e1006867, January 2018.

[158] Ceri A. Fielding, Rebecca Aicheler, Richard J. Stanton, Eddie C. Y. Wang, Song Han, Sepehr Seirafian, James Davies, Brian P. McSharry, Michael P. Weekes, P. Robin Antrobus, Virginie Prod'homme, Fabien P. Blanchet, Daniel Sugrue, Simone Cuff, Dawn Roberts, Andrew J. Davison, Paul J. Lehner, Gavin W. G. Wilkinson, and Peter Tomasec. Two Novel Human Cytomegalovirus NK Cell Evasion Functions Target MICA for Lysosomal Degradation. *PLOS Pathogens*, 10(5):e1004058, May 2014.

[159] Ceri A Fielding, Michael P Weekes, Luis V Nobre, Eva Ruckova, Gavin S Wilkie, Joao A Paulo, Chiwen Chang, Nicolás M Suárez, James A Davies, Robin Antrobus, Richard J Stanton, Rebecca J Aicheler, Hester Nichols, Borek Vojtesek, John Trowsdale, Andrew J Davison, Steven P Gygi, Peter Tomasec, Paul J Lehner, and Gavin W G Wilkinson. Control of immune ligands by members of a cytomegalovirus gene expansion suppresses natural killer cell activation. *eLife*, 6:e22206, February 2017.

[160] Bernard N Fields. Fields virology- cytomegaloviruses. In *Volume II*. Lippincott Williams & Wilkins, sixth edition, 2013.

[161] Kenneth N. Fish, Cecilia Soderberg-Naucler, Lisa K. Mills, Stephan Stenglein, and Jay A. Nelson. Human Cytomegalovirus Persistently Infects Aortic Endothelial Cells. *Journal of Virology*, 72(7):5661–5668, July 1998.

[162] Jay A. Fishman. Infection in solid-organ transplant recipients. *New England Journal of Medicine*, 2007.

[163] Jay A. Fishman. Infections in immunocompromised hosts and organ transplant recipients: Essentials. *Liver Transplantation*, 2011.

[164] Jean M. Fletcher, Milica Vukmanovic-Stejic, Padraic J. Dunne, Katie E. Birch, Joanne E. Cook, Sarah E. Jackson, Mike Salmon, Malcolm H. Rustin, and Arne N. Akbar. Cytomegalovirus-Specific CD4+ T Cells in Healthy Carriers Are Continuously Driven

to Replicative Exhaustion. *The Journal of Immunology*, 175(12):8218–8225, December 2005.

[165] T. W. H. Flinsenberg, L. Spel, M. Jansen, D. Koning, C. de Haar, M. Plantinga, R. Scholman, M. M. van Loenen, S. Nierkens, L. Boon, D. van Baarle, M. H. M. Heemskerk, J. J. Boelens, and M. Boes. Cognate CD4 T-Cell Licensing of Dendritic Cells Heralds Anti-Cytomegalovirus CD8 T-Cell Immunity after Human Allogeneic Umbilical Cord Blood Transplantation. *Journal of Virology*, 89(2):1058–1069, January 2015.

[166] Adriana Flores-Langarica, Jennifer L. Marshall, Saeeda Bobat, Elodie Mohr, Jessica Hitchcock, Ewan A. Ross, Ruth E. Coughlan, Mahmood Khan, Nico Van Rooijen, Ian R. Henderson, Ian C. M. MacLennan, and Adam F. Cunningham. T-zone localized monocyte-derived dendritic cells promote Th1 priming to Salmonella. *European Journal of Immunology*, 41(9):2654–2665, 2011.

[167] Bree Foley, Sarah Cooley, Michael R. Verneris, Julie Curtsinger, Xianghua Luo, Edmund K. Waller, Claudio Anasetti, Daniel Weisdorf, and Jeffrey S. Miller. Human Cytomegalovirus (CMV)-Induced Memory-like NKG2C+ NK Cells Are Transplantable and Expand In Vivo in Response to Recipient CMV Antigen. *The Journal of Immunology*, 189(10):5082–5088, November 2012.

[168] Chiara Fornara, Milena Furione, Alessia Arossa, Giuseppe Gerna, and Daniele Lilleri. Comparative magnitude and kinetics of human cytomegalovirus-specific CD4+ and CD8+ T-cell responses in pregnant women with primary versus remote infection and in transmitting versus non-transmitting mothers: Its utility for dating primary infection in pregnancy. *Journal of Medical Virology*, 88(7):1238–1246, 2016.

[169] Chiara Fornara, Daniele Lilleri, M. Grazia Revello, Milena Furione, Maurizio Zavattoni, Elisa Lenta, and Giuseppe Gerna. Kinetics of Effector Functions and Phenotype of Virus-Specific and $\Gamma\delta$ T Lymphocytes in Primary Human Cytomegalovirus Infection During Pregnancy. *Journal of Clinical Immunology*, 31(6):1054–1064, December 2011.

[170] Calum Forrest, Ariane Gomes, Matthew Reeves, and Victoria Male. NK Cell Memory to Cytomegalovirus: Implications for Vaccine Development. *Vaccines*, 8(3):394, September 2020.

[171] Aaron E Foster, David J Gottlieb, Mary Sartor, Mark S Hertzberg, and Kenneth F Bradstock. Cytomegalovirus-specific CD4+ and CD8+ T-cells follow a similar reconstitution pattern after allogeneic stem cell transplantation. *Biology of Blood and Marrow Transplantation*, 8(9):501–511, September 2002.

[172] Ashley E. Fouts, Pamela Chan, Jean-Philippe Stephan, Richard Vandlen, and Becket Feierbach. Antibodies against the gH/gL/UL128/UL130/UL131 Complex Comprise the

Majority of the Anti-Cytomegalovirus (Anti-CMV) Neutralizing Antibody Response in CMV Hyperimmune Globulin. *Journal of Virology*, 86(13):7444–7447, July 2012.

[173] Karen B. Fowler, Sergio Stagno, and Robert F. Pass. Maternal immunity and prevention of congenital cytomegalovirus infection. *Journal of the American Medical Association*, 2003.

[174] Karen B. Fowler, Sergio Stagno, Robert F. Pass, William J. Britt, Thomas J. Boll, and Charles A. Alford. The Outcome of Congenital Cytomegalovirus Infection in Relation to Maternal Antibody Status. *New England Journal of Medicine*, 326(10):663–667, March 1992.

[175] Yu-Zhi Fu, Shan Su, Yi-Qun Gao, Pei-Pei Wang, Zhe-Fu Huang, Ming-Ming Hu, Wei-Wei Luo, Shu Li, Min-Hua Luo, Yan-Yi Wang, and Hong-Bing Shu. Human Cytomegalovirus Tegument Protein UL82 Inhibits STING-Mediated Signaling to Evade Antiviral Immunity. *Cell Host & Microbe*, 21(2):231–243, February 2017.

[176] Stephan Fuhrmann, Mathias Streitz, Petra Reinke, Hans-Dieter Volk, and Florian Kern. T Cell Response to the Cytomegalovirus Major Capsid Protein (UL86) Is Dominated by Helper Cells with a Large Polyfunctional Component and Diverse Epitope Recognition. *The Journal of Infectious Diseases*, 197(10):1455–1458, May 2008.

[177] Tomoko Fujikawa, Kei Numazaki, Hideomi Asanuma, and Hiroyuki Tsutsumi. Human cytomegalovirus infection during pregnancy and detection of specific T cells by intracellular cytokine staining. *International Journal of Infectious Diseases*, 7(3):215–221, September 2003.

[178] Elisa Gabanti, Daniele Lilleri, Francesco Ripamonti, Francesca Bruno, Paola Zelini, Milena Furione, Anna A. Colombo, Emilio P. Alessandrino, and Giuseppe Gerna. Reconstitution of Human Cytomegalovirus–Specific CD4+ T Cells is Critical for Control of Virus Reactivation in Hematopoietic Stem Cell Transplant Recipients but Does Not Prevent Organ Infection. *Biology of Blood and Marrow Transplantation*, 21(12):2192–2202, December 2015.

[179] Florin Gabor, Gerhard Jahn, Daniel D. Sedmak, and Christian Sinzger. In vivo Downregulation of MHC Class I Molecules by HCMV Occurs During All Phases of Viral Replication but Is Not Always Complete. *Frontiers in Cellular and Infection Microbiology*, 10, 2020.

[180] Laila E. Gamadia, Ester B. M. Remmerswaal, Jan F. Weel, Frederieke Bemelman, René A. W. van Lier, and Ineke J. M. Ten Berge. Primary immune responses to human CMV: A critical role for IFN-γ–producing CD4+ T cells in protection against CMV disease. *Blood*, 101(7):2686–2692, April 2003.

[181] Laila E Gamadia, Rob J Rentenaar, René A. W van Lier, and Ineke J. M ten Berge. Properties of CD4+ T cells in human cytomegalovirus infection. *Human Immunology*, 65(5):486–492, May 2004.

[182] Soren Gantt, Erin Leister, Denise L. Jacobson, Isabelle Boucoiran, Meei-Li Huang, Keith R. Jerome, Gonzague Jourdain, Nicole Ngo-Giang-Huong, Sandra Burchett, and Lisa Frenkel. Risk of congenital cytomegalovirus infection among HIV-exposed uninfected infants is not decreased by maternal nelfinavir use during pregnancy. *Journal of medical virology*, 88(6):1051–1058, June 2016.

[183] Roi Gazit, Ben Zion Garty, Yehudith Monselise, Vered Hoffer, Yaron Finkelstein, Gal Markel, Gil Katz, Jacob Hanna, Hagit Achdout, Raizy Gruda, Tsufit Gonen-Gross, and Ofer Mandelboim. Expression of KIR2DL1 on the entire NK cell population: A possible novel immunodeficiency syndrome. *Blood*, 2004.

[184] A. P. Geballe, F. S. Leach, and E. S. Mocarski. Regulation of cytomegalovirus late gene expression: Gamma genes are controlled by posttranscriptional events. *Journal of Virology*, 57(3):864–874, March 1986.

[185] G. Gerna, D. Lilleri, A. Chiesa, P. Zelini, M. Furione, G. Comolli, C. Pellegrini, E. Sarchi, C. Migotto, M. Regazzi Bonora, F. Meloni, and E. Arbustini. Virologic and Immunologic Monitoring of Cytomegalovirus to Guide Preemptive Therapy in Solid-Organ Transplantation. *American Journal of Transplantation*, 11(11):2463–2471, 2011.

[186] G. Gerna, D. Lilleri, C. Fornara, G. Comolli, L. Lozza, C. Campana, C. Pellegrini, F. Meloni, and T. Rampino. Monitoring of Human Cytomegalovirus-Specific CD4+ and CD8+ T-Cell Immunity in Patients Receiving Solid Organ Transplantation. *American Journal of Transplantation*, 6(10):2356–2364, 2006.

[187] Giuseppe Gerna and Daniele Lilleri. Human cytomegalovirus (HCMV) infection/reinfection: Development of a protective HCMV vaccine. *The New Microbiologica*, 42(1):1–20, January 2019.

[188] Giuseppe Gerna, Elena Percivalle, Daniele Lilleri, Laura Lozza, Chiara Fornara, Gabriele Hahn, Fausto Baldanti, and M. Grazia Revello. Dendritic-cell infection by human cytomegalovirus is restricted to strains carrying functional UL131-128 genes and mediates efficient viral antigen presentation to CD8+ T cells. *The Journal of General Virology*, 86(Pt 2):275–284, February 2005.

[189] Giuseppe Gerna, Elena Percivalle, Antonella Sarasini, and M. Grazia Revello. Human Cytomegalovirus and Human Umbilical Vein Endothelial Cells: Restriction of Primary Isolation to Blood Samples and Susceptibilities of Clinical Isolates from Other Sources to Adaptation. *Journal of Clinical Microbiology*, 40(1):233–238, January 2002.

[190] Laura Gibson, Constance M. Barysauskas, Margaret McManus, Sheryl Dooley, Daniele Lilleri, Donna Fisher, Tumul Srivastava, Don J. Diamond, and Katherine Luzuriaga. Reduced Frequencies of Polyfunctional CMV-Specific T Cell Responses in Infants with Congenital CMV Infection. *Journal of Clinical Immunology*, 35(3):289–301, April 2015.

[191] Laura Gibson, Giampiero Piccinini, Daniele Lilleri, Maria Grazia Revello, Zhongde Wang, Susan Markel, Don J. Diamond, and Katherine Luzuriaga. Human cytomegalovirus proteins pp65 and immediate early protein 1 are common targets for CD8+ T cell responses in children with congenital or postnatal human cytomegalovirus infection. *Journal of Immunology (Baltimore, Md.: 1950)*, 172(4):2256–2264, February 2004.

[192] M J Gilbert, S R Riddell, C R Li, and P D Greenberg. Selective interference with class I major histocompatibility complex presentation of the major immediate-early protein following infection with human cytomegalovirus. *Journal of Virology*, 67(6):3461–3469, June 1993.

[193] Michel Gilliet, Wei Cao, and Yong-Jun Liu. Plasmacytoid dendritic cells: Sensing nucleic acids in viral infection and autoimmune diseases. *Nature Reviews Immunology*, 8(8):594–606, August 2008.

[194] Corrado Girmenia, Tiziana Lazzarotto, Francesca Bonifazi, Francesca Patriarca, Giuseppe Irrera, Fabio Ciceri, Franco Aversa, Franco Citterio, Umberto Cillo, Emanuele Cozzi, Enrico Gringeri, Fausto Baldanti, Rossana Cavallo, Pierangelo Clerici, Giovanni Barosi, and Paolo Grossi. Assessment and prevention of cytomegalovirus infection in allogeneic hematopoietic stem cell transplant and in solid organ transplant: A multidisciplinary consensus conference by the Italian GITMO, SITO, and AMCLI societies. *Clinical Transplantation*, 33(10):e13666, October 2019.

[195] Ben J. Glasgow and Annemarie K. Weisberger. A Quantitative and Cartographic Study of Retinal Microvasculopathy in Acquired Immunodeficiency Syndrome. *American Journal of Ophthalmology*, 118(1):46–56, July 1994.

[196] J. W. Gnann, J. Ahlmén, C. Svalander, L. Olding, M. B. Oldstone, and J. A. Nelson. Inflammatory cells in transplanted kidneys are infected by human cytomegalovirus. *The American Journal of Pathology*, 132(2):239–248, August 1988.

[197] Marie-Laure Golinski, Mélanie Demeules, Céline Derambure, Gaetan Riou, Maud Maho-Vaillant, Olivier Boyer, Pascal Joly, and Sébastien Calbo. CD11c+ B Cells Are Mainly Memory Cells, Precursors of Antibody Secreting Cells in Healthy Donors. *Frontiers in Immunology*, 11, 2020.

[198] Vita Golubovskaya and Lijun Wu. Different Subsets of T Cells, Memory, Effector Functions, and CAR-T Immunotherapy. *Cancers*, 8(3):36, March 2016.

[199] Aparecida Gomes Pinto Garcia, Evangelina Ferreira Fonseca, Regina Lucia De Souza Marques, and Yolanda Yamaki Lobato. Placental morphology in cytomegalovirus infection. *Placenta*, 1989.

[200] Christopher Goodwin, Jessica Ciesla, and Joshua Munger. Who's driving? Human cytomegalovirus, interferon, and NFκb signaling. *Viruses*, 10(9):447, 2018.

[201] M. Grazia Revello, Fausto Baldanti, Elena Percivalle, Antonella Sarasini, Luciana De-Giuli, Emilia Genini, Daniele Lilleri, Nazarena Labò, and Giuseppe Gerna. In vitro selection of human cytomegalovirus variants unable to transfer virus and virus products from infected cells to polymorphonuclear leukocytes and to grow in endothelial cells. *Journal of General Virology,*, 82(6):1429–1438, 2001.

[202] AE Greijer, JM van de Crommert, SJ Stevens, and JM Middeldorp. Molecular fine-specificity analysis of antibody responses to human cytomegalovirus and design of novel synthetic-peptide-based serodiagnostic assays. *Journal of clinical microbiology*, 37(1):179—188, January 1999.

[203] Paul D. Griffiths and Vincent C. Emery. Taming the transplantation troll by targeting terminase. *New England Journal of Medicine*, 2014.

[204] Paul D Griffiths, Anna Stanton, Erin McCarrell, Colette Smith, Mohamed Osman, Mark Harber, Andrew Davenport, Gareth Jones, David C Wheeler, James O'Beirne, Douglas Thorburn, David Patch, Claire E Atkinson, Sylvie Pichon, Paul Sweny, Marisa Lanzman, Elizabeth Woodford, Emily Rothwell, Natasha Old, Ruth Kinyanjui, Tanzina Haque, Sowsan Atabani, Suzanne Luck, Steven Prideaux, Richard SB Milne, Vincent C Emery, and Andrew K Burroughs. Cytomegalovirus glycoprotein-B vaccine with MF59 adjuvant in transplant recipients: A phase 2 randomised placebo-controlled trial. *The Lancet*, 377(9773):1256–1263, April 2011.

[205] Géraldine Grouard, Marie-Clotilde Rissoan, Luis Filgueira, Isabelle Durand, Jacques Banchereau, and Yong-Jun Liu. The Enigmatic Plasmacytoid T Cells Develop into Dendritic Cells with Interleukin (IL)-3 and CD40-Ligand. *Journal of Experimental Medicine*, 185(6):1101–1112, March 1997.

[206] V. Guérin, J.-H. Dalle, B. Pédron, M. Ouachée-Chardin, K. Yakouben, A. Baruchel, and G. Sterkers. Cellular immune parameters associated with spontaneous control of CMV in children who underwent transplantation. *Bone Marrow Transplantation*, 45(3):442–449, March 2010.

[207] Pierre Guermonprez, Yohan Gerber-Ferder, Kristine Vaivode, Pierre Bourdely, and Julie Helft. Chapter One - Origin and development of classical dendritic cells. In Claire Lhuillier and Lorenzo Galluzzi, editors, *International Review of Cell and Molecular Biology*, volume

349 of *Immunobiology of Dendritic Cells Part B*, pages 1–54. Academic Press, January 2019.

[208] Abraham Guerrero, Stanley R. Riddell, Jan Storek, Terry Stevens-Ayers, Barry Storer, John A. Zaia, Stephen Forman, Robert S. Negrin, Thomas Chauncey, William Bensinger, and Michael Boeckh. Cytomegalovirus Viral Load and Virus-Specific Immune Reconstitution after Peripheral Blood Stem Cell versus Bone Marrow Transplantation. *Biology of Blood and Marrow Transplantation*, 18(1):66–75, January 2012.

[209] Gaelle Guibert, Josiane Warszawski, Jerome Le Chenadec, Stephane Blanche, Yassine Benmebarek, Laurent Mandelbrot, Rolland Tubiana, Christine Rouzioux, and Marianne Leruez-Ville. Decreased Risk of Congenital Cytomegalovirus Infection in Children Born to HIV-1-Infected Mothers in the Era of Highly Active Antiretroviral Therapy. *Clinical Infectious Diseases*, 48(11):1516–1525, June 2009.

[210] Mónica Gumá, Ana Angulo, Carlos Vilches, Natalia Gómez-Lozano, Núria Malats, and Miguel López-Botet. Imprint of human cytomegalovirus infection on the NK cell receptor repertoire. *Blood*, 104(12):3664–3671, December 2004.

[211] Mónica Gumá, Matthias Budt, Andrea Sáez, Tamara Brckalo, Hartmut Hengel, Ana Angulo, and Miguel López-Botet. Expansion of CD94/NKG2C+ NK cells in response to human cytomegalovirus-infected fibroblasts. *Blood*, 107(9):3624–3631, May 2006.

[212] Mónica Gumá, Lisa K. Busch, Laura I. Salazar-Fontana, Beatriz Bellosillo, Carles Morte, Pilar García, and Miguel López-Botet. The CD94/NKG2C killer lectin-like receptor constitutes an alternative activation pathway for a subset of CD8+ T cells. *European Journal of Immunology*, 35(7):2071–2080, 2005.

[213] Gabriele Hahn, Maria Grazia Revello, Marco Patrone, Elena Percivalle, Giulia Campanini, Antonella Sarasini, Markus Wagner, Andrea Gallina, Gabriele Milanesi, Ulrich Koszinowski, Fausto Baldanti, and Giuseppe Gerna. Human Cytomegalovirus UL131-128 Genes Are Indispensable for Virus Growth in Endothelial Cells and Virus Transfer to Leukocytes. *Journal of Virology*, 78(18):10023–10033, September 2004.

[214] Ghady Haidar, Michael Boeckh, and Nina Singh. Cytomegalovirus Infection in Solid Organ and Hematopoietic Cell Transplantation: State of the Evidence. *The Journal of Infectious Diseases*, 221(Supplement_1):S23–S31, March 2020.

[215] Morgan Hakki, Stanley R. Riddell, Jan Storek, Rachel A. Carter, Terry Stevens-Ayers, Patrick Sudour, Kristen White, Lawrence Corey, and Michael Boeckh. Immune reconstitution to cytomegalovirus after allogeneic hematopoietic stem cell transplantation: Impact of host factors, drug therapy, and subclinical reactivation. *Blood*, 102(8):3060–3067, October 2003.

[216] J. Scott Hale and Rafi Ahmed. Memory T Follicular Helper CD4 T Cells. *Frontiers in Immunology*, 6, 2015.

[217] J. Scott Hale, Ben Youngblood, Donald R. Latner, Ata Ur Rasheed Mohammed, Lilin Ye, Rama S. Akondy, Tuoqi Wu, Smita S. Iyer, and Rafi Ahmed. Distinct Memory CD4+ T Cells with Commitment to T Follicular Helper- and T Helper 1-Cell Lineages Are Generated after Acute Viral Infection. *Immunity*, 38(4):805–817, April 2013.

[218] Ben Hammoud, Michael Schmueck, Annika M. Fischer, Henrike Fuehrer, Su-Jin Park, Levent Akyuez, Joerg C. Schefold, Martin J. Raftery, Günther Schönrich, Andreas M. Kaufmann, Hans-Dieter Volk, and Petra Reinke. HCMV-specific T-cell Therapy: Do Not Forget Supply of Help. *Journal of Immunotherapy*, 36(2):93, February 2013.

[219] S. Hanabuchi, M. Koyanagi, A. Kawasaki, N. Shinohara, A. Matsuzawa, Y. Nishimura, Y. Kobayashi, S. Yonehara, H. Yagita, and K. Okumura. Fas and its ligand in a general mechanism of T-cell-mediated cytotoxicity. *Proceedings of the National Academy of Sciences*, 91(11):4930–4934, May 1994.

[220] Meaghan H. Hancock, Lindsey B. Crawford, Andrew H. Pham, Jennifer Mitchell, Hillary M. Struthers, Andrew D. Yurochko, Patrizia Caposio, and Jay A. Nelson. Human Cytomegalovirus miRNAs Regulate TGF-β to Mediate Myelosuppression while Maintaining Viral Latency in CD34+ Hematopoietic Progenitor Cells. *Cell Host & Microbe*, 27(1):104–114.e4, January 2020.

[221] Muzlifah Haniffa, Amanda Shin, Venetia Bigley, Naomi McGovern, Pearline Teo, Peter See, Pavandip Singh Wasan, Xiao-Nong Wang, Frano Malinarich, Benoit Malleret, Anis Larbi, Pearlie Tan, Helen Zhao, Michael Poidinger, Sarah Pagan, Sharon Cookson, Rachel Dickinson, Ian Dimmick, Ruth F. Jarrett, Laurent Renia, John Tam, Colin Song, John Connolly, Jerry K. Y. Chan, Adam Gehring, Antonio Bertoletti, Matthew Collin, and Florent Ginhoux. Human Tissues Contain CD141hi Cross-Presenting Dendritic Cells with Functional Homology to Mouse CD103+ Nonlymphoid Dendritic Cells. *Immunity*, 37(1):60–73, July 2012.

[222] Ted H. Hansen and Marlene Bouvier. MHC class I antigen presentation: Learning from viral evasion strategies. *Nature Reviews Immunology*, 9(7):503–513, July 2009.

[223] D. Hargett and T. E. Shenk. Experimental human cytomegalovirus latency in CD14+ monocytes. *Proceedings of the National Academy of Sciences*, 2010.

[224] J. Hassan, S. Dooley, and W. Hall. Immunological response to cytomegalovirus in congenitally infected neonates. *Clinical & Experimental Immunology*, 147(3):465–471, 2007.

[225] Naomi Hayashi, Hiroshi Kimura, Tsuneo Morishima, Naoko Tanaka, Tatsuya Tsurumi, and Kiyotaka Kuzushima. Flow cytometric analysis of cytomegalovirus-specific cell-mediated immunity in the congenital infection. *Journal of Medical Virology*, 71(2):251–258, October 2003.

[226] Jon Hazeldine and Janet M. Lord. The impact of ageing on natural killer cell function and potential consequences for health in older adults. *Ageing Research Reviews*, 12(4):1069–1078, September 2013.

[227] Holger Hebart and Hermann Einsele. Clinical aspects of cmv infection after stem cell transplantation. *Human Immunology*, 65(5):432–436, May 2004.

[228] Nagendra R. Hegde, Roman A. Tomazin, Todd W. Wisner, Claire Dunn, Jessica M. Boname, David M. Lewinsohn, and David C. Johnson. Inhibition of HLA-DR Assembly, Transport, and Loading by Human Cytomegalovirus Glycoprotein US3: A Novel Mechanism for Evading Major Histocompatibility Complex Class II Antigen Presentation. *Journal of Virology*, 76(21):10929–10941, November 2002.

[229] H. Hengel, J. O. Koopmann, T. Flohr, W. Muranyi, E. Goulmy, G. J. Hämmerling, U. H. Koszinowski, and F. Momburg. A viral ER-resident glycoprotein inactivates the MHC-encoded peptide transporter. *Immunity*, 6(5):623–632, May 1997.

[230] Hartmut Hengel, Thomas Flohr, Günter J. Hämmerling, Ulrich H. Koszinowski, and FrankYR 1996 Momburg. Human Cytomegalovirus Inhibits Peptide Translocation into the Endoplasmic Reticulum for MHC Class I Assembly. *Journal of General Virology*, 77(9):2287–2296, September 1996.

[231] Pierre A. Henkart. Mechanism of Lymphocyte-Mediated Cytotoxicity. *Annual Review of Immunology*, 3(1):31–58, April 1985.

[232] Gabriele Hensel, Hemmo Meyer, Sabine Gärtner, Gabriele Brand, and Horst Franz Kern. Nuclear localization of the human cytomegalovirus tegument protein pp150 (ppUL32). *Journal of General Virology*, 76(7):1591–1601, 1995.

[233] Laura Hertel, Vashti G. Lacaille, Herbert Strobl, Elizabeth D. Mellins, and Edward S. Mocarski. Susceptibility of Immature and Mature Langerhans Cell-Type Dendritic Cells to Infection and Immunomodulation by Human Cytomegalovirus. *Journal of Virology*, 77(13):7563–7574, July 2003.

[234] E. W. Hewitt, S. S. Gupta, and P. J. Lehner. The human cytomegalovirus gene product US6 inhibits ATP binding by TAP. *EMBO Journal*, 2001.

[235] Guillaume Hoeffel, Anne-Claire Ripoche, Diana Matheoud, Michelina Nascimbeni, Nicolas Escriou, Pierre Lebon, Farhad Heshmati, Jean-Gérard Guillet, Monique Gannagé,

Sophie Caillat-Zucman, Nicoletta Casartelli, Olivier Schwartz, Henri De la Salle, Daniel Hanau, Anne Hosmalin, and Concepción Marañón. Antigen Crosspresentation by Human Plasmacytoid Dendritic Cells. *Immunity*, 27(3):481–492, September 2007.

[236] Tjadine M Holling, Erik Schooten, and Peter J van Den Elsen. Function and regulation of MHC class II molecules in T-lymphocytes: Of mice and men. *Human Immunology*, 65(4):282–290, April 2004.

[237] Nick Holmes. CD45: All is not yet crystal clear. *Immunology*, 117(2):145–155, February 2006.

[238] Chien-Li Holmes-Liew, Mark Holmes, Leone Beagley, Peter Hopkins, Daniel Chambers, Corey Smith, and Rajiv Khanna. Adoptive T-cell immunotherapy for ganciclovir-resistant CMV disease after lung transplantation. *Clinical & Translational Immunology*, 4(3):e35, March 2015.

[239] M. Homman-Loudiyi, K. Hultenby, W. Britt, and C. Söderberg-Nauclér. Envelopment of Human Cytomegalovirus Occurs by Budding into Golgi-Derived Vacuole Compartments Positive for gB, Rab 3, Trans-Golgi Network 46, and Mannosidase II. *Journal of Virology*, 77(5):3191–3203, March 2003.

[240] Kenya Honda, Hideyuki Yanai, Hideo Negishi, Masataka Asagiri, Mitsuharu Sato, Tatsuaki Mizutani, Naoya Shimada, Yusuke Ohba, Akinori Takaoka, Nobuaki Yoshida, and Tadatsugu Taniguchi. IRF-7 is the master regulator of type-I interferon-dependent immune responses. *Nature*, 434(7034):772–777, April 2005.

[241] Charlotte J. Houldcroft, Sarah E. Jackson, Eleanor Y. Lim, George X. Sedikides, Emma L. Davies, Claire Atkinson, Megan McIntosh, Ester B. M. Remmerswaal, Georgina Okecha, Frederike J. Bemelman, Richard J. Stanton, Matthew Reeves, and Mark R. Wills. Assessing Anti-HCMV Cell Mediated Immune Responses in Transplant Recipients and Healthy Controls Using a Novel Functional Assay. *Frontiers in Cellular and Infection Microbiology*, 10:275, 2020.

[242] Zhe-Fu Huang, Hong-Mei Zou, Bo-Wei Liao, Hong-Yan Zhang, Yan Yang, Yu-Zhi Fu, Su-Yun Wang, Min-Hua Luo, and Yan-Yi Wang. Human Cytomegalovirus Protein UL31 Inhibits DNA Sensing of cGAS to Mediate Immune Evasion. *Cell Host & Microbe*, 24(1):69–80.e4, July 2018.

[243] A. Humar and D. Snydman. Cytomegalovirus in Solid Organ Transplant Recipients. *American Journal of Transplantation*, 9(s4):S78–S86, 2009.

[244] Ian R. Humphreys, Carl de Trez, April Kinkade, Chris A. Benedict, Michael Croft, and Carl F. Ware. Cytomegalovirus exploits IL-10–mediated immune regulation in the salivary glands. *Journal of Experimental Medicine*, 204(5):1217–1225, May 2007.

[245] Morgan Huse, Emily J Quann, and Mark M Davis. Shouts, whispers and the kiss of death: Directional secretion in T cells. *Nature immunology*, 9(10):1105–1111, October 2008.

[246] Ariane Huygens, Sandra Lecomte, Marie Tackoen, Véronique Olislagers, Yves Delmarcelle, Wivine Burny, Michel Van Rysselberge, Corinne Liesnard, Martin Larsen, Victor Appay, Catherine Donner, and Arnaud Marchant. Functional Exhaustion Limits CD4+ and CD8+ T-Cell Responses to Congenital Cytomegalovirus Infection. *The Journal of Infectious Diseases*, 212(3):484–494, August 2015.

[247] Jiwon Hwang and Robert F. Kalejta. Proteasome-dependent, ubiquitin-independent degradation of Daxx by the viral pp71 protein in human cytomegalovirus-infected cells. *Virology*, 367(2):334–338, October 2007.

[248] Kazue Imai, Satoru Matsuyama, Satoshi Miyake, Kenji Suga, and Kei Nakachi. Natural cytotoxic activity of peripheral-blood lymphocytes and cancer incidence: An 11-year follow-up study of a general population. *The Lancet*, 356(9244):1795–1799, November 2000.

[249] K Inaba, M Inaba, N Romani, H Aya, M Deguchi, S Ikehara, S Muramatsu, and R M Steinman. Generation of large numbers of dendritic cells from mouse bone marrow cultures supplemented with granulocyte/macrophage colony-stimulating factor. *Journal of Experimental Medicine*, 176(6):1693–1702, December 1992.

[250] M. K. Isaacson, L. K. Juckem, and T. Compton. Virus entry and innate immune activation. In Thomas E. Shenk and Mark F. Stinski, editors, *Human Cytomegalovirus*, pages 85–100. Springer Berlin Heidelberg, Berlin, Heidelberg, 2008.

[251] Hiroki Isomura, Mark F. Stinski, Ayumi Kudoh, Sanae Nakayama, Satoko Iwahori, Yoshitaka Sato, and Tatsuya Tsurumi. The Late Promoter of the Human Cytomegalovirus Viral DNA Polymerase Processivity Factor Has an Impact on Delayed Early and Late Viral Gene Products but Not on Viral DNA Synthesis. *Journal of Virology*, 81(12):6197–6206, June 2007.

[252] Ann-Charlotte Iversen, Paula S. Norris, Carl F. Ware, and Chris A. Benedict. Human NK Cells Inhibit Cytomegalovirus Replication through a Noncytolytic Mechanism Involving Lymphotoxin-Dependent Induction of IFN-β. *The Journal of Immunology*, 175(11):7568–7574, December 2005.

[253] Mineo Iwata, Jeff Vieira, Michael Byrne, Heidi Horton, and Beverly Torok-Storb. Interleukin-1 (IL-1) Inhibits Growth of Cytomegalovirus in Human Marrow Stromal Cells: Inhibition Is Reversed Upon Removal of IL-1. *Blood*, 94(2):572–578, July 1999.

[254] S. E. Jackson, G. M. Mason, G. Okecha, J. G. P. Sissons, and M. R. Wills. Diverse specificities, phenotypes, and antiviral activities of cytomegalovirus-specific CD8+ t cells. *Journal of Virology*, 2014.

[255] Sarah E. Jackson, Gavin M. Mason, and Mark R. Wills. Human cytomegalovirus immunity and immune evasion. *Virus Research*, 157(2):151–160, May 2011.

[256] Sarah E. Jackson, George X. Sedikides, Gavin M. Mason, Georgina Okecha, and Mark R. Wills. Human Cytomegalovirus (HCMV)-Specific CD4+ T Cells Are Polyfunctional and Can Respond to HCMV-Infected Dendritic Cells In Vitro. *Journal of Virology*, 91(6), February 2017.

[257] Sarah E. Jackson, George X. Sedikides, Georgina Okecha, Emma L. Poole, John H. Sinclair, and Mark R. Wills. Latent Cytomegalovirus (CMV) Infection Does Not Detrimentally Alter T Cell Responses in the Healthy Old, But Increased Latent CMV Carriage Is Related to Expanded CMV-Specific T Cells. *Frontiers in Immunology*, 8:733, 2017.

[258] Sarah E. Jackson, George X. Sedikides, Georgina Okecha, and Mark R. Wills. Generation, maintenance and tissue distribution of T cell responses to human cytomegalovirus in lytic and latent infection. *Medical Microbiology and Immunology*, 208(3):375–389, August 2019.

[259] Claudia V. Jakubzick, Gwendalyn J. Randolph, and Peter M. Henson. Monocyte differentiation and antigen-presenting functions. *Nature Reviews Immunology*, 17(6):349–362, June 2017.

[260] Laura Jardine, Dawn Barge, Ashley Ames-Draycott, Sarah Pagan, Sharon Cookson, Gavin Spickett, Muzlifah Haniffa, Matthew Collin, and Venetia Bigley. Rapid Detection of Dendritic Cell and Monocyte Disorders Using CD4 as a Lineage Marker of the Human Peripheral Blood Antigen-Presenting Cell Compartment. *Frontiers in Immunology*, 4, 2013.

[261] David Jarrossay, Giorgio Napolitani, Marco Colonna, Federica Sallusto, and Antonio Lanzavecchia. Specialization and complementarity in microbial molecule recognition by human myeloid and plasmacytoid dendritic cells. *European Journal of Immunology*, 31(11):3388–3393, 2001.

[262] Michael A. Jarvis and Jay A. Nelson. Human Cytomegalovirus Tropism for Endothelial Cells: Not All Endothelial Cells Are Created Equal. *Journal of Virology*, 81(5):2095–2101, March 2007.

[263] Emilia Jaskula, Dorota Dlubek, Agnieszka Tarnowska, Janusz Lange, Monika Mordak-Domagala, Krzysztof Suchnicki, Mariola Sedzimirska, Agata Borowik, Sylwia Mizia,

and Andrzej Lange. Anti-CMV-IgG Positivity of Donors Is Beneficial for alloHSCT Recipients with Respect to the Better Short-Term Immunological Recovery and High Level of CD4+CD25high Lymphocytes. *Viruses*, 7(3):1391–1408, March 2015.

[264] Gaetan Jego, A. Karolina Palucka, Jean-Philippe Blanck, Cecile Chalouni, Virginia Pascual, and Jacques Banchereau. Plasmacytoid Dendritic Cells Induce Plasma Cell Differentiation through Type I Interferon and Interleukin 6. *Immunity*, 19(2):225–234, August 2003.

[265] C. Jenkins, W. Garcia, M. J. Godwin, J. V. Spencer, J. Lewis Stern, A. Abendroth, and B. Slobedman. Immunomodulatory properties of a viral homolog of human interleukin-10 expressed by human cytomegalovirus during the latent phase of infection. *Journal of Virology*, 82(7):3736–3750, April 2008.

[266] Christina Jenkins, Allison Abendroth, and Barry Slobedman. A Novel Viral Transcript with Homology to Human Interleukin-10 Is Expressed during Latent Human Cytomegalovirus Infection. *Journal of Virology*, 78(3):1440–1447, February 2004.

[267] Shujuan Jiang, Ying Qi, Rong He, Yujing Huang, Zhongyang Liu, Yanping Ma, Xin Guo, Yaozhong Shao, Zhengrong Sun, and Qiang Ruan. Human cytomegalovirus microRNA miR-US25-1-5p inhibits viral replication by targeting multiple cellular genes during infection. *Gene*, 570(1):108–114, October 2015.

[268] David C. Johnson and Ann B. Hill. Herpesvirus Evasion of the Immune System. In J. Lindsay Whitton, editor, *Antigen Presentation*, Current Topics in Microbiology and Immunology, pages 149–177. Springer, Berlin, Heidelberg, 1998.

[269] T. R. Jones, L. K. Hanson, L. Sun, J. S. Slater, R. M. Stenberg, and A. E. Campbell. Multiple independent loci within the human cytomegalovirus unique short region down-regulate expression of major histocompatibility complex class I heavy chains. *Journal of Virology*, 69(8):4830–4841, August 1995.

[270] T. R. Jones, E. J. Wiertz, L. Sun, K. N. Fish, J. A. Nelson, and H. L. Ploegh. Human cytomegalovirus US3 impairs transport and maturation of major histocompatibility complex class I heavy chains. *Proceedings of the National Academy of Sciences*, 93(21):11327–11333, October 1996.

[271] Sarah L. Jongbloed, Andrew J. Kassianos, Kylie J. McDonald, Georgina J. Clark, Xinsheng Ju, Catherine E. Angel, Chun-Jen J. Chen, P. Rod Dunbar, Robert B. Wadley, Varinder Jeet, Annelie J.E. Vulink, Derek N.J. Hart, and Kristen J. Radford. Human CD141+ (BDCA-3)+ dendritic cells (DCs) represent a unique myeloid DC subset that cross-presents necrotic cell antigens. *Journal of Experimental Medicine*, 207(6):1247–1260, May 2010.

[272] S Jonjic, W Mutter, F Weiland, M J Reddehase, and U H Koszinowski. Site-restricted persistent cytomegalovirus infection after selective long-term depletion of CD4+ T lymphocytes. *The Journal of Experimental Medicine*, 169(4):1199–1212, April 1989.

[273] Stipan Jonjić, Ivica Pavić, Bojan Polić, Irena Crnkovic, Pero Lučin, and Ulrich H. Koszinowski. Antibodies are not essential for the resolution of primary cytomegalovirus infection but limit dissemination of recurrent virus. *The Journal of Experimental Medicine*, 179(5):1713–1717, May 1994.

[274] Jennifer A. Juno, David van Bockel, Stephen J. Kent, Anthony D. Kelleher, John J. Zaunders, and C. Mee Ling Munier. Cytotoxic CD4 T Cells—Friend or Foe during Viral Infection? *Frontiers in Immunology*, 8, 2017.

[275] Anna Kabanova, Laurent Perez, Daniele Lilleri, Jessica Marcandalli, Gloria Agatic, Simone Becattini, Silvia Preite, Dario Fuschillo, Elena Percivalle, Federica Sallusto, Giuseppe Gerna, Davide Corti, and Antonio Lanzavecchia. Antibody-driven design of a human cytomegalovirus gHgLpUL128L subunit vaccine that selectively elicits potent neutralizing antibodies. *Proceedings of the National Academy of Sciences of the United States of America*, 111(50):17965–17970, December 2014.

[276] Norimitsu Kadowaki, Stephen Ho, Svetlana Antonenko, Rene de Waal Malefyt, Robert A. Kastelein, Fernando Bazan, and Yong-Jun Liu. Subsets of Human Dendritic Cell Precursors Express Different Toll-like Receptors and Respond to Different Microbial Antigens. *Journal of Experimental Medicine*, 194(6):863–870, September 2001.

[277] Susan M. Kaech and Weiguo Cui. Transcriptional control of effector and memory CD8+ T cell differentiation. *Nature reviews. Immunology*, 12(11):749–761, November 2012.

[278] M. Kahl, D. Siegel-Axel, S. Stenglein, G., Jahn, and C. Sinzger. Efficient Lytic Infection of Human Arterial Endothelial Cells by Human Cytomegalovirus Strains. *Journal of Virology*, 74(16):7628–7635, August 2000.

[279] Gunjan Kak, Mohsin Raza, and Brijendra K. Tiwari. Interferon-gamma (IFN-γ): Exploring its implications in infectious diseases. *Biomolecular Concepts*, 9(1):64–79, May 2018.

[280] Robert F. Kalejta and Emily R. Albright. Expanding the Known Functional Repertoire of the Human Cytomegalovirus pp71 Protein. *Frontiers in Cellular and Infection Microbiology*, 10, March 2020.

[281] Vera M. Kamp, Janesh Pillay, Jan-Willem J. Lammers, Peter Pickkers, Laurien H. Ulfman, and Leo Koenderman. Human suppressive neutrophils CD16bright/CD62Ldim exhibit decreased adhesion. *Journal of Leukocyte Biology*, 92(5):1011–1020, 2012.

[282] Takumi Kanesaki, Koichi Baba, Kazuko Tanaka, Michio Ishibashi, and Hyakuji Yabuuchi. Characterization of cytomegalovirus isolates recovered during repeated infection in renal transplant recipients. *Journal of Medical Virology*, 28(3):140–143, 1989.

[283] Soowon Kang, Hailey M. Brown, and Seungmin Hwang. Direct Antiviral Mechanisms of Interferon-Gamma. *Immune Network*, 18(5), October 2018.

[284] Theodore S. Kapellos, Lorenzo Bonaguro, Ioanna Gemünd, Nico Reusch, Adem Saglam, Emily R. Hinkley, and Joachim L. Schultze. Human Monocyte Subsets and Phenotypes in Major Chronic Inflammatory Diseases. *Frontiers in Immunology*, 10, 2019.

[285] Elvedina Kapic, Fahir Becic, and Jasna Kusturica. Basiliximab, mechanism of action and pharmacological properties. *Medicinski Arhiv*, 58(6):373–376, 2004.

[286] Arun Kapoor, Michael Forman, and Ravit Arav-Boger. Activation of Nucleotide Oligomerization Domain 2 (NOD2) by Human Cytomegalovirus Initiates Innate Immune Responses and Restricts Virus Replication. *PLOS ONE*, 9(3):e92704, March 2014.

[287] Bruce Kari and Richard Gehrz. A human cytomegalovirus glycoprotein complex designated gC-II is a major heparin-binding component of the envelope. *Journal of Virology*, 1992.

[288] Ahmad Karkhah, Mostafa Javanian, and Soheil Ebrahimpour. The role of regulatory T cells in immunopathogenesis and immunotherapy of viral infections. *Infection, Genetics and Evolution*, 59:32–37, April 2018.

[289] Klas Kärre, Hans Gustaf Ljunggren, Gerald Piontek, and Rolf Kiessling. Selective rejection of H–2-deficient lymphoma variants suggests alternative immune defence strategy. *Nature*, 319(6055):675–678, February 1986.

[290] T. Kasahara, J. J. Hooks, S. F. Dougherty, and J. J. Oppenheim. Interleukin 2-mediated immune interferon (IFN-gamma) production by human T cells and T cell subsets. *The Journal of Immunology*, 130(4):1784–1789, April 1983.

[291] Taro Kawai, Shintaro Sato, Ken J. Ishii, Cevayir Coban, Hiroaki Hemmi, Masahiro Yamamoto, Kenta Terai, Michiyuki Matsuda, Jun-ichiro Inoue, Satoshi Uematsu, Osamu Takeuchi, and Shizuo Akira. Interferon-α induction through Toll-like receptors involves a direct interaction of IRF7 with MyD88 and TRAF6. *Nature Immunology*, 5(10):1061–1068, October 2004.

[292] F. Kazazi, J. M. Mathijs, P. Foley, and A. L. Cunningham. Variations in CD4 expression by human monocytes and macrophages and their relationships to infection with the human immunodeficiency virus. *The Journal of General Virology*, 70 (Pt 10):2661–2672, October 1989.

[293] Jane Kelly-Rogers, Laura Madrigal-Estebas, Tony O'Connor, and Derek G. Doherty. Activation-Induced Expression of CD56 by T Cells Is Associated With a Reprogramming of Cytolytic Activity and Cytokine Secretion Profile In Vitro. *Human Immunology*, 67(11):863–873, November 2006.

[294] A. Kelso and A. L. Glasebrook. Secretion of interleukin 2, macrophage-activating factor, interferon, and colony-stimulating factor by alloreactive T lymphocyte clones. *The Journal of Immunology*, 132(6):2924–2931, June 1984.

[295] Aileen Kenneson and Michael J. Cannon. Review and meta-analysis of the epidemiology of congenital cytomegalovirus (CMV) infection. *Reviews in Medical Virology*, 17(4):253–276, 2007.

[296] F. Kern, I. P. Surel, N. Faulhaber, C. Frömmel, J. Schneider-Mergener, C. Schönemann, P. Reinke, and H. D. Volk. Target structures of the CD8(+)-T-cell response to human cytomegalovirus: The 72-kilodalton major immediate-early protein revisited. *Journal of Virology*, 73(10):8179–8184, October 1999.

[297] Florian Kern, Torsten Bunde, Nicole Faulhaber, Felix Kiecker, Elham Khatamzas, Ina-Maria Rudawski, Axel Pruss, Jan-Willem Gratama, Rudolf Volkmer-Engert, Ralf Ewert, Petra Reinke, Hans-Dieter Volk, and Louis J. Picker. Cytomegalovirus (CMV) phosphoprotein 65 makes a large contribution to shaping the T cell repertoire in CMV-exposed individuals. *The Journal of Infectious Diseases*, 185(12):1709–1716, June 2002.

[298] J. A. Kerry, M. A. Priddy, C. P. Kohler, T. L. Staley, D. Weber, T. R. Jones, and R. M. Stenberg. Translational regulation of the human cytomegalovirus pp28 (UL99) late gene. *Journal of Virology*, 71(2):981–987, February 1997.

[299] Lisa R. Keyes, Danna Hargett, Melisa Soland, Mariana G. Bego, Cyprian C. Rossetto, Graca Almeida-Porada, and Stephen St. Jeor. HCMV protein LUNA is required for viral reactivation from latently infected primary CD14+Cells. *PLoS ONE*, 2012.

[300] Naeem Khan, Donna Best, Rachel Bruton, Laxman Nayak, Alan B. Rickinson, and Paul A. H. Moss. T Cell Recognition Patterns of Immunodominant Cytomegalovirus Antigens in Primary and Persistent Infection. *The Journal of Immunology*, 178(7):4455–4465, April 2007.

[301] Supha Kijpittayarit, Albert J. Eid, Robert A. Brown, Carlos V. Paya, and Raymund R. Razonable. Relationship between Toll-Like Receptor 2 Polymorphism and Cytomegalovirus Disease after Liver Transplantation. *Clinical Infectious Diseases*, 44(10):1315–1320, May 2007.

[302] Taeg S. Kim and Thomas J. Braciale. Respiratory dendritic cell subsets differ in their capacity to support the induction of virus-specific cytotoxic CD8+ T cell responses. *PloS One*, 4(1):e4204, 2009.

[303] Christine A. King, Joan Baillie, and John H.YR 2006 Sinclair. Human cytomegalovirus modulation of CCR5 expression on myeloid cells affects susceptibility to human immunodeficiency virus type 1 infection. *Journal of General Virology*, 87(8):2171–2180, August 2006.

[304] Paul Klenerman and Annette Oxenius. T cell responses to cytomegalovirus. *Nature Reviews Immunology*, 2016.

[305] Mirjam Kool, Thomas Soullié, Menno van Nimwegen, Monique A.M. Willart, Femke Muskens, Steffen Jung, Henk C. Hoogsteden, Hamida Hammad, and Bart N. Lambrecht. Alum adjuvant boosts adaptive immunity by inducing uric acid and activating inflammatory dendritic cells. *Journal of Experimental Medicine*, 205(4):869–882, March 2008.

[306] S. V. Kotenko, S. Saccani, L. S. Izotova, O. V. Mirochnitchenko, and S. Pestka. Human cytomegalovirus harbors its own unique IL-10 homolog (cmvIL-10). *Proceedings of the National Academy of Sciences of the United States of America*, 97(4):1695–1700, February 2000.

[307] Sergei V. Kotenko, Grant Gallagher, Vitaliy V. Baurin, Anita Lewis-Antes, Meiling Shen, Nital K. Shah, Jerome A. Langer, Faruk Sheikh, Harold Dickensheets, and Raymond P. Donnelly. IFN-Λs mediate antiviral protection through a distinct class II cytokine receptor complex. *Nature Immunology*, 4(1):69–77, January 2003.

[308] Camille N. Kotton, Deepali Kumar, Angela M. Caliendo, Shirish Huprikar, Sunwen Chou, Lara Danziger-Isakov, Atul Humar, and on behalf of the The Transplantation Society International CMV Consensus Group. The Third International Consensus Guidelines on the Management of Cytomegalovirus in Solid-organ Transplantation. *Transplantation*, 102(6):900–931, June 2018.

[309] Shanna Kowalsky, Ronen Arnon, and Roberto Posada. Prevention of cytomegalovirus following solid organ transplantation: A literature review. *Pediatric Transplantation*, 17(6):499–509, 2013.

[310] Motoko Koyama, Daigo Hashimoto, Kazutoshi Aoyama, Ken-ichi Matsuoka, Kennosuke Karube, Hiroaki Niiro, Mine Harada, Mitsune Tanimoto, Koichi Akashi, and Takanori Teshima. Plasmacytoid dendritic cells prime alloreactive T cells to mediate graft-versus-host disease as antigen-presenting cells. *Blood*, 113(9):2088–2095, February 2009.

[311] H Krause, H Hebart, G Jahn, Ca Müller, and H Einsele. Screening for CMV-specific T cell proliferation to identify patients at risk of developing late onset CMV disease. *Bone Marrow Transplantation*, 19(11):1111–1116, June 1997.

[312] Benjamin A. Krishna, Emma L. Poole, Sarah E. Jackson, Martine J. Smit, Mark R. Wills, and John H. Sinclair. Latency-associated expression of human cytomegalovirus US28 attenuates cell signaling pathways to maintain latent infection. *mBio*, 2017.

[313] Benjamin A. Krishna, Amanda B. Wass, Abigail L. Dooley, and Christine M. O'Connor. CMV-encoded GPCR pUL33 activates CREB and facilitates its recruitment to the MIE locus for efficient viral reactivation. *Journal of Cell Science*, 134(jcs254268), January 2021.

[314] L. Król, J. Stuchlý, P. Hubáček, P. Keslová, P. Sedláček, J. Starý, O. Hrušák, and T. Kalina. Signature profiles of CMV-specific T-cells in patients with CMV reactivation after hematopoietic SCT. *Bone Marrow Transplantation*, 46(8):1089–1098, August 2011.

[315] J. Kruse, R. Mailhammer, H. Wernecke, A. Faissner, I. Sommer, C. Goridis, and M. Schachner. Neural cell adhesion molecules and myelin-associated glycoprotein share a common carbohydrate moiety recognized by monoclonal antibodies L2 and HNK-1. *Nature*, 1984.

[316] Sven Kuenzel, Andreas Till, Michael Winkler, Robert Häsler, Simone Lipinski, Sascha Jung, Joachim Grötzinger, Helmut Fickenscher, Stefan Schreiber, and Philip Rosenstiel. The Nucleotide-Binding Oligomerization Domain-Like Receptor NLRC5 Is Involved in IFN-Dependent Antiviral Immune Responses. *The Journal of Immunology*, 184(4):1990–2000, February 2010.

[317] Deepali Kumar, Peter Chin-Hong, Liise Kayler, David Wojciechowski, Ajit P. Limaye, A. Osama Gaber, Simon Ball, Aneesh K. Mehta, Matthew Cooper, Ted Blanchard, James MacDougall, and Camille N. Kotton. A prospective multicenter observational study of cell-mediated immunity as a predictor for cytomegalovirus infection in kidney transplant recipients. *American Journal of Transplantation*, 19(9):2505–2516, 2019.

[318] Espen Ø. Kvale, Jakob Dalgaard, Fridtjof Lund-Johansen, Halvor Rollag, Lorant Farkas, Karsten Midtvedt, Frode L. Jahnsen, Jan E. Brinchmann, and Johanna Olweus. CD11c+ dendritic cells and plasmacytoid DCs are activated by human cytomegalovirus and retain efficient T cell-stimulatory capability upon infection. *Blood*, 107(5):2022–2029, March 2006.

[319] Corinna La Rosa, Ajit P. Limaye, Aparna Krishnan, Jeff Longmate, and Don J. Diamond. Longitudinal Assessment of Cytomegalovirus (CMV)—Specific Immune Responses in

Liver Transplant Recipients at High Risk for Late CMV Disease. *The Journal of Infectious Diseases*, 195(5):633–644, March 2007.

[320] Raskit Lachmann, Martha Bajwa, Serena Vita, Helen Smith, Elizabeth Cheek, Arne Akbar, and Florian Kern. Polyfunctional T Cells Accumulate in Large Human Cytomegalovirus-Specific T Cell Responses. *Journal of Virology*, 86(2):1001–1009, January 2012.

[321] M. Lanari. Neonatal cytomegalovirus blood load and risk of sequelae in symptomatic and asymptomatic congenitally infected newborns. *Pediatrics*, 2006.

[322] MP Landini, MX Guan, G Jahn, W Lindenmaier, M Mach, A Ripalti, A Necker, T Lazzarotto, and B Plachter. Large-scale screening of human sera with cytomegalovirus recombinant antigens. *Journal of clinical microbiology*, 28(6):1375—1379, June 1990.

[323] Christelle Langlet, Samira Tamoutounour, Sandrine Henri, Hervé Luche, Laurence Ardouin, Claude Grégoire, Bernard Malissen, and Martin Guilliams. CD64 Expression Distinguishes Monocyte-Derived and Conventional Dendritic Cells and Reveals Their Distinct Role during Intramuscular Immunization. *The Journal of Immunology*, 188(4):1751–1760, February 2012.

[324] L. L. Lanier, A. M. Le, J. H. Phillips, N. L. Warner, and G. F. Babcock. Subpopulations of human natural killer cells defined by expression of the Leu-7 (HNK-1) and Leu-11 (NK-15) antigens. *Journal of Immunology (Baltimore, Md.: 1950)*, 131(4):1789–1796, October 1983.

[325] Lewis L. Lanier. Nk Cell Recognition. *Annual Review of Immunology*, 23(1):225–274, 2005.

[326] S. Larsson, C. Soderberg-Naucler, F. Z. Wang, and E. Moller. Cytomegalovirus DNA can be detected in peripheral blood mononuclear cells from all seropositive and most seronegative healthy blood donors over time. *Transfusion*, 38(3):271–278, 1998.

[327] Betty Lau, Emma Poole, Benjamin Krishna, Immaculada Montanuy, Mark R. Wills, Eain Murphy, and John Sinclair. The Expression of Human Cytomegalovirus MicroRNA MiR-UL148D during Latent Infection in Primary Myeloid Cells Inhibits Activin A-triggered Secretion of IL-6. *Scientific Reports*, 6(1):31205, August 2016.

[328] Helen M. Lazear, John W. Schoggins, and Michael S. Diamond. Shared and Distinct Functions of Type I and Type III Interferons. *Immunity*, 50(4):907–923, April 2019.

[329] V. T. K. Le, M. Trilling, and H. Hengel. The cytomegaloviral protein pUL138 acts as potentiator of tumor necrosis factor (TNF) receptor 1 surface density to enhance ULb'-Encoded modulation of TNF- signaling. *Journal of Virology*, 2011.

[330] Andrew W. Lee, Nan Wang, Tara M.C. Hornell, James J. Harding, Chetan Deshpande, Laura Hertel, Vashti Lacaille, Achal Pashine, Claudia Macaubas, Edward S. Mocarski, and Elizabeth D. Mellins. Human cytomegalovirus decreases constitutive transcription of MHC class II genes in mature Langerhans cells by reducing CIITA transcript levels. *Molecular immunology*, 48(9-10):1160–1167, May 2011.

[331] Seong Ok Lee, Sujin Hwang, Junghyun Park, Boyoun Park, Bong Suk Jin, Sungwook Lee, Eunkyung Kim, Sunglim Cho, Youngkyun Kim, Kwangmin Cho, Jinwook Shin, and Kwangseog Ahn. Functional dissection of HCMV US11 in mediating the degradation of MHC class I molecules. *Biochemical and Biophysical Research Communications*, 2005.

[332] Seung-Hwan Lee, Sonia Girard, Denis Macina, Maria Busà, Ahmed Zafer, Abdelmajid Belouchi, Philippe Gros, and Silvia M. Vidal. Susceptibility to mouse cytomegalovirus is associated with deletion of an activating natural killer cell receptor of the C-type lectin superfamily. *Nature Genetics*, 28(1):42–45, May 2001.

[333] Ann M. Leen, Catherine M. Bollard, Adam M. Mendizabal, Elizabeth J. Shpall, Paul Szabolcs, Joseph H. Antin, Neena Kapoor, Sung-Yun Pai, Scott D. Rowley, Partow Kebriaei, Bimalangshu R. Dey, Bambi J. Grilley, Adrian P. Gee, Malcolm K. Brenner, Cliona M. Rooney, and Helen E. Heslop. Multicenter study of banked third-party virus-specific T cells to treat severe viral infections after hematopoietic stem cell transplantation. *Blood*, 121(26):5113–5123, June 2013.

[334] Christian H. K. Lehmann, Anna Baranska, Gordon F. Heidkamp, Lukas Heger, Kirsten Neubert, Jennifer J. Lühr, Alana Hoffmann, Katharina C. Reimer, Christin Brückner, Simone Beck, Michaela Seeling, Melissa Kießling, Didier Soulat, Anne B. Krug, Jeffrey V. Ravetch, Jeanette H. W. Leusen, Falk Nimmerjahn, and Diana Dudziak. DC subset-specific induction of T cell responses upon antigen uptake via Fcγ receptors in vivo. *The Journal of Experimental Medicine*, 214(5):1509–1528, May 2017.

[335] P J Lehner, J T Karttunen, G W Wilkinson, and P Cresswell. The human cytomegalovirus US6 glycoprotein inhibits transporter associated with antigen processing-dependent peptide translocation. *Proceedings of the National Academy of Sciences of the United States of America*, 1997.

[336] Paul J. Lehner, Jaana T. Karttunen, Gavin W. G. Wilkinson, and Peter Cresswell. The human cytomegalovirus US6 glycoprotein inhibits transporter associated with antigen processing-dependent peptide translocation. *Proceedings of the National Academy of Sciences*, 94(13):6904–6909, June 1997.

[337] Josef Leibold, Judith Feucht, Ameli Halder, Stefan Stevanovic, Simone Kayser, Rupert Handgretinger, and Tobias Feuchtinger. Induction of Thelper1-driven Antiviral T-cell

Lines for Adoptive Immunotherapy Is Determined by Differential Expression of IFN-γ and T-cell Activation Markers. *Journal of Immunotherapy*, 35(9):661, November 2012.

[338] Niels A. W. Lemmermann and Matthias J. Reddehase. Refining human T-cell immunotherapy of cytomegalovirus disease: A mouse model with 'humanized' antigen presentation as a new preclinical study tool. *Medical Microbiology and Immunology*, 205(6):549–561, December 2016.

[339] Karl Lennert and Wolfgang Remmele. Karyometrische Untersuchungen an Lymphknotenzellen des Menschen. *Acta Haematologica*, 19(2):99–113, 1958.

[340] Josh Levitsky, Alison G. Freifeld, Susan Puumala, Kim Bargenquast, Penny Hardiman, Catherine Gebhart, Lucy Wrenshall, Alan Langnas, and Andre C. Kalil. Cytomegalovirus viremia in solid organ transplantation: Does the initial viral load correlate with risk factors and outcomes? *Clinical Transplantation*, 22(2):222–228, 2008.

[341] C. R. Li, P. D. Greenberg, M. J. Gilbert, J. M. Goodrich, and S. R. Riddell. Recovery of HLA-restricted cytomegalovirus (CMV)-specific T-cell responses after allogeneic bone marrow transplant: Correlation with CMV disease and effect of ganciclovir prophylaxis. *Blood*, 83(7):1971–1979, April 1994.

[342] Tuo Li, Jin Chen, and Ileana M. Cristea. Human Cytomegalovirus Tegument Protein pUL83 Inhibits IFI16-Mediated DNA Sensing for Immune Evasion. *Cell Host & Microbe*, 14(5):591–599, November 2013.

[343] Wei Liao, Jian-Xin Lin, and Warren J. Leonard. IL-2 Family Cytokines: New Insights into the Complex Roles of IL-2 as a Broad Regulator of T helper Cell Differentiation. *Current Opinion in Immunology*, 23(5):598–604, October 2011.

[344] A. K. Lidehäll, M.-L. Engman, F. Sund, G. Malm, I. Lewensohn-Fuchs, U. Ewald, T. H. Tötterman, E. Karltorp, O. Korsgren, and B.-M. Eriksson. Cytomegalovirus-Specific CD4 and CD8 T Cell Responses in Infants and Children. *Scandinavian Journal of Immunology*, 77(2):135–143, 2013.

[345] D. Lilleri, P. Zelini, C. Fornara, G. Comolli, and G. Gerna. Inconsistent Responses of Cytomegalovirus-Specific T Cells to pp65 and IE-1 versus Infected Dendritic Cells in Organ Transplant Recipients. *American Journal of Transplantation*, 7(8):1997–2005, 2007.

[346] Daniele Lilleri, Chiara Fornara, Antonella Chiesa, Daniela Caldera, Emilio Paolo Alessandrino, and Giuseppe Gerna. Human cytomegalovirus-specific CD4+ and CD8+ T-cell reconstitution in adult allogeneic hematopoietic stem cell transplant recipients and immune control of viral infection. *Haematologica*, 93(2):248–256, February 2008.

[347] Daniele Lilleri, Chiara Fornara, Milena Furione, Maurizio Zavattoni, Maria Grazia Revello, and Guiseppe Gerna. Development of Human Cytomegalovirus—Specific T Cell Immunity during Primary Infection of Pregnant Women and Its Correlation with Virus Transmission to the Fetus. *The Journal of Infectious Diseases*, 195(7):1062–1070, April 2007.

[348] Daniele Lilleri, Chiara Fornara, Maria Grazia Revello, and Giuseppe Gerna. Human Cytomegalovirus-specific Memory CD8+ and CD4+ T Cell Differentiation after Primary Infection. *The Journal of Infectious Diseases*, 198(4):536–543, August 2008.

[349] Daniele Lilleri, Giuseppe Gerna, Chiara Fornara, Laura Lozza, Rita Maccario, and Franco Locatelli. Prospective simultaneous quantification of human cytomegalovirus-specific CD4+ and CD8+ T-cell reconstitution in young recipients of allogeneic hematopoietic stem cell transplants. *Blood*, 108(4):1406–1412, August 2006.

[350] Daniele Lilleri, Anna Kabanova, Maria Grazia Revello, Elena Percivalle, Antonella Sarasini, Emilia Genini, Federica Sallusto, Antonio Lanzavecchia, Davide Corti, and Giuseppe Gerna. Fetal Human Cytomegalovirus Transmission Correlates with Delayed Maternal Antibodies to gH/gL/pUL128-130-131 Complex during Primary Infection. *PLoS ONE*, 8(3), March 2013.

[351] Daniele Lilleri, Paola Zelini, Chiara Fornara, Federica Zavaglio, Teresa Rampino, Laurent Perez, Elisa Gabanti, and Giuseppe Gerna. Human cytomegalovirus (HCMV)-specific T cell but not neutralizing or IgG binding antibody responses to glycoprotein complexes gB, gHgLgO, and pUL128L correlate with protection against high HCMV viral load reactivation in solid-organ transplant recipients. *Journal of Medical Virology*, 90(10):1620–1628, October 2018.

[352] Eleanor Y. Lim, Sarah E. Jackson, and Mark R. Wills. The CD4+ T Cell Response to Human Cytomegalovirus in Healthy and Immunocompromised People. *Frontiers in Cellular and Infection Microbiology*, 10, 2020.

[353] Ajit P. Limaye, Margaret L. Green, Bradley C. Edmison, Terry Stevens-Ayers, Sam Chatterton-Kirchmeier, Adam P. Geballe, Nina Singh, and Michael Boeckh. Prospective Assessment of Cytomegalovirus Immunity in High-Risk Donor-Seropositive/Recipient-Seronegative Liver Transplant Recipients Receiving Either Preemptive Therapy or Antiviral Prophylaxis. *The Journal of Infectious Diseases*, 220(5):752–760, July 2019.

[354] Brett D Lindenbach. Chapter 24 measuring HCV infectivity produced in cell culture and in vivo. *Hepatitis C: Methods and Protocols*, 2009.

[355] M. D. Lindsley, D. J. Torpey, and C. R. Rinaldo. HLA-DR-restricted cytotoxicity of cytomegalovirus-infected monocytes mediated by Leu-3-positive T cells. *Journal of Immunology (Baltimore, Md.: 1950)*, 136(8):3045–3051, April 1986.

[356] Chan-Wang J. Lio, Bryan McDonald, Mariko Takahashi, Rekha Dhanwani, Nikita Sharma, Jenny Huang, Elise Pham, Chris A. Benedict, and Sonia Sharma. cGAS-STING Signaling Regulates Initial Innate Control of Cytomegalovirus Infection. *Journal of Virology*, 90(17):7789–7797, September 2016.

[357] Nicolle H. R. Litjens, Ling Huang, Burç Dedeoglu, Ruud W. J. Meijers, Jaap Kwekkeboom, and Michiel G. H. Betjes. Protective Cytomegalovirus (CMV)-Specific T-Cell Immunity Is Frequent in Kidney Transplant Patients without Serum Anti-CMV Antibodies. *Frontiers in Immunology*, 8, 2017.

[358] Hans-Gustaf Ljunggren and Klas Kärre. In search of the 'missing self': MHC molecules and NK cell recognition. *Immunology Today*, 11:237–244, January 1990.

[359] R. M. Locksley, S. L. Reiner, F. Hatam, D. R. Littman, and N. Killeen. Helper T cells without CD4: Control of leishmaniasis in CD4-deficient mice. *Science*, 261(5127):1448–1451, September 1993.

[360] Maria Ovidia López-Oliva, Virginia Martinez, Agueda Buitrago, Carlos Jiménez, Begoña Rivas, Fernando Escuin, María José Santana, Rafael Selgas, and Teresa Bellón. Pretransplant CD8 T-cell response to IE-1 discriminates seropositive kidney recipients at risk of developing CMV infection posttransplant. *Transplantation*, 97(8):839–845, April 2014.

[361] Sandra Lopez-Vergès, Jeffrey M Milush, Suchitra Pandey, Vanessa a York, Janice Arakawa-Hoyt, Hanspeter Pircher, Phillip J Norris, Douglas F Nixon, and Lewis L Lanier. CD57 defines a functionally distinct population of mature NK cells in the human CD56dimCD16+ NK cell subset. *Blood*, 2010.

[362] Sandra Lopez-Vergès, Jeffrey M. Milush, Brian S. Schwartz, Marcelo J. Pando, Jessica Jarjoura, Vanessa A. York, Jeffrey P. Houchins, Steve Miller, Sang-Mo Kang, Phillip J. Norris, Douglas F. Nixon, and Lewis L. Lanier. Expansion of a unique CD57+NKG2Chi natural killer cell subset during acute human cytomegalovirus infection. *Proceedings of the National Academy of Sciences*, 108(36):14725–14732, September 2011.

[363] F Louache, N Debili, A Marandin, L Coulombel, and W Vainchenker. Expression of CD4 by human hematopoietic progenitors [see comments]. *Blood*, 84(10):3344–3355, November 1994.

[364] Bente Lowin, Michael Hahne, Chantal Mattmann, and Jürg Tschopp. Cytolytic T-cell cytotoxicity is mediated through perforin and Fas lytic pathways. *Nature*, 370(6491):650–652, August 1994.

[365] Rishi Vishal Luckheeram, Rui Zhou, Asha Devi Verma, and Bing Xia. CD4+T Cells: Differentiation and Functions. *Clinical and Developmental Immunology*, 2012, 2012.

[366] Yvonne Lueder, Katrin Heller, Christiane Ritter, Kirsten A. Keyser, Karen Wagner, Xiaokun Liu, Martin Messerle, Felix R. Stahl, Stephan Halle, and Reinhold Förster. Control of primary mouse cytomegalovirus infection in lung nodular inflammatory foci by cooperation of interferon-gamma expressing CD4 and CD8 T cells. *PLOS Pathogens*, 14(8):e1007252, August 2018.

[367] Vera Lukashchuk, Steven McFarlane, Roger D. Everett, and Chris M. Preston. Human Cytomegalovirus Protein pp71 Displaces the Chromatin-Associated Factor ATRX from Nuclear Domain 10 at Early Stages of Infection. *Journal of Virology*, 82(24):12543–12554, December 2008.

[368] C. Lumbreras, O. Manuel, O. Len, I. J. M. ten Berge, D. Sgarabotto, and H. H. Hirsch. Cytomegalovirus infection in solid organ transplant recipients. *Clinical Microbiology and Infection*, 20:19–26, September 2014.

[369] H. A. Lumgair, N. Rolando, J. O'Beirne, D. Sharma, and P. D. Griffiths. Transient residence of a seropositive organ is sufficient to transfer human cytomegalovirus to a seronegative recipient. *Transplant Infectious Disease: An Official Journal of the Transplantation Society*, 16(3):501–504, June 2014.

[370] Manfred B Lutz, Nicole Kukutsch, Alexandra L. J Ogilvie, Susanne Rößner, Franz Koch, Nikolaus Romani, and Gerold Schuler. An advanced culture method for generating large quantities of highly pure dendritic cells from mouse bone marrow. *Journal of Immunological Methods*, 223(1):77–92, February 1999.

[371] Kelli P. A. MacDonald, David J. Munster, Georgina J. Clark, Andrzej Dzionek, Juergen Schmitz, and Derek N. J. Hart. Characterization of human blood dendritic cell subsets. *Blood*, 100(13):4512–4520, December 2002.

[372] John D. MacMicking. Interferon-inducible effector mechanisms in cell-autonomous immunity. *Nature Reviews Immunology*, 12(5):367–382, May 2012.

[373] Edward De Maeyer and Jaqueline De Maeyer-Guignard. Type I Interferons. *International Reviews of Immunology*, July 2009.

[374] Karl-Johan Malmberg, Vivien Beziat, and Hans-Gustaf Ljunggren. Spotlight on NKG2C and the human NK-cell response to CMV infection. *European Journal of Immunology*, 42(12):3141–3145, December 2012.

[375] Arundhati Mandal and Chandra Viswanathan. Natural killer cells: In health and disease. *Hematology/Oncology and Stem Cell Therapy*, 8(2):47–55, June 2015.

[376] O. Mandelboim, P. Malik, D.M. Davis, C.H. Jo, J.E. Boyson, and J.L. Strominger. Human CD16 as a lysis receptor mediating direct natural killer cell cytotoxicity. *Proceedings of the National Academy of Sciences of the United States of America*, 96(10):5640–5644, 1999.

[377] Anna Mania, Paweł Kemnitz, Kamila Cudnoch, Katarzyna Mazur-Melewska, Magdalena Figlerowicz, and Wojciech Służewski. Clinical condition and transmission of coinfections with human cytomegalovirus in infants of HIV-1 infected mothers in the era of mother-to-child-transmission prophylaxis. *Early Human Development*, 89(2):119–124, February 2013.

[378] Oriol Manuel, Xiaoli L. Pang, Atul Humar, Deepali Kumar, Karen Doucette, and Jutta K. Preiksaitis. An Assessment of Donor-to-Recipient Transmission Patterns of Human Cytomegalovirus by Analysis of Viral Genomic Variants. *The Journal of Infectious Diseases*, 199(11):1621–1628, June 2009.

[379] Rekha Marimuthu, Habib Francis, Suat Dervish, Stephen C.H. Li, Heather Medbury, and Helen Williams. Characterization of Human Monocyte Subsets by Whole Blood Flow Cytometry Analysis. *Journal of Visualized Experiments : JoVE*, (140), October 2018.

[380] Sabrina Mariotti, Valeria Sargentini, Cinzia Marcantonio, Emiliano Todero, Raffaela Teloni, Maria Cristina Gagliardi, Anna Rita Ciccaglione, and Roberto Nisini. T-cell-mediated and antigen-dependent differentiation of human monocyte into different dendritic cell subsets: A feedback control of Th1/Th2 responses. *The FASEB Journal*, 22(9):3370–3379, 2008.

[381] Gavin M. Mason, Sarah Jackson, Georgina Okecha, Emma Poole, J. G. Patrick Sissons, John Sinclair, and Mark R. Wills. Human Cytomegalovirus Latency-Associated Proteins Elicit Immune-Suppressive IL-10 Producing CD4+ T Cells. *PLOS Pathogens*, 9(10):e1003635, October 2013.

[382] Errin O Matechak, Nigel Killeen, Stephen M Hedrick, and B. J Fowlkes. MHC Class II–Specific T Cells Can Develop in the CD8 Lineage When CD4 Is Absent. *Immunity*, 4(4):337–347, April 1996.

[383] F. M. Mattes, E. G. Hainsworth, A. F. Hassan Walker, A. K. Burroughs, P. Sweny, P. D. Griffiths, and V. C. Emery. Kinetics of Cytomegalovirus Load Decrease in Solid-Organ Transplant Recipients after Preemptive Therapy with Valganciclovir. *The Journal of Infectious Diseases*, 191(1):89–92, January 2005.

[384] Atibordee Meesing, Roshini S. Abraham, and Raymund R. Razonable. Clinical Correlation of Cytomegalovirus Infection With CMV-specific CD8+ T-cell Immune Competence Score and Lymphocyte Subsets in Solid Organ Transplant Recipients. *Transplantation*, 103(4):832–838, April 2019.

[385] Atibordee Meesing and Raymund R. Razonable. New Developments in the Management of Cytomegalovirus Infection After Transplantation. *Drugs*, 78(11):1085–1103, July 2018.

[386] Federico Mele, Chiara Fornara, David Jarrossay, Milena Furione, Alessia Arossa, Arsenio Spinillo, Antonio Lanzavecchia, Giuseppe Gerna, Federica Sallusto, and Daniele Lilleri. Phenotype and specificity of T cells in primary human cytomegalovirus infection during pregnancy: IL-7Rpos long-term memory phenotype is associated with protection from vertical transmission. *PLOS ONE*, 12(11):e0187731, November 2017.

[387] Juan Damián Mena-Romo, Pilar Pérez Romero, Cecilia Martín-Gandul, Miguel Ángel Gentil, Gonzalo Suárez-Artacho, Ernesto Lage, Magdalena Sánchez, and Elisa Cordero. CMV-specific T-cell immunity in solid organ transplant recipients at low risk of CMV infection. Chronology and applicability in preemptive therapy. *Journal of Infection*, 75(4):336–345, October 2017.

[388] Marc Mendelson, Simon Monard, Patrick Sissons, and John Sinclair. Detection of endogenous human cytomegalovirus in CD34+bone marrow progenitors. *Journal of General Virology*, 1996.

[389] Matthew M. Meredith, Kang Liu, Guillaume Darrasse-Jeze, Alice O. Kamphorst, Heidi A. Schreiber, Pierre Guermonprez, Juliana Idoyaga, Cheolho Cheong, Kai-Hui Yao, Rachel E. Niec, and Michel C. Nussenzweig. Expression of the zinc finger transcription factor zDC (Zbtb46, Btbd4) defines the classical dendritic cell lineage. *The Journal of Experimental Medicine*, 209(6):1153–1165, June 2012.

[390] Mesfin K. Meshesha, Zvi Bentwich, Semaria A. Solomon, and Yonat Shemer Avni. In vivo expression of human cytomegalovirus (HCMV) microRNAs during latency. *Gene*, 575(1):101–107, January 2016.

[391] H H Meyer, A Ripalti, M P Landini, K Radsak, H F Kern, and G M Hensel. Human cytomegalovirus late-phase maturation is blocked by stably expressed UL32 antisense mRNA in astrocytoma cells. *Journal of General Virology*, 78(10):2621–2631, 1997.

[392] Charles Millson, Aisling Considine, Matthew E. Cramp, Andrew Holt, Stefan Hubscher, John Hutchinson, Kate Jones, Joanna Leithead, Steven Masson, Krish Menon, Darius Mirza, James Neuberger, Raj Prasad, Anthony Pratt, Wendy Prentice, Liz Shepherd, Ken Simpson, Doug Thorburn, Rachel Westbrook, and Dhiraj Tripathi. Adult liver transplantation: UK clinical guideline - part 2: Surgery and post-operation. *Frontline Gastroenterology*, 11(5):385–396, September 2020.

[393] Hans-Willi Mittrücker, Alexander Visekruna, and Magdalena Huber. Heterogeneity in the Differentiation and Function of CD8+ T Cells. *Archivum Immunologiae et Therapiae Experimentalis*, 62(6):449–458, December 2014.

[394] Edward S. Mocarski. Betaherpes viral genes and their functions. In *Human Herpesviruses: Biology, Therapy, and Immunoprophylaxis*. Cambridge University Press, Cambridge, 2007.

[395] Edward S. Mocarski, Lenore Pereira, and A. LouiseYR 1988 McCormick. Human Cytomegalovirus ICP22, the Product of the HWLF1 Reading Frame, Is an Early Nuclear Protein that Is Released from Cells. *Journal of General Virology*, 69(10):2613–2621, October 1988.

[396] Edward S Mocarski, Thomas Shenk, and Robert F Pass. Cytomegaloviruses. In *Fields Virology*. 2007.

[397] Jessica M Moffat, Justine D Mintern, and Jose A Villadangos. Control of MHC II antigen presentation by ubiquitination. *Current Opinion in Immunology*, 25(1):109–114, February 2013.

[398] Elisa Montaldo, Genny Del Zotto, Mariella Della Chiesa, Maria Cristina Mingari, Alessandro Moretta, Andrea De Maria, and Lorenzo Moretta. Human NK cell receptors/markers: A tool to analyze NK cell development, subsets and function. *Cytometry Part A*, 83A(8):702–713, 2013.

[399] Alessandro Moretta, Cristina Bottino, Massimo Vitale, Daniela Pende, Claudia Cantoni, Maria Cristina Mingari, Roberto Biassoni, and Lorenzo Moretta. Activating Receptors and Coreceptors Involved in Human Natural Killer Cell-Mediated Cytolysis. *Annual Review of Immunology*, 19(1):197–223, April 2001.

[400] T. R. Mosmann, H. Cherwinski, M. W. Bond, M. A. Giedlin, and R. L. Coffman. Two types of murine helper T cell clone. I. Definition according to profiles of lymphokine activities and secreted proteins. *The Journal of Immunology*, 136(7):2348–2357, April 1986.

[401] Magdalena Moutaftsi, Paul Brennan, Stephen A. Spector, and Zsuzsanna Tabi. Impaired Lymphoid Chemokine-Mediated Migration due to a Block on the Chemokine Receptor Switch in Human Cytomegalovirus-Infected Dendritic Cells. *Journal of Virology*, 78(6):3046–3054, March 2004.

[402] Annick Muhlethaler-Mottet, Wilma Di Berardino, Luc A. Otten, and Bernard Mach. Activation of the MHC Class II Transactivator CIITA by Interferon-γ Requires Cooperative Interaction between Stat1 and USF-1. *Immunity*, 8(2):157–166, February 1998.

[403] E. Murphy and Thomas E. Shenk. Human cytomegalovirus genome. *Current Topics in Microbiology and Immunology*, 2008.

[404] Jane C. Murphy, Wolfgang Fischle, Eric Verdin, and John H. Sinclair. Control of cytomegalovirus lytic gene expression by histone acetylation. *EMBO Journal*, 2002.

[405] D. Myerson, R. C. Hackman, J. A. Nelson, D. C. Ward, and J. K. McDougall. Widespread presence of histologically occult cytomegalovirus. *Human Pathology*, 15(5):430–439, May 1984.

[406] Daphna Nachmani, Albert Zimmermann, Esther Oiknine Djian, Yiska Weisblum, Yoav Livneh, Vu Thuy Khanh Le, Eithan Galun, Vaclav Horejsi, Ofer Isakov, Noam Shomron, Dana G. Wolf, Hartmut Hengel, and Ofer Mandelboim. MicroRNA Editing Facilitates Immune Elimination of HCMV Infected Cells. *PLOS Pathogens*, 10(2):e1003963, February 2014.

[407] Faramarz Naeim, P. Nagesh Rao, Sophie X. Song, and Ryan T. Phan. Chapter 2 - Principles of Immunophenotyping. In Faramarz Naeim, P. Nagesh Rao, Sophie X. Song, and Ryan T. Phan, editors, *Atlas of Hematopathology (Second Edition)*, pages 29–56. Academic Press, January 2018.

[408] Hideki Nakano, Kaifeng Lisa Lin, Manabu Yanagita, Chantal Charbonneau, Donald N. Cook, Terutaka Kakiuchi, and Michael D. Gunn. Blood-derived inflammatory dendritic cells in lymph nodes stimulate acute T helper type 1 immune responses. *Nature Immunology*, 10(4):394–402, April 2009.

[409] Yoichiro Natori, Atul Humar, Shahid Husain, Coleman Rotstein, Eberhard Renner, Lianne Singer, S. Joseph Kim, and Deepali Kumar. Recurrence of CMV Infection and the Effect of Prolonged Antivirals in Organ Transplant Recipients. *Transplantation*, 101(6):1449–1454, June 2017.

[410] G. Nebbia, F. M. Mattes, C. Smith, E. Hainsworth, J. Kopycinski, A. Burroughs, P. D. Griffiths, P. Klenerman, and V. C. Emery. Polyfunctional Cytomegalovirus-Specific CD4+ and pp65 CD8+ T Cells Protect Against High-Level Replication After Liver

Transplantation. *American Journal of Transplantation*, 8(12):2590–2599, December 2008.

[411] Jacques Neefjes, Marlieke L. M. Jongsma, Petra Paul, and Oddmund Bakke. Towards a systems understanding of MHC class I and MHC class II antigen presentation. *Nature Reviews Immunology*, 11(12):823–836, December 2011.

[412] M. Neuenhahn, J. Albrecht, M. Odendahl, F. Schlott, G. Dössinger, M. Schiemann, S. Lakshmipathi, K. Martin, D. Bunjes, S. Harsdorf, E. M. Weissinger, H. Menzel, M. Verbeek, L. Uharek, N. Kröger, E. Wagner, G. Kobbe, T. Schroeder, M. Schmitt, G. Held, W. Herr, L. Germeroth, H. Bonig, T. Tonn, H. Einsele, D. H. Busch, and G. U. Grigoleit. Transfer of minimally manipulated CMV-specific T cells from stem cell or third-party donors to treat CMV infection after allo-HSCT. *Leukemia*, 31(10):2161–2171, October 2017.

[413] Natalie E. Nierenberg, Debra D. Poutsiaka, Jennifer K. Chow, Jeffrey Cooper, Lori Lyn Price, Richard B. Freeman, Richard Rohrer, and David R. Snydman. Pretransplant lymphopenia is a novel prognostic factor in cytomegalovirus and noncytomegalovirus invasive infections after liver transplantation. *Liver Transplantation*, 20(12):1497–1507, 2014.

[414] Kei Numazaki, Tomoko Fujikawa, and Hideomi Asanuma. Immunological evaluation and clinical aspects of children with congenital cytomegalovirus infection. *Congenital Anomalies*, 42(3):181–186, September 2002.

[415] U O'Doherty, M Peng, S Gezelter, W J Swiggard, M Betjes, N Bhardwaj, and R M Steinman. Human blood contains two subsets of dendritic cells, one immunologically mature and the other immature. *Immunology*, 82(3):487–493, July 1994.

[416] Mari Ohmura-Hoshino, Yohei Matsuki, Masami Aoki, Eiji Goto, Mari Mito, Mika Uematsu, Terutaka Kakiuchi, Hak Hotta, and Satoshi Ishido. Inhibition of MHC Class II Expression and Immune Responses by c-MIR. *The Journal of Immunology*, 177(1):341–354, July 2006.

[417] Anna E. Oja, Felipe A. Vieira Braga, Ester B. M. Remmerswaal, Natasja A. M. Kragten, Kirsten M. L. Hertoghs, Jianmin Zuo, Paul A. Moss, René A. W. van Lier, Klaas P. J. M. van Gisbergen, and Pleun Hombrink. The Transcription Factor Hobit Identifies Human Cytotoxic CD4+ T Cells. *Frontiers in Immunology*, 8, 2017.

[418] Shinya Omoto and Edward S. Mocarski. Transcription of True Late ($\Gamma 2$) Cytomegalovirus Genes Requires UL92 Function That Is Conserved among Beta- and Gammaherpesviruses. *Journal of Virology*, 88(1):120–130, January 2014.

[419] Jordan S Orange. Human natural killer cell deficiencies and susceptibility to infection. *Microbes and Infection*, 4(15):1545–1558, 2002.

[420] Annette Pachnio, Miriam Ciaurriz, Jusnara Begum, Neeraj Lal, Jianmin Zuo, Andrew Beggs, and Paul Moss. Cytomegalovirus Infection Leads to Development of High Frequencies of Cytotoxic Virus-Specific CD4+ T Cells Targeted to Vascular Endothelium. *PLOS Pathogens*, 12(9):e1005832, September 2016.

[421] Annette Pachnio, Jianmin Zuo, Gordon B. Ryan, Jusnara Begum, and Paul A. H. Moss. The Cellular Localization of Human Cytomegalovirus Glycoprotein Expression Greatly Influences the Frequency and Functional Phenotype of Specific CD4+ T Cell Responses. *The Journal of Immunology*, 195(8):3803–3815, October 2015.

[422] Aurora Páez-Vega, Antonio Poyato, Alberto Rodriguez-Benot, Lluis Guirado, Jesús Fortún, Oscar Len, Edson Abdala, María C. Fariñas, Elisa Cordero, Carmen de Gracia, Domingo Hernández, Rafael González, Julián Torre-Cisneros, Sara Cantisán, Aurora Páez-Vega, Alberto Rodriguez-Benot, Jesús Fortún, Oscar Len, María C. Fariñas, Elisa Cordero, Julián Torre-Cisneros, Alberto Rodriguez-Benot, Lluis Guirado, and Domingo Hernández. Analysis of spontaneous resolution of cytomegalovirus replication after transplantation in CMV-seropositive patients with pretransplant CD8+IFNG+ response. *Antiviral Research*, 155:97–105, July 2018.

[423] Jennifer Paijo, Marius Döring, Julia Spanier, Elena Grabski, Mohammed Nooruzzaman, Tobias Schmidt, Gregor Witte, Martin Messerle, Veit Hornung, Volkhard Kaever, and Ulrich Kalinke. cGAS Senses Human Cytomegalovirus and Induces Type I Interferon Responses in Human Monocyte-Derived Cells. *PLOS Pathogens*, 12(4):e1005546, April 2016.

[424] Chaoyun Pan, Dihan Zhu, Yan Wang, Limin Li, Donghai Li, Fenyong Liu, Chen-Yu Zhang, and Ke Zen. Human Cytomegalovirus miR-UL148D Facilitates Latent Viral Infection by Targeting Host Cell Immediate Early Response Gene 5. *PLoS pathogens*, 12(11):e1006007, November 2016.

[425] G. S. Pari. Nuts and bolts of human cytomegalovirus lytic DNA replication. *Current Topics in Microbiology and Immunology*, 2008.

[426] G. S. Pari, M. A. Kacica, and D. G. Anders. Open reading frames UL44, IRS1/TRS1, and UL36-38 are required for transient complementation of human cytomegalovirus oriLyt-dependent DNA synthesis. *Journal of Virology*, 67(5):2575–2582, May 1993.

[427] Boyoun Park, Eric Spooner, Brandy L. Houser, Jack L. Strominger, and Hidde L. Ploegh. The HCMV membrane glycoprotein US10 selectively targets HLA-G for degradation. *Journal of Experimental Medicine*, 207(9):2033–2041, August 2010.

[428] Robert F. Pass, Changpin Zhang, Ashley Evans, Tina Simpson, William Andrews, Meei-Li Huang, Lawrence Corey, Janie Hill, Elizabeth Davis, Cynthia Flanigan, and Gretchen Cloud. Vaccine Prevention of Maternal Cytomegalovirus Infection. *New England Journal of Medicine*, 360(12):1191–1199, March 2009.

[429] S. S. Patel, A. D. Duby, D. L. Thiele, and P. E. Lipsky. Phenotypic and functional characterization of human T cell clones. *The Journal of Immunology*, 141(11):3726–3736, December 1988.

[430] Marco Patrone, Massimiliano Secchi, Eleonora Bonaparte, Gabriele Milanesi, and Andrea Gallina. Cytomegalovirus UL131-128 Products Promote gB Conformational Transition and gB-gH Interaction during Entry into Endothelial Cells. *Journal of Virology*, 81(20):11479–11488, October 2007.

[431] C E Patterson and T Shenk. Human cytomegalovirus UL36 protein is dispensable for viral replication in cultured cells. *Journal of virology*, 73(9):7126–7131, 1999.

[432] Steven Patterson, Jacqueline Gross, Nicholas English, Arthur Stackpoole, Penelope Bedford, and Stella C.YR 1995 Knight. CD4 expression on dendritic cells and their infection by human immunodeficiency virus. *Journal of General Virology*, 76(5):1155–1163, May 1995.

[433] Franciane Paul, Sandra Pellegrini, and Gilles Uzé. IFNA2: The prototypic human alpha interferon. *Gene*, 567(2):132–137, August 2015.

[434] Jay S. Pepose, Cheryl Newman, Michael C. Bach, Thomas C. Quinn, Richard F. Ambinder, Gary N. Holland, Peter S. Hodstrom, Henry M. Frey, and Robert Y. Foos. Pathologic Features of Cytomegalovirus Retinopathy after Treatment with the Antiviral Agent Ganciclovir. *Ophthalmology*, 94(4):414–424, April 1987.

[435] Emma K. Persson, Heli Uronen-Hansson, Monika Semmrich, Aymeric Rivollier, Karin Hägerbrand, Jan Marsal, Sigurdur Gudjonsson, Ulf Håkansson, Boris Reizis, Knut Kotarsky, and William W. Agace. IRF4 Transcription-Factor-Dependent CD103+CD11b+ Dendritic Cells Drive Mucosal T Helper 17 Cell Differentiation. *Immunity*, 38(5):958–969, May 2013.

[436] David H. Peters, Andrew Fitton, Greg L. Plosker, and Diana Faulds. Tacrolimus. *Drugs*, 46(4):746–794, October 1993.

[437] Minh-Trang Phan, Sejong Chun, Sun-Hee Kim, Alaa Kassim Ali, Seung-Hwan Lee, Seokho Kim, Soo-Hyun Kim, and Duck Cho. Natural killer cell subsets and receptor expression in peripheral blood mononuclear cells of a healthy Korean population: Reference range, influence of age and sex, and correlation between NK cell receptors and cytotoxicity. *Human Immunology*, 78(2):103–112, February 2017.

[438] Paola Pierucci, Monique Malouf, Allan R. Glanville, Leone Beagley, Corey Smith, and Rajiv Khanna. Novel autologous T-cell therapy for drug-resistant cytomegalovirus disease after lung transplantation. *The Journal of Heart and Lung Transplantation*, 35(5):685–687, May 2016.

[439] Matthew R. Pipeling, Emily R. John, Jonathan B. Orens, Noah Lechtzin, and John F. McDyer. Primary cytomegalovirus phosphoprotein 65-specific CD8+ T-cell responses and T-bet levels predict immune control during early chronic infection in lung transplant recipients. *The Journal of Infectious Diseases*, 204(11):1663–1671, December 2011.

[440] Hidde L. Ploegh. Viral Strategies of Immune Evasion. *Science*, 280(5361):248–253, April 1998.

[441] S A Plotkin, T Furukawa, N Zygraich, and C Huygelen. Candidate cytomegalovirus strain for human vaccination. *Infection and Immunity*, 12(3):521–527, September 1975.

[442] E. R. Podack. Molecular mechanisms of cytolysis by complement and by cytolytic lymphocytes. *Journal of Cellular Biochemistry*, 30(2):133–170, 1986.

[443] E R Podack and P J Konigsberg. Cytolytic T cell granules. Isolation, structural, biochemical, and functional characterization. *Journal of Experimental Medicine*, 160(3):695–710, September 1984.

[444] J. Podlech, R. Holtappels, N. Wirtz, H. P. Steffens, and M. J. Reddehase. Reconstitution of CD8 T cells is essential for the prevention of multiple-organ cytomegalovirus histopathology after bone marrow transplantation. *The Journal of General Virology*, 79 (Pt 9):2099–2104, September 1998.

[445] Jürgen Podlech, Rafaela Holtappels, Marcus-Folker Pahl-Seibert, Hans-Peter Steffens, and Matthias J. Reddehase. Murine Model of Interstitial Cytomegalovirus Pneumonia in Syngeneic Bone Marrow Transplantation: Persistence of Protective Pulmonary CD8-T-Cell Infiltrates after Clearance of Acute Infection. *Journal of Virology*, 74(16):7496–7507, August 2000.

[446] Hendrik Poeck, Moritz Wagner, Julia Battiany, Simon Rothenfusser, Daniela Wellisch, Veit Hornung, Bernd Jahrsdorfer, Thomas Giese, Stefan Endres, and Gunther Hartmann. Plasmacytoid dendritic cells, antigen, and CpG-C license human B cells for plasma cell differentiation and immunoglobulin production in the absence of T-cell help. *Blood*, 103(8):3058–3064, April 2004.

[447] Bojan Polić, Hartmut Hengel, Astrid Krmpotić, Joanne Trgovcich, Ivica Pavić, Pero Lučin, Stipan Jonjić, and Ulrich H. Koszinowski. Hierarchical and Redundant Lymphocyte Subset Control Precludes Cytomegalovirus Replication during Latent Infection. *The Journal of Experimental Medicine*, 188(6):1047–1054, September 1998.

[448] E. Poole, A. Walther, K. Raven, C. A. Benedict, G. M. Mason, and J. Sinclair. The myeloid transcription factor GATA-2 regulates the viral UL144 gene during human cytomegalovirus latency in an isolate-specific manner. *Journal of Virology*, 2013.

[449] Emma Poole, Selmir Avdic, Jemima Hodkinson, Sarah Jackson, Mark Wills, Barry Slobedman, and John Sinclair. Latency-associated viral interleukin-10 (IL-10) encoded by human cytomegalovirus modulates cellular IL-10 and CCL8 Secretion during latent infection through changes in the cellular microRNA hsa-miR-92a. *Journal of Virology*, 88(24):13947–13955, December 2014.

[450] Emma Poole, Ian Groves, Sarah Jackson, Mark Wills, and John Sinclair. Using Primary Human Cells to Analyze Human Cytomegalovirus Biology. In Andrew D. Yurochko, editor, *Human Cytomegaloviruses: Methods and Protocols*, Methods in Molecular Biology, pages 51–81. Springer US, New York, NY, 2021.

[451] Emma Poole, Matthew Reeves, and John H. Sinclair. The Use of Primary Human Cells (Fibroblasts, Monocytes, and Others) to Assess Human Cytomegalovirus Function. In Andrew D. Yurochko and William E. Miller, editors, *Human Cytomegaloviruses: Methods and Protocols*, Methods in Molecular Biology, pages 81–98. Humana Press, Totowa, NJ, 2014.

[452] B. Pourgheysari, K. P. Piper, A. McLarnon, J. Arrazi, R. Bruton, F. Clark, M. Cook, P. Mahendra, C. Craddock, and P. a. H. Moss. Early reconstitution of effector memory CD4+ CMV-specific T cells protects against CMV reactivation following allogeneic SCT. *Bone Marrow Transplantation*, 43(11):853–861, June 2009.

[453] Batoul Pourgheysari, Naeem Khan, Donna Best, Rachel Bruton, Laxman Nayak, and Paul A. H. Moss. The Cytomegalovirus-Specific CD4+ T-Cell Response Expands with Age and Markedly Alters the CD4+ T-Cell Repertoire. *Journal of Virology*, 81(14):7759–7765, July 2007.

[454] Jutta K. Preiksaitis, Daniel C. Brennan, Jay Fishman, and Upton Allen. Canadian Society of Transplantation Consensus Workshop on Cytomegalovirus Management in Solid Organ Transplantation Final Report. *American Journal of Transplantation*, 5(2):218–227, 2005.

[455] V. Prod'homme, C. Griffin, R. J. Aicheler, E. C. Y. Wang, B. P. McSharry, C. R. Rickards, R. J. Stanton, L. K. Borysiewicz, M. Lopez-Botet, G. W. G. Wilkinson, and P. Tomasec. The human cytomegalovirus MHC class I homolog UL18 inhibits LIR-1+ but activates LIR-1- NK cells. *The Journal of Immunology*, 2007.

[456] Virginie Prod'homme, Daniel M. Sugrue, Richard J. Stanton, Akio Nomoto, James Davies, Carole R. Rickards, Daniel Cochrane, Melanie Moore, Gavin W.G. Wilkinson,

and Peter Tomasec. Human cytomegalovirus UL141 promotes efficient downregulation of the natural killer cell activating ligand CD112. *Journal of General Virology*, 2010.

[457] PubChem. Azathioprine. https://pubchem.ncbi.nlm.nih.gov/compound/2265.

[458] Gerald V. Quinnan, Nigar Kirmani, Alain H. Rook, Jody F. Manischewitz, Lozannie Jackson, Gail Moreschi, George W. Santos, Rein Saral, and William H. Burns. Cytotoxic T Cells in Cytomegalovirus Infection. *New England Journal of Medicine*, 307(1):7–13, July 1982.

[459] Afsar Rahbar, Inti Peredo, Nina Wolmer Solberg, Chato Taher, Mensur Dzabic, Xinling Xu, Petra Skarman, Olesja Fornara, Charlotte Tammik, Koon Yaiw, Vanessa Wilhelmi, Alice Assinger, Giuseppe Stragliotto, and Cecilia Söderberg-Naucler. Discordant humoral and cellular immune responses to Cytomegalovirus (CMV) in glioblastoma patients whose tumors are positive for CMV. *Oncoimmunology*, 4(2), February 2015.

[460] Amin Rahemtulla, Thomas M. Kündig, Arumugabadiv Narendran, Martin F. Bachmann, Michael Julius, Christopher J. Paige, Pamela S. Ohashi, Rolf M. Zinkernagel, and Tak W. Mak. Class II major histocompatibility complex-restricted T cell function in CD4-deficient mice. *European Journal of Immunology*, 24(9):2213–2218, 1994.

[461] Michael A. Rak, Jason Buehler, Sebastian Zeltzer, Justin Reitsma, Belen Molina, Scott Terhune, and Felicia Goodrum. Human Cytomegalovirus UL135 Interacts with Host Adaptor Proteins To Regulate Epidermal Growth Factor Receptor and Reactivation from Latency. *Journal of Virology*, 92(20), October 2018.

[462] Gwendalyn J Randolph, Claudia Jakubzick, and Chunfeng Qu. Antigen presentation by monocytes and monocyte-derived cells. *Current Opinion in Immunology*, 20(1):52–60, February 2008.

[463] N A Rao, J Zhang, and S Ishimoto. Role of retinal vascular endothelial cells in development of CMV retinitis. *Transactions of the American Ophthalmological Society*, 96:111–126, 1998.

[464] Jeffrey V. Ravetch and Silvia Bolland. IgG Fc Receptors. *Annual Review of Immunology*, 19(1):275–290, April 2001.

[465] Raymund R. Razonable. Immune-based therapies for cytomegalovirus infection. *Immunotherapy*, 2010.

[466] Raymund R. Razonable and Randall T. Hayden. Clinical Utility of Viral Load in Management of Cytomegalovirus Infection after Solid Organ Transplantation. *Clinical Microbiology Reviews*, 26(4):703–727, October 2013.

[467] R. W. Read, J. A. Zhang, S. I. Ishimoto, and N. A. Rao. Evaluation of the role of human retinal vascular endothelial cells in the pathogenesis of CMV retinitis. *Ocular Immunology and Inflammation*, 7(3-4):139–146, December 1999.

[468] M. J. Reddehase, S. Jonjić, F. Weiland, W. Mutter, and U. H. Koszinowski. Adoptive immunotherapy of murine cytomegalovirus adrenalitis in the immunocompromised host: CD4-helper-independent antiviral function of CD8-positive memory T lymphocytes derived from latently infected donors. *Journal of Virology*, 62(3):1061–1065, March 1988.

[469] M J Reddehase, W Mutter, K Münch, H J Bühring, and U H Koszinowski. CD8-positive T lymphocytes specific for murine cytomegalovirus immediate-early antigens mediate protective immunity. *Journal of Virology*, 61(10):3102–3108, October 1987.

[470] M J Reddehase, F Weiland, K Münch, S Jonjic, A Lüske, and U H Koszinowski. Interstitial murine cytomegalovirus pneumonia after irradiation: Characterization of cells that limit viral replication during established infection of the lungs. *Journal of Virology*, 55(2):264–273, August 1985.

[471] M. Reeves and J. Sinclair. Aspects of Human Cytomegalovirus Latency and Reactivation. In Thomas E. Shenk and Mark F. Stinski, editors, *Human Cytomegalovirus*, Current Topics in Microbiology and Immunology, pages 297–313. Springer, Berlin, Heidelberg, 2008.

[472] M. B. Reeves, P. J. Lehner, J. G P Sissons, and J. H. Sinclair. An in vitro model for the regulation of human cytomegalovirus latency and reactivation in dendritic cells by chromatin remodelling. *Journal of General Virology*, 2005.

[473] M. B. Reeves, P. A. MacAry, P. J. Lehner, J. G. P. Sissons, and J. H. Sinclair. Latency, chromatin remodeling, and reactivation of human cytomegalovirus in the dendritic cells of healthy carriers. *Proceedings of the National Academy of Sciences*, 2005.

[474] Matthew B Reeves and John H Sinclair. Circulating dendritic cells isolated from healthy seropositive donors are sites of human cytomegalovirus reactivation in vivo. *Journal of virology*, 2013.

[475] Barbara Reinhardt, Peter Schaarschmidt, Andrea Bossert, Anke Lüske, Günter Finkenzeller, Thomas Mertens, and DetlefYR 2005 Michel. Upregulation of functionally active vascular endothelial growth factor by human cytomegalovirus. *Journal of General Virology*, 86(1):23–30, January 2005.

[476] E. L. Reinherz, S. C. Meuer, and S. F. Schlossman. The human T cell receptor: Analysis with cytotoxic T cell clones. *Immunological Reviews*, 74:83–112, 1983.

[477] Boris Reizis, Anna Bunin, Hiyaa S. Ghosh, Kanako L. Lewis, and Vanja Sisirak. Plasmacytoid Dendritic Cells: Recent Progress and Open Questions. *Annual Review of Immunology*, 29(1):163–183, March 2011.

[478] R. J Rentenaar, L. E Gamadia, N van der Hoek, F. N. J van Diepen, R Boom, J. F. L Weel, R. A. W van Lier, and I. J. M ten Berge. CD4+ T-cell dynamics in primary cytomegalovirus infection. *Transplantation Proceedings*, 33(3):2313–2314, May 2001.

[479] Rob J. Rentenaar, Laila E. Gamadia, Nicolette van derHoek, Frank N. J. van Diepen, René Boom, Jan F. L. Weel, Pauline M. E. Wertheim-van Dillen, René A. W. van Lier, and Ineke J. M. ten Berge. Development of virus-specific $CD4^+$ T cells during primary cytomegalovirus infection. *The Journal of Clinical Investigation*, 105(4):541–548, February 2000.

[480] Jon D. Reuter, Jean H. Wilson, Kimberly E. Idoko, and Anthony N. van den Pol. CD4+ T-Cell Reconstitution Reduces Cytomegalovirus in the Immunocompromised Brain. *Journal of Virology*, 79(15):9527–9539, August 2005.

[481] Maria Grazia Revello, Daniele Lilleri, Maurizio Zavattoni, Milena Furione, Emilia Genini, Giuditta Comolli, and Giuseppe Gerna. Lymphoproliferative Response in Primary Human Cytomegalovirus (HCMV) Infection Is Delayed in HCMV Transmitter Mothers. *The Journal of Infectious Diseases*, 193(2):269–276, January 2006.

[482] Jake William Rhodes, Orion Tong, Andrew Nicholas Harman, and Stuart Grant Turville. Human Dendritic Cell Subsets, Ontogeny, and Impact on HIV Infection. *Frontiers in Immunology*, 10, 2019.

[483] H. Ribbert. Ueber protozoenartige Zellen in der Niere eines syphilitischen Neugeborenen und in der Parotis von Kindern. *Zbl All Pathol*, 15:945–948, 1904.

[484] Raphaëlle Riou, Céline Bressollette-Bodin, David Boutoille, Katia Gagne, Audrey Rodallec, Maeva Lefebvre, François Raffi, David Senitzer, Berthe-Marie Imbert-Marcille, and Christelle Retière. Severe Symptomatic Primary Human Cytomegalovirus Infection despite Effective Innate and Adaptive Immune Responses. *Journal of Virology*, 91(5), February 2017.

[485] A. Ripalti, M. C. Boccuni, F. Campanini, and M. P. Landini. Cytomegalovirus-mediated induction of antisense mRNA expression to UL44 inhibits virus replication in an astrocytoma cell line: Identification of an essential gene. *Journal of Virology*, 69(4):2047–2057, April 1995.

[486] J. Ritter, V. Seitz, H. Balzer, R. Gary, D. Lenze, S. Moi, S. Pasemann, A. Seegebarth, M. Wurdack, S. Hennig, A. Gerbitz, and M. Hummel. Donor CD4 T Cell Diversity

Determines Virus Reactivation in Patients After HLA-Matched Allogeneic Stem Cell Transplantation. *American Journal of Transplantation*, 15(8):2170–2179, 2015.

[487] W. H. Roberts, J. M. Sneddon, J. Waldman, and R. E. Stephens. Cytomegalovirus infection of gastrointestinal endothelium demonstrated by simultaneous nucleic acid hybridization and immunohistochemistry. *Archives of Pathology & Laboratory Medicine*, 113(5):461–464, May 1989.

[488] Rolla B. Hill, Jr., David T. Rowlands, Jr. and David Rifkind. Infectious pulmonary disease in patients receiving immunosuppressive therapy for organ transplantation. *The New England Journal of Medicine*, (271):1021–1027, 1964.

[489] Shannon A. Ross, Nitin Arora, Zdenek Novak, Karen B. Fowler, William J. Britt, and Suresh B. Boppana. Cytomegalovirus Reinfections in Healthy Seroimmune Women. *The Journal of Infectious Diseases*, 201(3):386–389, February 2010.

[490] Cyprian C. Rossetto, Margaret Tarrant-Elorza, and Gregory S. Pari. Cis and trans acting factors involved in human cytomegalovirus experimental and natural latent infection of CD14 (+) monocytes and CD34 (+) cells. *PLoS Pathogens*, 2013.

[491] W P Rowe, J W Hartley, S Waterman, H C Turner, and R J Huebner. Cytopathogenic agent resembling human salivary gland virus recovered from tissue cultures of human adenoids. *Proceedings of the Society for Experimental Biology and Medicine*, 92(2):418–24, June 1956.

[492] Yuri P. Rubtsov, Jeffrey P. Rasmussen, Emil Y. Chi, Jason Fontenot, Luca Castelli, Xin Ye, Piper Treuting, Lisa Siewe, Axel Roers, William R. Henderson, Werner Muller, and Alexander Y. Rudensky. Regulatory T Cell-Derived Interleukin-10 Limits Inflammation at Environmental Interfaces. *Immunity*, 28(4):546–558, April 2008.

[493] Brent J. Ryckman, Barb L. Rainish, Marie C. Chase, Jamie A. Borton, Jay A. Nelson, Michael A. Jarvis, and David C. Johnson. Characterization of the Human Cytomegalovirus gH/gL/UL128-131 Complex That Mediates Entry into Epithelial and Endothelial Cells. *Journal of Virology*, 82(1):60–70, January 2008.

[494] Steffanie Sabbaj, Robert F. Pass, Sylvie Pichon, and Paul A. Goepfert. Glycoprotein B Vaccine Is Capable of Boosting Both Antibody and CD4 T-Cell Responses to Cytomegalovirus in Chronically Infected Women. *The Journal of Infectious Diseases*, 203(11):1534–1541, June 2011.

[495] Anthony J. Sadler and Bryan R. G. Williams. Interferon-inducible antiviral effectors. *Nature Reviews Immunology*, 8(7):559–568, July 2008.

[496] R. T. Saffert and R. F. Kalejta. Inactivating a cellular intrinsic immune defense mediated by daxx is the mechanism through which the human cytomegalovirus pp71 protein stimulates viral immediate-early gene expression. *Journal of Virology*, 2006.

[497] Kerstin Laib Sampaio, Yolaine Cavignac, York-Dieter Stierhof, and Christian Sinzger. Human Cytomegalovirus Labeled with Green Fluorescent Protein for Live Analysis of Intracellular Particle Movements. *Journal of Virology*, 79(5):2754–2767, March 2005.

[498] R. San-Juan, D. Navarro, A. García-Reyne, M. Montejo, P. Muñoz, J. Carratala, O. Len, J. Fortun, B. Muñoz-Cobo, E. Gimenez, A. Eworo, N. Sabe, Y. Meije, P. Martín-Davila, A. Andres, J. Delgado, C. Jimenez, P. Amat, M. Fernández-Ruiz, F. López-Medrano, C. Lumbreras, J. M. Aguado, and REIPI Network. Effect of long-term prophylaxis in the development of cytomegalovirus-specific T-cell immunity in D+/R- solid organ transplant recipients. *Transplant Infectious Disease: An Official Journal of the Transplantation Society*, 17(5):637–646, October 2015.

[499] V. Sanchez, E. Sztul, and W. J. Britt. Human cytomegalovirus pp28 (UL99) localizes to a cytoplasmic compartment which overlaps the endoplasmic reticulum-golgi-intermediate compartment. *Journal of Virology*, 74(8):3842–3851, April 2000.

[500] Veronica Sanchez, Kenneth D. Greis, Elizabeth Sztul, and William J. Britt. Accumulation of Virion Tegument and Envelope Proteins in a Stable Cytoplasmic Compartment during Human Cytomegalovirus Replication: Characterization of a Potential Site of Virus Assembly. *Journal of Virology*, 74(2):975–986, January 2000.

[501] Praneet K. Sandhu and Nicholas J. Buchkovich. Human Cytomegalovirus Decreases Major Histocompatibility Complex Class II by Regulating Class II Transactivator Transcript Levels in a Myeloid Cell Line. *Journal of Virology*, 94(7), March 2020.

[502] Andrea J. Sant and Andrew McMichael. Revealing the role of CD4+ T cells in viral immunity. *The Journal of Experimental Medicine*, 209(8):1391–1395, July 2012.

[503] Stefano M. Santini, Caterina Lapenta, Mariantonia Logozzi, Stefania Parlato, Massimo Spada, Tiziana Di Pucchio, and Filippo Belardelli. Type I Interferon as a Powerful Adjuvant for Monocyte-Derived Dendritic Cell Development and Activity in Vitro and in Hu-Pbl-Scid Mice. *Journal of Experimental Medicine*, 191(10):1777–1788, May 2000.

[504] Ansuman T. Satpathy, Wumesh Kc, Jörn C. Albring, Brian T. Edelson, Nicole M. Kretzer, Deepta Bhattacharya, Theresa L. Murphy, and Kenneth M. Murphy. Zbtb46 expression distinguishes classical dendritic cells and their committed progenitors from other immune lineages. *The Journal of Experimental Medicine*, 209(6):1135–1152, June 2012.

[505] A. A. Scalzo, N. A. Fitzgerald, A. Simmons, A. B. La Vista, and G. R. Shellam. Cmv-1, a genetic locus that controls murine cytomegalovirus replication in the spleen. *The Journal of Experimental Medicine*, 171(5):1469–1483, May 1990.

[506] Anthony A. Scalzo, Paul A. Lyons, Nicola A. Fitzgerald, Catherine A. Forbes, Wayne M. Yokoyama, and Geoffrey R. Shellam. Genetic Mapping of Cmv1 in the Region of Mouse Chromosome 6 Encoding the NK Gene Complex-Associated Loci Ly49 and musNKR-P1. *Genomics*, 27(3):435–441, June 1995.

[507] Andreas Schlitzer, Naomi McGovern, Pearline Teo, Teresa Zelante, Koji Atarashi, Donovan Low, Adrian W. S. Ho, Peter See, Amanda Shin, Pavandip Singh Wasan, Guillaume Hoeffel, Benoit Malleret, Alexander Heiseke, Samantha Chew, Laura Jardine, Harriet A. Purvis, Catharien M. U. Hilkens, John Tam, Michael Poidinger, E. Richard Stanley, Anne B. Krug, Laurent Renia, Baalasubramanian Sivasankar, Lai Guan Ng, Matthew Collin, Paola Ricciardi-Castagnoli, Kenya Honda, Muzlifah Haniffa, and Florent Ginhoux. IRF4 Transcription Factor-Dependent CD11b+ Dendritic Cells in Human and Mouse Control Mucosal IL-17 Cytokine Responses. *Immunity*, 38(5):970–983, May 2013.

[508] Heinrich Schlums, Frank Cichocki, Bianca Tesi, Jakob Theorell, Vivien Beziat, Tim D. Holmes, Hongya Han, Samuel C. C. Chiang, Bree Foley, Kristin Mattsson, Stella Larsson, Marie Schaffer, Karl-Johan Malmberg, Hans-Gustaf Ljunggren, Jeffrey S. Miller, and Yenan T. Bryceson. Cytomegalovirus Infection Drives Adaptive Epigenetic Diversification of NK Cells with Altered Signaling and Effector Function. *Immunity*, 42(3):443–456, March 2015.

[509] Carol T. Schnizlein-Bick, Francis F. Mandy, Maurice R. G. O'Gorman, Helene Paxton, Janet K. A. Nicholson, Lance E. Hultin, Rebecca S. Gelman, Cynthia L. Wilkening, and Daniella Livnat. Use of CD45 gating in three and four-color flow cytometric immunophenotyping: Guideline from the national institute of allergy and infectious diseases, division of AIDS. *Cytometry*, 50(2):46–52, 2002.

[510] K. Schroder. Interferon- : An overview of signals, mechanisms and functions. *Journal of Leukocyte Biology*, 2003.

[511] S. Schwele, A. M. Fischer, G. Brestrich, M. W. Wlodarski, L. Wagner, M. Schmueck, A. Roemhild, S. Thomas, M. H. Hammer, N. Babel, A. Kurtz, J. P. Maciejewski, P. Reinke, and H.-D. Volk. Cytomegalovirus-Specific Regulatory and Effector T Cells Share TCR Clonality—Possible Relation to Repetitive CMV Infections. *American Journal of Transplantation*, 12(3):669–681, 2012.

[512] Peter See, Charles-Antoine Dutertre, Jinmiao Chen, Patrick Günther, Naomi McGovern, Sergio Erdal Irac, Merry Gunawan, Marc Beyer, Kristian Händler, Kaibo Duan,

Hermi Rizal Bin Sumatoh, Nicolas Ruffin, Mabel Jouve, Ester Gea-Mallorquí, Raoul C. M. Hennekam, Tony Lim, Chan Chung Yip, Ming Wen, Benoit Malleret, Ivy Low, Nurhidaya Binte Shadan, Charlene Foong Shu Fen, Alicia Tay, Josephine Lum, Francesca Zolezzi, Anis Larbi, Michael Poidinger, Jerry K. Y. Chan, Qingfeng Chen, Laurent Rénia, Muzlifah Haniffa, Philippe Benaroch, Andreas Schlitzer, Joachim L. Schultze, Evan W. Newell, and Florent Ginhoux. Mapping the human DC lineage through the integration of high-dimensional techniques. *Science*, 356(6342), June 2017.

[513] Einat Seidel, Vu Thuy Khanh Le, Yotam Bar-On, Pinchas Tsukerman, Jonatan Enk, Rachel Yamin, Natan Stein, Dominik Schmiedel, Esther Oiknine Djian, Yiska Weisblum, Boaz Tirosh, Peter Stastny, Dana G. Wolf, Hartmut Hengel, and Ofer Mandelboim. Dynamic Co-evolution of Host and Pathogen: HCMV Downregulates the Prevalent Allele MICA$_*$008 to Escape Elimination by NK Cells. *Cell Reports*, 10(6):968–982, February 2015.

[514] Jun-Young Seo, Hyejin Jeon, Sookyung Hong, and William J. Britt. Distinct functional domains within the acidic cluster of tegument protein pp28 required for trafficking and cytoplasmic envelopment of human cytomegalovirus. *The Journal of General Virology*, 97(10):2677–2683, October 2016.

[515] M. Sester, U. Sester, B. Gärtner, G. Heine, M. Girndt, N. Mueller-Lantzsch, A. Meyerhans, and H. Köhler. Levels of virus-specific CD4 T cells correlate with cytomegalovirus control and predict virus-induced disease after renal transplantation. *Transplantation*, 71(9):1287–1294, May 2001.

[516] Martina Sester, Urban Sester, Barbara Gärtner, Boris Kubuschok, Matthias Girndt, Andreas Meyerhans, and Hans Köhler. Sustained High Frequencies of Specific CD4 T Cells Restricted to a Single Persistent Virus. *Journal of Virology*, 76(8):3748–3755, April 2002.

[517] Paul Sheppard, Wayne Kindsvogel, Wenfeng Xu, Katherine Henderson, Stacy Schlutsmeyer, Theodore E. Whitmore, Rolf Kuestner, Ursula Garrigues, Carl Birks, Jenny Roraback, Craig Ostrander, Dennis Dong, Jinu Shin, Scott Presnell, Brian Fox, Betty Haldeman, Emily Cooper, David Taft, Teresa Gilbert, Francis J. Grant, Monica Tackett, William Krivan, Gary McKnight, Chris Clegg, Don Foster, and Kevin M. Klucher. IL-28, IL-29 and their class II cytokine receptor IL-28R. *Nature Immunology*, 4(1):63–68, January 2003.

[518] Jeoung-Sook Shin, Melanie Ebersold, Marc Pypaert, Lelia Delamarre, Adam Hartley, and Ira Mellman. Surface expression of MHC class II in dendritic cells is controlled by regulated ubiquitination. *Nature*, 444(7115):115–118, November 2006.

[519] Mari L. Shinohara, Linrong Lu, Jing Bu, Miriam B. F. Werneck, Koichi S. Kobayashi, Laurie H. Glimcher, and Harvey Cantor. Osteopontin expression is essential for interferon-α production by plasmacytoid dendritic cells. *Nature Immunology*, 7(5):498–506, May 2006.

[520] Miri Shnayder, Aharon Nachshon, Benjamin Krishna, Emma Poole, Alina Boshkov, Amit Binyamin, Itay Maza, John Sinclair, Michal Schwartz, and Noam Stern-Ginossar. Defining the Transcriptional Landscape during Cytomegalovirus Latency with Single-Cell RNA Sequencing. *mBio*, 9(2), March 2018.

[521] Protul A. Shrikant, Rajesh Rao, Qingsheng Li, Joshua Kesterson, Cheryl Eppolito, Axel Mischo, and Pankaj Singhal. Regulating functional cell fates in CD8 T cells. *Immunologic Research*, 46(1-3):12–22, March 2010.

[522] Leonard D. Shultz, Michael A. Brehm, J. Victor Garcia, and Dale L. Greiner. Humanized mice for immune system investigation: Progress, promise and challenges. *Nature reviews. Immunology*, 12(11):786–798, November 2012.

[523] Frederick P. Siegal, Norimitsu Kadowaki, Michael Shodell, Patricia A. Fitzgerald-Bocarsly, Kokila Shah, Stephen Ho, Svetlana Antonenko, and Yong-Jun Liu. The Nature of the Principal Type 1 Interferon-Producing Cells in Human Blood. *Science*, 284(5421):1835–1837, June 1999.

[524] Maria C. Silva, Qian-Chun Yu, Lynn Enquist, and Thomas Shenk. Human Cytomegalovirus UL99-Encoded pp28 Is Required for the Cytoplasmic Envelopment of Tegument-Associated Capsids. *Journal of Virology*, 77(19):10594–10605, October 2003.

[525] John Sinclair and PatrickYR 2006 Sissons. Latency and reactivation of human cytomegalovirus. *Journal of General Virology*, 87(7):1763–1779, July 2006.

[526] John H. Sinclair and Matthew B. Reeves. Human cytomegalovirus manipulation of latently infected cells. *Viruses*, 2013.

[527] H Sindre, G E Tjønnfjord, H Rollag, T Ranneberg-Nilsen, O P Veiby, S Beck, M Degré, and K Hestdal. Human cytomegalovirus suppression of and latency in early hematopoietic progenitor cells. *Blood*, 1996.

[528] Dinah S. Singer and Ballachanda Nanjappa Devaiah. CIITA and Its Dual Roles in MHC Gene Transcription. *Frontiers in Immunology*, 4, 2013.

[529] C. Sinzger, M. Digel, and G. Jahn. Cytomegalovirus Cell Tropism. In Thomas E. Shenk and Mark F. Stinski, editors, *Human Cytomegalovirus*, Current Topics in Microbiology and Immunology, pages 63–83. Springer, Berlin, Heidelberg, 2008.

[530] C. Sinzger, A. Grefte, B. Plachter, A. S. Gouw, T. H. The, and G. Jahn. Fibroblasts, epithelial cells, endothelial cells and smooth muscle cells are major targets of human cytomegalovirus infection in lung and gastrointestinal tissues. *The Journal of General Virology*, 76 (Pt 4):741–750, April 1995.

[531] C. Sinzger, K. Schmidt, J. Knapp, M. Kahl, R. Beck, J. Waldman, H. Hebart, H. Einsele, and G. YR 1999 Jahn. Modification of human cytomegalovirus tropism through propagation in vitro is associated with changes in the viral genome. *Journal of General Virology*, 80(11):2867–2877, November 1999.

[532] Christian Sinzger, Kathrin Eberhardt, Yolaine Cavignac, Christof Weinstock, Tobias Kessler, Gerhard Jahn, and Jean-LucYR 2006 Davignon. Macrophage cultures are susceptible to lytic productive infection by endothelial-cell-propagated human cytomegalovirus strains and present viral IE1 protein to CD4+ T cells despite late downregulation of MHC class II molecules. *Journal of General Virology*, 87(7):1853–1862, July 2006.

[533] Christian Sinzger, Gabriele Hahn, Margarete Digel, Ruth Katona, Kerstin Laib Sampaio, Martin Messerle, Hartmut Hengel, Ulrich Koszinowski, Wolfram Brune, and BarbaraYR 2008 Adler. Cloning and sequencing of a highly productive, endotheliotropic virus strain derived from human cytomegalovirus TB40/E. *Journal of General Virology*, 89(2):359–368, February 2008.

[534] Simona Sivori, Paola Vacca, Genny Del Zotto, Enrico Munari, Maria Cristina Mingari, and Lorenzo Moretta. Human NK cells: Surface receptors, inhibitory checkpoints, and translational applications. *Cellular & Molecular Immunology*, 16(5):430–441, May 2019.

[535] A Skaletskaya, L M Bartle, T Chittenden, A L McCormick, E S Mocarski, and V S Goldmacher. A cytomegalovirus-encoded inhibitor of apoptosis that suppresses caspase-8 activation. *Proceedings of the National Academy of Sciences of the United States of America*, 2001.

[536] Brian Skaug and Zhijian J. Chen. Emerging role of ISG15 in antiviral immunity. *Cell*, 143(2):187–190, October 2010.

[537] T. N. Small, E. B. Papadopoulos, F. Boulad, P. Black, H. Castro-Malaspina, B. H. Childs, N. Collins, A. Gillio, D. George, A. Jakubowski, G. Heller, M. Fazzari, N. Kernan, S. MacKinnon, P. Szabolcs, J. W. Young, and R. J. O'Reilly. Comparison of Immune Reconstitution After Unrelated and Related T-Cell–Depleted Bone Marrow Transplantation: Effect of Patient Age and Donor Leukocyte Infusions. *Blood*, 93(2):467–480, January 1999.

[538] Corey Smith, Leone Beagley, Sweera Rehan, Michelle A. Neller, Pauline Crooks, Matthew Solomon, Chien-Li Holmes-Liew, Mark Holmes, Scott C. McKenzie, Peter Hopkins, Scott Campbell, Ross S. Francis, Daniel C. Chambers, and Rajiv Khanna. Autologous Adoptive T-cell Therapy for Recurrent or Drug-resistant Cytomegalovirus Complications in Solid Organ Transplant Recipients: A Single-arm Open-label Phase I Clinical Trial. *Clinical Infectious Diseases*, 68(4):632–640, February 2019.

[539] Rebecca Marie Smith, Srivenkat Kosuri, and Julie Anne Kerry. Role of Human Cytomegalovirus Tegument Proteins in Virion Assembly. *Viruses*, 6(2):582–605, February 2014.

[540] Samantha L. Smith, Philippa R. Kennedy, Kevin B. Stacey, Jonathan D. Worboys, Annie Yarwood, Seungmae Seo, Everardo Hegewisch Solloa, Brandon Mistretta, Sujash S. Chatterjee, Preethi Gunaratne, Kimaada Allette, Ying-Chih Wang, Melissa Laird Smith, Robert Sebra, Emily M. Mace, Amir Horowitz, Wendy Thomson, Paul Martin, Steve Eyre, and Daniel M. Davis. Diversity of peripheral blood human NK cells identified by single-cell RNA sequencing. *Blood Advances*, 4(7):1388–1406, April 2020.

[541] Wendell Smith, Peter Tomasec, Rebecca Aicheler, Andrea Loewendorf, Ivana Nemčovičová, Eddie C. Y. Wang, Richard J. Stanton, Matt Macauley, Paula Norris, Laure Willen, Eva Ruckova, Akio Nomoto, Pascal Schneider, Gabriele Hahn, Dirk M. Zajonc, Carl F. Ware, Gavin W. G. Wilkinson, and Chris A. Benedict. Human Cytomegalovirus Glycoprotein UL141 Targets the TRAIL Death Receptors to Thwart Host Innate Antiviral Defenses. *Cell Host & Microbe*, 13(3):324–335, March 2013.

[542] Christopher M. Snyder, Andrea Loewendorf, Elizabeth L. Bonnett, Michael Croft, Chris A. Benedict, and Ann B. Hill. CD4+ T Cell Help Has an Epitope-Dependent Impact on CD8+ T Cell Memory Inflation during Murine Cytomegalovirus Infection. *Journal of immunology (Baltimore, Md. : 1950)*, 183(6):3932–3941, September 2009.

[543] Cecilia Söderberg-Nauclér, Kenneth N. Fish, and Jay A. Nelson. Reactivation of latent human cytomegalovirus by allogeneic stimulation of blood cells from healthy donors. *Cell*, 1997.

[544] Carlos Solano, Isana Benet, María A. Clari, José Nieto, Rafael de la Cámara, Javier López, Juan C. Hernández-Boluda, María J. Remigia, Isidro Jarque, María L. Calabuig, Ana Garcia-Noblejas, Juan Alberola, Amparo Tamarit, Concepción Gimeno, and David Navarro. Enumeration of cytomegalovirus-specific interferonγ CD8+ and CD4+ T cells early after allogeneic stem cell transplantation may identify patients at risk of active cytomegalovirus infection. *Haematologica*, 93(9):1434–1436, September 2008.

[545] Juliet V. Spencer, Kristen M. Lockridge, Peter A. Barry, Gaofeng Lin, Monica Tsang, Mark E. T. Penfold, and Thomas J. Schall. Potent immunosuppressive activities of

cytomegalovirus-encoded interleukin-10. *Journal of Virology*, 76(3):1285–1292, February 2002.

[546] H. Spits, H. Yssel, A. Voordouw, and J. E. de Vries. The role of T8 in the cytotoxic activity of cloned cytotoxic T lymphocyte lines specific for class II and class I major histocompatibility complex antigens. *Journal of Immunology (Baltimore, Md.: 1950)*, 134(4):2294–2298, April 1985.

[547] Edward F. Srour, Tom Leemhuis, Laura Jenski, Robert Redmond, and Jan Jansen. Cytolytic activity of human natural killer cell subpopulations isolated by four-color immunofluorescence flow cytometric cell sorting. *Cytometry*, 11(3):442–446, 1990.

[548] Michael St. Paul and Pamela S. Ohashi. The Roles of CD8+ T Cell Subsets in Antitumor Immunity. *Trends in Cell Biology*, 30(9):695–704, September 2020.

[549] Sergio Stagno, Robert F. Pass, Gretchen Cloud, William J. Britt, Ronald E. Henderson, Philip D. Walton, Dean A. Veren, Frank Page, and Charles A. Alford. Primary cytomegalovirus infection in pregnancy: Incidence, transmission to fetus, and clinical outcome. *The Journal of the American Medical Association*, 1986.

[550] Richard J. Stanton, Katarina Baluchova, Derrick J. Dargan, Charles Cunningham, Orla Sheehy, Sepehr Seirafian, Brian P. McSharry, M. Lynne Neale, James A. Davies, Peter Tomasec, Andrew J. Davison, and Gavin W. G. Wilkinson. Reconstruction of the complete human cytomegalovirus genome in a BAC reveals RL13 to be a potent inhibitor of replication. *The Journal of Clinical Investigation*, 120(9):3191–3208, September 2010.

[551] Richard J. Stanton, Virginie Prod'homme, Marco A. Purbhoo, Melanie Moore, Rebecca J. Aicheler, Marcus Heinzmann, Susanne M. Bailer, Jürgen Haas, Robin Antrobus, Michael P. Weekes, Paul J. Lehner, Borivoj Vojtesek, Kelly L. Miners, Stephen Man, Gavin S. Wilkie, Andrew J. Davison, Eddie C. Y. Wang, Peter Tomasec, and Gavin W. G. Wilkinson. HCMV pUL135 Remodels the Actin Cytoskeleton to Impair Immune Recognition of Infected Cells. *Cell Host & Microbe*, 16(2):201–214, August 2014.

[552] Hans-Peter Steffens, Sabine Kurz, Rafaela Holtappels, and Matthias J. Reddehase. Preemptive CD8 T-Cell Immunotherapy of Acute Cytomegalovirus Infection Prevents Lethal Disease, Limits the Burden of Latent Viral Genomes, and Reduces the Risk of Virus Recurrence. *Journal of Virology*, 72(3):1797–1804, March 1998.

[553] V. Steimle, C. A. Siegrist, A. Mottet, B. Lisowska-Grospierre, and B. Mach. Regulation of MHC class II expression by interferon-gamma mediated by the transactivator gene CIITA. *Science*, 265(5168):106–109, July 1994.

[554] Noam Stern-Ginossar, Naama Elefant, Albert Zimmermann, Dana G. Wolf, Nivin Saleh, Moshe Biton, Elad Horwitz, Zafnat Prokocimer, Mark Prichard, Gabriele Hahn, Debra Goldman-Wohl, Caryn Greenfield, Simcha Yagel, Hartmut Hengel, Yael Altuvia, Hanah Margalit, and Ofer Mandelboim. Host Immune System Gene Targeting by a Viral miRNA. *Science*, 317(5836):376–381, July 2007.

[555] Noam Stern-Ginossar and Ofer Mandelboim. Chapter Eleven - Receptors on NK cells. In Michael T. Lotze and Angus W. Thomson, editors, *Natural Killer Cells*, pages 155–168. Academic Press, San Diego, January 2010.

[556] M. F. Stinski. Sequence of protein synthesis in cells infected by human cytomegalovirus: Early and late virus-induced polypeptides. *Journal of Virology*, 26(3):686–701, June 1978.

[557] Sarah Straschewski, Marco Patrone, Paul Walther, Andrea Gallina, Thomas Mertens, and Giada Frascaroli. Protein pUL128 of Human Cytomegalovirus Is Necessary for Monocyte Infection and Blocking of Migration. *Journal of Virology*, 85(10):5150–5158, May 2011.

[558] Yvonne Suessmuth, Rithun Mukherjee, Benjamin Watkins, Divya T. Koura, Knut Finstermeier, Cindy Desmarais, Linda Stempora, John T. Horan, Amelia Langston, Muna Qayed, Hanna J. Khoury, Audrey Grizzle, Jennifer A. Cheeseman, Jason A. Conger, Jennifer Robertson, Aneesah Garrett, Allan D. Kirk, Edmund K. Waller, Bruce R. Blazar, Aneesh K. Mehta, Harlan S. Robins, and Leslie S. Kean. CMV reactivation drives post-transplant T-cell reconstitution and results in defects in the underlying TCRβ repertoire. *Blood*, 125(25):3835–3850, June 2015.

[559] Joseph C. Sun, Joshua N. Beilke, and Lewis L. Lanier. Adaptive immune features of natural killer cells. *Nature*, 457(7229):557–561, January 2009.

[560] Anette Sundstedt, Emma J. O'Neill, Kirsty S. Nicolson, and David C. Wraith. Role for IL-10 in Suppression Mediated by Peptide-Induced Regulatory T Cells In Vivo. *The Journal of Immunology*, 170(3):1240–1248, February 2003.

[561] Indran Sv and Britt Wj. A role for the small GTPase Rab6 in assembly of human cytomegalovirus. *Journal of Virology*, 85(10):5213–5219, March 2011.

[562] Susan L. Swain, K. Kai McKinstry, and Tara M. Strutt. Expanding roles for CD4+ T cells in immunity to viruses. *Nature reviews. Immunology*, 12(2):136–148, January 2012.

[563] Melissa Swiecki and Marco Colonna. The multifaceted biology of plasmacytoid dendritic cells. *Nature Reviews Immunology*, 15(8):471–485, August 2015.

[564] Andrew W. Sylwester, Bridget L. Mitchell, John B. Edgar, Cara Taormina, Christian Pelte, Franziska Ruchti, Paul R. Sleath, Kenneth H. Grabstein, Nancy A. Hosken, Florian Kern, Jay A. Nelson, and Louis J. Picker. Broadly targeted human cytomegalovirus-specific CD4+ and CD8+ T cells dominate the memory compartments of exposed subjects. *The Journal of Experimental Medicine*, 202(5):673–685, September 2005.

[565] Andrea L. Szymczak-Workman, Kate M. Vignali, and Dario A A Vignali. Design and construction of 2A peptide-linked multicistronic vectors. *Cold Spring Harbor Protocols*, 2012.

[566] Hiroyuki Takaba and Hiroshi Takayanagi. The Mechanisms of T Cell Selection in the Thymus. *Trends in Immunology*, 38(11):805–816, November 2017.

[567] Arata Takeuchi and Takashi Saito. CD4 CTL, a cytotoxic subset of CD4+T cells, their differentiation and function. *Frontiers in Immunology*, 8(FEB):1–7, 2017.

[568] Ritesh Tandon and Edward S. Mocarski. Control of Cytoplasmic Maturation Events by Cytomegalovirus Tegument Protein pp150. *Journal of Virology*, 82(19):9433–9444, October 2008.

[569] Jean Taylor-Wiedeman, J. G. P. Sissons, L. K. Borysiewicz, and J. H. Sinclair. Monocytes are a major site of persistence of human cytomegalovirus in peripheral blood mononuclear cells. *Journal of General Virology,*, 72(9):2059–2064, 1991.

[570] Jean Taylor-Wiedeman, Patrick Sissons, and John Sinclair. Induction of endogenous human cytomegalovirus gene expression after differentiation of monocytes from healthy carriers. *Journal of Virology*, 1994.

[571] Daniel J. Tenney and Anamaris M. Colberg-Poley. Expression of the human cytomegalovirus UL36–38 immediate early region during permissive infection. *Virology*, 182(1):199–210, May 1991.

[572] Fredrik Terlutter, Richard Caspell, Tobias M. Nowacki, Alexander Lehmann, Ruliang Li, Ting Zhang, Anna Przybyla, Stefanie Kuerten, and Paul V. Lehmann. Direct Detection of T- and B-Memory Lymphocytes by ImmunoSpot® Assays Reveals HCMV Exposure that Serum Antibodies Fail to Identify. *Cells*, 7(5), May 2018.

[573] Nadia Terrazzini, Martha Bajwa, Serena Vita, Elizabeth Cheek, David Thomas, Nabila Seddiki, Helen Smith, and Florian Kern. A Novel Cytomegalovirus-Induced Regulatory-Type T-Cell Subset Increases in Size During Older Life and Links Virus-Specific Immunity to Vascular Pathology. *The Journal of Infectious Diseases*, 209(9):1382–1392, May 2014.

[574] Ugo Testa, Elvira Pelosi, and Arthur Frankel. CD 123 is a membrane biomarker and a therapeutic target in hematologic malignancies. *Biomarker Research*, 2(1):4, February 2014.

[575] Christoph A. Thaiss, Verena Semmling, Lars Franken, Hermann Wagner, and Christian Kurts. Chemokines: A New Dendritic Cell Signal for T Cell Activation. *Frontiers in Immunology*, 2, 2011.

[576] The UniProt Consortium. UniProt: The universal protein knowledgebase in 2021. *Nucleic Acids Research*, 49(D1):D480–D489, January 2021.

[577] Derek J. Theisen, Jesse T. Davidson, Carlos G. Briseño, Marco Gargaro, Elvin J. Lauron, Qiuling Wang, Pritesh Desai, Vivek Durai, Prachi Bagadia, Joshua R. Brickner, Wandy L. Beatty, Herbert W. Virgin, William E. Gillanders, Nima Mosammaparast, Michael S. Diamond, L. David Sibley, Wayne Yokoyama, Robert D. Schreiber, Theresa L. Murphy, and Kenneth M. Murphy. WDFY4 is required for cross-presentation in response to viral and tumor antigens. *Science (New York, N.Y.)*, 362(6415):694–699, November 2018.

[578] Graham D. Thomas, Anouk A.J. Hamers, Catherine Nakao, Paola Marcovecchio, Angela M. Taylor, Chantel McSkimming, Anh Tram Nguyen, Coleen A. McNamara, and Catherine C. Hedrick. Human Blood Monocyte Subsets. *Arteriosclerosis, Thrombosis, and Vascular Biology*, 37(8):1548–1558, August 2017.

[579] Simone Thomas, Sebastian Klobuch, Jürgen Podlech, Bodo Plachter, Petra Hoffmann, Angelique Renzaho, Matthias Theobald, Matthias J. Reddehase, Wolfgang Herr, and Niels A. W. Lemmermann. Evaluating Human T-Cell Therapy of Cytomegalovirus Organ Disease in HLA-Transgenic Mice. *PLoS Pathogens*, 11(7), July 2015.

[580] Peter Tomasec, Veronique M. Braud, Carole Rickards, Martin B. Powell, Brian P. McSharry, Stephan Gadola, Vincenzo Cerundolo, Leszek K. Borysiewicz, Andrew J. McMichael, and Gavin W. G. Wilkinson. Surface Expression of HLA-E, an Inhibitor of Natural Killer Cells, Enhanced by Human Cytomegalovirus gpUL40. *Science*, 287(5455):1031–1033, February 2000.

[581] Peter Tomasec, Eddie C. Y. Wang, Andrew J. Davison, Borivoj Vojtesek, Melanie Armstrong, Cora Griffin, Brian P. McSharry, Rebecca J. Morris, Sian Llewellyn-Lacey, Carole Rickards, Akio Nomoto, Christian Sinzger, and Gavin W. G. Wilkinson. Downregulation of natural killer cell–activating ligand CD155 by human cytomegalovirus UL141. *Nature Immunology*, 6(2):181–188, February 2005.

[582] Roman Tomazin, Jessica Boname, Nagendra R. Hegde, David M. Lewinsohn, Yoram Altschuler, Thomas R. Jones, Peter Cresswell, Jay A. Nelson, Stanley R. Riddell, and

David C. Johnson. Cytomegalovirus US2 destroys two components of the MHC class II pathway, preventing recognition by CD4 + T cells. *Nature Medicine*, 5(9):1039–1043, September 1999.

[583] N. Tormo, C. Solano, I. Benet, M. A. Clari, J. Nieto, R. de la Cámara, J. López, N. López-Aldeguer, J. C. Hernández-Boluda, M. J. Remigia, A. Garcia-Noblejas, C. Gimeno, and D. Navarro. Lack of prompt expansion of cytomegalovirus pp65 and IE-1-specific IFNγ CD8 + and CD4 + T cells is associated with rising levels of pp65 antigenemia and DNAemia during pre-emptive therapy in allogeneic hematopoietic stem cell transplant recipients. *Bone Marrow Transplantation*, 45(3):543–549, March 2010.

[584] N. Tormo, C. Solano, I. Benet, J. Nieto, R. de la Cámara, J. López, A. Garcia-Noblejas, B. Muñoz-Cobo, E. Costa, M. A. Clari, J. C. Hernández-Boluda, M. J. Remigia, and D. Navarro. Reconstitution of CMV pp65 and IE-1-specific IFN-γ CD8 + and CD4 + T-cell responses affording protection from CMV DNAemia following allogeneic hematopoietic SCT. *Bone Marrow Transplantation*, 46(11):1437–1443, November 2011.

[585] Nuria Tormo, Carlos Solano, Isabel Benet, José Nieto, Rafael de la Cámara, Ana Garcia-Noblejas, María Ángeles Clari, Marifina Chilet, Javier López, Juan Carlos Hernández-Boluda, María José Remigia, and David Navarro. Kinetics of cytomegalovirus (CMV) pp65 and IE-1-specific IFNγ CD8+ and CD4+ T cells during episodes of viral DNAemia in allogeneic stem cell transplant recipients: Potential implications for the management of active CMV infection. *Journal of Medical Virology*, 82(7):1208–1215, 2010.

[586] Adriana Tovar-Salazar, Julie Patterson-Bartlett, Renee Jesser, and Adriana Weinberg. Regulatory function of cytomegalovirus-specific CD4+CD27-CD28- T cells. *Virology*, 398(2):158–167, March 2010.

[587] James C. Towler, Bahram Ebrahimi, Brian Lane, Andrew J. Davison, and Derrick J. Dargan. Human cytomegalovirus transcriptome activity differs during replication in human fibroblast, epithelial and astrocyte cell lines. *Journal of General Virology*, 2012.

[588] G Trinchieri, D Santoli, R R Dee, and B B Knowles. Anti-viral activity induced by culturing lymphocytes with tumor-derived or virus-transformed cells. Identification of the anti-viral activity as interferon and characterization of the human effector lymphocyte subpopulation. *Journal of Experimental Medicine*, 147(5):1299–1313, May 1978.

[589] Wenwei Tu, Sharon Chen, Margaret Sharp, Corry Dekker, Anne Marie Manganello, Eileen C. Tongson, Holden T. Maecker, Tyson H. Holmes, Zhaoti Wang, George Kemble, Stuart Adler, Ann Arvin, and David B. Lewis. Persistent and selective deficiency of CD4+ T cell immunity to cytomegalovirus in immunocompetent young children. *Journal of Immunology (Baltimore, Md.: 1950)*, 172(5):3260–3267, March 2004.

[590] Aaron J. Tyznik, Joseph C. Sun, and Michael J. Bevan. The CD8 Population in CD4-deficient Mice Is Heavily Contaminated with MHC Class II–restricted T Cells. *The Journal of Experimental Medicine*, 199(4):559–565, February 2004.

[591] Mathias Uhlén, Max J. Karlsson, Andreas Hober, Anne-Sophie Svensson, Julia Scheffel, David Kotol, Wen Zhong, Abdellah Tebani, Linnéa Strandberg, Fredrik Edfors, Evelina Sjöstedt, Jan Mulder, Adil Mardinoglu, Anna Berling, Siri Ekblad, Melanie Dannemeyer, Sara Kanje, Johan Rockberg, Magnus Lundqvist, Magdalena Malm, Anna-Luisa Volk, Peter Nilsson, Anna Månberg, Tea Dodig-Crnkovic, Elisa Pin, Martin Zwahlen, Per Oksvold, Kalle von Feilitzen, Ragna S. Häussler, Mun-Gwan Hong, Cecilia Lindskog, Fredrik Ponten, Borbala Katona, Jimmy Vuu, Emil Lindström, Jens Nielsen, Jonathan Robinson, Burcu Ayoglu, Diana Mahdessian, Devin Sullivan, Peter Thul, Frida Danielsson, Charlotte Stadler, Emma Lundberg, Göran Bergström, Anders Gummesson, Bjørn G. Voldborg, Hanna Tegel, Sophia Hober, Björn Forsström, Jochen M. Schwenk, Linn Fagerberg, and Åsa Sivertsson. The human secretome. *Science Signaling*, 12(609), November 2019.

[592] Mathias Uhlen, Max J. Karlsson, Wen Zhong, Abdellah Tebani, Christian Pou, Jaromir Mikes, Tadepally Lakshmikanth, Björn Forsström, Fredrik Edfors, Jacob Odeberg, Adil Mardinoglu, Cheng Zhang, Kalle von Feilitzen, Jan Mulder, Evelina Sjöstedt, Andreas Hober, Per Oksvold, Martin Zwahlen, Fredrik Ponten, Cecilia Lindskog, Åsa Sivertsson, Linn Fagerberg, and Petter Brodin. A genome-wide transcriptomic analysis of protein-coding genes in human blood cells. *Science*, 366(6472), December 2019.

[593] Mahadevaiah Umashankar, Michael Rak, Farah Bughio, Patricia Zagallo, Katie Caviness, and Felicia D. Goodrum. Antagonistic Determinants Controlling Replicative and Latent States of Human Cytomegalovirus Infection. *Journal of Virology*, 88(11):5987–6002, June 2014.

[594] Leonie Unterholzner, Sinead E. Keating, Marcin Baran, Kristy A. Horan, Søren B. Jensen, Shruti Sharma, Cherilyn M. Sirois, Tengchuan Jin, Eicke Latz, T. Sam Xiao, Katherine A. Fitzgerald, Søren R. Paludan, and Andrew G. Bowie. IFI16 is an innate immune sensor for intracellular DNA. *Nature Immunology*, 11(11):997–1004, November 2010.

[595] Yanet Valdez, Weiling Mah, Monte M. Winslow, Lixin Xu, Peter Ling, and Sarah E. Townsend. Major histocompatibility complex class II presentation of cell-associated antigen is mediated by CD8alpha+ dendritic cells in vivo. *The Journal of Experimental Medicine*, 195(6):683–694, March 2002.

[596] Jorge Valle-Arroyo, Rocío Aguado, Aurora Páez-Vega, Ana B. Pérez, Rafael González, Gema Fornés, Julián Torre-Cisneros, and Sara Cantisán. Lack of cytomegalovirus

(CMV)-specific cell-mediated immune response using QuantiFERON-CMV assay in CMV-seropositive healthy volunteers: Fact not artifact. *Scientific Reports*, 10(1):7194, April 2020.

[597] P. L. J. van der Heiden, H. M. van Egmond, S. A. J. Veld, M. van de Meent, M. Eefting, L. C. de Wreede, C. J. M. Halkes, J. H. F. Falkenburg, W. A. F. Marijt, and I. Jedema. CMV seronegative donors: Effect on clinical severity of CMV infection and reconstitution of CMV-specific immunity. *Transplant Immunology*, 49:54–58, August 2018.

[598] Pim van der Heiden, Erik Marijt, Fred Falkenburg, and Inge Jedema. Control of Cytomegalovirus Viremia after Allogeneic Stem Cell Transplantation: A Review on CMV-Specific T Cell Reconstitution. *Biology of Blood and Marrow Transplantation*, 24(9):1776–1782, September 2018.

[599] Ester M. M. van Leeuwen, Ester B. M. Remmerswaal, Mirjam H. M. Heemskerk, Ineke J. M. ten Berge, and Rene A. W. van Lier. Strong selection of virus-specific cytotoxic CD4+ T-cell clones during primary human cytomegalovirus infection. *Blood*, 108(9):3121–3127, November 2006.

[600] Ester M. M. van Leeuwen, Ester B. M. Remmerswaal, Mireille T. M. Vossen, Ajda T. Rowshani, Pauline M. E. Wertheim-van Dillen, René A. W. van Lier, and Ineke J. M. ten Berge. Emergence of a CD4+CD28- Granzyme B+, Cytomegalovirus-Specific T Cell Subset after Recovery of Primary Cytomegalovirus Infection. *The Journal of Immunology*, 173(3):1834–1841, August 2004.

[601] Guillaume van Niel, Richard Wubbolts, Toine ten Broeke, Sonja I. Buschow, Ferry A. Ossendorp, Cornelis J. Melief, Graca Raposo, Bas W. van Balkom, and Willem Stoorvogel. Dendritic Cells Regulate Exposure of MHC Class II at Their Plasma Membrane by Oligoubiquitination. *Immunity*, 25(6):885–894, December 2006.

[602] J van Zanten, M van der Giessen, WJ van Son, and TH The. Antibody responses to human cytomegalovirus-specific polypeptides studied by immunoblotting in relation to viral load during cytomegalovirus infection. *Journal of medical virology*, 39(1):80—87, January 1993.

[603] Bryan Vander Lugt, Aly A. Khan, Jason A. Hackney, Smita Agrawal, Justin Lesch, Meijuan Zhou, Wyne P. Lee, Summer Park, Min Xu, Jason DeVoss, Chauncey J. Spooner, Cecile Chalouni, Lelia Delamarre, Ira Mellman, and Harinder Singh. Transcriptional programming of dendritic cells for enhanced MHC class II antigen presentation. *Nature Immunology*, 15(2):161–167, February 2014.

[604] Stefania Varani, Madeleine Cederarv, Sari Feld, Charlotte Tammik, Giada Frascaroli, Maria P. Landini, and Cecilia Söderberg-Nauclér. Human Cytomegalovirus Differentially

Controls B Cell and T Cell Responses through Effects on Plasmacytoid Dendritic Cells. *The Journal of Immunology*, 179(11):7767–7776, December 2007.

[605] S. Variend and R. G. Pearse. Sudden infant death and cytomegalovirus inclusion disease. *Journal of Clinical Pathology*, 39(4):383–386, April 1986.

[606] Shilpi Verma, Daniela Weiskopf, Ankan Gupta, Bryan McDonald, Bjoern Peters, Alessandro Sette, and Chris A. Benedict. Cytomegalovirus-Specific CD4 T Cells Are Cytolytic and Mediate Vaccine Protection. *Journal of Virology*, 90(2):650–658, December 2015.

[607] José A. Villadangos and Louise Young. Antigen-Presentation Properties of Plasmacytoid Dendritic Cells. *Immunity*, 29(3):352–361, September 2008.

[608] Alexandra-Chloé Villani, Rahul Satija, Gary Reynolds, Siranush Sarkizova, Karthik Shekhar, James Fletcher, Morgane Griesbeck, Andrew Butler, Shiwei Zheng, Suzan Lazo, Laura Jardine, David Dixon, Emily Stephenson, Emil Nilsson, Ida Grundberg, David McDonald, Andrew Filby, Weibo Li, Philip L. De Jager, Orit Rozenblatt-Rosen, Andrew A. Lane, Muzlifah Haniffa, Aviv Regev, and Nir Hacohen. Single-cell RNA-seq reveals new types of human blood dendritic cells, monocytes and progenitors. *Science (New York, N.Y.)*, 356(6335), April 2017.

[609] Mai Vo, Alexis Aguiar, Michael A. McVoy, and Laura Hertel. Cytomegalovirus Strain TB40/E Restrictions and Adaptations to Growth in ARPE-19 Epithelial Cells. *Microorganisms*, 8(4):615, April 2020.

[610] Valentina Voigt, Catherine A. Forbes, Joanne N. Tonkin, Mariapia A. Degli-Esposti, Hamish R. C. Smith, Wayne M. Yokoyama, and Anthony A. Scalzo. Murine cytomegalovirus m157 mutation and variation leads to immune evasion of natural killer cells. *Proceedings of the National Academy of Sciences*, 100(23):13483–13488, November 2003.

[611] Harald von Boehmer. Mechanisms of suppression by suppressor T cells. *Nature Immunology*, 6(4):338–344, April 2005.

[612] Linda M. Wakim, Jason Waithman, Nico van Rooijen, William R. Heath, and Francis R. Carbone. Dendritic Cell-Induced Memory T Cell Activation in Nonlymphoid Tissues. *Science*, 319(5860):198–202, January 2008.

[613] W. J. Waldman, W. H. Roberts, D. H. Davis, M. V. Williams, D. D. Sedmak, and R. E. Stephens. Preservation of natural endothelial cytopathogenicity of cytomegalovirus by propagation in endothelial cells. *Archives of Virology*, 117(3-4):143–164, 1991.

[614] W. James Waldman, Jeffrey M. Sneddon, Ralph E. Stephens, and William H. Roberts. Enhanced endothelial cytopathogenicity induced by a cytomegalovirus strain propagated in endothelial cells. *Journal of Medical Virology*, 28(4):223–230, 1989.

[615] Edmund K. Waller, Brent R. Logan, Mingwei Fei, Stephanie J. Lee, Dennis Confer, Alan Howard, Shanmuganathan Chandrakasan, Claudio Anasetti, Shanelle M. Fernando, and Cynthia R. Giver. Kinetics of immune cell reconstitution predict survival in allogeneic bone marrow and G-CSF–mobilized stem cell transplantation. *Blood Advances*, 3(15):2250–2263, August 2019.

[616] Elizabeth A. Walter, Philip D. Greenberg, Mark J. Gilbert, Rosalynde J. Finch, Käthe S. Watanabe, E. Donnall Thomas, and Stanley R. Riddell. Reconstitution of Cellular Immunity against Cytomegalovirus in Recipients of Allogeneic Bone Marrow by Transfer of T-Cell Clones from the Donor. *New England Journal of Medicine*, 333(16):1038–1044, October 1995.

[617] Senta M. Walton, Sanja Mandaric, Nicole Torti, Albert Zimmermann, Hartmut Hengel, and Annette Oxenius. Absence of Cross-Presenting Cells in the Salivary Gland and Viral Immune Evasion Confine Cytomegalovirus Immune Control to Effector CD4 T Cells. *PLOS Pathogens*, 7(8):e1002214, August 2011.

[618] Senta M. Walton, Nicole Torti, Sanja Mandaric, and Annette Oxenius. T-cell help permits memory CD8+ T-cell inflation during cytomegalovirus latency. *European Journal of Immunology*, 41(8):2248–2259, August 2011.

[619] Senta M. Walton, Philippe Wyrsch, Michael W. Munks, Albert Zimmermann, Hartmut Hengel, Ann B. Hill, and Annette Oxenius. The Dynamics of Mouse Cytomegalovirus-Specific CD4 T Cell Responses during Acute and Latent Infection. *The Journal of Immunology*, 181(2):1128–1134, July 2008.

[620] Joseph L. Waner and Julia A. Nierenberg. Natural killing (NK) of cytomegalovirus (CMV)-infected fibroblasts: A comparison between two strains of CMV, uninfected fibroblasts, and K562 cells. *Journal of Medical Virology*, 1985.

[621] Dai Wang and Thomas Shenk. Human Cytomegalovirus UL131 Open Reading Frame Is Required for Epithelial Cell Tropism. *Journal of Virology*, 79(16):10330–10338, August 2005.

[622] Dai Wang and Thomas Shenk. Human cytomegalovirus virion protein complex required for epithelial and endothelial cell tropism. *Proceedings of the National Academy of Sciences of the United States of America*, 102(50):18153–18158, December 2005.

[623] Eddie C. Y. Wang, Brian McSharry, Christelle Retiere, Peter Tomasec, Sheila Williams, Leszek K. Borysiewicz, Veronique M. Braud, and Gavin W. G. Wilkinson. UL40-mediated NK evasion during productive infection with human cytomegalovirus. *Proceedings of the National Academy of Sciences*, 99(11):7570–7575, May 2002.

[624] Eddie C. Y. Wang, Mariana Pjechova, Katie Nightingale, Virginia-Maria Vlahava, Mihil Patel, Eva Ruckova, Simone K. Forbes, Luis Nobre, Robin Antrobus, Dawn Roberts, Ceri A. Fielding, Sepehr Seirafian, James Davies, Isa Murrell, Betty Lau, Gavin S. Wilkie, Nicolás M. Suárez, Richard J. Stanton, Borivoj Vojtesek, Andrew Davison, Paul J. Lehner, Michael P. Weekes, Gavin W. G. Wilkinson, and Peter Tomasec. Suppression of costimulation by human cytomegalovirus promotes evasion of cellular immune defenses. *Proceedings of the National Academy of Sciences*, 115(19):4998–5003, May 2018.

[625] N. Wara-Aswapati, J. A. Boch, and P. E. Auron. Activation of interleukin 1beta gene transcription by human cytomegalovirus: Molecular mechanisms and relevance to periodontitis. *Oral Microbiology and Immunology*, 18(2):67–71, April 2003.

[626] Colin Watts. The endosome–lysosome pathway and information generation in the immune system. *Biochimica et Biophysica Acta (BBA) - Proteins and Proteomics*, 1824(1):14–21, January 2012.

[627] Carsten Watzl and Eric O. Long. Signal Transduction During Activation and Inhibition of Natural Killer Cells. *Current Protocols in Immunology*, 90(1):11.9B.1–11.9B.17, 2010.

[628] Michael P. Weekes, Shireen Y.L. Tan, Emma Poole, Suzanne Talbot, Robin Antrobus, Duncan L. Smith, Christina Montag, Steven P. Gygi, John H. Sinclair, and Paul J. Lehner. Latency-associated degradation of the MRP1 drug transporter during latent human cytomegalovirus infection. *Science*, 2013.

[629] Michael P. Weekes, Mark R. Wills, J. G. Patrick Sissons, and Andrew J. Carmichael. Long-Term Stable Expanded Human CD4+ T Cell Clones Specific for Human Cytomegalovirus Are Distributed in Both CD45RAhigh and CD45ROhigh Populations. *The Journal of Immunology*, 173(9):5843–5851, November 2004.

[630] Ellen J. Wehrens, Kurt A. Wong, Ankan Gupta, Ayesha Khan, Chris A. Benedict, and Elina I. Zuniga. IL-27 regulates the number, function and cytotoxic program of antiviral CD4 T cells and promotes cytomegalovirus persistence. *PLOS ONE*, 13(7):e0201249, July 2018.

[631] K. L. Weiland, N. L. Oien, F. Homa, and M. W. Wathen. Functional analysis of human cytomegalovirus polymerase accessory protein. *Virus Research*, 34(3):191–206, December 1994.

[632] Orr-El Weizman, Eric Song, Nicholas M. Adams, Andrew D. Hildreth, Luke Riggan, Chirag Krishna, Oscar A. Aguilar, Christina S. Leslie, James R. Carlyle, Joseph C. Sun, and Timothy E. O'Sullivan. Mouse cytomegalovirus-experienced ILC1s acquire a memory response dependent on the viral glycoprotein m12. *Nature Immunology*, 20(8):1004–1011, August 2019.

[633] Stefan A. Welte, Christian Sinzger, Stefan Z. Lutz, Harpreet Singh-Jasuja, Kerstin Laib Sampaio, Ute Eknigk, Hans-Georg Rammensee, and Alexander Steinle. Selective intracellular retention of virally induced NKG2D ligands by the human cytomegalovirus UL16 glycoprotein. *European Journal of Immunology*, 33(1):194–203, 2003.

[634] Suzanne P. M. Welten, Anke Redeker, Kees L. Franken, Chris A. Benedict, Hideo Yagita, Felix M. Wensveen, Jannie Borst, Cornelis J. M. Melief, René A. W. van Lier, Klaas P. J. M. van Gisbergen, and Ramon Arens. CD27-CD70 Costimulation Controls T Cell Immunity during Acute and Persistent Cytomegalovirus Infection. *Journal of Virology*, 87(12):6851–6865, June 2013.

[635] Kristen N. Westdorp, Andrea Sand, Nathaniel J. Moorman, and Scott S. Terhune. Cytomegalovirus Late Protein pUL31 Alters Pre-rRNA Expression and Nuclear Organization during Infection. *Journal of Virology*, 91(18), September 2017.

[636] EF Wheelock. Interferon-like virus-inhibitor induced in human leukocytes by phytohemagglutinin. *Science*, 1965.

[637] EA White and DH Spector. Early CMV gene expression and function. In AM Arvin, G Campadelli-Fiume, ES Mocarski, and Et Al, editors, *Human Herpesviruses: Biology, Therapy, and Immunoprophylaxis*, pages 264–294. Cambridge University Press, 2011.

[638] Emmanuel J. H. J. Wiertz, Domenico Tortorella, Matthew Bogyo, Joyce Yu, Walther Mothes, Thomas R. Jones, Tom A. Rapoport, and Hidde L. Ploegh. Sec6l-mediated transfer of a membrane protein from the endoplasmic reticulum to the proteasome for destruction. *Nature*, 384(6608):432–438, December 1996.

[639] Emmanuel J.H.J. Wiertz, Thomas R. Jones, Lei Sun, Matthew Bogyo, Hans J. Geuze, and Hidde L. Ploegh. The human cytomegalovirus US11 gene product dislocates MHC class I heavy chains from the endoplasmic reticulum to the cytosol. *Cell*, 1996.

[640] C. A. Wiley and J. A. Nelson. Role of human immunodeficiency virus and cytomegalovirus in AIDS encephalitis. *The American Journal of Pathology*, 133(1):73–81, October 1988.

[641] Gavin W. G. Wilkinson, Andrew J. Davison, Peter Tomasec, Ceri A. Fielding, Rebecca Aicheler, Isa Murrell, Sepher Seirafian, Edward C. Y. Wang, Michael Weekes, Paul J.

Lehner, Gavin S. Wilkie, and Richard J. Stanton. Human cytomegalovirus: Taking the strain. *Medical Microbiology and Immunology*, 204(3):273–284, June 2015.

[642] Gavin W. G. Wilkinson, Peter Tomasec, Richard J. Stanton, Melanie Armstrong, Virginie Prod'homme, Rebecca Aicheler, Brian P. McSharry, Carole R. Rickards, Daniel Cochrane, Sian Llewellyn-Lacey, Eddie C. Y. Wang, Cora A. Griffin, and Andrew J. Davison. Modulation of natural killer cells by human cytomegalovirus. *Journal of Clinical Virology*, 41(3):206–212, March 2008.

[643] Mark R. Wills, Georgina Okecha, Michael P. Weekes, Maher K. Gandhi, Patrick J. G. Sissons, and Andrew J. Carmichael. Identification of naive or antigen-experienced human CD8(+) T cells by expression of costimulation and chemokine receptors: Analysis of the human cytomegalovirus-specific CD8(+) T cell response. *Journal of Immunology (Baltimore, Md.: 1950)*, 168(11):5455–5464, June 2002.

[644] Mark R. Wills, Emma Poole, Betty Lau, Ben Krishna, and John H. Sinclair. The immunology of human cytomegalovirus latency: Could latent infection be cleared by novel immunotherapeutic strategies? *Cellular & Molecular Immunology*, 12(2):128–138, March 2015.

[645] Nikolaus Wirtz, Sina I. Schader, Rafaela Holtappels, Christian O. Simon, Niels A. W. Lemmermann, Matthias J. Reddehase, and Jürgen Podlech. Polyclonal cytomegalovirus-specific antibodies not only prevent virus dissemination from the portal of entry but also inhibit focal virus spread within target tissues. *Medical Microbiology and Immunology*, 197(2):151–158, June 2008.

[646] Barbara Withers, Emily Blyth, Leighton E. Clancy, Agnes Yong, Chris Fraser, Jane Burgess, Renee Simms, Rebecca Brown, David Kliman, Ming-Celine Dubosq, David Bishop, Gaurav Sutrave, Chun Kei Kris Ma, Peter J. Shaw, Kenneth P. Micklethwaite, and David J. Gottlieb. Long-term control of recurrent or refractory viral infections after allogeneic HSCT with third-party virus-specific T cells. *Blood Advances*, 1(24):2193–2205, November 2017.

[647] S. D. Wright, R. A. Ramos, P. S. Tobias, R. J. Ulevitch, and J. C. Mathison. CD14, a receptor for complexes of lipopolysaccharide (LPS) and LPS binding protein. *Science*, 249(4975):1431–1433, September 1990.

[648] Zeguang Wu, Christian Sinzger, Giada Frascaroli, Johanna Reichel, Carina Bayer, Li Wang, Reinhold Schirmbeck, and Thomas Mertens. Human Cytomegalovirus-Induced NKG2Chi CD57hi Natural Killer Cells Are Effectors Dependent on Humoral Antiviral Immunity. *Journal of Virology*, 87(13):7717–7725, July 2013.

[649] Aparecida Yulie Yamamoto, Marisa Marcia Mussi-Pinhata, Suresh B. Boppana, Zdenek Novak, Virginia M. Wagatsuma, Patricia de Frizzo Oliveira, Geraldo Duarte, and William J. Britt. Human cytomegalovirus reinfection is associated with intrauterine transmission in a highly cytomegalovirus-immune maternal population. *American Journal of Obstetrics and Gynecology*, 202(3):297.e1–297.e8, March 2010.

[650] Y. Yamashita, K. Shimokata, S. Mizuno, H. Yamaguchi, and Y. Nishiyama. Down-regulation of the surface expression of class I MHC antigens by human cytomegalovirus. *Virology*, 193(2):727–736, April 1993.

[651] Yan Yan, Renfang Chen, Xu Wang, Kai Hu, Lihua Huang, Mengji Lu, and Qinxue Hu. CCL19 and CCR7 Expression, Signaling Pathways, and Adjuvant Functions in Viral Infection and Prevention. *Frontiers in Cell and Developmental Biology*, 7, October 2019.

[652] Lele Ye, Yunyun Qian, Weijie Yu, Gangqiang Guo, Hong Wang, and Xiangyang Xue. Functional Profile of Human Cytomegalovirus Genes and Their Associated Diseases: A Review. *Frontiers in Microbiology*, 11, 2020.

[653] Kok-Hooi Yew, Bonnie Carsten, and Christopher Harrison. Scavenger receptor A1 is required for sensing HCMV by endosomal TLR-3/-9 in monocytic THP-1 cells. *Molecular Immunology*, 47(4):883–893, January 2010.

[654] Yue Yin and Herman W. Favoreel. Herpesviruses and the Type III Interferon System. *Virologica Sinica*, January 2021.

[655] Louise J. Young, Nicholas S. Wilson, Petra Schnorrer, Anna Proietto, Toine ten Broeke, Yohei Matsuki, Adele M. Mount, Gabrielle T. Belz, Meredith O'Keeffe, Mari Ohmura-Hoshino, Satoshi Ishido, Willem Stoorvogel, William R. Heath, Ken Shortman, and Jose A. Villadangos. Differential MHC class II synthesis and ubiquitination confers distinct antigen-presenting properties on conventional and plasmacytoid dendritic cells. *Nature Immunology*, 9(11):1244–1252, November 2008.

[656] Dong Yu, Maria C. Silva, and Thomas Shenk. Functional map of human cytomegalovirus AD169 defined by global mutational analysis. *Proceedings of the National Academy of Sciences*, 100(21):12396–12401, October 2003.

[657] Tae Jin Yun, Suzu Igarashi, Haoquan Zhao, Oriana A. Perez, Marcus R. Pereira, Emmanuel Zorn, Yufeng Shen, Felicia Goodrum, Adeeb Rahman, Peter A. Sims, Donna L. Farber, and Boris Reizis. Human plasmacytoid dendritic cells mount a distinct antiviral response to virus-infected cells. *Science Immunology*, 6(58), April 2021.

[658] G Zauli, G Furlini, M Vitale, MC Re, D Gibellini, L Zamai, G Visani, P Borgatti, S Capitani, and M La Placa. A subset of human CD34+ hematopoietic progenitors

express low levels of CD4, the high-affinity receptor for human immunodeficiency virus-type 1. *Blood*, 84(6):1896–1905, September 1994.

[659] Biao Zheng, Zeynep Z. Ozen, Shutong Cao, Ye Zhang, and Shuhua Han. CD4-deficient T helper cells are capable of supporting somatic hypermutation and affinity maturation of germinal center B cells. *European Journal of Immunology*, 32(11):3315–3325, November 2002.

[660] Hua Zhu, Jiang-Ping Cong, and Thomas Shenk. Use of differential display analysis to assess the effect of human cytomegalovirus infection on the accumulation of cellular RNAs: Induction of interferon-responsive RNAs. *Proceedings of the National Academy of Sciences*, 94(25):13985–13990, December 1997.

[661] Jianhui Zhu, Gene M. Shearer, Francesco M. Marincola, James E. Norman, David Rott, Jian-Ping Zou, and Stephen E. Epstein. Discordant cellular and humoral immune responses to cytomegalovirus infection in healthy blood donors: Existence of a Th1-type dominant response. *International Immunology*, 13(6):785–790, June 2001.

[662] H. W. L. Ziegler-Heitbrock and R. J. Ulevitch. CD14: Cell surface receptor and differentiation marker. *Immunology Today*, 14(3):121–125, January 1993.

[663] Loems Ziegler-Heitbrock, Petronela Ancuta, Suzanne Crowe, Marc Dalod, Veronika Grau, Derek N. Hart, Pieter J. M. Leenen, Yong-Jun Liu, Gordon MacPherson, Gwendalyn J. Randolph, Juergen Scherberich, Juergen Schmitz, Ken Shortman, Silvano Sozzani, Herbert Strobl, Marek Zembala, Jonathan M. Austyn, and Manfred B. Lutz. Nomenclature of monocytes and dendritic cells in blood. *Blood*, 116(16):e74–e80, October 2010.

[664] Donato Zipeto, Fausto Baldanti, Elena Percivalle, Giuseppe Gerna, and Gabriele Milanesi. Identification of a human cytomegalovirus mutant in the pp150 matrix phosphoprotein gene with a growth-defective phenotype. *Journal of General Virology*, 74(8):1645–1648, August 1993.

[665] Jasmin Zischke, Panagiota Mamareli, Claudia Pokoyski, Ildar Gabaev, Sabine Buyny, Roland Jacobs, Christine S. Falk, Matthias Lochner, Tim Sparwasser, Thomas F. Schulz, and Penelope C. Kay-Fedorov. The human cytomegalovirus glycoprotein pUL11 acts via CD45 to induce T cell IL-10 secretion. *PLOS Pathogens*, 13(6):e1006454, June 2017.

Appendices

A Characteristics of healthy donors

Donor	Gender	Age	HCMV serostatus
AQUARIA 02	Female	31	Positive
AQUARIA 03	Female	32	Positive
AQUARIA 04	Female	39	Positive
AQUARIA 06	Female	68	Positive
AQUARIA 07	Male	74	Negative
AQUARIA 08	Male	71	Positive
AQUARIA 09	Female	75	Positive
AQUARIA 10	Female	39	Positive
AQUARIA 11	Female	76	Negative
AQUARIA 12	Female	41	Negative
AQUARIA 13	Male	40	Negative
AQUARIA 14	Female	73	Positive
AQUARIA 16	Male	41	Negative
AQUARIA 17	Male	75	Negative
AQUARIA 18	Female	76	Negative
AQUARIA 19	Female	76	Negative
AQUARIA 20	Male	36	Negative
AQUARIA 21	Female	74	Positive
AQUARIA 22	Female	76	Positive
AQUARIA 23	Female	39	Negative
AQUARIA 24	Female	74	Positive
AQUARIA 25	Female	39	Positive
AQUARIA 26	Male	38	Positive

Table A: Characteristics of healthy donors

B Individual results of viral dissemination assays performed on PBMCs from healthy donors

(A) Seropositive donors, PBMCs

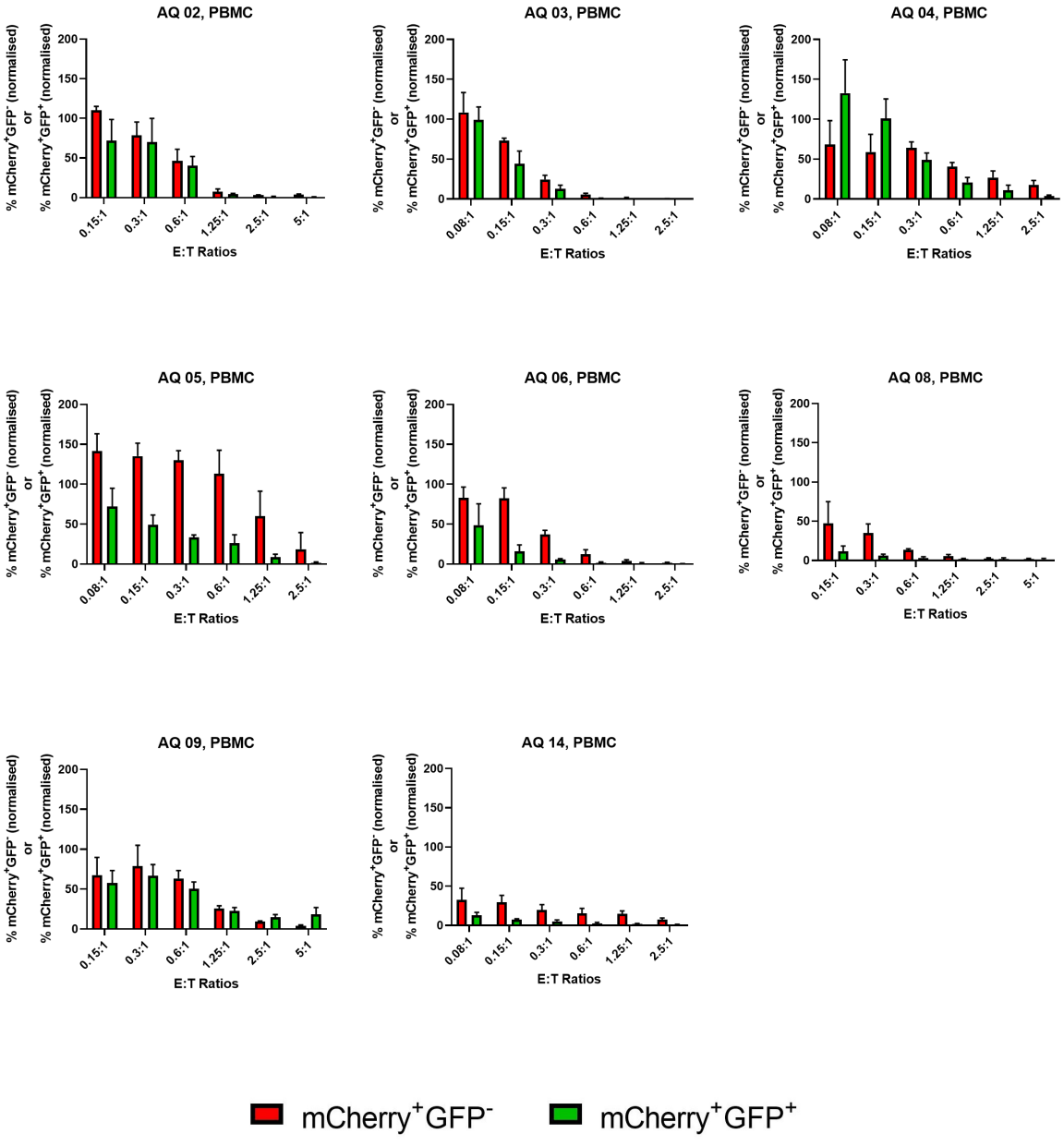

(B) Seronegative donors, PBMCs

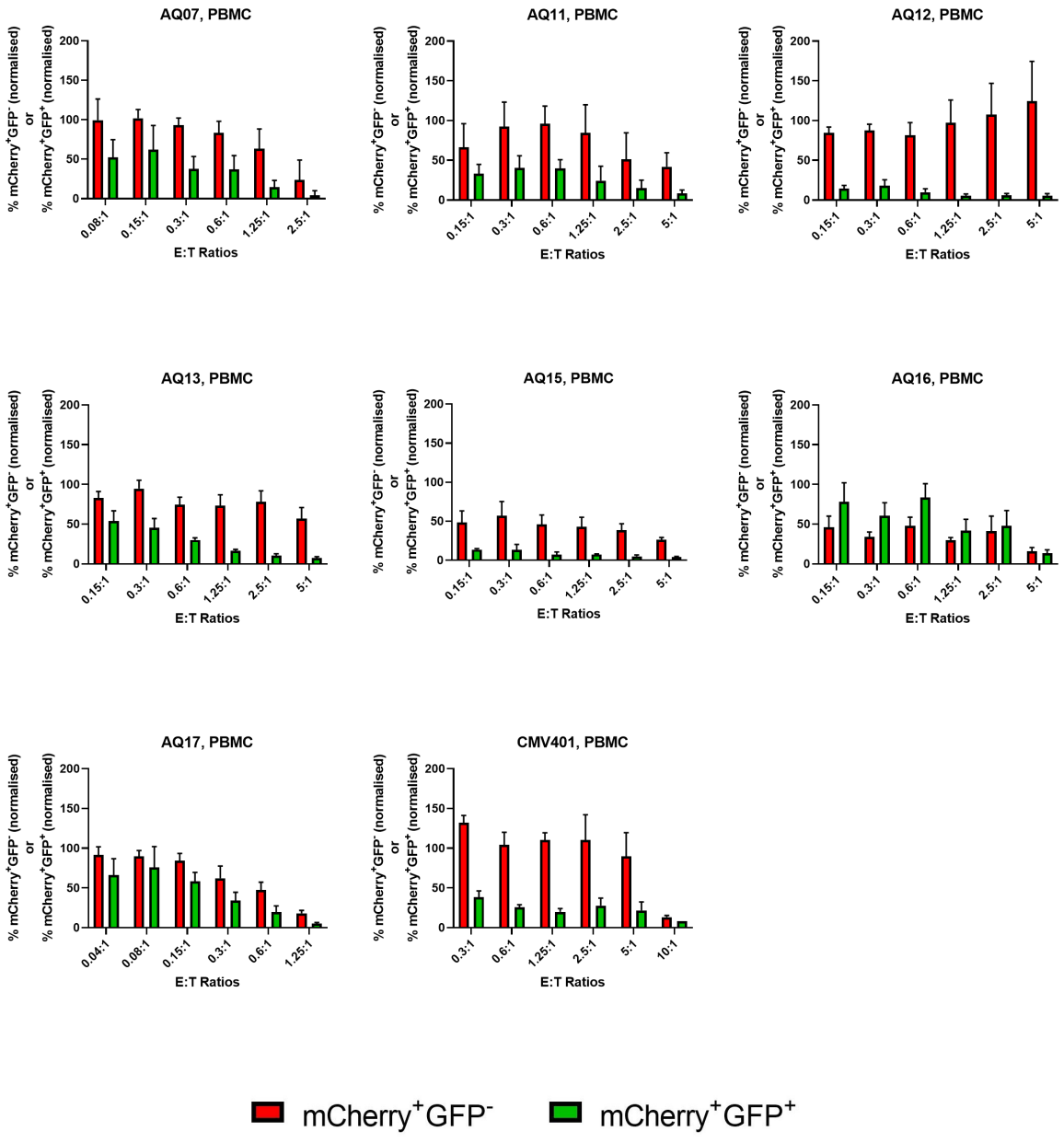

Figure B: Individual results of viral dissemination assays performed on PBMCs from healthy donors

Error bars represent SD of triplicate wells.

C Post-separation purities of $CD4^+$ cells from healthy donors

Donor	Live cells (%)	$CD3^+$ (% of Live cells)	$CD4^+$ (% of $CD3^+$ cells)
AQUARIA 02	95.1	99.7	99.5
AQUARIA 03	91.8	91.2	95.4
AQUARIA 04	94.2	99.8	99.7
AQUARIA 06	99.9	99.1	94.1
AQUARIA 07	92.5	99.5	99.5
AQUARIA 08	100	99.9	98.7
AQUARIA 09	100	97.5	85.8
AQUARIA 10	87.5	97.4	96.8
AQUARIA 11	99.7	93.9	95.9
AQUARIA 12	100	99.6	97.3
AQUARIA 13	90.3	97.5	97
AQUARIA 14	90.4	97.9	98.8
AQUARIA 16	100	99.3	92.6
AQUARIA 17	90.8	97.2	98.6
AQUARIA 18	100	99.5	97.8
AQUARIA 19	99.9	98.4	89.3
AQUARIA 20	95.5	99.3	99.6
AQUARIA 21	100	98.9	95.7
AQUARIA 22	99.9	98.7	89.7
AQUARIA 23	100	99.3	91.1
AQUARIA 24	100	98.2	97.1
AQUARIA 25	100	99.5	97.6
AQUARIA 26	100	99.5	97.1

Table C: Post-separation purities of $CD4^+$ T cells from healthy donors

D Individual results of viral dissemination assays performed on CD4$^+$ cells from healthy donors

(A) Seropositive donors, CD4$^+$ cells

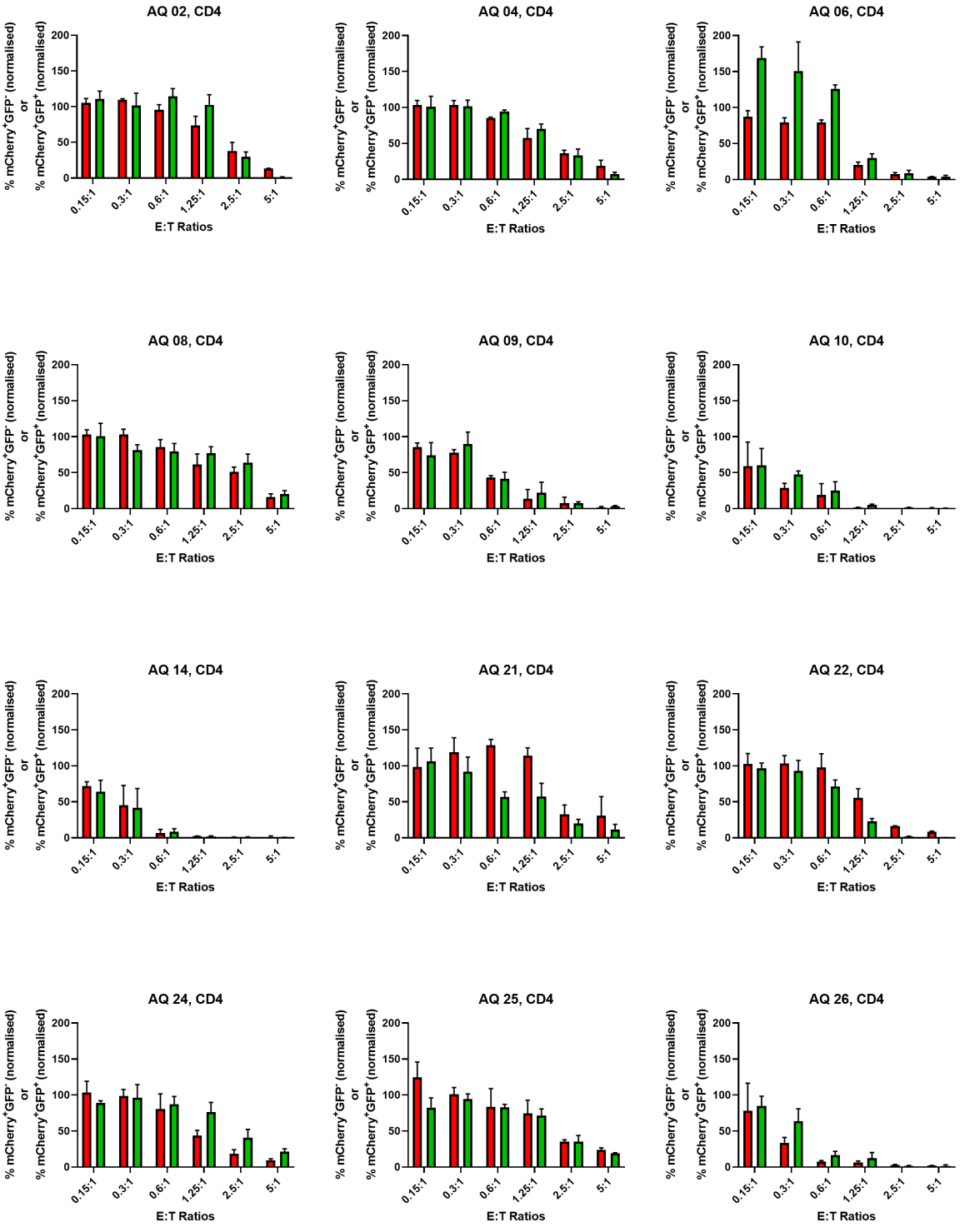

(B) Seronegative donors, $CD4^+$ cells

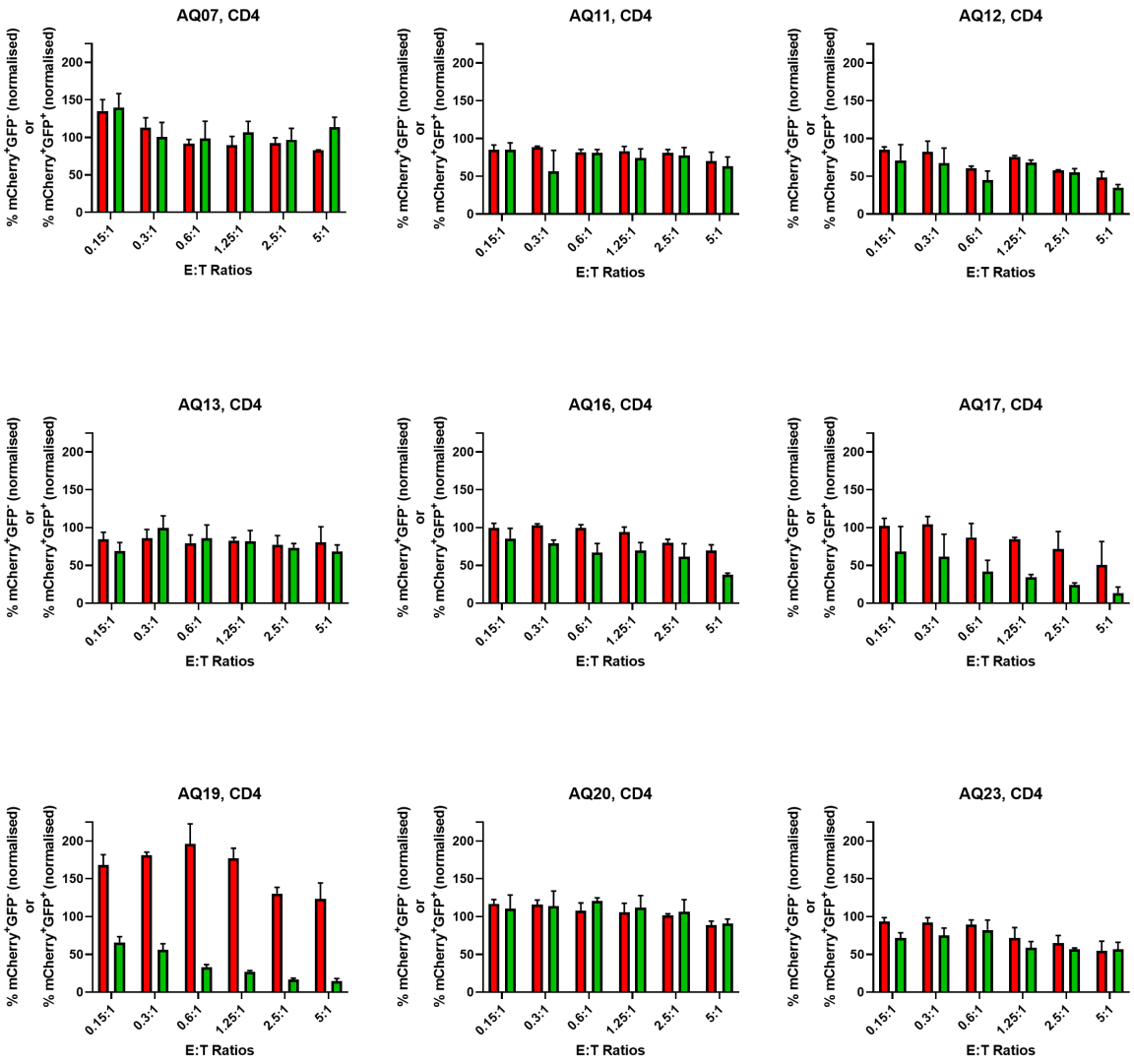

Figure D: Individual results of viral dissemination assays performed on $CD4^+$ cells from healthy donors

Error bars represent SD of triplicate wells.

E Post-separation purities of CD8$^+$ T cells from healthy donors

Donor	Live cells (%)	CD3$^+$ (% of Live cells)	CD8$^+$ (% of CD3$^+$ cells)
AQUARIA 02	98.5	94.7	90.2
AQUARIA 03	99.2	96.7	93.7
AQUARIA 04		30.2	76.9
AQUARIA 05	88.1	78.6	88.9
AQUARIA 06	96.2	92.4	86.6
AQUARIA 07	89.2	88.1	88.3
AQUARIA 08	98.1	51.1	98.5
AQUARIA 09	96.3	71.3	99.4
AQUARIA 11	92.4	89.5	80.8
AQUARIA 12	98.7	94.1	60.5
AQUARIA 13	99.5	90.8	59.7
AQUARIA 14	96.4	93.2	88.5
AQUARIA 15	96.6	92.3	94.6
AQUARIA 16	95.9	95.7	90.3

Table E: Post-separation purities of CD8$^+$ T cells from healthy donors

F Individual results of viral dissemination assays performed on CD8$^+$ T cells from healthy donors

(A) Seropositive donors, CD8$^+$ T cells

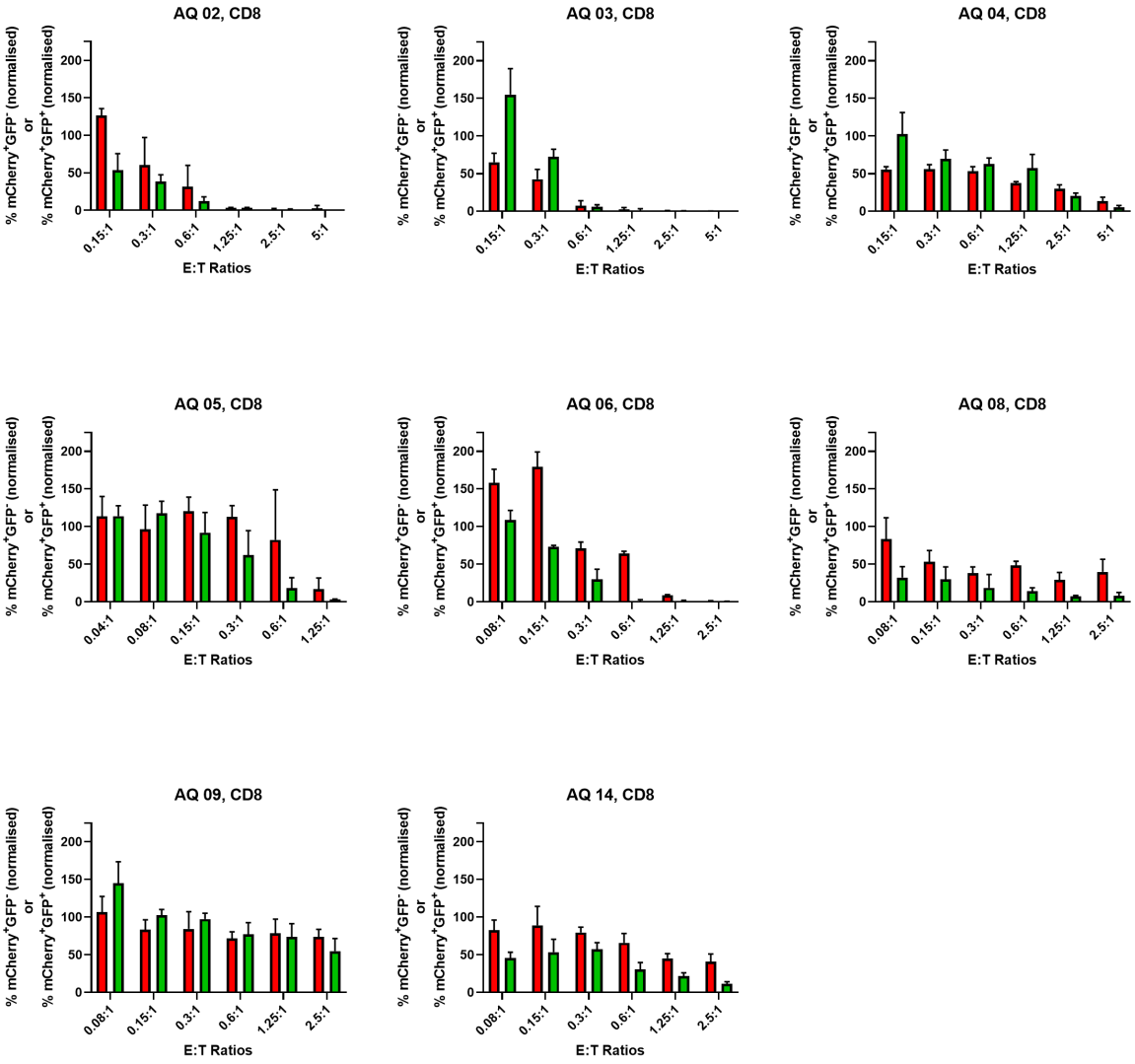

(B) Seronegative donors, $CD8^+$ T cells

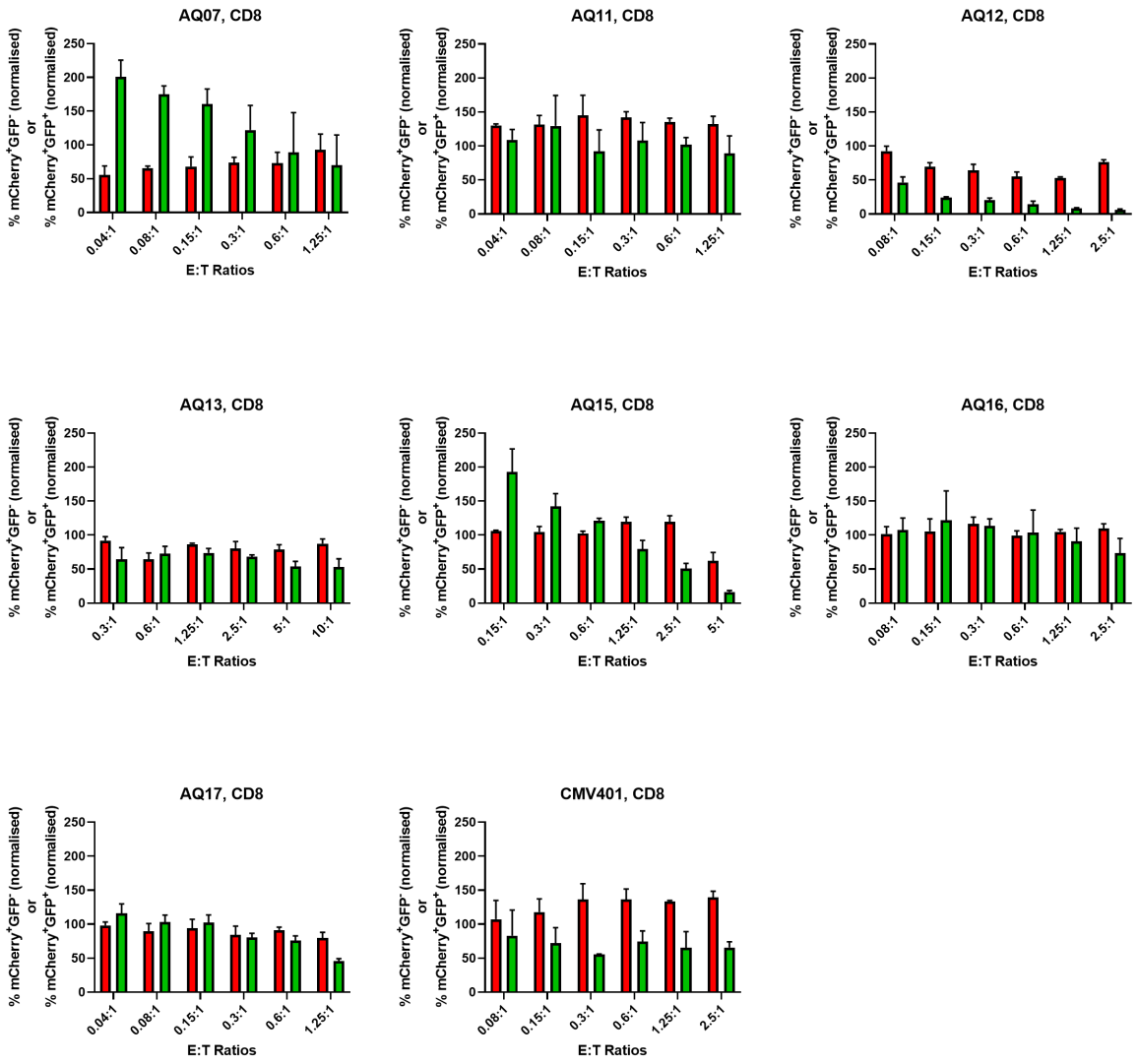

Figure F: Individual results of viral dissemination assays performed on $CD8^+$ T cells from healthy donors

Error bars represent SD of triplicate wells.

G Post-separation purities of NK cells from healthy donors

Donor	Live cells (%)	$CD3^-$ (% of Live cells)	$CD56^{dim}$ (% of $CD3^-$ cells)	$CD56^{bright}$ (% of $CD3^-$ cells)
AQUARIA 02	98.5	95	73.29	15.25
AQUARIA 03	99.2	97.6	95.37	2.28
AQUARIA 04	78.8	92.5	69.33	25.84
AQUARIA 05	87.8	99.5	86.47	2.62
AQUARIA 06	80.3	97	80.91	18.01
AQUARIA 07	89.4	99.9	96.54	1.51
AQUARIA 08	94.9	99.4	89.27	4.3
AQUARIA 09	95.7	99.9	92.86	3.03
AQUARIA 11	94.8	100	82.7	0.2
AQUARIA 12	98.5	99.7	97.1	1.5
AQUARIA 13	93.2	98.9	98.8	0.2
AQUARIA 14	90.8	99.7	90.28	1.74
AQUARIA 15	86.6	99.3	82.95	9.95
AQUARIA 16	96.9	99.5	73.1	2

Table G: Post-separation purities of NK cells from healthy donors

H Individual results of viral dissemination assays performed on NK cells from healthy donors

(A) Seropositive donors, NK cells

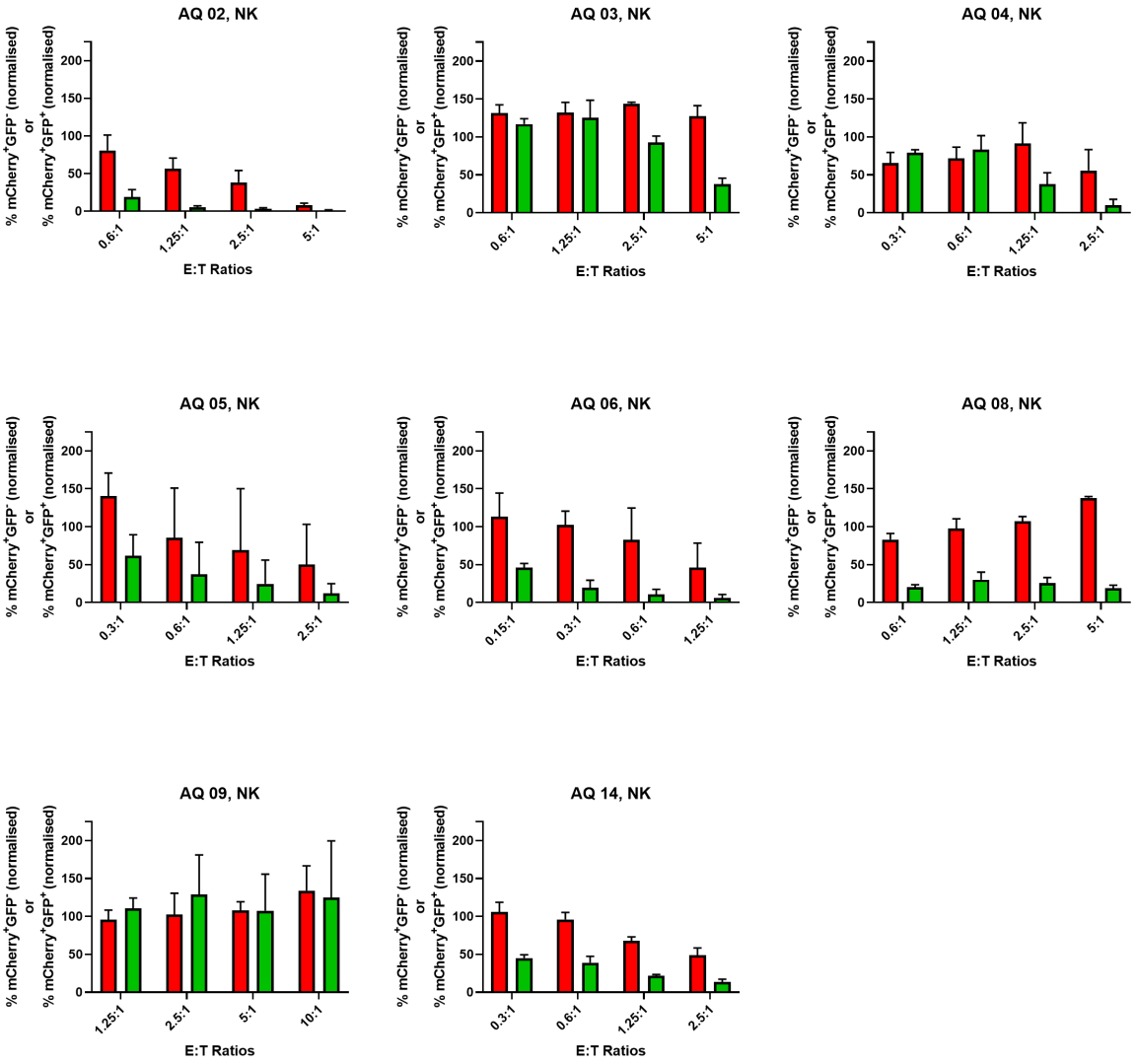

(B) Seronegative donors, NK cells

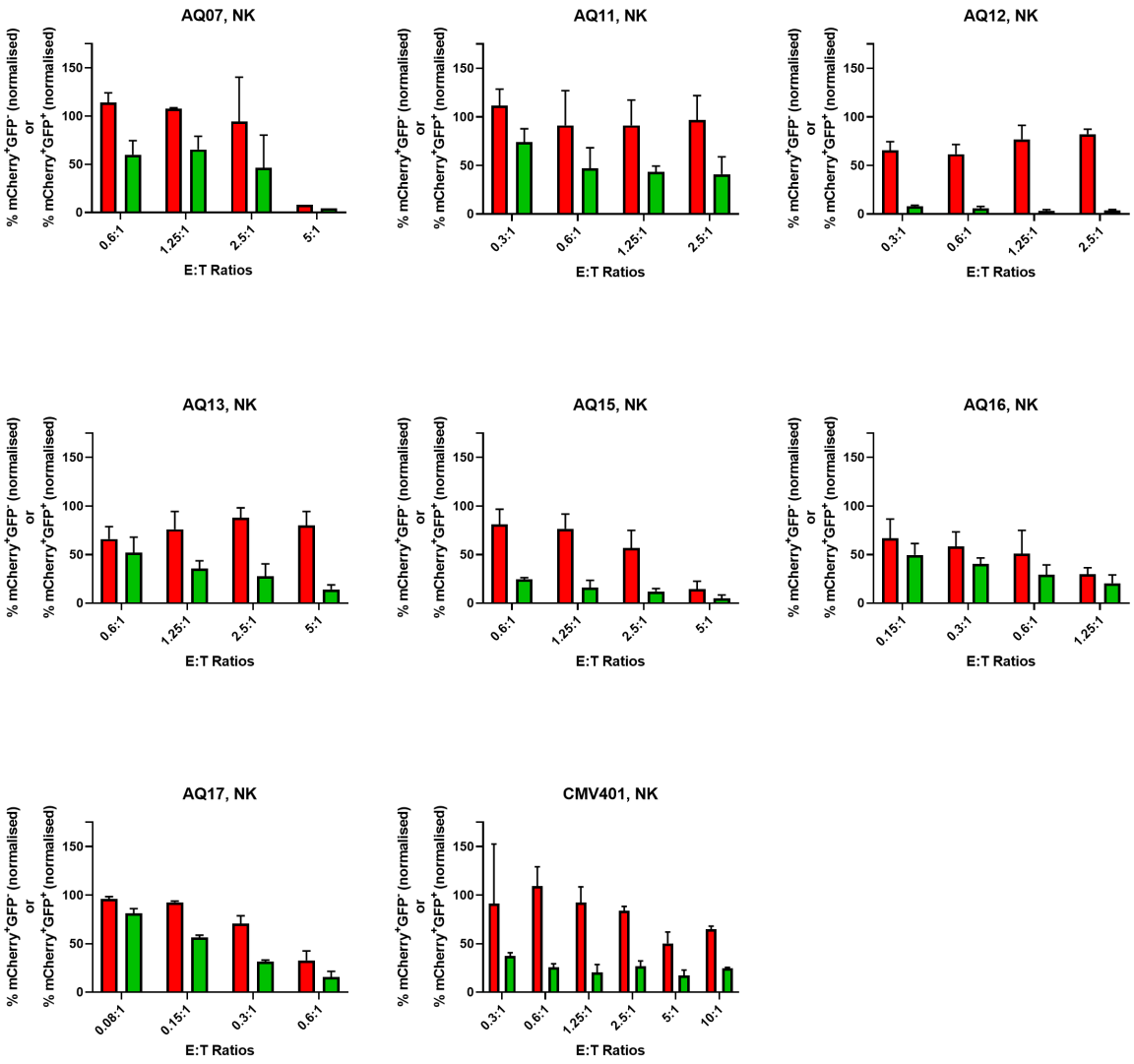

Figure H: Individual results of viral dissemination assays performed on NK cells from healthy donors

Error bars represent SD of triplicate wells.

I Post-separation purity of cell populations used in Figs.5.10B & 5.10C

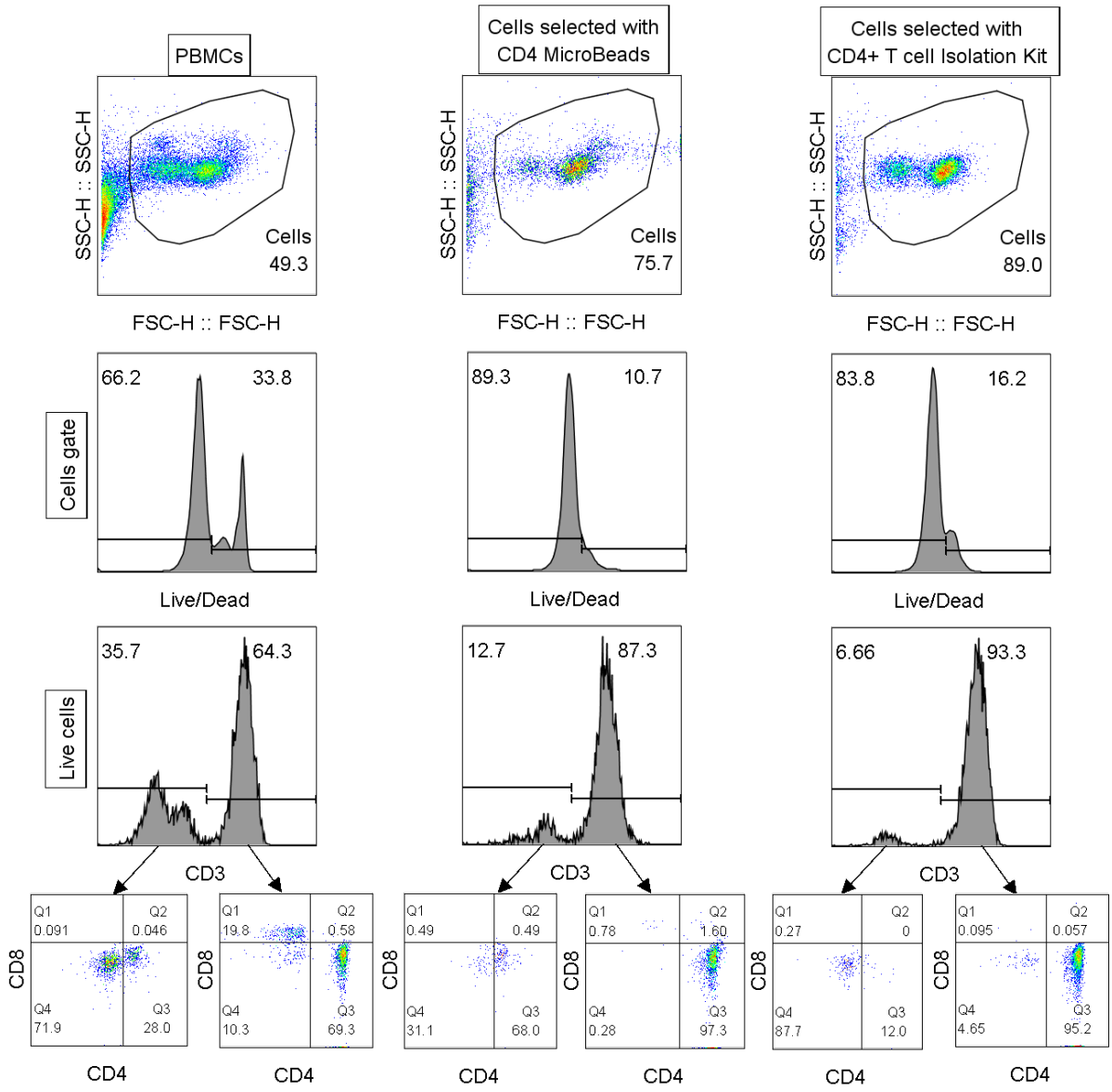

Figure I: Post-separation purity of cell populations used in Figs.5.10B & 5.10C
Cells were stained with Live/Dead FarRed, CD3-FITC, CD4-PE and CD8-PerCP-Cy5.5. Left column shows PBMCs, middle column shows purities of cells isolated by positive selection on MACS with CD4 MicroBeads, right column shows cells isolated by depletion on MACS with $CD4^+$ T cell Isolation Kit. Last row shows CD4 and CD8 stains on the $CD3^-$ and $CD3^+$ cells from each population.

J Characteristics of individual transplant recipients

Patient	Organ transplanted	Donor CMV serostatus	Recipient CMV serostatus
R01-037	Kidney	D^+	R^-
R01-079	Liver	D^+	R^-
R01-081	Liver	D^+	R^-
R02-005	Liver	D^+	R^+
R02-011	Liver	D^+	R^+
R02-015	Liver	D^-	R^+
R02-058	Kidney	D^+	R^+
R02-079	Kidney	D^+	R^+
R02-109	Kidney	D^+	R^+
R02-125	Kidney	D^+	R^+
R02-129	Liver	D^+	R^+
R02-171	Liver	D^+	R^+
R02-174	Liver	D^-	R^+
R02-184	Kidney	D^+	R^+
R02-185	Kidney	D^+	R^+

Table J: Characteristics of individual transplant recipients

K Individual results of viral dissemination assays performed on PBMCs from transplant recipients

(A) D^+R^- Viraemic

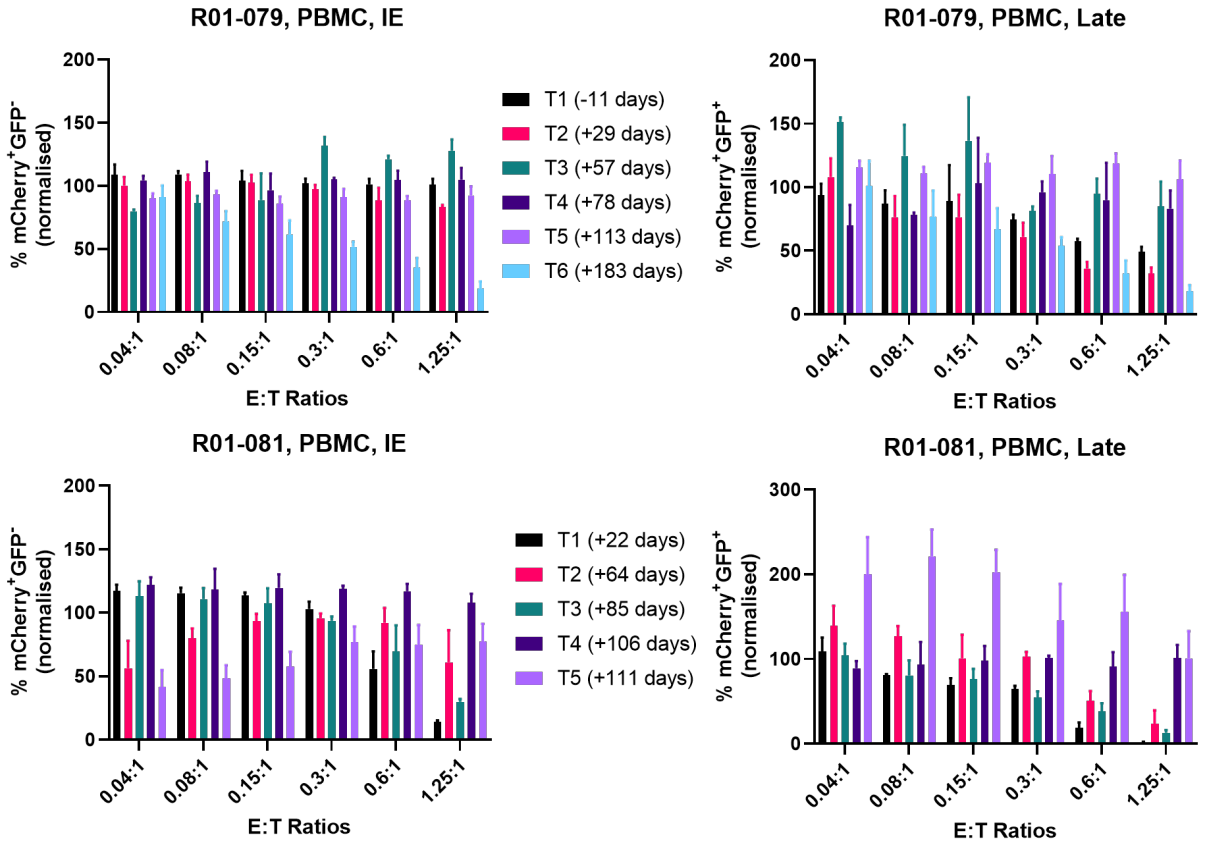

(B) D^+R^+ Viraemic

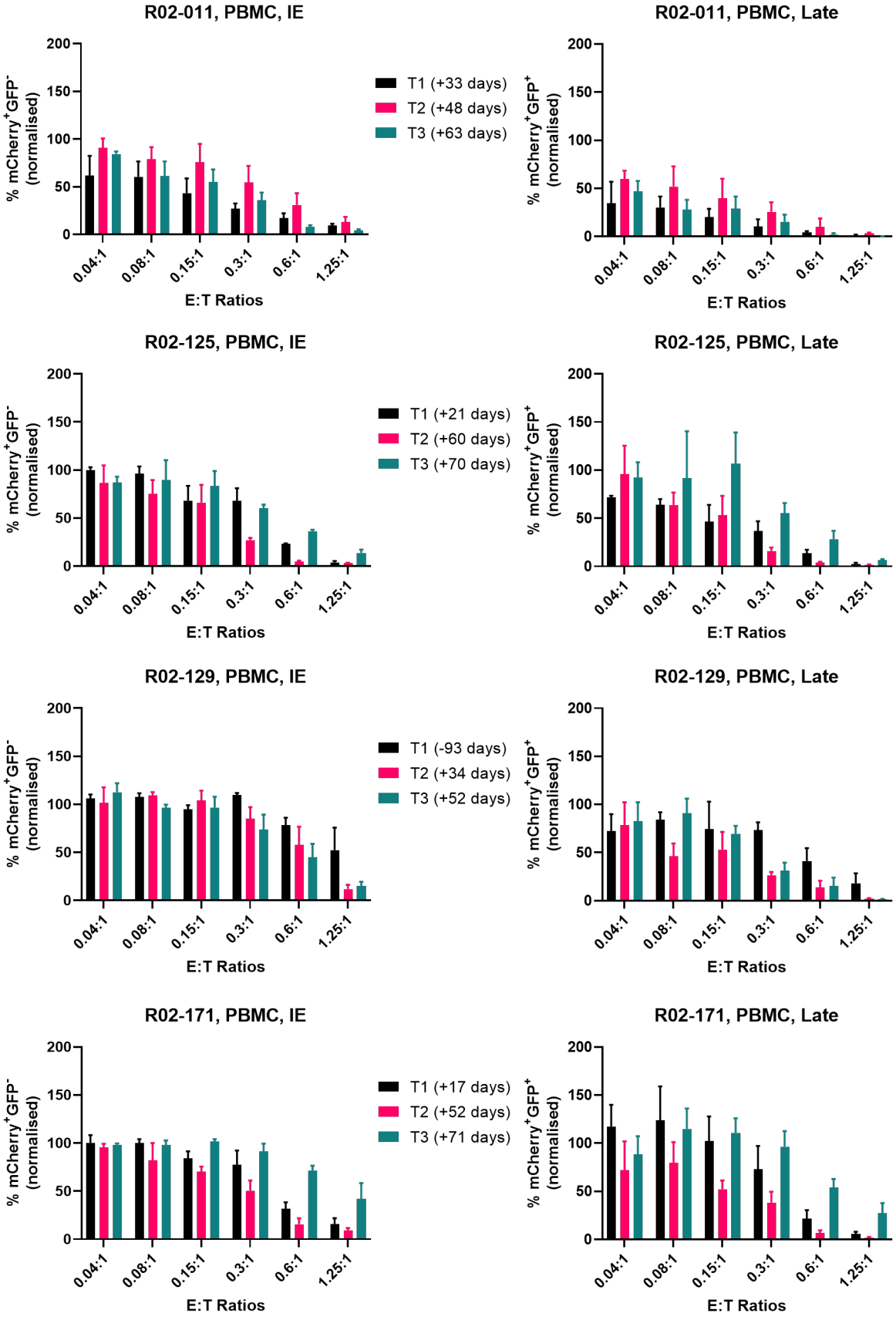

(C) D^+R^- Non-viraemic

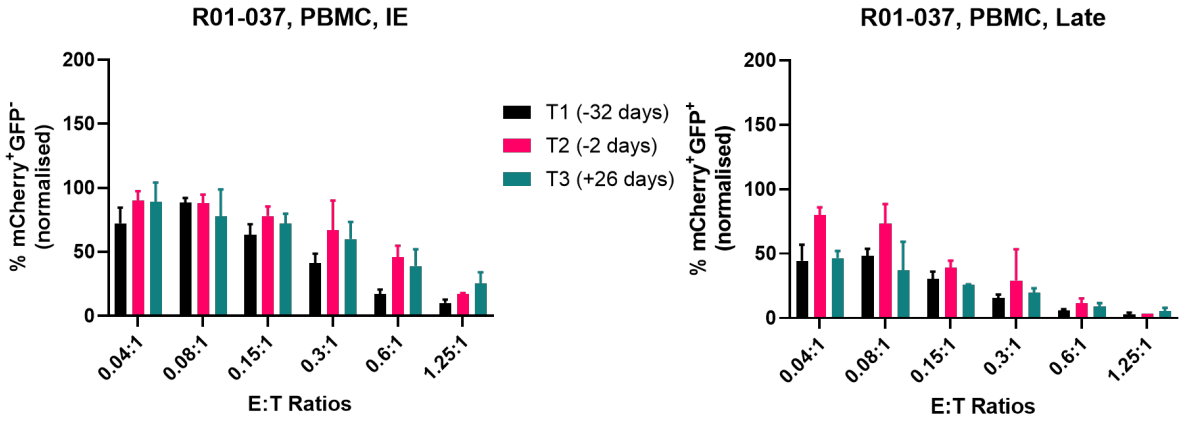

(D) D^-R^+ Non-viraemic

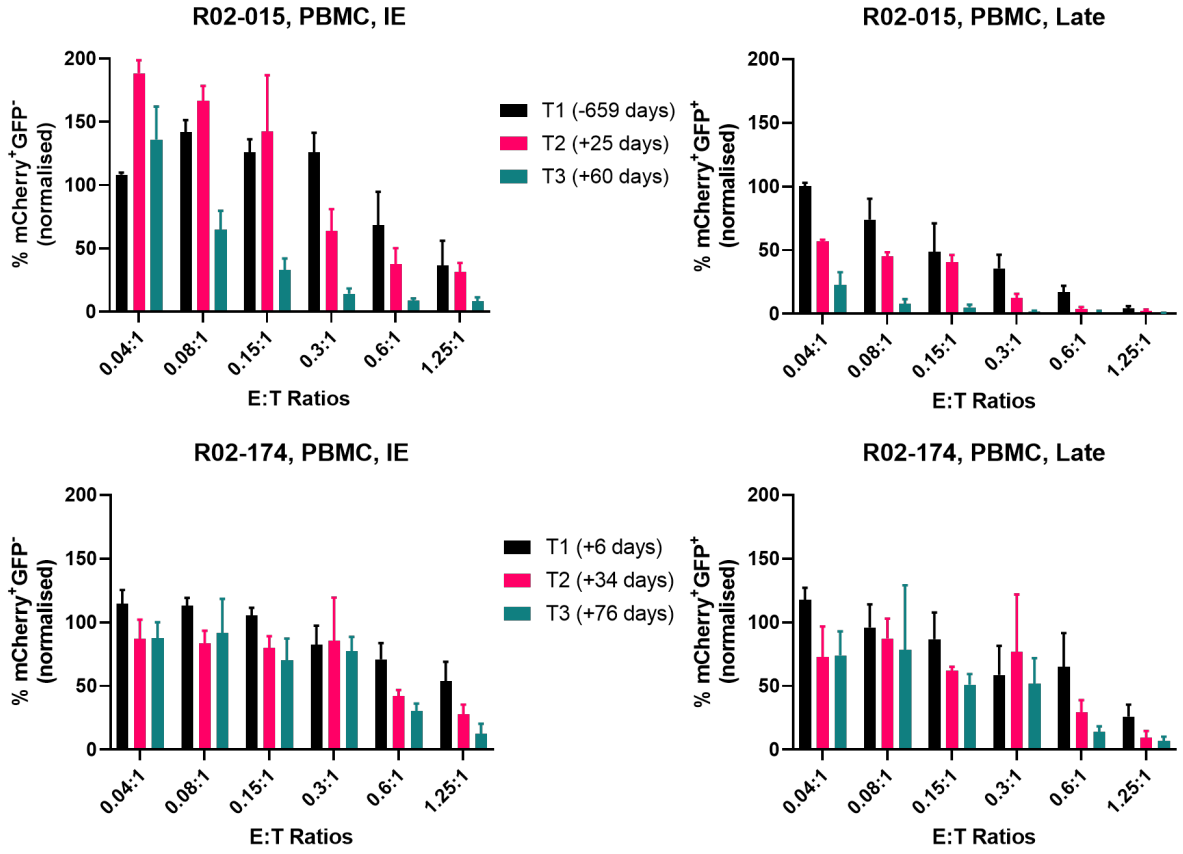

(E) D^+R^+ Non-viraemic

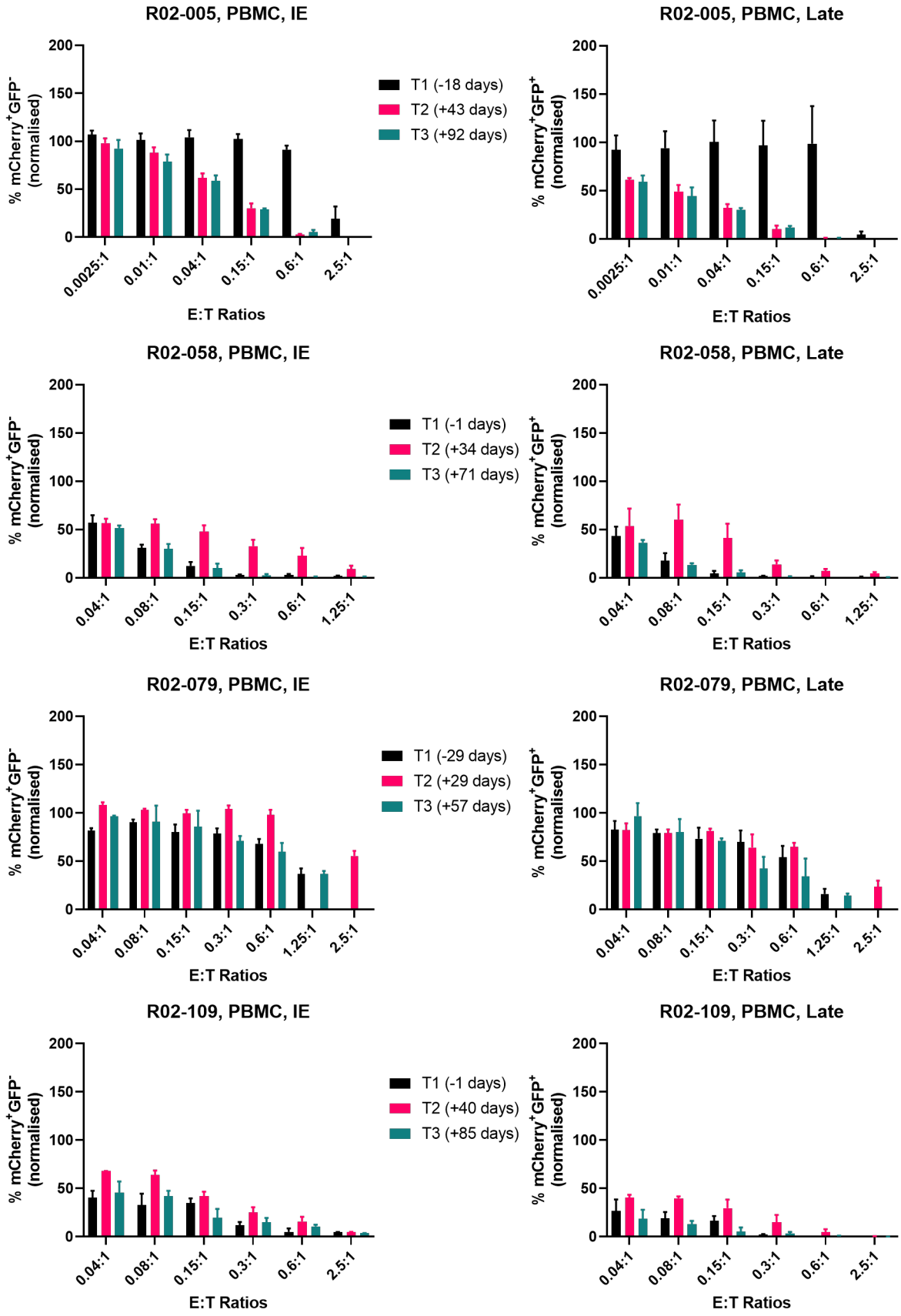

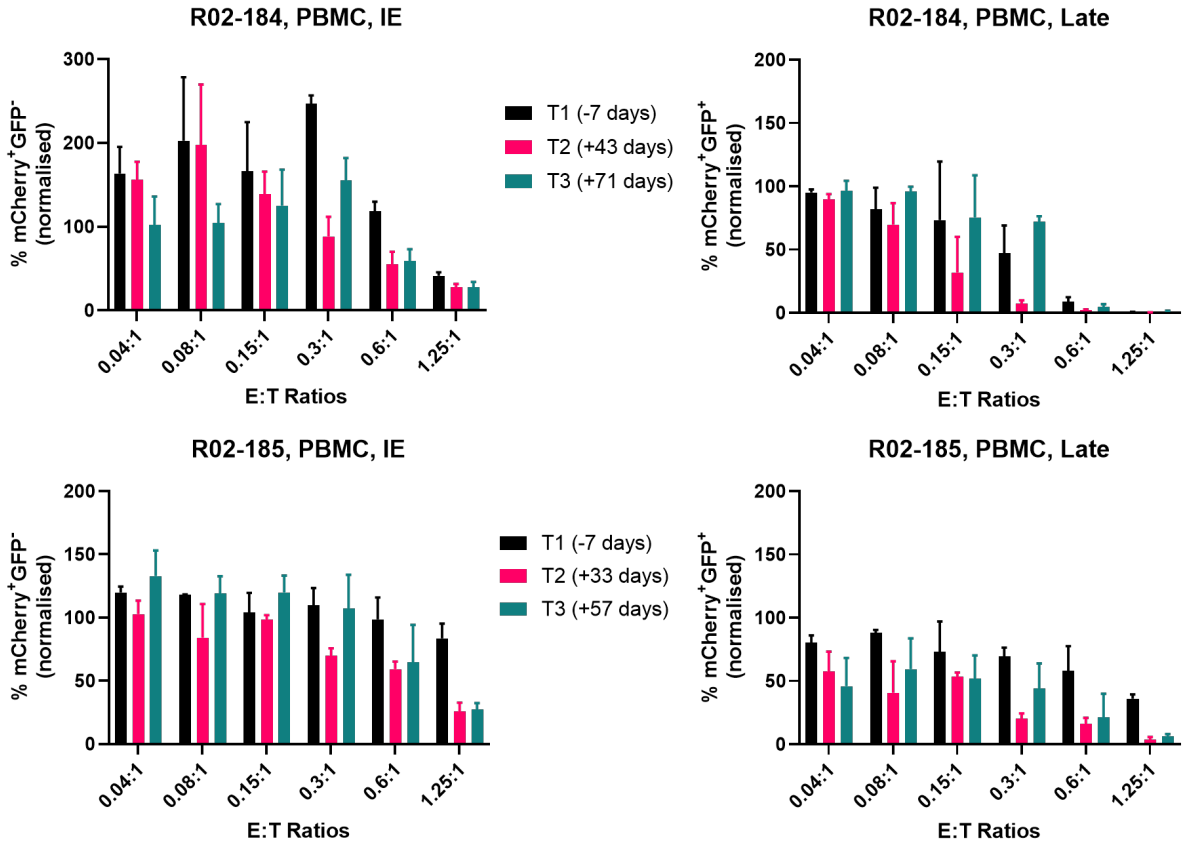

Figure K: Individual results of viral dissemination assays performed on PBMCs from transplant recipients

T1 = Timepoint 1; T2 = Timepoint 2; T3 = Timepoint 3; T4 = Timepoint 4; T5 = Timepoint 5; T6 = Timepoint 6. Number of days pre- or post-transplant that sample was taken from is given in brackets in legend of each graph. Error bars represent SD of triplicate wells.

L Post-separation purities of CD4$^+$ cells from transplant recipients

Donor	Timepoint	Live cells (%)	CD3$^+$ (% of Live cells)	CD4$^+$ (% of CD3$^+$)
R01-079	1	97.7	97.8	95
	2	97	99	99
	3	99.3	99.6	99.6
	4	91.9	93.1	96.4
	5	67.5	98.5	94.3
	6	96.4	98.9	97.4
R01-081	1	90.1	97.9	96.6
	2	81.4	98.3	96.9
	3	13.2	91	83.1
R02-011	1	98.2	95.2	96.2
	2	96.3	99.5	99.2
	3	94.3	97.8	98.4
R02-125	1	82.9	98	91.7
	2	96.6	98.2	73.8
	3	94.6	99.4	96.5
R02-129	1	94.2	99.5	98.9
	2	91	99.1	98.1
	3	96.8	98.8	86.5
R02-171	1	94.7	97.6	99.4
	2	93.9	97.2	96.6
	3	95.4	99.3	99.3
R01-037	1	94	97.6	96.6
	2	96.9	99.3	98.5
	3	89.9	98.1	98.4
R02-015	1			
	2			
	3	92.6	99.2	99.3
R02-174	1	99.9	97.7	95.1
	2	97.3	97.9	96.4
	3	99.6	98.2	98.4
R02-079	1	82.6	81.2	96.4
	2	75.9	98.3	88.5
	3	87.4	90.8	77.6

Table L continued from previous page

Donor	Timepoint	Live cells (%)	$CD3^+$ (% of Live cells)	$CD4^+$ (% of $CD3^+$)
R02-109	1	93.7	99	99
	2	92.1	97.4	82.9
	3	84.1	95.5	81.4
R02-184	1	87.6	96.8	98.6
	2	75.9	94.9	97
	3	82.5	97.5	98.5
R02-185	1	78.3	96.5	96
	2	73.5	98.3	97.7
	3	40.6	97.4	93.3

Table L: Post-separation purities of $CD4^+$ cells from transplant recipients

M Individual results of viral dissemination assays performed on CD4$^+$ cells from transplant recipients

(A) D^+R^- Viraemic

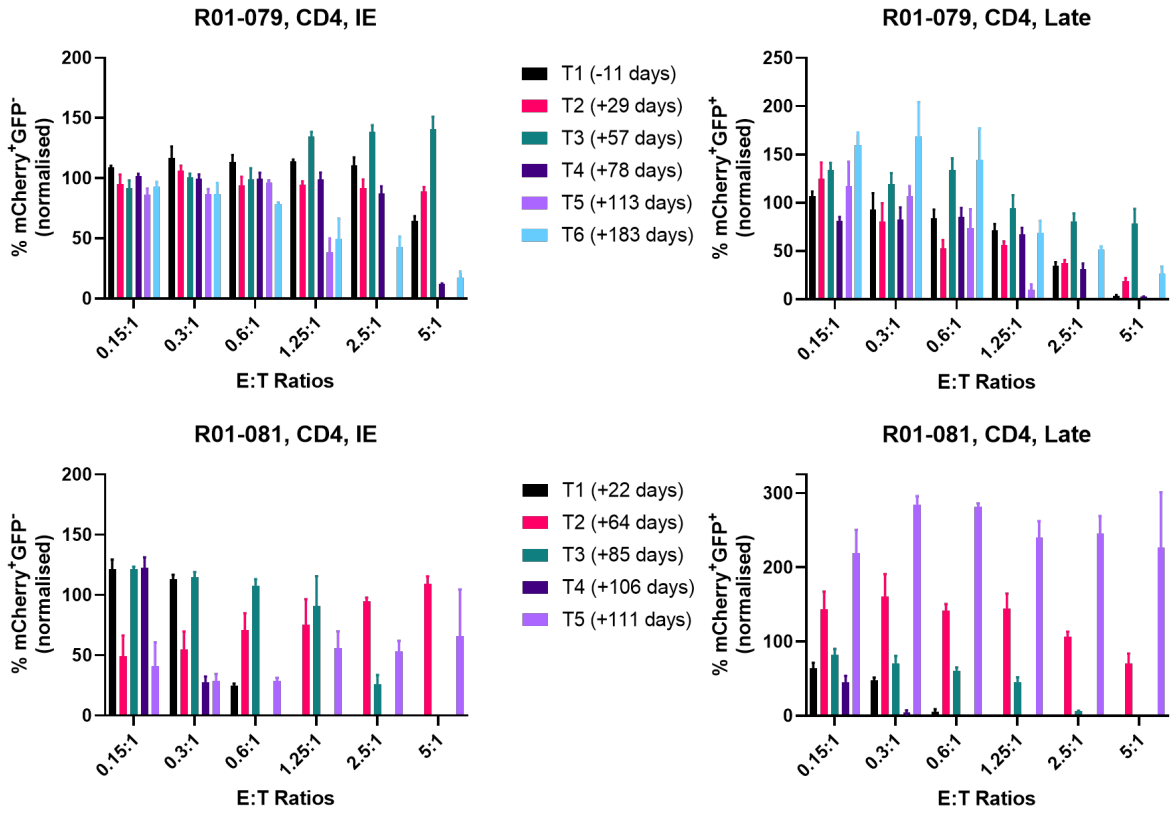

(B) D^+R^+ Viraemic

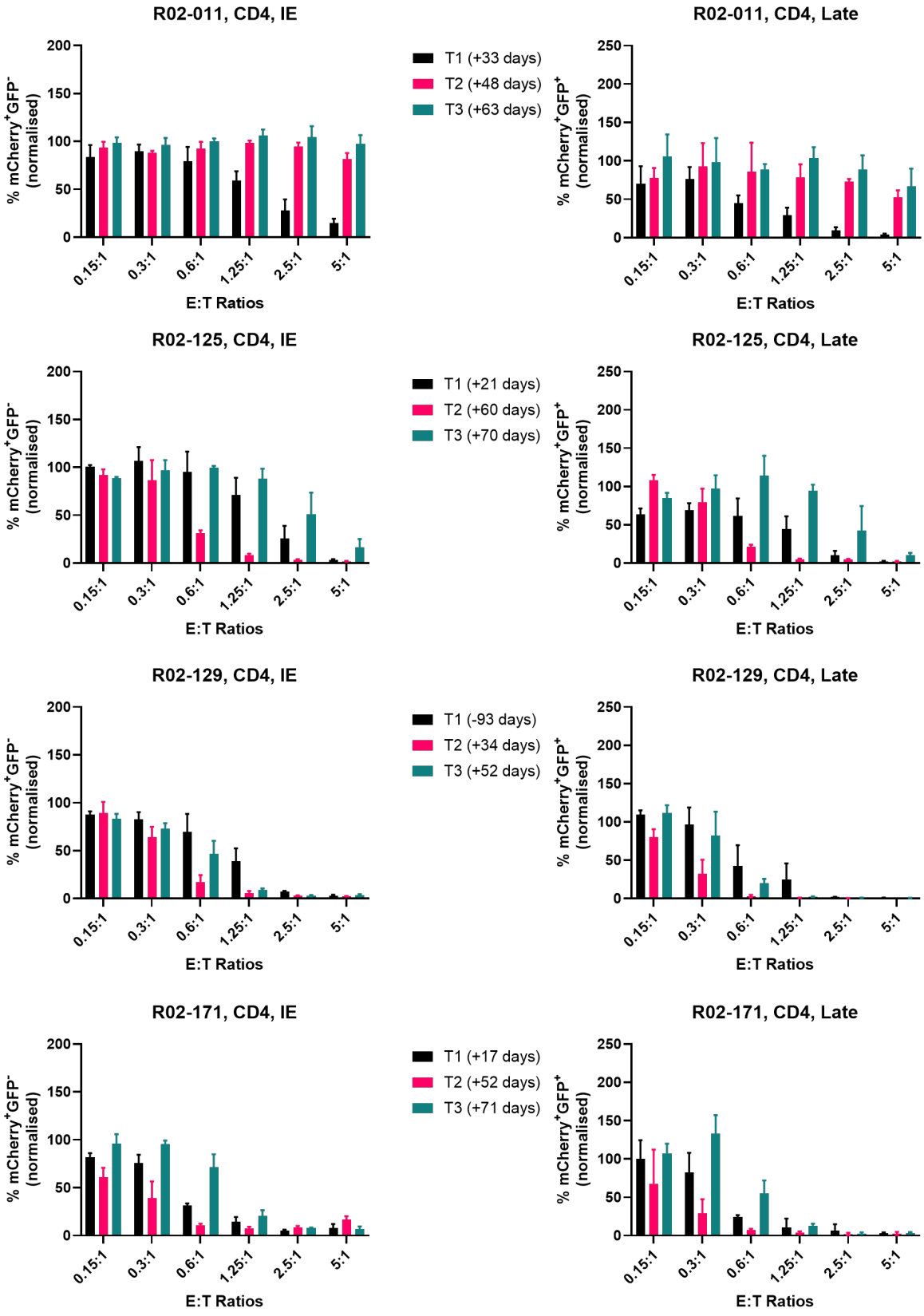

(C) D^+R^- Non-viraemic

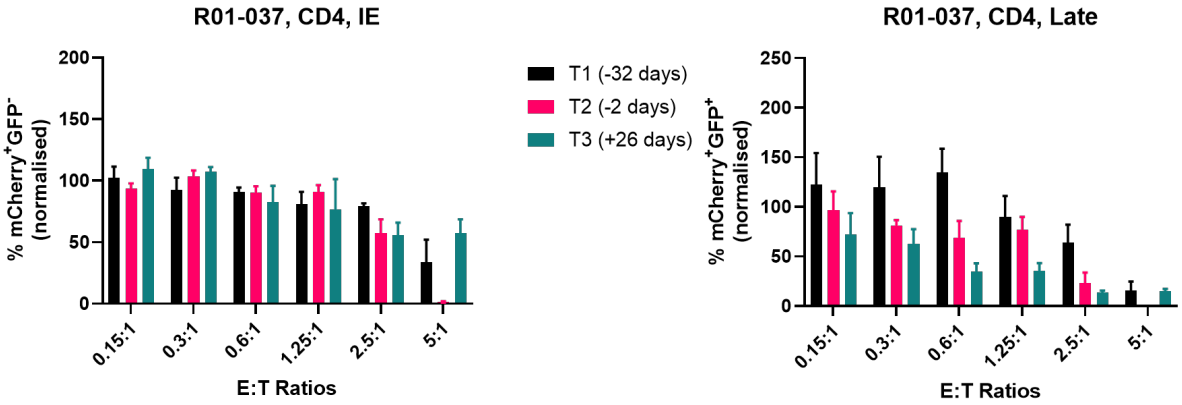

(D) D^-R^+ Non-viraemic

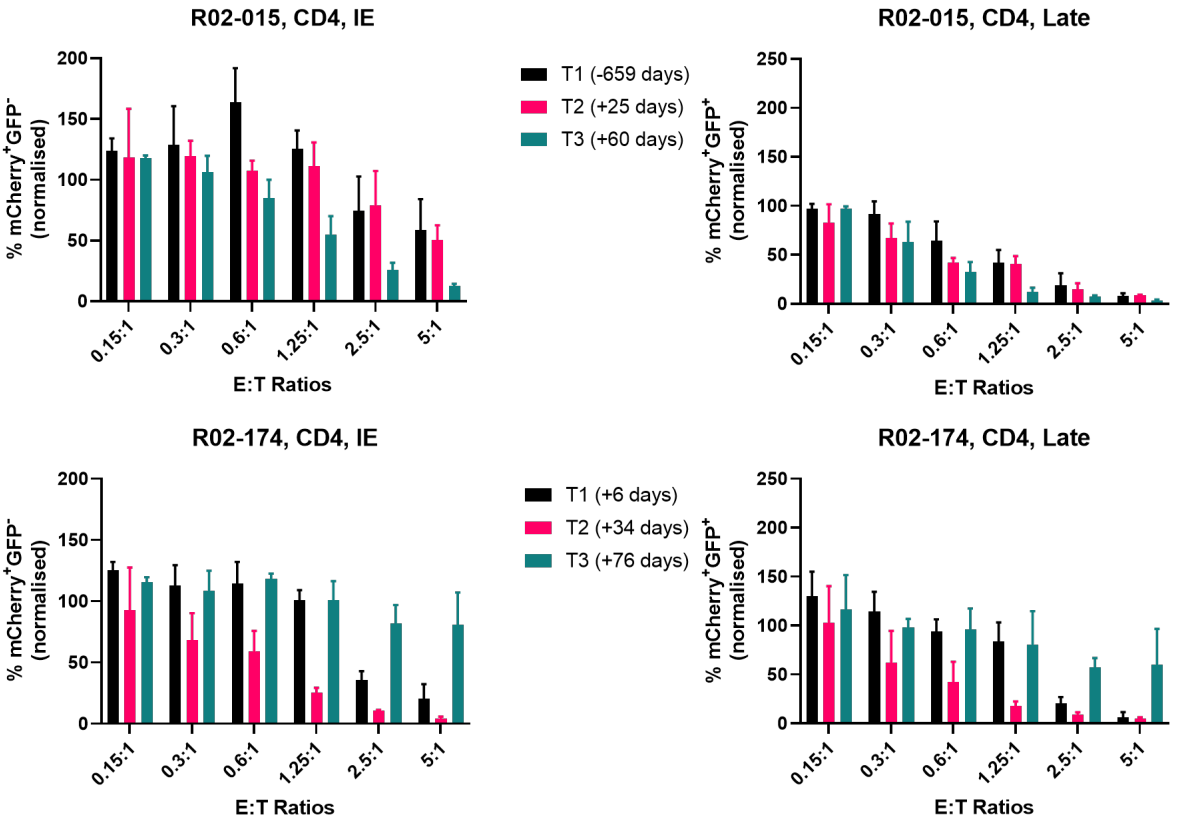

(E) D^+R^+ Non-viraemic

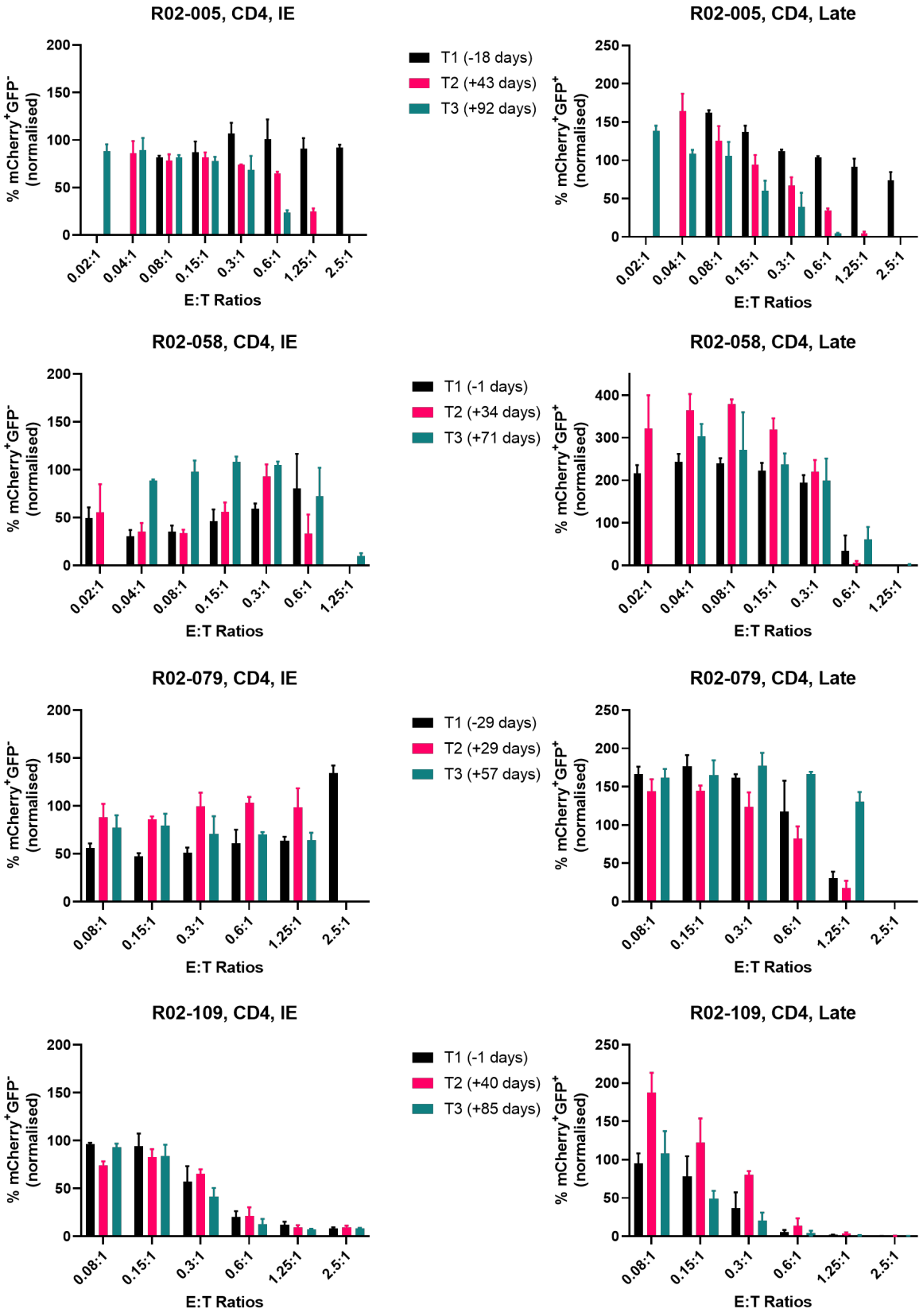

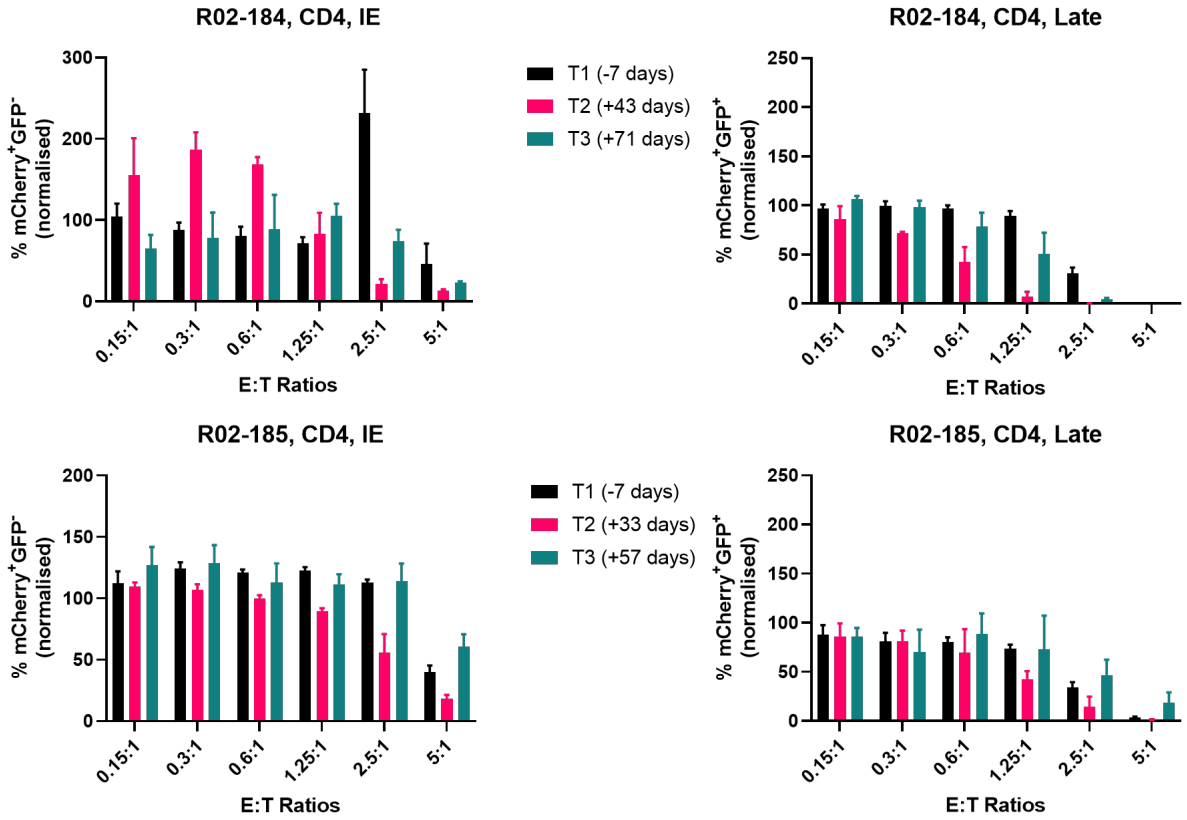

Figure M: Individual results of viral dissemination assays performed on CD4$^+$ cells from transplant recipients

T1 = Timepoint 1; T2 = Timepoint 2; T3 = Timepoint 3; T4 = Timepoint 4; T5 = Timepoint 5; T6 = Timepoint 6. Number of days pre- or post-transplant that sample was taken from is given in brackets in legend of each graph. Error bars represent SD of triplicate wells.

N Post-separation purities of CD8$^+$ T cells from transplant recipients

Donor	Timepoint	Live cells (%)	CD3$^+$ (% of Live cells)	CD8$^+$ (% of CD3$^+$)
R01-079	1	98.2	88.6	59.7
	2	99.2	88.7	89.7
	3	99.6	91.2	80
	4	95.3	91.9	80.1
	5	59.1	85	58
	6	91.8	96.7	89.1
R01-081	1	74.7	76.3	81.6
	2	71.8	90	89.4
	3			
R02-011	1	74.8	67.3	73.1
	2	85	78.8	74.3
	3	65.6	78.6	69.8
R02-125	1	70.4	72.6	58.4
	2	96.6	92.6	11.3
	3	87.5	94.2	73.9
R02-129	1	92.1	88.5	71.4
	2	82.5	79.1	61.7
	3	85.4	70.2	4.4
R02-171	1	83.6	89.4	78.8
	2	83.7	81.2	78.5
	3	89.6	91.6	85.3
R01-037	1	96.6	95.3	95.4
	2	96.4	92.9	95.4
	3	93.6	98.2	97.2
R02-015	1	85.4	81.9	97.9
	2	91.4	97	92.4
	3			
R02-174	1	97.4	72.2	80.5
	2	90.3	76.4	78.9
	3	94.1	81.6	83.5
R02-079	1	94.5	97.7	
	2	90.2	97.8	
	3	89.8	99.1	

Table N continued from previous page

Donor	Timepoint	Live cells (%)	CD3$^+$ (% of Live cells)	CD8$^+$ (% of CD3$^+$)
R02-109	1	91.6	99.4	
	2	94.3	93.8	
	3	94.2	94.2	
R02-184	1	88.2	84.1	99.3
	2	80.5	85.3	99.1
	3	89.3	86.2	98.9
R02-185	1	42	77	72.7
	2	55.3	91.2	85
	3	39.3	93.1	84.5
R02-005	1	22	92	
	2	27.5	90.5	
	3	19.1	90.9	

Table N: Post-separation purities of CD8$^+$ T cells from transplant recipients

O Individual results of viral dissemination assays performed on CD8$^+$ T cells from transplant recipients

(A) D^+R^- Viraemic

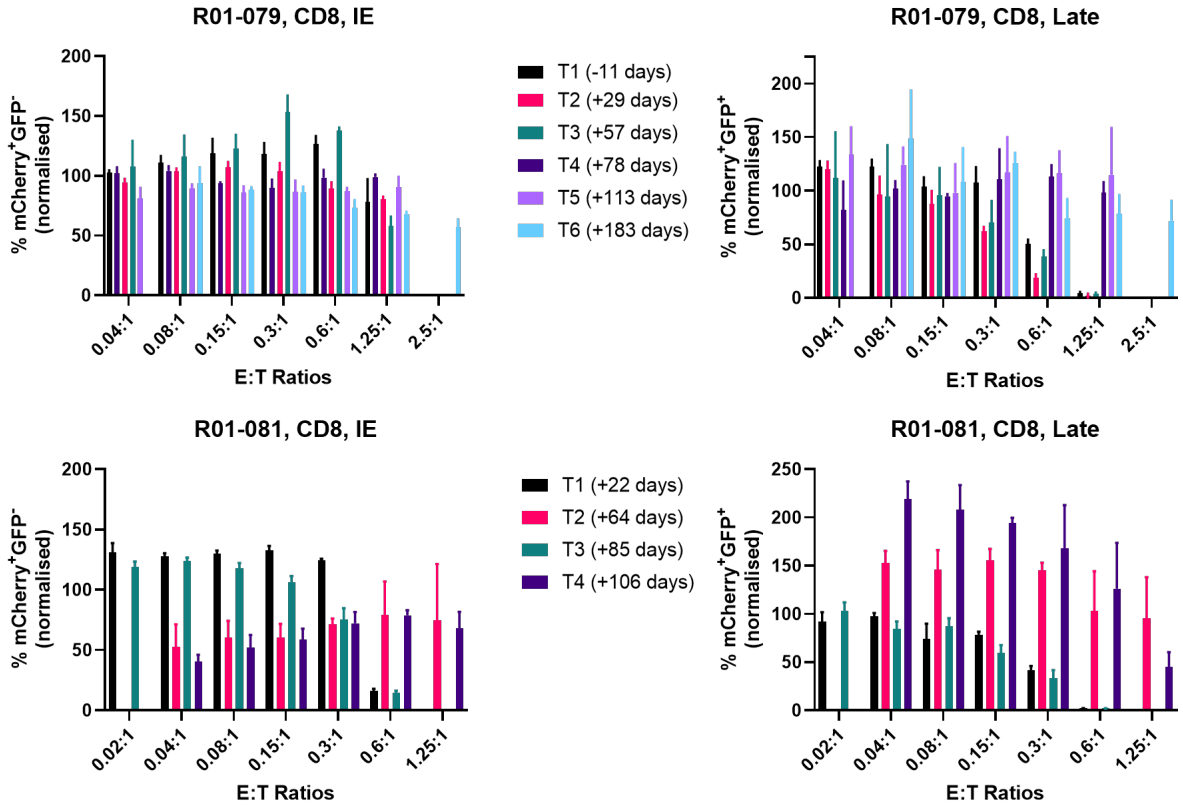

(B) D^+R^+ Viraemic

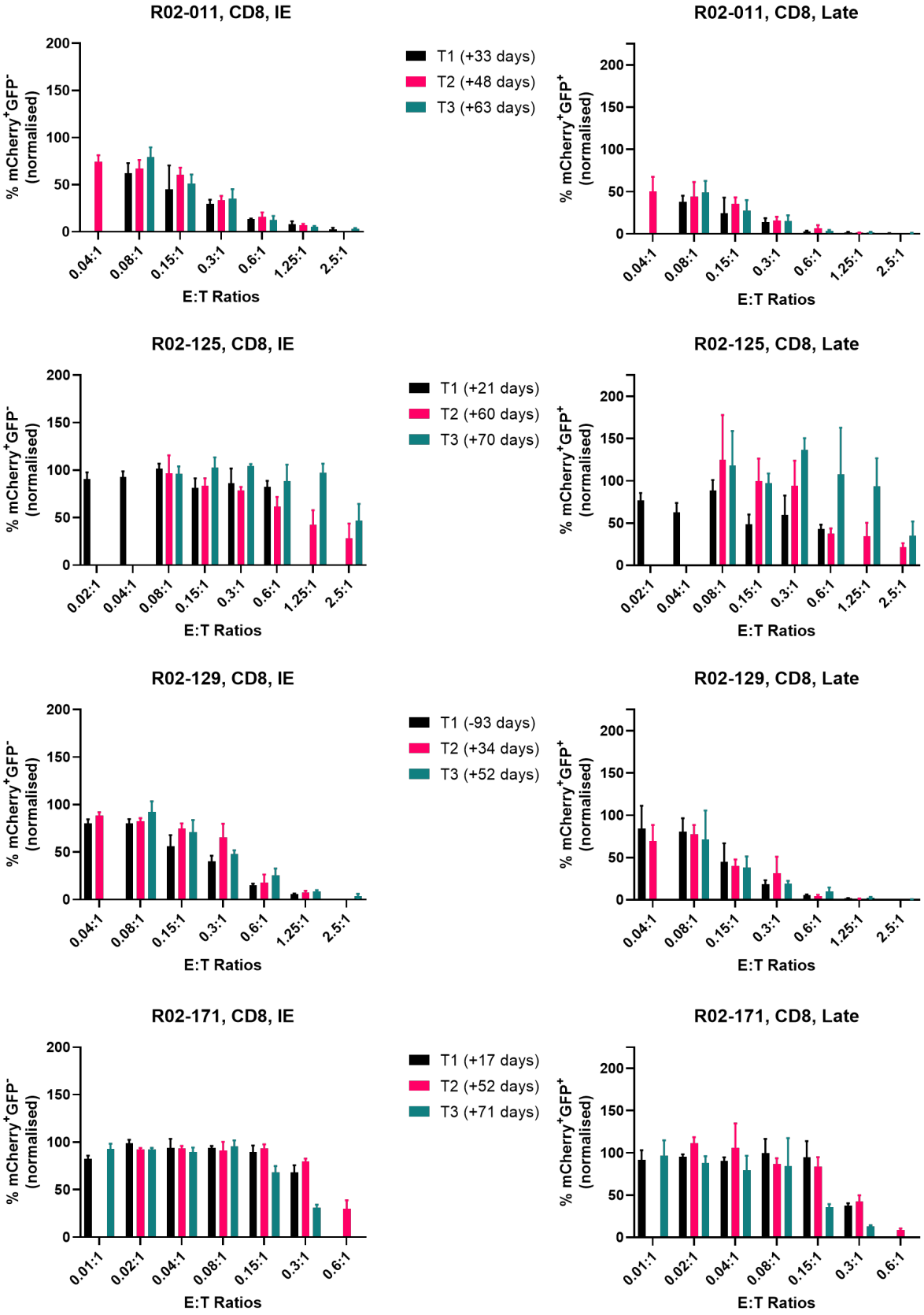

(C) D^+R^- Non-viraemic

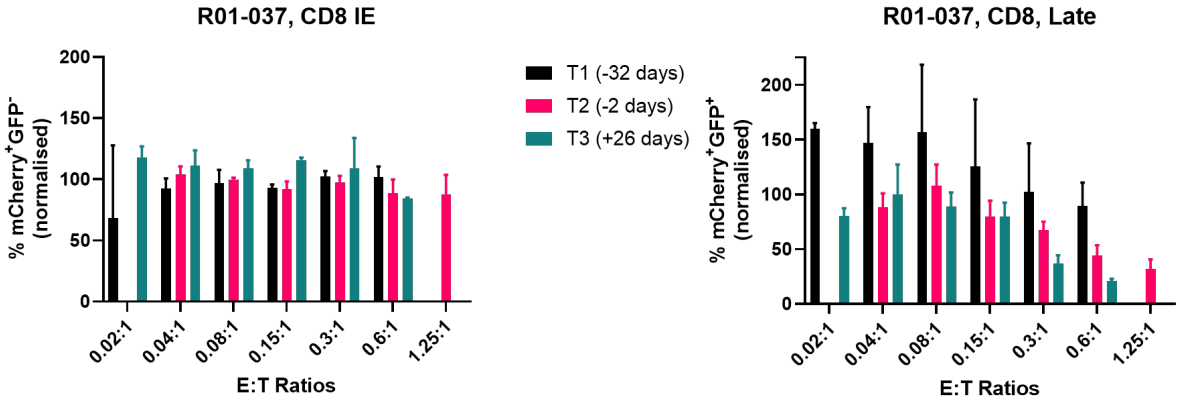

(D) D^-R^+ Non-viraemic

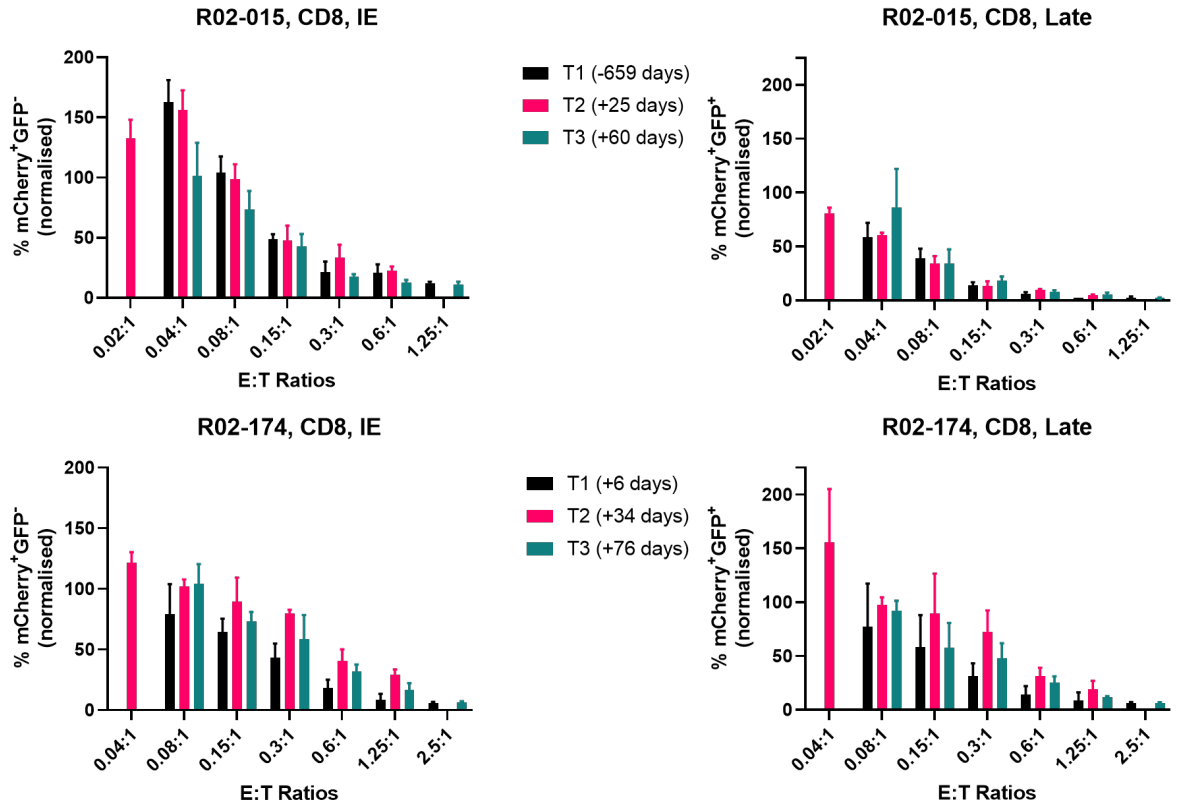

(E) D^+R^+ Non-viraemic

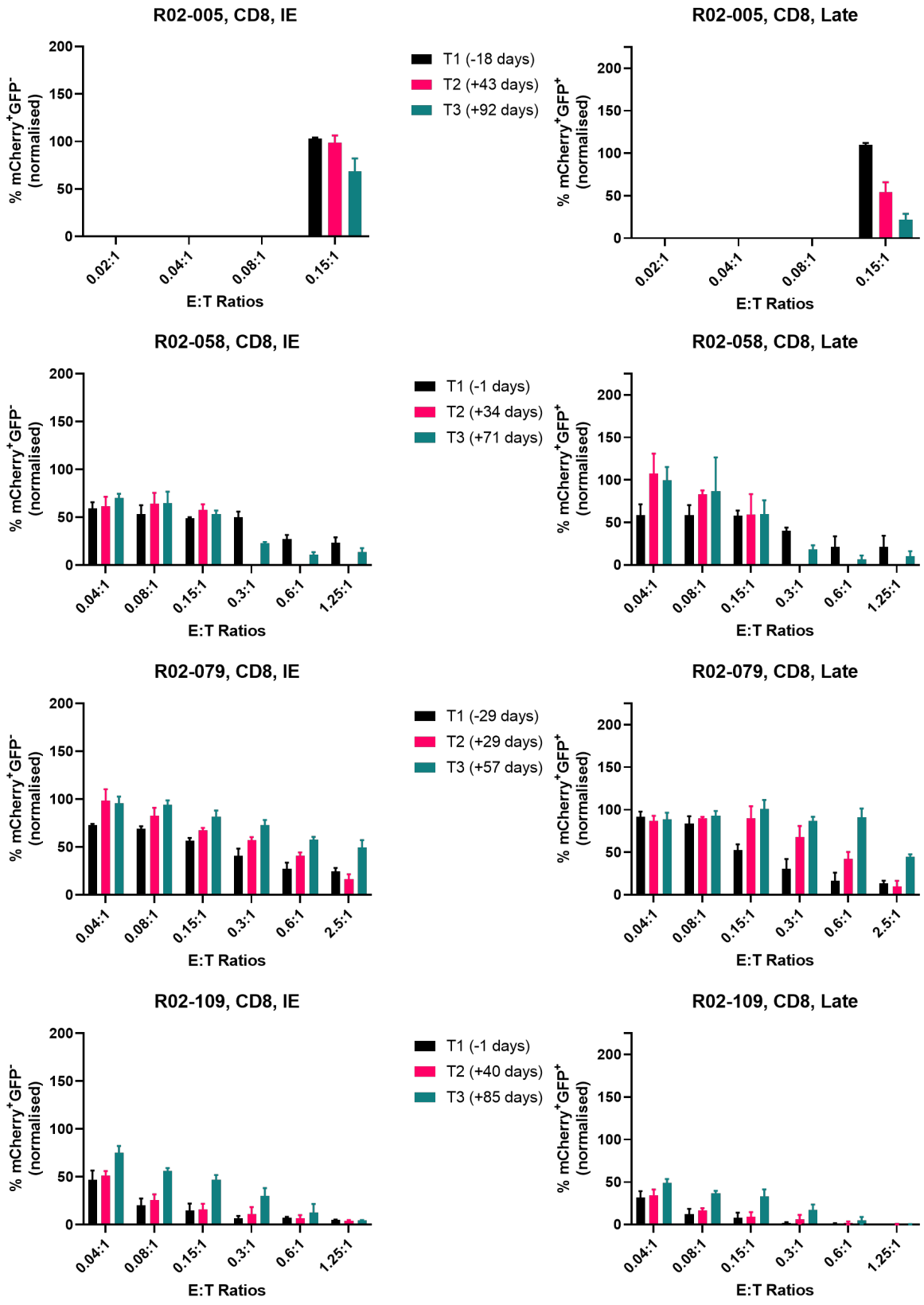

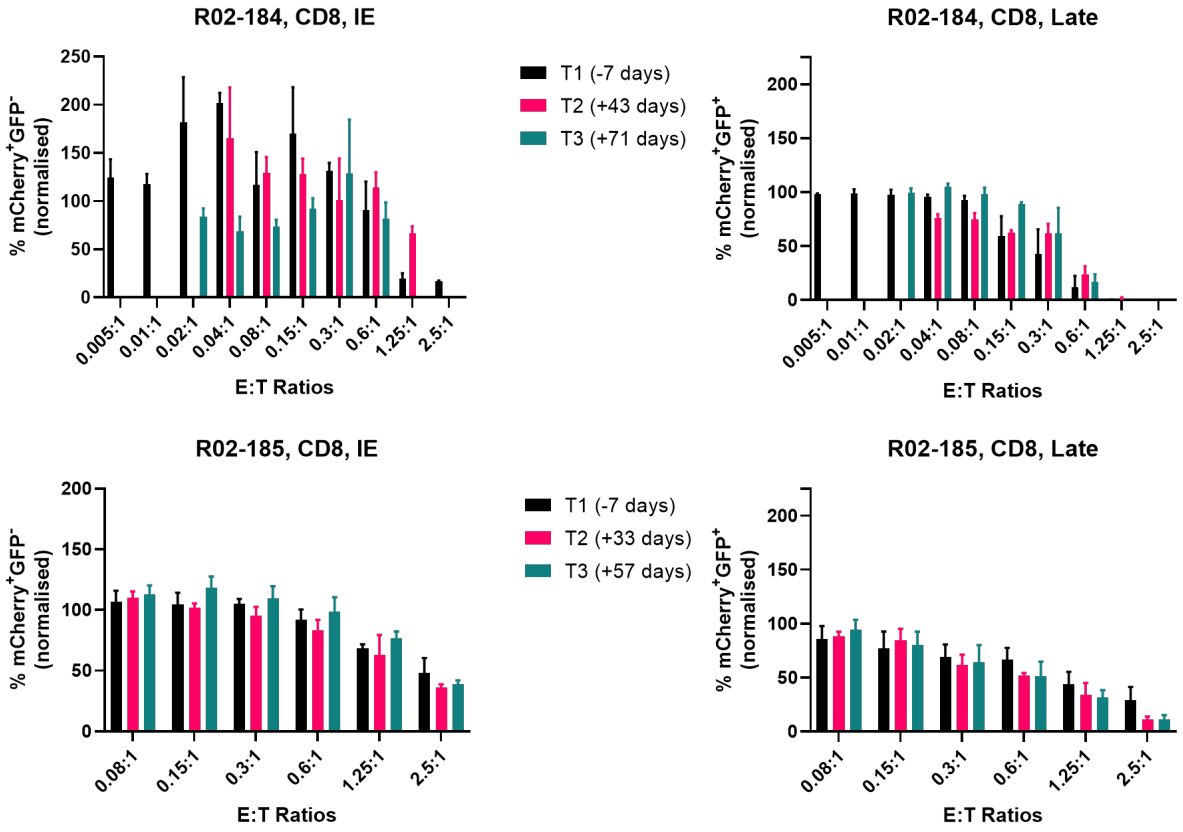

Figure O: Individual results of viral dissemination assays performed on CD8$^+$ T cells from transplant recipients

T1 = Timepoint 1; T2 = Timepoint 2; T3 = Timepoint 3; T4 = Timepoint 4; T5 = Timepoint 5; T6 = Timepoint 6. Number of days pre- or post-transplant that sample was taken from is given in brackets in legend of each graph. Error bars represent SD of triplicate wells.

P Post-separation purities of NK cells from transplant recipients

Donor	Timepoint	Live cells (%)	$CD3^-$ (% of Live cells)	$CD56^{dim}$ (% of $CD3^-$)	$CD56^{bright}$ (% of $CD3^-$)
R01-079	1	98.2	99.7	33.2	66.4
	2	98.9	99.8	17.7	82
	3	98.4	99.8	87	89.4
	4	86.8	85.1	53.6	35.4
	5	81.7	85	61.2	21.2
	6	90.2	95.9	30.6	36
R01-081	1	87	98.5	97.3	25
	2	71	92.4	92.4	50
	3				
R02-011	1	99.1	97.4	66.4	24.1
	2	99.7	98.7	61.9	26.5
	3	99.5	91.6	77.2	2.4
R02-125	1	92.6	100	75.8	16.6
	2	96.1	100	45.1	0.3
	3	88.8	97.5	56.8	2.8
R02-129	1	96.6	96.9	82.1	10
	2	91.9	96.7	84.8	2.3
	3	95.9	99.7	63.4	0.1
R02-171	1	88.9	99.2	39.7	47.4
	2	83.1	99.7	31.9	38.1
	3	85.6	99.8	44.8	48.3
R01-037	1	99.1	94.4	89.7	8.4
	2	98.5	92.5	76.2	21.2
	3	99.4	95.1	74.2	25.2
R02-015	1	73.6	98.8	67.1	19.4
	2				
	3	87.8	95.8	58.7	5.2
R02-174	1	88.2	99.4	42.7	0.1
	2	80.2	98.8	48.7	2.1
	3	88.6	99.6	40.5	6.5
R02-079	1*	60.3	45.1	97.3	0
	2*	57.9	89.1	95.9	4.08
	3				

Table P continued from previous page

Donor	Timepoint	Live cells (%)	$CD3^-$ (% of Live cells)	$CD56^{dim}$ (% of $CD3^-$)	$CD56^{bright}$ (% of $CD3^-$)
R02-109	1	94.8	67.3	54.8	24.1
	2	93.8	99.7	63.9	35.8
	3	92.2	56.8	53.7	19.7
R02-184	1				
	2	76	97.1	91.5	4.91
	3	77.4	99.1	95.4	2.17
R02-185	1	84.6	98.6	74.1	19.4
	2	85.9	98.1	53.4	41.5
	3	86.8	98.7	42.8	50.6

Table P: Post-separation purities of NK cells from transplant recipients
*Very few cells in sample

Q Individual results of viral dissemination assays performed on NK cells from transplant recipients

(A) D^+R^- Viraemic

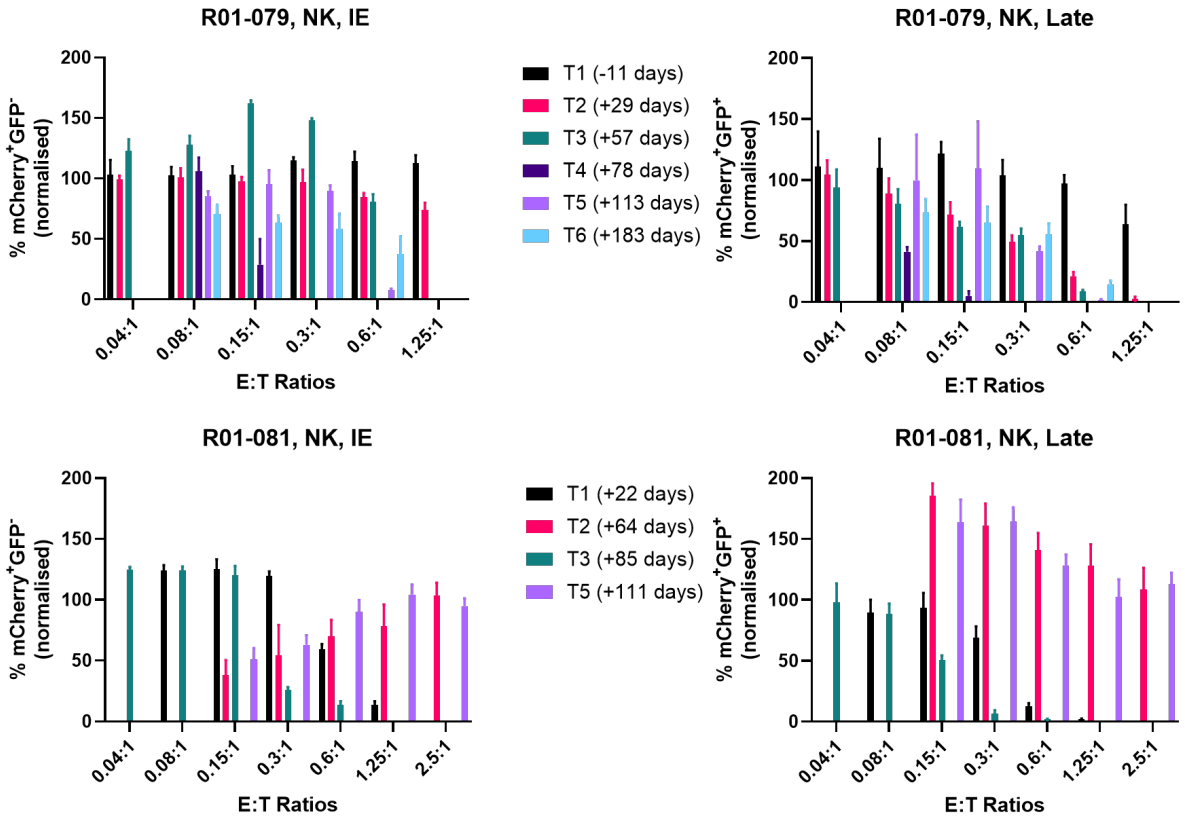

(B) D^+R^+ Viraemic

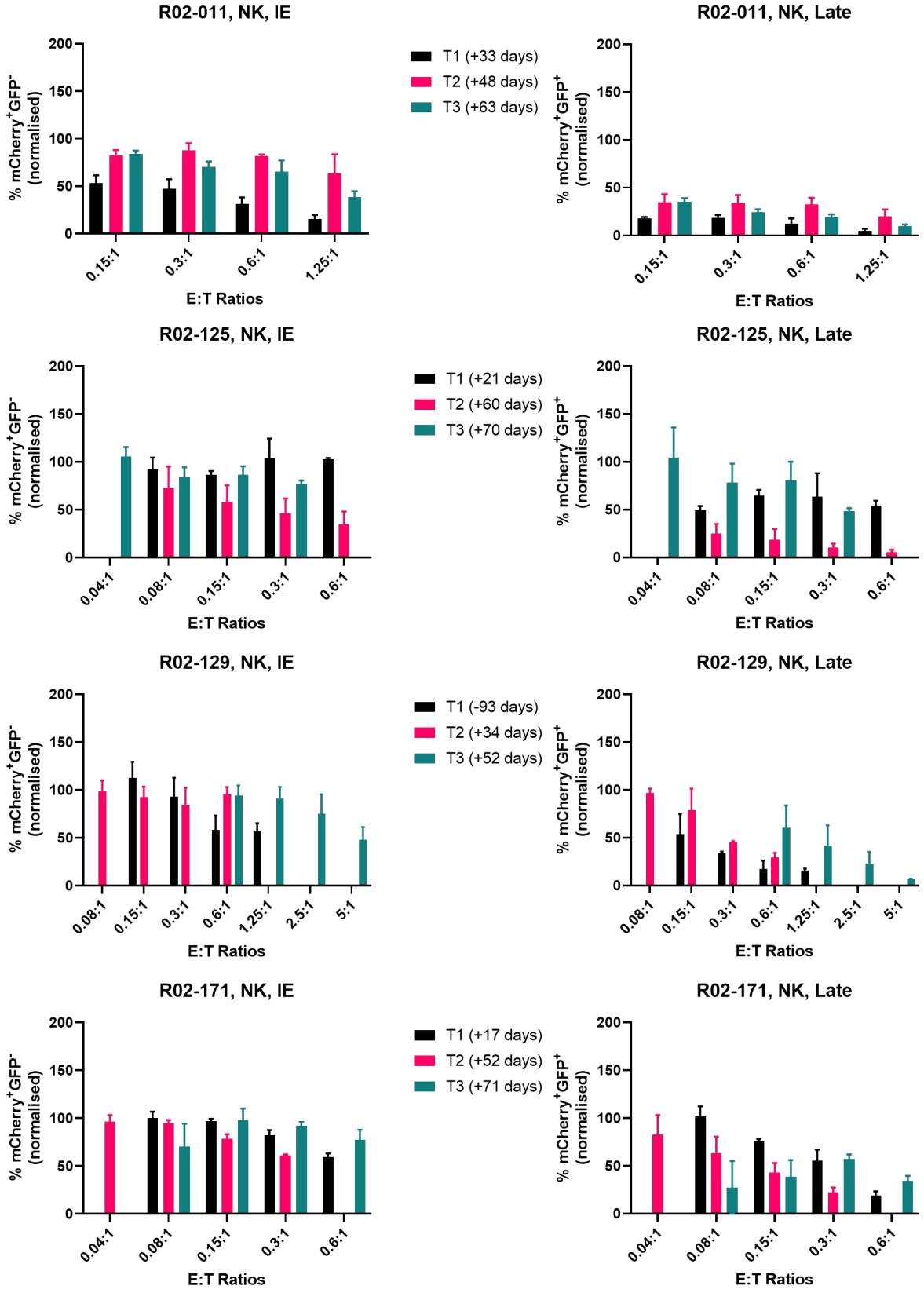

(C) D^+R^- Non-viraemic

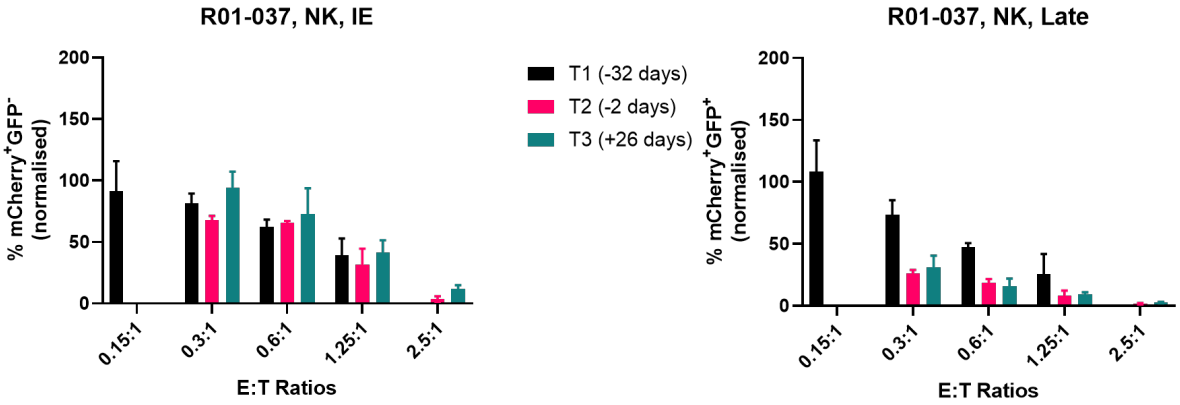

(D) D^-R^+ Non-viraemic

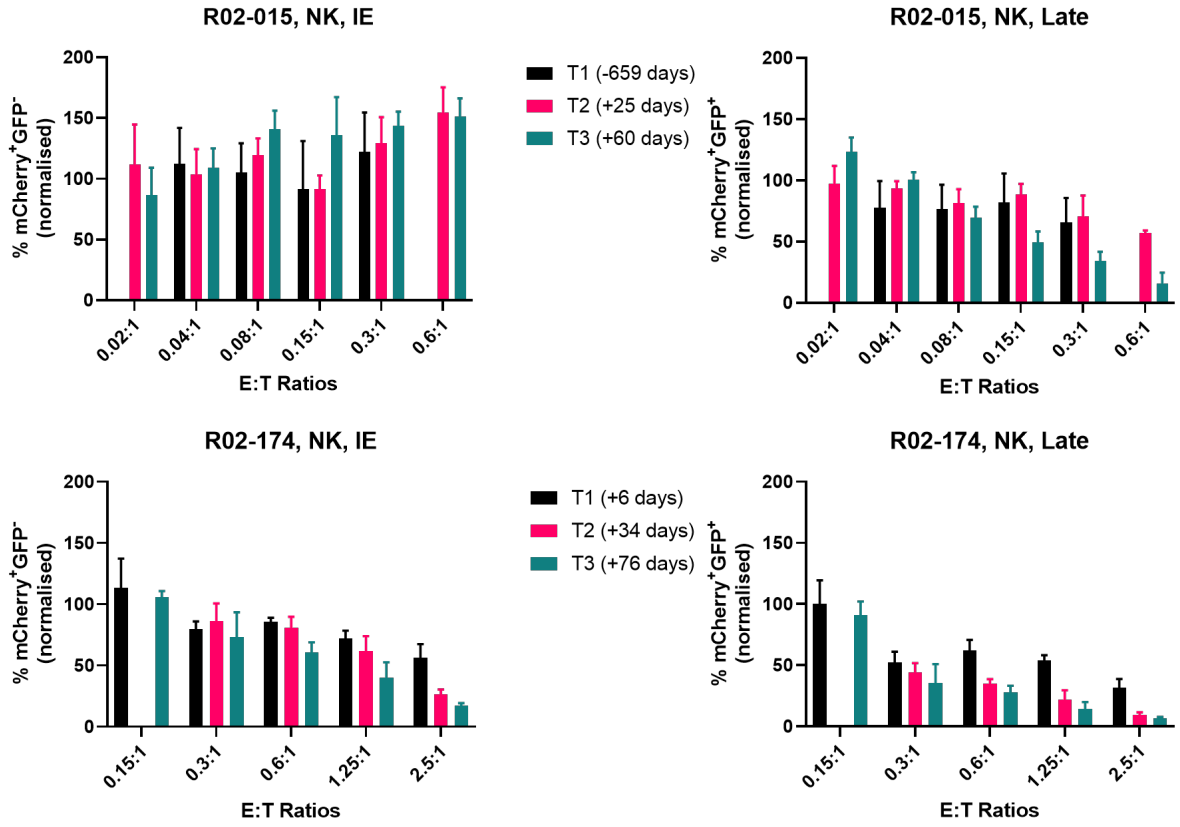

(E) D^+R^+ Non-viraemic

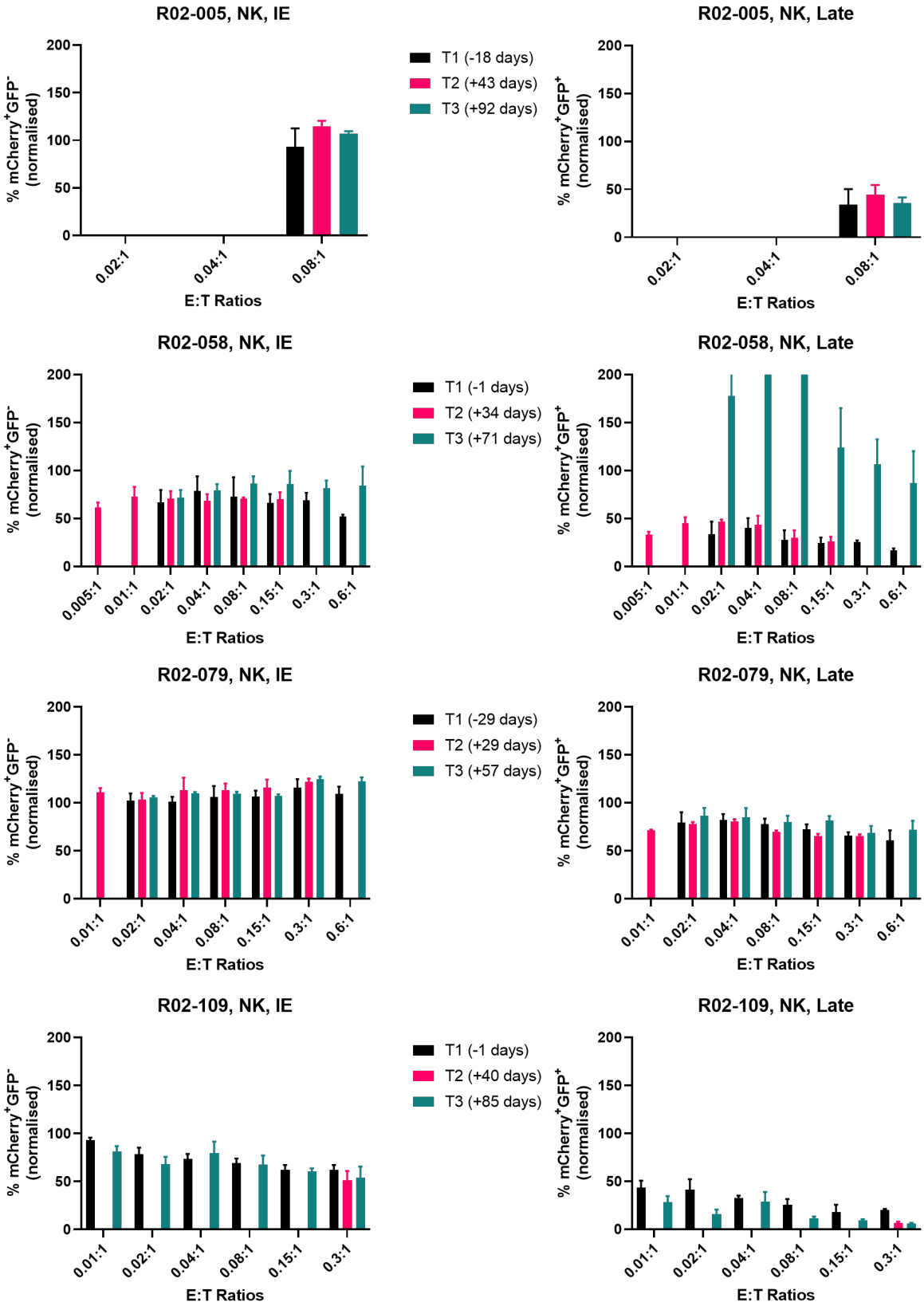

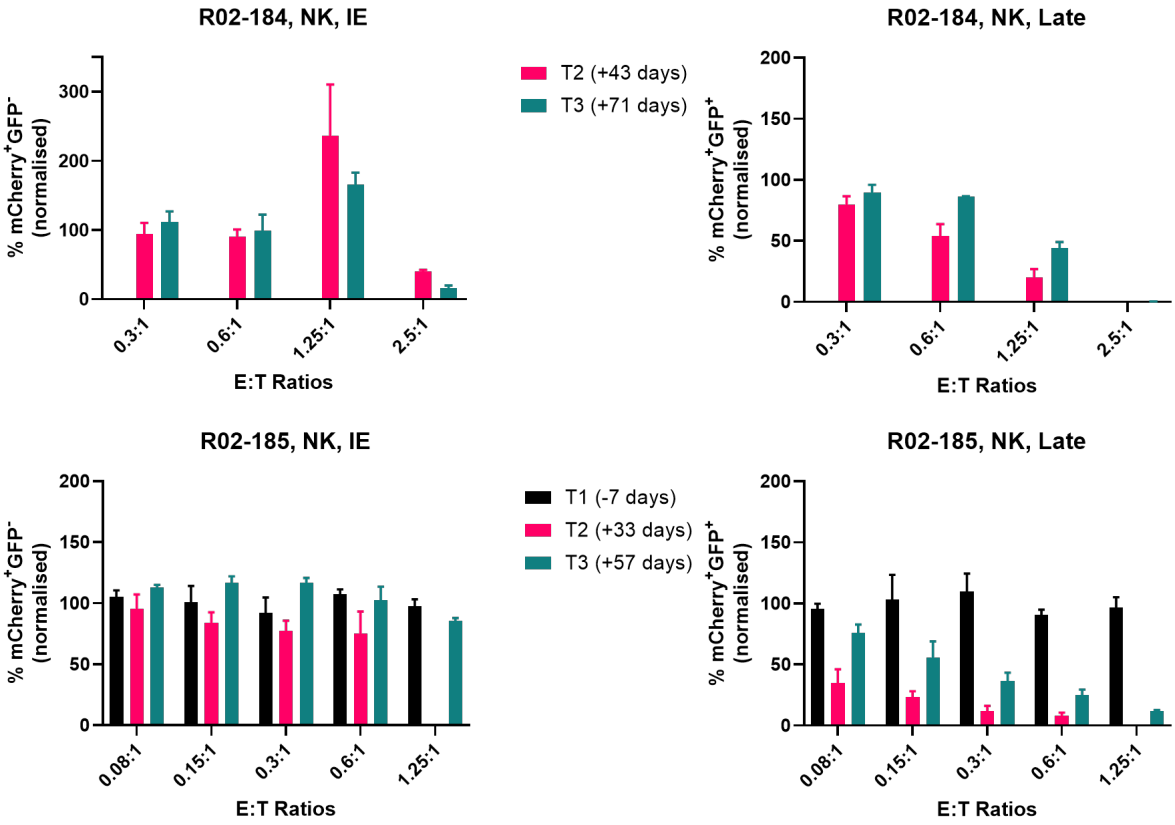

Figure Q: Individual results of viral dissemination assays performed on NK cells from transplant recipients

T1 = Timepoint 1; T2 = Timepoint 2; T3 = Timepoint 3; T4 = Timepoint 4; T5 = Timepoint 5; T6 = Timepoint 6. Number of days pre- or post-transplant that sample was taken from is given in brackets in legend of each graph. Error bars represent SD of triplicate wells.

R List of publications authored related to this project

1. Lim, E. Y., Jackson, S. E., & Wills, M. R. (2020). The $CD4^+$ T Cell Response to Human Cytomegalovirus in Healthy and Immunocompromised People. *Frontiers in cellular and infection microbiology,* 10, 202. https://doi.org/10.3389/fcimb.2020.00202

2. Houldcroft, C. J., Jackson, S. E., Lim, E. Y., Sedikides, G. X., Davies, E. L., Atkinson, C., McIntosh, M., Remmerswaal, E., Okecha, G., Bemelman, F. J., Stanton, R. J., Reeves, M., & Wills, M. R. (2020). Assessing Anti-HCMV Cell Mediated Immune Responses in Transplant Recipients and Healthy Controls Using a Novel Functional Assay. *Frontiers in cellular and infection microbiology,* 10, 275. https://doi.org/10.3389/fcimb.2020.00275